

Human Milk Oligosaccharides as a Defense
Against Infectious Diseases

By

Kelly Marie Craft

Dissertation

Submitted to the Faculty of the
Graduate School of Vanderbilt University
in partial fulfillment of the requirements

for the degree of

DOCTOR OF PHILOSOPHY

in

Chemistry

May 10, 2019

Nashville, Tennessee

Approved:

Steven D. Townsend, Ph.D.

Brian O. Bachmann, Ph.D.

Jennifer A. Gaddy, Ph.D.

Gary A. Sulikowski, Ph.D.

ACKNOWLEDGMENTS

First and foremost, I would like to thank my advisor Prof. Steven D. Townsend for his invaluable mentorship and support during my time at Vanderbilt. I cannot speak highly enough of him as a mentor, scientist, or person. Before joining Steve's lab, I had been in plenty of chemistry classes and done well, but I had had limited research experience. As I know Steve enjoys telling people, when I first joined his lab, I had a few moments where my inexperienced chemistry hands were on full display. Thankfully, my hands have improved since then as has my general chemical knowledge. While the time and effort I put in to improve as a chemist have of course been important in my graduate career, my success at Vanderbilt is quite truly a testament to Steve and his capabilities as a mentor and as a scientist. Most of what I have learned as an experimentalist is thanks to Steve and his guidance. He has always been willing and able to help me and to meet me where I needed in terms of mentorship. He has also always fostered a highly collaborative environment and has believed in me and my ideas even when I did not.

In addition to my immense gratitude to him for his mentorship in research, I am also extremely grateful for the care he puts into ensuring his student's well-being and happiness. Steve has always provided me with a safe space to share not only my frustrations but also my triumphs. Whether it was talking me down when I walked into his office so mad I had tears in my eyes or laughing with me as we swapped horror stories, my conversations with Steve are something I will carry with me forever. In short, it has been an absolute pleasure getting to work with him these past five years, and I thank him for letting me be a part of his lab at its beginning.

I would also like to thank my remaining committee members Prof. Brian O. Bachmann, Prof. Jennifer A. Gaddy, and Prof Garry A. Sulikowski for all the support and advice they have given me throughout the years. They have proved to be a wonderful support system and have pushed me continually to keep improving. I am forever grateful for the effort they put in to help me develop as a scientist. I would especially like to thank Jen for her generous mentorship and support. I came to Vanderbilt as a chemist, and thanks to Jen, I leave as a chemist who also at least somewhat knows her way around a biology lab. Prior to working in Jen's lab, I had no microbiology research experience, so teaching me the ins and outs of a biology lab was no easy task. However, Jen was up for the challenge and has been instrumental in my development as a chemist who gets to moonlight as a biologist. Again, I will be forever grateful for her mentorship, her willingness to let me use her lab space and supplies, and her willingness to take special trips down the elevator to let me into lab (I still don't have card access).

Additionally, I have to thank Dr. Ryan S. Doster and Jacky Lu of the Gaddy lab for all their help throughout the years. Ryan was there at the beginning of my time in the Gaddy lab, and he has been willing to help me learn from day one. Ryan helped me learn how to design biological assays, how to prepare and run those assays, and how to interpret data. Jacky has been a great source of help and friendship over the last few years. He has always been ready and willing to help me with anything I needed in the Gaddy lab, including making several trips into lab on a Sunday to subculture bacteria for me to use the following day (I still don't have access to the building). I also have to thank Jacky and Ryan for the countless trips they too made down the elevators to let me into lab. Have I mentioned that I don't have access to the building yet?

I have also been fortunate enough to have a wonderful group of people around me in the chemistry department. First, I want to acknowledge Jade Bing and Audrey Yniguez-Gutierrez. Jade, Audrey, and I first met on visitation weekend and I am so thankful that we did. During my time at Vanderbilt, Jade and Audrey have not only pushed me to become a better scientist, they have also been invaluable sources of friendship and support. While my graduate school career has had its high points, it has certainly had its fair share of low points. Having friends like Jade and Audrey who could pick me up when I was down or celebrate with me when one of us had a good day was without a doubt integral to my ability to survive graduate school and to do so with my sanity at least mostly intact.

I also have to thank the other members of the Townsend lab. First, I would like to thank John Hayes who served as a mentor to me when I first joined. Even though he had been in the lab for less than a year, he took my questions like a seasoned pro. I thank him for answering all my questions and for challenging me with follow-up questions of his own. Next, I would like to thank Jamin Keith. Jamin...we made it! Jamin and I joined the lab together and though we may not have always seen eye to eye, I am very thankful to have taken this walk together. Thank you Jamin for being a constant source of knowledge and entertainment, and I wish you the best with your next chapter. Oh, and now I can tell you, I'm the one who put water in the unlabeled acetone bottle that you used one day to wash out your column fractions. Sorry. Next, I would like to thank Eric Huseman. Eric is one of the most knowledgeable and kindest people I have ever met and thank goodness for that. I have found that having someone who is willing and able to answer all of your

stupid questions without judgment is an invaluable asset. Eric, thank you so much for being that person for me.

I would also like to thank the remaining Townsend lab members Schuyler Chambers, Johny Nguyen, Lianyan Xu, Rebecca Moore, and Cleo Evans. Johny, you have been a fantastic deskmate, and I have enjoyed our conversations and your infectious positivity. Schuyler, thank you for your knowledge and for putting up with all my ordering requests. I wish you the best of luck as you continue on with the HMO project, and I cannot wait to see what you accomplish. Lianyan, Rebecca, and Cleo, it has been a pleasure getting to know you, and I am excited to see what your graduate careers have in store! Lastly, I have had the pleasure of working with several talented undergraduate students. I am extremely grateful for Harrison Thomas who worked long hours with me to generate growth curves and count colonies for days on end. Thank you for your constant willingness to work, your immense kindness, and your fantastic sterile technique. I would also like to thank Rishub Das. Rishub was the first student I had the opportunity to mentor, and I thank him for being patient with me. It was a pleasure to work with him, and I thank him for his extensive HMO isolation efforts.

In addition to a solid support system at Vanderbilt, I have also been and continue to be blessed with a solid support system outside of work. This support system first and foremost consists of my mom and dad as well as my sisters Meghan and Tessa. I cannot begin to describe how much your love and support have helped me become who I am today. Thank you for always being there for me whether that be celebrating a success or listening patiently while I vented about frustrations about work or life. I know those venting sessions were sometimes all too frequent. I also have to thank Jamie, Jennifer, and

Richelle for being some of the best friends anyone could ask for. Thank you for your constant friendship and support and for dealing with my often hectic schedule. Finally, I would like to thank my church family. They have always made me feel at home and welcome. They have been a constant bright spot even when work and life felt overwhelming, and, for that, I am forever grateful.

Finally, I would like to thank all of my chemistry teachers, professors, and mentors who helped me prior to my start at Vanderbilt. I feel strongly that one's passion for a subject is largely shaped by the teachers they encounter along the way. Thankfully, throughout my education, I have had chemistry teachers that have inspired me and helped me to develop a love for chemistry. To my high school chemistry teacher, Mr. Jones, thank you for sharing your passion for chemistry with me and for introducing me to organic chemistry. It was the experience I had in your classes that inspired me to major in chemistry. To my chemistry professors at Birmingham-Southern College, thank you for your passion, commitment, and knowledge. In particular, I would like to thank my undergraduate research advisor Prof. David A. Schedler. The experiences I had in your class and in your research lab led me to pursue graduate studies in organic chemistry. Your support, passion, and mentorship were instrumental in directing my career path, and, for that, I thank you.

TABLE OF CONTENTS

	Page
ACKNOWLEDGMENTS	ii
LIST OF TABLES	xii
LIST OF FIGURES	xvi
LIST OF SCHEMES.....	xxviii
LIST OF ABBREVIATIONS	xxxii
CHAPTER	
1. Antibiotics and the Evolution of Resistance	1
1.1 Introduction	1
1.2 Mechanisms of Antibiotic Action	6
1.2.1 Introduction.....	6
1.2.2 Cell Wall-Targeting Antibiotics.....	7
1.2.3 Cell Membrane-Targeting Antibiotics.....	14
1.2.4 Protein Synthesis-Targeting Antibiotics	18
1.2.5 DNA and RNA-Targeting Antibiotics.....	23
1.2.6 Folate Biosynthesis-Targeting Antibiotics	29
1.3 Mechanisms of Antibiotic Resistance.....	32
1.3.1 Introduction.....	32
1.3.2 Prevention of Antibiotic Target Engagement	34
1.3.3 Modification of Antibiotic Structure	36
1.3.4 Modification of Antibiotic Target	41
1.4 The ESKAPE Pathogens	48
1.5 Alternative Approaches to Current Antibiotic Monotherapy.....	54

1.5.1 Multi-Antibiotic Combination Therapies	55
1.5.2 Antibiotic and Antibiotic Adjuvant Combination Therapies.....	57
1.5.3 Antivirulence Antibiotics.....	60
1.5.4 Narrow-Spectrum Antibiotics	61
1.6 Conclusions and Future Outlook.....	63
1.7 References	64
2. Human Milk Oligosaccharides: A Source of Protection Against Infectious Diseases.....	76
2.1 Infant Feeding: A Brief History	76
2.2 Human Milk Composition	78
2.2.1 Fats	79
2.2.2 Proteins	81
2.2.3 Carbohydrates.....	86
2.3 Human Milk Oligosaccharides: Discovery and Early Research	91
2.4 Human Milk Oligosaccharides: Structure and Biosynthesis.....	97
2.5 Human Milk Oligosaccharides: Health Benefits	113
2.5.1 Prebiotics.....	113
2.5.2 Antiadhesive Antimicrobials.....	121
2.6 Conclusions and Future Outlook.....	125
2.7 References	127
3. Evaluation of the Antibacterial Properties of Heterogeneous Human Milk Oligosaccharides Against <i>Streptococcus agalactiae</i> , <i>Staphylococcus</i> <i>aureus</i> , and <i>Acinetobacter baumannii</i>	140
3.1 Group B <i>Streptococcus</i>	140

3.1.1 Group B <i>Streptococcus</i> : An Introduction	140
3.1.2 Clinical Manifestations and Modes of Transmission	140
3.1.3 Types of GBS Disease and Methods for Prevention and Treatment.....	142
3.1.4 GBS Virulence Factors	147
3.1.5 Maternal-Derived Sources of Protection Against GBS	153
3.1.6 HMOs as a Source of Protection Against GBS: Previous Work.....	155
3.2 Evaluation of Antimicrobial and Antibiofilm Properties of Heterogenous HMOs	161
3.2.1 HMO Isolation and Blood Group Characterization.....	162
3.2.2 Evaluation of Antimicrobial and Antibiofilm Activities of HMOs Against GBS	163
3.2.3 Evaluation of Antimicrobial and Antibiofilm Activities of HMOs Against <i>Staphylococcus aureus</i> and <i>Acinetobacter</i> <i>baumannii</i>	169
3.3 Investigation of HMO Antimicrobial Mechanism of Action.....	180
3.3.1 Evaluation of Heterogeneous HMOs in Antibiotic Combination Therapies	180
3.3.2 Evaluation of HMO Antimicrobial Mechanism of Action.....	192
3.4 Conclusions and Future Outlook.....	194
3.5 Experimental Methods	196
3.5.1 General Methods and Materials	196
3.5.2 Evaluation of Antimicrobial and Antibiofilm Activities of HMOs Against GBS, <i>Staphylococcus aureus</i> and <i>Acinetobacter</i> <i>baumannii</i>	197
3.5.3 Investigation of HMO Antimicrobial Mechanism of Action	201
3.6 References	204
Appendix A1: Data and Spectra Relevant to Chapter 3.....	217

4. Synthesis of Lacto- <i>N</i> -Tetraose	251
4.1 Rationale for the Synthesis of Lacto- <i>N</i> -Tetraose	251
4.2 Methods for Oligosaccharide Synthesis.....	253
4.3 Chemical Approaches for Oligosaccharide Synthesis	254
4.3.1 Glycoside Bond Formation: The Glycosylation Reaction.....	254
4.3.2 The Anomeric Effect.....	256
4.3.3 Protecting Groups.....	257
4.3.4 Solvent Effects	261
4.3.5 Glycosyl Donors	263
4.4 Previous Syntheses of Lacto- <i>N</i> -Tetraose and Derivatives.....	270
4.4.1 Introduction.....	270
4.4.2 Tejima et al. LNT Synthesis (Chemical)	271
4.4.3 Schmidt et al. LNT Synthesis (Chemical)	273
4.4.4 Chen et al. LNT-ProN ₃ Synthesis (Chemical).....	277
4.4.5 Wong et al. Linker-Attached Lc ₄ Synthesis (Chemical)	280
4.4.6 Albermann et al. LNT Synthesis (Enzymatic)	282
4.5 Synthesis of Lacto- <i>N</i> -Tetraose	285
4.5.1 Synthetic Strategy	285
4.5.2 Synthesis of Glucosamine Acceptor 4.52	286
4.5.3 Synthesis of Lacto- <i>N</i> -Biose Donor 4.54	287
4.5.4 Synthesis of Lactose Acceptor 4.53	291
4.5.5 Synthesis of Lacto- <i>N</i> -Tetraose	294
4.5.6 Second-Generation Approach to Lacto- <i>N</i> -Tetraose	296
4.5.7 Second-Generation Approach to Lacto- <i>N</i> -Biose Donor 4.72	300
4.5.8 Deprotection of Tetrasaccharide 4.76 to Afford Lacto- <i>N</i> -Tetraose	305

4.6 Conclusion	307
4.7 Experimental Methods	308
4.8 References	335
Appendix A2: Spectra Relevant to Chapter 4	344
5. Evaluation of the Antibacterial Properties of Homogeneous Human Milk Oligosaccharides Against <i>Streptococcus agalactiae</i>	365
5.1 Introduction	365
5.2 Rationale for Inclusion of Acidic, Sialylated HMOs	365
5.3 Antimicrobial and Antibiofilm Activities of Homogenous Acidic, Sialylated HMOs	370
5.4 Rationale for Inclusion of Neutral, Fucosylated and Non-Fucosylated HMOs.....	377
5.5 Antimicrobial and Antibiofilm Activities of Homogenous Neutral, Fucosylated and Non-Fucosylated HMOs.....	381
5.6 Summary of Homogenous HMO Evaluation Results	390
5.7 Antimicrobial and Antibiofilm Activities of Simple HMO Mixtures	393
5.8 Antimicrobial and Antibiofilm Activities of 1-Amino-2'-Fucosyllactose...	398
5.9 Conclusions and Future Outlook.....	403
5.10 Experimental Methods	403
5.11 References	408
Appendix A3: Spectra and Data Relevant to Chapter 5.....	414

LIST OF TABLES

Table	Page
1.1 World Health Organization Priority Pathogen List for R&D of New Antibiotics	6
1.2 General bacterial resistance mechanisms against common classes of antibiotics.....	33
1.3 Enzymatic Strategies for Antibiotic Structural Modification and Inactivation.....	41
1.4 The ESKAPE Pathogens	49
2.1 HMO Monosaccharide Building Blocks	97
2.2 <i>Le</i> and <i>Se</i> Gene-Encoded Fucosyltransferases.....	109
2.3 HMO-Promoted Growth of Symbiotic Bacteria	115
2.4 Protection Against Infectious Disease Derived from Antiadhesive Antimicrobial Functions of HMOs	122
3.1 Types of GBS Disease	144
3.2 Secretor and Lewis Blood Group Assignments of Five Donor Milk Samples.....	157
3.3 Secretor and Lewis Blood Group Assignments of Fourteen Donor Milk Samples	163
3.4 Lewis Blood Group Distribution for Nineteen Donor Milk Samples.....	163
3.5 Antimicrobial Activity of Heterogeneous HMO Extracts Against Three Strains of <i>S. agalactiae</i> (GBS)	165
3.6 Antibiofilm Activity of Heterogeneous HMO Extracts Against Three Strains of <i>S. agalactiae</i> (GBS)	168
3.7 Important Pathogens Responsible for Infection During Pediatric Age	170

3.8	Antimicrobial Activity of Heterogeneous HMO Extracts Against <i>S. aureus</i> and <i>A. baumannii</i>	171
3.9	Antibiofilm Activity of Heterogeneous HMO Extracts Against <i>S. aureus</i> and <i>A. baumannii</i>	174
3.10	Antimicrobial Activity of Three Additional Heterogeneous HMO Extracts Against Three Strains of <i>S. agalactiae</i> (GBS).....	183
3.11	Antibiofilm Activity of Three Additional Heterogeneous HMO Extracts Against Three Strains of <i>S. agalactiae</i> (GBS).....	184
3.12	HMO IC ₅₀ Values Against Three Strains of <i>S. agalactiae</i> (GBS)	185
3.13	Antibiotic Sensitization Data for HMOs Against Three Strains of <i>S. agalactiae</i> (GBS) in THB.....	187
3.14	Antibiotic Sensitization Data for HMOs Against Three Strains of <i>S. agalactiae</i> (GBS) in THB + 1% Glucose.....	187
3.15	Antibiotic Sensitization Data for HMOs Against <i>S. aureus</i> in THB + 1% Glucose.....	189
3.16	Antibiotic Sensitization Data for HMOs Against <i>A. baumannii</i> in THB ..	190
3.17	Bacterial Strains	196
A1.1	Antibiotic Sensitization Data for HMOs Against <i>S. aureus</i> in THB.....	249
A1.2	Antibiotic Sensitization Data for HMOs Against <i>A. baumannii</i> in THB + 1% Glucose.....	249
A1.3	Results of LIVE/DEAD BacLight Assay for Treatment of Three Strains of <i>S. agalactiae</i> (GBS) with Heterogenous HMO Extracts.....	250
4.1	Synthesis of Lacto- <i>N</i> -Biose Disaccharide 4.59 and Orthoacetate 4.60	288
4.2	Attempted Glycosylations to Yield LNT Tetrasaccharide 4.70	294
4.3	Attempted Glycosylations to Yield LNB Disaccharide 4.79	301
A2.1	Synthetic and Natural Lacto- <i>N</i> -Tetraose in D ₂ O	364

5.1	Summary of Antimicrobial and Antibiofilm Activities of Single-Entity HMOs Against Two Strains of GBS	391
5.2	HMO Extract Mimic Composition.....	394
A3.1	Effects of Sialylated HMOs on GB590 Growth Over 24 h.....	415
A3.2	Effects of Sialylated HMOs on GB2 Growth Over 24 h.....	416
A3.3	Effects of Sialylated HMOs on GB590 Viability Over 24 h.....	417
A3.4	Effects of Sialylated HMOs on GB2 Viability Over 24 h.....	418
A3.5	Effects of Sialylated HMOs on GB590 Biofilm Production at 24 h	419
A3.6	Effects of Sialylated HMOs on GB2 Biofilm Production at 24 h	419
A3.7	Effects of Neutral, Fucosylated HMOs on GB590 Growth Over 24 h.....	420
A3.8	Effects of Neutral, Nonfucosylated HMOs on GB590 Growth Over 24 h.....	421
A3.9	Effects of Neutral, Fucosylated HMOs on GB2 Growth Over 24 h.....	422
A3.10	Effects of Neutral, Nonfucosylated HMOs on GB2 Growth Over 24 h.....	423
A3.11	Effects of Neutral, Fucosylated HMOs on GB590 Viability Over 24 h.....	424
A3.12	Effects of Neutral, Nonfucosylated HMOs on GB590 Viability Over 24 h.....	425
A3.13	Effects of Neutral, Fucosylated HMOs on GB2 Viability Over 24 h.....	426
A3.14	Effects of Neutral, Nonfucosylated HMOs on GB2 Viability Over 24 h.....	427
A3.15	Effects of Neutral, Fucosylated HMOs on GB590 Biofilm Production at 24 h	428

A3.16	Effects of Neutral, Nonfucosylated HMOs on GB590 Biofilm Production at 24 h	428
A3.17	Effects of Neutral, Fucosylated HMOs on GB2 Biofilm Production at 24 h	429
A3.18	Effects of Neutral, Nonfucosylated HMOs on GB2 Biofilm Production at 24 h	429
A3.19	Effects of HMO Mixtures on GB590 Growth Over 24 h	430
A3.20	Effects of HMO Mixtures on GB590 Viability Over 24 h.....	430
A3.21	Effects of HMO Mixtures on GB2 Growth Over 24 h	431
A3.22	Effects of HMO Mixtures on GB590 Viability Over 24 h.....	431
A3.23	Effects of HMO Mixtures on GB590 Biofilm Production at 24 h.....	432
A3.24	Effects of HMO Mixtures on GB2 Biofilm Production at 24 h.....	432
A3.25	Effects of 1-Amino-2'-Fucosyllactose (Amino-2'-FL) on GB590 Growth Over 24 h.....	433
A3.26	Effects of 1-Amino-2'-Fucosyllactose (Amino-2'-FL) on GB590 Viability Over 24 h	433
A3.27	Effects of 1-Amino-2'-Fucosyllactose (Amino-2'-FL) on GB2 Growth Over 24 h.....	434
A3.28	Effects of 1-Amino-2'-Fucosyllactose (Amino-2'-FL) on GB2 Viability Over 24 h	434
A3.29	Effects of 1-Amino-2'-Fucosyllactose (Amino-2'-FL) on GB590 Biofilm Production at 24 h.....	435
A3.30	Effects of 1-Amino-2'-Fucosyllactose (Amino-2'-FL) on GB2 Biofilm Production 24 h.....	435

LIST OF FIGURES

Figure		Page
1.1	Timeline of antibiotic discovery	1
1.2	Structures of selected early antibiotics Salvarsan (1.1), Prontosil (1.2), and penicillin G (1.3)	2
1.3	Selection for antibiotic resistance.....	4
1.4	Timeline of antibiotic resistance development.....	5
1.5	Major classes of antibiotic bacterial cell targets	7
1.6	General compositional differences between Gram-positive and Gram-negative bacterial cell envelopes	8
1.7	Typical repeating unit of the peptidoglycan bacterial cell wall	9
1.8	Structures of common β -lactams of the penicillin, carbapenem, and cephalosporin sub-classes.....	10
1.9	Mechanism of penicillin (β -lactam)-mediated inhibition of transpeptidase (TPase) action in peptidoglycan (PG) cell wall synthesis	11
1.10	Mechanism of vancomycin-mediated inhibition of transpeptidase (TPase) and transglycosylase (TGase) action in peptidoglycan (PG) cell wall synthesis.....	12
1.11	Structures of Fosfomycin (1.13) and Bacitracin (1.14)	13
1.12	Fosfomycin-mediated inhibition of peptidoglycan (PG) strand synthesis	14
1.13	Gram-positive and Gram-negative cell envelopes	15
1.14	Structures of common lipopolysaccharide (LPS) components	16
1.15	Structures of polymyxins B (1.24) and E (1.25).....	17

1.16	Structures of daptomycin (DAP, 1.26) and its bacterial cell membrane target, phosphatidylglycerol (1.27)	18
1.17	Structures of select ribosomal-protein synthesis-targeting antibiotics	19
1.18	Steps of ribosomal-protein synthesis	20
1.19	Protein synthesis target sites of aminoglycosides (AGs), lincosamides, macrolides, oxazolidinones, and tetracyclines	21
1.20	Schematic depiction of bacterial DNA replication.....	23
1.21	Structures of select quinolone antibiotics	24
1.22	Mechanism of quinolone-mediated cell death	25
1.23	Process of bacterial transcription	26
1.24	Structures of select rifamycin antibiotics	27
1.25	Structure of fidaxomicin (1.43)	29
1.26	Bacterial folate biosynthetic pathway	30
1.27	Folate synthesis-targeting antibiotics	31
1.28	Prevention of antibiotic target engagement as a resistance mechanism.....	34
1.29	Modification of antibiotic structure as a resistance mechanism.....	36
1.30	Mechanism of β -lactamase-mediated resistance to penicillin (1.3)	37
1.31	Structure of the extended-spectrum cephalosporin cefotaxime (1.53)	38
1.32	Structure of the aminoglycoside antibiotic kanamycin A (1.54)	39
1.33	Mechanisms for structural modification of the aminoglycoside (AG) kanamycin A by select AG modifying enzymes (AMEs).....	39

1.34	Structures of kanamycin A (1.54) and kanamycin A-derived amikacin (1.29)	40
1.35	Modification of antibiotic cellular target as a resistance mechanism	41
1.36	Bacterial RNA polymerase (RNAP) core enzyme subunit composition...	42
1.37	Schematic depiction of the water-ion bridge that facilitates quinolone (ex. ciprofloxacin (1.37)) binding to topoisomerase II (Topo II)	43
1.38	Alterations to terminal D-Ala-D-Ala dipeptide of peptidoglycan (PG) strands that confer resistance to vancomycin (1.12).....	46
1.39	Structure of the common carbapenem core and the carbapenem antibiotics imipenem (1.55), doripenem (1.56), and meropenem (1.57)..	51
1.40	Structures of antibiotics typically used in multi-drug therapy for <i>Mycobacterium tuberculosis</i> infections.....	55
1.41	Structures of folate synthesis-targeting antibiotics typically used in combination therapies	56
1.42	Structures of ribosome-targeting streptogramins used together in combination therapies	57
1.43	Classification of antibiotic adjuvants and corresponding examples from each adjuvant class	58
1.44	Structures of the components of Augmentin, amoxicillin (1.67) and clavulanic acid (1.64)	59
2.1	Human milk macromolecular composition.....	79
2.2	Structure and composition of human milk fat globules	80
2.3	Structure of lactose (2.1)	86
2.4	HMO structure and biosynthesis.....	88
2.5	Human milk versus bovine milk macromolecular compositions	89
2.6	Structures of 2'-fucosyllactose (2'-FL, 2.8) and 3-fucosyllactose (3-FL, 2.9)	93

2.7	Selected HMO structures.....	94
2.8	HMO biosynthetic blueprint and selected HMO structures	98
2.9	Structures of blood group antigens.....	102
2.10	Structural similarities between blood group antigens H (2.23) and Le ^b (2.25) and human milk-derived oligosaccharide 2'-fucosyllactose (2'-FL, 2.8).....	104
2.11	Experimental evidence that the fucosyltransferase (FUT) responsible for formation of the Fuc α 1-4GlcNAc bond of Lewis blood group antigens is also responsible for formation of the Fuc α 1-4GlcNAc bond of HMOs like LNFP II (2.11) and LNDFH I (2.26).....	106
2.12	Experimental evidence that the fucosyltransferase (FUT) responsible for formation of the Fuc α 1-4GlcNAc bond of Lewis blood group antigens might also responsible for formation of the Fuc α 1-3GlcNAc bond of HMOs like DFL (2.12), 3-FL (2.9), and LNDF III (2.12).....	108
2.13	Human milk groups based on HMO fucosylation patterns.....	110
2.14	Structures of selected HMOs previously shown to promote the growth of several species of <i>Bacteroides</i>	114
2.15	Glycosidases and transport-related genes located in the HMO utilization cluster	117
2.16	Example cleavage sites of the glycosidases in the HMO utilization gene cluster of <i>Bifidobacterium longum</i> subsp. <i>infantis</i> on the HMO sialylfucosyllacto- <i>N</i> -tetraose (S-LNF II or F-LST a, 2.29).	117
2.17	HMO metabolic pathways in <i>B. longum</i> subsp. <i>infantis</i> and <i>B. bifidum</i>	119
2.18	The bifid shunt hexose fermentative pathway.....	120
2.19	Antiadhesive antimicrobial activity of 2'-fucosyllactose (2'-FL) against <i>Campylobacter jejuni</i>	123
3.1	Current CDC antibiotic selection guidelines for intrapartum antibiotic prophylaxis (IAP) against early-onset GBS disease (EOD)	145
3.2	Structures of the repeating units of the Group B <i>Streptococcus</i> (GBS) capsular polysaccharides (CPS) for serotypes Ia, Ib, and II-XI.....	148

3.3	The biofilm life cycle	150
3.4	Structures of LS-tetrasaccharide a (LST a) and lacto- <i>N</i> -tetraose (LNT)	155
3.5	Effect of heterogeneous HMOs dosed at ca. 5 mg/mL on viability of GBS CNCTC 10/84 in THB.....	157
3.6	Effect of heterogeneous HMOs dosed at ca. 5 mg/mL on viability of GBS CNCTC 10/84 in THB + 1% glucose (glc)	158
3.7	Effects of heterogeneous HMOs dosed at ca. 5 mg/mL on GBS CNCTC 10/84 biofilm production after 24 h of growth	159
3.8	SEM micrographs of GBS CNCTC 10/84 biofilm formation after 24 h.....	160
3.9	Isolation of HMOs from whole milk workflow	162
3.10	Effects of various concentrations of <i>N</i> -acetylcysteine (NAC) on <i>S. aureus</i> strain USA300 growth and biofilm formation after 24 h of growth.....	176
3.11	Effect of co-treatment of HMOs and varying concentrations of <i>N</i> -acetylcysteine (NAC) on <i>S. aureus</i> strain USA300 growth after 24 h ...	178
3.12	Effect of co-treatment of HMOs and varying concentrations of <i>N</i> -acetylcysteine (NAC) on <i>S. aureus</i> strain USA300 biofilm formation after 24 h	179
3.13	Second-generation isolation of HMOs from whole milk workflow	182
3.14	IC ₅₀ curves for HMO cocktail against three GBS strains in THB and THB + 1% glucose (glc).....	186
3.15	LIVE/DEAD BacLight assay to evaluate bacterial cell membrane integrity	193
A1.1	¹ H NMR (400 MHz, D ₂ O) and ¹³ C NMR (100 MHz, D ₂ O) spectra of HMOs isolated from Donor 14	218
A1.2	Matrix-assisted laser desorption/ionization (MALDI) full size MS spectra for HMO mixtures isolated from Donors 0, 5, 7, 8,14, 17, and 18.....	219

A1.3	Matrix-assisted laser desorption/ionization (MALDI) full size MS spectra for HMO mixtures isolated from Donors 19, 24, 29, 31,32, 34, and 37.....	220
A1.4	Matrix-assisted laser desorption/ionization (MALDI) partial MS spectra from m/z 630-730 for HMO mixtures isolated from Donors 0, 5, 7, 8, 14, 17, and 18.....	221
A1.5	Matrix-assisted laser desorption/ionization (MALDI) partial MS spectra from m/z 630-730 for HMO mixtures isolated from Donors 19, 24, 29, 31, 32, 34, and 37.....	222
A1.6	Matrix-assisted laser desorption/ionization (MALDI) partial MS spectra from m/z 1010-1060 for HMO mixtures isolated from Donors 0, 5, 7, 8, 14, 17, and 18.....	223
A1.7	Matrix-assisted laser desorption/ionization (MALDI) partial MS spectra from m/z 1010-1060 for HMO mixtures isolated from Donors 19, 24, 29, 31, 32, 34, and 37.....	224
A1.8	Matrix-assisted laser desorption/ionization (MALDI) MS/MS spectra of selected m/z 657.2 ion for HMO mixtures isolated from Donors 0, 5, 7, 8, 14, 17, and 18.....	225
A1.9	Matrix-assisted laser desorption/ionization (MALDI) MS/MS spectra of selected m/z 657.2 ion for HMO mixtures isolated from Donors 19, 24, 29, 31, 32, 34, and 37.....	226
A1.10	Matrix-assisted laser desorption/ionization (MALDI) MS/MS spectra of selected m/z 1022.2 ion for HMO mixtures isolated from Donors 0, 5, 7, 8, 14, 17, and 18.....	227
A1.11	Matrix-assisted laser desorption/ionization (MALDI) MS/MS partial spectra of selected m/z 1022.2 ion (from m/z 700-900) for HMO mixtures isolated from Donors 0, 5, 7, 8, 14, 17, and 18.....	228
A1.12	Matrix-assisted laser desorption/ionization (MALDI) MS/MS spectra of selected m/z 1022.2 ion for HMO mixtures isolated from Donors 19, 24, 29, 31, 32, 34, and 37.....	229
A1.13	Matrix-assisted laser desorption/ionization (MALDI) MS/MS partial spectra of selected m/z 1022.2 ion (from m/z 700-900) for HMO mixtures isolated from Donors 19, 24, 29, 31, 32, 34, and 37.....	230
A1.14	General HMO composition of two distinct donors.....	231

A1.15	Biofilm formation for <i>S. agalactiae</i> strain CNCTC 10/84 after 24 H of growth in THB media alone or in the presence of ca. 5 mg/mL HMOs from various donors.....	232
A1.16	Biomass for <i>S. agalactiae</i> strain CNCTC 10/84 after 24 H of growth in THB media alone or in the presence of ca. 5 mg/mL HMOs from various donors.....	232
A1.17	Biofilm to biomass ratio of <i>S. agalactiae</i> strain CNCTC 10/84 after 24 H of growth in THB media alone or in the presence of ca. 5 mg/mL HMOs from various donors.....	233
A1.18	Biofilm to biomass ratio of <i>S. agalactiae</i> strain CNCTC 10/84 after 24 H of growth in THB media alone or in the presence of ca. 5 mg/mL HMOs from various donors excluding Donor 8.....	233
A1.19	Biofilm for <i>S. agalactiae</i> strain CNCTC 10/84 after 24 H of growth in THB + 1% glucose media alone or in the presence of ca. 5 mg/mL HMOs from various donors.....	234
A1.20	Biomass for <i>S. agalactiae</i> strain CNCTC 10/84 after 24 H of growth in THB + 1% glucose media alone or in the presence of ca. 5 mg/mL HMOs from various donors.....	234
A1.21	Biofilm to biomass ratio of <i>S. agalactiae</i> strain CNCTC 10/84 after 24 H of growth in THB + 1% glucose media alone or in the presence of ca. 5 mg/mL HMOs from various donors	235
A1.22	Biofilm for <i>S. agalactiae</i> strain GB590 after 24 H of growth in THB media alone or in the presence of ca. 5 mg/mL HMOs from various donors.....	235
A1.23	Biomass for <i>S. agalactiae</i> strain GB590 after 24 H of growth in THB media alone or in the presence of ca. 5 mg/mL HMOs from various donors.....	236
A1.24	Biofilm to biomass ratio of <i>S. agalactiae</i> strain GB590 after 24 H of growth in THB media alone or in the presence of ca. 5 mg/mL HMOs from various donors.....	236
A1.25	Biofilm to biomass ratio for <i>S. agalactiae</i> strain GB590 after 24 H of growth in THB media alone or in the presence of ca. 5 mg/mL HMOs from various donors excluding Donor 8.....	237
A1.26	Biofilm for <i>S. agalactiae</i> strain GB590 after 24 H of growth in THB + 1% glucose media alone or in the presence of ca. 5 mg/mL HMOs from various donors.....	237

A1.27	Biomass for <i>S. agalactiae</i> strain GB590 after 24 H of growth in THB + 1% glucose media alone or in the presence of ca. 5 mg/mL HMOs from various donors.....	238
A1.28	Biofilm to biomass ratio of <i>S. agalactiae</i> strain GB590 after 24 H of growth in THB + 1% glucose media alone or in the presence of ca. 5 mg/mL HMOs from various donors	238
A1.29	Biofilm for <i>S. agalactiae</i> strain GB2 after 24 H of growth in THB media alone or in the presence of ca. 5 mg/mL HMOs from various donors.....	239
A1.30	Biomass for <i>S. agalactiae</i> strain GB2 after 24 H of growth in THB media alone or in the presence of ca. 5 mg/mL HMOs from various donors.....	239
A1.31	Biofilm to biomass ratio of <i>S. agalactiae</i> strain GB2 after 24 H of growth in THB media alone or in the presence of ca. 5 mg/mL HMOs from various donors.....	240
A1.32	Biofilm to biomass ratio for <i>S. agalactiae</i> strain CNCTC 10/84 after 24 H of growth in THB media alone or in the presence of ca. 5 mg/mL HMOs from various donors excluding Donor 8	240
A1.33	Biofilm for <i>S. agalactiae</i> strain GB2 after 24 H of growth in THB + 1% glucose media alone or in the presence of ca. 5 mg/mL HMOs from various donors	241
A1.34	Biomass for <i>S. agalactiae</i> strain GB2 after 24 H of growth in THB + 1% glucose media alone or in the presence of ca. 5 mg/mL HMOs from various donors.....	241
A1.35	Biofilm to biomass ratio of <i>S. agalactiae</i> strain GB2 after 24 H of growth in THB + 1% glucose media alone or in the presence of ca. 5 mg/mL HMOs from various donors.....	242
A1.36	Biofilm formation for <i>S. aureus</i> USA300 after 24 H of growth in THB media alone or in the presence of ca. 5 mg/mL HMOs from various donors.....	242
A1.37	Biomass for <i>S. aureus</i> strain USA300 after 24 H of growth in THB media alone or in the presence of ca. 5 mg/mL HMOs from various donors.....	243
A1.38	Biofilm to biomass ratio of <i>S. aureus</i> strain USA300 after 24 H of growth in THB media alone or in the presence of ca. 5 mg/mL HMOs from various donors.....	243

A1.39	Biofilm formation for <i>S. aureus</i> strain USA300 after 24 H of growth in THB + 1% glucose media alone or in the presence of ca. 5 mg/mL HMOs from various donors.....	244
A1.40	Biomass for <i>S. aureus</i> strain USA300 after 24 H of growth in THB + 1% glucose media alone or in the presence of ca. 5 mg/mL HMOs from various donors.....	244
A1.41	Biofilm to biomass ratio of <i>S. aureus</i> strain USA300 after 24 H of growth in THB + 1% glucose media alone or in the presence of ca. 5 mg/mL HMOs from various donors	245
A1.42	Biofilm formation for <i>A. baumannii</i> strain ATCC 19606 after 24 H of growth in THB media alone or in the presence of ca. 5 mg/mL HMOs from various donors.....	245
A1.43	Biomass for <i>A. baumannii</i> strain ATCC 19606 after 24 H of growth in THB media alone or in the presence of ca. 5 mg/mL HMOs from various donors.....	246
A1.44	Biofilm to biomass ratio of <i>A. baumannii</i> strain ATCC 19606 after 24 H of growth in media alone or in the presence of ca. 5 mg/mL HMOs from various donors.....	246
A1.45	Biofilm formation for <i>A. baumannii</i> strain ATCC 19606 after 24 H of growth in THB + 1% glucose media alone or in the presence of ca. 5 mg/mL HMOs from various donors.....	247
A1.46	Biomass for <i>A. baumannii</i> strain ATCC 19606 after 24 H of growth in THB + 1% glucose media alone or in the presence of ca. 5 mg/mL HMOs from various donors.....	247
A1.47	Biofilm to biomass ratio of <i>A. baumannii</i> strain ATCC 19606 after 24 H of growth in THB + 1% glucose media alone or in the presence of ca. 5 mg/mL HMOs from various donors	248
4.1	Structure of lacto- <i>N</i> -tetraose (LNT, 2.4).....	252
4.2	Conventional carbohydrate carbon numbering and α/β and <i>cis/trans</i> designations for monosaccharides and larger	255
4.3	Common oxygen and nitrogen protecting groups in carbohydrate chemistry	258
4.4	Arming and disarming effects of protecting groups.....	260

4.5	Common classes of glycosyl donor	263
4.6	Structures of Lc ₄ ceramide (4.39), IV ² Fuc-Lc ₄ ceramide (4.40), and linker-attached Lc ₄ , 4.41	280
A2.1	¹ H NMR (400 MHz, CDCl ₃) and ¹³ C (100 MHz, CDCl ₃) spectra of 4.56	345
A2.2	¹ H NMR (400 MHz, MeOD) and ¹³ C (100 MHz, MeOD) spectra of 4.57	346
A2.3	¹ H NMR (400 MHz, CDCl ₃) and ¹³ C (100 MHz, CDCl ₃) spectra of 4.52	347
A2.4	¹ H NMR (400 MHz, CDCl ₃) and ¹³ C (100 MHz, CDCl ₃) spectra of 4.59	348
A2.5	¹ H NMR (400 MHz, CDCl ₃) and ¹³ C (100 MHz, CDCl ₃) spectra of 4.60	349
A2.6	¹ H NMR (400 MHz, CDCl ₃) and ¹³ C (100 MHz, CDCl ₃) spectra of 4.63	350
A2.7	¹ H NMR (400 MHz, CDCl ₃) and ¹³ C (100 MHz, CDCl ₃) spectra of 4.54	351
A2.8	¹ H NMR (400 MHz, CDCl ₃) and ¹³ C (100 MHz, CDCl ₃) spectra of 4.64	352
A2.9	¹ H NMR (400 MHz, CDCl ₃) and ¹³ C (100 MHz, CDCl ₃) spectra of 4.66	353
A2.10	¹ H NMR (400 MHz, CDCl ₃) and ¹³ C (100 MHz, CDCl ₃) spectra of A1	354
A2.11	¹ H NMR (400 MHz, CDCl ₃) and ¹³ C (100 MHz, CDCl ₃) spectra of 4.53	355
A2.12	¹ H NMR (400 MHz, CDCl ₃) and ¹³ C (100 MHz, CDCl ₃) spectra of 4.71	356
A2.13	¹ H NMR (400 MHz, CDCl ₃) and ¹³ C (100 MHz, CDCl ₃) spectra of 4.72	357
A2.14	¹ H NMR (600 MHz, CDCl ₃) and ¹³ C (100 MHz, CDCl ₃) spectra of 4.75	358

A2.15	¹ H NMR (400 MHz, CDCl ₃) and ¹³ C (100 MHz, CDCl ₃) spectra of 4.76	359
A2.16	¹ H NMR (400 MHz, CDCl ₃) and ¹³ C (100 MHz, CDCl ₃) spectra of 4.78	360
A2.17	¹ H NMR (400 MHz, CDCl ₃) and ¹³ C (100 MHz, CDCl ₃) spectra of 4.77	361
A2.18	¹ H NMR (400 MHz, CDCl ₃) and ¹³ C (150 MHz, CDCl ₃) spectra of 4.79 (β).....	362
A2.19	¹ H NMR (400 MHz, D ₂ O) and ¹³ C (100 MHz, D ₂ O) spectra of (2.4)	363
5.1	Structure of sialyl-Lewis X (sLe ^x , 5.1).....	367
5.2	Structures of sialylated HMOs evaluated for antibacterial activity against GBS	369
5.3	Effects of homogenous and heterogenous HMOs dosed at ca. 5 mg/mL on the growth and viability of GB590 in Todd-Hewitt Broth....	372
5.4	Effects of homogenous and heterogenous HMOs dosed at ca. 5 mg/mL on the growth and viability of GB2 in Todd-Hewitt Broth.....	373
5.5	Effects of homogeneous HMOs dosed at ca. 5 mg/mL on GBS biofilm production after 24 h of growth in Todd-Hewitt Broth	376
5.6	Structures of neutral HMOs previously assayed for antimicrobial activity against GBS.....	379
5.7	Structures of neutral HMOs assayed for antibacterial activity against GBS	380
5.8	Effects of single-entity, neutral HMOs dosed at ca. 5 mg/mL on the growth of GB590 in Todd-Hewitt Broth	382
5.9	Effects of single-entity, neutral HMOs dosed at ca. 5 mg/mL on the viability of GB590 in Todd-Hewitt Broth	383
5.10	Effects of single-entity, neutral HMOs dosed at ca. 5 mg/mL on the growth of GB2 in Todd-Hewitt Broth	386
5.11	Effects of single-entity, neutral HMOs dosed at ca. 5 mg/mL on the viability of GB2 in Todd-Hewitt Broth	387

5.12	Effects of single-entity, neutral HMOs dosed at ca. 5 mg/mL on GBS biofilm production after 24 h of growth in Todd-Hewitt Broth	389
5.13	Effects of heterogeneous HMO mixtures dosed at ca. 5 mg/mL on the growth and viability of GB590 in Todd-Hewitt Broth.....	395
5.14	Effects of heterogenous HMO mixtures dosed at ca. 5 mg/mL on the growth and viability of GB2 in Todd-Hewitt Broth.....	396
5.15	Effects of heterogeneous HMO mixtures dosed at ca. 5 mg/mL on GBS biofilm production after 24 h of growth in Todd-Hewitt Broth.....	397
5.16	Effects lactose (2.1), 2'-FL (2.8), and amino 2'-FL (5.10) dosed at ca. 5 mg/mL on the growth and viability of GB590 in Todd-Hewitt Broth.....	400
5.17	Effects lactose (2.1), 2'-FL (2.8), and amino 2'-FL (5.10) dosed at ca. 5 mg/mL on the growth and viability of GB2 in Todd-Hewitt Broth.....	401
5.18	Effects lactose (2.1), 2'-FL (2.8), and amino 2'-FL (5.10) dosed at ca. 5 mg/mL on GBS biofilm production after 24 h of growth in Todd-Hewitt Broth.....	402
A3.1	¹ H NMR (400 MHz, D ₂ O) comparison of 2'-FL (2.8) and 1-amino-2'-FL, 5.10	436
A3.2	¹³ C NMR (100 MHz, D ₂ O) comparison of 2'-FL (2.8) and 1-amino-2'-FL, 5.10	437

LIST OF SCHEMES

Schemes	Page
2.1 Enzymatic hydrolysis of lactose into glucose and galactose by β -galactosidase (β -Gal).....	87
2.2 Lactose biosynthesis.....	100
2.3 Activity of a hypothesized <i>H</i> gene-encoded fucosyltransferase (FUT).....	103
2.4 Activity of a hypothesized <i>Le</i> gene-encoded fucosyltransferase (FUT).....	105
2.5 Additional hypothesized activity of an <i>Le</i> gene-encoded fucosyltransferase (FUT).....	107
2.6 Patterns of sialyltransferase (ST)-catalyzed addition of <i>N</i> -acetylneuraminic acid (Neu5Ac) to oligosaccharide chains	111
4.1 The chemical glycosylation reaction	254
4.2 Mechanistic continuum for a glycosylation reaction.....	256
4.3 The anomeric effect.....	257
4.4 Neighboring group participation (NGP).....	259
4.5 Solvent participation in glycosylation reactions.....	262
4.6 Participation of acetonitrile solvent in glycosylations	262
4.7 Preparation and use of glycosyl bromides and chlorides.....	264
4.8 Common methods for the synthesis of glycosyl fluorides	266
4.9 Synthesis of trichloroacetimidate glycosyl donors	267
4.10 Reactions of trichloroacetimidates.....	269

4.11	Thioglycoside preparation and donor interconversion	270
4.12	Tejima's retrosynthetic analysis of LNT	271
4.13	Augé and Veyrières' synthesis of oxazoline LNB donor 4.1	272
4.14	Tejima's synthesis of LNT (2.4)	272
4.15	Selected example of dimethylmaleoyl (DMM) amino protecting group in carbohydrate synthesis.....	274
4.16	Schmidt's retrosynthetic analysis of LNT (2.4).....	274
4.17	LNT building block synthesis	275
4.18	Schmidt's synthesis of LNT (2.4).....	276
4.19	Chen's retrosynthetic analysis of LNT-ProN ₃ 4.29	277
4.20	Synthesis of LNB donor 4.32	278
4.21	Synthesis of lactose derivative 4.34	279
4.22	Chen's synthesis of LNT-ProN ₃ 4.29	280
4.23	Synthesis of LNB donors 4.44 and 4.46	281
4.24	Wong's one-pot, two-glycosylation method to linker-attached Lc ₄ , 4.41	282
4.25	Wang's enzymatic synthesis of benzyl β-lacto- <i>N</i> -tetraoside 4.49 using recombinant LgtA and WbgO.....	283
4.26	Albermann's <i>in vivo</i> synthesis of lacto- <i>N</i> -triose (LNT II, 4.51) and lacto- <i>N</i> -tetraose (LNT, 2.4) in recombinant <i>E. coli</i> cells using Leloir glycosyltransferases and intracellular nucleotide sugars.....	284
4.27	Retrosynthetic analysis of LNT (2.4).....	285
4.28	Synthesis of glucosamine acceptor 4.52	287

4.29	Synthesis of galactose donor 4.18	287
4.30	Mechanistic explanation for the formation of undesired orthoacetate 4.60 and desired β -linked disaccharide 4.59 glycosylation products	289
4.31	Synthesis of lacto- <i>N</i> -biose donor 4.54	291
4.32	First-generation approach to β -benzyl lactoside 4.64	292
4.33	Synthesis of lactose acceptor 4.53	293
4.34	Synthesis of second-generation, peracetylated LNB donor 4.72	296
4.35	Hypothesized result of second-generation glycosylation towards LNT tetrasaccharide 4.73	298
4.36	Synthesis of fully protected LNT tetrasaccharide 4.76	299
4.37	Synthesis of second-generation, acetylated glucosamine acceptor 4.77	300
4.38	Proposed mechanistic explanation for the formation of both α and β glycosides despite a C2 participating functionality on galactose donor 4.18	303
4.39	Deprotection of fully protected LNT tetrasaccharide 4.76 to yield LNT (2.4).....	306
5.1	Synthesis of 1-amino-2'-fucosyllactose (amino 2'-FL, 5.10).....	399

LIST OF ABBREVIATIONS

2'-FL	2'-fucosyllactose
2,2-DMP	2,2-dimethoxypropane
3-FL	3-fucosyllactose
3'-SL	3'-sialyllactose
6'-GL	6'-galactosyllactose
15-c-5	15-crown-5
18-c-8	18-crown-8
Å	ångström
AAC	aminoglycoside <i>N</i> -acetyltransferase
AAP	American Academy of Pediatrics
ABC	ATP-dependent binding cassette
Ac	acetyl
Ac ₂ O	acetic anhydride
AcOH	acetic acid
ADP	adenosine diphosphate
AG	aminoglycoside
AgClO ₄	silver perchlorate
Ag ₂ CO ₃	silver carbonate
AgOTf	silver triflate
AHL	<i>N</i> -acyl L-homoserine lactone
aHMO	acidic, sialylated HMO extract
AI	autoinducer
AIP	autoinducing peptide
AlCl ₃	aluminum chloride
AME	aminoglycoside-modifying enzyme
AMP	antimicrobial peptide
AMR	antimicrobial resistance
amu	atomic mass unit
ANT	aminoglycoside <i>O</i> -nucleotidyl- or -adenylyltransferase
APH	aminoglycoside <i>O</i> -phosphotransferase
app	apparent
aq.	aqueous
ATP	adenosine triphosphate
BaO	barium oxide
Ba(OH) ₂ •8H ₂ O	barium hydroxide octahydrate
BDMA	benzaldehyde dimethyl acetal
BDNF	brain-derived neurotrophic factor
BF ₃ •Oet ₂	boron trifluoride diethyl etherate
β-gal	β-galactosidase
BMO	bovine milk oligosaccharide
Bn	benzyl
BnBr	benzyl bromide

BnOH	benzyl alcohol
br	broad
BSI	bloodstream infection
BSSL	bile salt-stimulating lipase
Bu ₂ SnO	dibutyltin oxide
<i>t</i> BuOH	<i>tert</i> -butanol
BzCl	benzoyl chloride
°C	degrees Celsius
calcd	calculated
cat.	catalytic
CAZY	carbohydrate-active enzymes
CDC	Centers for Disease Control
CDI	<i>Clostridium difficile</i> infection
CDCl ₃	chloroform- <i>d</i>
CE	capillary electrophoresis
CF	cystic fibrosis
CFU	colony forming units
CH ₃ Cl	chloroform
CH ₃ CN	acetonitrile
CH ₃ C(OCH ₃) ₃	trimethyl orthoacetate
CHDL	carbapenem hydrolyzing oxacillinase
CIP	contact ion pair
Cl ₃ CCN	trichloroacetonitrile
CMP	cytidine monophosphate
COSY	correlation spectroscopy
Cp ₂ HfCl ₂	bis(cyclopentadienyl)hafnium(IV) dichloride
Cp ₂ ZrCl ₂	bis(cyclopentadienyl)zirconium(IV) dichloride
CRKP	carbapenem-resistant <i>Klebsiella pneumoniae</i>
CPS	capsular polysaccharide
CSA	10-camphorsulfonic acid
CSLM	confocal laser scanning microscopy
d	doublet
DAP	2,6-diaminopimelic acid; daptomycin
DAST	(diethylamino)sulfur trifluoride
DBU	1,8-diazabicyclo[5.4.0]undec-7-ene
DCM	dichloromethane
dd	doublet of doublets
DFL	difucosyllactose
DHFR	dihydrofolate reductase
DHFS	dihydrofolate synthase
DHPS	dihydropteroate synthase
DMAP	4-dimethylaminopyridine
DMAPA	3-(dimethylamino)-1-propylamine
DMF	dimethylformamide
DMM	dimethylmaleoyl

DMMA	dimethyl maleoyl anhydride
DMTST	dimethyl(methylthio) sulfonium triflate
DNA	deoxyribonucleic acid
D ₂ O	deuterium oxide
DRI	device-related infection
DSLNT	disialyllacto- <i>N</i> -tetraose
EC	elongation complex
EDC	1-ethyl-3-(3-dimethylaminopropyl)carbodiimide
EGF	epidermal growth factor
EOD	early-onset disease (GBS)
EPEC	enteropathogenic <i>Escherichia coli</i>
Epo	erythropoietin
EPS	extracellular polymeric matrix
eq	equivalence
Erm	erythromycin ribosomal methylation
ESBL	extended-spectrum β -lactamase
ESI	electrospray ionization
Et ₃ N	triethylamine
EtOAc	ethyl acetate
EtOH	ethanol
EtSH	ethanethiol
FAB	fast atom bombardment
FT-ICR	Fourier transform ion cyclotron resonance
Fuc	fucose
FUT	fucosyltransferase
g	gram
Gal	galactose
GalNAc	<i>N</i> -acetylgalactosamine
GBS	Group B <i>Streptococcus</i> , <i>Streptococcus agalactiae</i>
GDP	guanosine diphosphate
GI	gastrointestinal
Glc	glucose
GlcNAc	<i>N</i> -acetylglucosamine
GNB	galacto- <i>N</i> -biose
Gnd•Cl	guanidinium chloride
GSL	glycosphingolipid
GST	glutathione S-transferase
GTP	guanosine triphosphate
GT	glycosyltransferase
h; H	hour
HABA	(<i>S</i>)-2-hydroxyaminobutyric acid
HAI	hospital-acquired infection
HBGA	histo-blood group antigen
HBr	hydrobromic acid
HCl	hydrochloric acid

hep	L-glycero-D-manno heptose
HF	hydrofluoric acid
HgBr ₂	mercury(II) bromide
Hg(CN) ₂	mercuric cyanide; mercury(II) cyanide
HgNa	sodium amalgam; mercuric sodium
HgO	mercury(II) oxide
HGT	horizontal gene transfer
HIV	human immunodeficiency virus
HLT	heat-labile enterotoxin
HMBC	heteronuclear multiple bond correlation
HMO	human milk oligosaccharide
HPEAC	high pH anion-exchange chromatography
HPLC	high performance liquid chromatography
HPPK	6-hydroxymethyl-7,8-dihydropterin pyrophosphokinase
HRMS	high resolution mass spectrometry
HSQC	heteronuclear single quantum coherence spectroscopy
Hz	hertz
IAP	intrapartum antibiotic prophylaxis
IC ₅₀	half maximal inhibitory concentration
IDCP	iodonium dicollidine perchlorate
IGF	insulin-like growth factor
IL	interleukin
IM	inner membrane
ImH	imidazole
INF _γ	interferon gamma
<i>J</i>	coupling constant
K ₂ CO ₃	potassium bicarbonate
Kdo	2-keto-3-deoxy-D-manno-octulosonic acid
L	liter
Lac	lactose; lactate
LacNAc	<i>N</i> -acetyllactosamine
LacY	lactose permease Y
LacZ	lactose permease Z
Lc	lactotetraosylceramide
LDFH	lacto-difucosyltetraose
Le	Lewis
Lev	levulinic
LevOH	levulinic acid
LgtA	β1-3 GlcNAc-transferase from <i>Neisseria meningitidis</i>
LNB	lacto- <i>N</i> -biose
LNDFH I	lacto- <i>N</i> -difucohexaose I
LNFP I, II, III,	lacto- <i>N</i> -fucopentaose I, II, III, IV, V
LNH	lacto- <i>N</i> -hexaose
LNnDFH	lacto- <i>N</i> -neodifucohexaose
LNnFP	lacto- <i>N</i> -neofucopentaose

LNnH	lacto- <i>N</i> -neohexaose
LNnO	lacto- <i>N</i> -neooctaose
LNnT	lacto- <i>N</i> -neotetraose
LNT	lacto- <i>N</i> -tetraose
LNT II	lacto- <i>N</i> -triose
LOA	lactose octaacetate
LOD	late-onset disease (GBS)
LOS	lipooligosaccharide
LPS	lipopolysaccharide
LRMS	low resolution mass spectrometry
LST	sialyllacto- <i>N</i> -tetraose
LST a, b, c	LS tetrasaccharide a, b, c
m	multiplet
M	molar
MALDI	matrix-assisted laser desorption/ionization
MBL	metallo- β -lactamase
mCPBA	<i>meta</i> -chloroperoxybenzoic acid
MDR	multi-drug resistant
MeOD	methanol- <i>d</i>
MeOH	methanol
MeOTf	methyl trifluoromethanesulfonate/triflate
MFGE8	milk fat globule epidermal growth factor VIII
MFGM	milk fat globule protein
MgSO ₄	magnesium sulfate
MHz	megahertz
MIC	minimum inhibitory concentration
mL	milliliter
MLS _B	macrolide-lincosamide-streptogramin B
mmol	millimole
MnCl ₂	manganese(II) chloride
MOI	multiplicity of infection
mol	mole
MRSA	methicillin-resistant <i>Staphylococcus aureus</i>
ms	molecular sieves
MS	mass spectrometry
MUC1	mucin
MurA	UDP- <i>N</i> -acetylglucosamine enolpyruvyl transferase
MurAc; NAG	<i>N</i> -acetylmuramic acid
N	normal
NAC	<i>N</i> -acetylcysteine (Ac-CYS-OH)
NaCl	sodium chloride
NAD ⁺	oxidized nicotinamide adenine dinucleotide
NADH	reduced nicotinamide adenine dinucleotide
NaH	sodium hydride
NaHCO ₃	sodium bicarbonate

NaN ₃	sodium azide
NaOH	sodium hydroxide
NaOMe	sodium methoxide
NBS	<i>N</i> -bromosuccinimide
NEC	necrotizing enterocolitis
Neu5Ac	<i>N</i> -acetylneuraminic acid
NGP	neighboring group participation
NH ₃	ammonia
NH ₂ •NH ₂ •AcOH	hydrazine acetate
NIS	<i>N</i> -iodosuccinimide
nHMO	neutral, non-sialylated HMO extract
NMR	nuclear magnetic resonance
NO ₂ CH ₃	nitromethane
OD	optical density
OM	outer membrane
OX	oxacillinase
p	pentet
P	phosphate
pABA	<i>para</i> -aminobenzoic acid
PBS	phosphate buffered saline
PBP	penicillin binding protein
PCl ₅	phosphorus pentachloride
Pd/C	palladium on carbon
Pd(OH) ₂	palladium hydroxide; Pearlman's catalyst
PG	peptidoglycan
Ph	phenyl
PhH	benzene
PhCH ₃	toluene
pHMO	pooled HMO extract
PhSOTf	benzenesulfonyl triflate
P _i	inorganic phosphate
PI	propidium iodide
P ₂ O ₅	phosphorus pentoxide
Ppi	pyrophosphate
ppm	parts per million
ProN ₃	propyl azide
pTsOH	<i>para</i> -toluenesulfonic acid
pyr	pyridine
q	quartet
Qnr	quinolone resistance protein
QS	quorum sensing
RBC	red blood cell
R _f	retention factor
RMT	ribosomal methyltransferase
RNA	ribonucleic acid

RNAP	RNA polymerase
RPP	ribosomal protection protein
rRNA	ribosomal RNA
rt	room temperature
s	singlet
SCFA	short chain fatty acid
Se	Secretor
SEM	scanning electron microscopy
SEM	standard error of the mean
Sia	sialic acid
SIDS	sudden infant death syndrome
SigA	secretory immunoglobulin A
sLe ^x	sialyl-Lewis X
SnCl ₂	tin(II) chloride
SSB	single-stranded DNA-binding
SSIP	solvent-separated ion pair
ST	sialyltransferase
t	triplet
TBAB	tetra- <i>n</i> -butylammonium bromide
TBAF	tetra- <i>n</i> -butylammonium fluoride
TBAI	tetra- <i>n</i> -butylammonium iodide
TBDMS/TBS	<i>tert</i> -butyldiphenyl silyl
TBDPS	<i>tert</i> -butyldimethyl silyl
TcdA, B	<i>Clostridium difficile</i> endotoxin A, B
TDS	dimethylhexylsilyl
TEAC	tetraethylammonium chloride
TFA	trifluoroacetic acid
TfOH	Trifluoromethanesulfonic/triflic acid
TGF	transforming growth factor
THB	Todd-Hewitt Broth
THF	Tetrahydrofuran; tetrahydrofolate
TIPS	triisopropylsilyl
TLC	thin-layer chromatography
TMSOTf	trimethylsilyl trifluoromethanesulfonate/triflate
TNF	tumor necrosis factor
TOF	time of flight
Topo	topoisomerase
Troc	2,2,2-trichloroethyl
Troc-Cl	2,2,2-trichloroethyl chloroformate
TsCl	<i>para</i> -toluenesulfonyl chloride; tosyl chloride
UDP	uridine diphosphate
μL	microliter
UPEC	uropathogenic <i>Escherichia coli</i>
UTI	urinary tract infection
UTP	uridine triphosphate

VEGF	vascular endothelial growth factor
VISA	vancomycin-intermediate <i>Staphylococcus aureus</i>
VRE	vancomycin-resistant <i>Enterococcus faecium</i>
VRSA	vancomycin-resistant <i>Staphylococcus aureus</i>
WbgO	β 1-3-galactosyltransferase from <i>E. coli</i> O55:H7
WHO	World Health Organization
wt	weight
XDR	extensively drug-resistant
xs	excess

CHAPTER 1

Antibiotics and the Evolution of Resistance

1.1 Introduction

One of the most important advances in modern medicine is the discovery and development of antibiotics. Antibiotics are loosely defined as molecules with the capacity to inhibit the growth of and/or destroy bacteria and other micro-organisms. Their history can be traced back to the pioneering work of Paul Ehrlich at the end of the nineteenth century (**Figure 1.1**).^{1,2} As a compliment to his work that would come to define what is now known as immunology, Ehrlich hypothesized that a pathogen could be treated with a chemical substance that had a high affinity and selectivity for the pathogen.³ This idea of a “magic bullet” was validated with Ehrlich’s discovery of diamidodioxarsenobenzol, better known as Salvarsan (**1.1**), as an effective treatment against the causative agent of syphilis, *Treponema pallidum* (**Figure 1.2**).^{3,4}

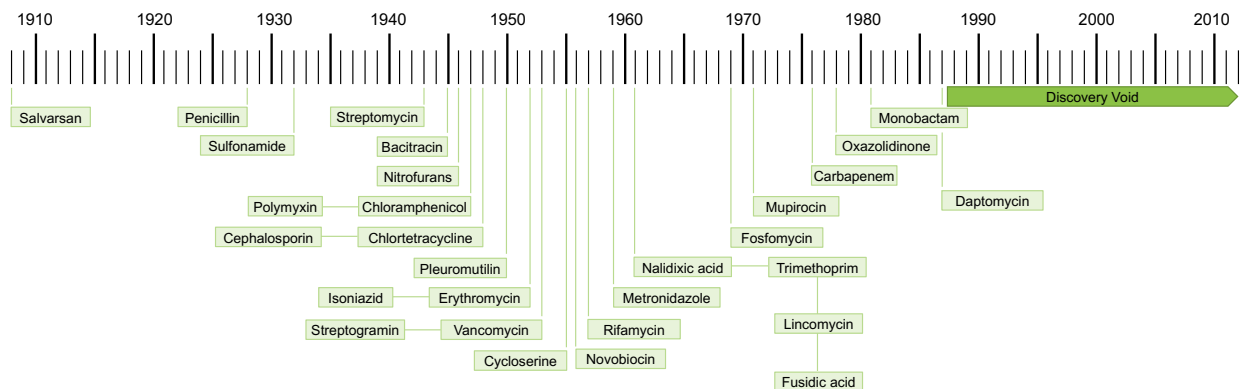


Figure 1.1. Timeline of antibiotic discovery.

Taking inspiration from the seminal work of Ehrlich, the Friedrich Bayer Company began to investigate the possibility that synthetic compounds could be used to treat bacterial diseases.^{2, 5, 6} The targeted hypothesis that dyes could serve as antimicrobial agents ultimately lead to the discovery of sulphamido-chrysoidine, better known as Prontosil (**1.2**), in the 1930s as a potent compound for the treatment of streptococcal infections (**Figure 1.2**). Importantly, this discovery, credited to Gerhard Domagk, ushered in the development of additional sulfa drugs.

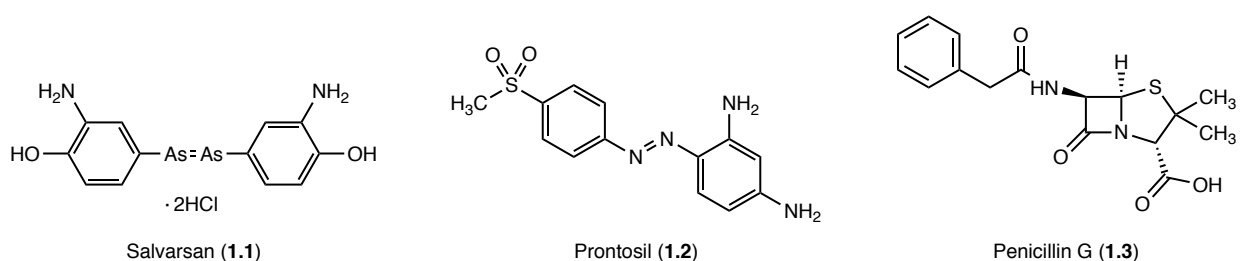


Figure 1.2. Structures of selected early antibiotics Salvarsan (**1.1**), Prontosil (**1.2**), and penicillin G (**1.3**).

Even though penicillin (**1.3**) would not find clinical significance until the early 1940s (after the introduction of Prontosil), Alexander Fleming's discovery of penicillin in 1928 is largely considered the start of the "antibiotic era" (**Figure 1.2**).^{5, 7} Moreover, the discovery of penicillin, an antibiotic derived from the fungus originally believed to be *Penicillium rubrum*, served to shift the focus of antibiotic discovery from synthetic small molecules to natural products.^{4, 8} This shift is considered to have paved the way for the so-called "golden era" of antibiotic discovery (1945-1960). This era saw the discovery of the majority of antibiotic classes now in clinical use and was followed by an era of antibiotic medicinal chemistry (1970-1980). The medicinal chemistry era is characterized by extensive chemical elaboration of many of the scaffolds originally identified during the "golden age" as a means to improve drug pharmacology and avoid antibiotic resistance.

In contrast to the many highly productive and fruitful decades of antibiotic discovery and development of the mid-twentieth century, the last few decades have seen a dramatic decrease in the rate of discovery of new and clinically viable antibiotics.^{4, 9} One explanation for this decline is that the antibiotics discovered around the 1950s were simply the “low hanging fruit.” Related to this notion is the idea that we may have exhausted soil bacteria, which are the source of a significant number of currently used antibiotics, as sources of new drugs.

In addition to these scientific explanations, there are also economic factors that have contributed to the antibiotic discovery void. Most pharmaceutical companies have limited investments in the development of new antibiotics due in large part to the generally poor return on investment seen for antibiotic development.^{2, 9, 10} Indeed, from a financial standpoint, it is more advantageous for companies to invest in drugs for chronic diseases, which are taken over long periods of time, than in antibiotics that are taken for only a short amount of time. Additionally, the ability of bacteria to develop resistance to antibiotics, often within a short window after initial introduction of an antibiotic, increases the risk of investing in new antibiotic development.

Antibiotic resistance is a natural, evolutionary response to the strong selective pressure that results from antibiotic exposure (**Figure 1.3**).⁹ In this sense, antibiotic treatment is a double-edged sword. On the one hand, antibiotics have revolutionized medicine by allowing us to treat a host of previously untreatable infections. On the other hand, continued exposure of pathogenic species to antibiotics drives the evolutionary response that ultimately gives rise to resistant organisms that render antibiotics obsolete. Indicative of this reality, since the introduction of penicillin in the clinic in the 1940s,

resistance to all classes of antibiotics has emerged (**Figure 1.4**).^{9, 11} Moreover, multi-drug resistant (MDR) bacterial species are becoming increasingly common.

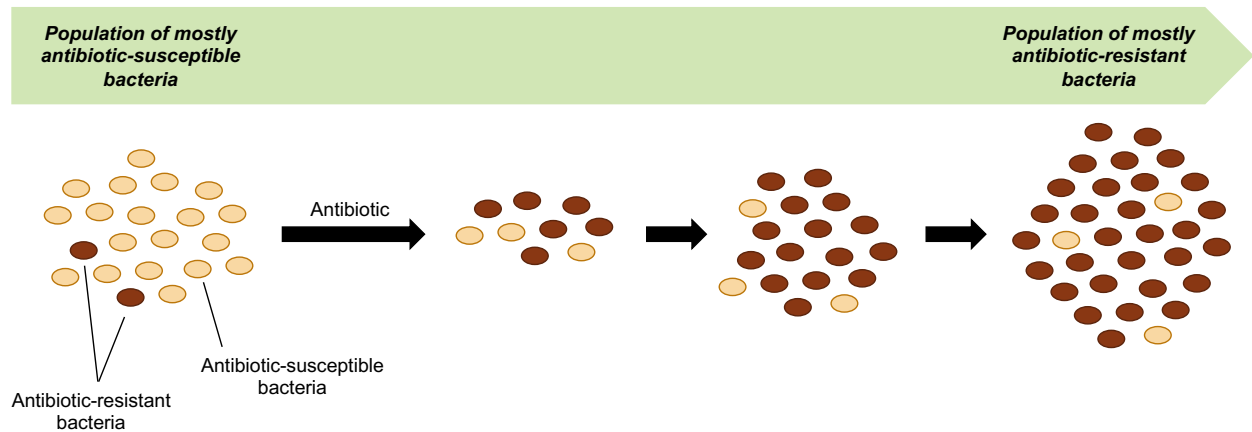


Figure 1.3. Selection for antibiotic resistance. Antibiotic exposure eliminates most antibiotic-susceptible bacteria, but the antibiotic-resistant bacteria survive. The antibiotic-resistant bacteria can then proliferate to create a population of mostly resistant bacteria.

While antibiotic resistance is not a phenomenon restricted to the 20th and 21st centuries, these centuries have seen an increase in the prevalence and diversity of resistant organisms.^{4, 10} This increase is largely attributable to the widespread overuse and misuse of antibiotics. Alarming, the increasing prevalence of antibiotic resistance coupled with a dramatically slowed rate of novel antibiotic discovery has created an environment wherein antimicrobial resistance is one of the most serious threats to human health. Common illnesses, such as pneumonia, as well as the world's most prevalent infectious diseases—human immunodeficiency virus (HIV), malaria, and tuberculosis—are becoming increasingly difficult to treat due to drug resistance. Additionally, infections caused by antibiotic-resistant bacteria continue to challenge physicians.

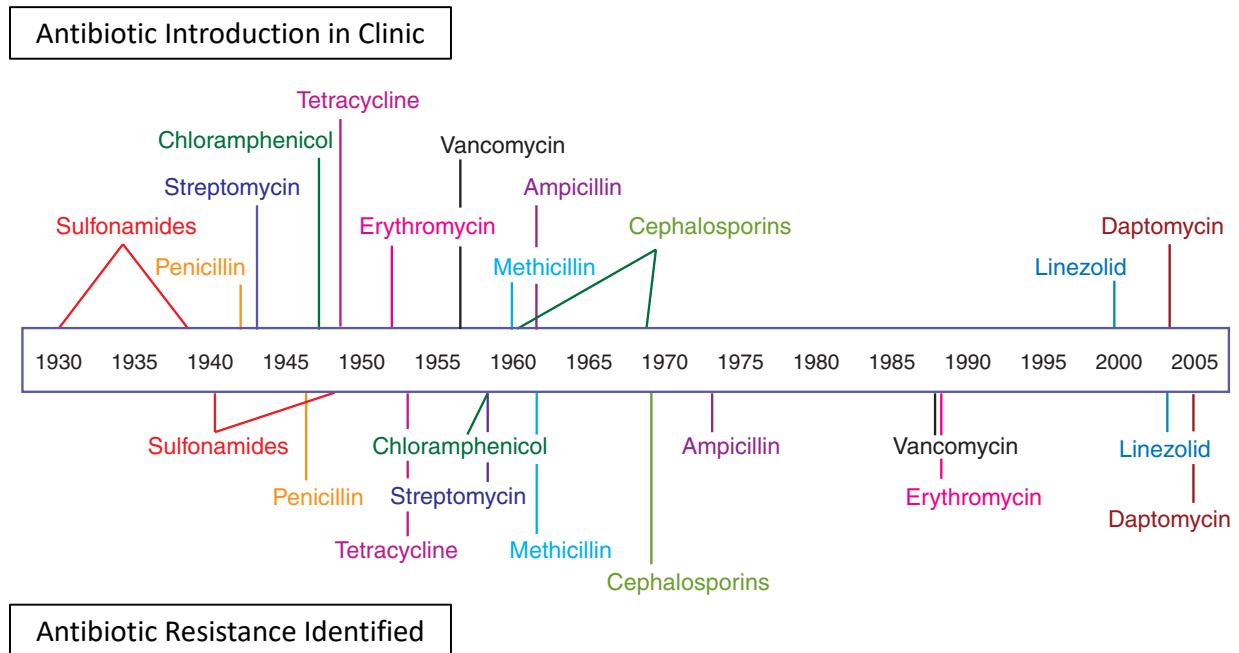


Figure 1.4. Timeline of antibiotic resistance development (figure adapted from reference 11).

The extensive problem of resistant infections prompted the World Health Organization (WHO) to develop a classification system to rank priority pathogens based on the urgency for new treatments (**Table 1.1**).¹² Moreover, there now exists a cohort of bacterial pathogens termed the ESKAPE pathogens (see section 1.4), which are characterized by their abilities to resist the action of multiple antibiotics.^{13, 14} These MDR bacteria are often referred to colloquially as superbugs, and several of these species are effectively untreatable with our current arsenal of antibiotics.⁴

In order to develop new techniques to address the growing problem of antimicrobial resistance, it is important to understand how this problem first came to be and how it evolved into the epidemic it is today. Indeed, gaining a deeper understanding of the modes of bacterial resistance as well as the sources of this resistance has already

led to the development of several new strategies to combat bacterial pathogens. Many of these will be presented later in the chapter.

Table 1.1. World Health Organization Priority Pathogen List for R&D of New Antibiotics^a

Priority Level 1: Critical	
Pathogen	Resistance
<i>Acinetobacter baumannii</i>	Carbapenem
<i>Pseudomonas aeruginosa</i>	Carbapenem
<i>Enterobacteriaceae</i> ^b	Carbapenem, 3 rd gen. Cephalosporin
Priority 2: High	
Pathogen	Resistance
<i>Enterococcus faecium</i>	Vancomycin
<i>Staphylococcus aureus</i>	Methicillin, Vancomycin
<i>Helicobacter pylori</i>	Clarithromycin
<i>Campylobacter</i>	Fluoroquinolone
<i>Salmonella</i>	Fluoroquinolone
<i>Neisseria gonorrhoeae</i>	3 rd gen. Cephalosporin, Fluoroquinolone
Priority 2: Medium	
Pathogen	Resistance
<i>Streptococcus pneumoniae</i>	Penicillin
<i>Haemophilus influenzae</i>	Ampicillin
<i>Shigella</i>	Fluoroquinolone

^a*Mycobacteria* was not included as it is already a globally established priority for which innovative new treatments are urgently needed

^b*Enterobacteriaceae* includes: *Klebsiella pneumoniae*, *Escherichia coli*, *Enterobacter* spp., *Serratia* spp., *Proteus* spp., and *Providencia* spp, *Morganella* spp.

1.2 Mechanisms of Antibiotic Action

1.2.1 Introduction

Antibiotics can be classified by the cellular component or system they affect and whether they induce cell death (bactericidal) or inhibit cell growth (bacteriostatic).^{9, 15, 16}

In order to affect pathogen death or interrupt pathogen growth, antibiotics target essential bacterial machinery. Consistent with this strategy, there are five major targets of antibiotics: the cell wall, the cell membrane, protein synthesis, DNA and RNA synthesis, and folic acid metabolism (**Figure 1.5**). Importantly, these targets are either sufficiently different or absent from eukaryotic cells (including human cells). For example, although cell walls are essential for bacterial survival, these structures are not found in eukaryotic cells. Additionally, while both bacterial cells and eukaryotic cells possess ribosomes, the structures of the ribosomes are sufficiently different that cross-inhibition is not observed.

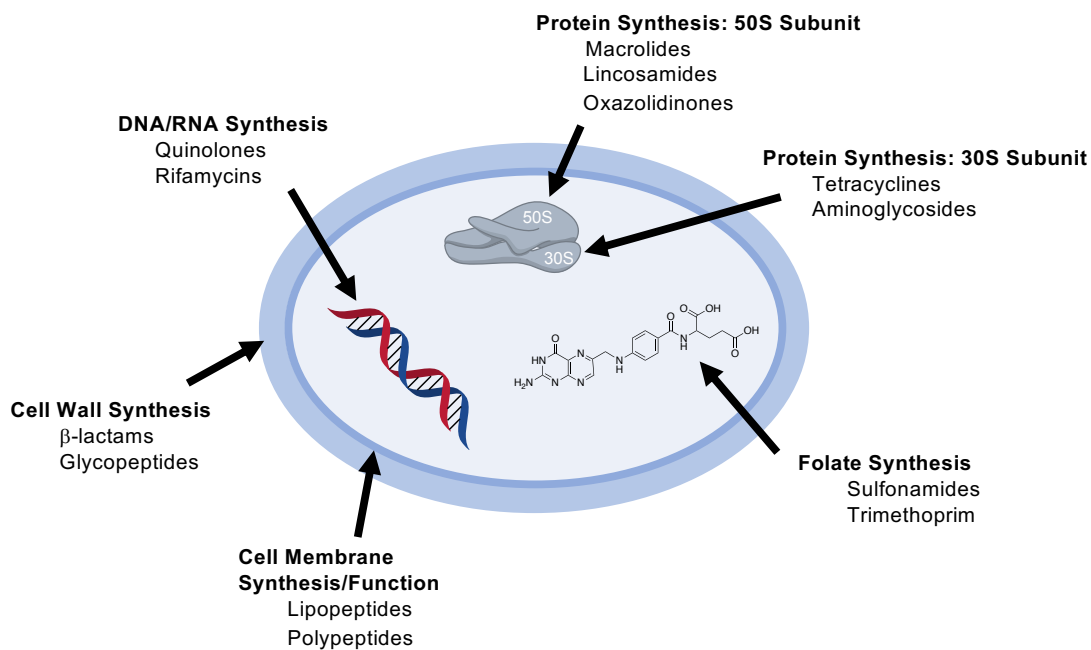


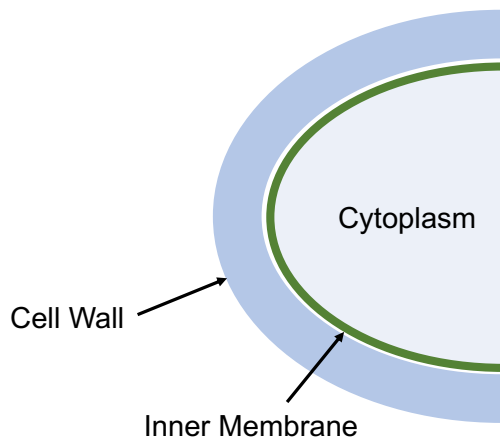
Figure 1.5. Major classes of antibiotic bacterial cell targets.

1.2.2 Cell Wall-Targeting Antibiotics

Bacterial cells are surrounded by a bacterial envelope that serves as protection from a hostile environment while also allowing for passage of select nutrients into the cell.¹⁷ Importantly, the composition of this envelope is what gives rise to the Gram-positive versus Gram-negative bacterial classification (**Figure 1.6**). In Gram-positive bacteria, the

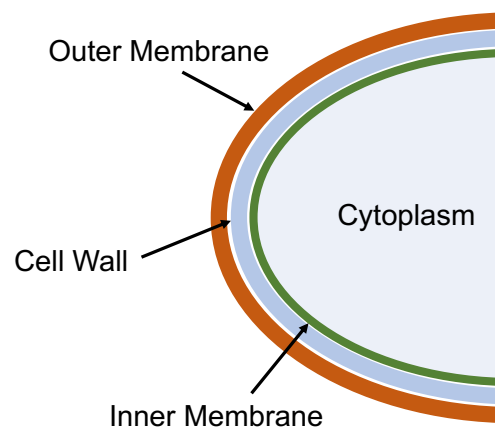
cell envelope is composed of a thick, outer peptidoglycan (PG) cell wall and an inner phospholipid bilayer membrane. While Gram-negative cell envelopes also contain a PG cell wall and an inner membrane, the cell wall is significantly thinner than that of Gram-positive cell envelopes. It is this difference in thickness that allows for experimental differentiation between Gram-positive and Gram-negative cells. The Gram stain is a crystal violet stain developed by Christian Gram that stains the PG of the bacterial cell wall. Because Gram-positive bacteria have a thick PG layer, they are able to retain a large amount of the Gram stain and thus are distinctly colored purple. Gram-negative bacteria, however, with their thin PG layer are not able to retain a large amount of Gram stain and can thus be counterstained with safranin or fuchsine to yield pink-colored cells.

A.



Gram-positive cell envelope

B.



Gram-negative cell envelope

Figure 1.6. General compositional differences between Gram-positive and Gram-negative bacterial cell envelopes.

In addition to a thinner cell wall, Gram-negative cells are also differentiated from Gram-positive cells by the presence of an outer membrane (OM) in their cell envelopes (**Figure 1.6B**). This feature is absent in the Gram-positive cell envelope. The OM is a lipid

bilayer composed of glycolipids, most notably lipopolysaccharides (LPSs), that extend beyond the outer leaflet of the OM (see section 1.2.3). The OM affords Gram-negative bacteria an additional layer of protection compared to Gram-positive species and is largely responsible for the increased difficulty of treating Gram-negative bacterial infections (see section 1.3.2).

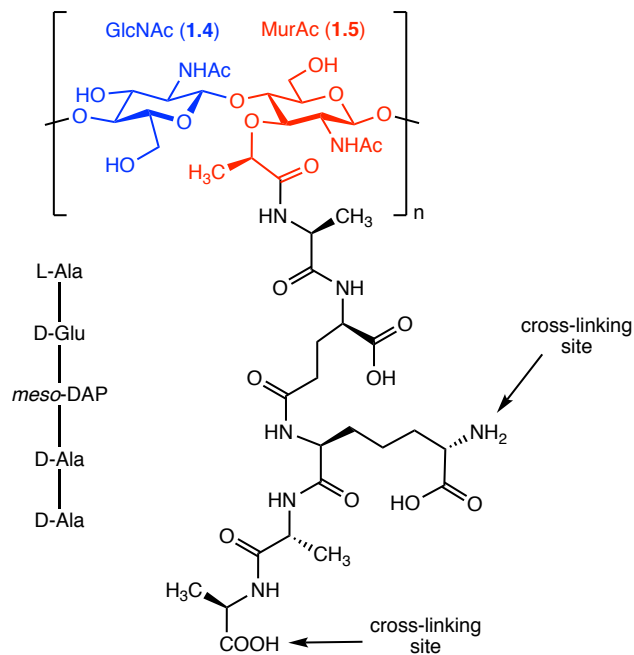


Figure 1.7. Typical repeating unit of the peptidoglycan bacterial cell wall.

In both Gram-positive and Gram-negative species, the rigid PG cell wall confers strength and structural integrity to the cell it surrounds.^{16, 17} In a similar vein, this layer determines cell shape. In terms of general composition, the PG layer is composed of linear glycan strands cross-linked by short peptide chains (**Figure 1.7**).¹⁸ The glycan strands consist of alternating *N*-acetylglucosamine (GlcNAc or NAM, **1.4**) and *N*-acetylmuramic acid (MurAc or NAG, **1.5**) residues linked via β 1-4 glycosidic bonds. Key to the cross-linking of these strands is a short peptide chain that is attached to the lactoyl group of the MurAc residues. The composition of this chain is most commonly L-Ala-D-

Glu-*meso*-DAP-D-Ala-D-Ala (*meso*-DAP or *meso*-A₂pm corresponds to D,L-2,6-diaminopimelic acid) (**Figure 1.7**). Crosslinking between glycan strands typically occurs at the subterminal D-Ala or DAP residues directly or through a short peptide bridge. Notably, the higher the degree of cross-linking in the PG, the higher the strength against osmotic lysis.^{16, 19}

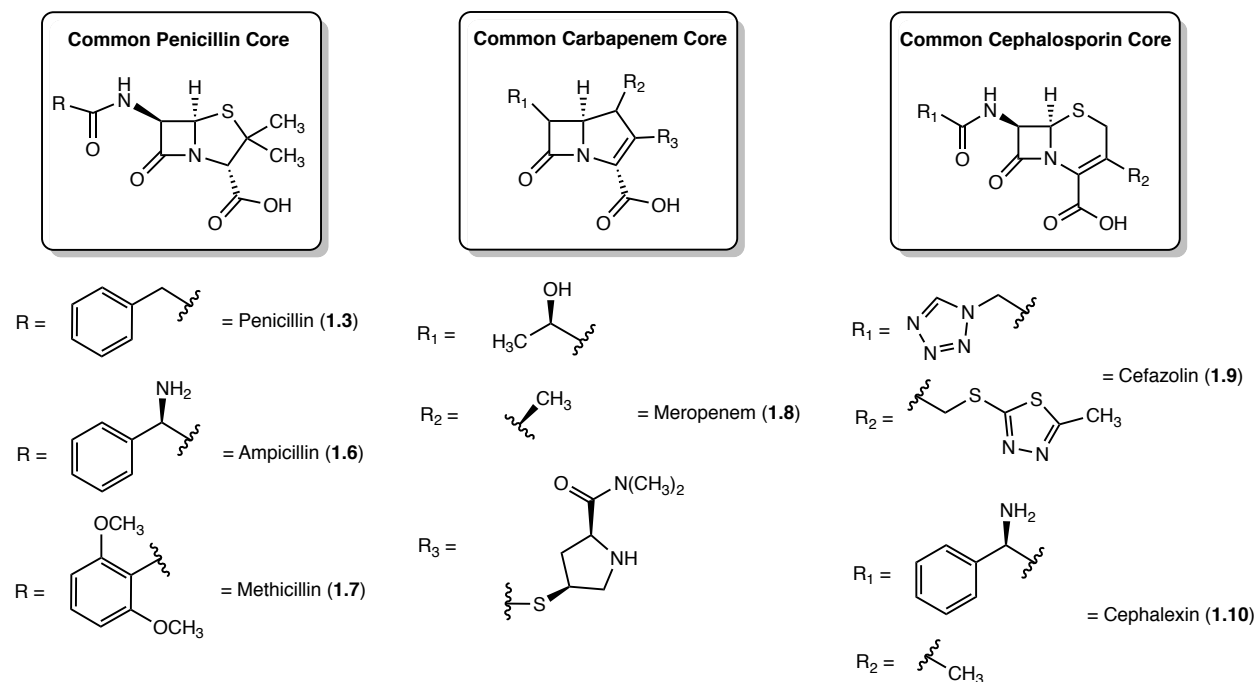


Figure 1.8. Structures of common β -lactams of the penicillin, carbapenem, and cephalosporin sub-classes.

Penicillin binding proteins (PBPs) are membrane-associated enzymes that are responsible for the synthesis and maintenance of the PG.²⁰ Importantly, PBPs are bifunctional enzymes possessing both transglycosylase and transpeptidase domains. Transglycosylases polymerize the disaccharide pentapeptide monomeric units while transpeptidases cross-link the short peptide chains of adjacent PG strands. As evidenced by their name, PBPs are the cellular targets of penicillin (1.3), the seminal β -lactam. PBPs

are also the cellular targets of other antibiotics of the β -lactam class including other penicillins, carbapenems, and cephalosporins (**Figure 1.8**).^{16, 19, 20}

β -lactams are bactericidal and exert their antibiotic action by blocking the cross-linking of PG strands through inhibition of the transpeptidase domain of PBPs (**Figure 1.9**).^{16, 19} As an analog of the terminal D-Ala-D-Ala dipeptide of the PG, β -lactams serve as pseudosubstrates and acylate the transpeptidase active site of PBPs to generate a ring-opened, penicilloylated PBP (**1.11**). This intermediate is unable to perform normal crosslinking of the PG strands which yields a weakened PG. Importantly, the penicilloylated PBP intermediate is hydrolyzed very slowly meaning that transpeptidase activity is blocked for prolonged periods.

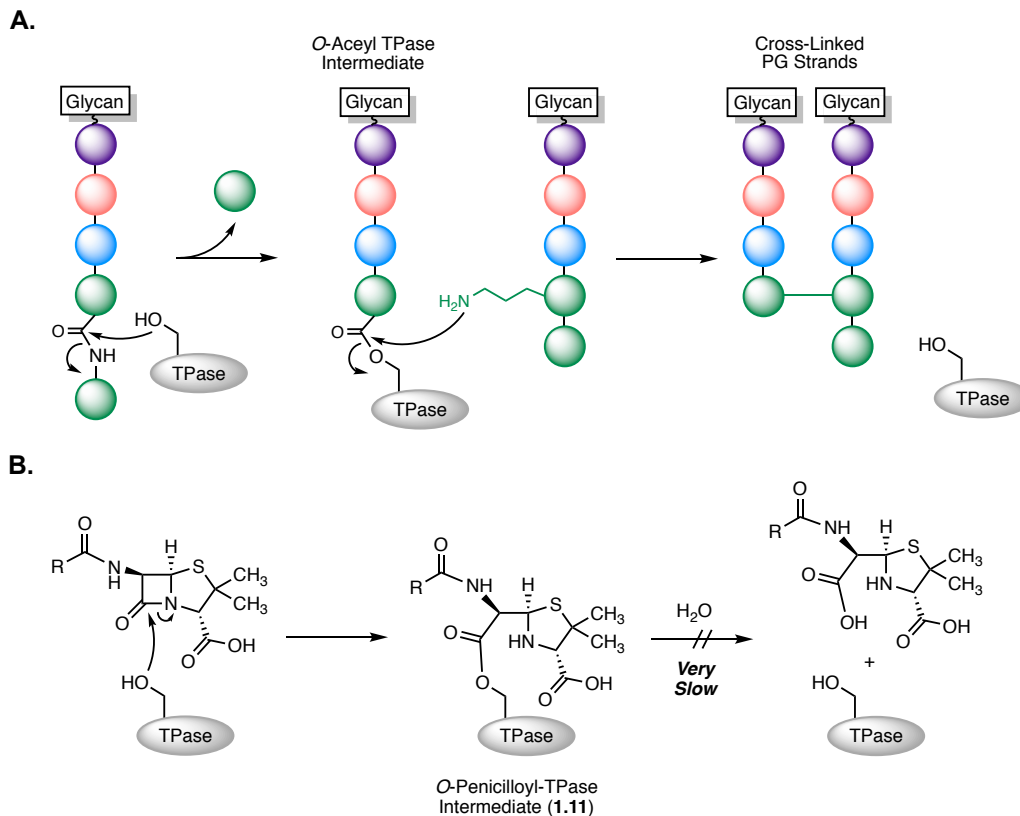


Figure 1.9. Mechanism of penicillin (β -lactam)-mediated inhibition of transpeptidase (TPase) action in peptidoglycan (PG) cell wall synthesis. **(A)** TPase cross-linking of PG strands in PG layer biosynthesis. **(B)** Inhibition of TPase activity by penicillins through covalent modification of the TPase active site by penicillin binding.

Glycopeptide antibiotics, such as vancomycin (**1.12**), also target the transpeptidase activity of PBPs and are similarly bactericidal.^{16, 19} However, in contrast to β -lactams that interact directly with the PBP to inhibit cross-linking, glycopeptides inhibit cross-linking by interacting with the PG units at the terminal D-Ala-D-Ala dipeptide (**Figure 1.10**). This interaction, characterized for vancomycin by five hydrogen bonds to the terminal D-Ala-D-Ala dipeptide, prevents a PG unit from reacting with either transglycosylases or transpeptidases. Again, this serves to reduce the amount of cross-linking in the PG which leads to a weaker cell that is more prone to lysis. Notably, because β -lactams and glycopeptides exert their effects on different aspects of the cross-linking reaction (enzyme and substrate, respectively), they have been found to work synergistically when used together, i.e. their combined activity is greater than the additive activity of each antibiotic when used alone.

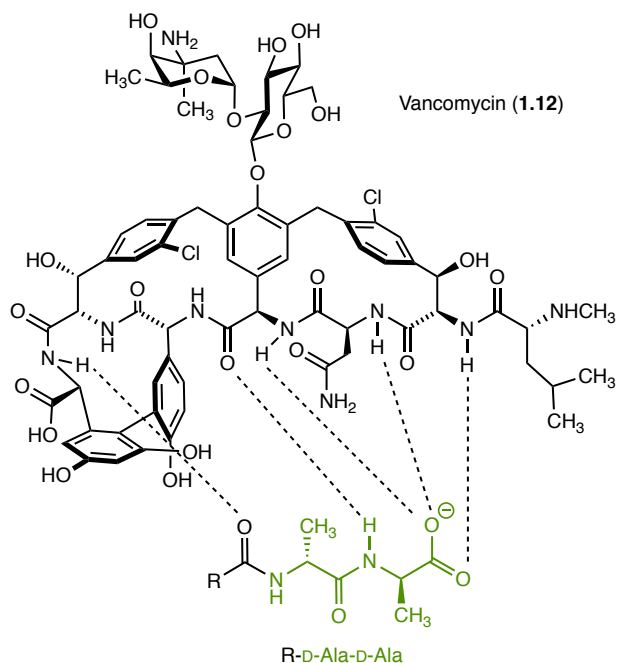


Figure 1.10. Mechanism of vancomycin-mediated inhibition of transpeptidase (TPase) and transglycosylase (TGase) action in peptidoglycan (PG) cell wall synthesis. Vancomycin forms five hydrogen bonds with the terminal D-Ala-D-Ala dipeptide of a PG strand. This steric interference prohibits the dipeptide from reacting with TPases or TGases, which inhibits cross-linking of PG strands.

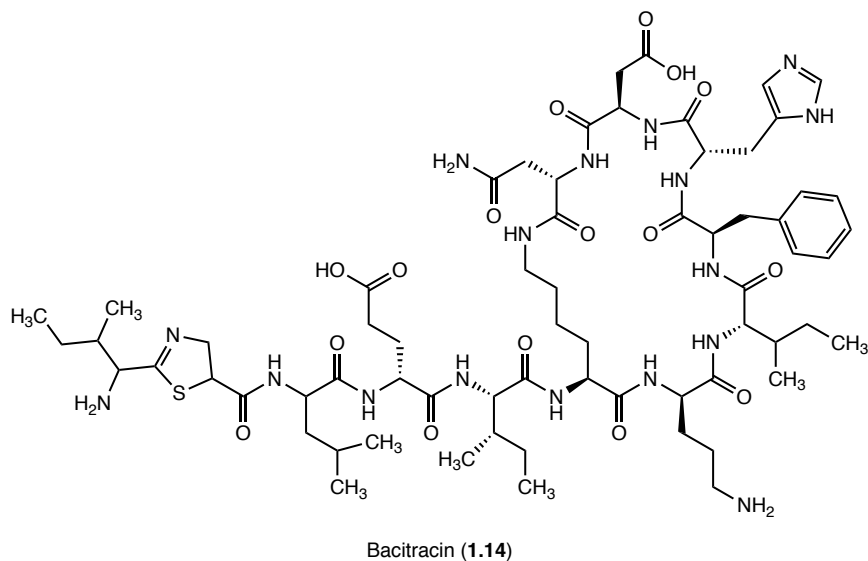
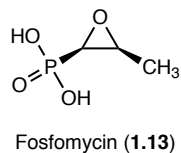


Figure 1.11. Structures of Fosfomicin (**1.13**) and Bacitracin (**1.14**). Fosfomicin and Bacitracin inhibit the synthesis and transport of peptidoglycan (PG) units, respectively.

Antibiotics also exist that inhibit the synthesis or transport of individual PG units, like fosfomicin (**1.13**) and bacitracin (**1.14**) (**Figure 1.11**). Fosfomicin and related phosphonic acids inhibit the synthesis of PG strands by interfering with the first committed step of PG synthesis: the formation of MurAc.^{21, 22} UDP-*N*-acetylglucosamine enolpyruvyl transferase (MurA) catalyzes the transfer of an enolpyruvyl moiety from phosphoenolpyruvate (PEP, **1.15**) to the C3'-hydroxyl of UDP-GlcNAc (**1.16**) to generate UDP-GlcNAc enolpyruvate (**1.17**); UDP-GlcNAc enolpyruvate (**1.17**) is a precursor for UDP-MurAc (**Figure 1.12A**). Similar to the β -lactams, Fosfomicin covalently modifies the active site of its target enzyme (MurA) which consequently inactivates the enzyme (**Figure 1.12B**). Conversely, the polypeptide antibiotic bacitracin exerts its antibiotic action by inhibiting the transport of PG units to the cell wall by interfering with the dephosphorylation of C₅₅-isoprenyl pyrophosphate; this dephosphorylation is essential to regenerate the lipid carrier that transports PG building blocks to the cell wall.^{16, 23}

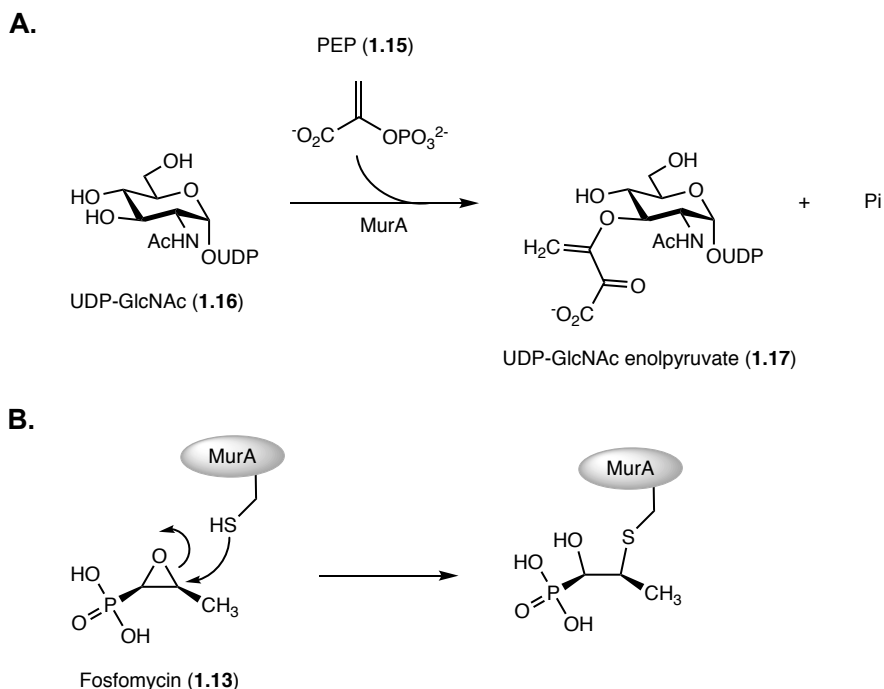


Figure 1.12. Fosfomycin-mediated inhibition of peptidoglycan (PG) strand synthesis. **(A)** The first committed step of PG strand synthesis is the synthesis of MurAc. MurAc synthesis begins with MurA-catalyzed transfer of an enolpyruvyl moiety to UDP-GlcNAc (1.16). **(B)** Fosfomycin inhibits the action of MurA through covalent modification of an active site cysteine residue. Abbreviations: UDP, uridine diphosphate; PEP, phosphoenolpyruvate (1.15); MurA, UDP-*N*-acetylglucosamine enolpyruvyl transferase.

1.2.3 Cell Membrane-Targeting Antibiotics

As previously mentioned, the bacterial cell membrane differs in composition and arrangement of constituent parts from the eukaryotic membrane. One of the most important differences is the presence of exposed anionic lipids on the surface of bacterial membranes; in eukaryotic membranes, anionic lipids are isolated to the lipid monolayer facing the cell interior.²⁴ In Gram-positive bacteria, teichoic and lipoteichoic acids extend from the inner membrane and the PG and are ultimately exposed to the extracellular environment (**Figure 1.13A**). In the OM of Gram-negative bacteria, LPS constitutes the major lipid component and is critical to the barrier function of the OM (**Figure 1.13B**).¹⁷

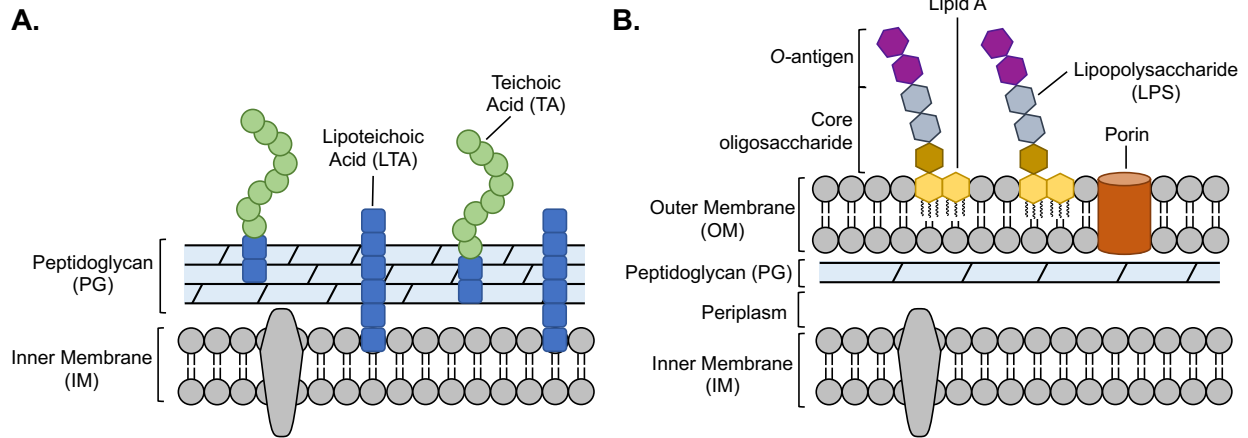


Figure 1.13. Gram-positive and Gram-negative cell envelopes.

General architecture of the LPS is shown in **Figure 1.13B**.^{25, 26} Lipid A (**1.18**), a glucosamine disaccharide phospholipid (**Figure 1.14**), is the innermost portion of the LPS and serves as a highly hydrophobic anchor of the LPS to the outer monolayer of the membrane.^{17, 25} Covalently attached to the lipid A component is the core oligosaccharide component of LPS that can be further broken down into the inner and outer core. The inner core is composed of less common sugars such as 2-keto-3-deoxy-D-mannooctulosonic acid (Kdo, **1.19**) and L-glycero-D-manno heptose (hep, **1.20**) (**Figure 1.14**). Conversely, the outer core is typically comprised of common hexaose sugars like glucose (Glc, **1.21**), galactose (Gal, **1.22**), GlcNAc (**1.4**), and *N*-acetylgalactosamine (GalNAc, **1.23**) (**Figure 1.14**). Notably, the carbohydrate residues in the inner and outer cores can be modified with phosphate- and pyrophosphate-containing functionalities. The binding of these negatively-charged functionalities, as well as the negatively-charged phosphate groups of lipid A, to Mg^{2+} or Ca^{2+} ions helps to facilitate tight packing of LPS molecules. Finally, a polymer of repeating saccharide units termed the *O*-polysaccharide, -chain, or -antigen is bound typically to the core oligosaccharide component. Importantly, the composition of this polymer varies among bacterial strains.

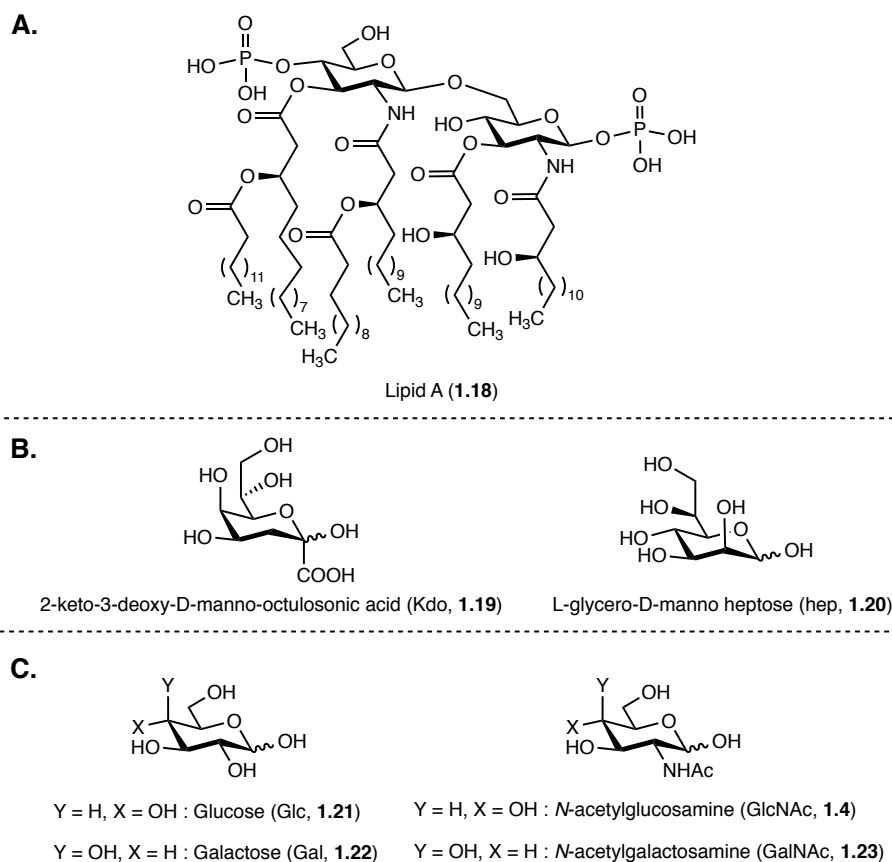


Figure 1.14. Structures of common lipopolysaccharide (LPS) components. **(A)** Structure of lipid A (1.18) as found in *E. coli*. Structures of common monosaccharides in the outer oligosaccharide core. **(B)** Structures of common monosaccharides in the inner oligosaccharide core.

To take advantage of the unique anionic nature of bacterial cell membranes, many antimicrobials are cationic (at physiological pH) as the favorable electrostatic interaction between drug and membrane facilitates greater selectivity for the bacterial membrane. Notably, cationic antimicrobials are an important form of treatment against Gram-negative bacteria. One class of cationic cell membrane-targeting antibiotics is the antimicrobial peptide (AMP). AMPs interact with the bacterial cell membrane to produce membrane perturbation and/or disintegration.^{21, 27, 28} For example, AMPs can be inserted into the membrane bilayer to form transmembrane pores. Moreover, in some cases, AMPs can translocate across the membrane and engage cytoplasmic targets.

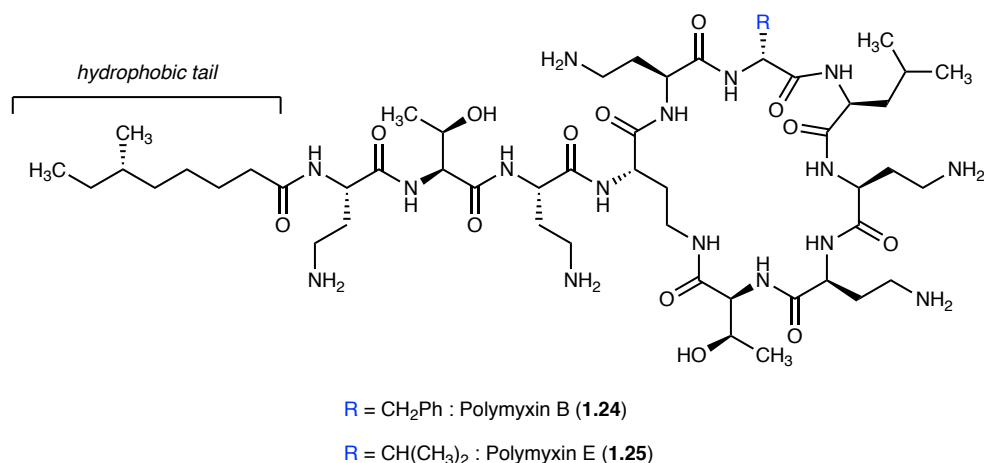


Figure 1.15. Structures of polymyxins B (1.24) and E (1.25).

Two common AMPs are the cyclopeptide antibiotics polymyxin B (1.24) and colistin (polymyxin E, 1.25) (Figure 1.15).^{21, 29} Polymyxins induce membrane destabilization by first displacing Mg^{2+} and Ca^{2+} ions and binding to the lipid A component of the LPS. The hydrophobic portion of the polymyxin is then inserted into the OM which weakens the tight packing between adjacent lipid A molecules.³⁰ Once a sufficient level of OM destabilization has been reached, the polymyxin can cross the OM and engage the IM. Polymyxin interaction with the IM leads to membrane thinning and eventual lysis and cell death. As Gram-positive species lack LPS, polymyxins are typically inactive against this class of bacteria.^{15, 31}

Daptomycin (DAP, 1.26) is a related lipopeptide antibiotic that is effective against Gram-positive bacteria but generally ineffective against Gram-negative species (Figure 1.16).^{32, 33} Analogous to the polymyxins that are effective against Gram-negative bacteria, DAP binds the Gram-positive membrane which leads to membrane destabilization and ultimately cell death. However, rather than targeting lipid A, DAP targets the anionic phospholipid phosphatidylglycerol (1.27) of the cell membrane (Figure 1.16). It has been hypothesized that the limited activity of DAP against Gram-negative

species is due to a significantly decreased prevalence of phospholipid phosphatidylglycerol in Gram-negative membranes. Importantly, prior to engaging phospholipid phosphatidylglycerols, DAP first binds Ca^{2+} ions to form DAP micelles that are hypothesized to aid in the delivery of DAP to the membrane. Once it has engaged phospholipid phosphatidylglycerols, it is proposed that DAP inserts its lipophilic tail into the cell membrane which leads to membrane destabilization and the formation of pore-like structures. The newly formed pore-like structures then facilitate potassium ion efflux which is followed by DNA, RNA, and protein synthesis arrest.

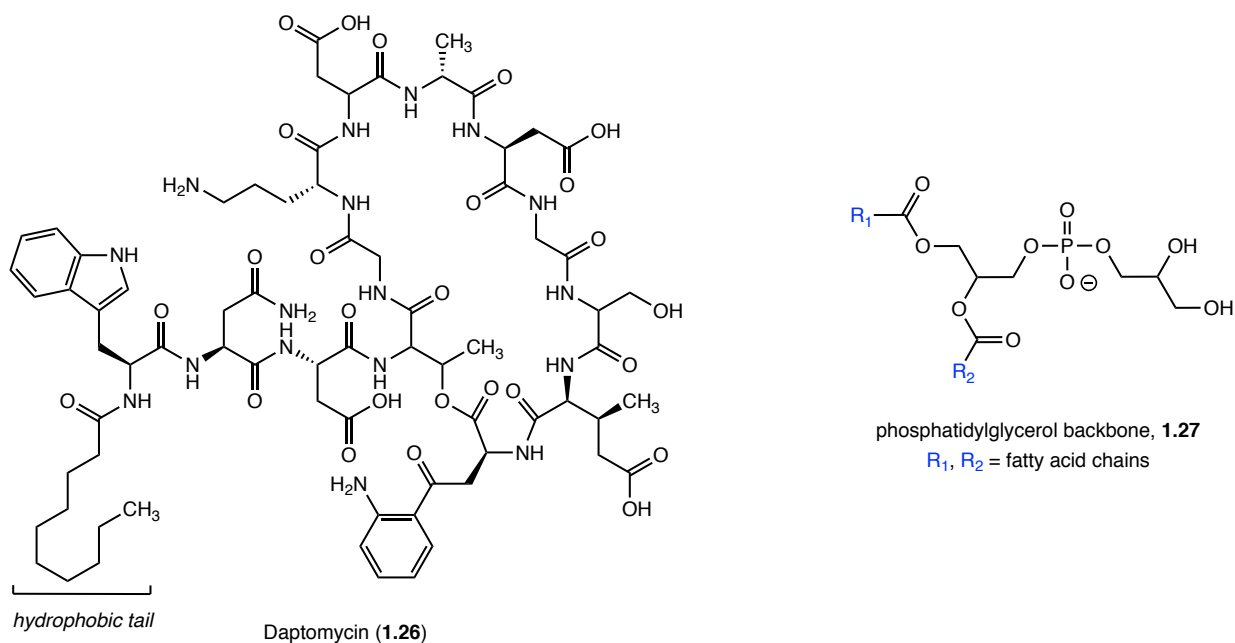


Figure 1.16. Structures of daptomycin (DAP, **1.26**) and its bacterial cell membrane target, phosphatidylglycerol (**1.27**).

1.2.4 Protein Synthesis-Targeting Antibiotics

The ribosome, i.e. the protein-synthesizing factory of the cell, is the target of numerous classes of antibiotics including the aminoglycosides (AGs), lincosamides, macrolides, oxazolidinones, and tetracyclines (**Figure 1.17**).

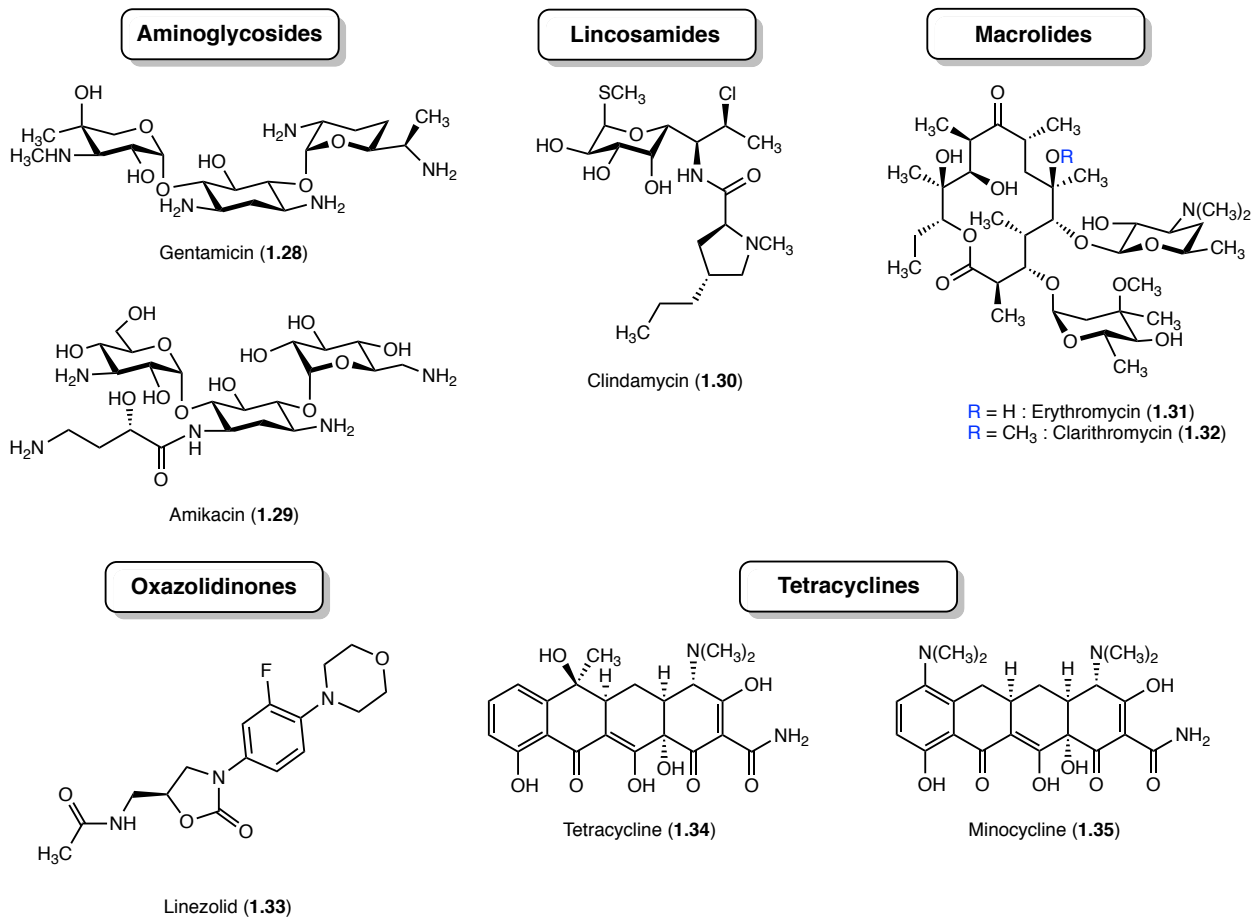


Figure 1.17. Structures of select ribosomal protein synthesis-targeting antibiotics.

Protein assembly can be divided into four main steps: initiation, elongation, termination, and recycling (**Figure 1.18**).^{16, 34} Initiation begins with formation of a 70S ribosome, composed of the 50S and 30S ribonucleoprotein subunits, in complex with the mRNA start codon (typically AUG) and initiator tRNA (usually fMet-tRNA). Once the mRNA start codon and initiator tRNA are properly positioned at the ribosomal P-site, elongation of the protein can occur. Elongation commences with delivery of an aminoacylated tRNA (aa-tRNA) to the A-site (adjacent to the P-site) of the 70S ribosome. The amino acid attached to the P-site tRNA is then transferred to the A-site aa-tRNA to form a peptide bond. The tRNAs in the A- and P-sites are then translocated to the P- and

E-sites to ready the ribosome for additional peptide bond formation. Elongation continues until a stop codon is encountered. When a stop codon is reached, the polypeptide chain is released from the ribosome (termination). The post-termination complex is then disassembled to allow the constituent parts to be recycled for the next round of protein translation (recycling).

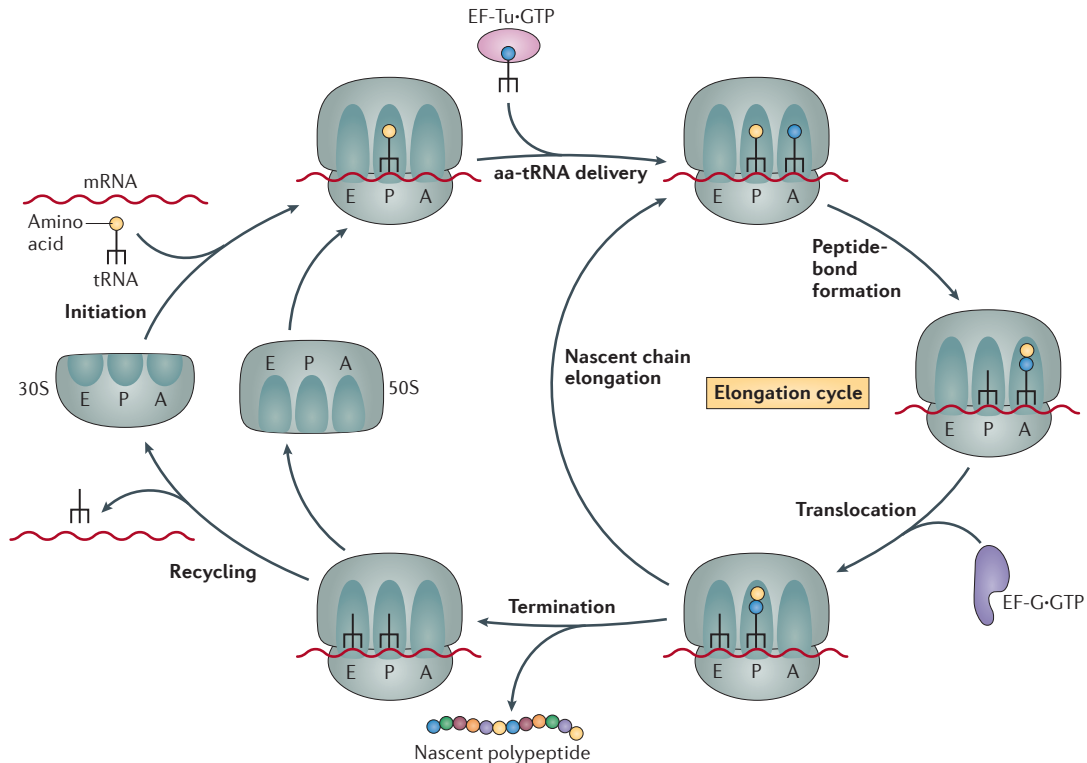


Figure 1.18. Steps of ribosomal-protein synthesis (figure adapted from reference 34). Abbreviations: tRNA, transfer ribonucleic acid; mRNA, messenger ribonucleic acid; EF-Tu-GTP, elongation factor thermos unstable-guanosine triphosphate; aa-tRNA, aminoacyl transfer ribonucleic acid.

The majority of known ribosome-targeting antibiotics target the elongation step of protein synthesis (**Figure 1.19**).^{16, 34} This inhibition can occur via binding of the antibiotic to either the 50S or 30S ribosomal subunits. The 30S subunit is the site of base-pairing interactions between mRNA codons and aa-tRNA anticodons that facilitate selection of the cognate aa-tRNA.³⁵ Conversely, the 50S subunit is the site of peptide bond formation;

bond formation occurs in the peptidyl transferase center (PTC) located within the 50S subunit.

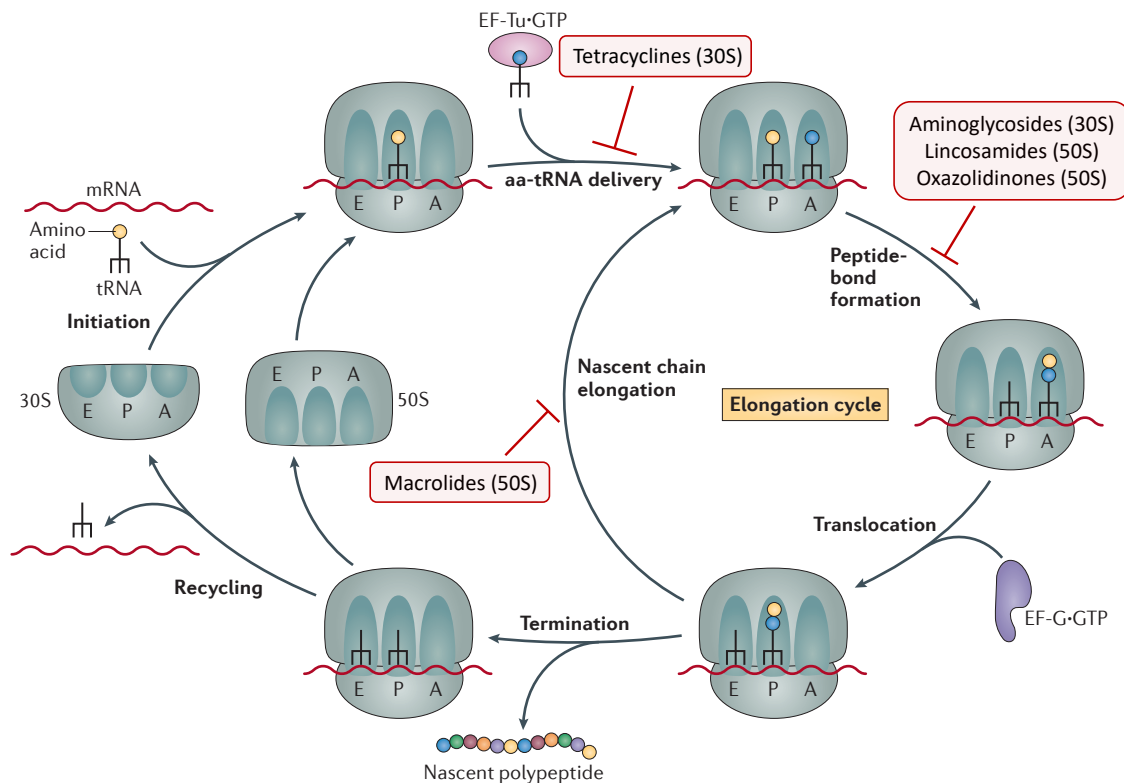


Figure 1.19. Protein synthesis target sites of aminoglycosides (AGs), lincosamides, macrolides, oxazolidinones, and tetracyclines (figure adapted from reference 34). Information in parentheses following antibiotic class names corresponds to the ribosomal subunit target of the antibiotic class.

Tetracyclines bind the 30S subunit at a site that overlaps with the position of the anticodon stem loop of the tRNA in the A-site.^{16, 34} The steric bulk imposed by the bound tetracycline blocks the delivery of aa-tRNAs to the A-site, which effectively halts protein elongation (**Figure 1.19**). AGs also interact with the 30S subunit. Importantly, AGs are the only ribosome-targeting antibiotic class that are broadly bactericidal. AGs bind the 16S rRNA (ribosomal ribonucleic acid) of the 30S subunit which induces a conformational change. This change subsequently promotes the binding of non-cognate tRNAs to the mRNA at the ribosome. This tRNA mismatching (translational misreading) can lead to the

production of faulty proteins that can then be incorporated into the cellular structure. Notably, the incorporation of mistranslated proteins into the cell membrane increases cell permeability which allows for greater influx of AGs into the intracellular environment.³⁶

While lincosamides, macrolides, and oxazolidinones also target the elongation step of protein synthesis, they do so by binding the 50S near the PTC rather than binding the 30S ribosomal subunit.^{16, 34} Lincosamides bind the PTC at a site that overlaps with aa-tRNA in the A-site. This steric bulk blocks peptide bond formation by blocking delivery of aa-tRNAs to the A-site (**Figure 1.19**). While oxazolidinones also bind the PTC at the A-site, their binding is thought to inhibit formation of the initial peptide bond by perturbing the position of the initial P-site tRNA.^{34, 37} This perturbation effectively blocks assembly of the 70S, mRNA start codon, and initiator tRNA complex thereby preventing commencement of mRNA translation. In contrast to lincosamides and oxazolidinones, macrolides bind the 50S subunit within the ribosomal exit tunnel, a site adjacent to the PTC; during peptide elongation, the growing peptide chain passes through the ribosomal exit tunnel to the cytoplasm where protein folding occurs.³⁴ This binding inhibits elongation of short nascent peptide chains which leads to peptidyl-tRNA drop off (release of peptidyl-tRNAs from the ribosome) and abortion of translation.^{34, 38}

Antibiotics that target the remaining steps of protein synthesis (initiation, termination, and recycling) as well as those that specifically target the translocation of growing peptide chains from the A- to P-sites are reviewed elsewhere.^{34, 39, 40}

1.2.5 DNA and RNA-Targeting Antibiotics

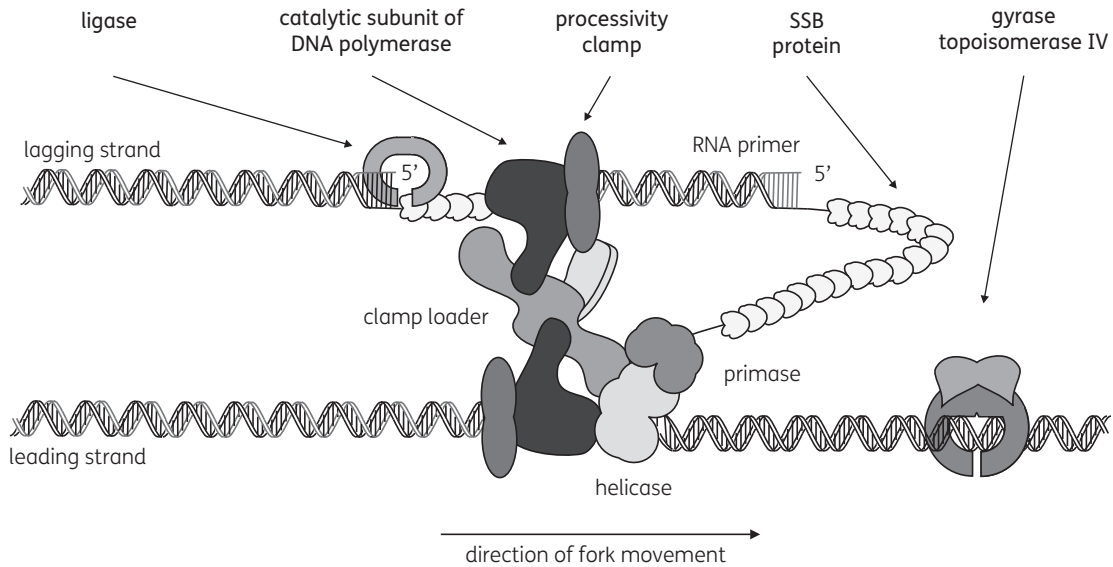


Figure 1.20. Schematic depiction of bacterial DNA replication (figure adapted from reference 41). For simplicity, DNA replication initiation and regulator proteins have been omitted. Abbreviations: DNA, deoxyribonucleic acid; SSB, single-stranded DNA-binding.

DNA replication is essential for cell survival and has thus become an attractive antibiotic target.^{16, 24, 41} Successful replication requires a multi-protein complex, termed the replisome, which is composed of the following proteins: DNA polymerase, processivity or sliding clamp, clamp ladder, helicase, primase, and single-stranded DNA-binding (SSB) (**Figure 1.20**).^{41, 42} In addition to the replisome complex, DNA ligase and the type II topoisomerases (Topo IIs) DNA gyrase and topoisomerase IV (Topo IV) are crucial for DNA replication (**Figure 1.20**). For replication to begin, double-stranded DNA must first be unwound and the two strands separated at what is termed a replication fork. Importantly, ahead of this fork, DNA gyrase introduces negative supercoiling that relaxes the DNA helix which allows replication to proceed. Topo IV similarly works to alleviate torsional stress in DNA, though it does so by removing knots that accumulate in the bacterial chromosome. Additionally, after replication, Topo IV catalyzes decatenation of

the two DNA molecules; the bacterial chromosome is typically circular, thus replication produces two rings that must be separated from one another. While any of the proteins involved in DNA replication are theoretically viable and effective drug targets, clinical antibiotics have largely been limited to Topo II inhibitors that target DNA gyrase and/or Topo IV.^{16, 41}

Of the Topo II inhibitors, the quinolones are the most successful and widely-used class of antibiotic.⁴² The earliest member of this class, nalidixic acid (**1.36**), was introduced into the clinic in the 1960s (**Figure 1.21**).⁴³ Since the 1960s, numerous second-generation quinolones, such as ciprofloxacin (**1.37**) and levofloxacin (**1.38**), have been introduced that feature improved efficacy against DNA gyrase, greater cell penetration in Gram-positive species, and improved pharmacodynamics and kinetics (**Figure 1.21**). The most notable features of these second-generation compounds are the introduction of a fluorine at the C6 position of the quinolone skeleton as well as a ringed substituent at the C7 position. Notably, due to the inclusion of a fluorine atom, quinolone antibiotics are now often referred to as fluoroquinolones.

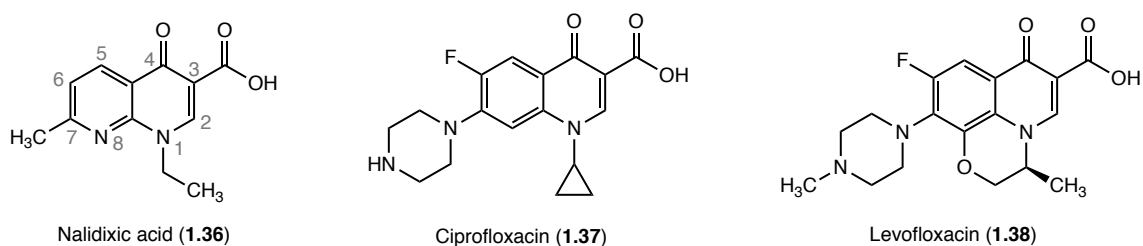


Figure 1.21. Structures of select quinolone antibiotics. The accepted numbering scheme for positions on the quinolone skeleton are denoted on the structure of nalidixic acid (**1.36**).

The actions of DNA gyrase and Topo IV require the generation of double-stranded breaks in the bacterial chromosome. While these genome fragmentations are necessary, quinolone antibiotics exert their action by exploiting Topo II-mediated genome

fragmentation.^{16, 41, 43} Quinolones bind non-covalently to the Topo II-cleaved DNA complex by intercalating into the DNA. This action stabilizes the complex and consequently prolongs the lifetime of double-stranded DNA breaks. When the replication process encounters quinolone-stabilized gyrase- or Topo IV-DNA cleavage complexes, the complexes are converted to permanent chromosomal breaks. If enough breaks are created, they can ultimately lead to cell death (**Figure 1.22**). Because of the ability of quinolones to effectively convert Topo II enzymes into cellular toxins, they are often referred to as “topoisomerase poisons.”

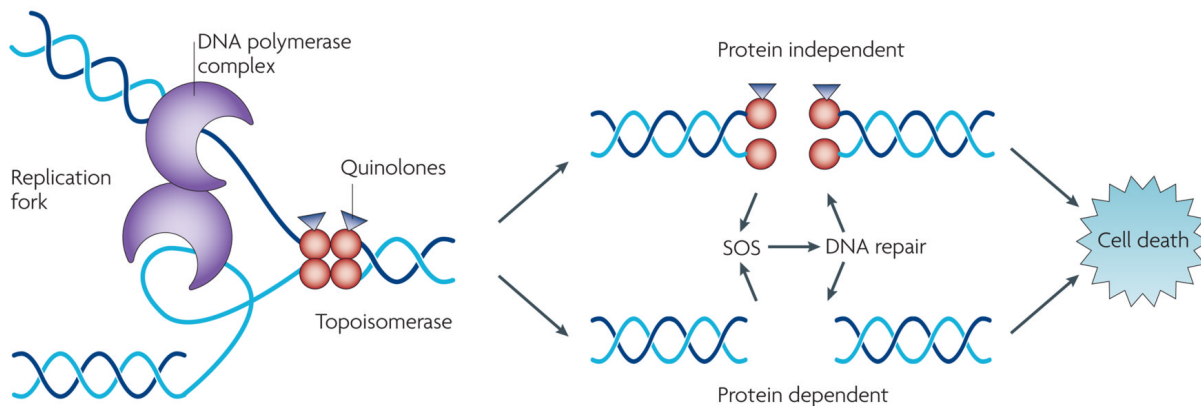


Figure 1.22. Mechanism of quinolone-mediated cell death (figure adapted from reference 16). Quinolones trap Topo II enzymes as a drug-enzyme-DNA complex. When this complex is encountered by the replisome, or DNA polymerase complex, lethal, double-stranded DNA breaks are released. The release of these strands triggers the SOS response and other DNA repair pathways. If strand breaks overwhelm these responses, cell death can occur.

Much like the inhibition of DNA replication, the inhibition of bacterial transcription can have a catastrophic effect on cellular viability. Transcription, i.e. the process by which RNA is synthesized from template DNA, is facilitated by RNA polymerase (RNAP) and numerous protein transcription factors (**Figure 1.23**).^{44, 45}

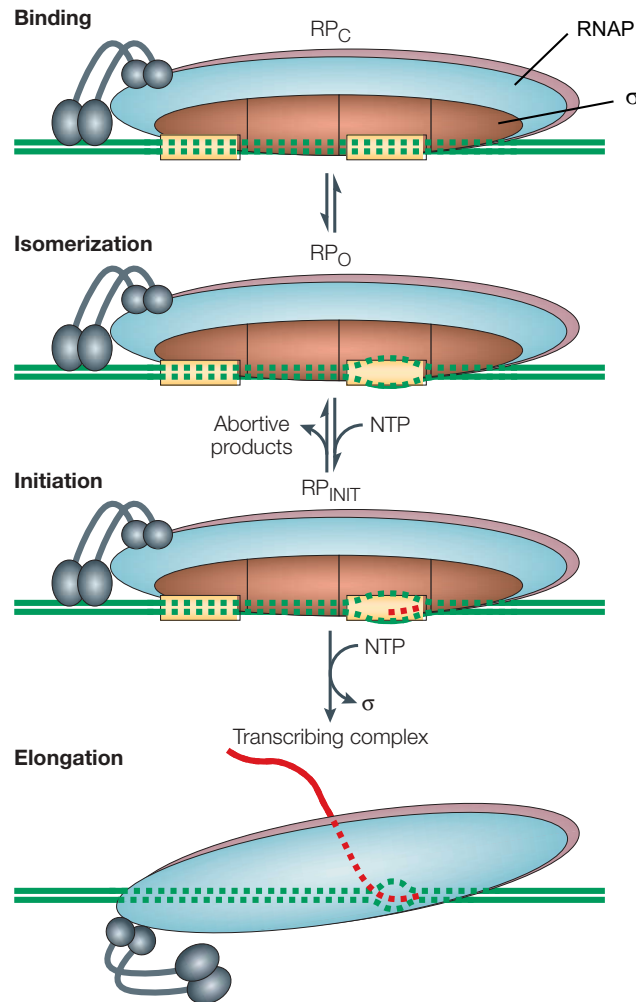


Figure 1.23. Process of bacterial transcription (figure adapted from reference 44). RNA polymerase (RNAP) forms a complex with initiation factor σ , and the resulting complex binds double-stranded DNA to form a closed complex (RP_C). Dashed lines indicate that DNA is bound by RNAP. Duplex DNA is next unwound to form the open complex (RP_O). The initiation complex (RP_{INIT}) is formed as synthesis of the DNA-template-directed RNA chain begins. The dashed red line indicates a growing RNA chain bound by RNAP. Finally, σ is released and RNAP undergoes a conformational change to facilitate elongation of the RNA chain. The solid red line indicates an elongated RNA chain. Abbreviations: NTP, nucleotide triphosphate.

For transcription to begin, RNAP must first associate with an initiation factor, σ , to form a complex that is poised to bind DNA at a promoter region.^{44, 45} Following promoter recognition, the double stranded DNA near the transcript start site is unwound to form an open promoter complex and initiation of RNA synthesis begins. Once approximately

twelve nucleotides of RNA have been synthesized, σ is released and RNAP undergoes a conformational change to form a transcription elongation complex (EC). Elongation of the DNA-template-directed RNA chain continues until a transcription termination signal is reached. RNAP is then released from the template DNA to allow for initiation of another round of transcription. Because RNAP and its associated transcription factors are highly conserved across bacterial species, antibiotics that target RNAP have the potential to be broad-spectrum drugs. Moreover, because bacterial RNAP and the associated transcription factors differ significantly from those of eukaryotes, antibiotics that target RNA synthesis have a low potential for cytotoxic effects.

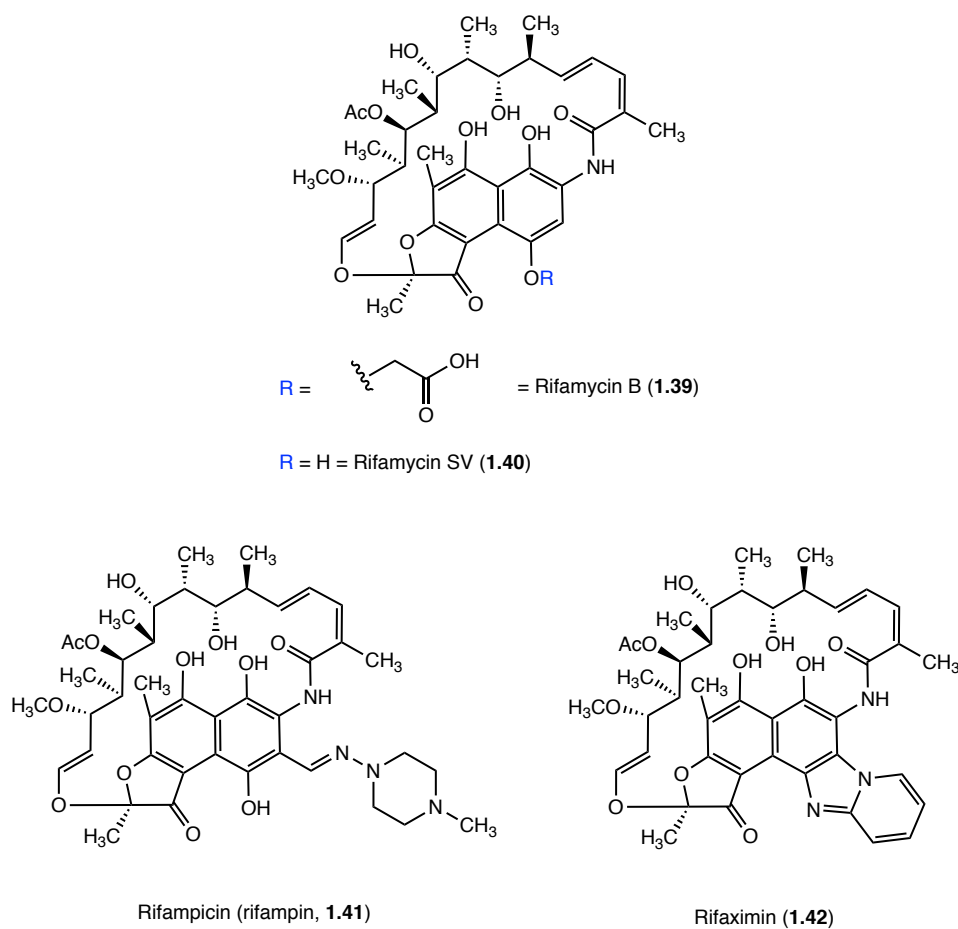


Figure 1.24. Structures of select rifamycin antibiotics.

Rifamycins were the first RNAP-targeting class of antibiotic discovered, and, today, this class is one of only a few approved for clinical use.⁴⁵ Structurally, rifamycins are part of the ansamycin antibiotic family, a family whose structures are defined by an aromatic residue bridged at nonadjacent positions by an aliphatic chain (**Figure 1.24**).⁴⁶ Derived from rifamycin B (**1.39**), which was isolated from the metabolites of *Amycolatopsis mediterranei*, rifamycin SV (**1.40**) was the first of its class to be approved for clinical use. Subsequent structural modifications to yield compounds like rifampicin (**1.41**, also known as rifampin) and rifaximin (**1.42**) were made to improve pharmacokinetics and reduce affinity for eukaryotic RNAPs rather than to modify the mechanism of antibiotic action.

Rifamycins inhibit the initiation phase of transcription by binding DNA-bound, actively-transcribing RNAP with high affinity at a site close to the active site.^{16, 45, 46} Importantly, the rifamycin binding site is located within the channel formed by the RNAP complex through which newly synthesized RNA chains emerge. Thus, the binding of rifamycin sterically hinders the growth of RNA. It is important to note, however, that this inhibition is unique to the initiation phase. Indeed, once RNA synthesis has progressed past an early stage and the growing RNA chain is several nucleotides long, the process is no longer sensitive to rifamycin treatment.

Fidaxomicin (**1.43**) is another approved RNAP-targeting antibiotic that possess selective antibacterial activity against Gram-positive species, especially *Clostridium difficile* (**Figure 1.25**).^{45, 47, 48} Like the rifamycins, fidaxomicin inhibits the action of RNAP at the initiation phase of transcription. However, fidaxomicin exerts its action earlier in transcription than the rifamycins. Fidaxomicin binds the DNA-bound RNAP complex and prevents initial separation of DNA strands, i.e. formation of the open complex, by the

initiation factor, σ . The engagement of fidaxomicin with σ is what is hypothesized to explain the limited spectrum of fidaxomicin antibacterial activity as σ subunits differ across bacterial species.⁴⁸

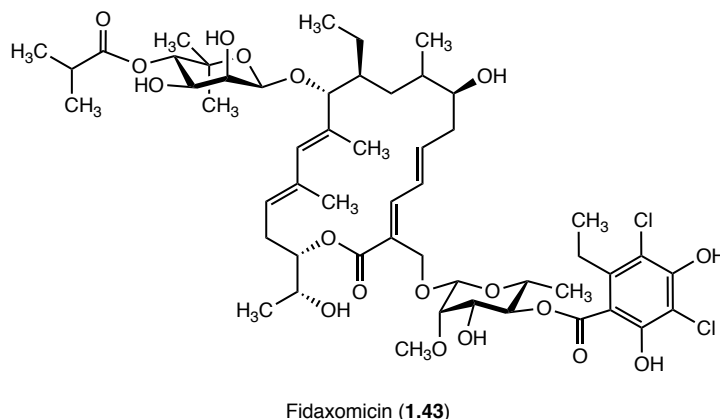


Figure 1.25. Structure of fidaxomicin (1.43).

1.2.6 Folate Biosynthesis-Targeting Antibiotics

In both prokaryotic and eukaryotic cells, folate cofactors are necessary for the biosynthesis of a diverse range of critical cellular components in nucleobases, proteins, and other cofactors.⁴⁹⁻⁵¹ Due to its essential role in nucleic acid synthesis, inhibition of the folate biosynthetic pathway prevents cell growth and proliferation. Consequently, folate biosynthesis represents another attractive antibiotic cellular target. To make this target even more attractive, while bacteria rely on *de novo* folate biosynthesis, humans lack this biosynthetic pathway and instead must obtain folate from their diet (in the form of the vitamin B9, folic acid). Thus, antibiotics targeting bacterial folate synthesis act only on the desired bacterial target.

The folate biosynthetic pathway is depicted in **Figure 1.26**. The pathway begins with guanosine triphosphate (GTP, **1.44**) which over several steps is converted to 6-hydroxymethyl-7,8-dihydropterin **1.45**.^{49, 51} 6-hydroxymethyl-7,8-dihydropterin

pyrophosphokinase (HPPK) then catalyzes ATP-dependent phosphorylation of **1.45** to yield 6-hydroxymethyl-7,8-dihydropterin pyrophosphate **1.46**. Next, dihydropteroate synthase (DHPS) catalyzes the condensation of **1.46** with *para*-aminobenzoic acid (pABA, **1.47**) to generate 7,8-dihydropteroate **1.48**. Intermediate **1.48** is converted to 7,8-dihydrofolate **1.49** via dihydrofolate synthase (DHFS)-mediated coupling with L-glutamate. Finally, **1.49** is reduced by dihydrofolate reductase (DHFR) to afford tetrahydrofolate (THF, **1.50**). THF can then be converted into various cofactors for use in a number of one carbon metabolic processes.

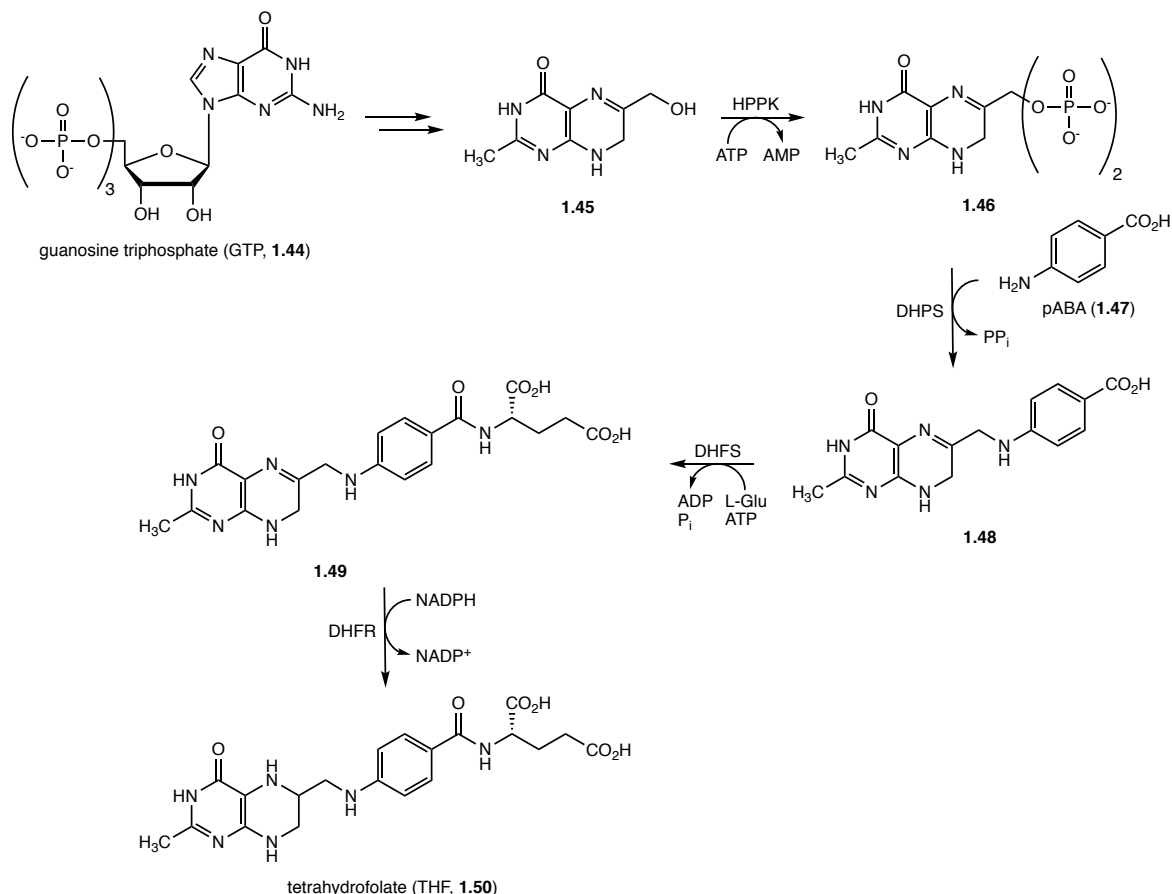
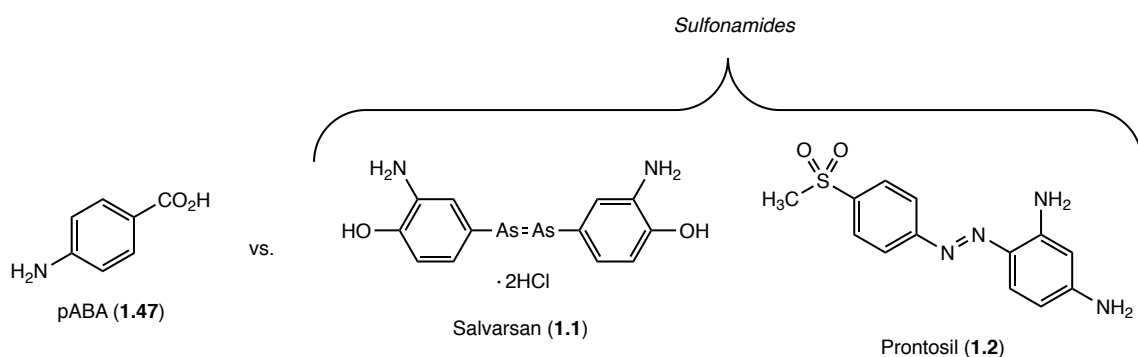


Figure 1.26. Bacterial folate biosynthetic pathway. Abbreviations: HPPK, 6-hydroxymethyl-7,8-dihydropterin pyrophosphokinase; ATP, adenosine triphosphate; AMP, adenosine monophosphate; pABA, *para*-aminobenzoic acid; DHPS, dihydropteroate synthase; PP_i, pyrophosphate; DHFS, dihydrofolate synthase; L-glu, L-glutamate; ADP, adenosine diphosphate; P_i, inorganic phosphate; DHFR, dihydrofolate reductase; NADPH, reduced nicotinamide adenine dinucleotide phosphate; NADP⁺, oxidized nicotinamide adenine dinucleotide phosphate; THF, tetrahydrofolate.

The sulfonamides, the first widely used synthetic antibiotics, target bacterial folate biosynthesis.⁴⁹ Due to their shared structural features (**Figure 1.27**), sulfonamide antibiotics act as mimics of pABA and can serve as alternative substrates for DHPS. By serving as an alternative substrate, sulfonamides effectively deplete the folate pool which inhibits cellular growth. The related diaminopyrimidine class of antibiotic, including trimethoprim (**1.51**), inhibits folate biosynthesis by inhibiting the action of DHFR.^{49, 52, 53} It is important to note, however, that both bacterial and human cells possess DHFR; in humans, DHFR reduces the folic acid obtained through diet to dihydrofolate then to THF. Thus, antibiotics targeting DHFR must be selective for the bacterial enzyme. The high selectivity of trimethoprim as an inhibitor of bacterial DHFR confers an advantage for this antibiotic over methotrexate (**1.52**), which features lowered selectivity for bacterial DHFR over human DHFR.⁵³

A.



B.

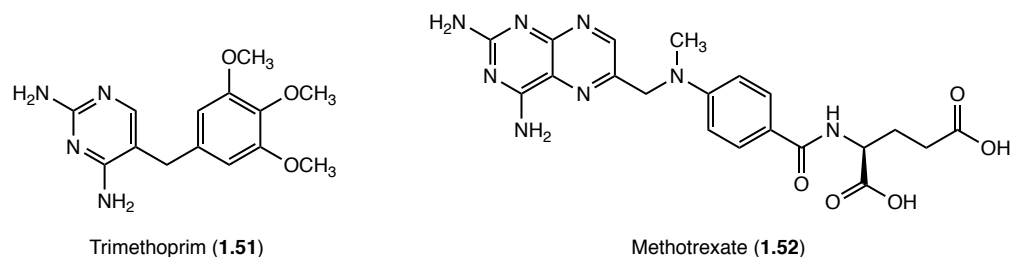


Figure 1.27. Folate synthesis-targeting antibiotics. **(A)** Structural comparison between *para*-aminobenzoic acid (pABA) and select sulfonamide antibiotics. **(B)** Structures of the diaminopyrimidine antibiotics trimethoprim (**1.51**) and methotrexate (**1.52**).

1.3 Mechanisms of Antibiotic Resistance

1.3.1 Introduction

Bacterial antibiotic resistance mechanisms can be divided into three general categories: prevention of antibiotic target engagement, modification of antibiotic structure, and modification or bypass of antibiotic target.^{9, 54} The first of these mechanistic classes results from decreased antibiotic penetration or active antibiotic efflux from the cell. Decreased antibiotic penetration, in particular, is an important resistance mechanism for Gram-negative pathogens due to their unique OM. For example, vancomycin is not active against Gram-negative bacteria due to its inability to traverse the OM to reach its cell wall target.⁵⁴ Examples of other general resistance mechanisms (not including decreased antibiotic penetration) for several common antibiotics are provided in **Table 1.2.**^{7, 19} Several of these specific examples will be discussed in more depth below.

In addition to the various methods bacteria use to resist antibiotic action, there are multiple ways bacteria can acquire resistance mechanisms. The first general strategy is through vertical transmission of a resistance mechanism from a resistant bacterium to its progeny.⁹ For example, resistance to quinolone antibiotics can be vertically transmitted as this resistance arises from point mutations in the genes encoding DNA gyrase and Topo IV. The second strategy involves transfer via mobile genetic elements, such as plasmids, that carry one or more resistance genes.^{9, 19} This type of transfer, known as horizontal gene transfer (HGT), is capable of transferring resistance mechanisms both vertically to bacterial progeny and horizontally to other bacteria. Importantly, HGT is not limited to intra-genera transfer. For example, the resistance mechanisms that have emerged in clinically relevant pathogenic species parallel the resistance mechanisms

found in environmental, antibiotic-producing bacteria and other non-pathogenic soil bacteria; the majority of soil bacteria have been found to be MDR as these species have had to adapt to life in an environment rich with potentially toxic small bioactive molecules.

Table 1.2. General bacterial resistance mechanisms against common classes of antibiotics

Antibiotic Class	Example	Antibiotic Target	Bacterial Resistance Mechanism
β -lactams	Penicillin	Penicillin-binding proteins (cell wall)	1. Modification of antibiotic structure 2. Modification/bypass of antibiotic target
Antimicrobial peptides	Polymyxin	Cell membrane	1. Modification/bypass of antibiotic target 2. Antibiotic efflux
Aminoglycosides	Gentamicin	30S ribosomal subunit (protein synthesis)	1. Modification of antibiotic structure 2. Modification/bypass of antibiotic target 3. Antibiotic efflux
Glycopeptides	Vancomycin	Terminal D-Ala-D-Ala of peptidoglycan and lipid II (cell wall)	1. Modification/bypass of antibiotic target
Macrolides	Erythromycin	50S ribosomal subunit (protein synthesis)	1. Modification/bypass of antibiotic target 2. Antibiotic efflux
Oxazolidinones	Linezolid	50S ribosomal subunit (protein synthesis)	1. Modification/bypass of antibiotic target 2. Antibiotic efflux
Quinolines	Ciprofloxacin	Topoisomerase II (DNA replication)	1. Modification of antibiotic structure 2. Modification/bypass of antibiotic target 3. Antibiotic efflux
Rifamycins	Rifampin	RNA polymerase (RNA synthesis)	1. Modification of antibiotic structure 2. Modification/bypass of antibiotic target 3. Antibiotic efflux
Sulfonamides	Prontosil	Dihydropteroate synthase (folate biosynthesis)	1. Modification/bypass of antibiotic target 2. Antibiotic efflux
Tetracyclines	Minocycline	50S ribosomal subunit (protein synthesis)	1. Modification/bypass of antibiotic target 2. Antibiotic efflux

1.3.2 Prevention of Antibiotic Target Engagement

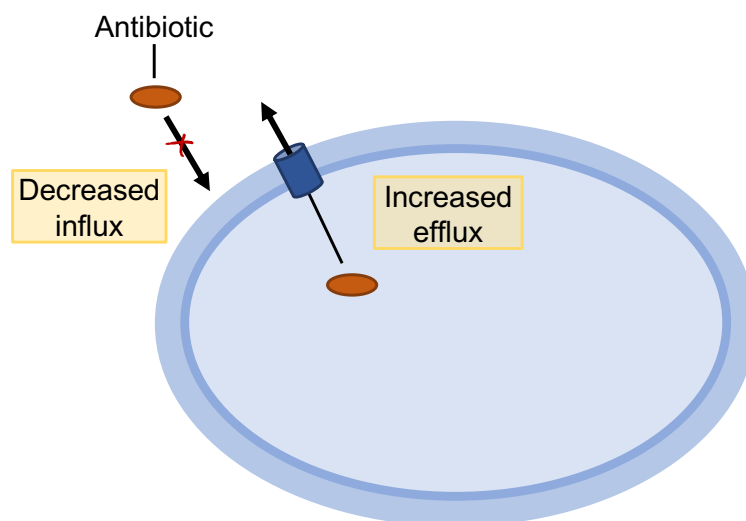


Figure 1.28. Prevention of antibiotic target engagement as a resistance mechanism.

Bacteria can prevent antibiotics from engaging their intended targets by decreasing antibiotic penetration into the intracellular environment, actively pumping antibiotics out of the intracellular environment using efflux pumps, or a combination of the two (**Figure 1.28**). As previously mentioned, the first of these mechanisms is characteristic of Gram-negative bacteria due to their unique OM. In fact, the only known function of this OM is to act as a protective barrier.¹⁷ Of the components of the OM, the LPS and porin protein channels play particularly critical roles in limiting the penetration of toxic compounds like intracellular-targeting antibiotics (see **Figure 1.13**).

The LPS is especially effective at limiting the influx of hydrophobic antibiotics such as the macrolides, rifamycins, and AMPs.^{17, 55} This protection is afforded by the tight packing of individual LPS strands. LPS strands can bind tightly due to the majority of their acyl chains being saturated. Additionally, avid binding of LPS strands to one another is improved in the presence of divalent cations like Mg^{2+} that can neutralize the negatively-

charged phosphate groups of the strands. In contrast to the LPS, porins serve to limit the influx of small, hydrophilic antibiotics. Porins, the most abundant OM proteins, are open, water-filled channels that facilitate the transfer of nutrients to the intracellular environment.^{55, 56} Important in terms of pathogenicity, porins limit the diffusion of small molecules to hydrophilic molecules smaller than approximately 700 Daltons.¹⁷ As small hydrophilic antibiotics such as the β -lactams, tetracyclines, and quinolones are not able to diffuse across the hydrophobic LPS, lipid bilayer OM, they rely on porins for passage into the cell.^{55, 56} Given the dependence of hydrophilic antibiotics on porin channels, resistant bacteria often downregulate porin expression or alter porin architecture to limit the influx of hydrophilic antibiotics. Indeed, these changes have been reported in a variety of species including *Enterobacter aerogenes*, *Escherichia coli*, *Klebsiella pneumoniae*, *Pseudomonas aeruginosa*, and *Neisseria gonorrhoeae*.⁵⁵

Efflux pumps are also a common method used by both Gram-positive and Gram-negative species to limit the ability of intracellular-targeting antibiotics to reach their desired targets in concentrations sufficient to inhibit the target's cellular function.^{19, 57-60} These pumps are membrane-associated, active transporter proteins that allow microbes to regulate their intracellular environment by expelling toxic substances such as antibiotics, heavy metals, detergents, antiseptics, metabolites, etc.^{59, 60} In this sense, efflux pumps are able to expel an antibiotic from the cell faster than the antibiotic is able to accumulate intracellularly to reach lethal concentrations.

Efflux as a mechanism of antibiotic resistance was first described in 1980 by McMurry et al. in *E. coli* as a means to protect against tetracycline.^{57, 60, 61} While it was originally hypothesized that this resistance mechanism was unique to tetracycline

antibiotics due to HGT from tetracycline-producing species, it has since been found that a single efflux pump can extrude a wide range of antibiotics. These types of efflux pumps have appropriately been termed MDR efflux pumps.^{57, 62} It is important to note, however, that there do exist efflux systems that are highly specific for a particular class of antibiotic. For example, the TetA efflux pump is highly selective for tetracycline antibiotics. Another important finding regarding efflux as a resistance mechanism was the discovery of a chromosomally-encoded efflux pump in *E. coli*, i.e. not obtained via HGT. This demonstrated that acquisition of antibiotic efflux pumps was not limited to HGT from antibiotic-producing microbes.^{57, 62} This notion was further supported by the finding that synthetic quinolone antibiotics are a favored substrate of bacterial MDR pumps.^{43, 60}

1.3.3 Modification of Antibiotic Structure

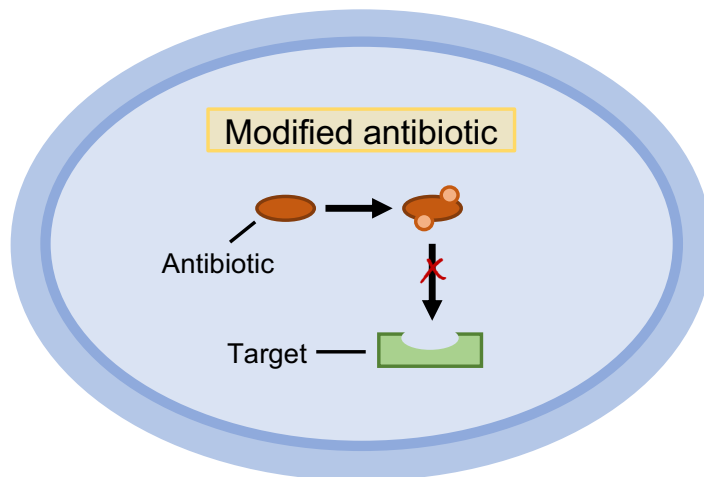


Figure 1.29. Modification of antibiotic structure as a resistance mechanism.

In contrast to the often broadly-applicable influx and efflux resistance mechanisms, enzymatic modification of an antibiotic is a highly specific resistance mechanism whose goal is to alter the structure of a drug enough to render it inactive (**Figure 1.29**). A

quintessential example of this type of resistance is the production of β -lactamases. These enzymes hydrolyze the β -lactam ring of penicillins and other β -lactams. As this ring is the antimicrobial warhead of β -lactam antibiotics, its hydrolysis renders these drugs inactive (**Figure 1.30**).

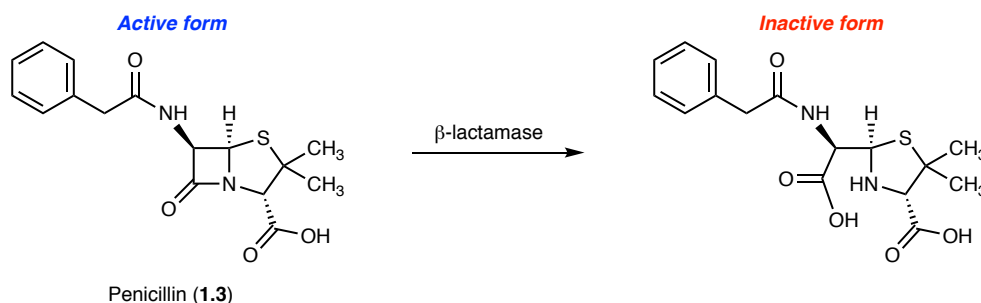


Figure 1.30. Mechanism of β -lactamase-mediated resistance to penicillin (1.3).

β -lactamases were first described by Abraham and Chain in 1940; Abraham and Chain identified an enzyme (penicillinase) in *E. coli* that was capable of destroying penicillin (1.3) and that was absent from penicillin-sensitive *S. aureus*.^{63, 64} In 1944, Kirby published similar reports detailing the presence of a penicillinase in penicillin-resistant strains of *S. aureus*.⁶⁵⁻⁶⁷ By the end of the 1940s, the majority of hospital isolates of *S. aureus* were resistant to penicillin.⁶⁶ From the hospital, penicillin-resistant *S. aureus* (PRSA) strains spread to the community, and by the 1950s and 1960s, community-associated PRSA strains had become pandemic.⁶⁸ Today, over 90% of staphylococcal isolates produce β -lactamase and are consequently resistant to penicillin.⁶⁹

Due to the increasing prevalence of β -lactamase-producing isolates, new β -lactam antibiotics were developed in an attempt to overcome this resistance. However, bacteria have proven to be highly adaptable to these changes. For example, only a few years after the discovery of ampicillin (1.6, **Figure 1.8**) in 1958, plasmid-encoded β -lactamases

capable of hydrolyzing ampicillin were identified in *E. coli* and *K. pneumoniae*.^{70, 71} A similar trend is seen with the extended-spectrum cephalosporins, such as cefotaxime (1.53, Figure 1.31).

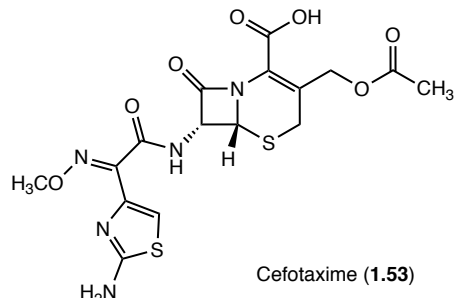
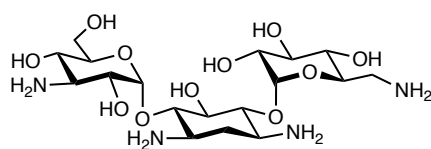


Figure 1.31. Structure of the extended-spectrum cephalosporin cefotaxime (1.53).

The extended-spectrum cephalosporins were developed to combat the increasing occurrence of ampicillin-hydrolyzing β -lactamases. However, shortly after these antibiotics gained widespread clinical application in the early 1980s, a β -lactamase capable of hydrolyzing extended-spectrum cephalosporins was identified in several strains of *K. pneumoniae*.^{71, 72} Shortly after this initial report, additional β -lactamases were discovered that conferred resistance to extended-spectrum cephalosporins. Today, over 150 extended-spectrum β -lactamases (ESBLs) have been described in species such as species of the Enterobacteriaceae family, *P. aeruginosa*, *E.coli*, and *K. pneumoniae*.^{66, 71} Notably, resistance to β -lactams in Gram-negative species is most commonly due to acquisition of β -lactamases while in Gram-positive species resistance is most commonly due to alternations in β -lactam cellular target (see section 1.3.4).^{66, 73}

Another well-known example of resistance facilitated by modification of antibiotic structure is the resistance conferred against AGs by the production of aminoglycoside modifying enzymes (AMEs). AME-mediated modification of AGs is the most common mechanism of AG resistance and is used by a wide range of Gram-positive and Gram-

negative species.^{36, 54, 74} Importantly, AMEs are highly mobile, i.e. the genes encoding these enzymes are found on a variety of transposable genetic elements. Concurrently, the majority of pathogenic bacteria acquire AME-mediated resistance via HGT.⁷⁴ Notably, the widespread dissemination of AMEs has rendered AGs like kanamycin (**1.54**, **Figure 1.32**) largely obsolete.³⁴



Kanamycin A (**1.54**)

Figure 1.32. Structure of the aminoglycoside antibiotic kanamycin A (**1.54**).

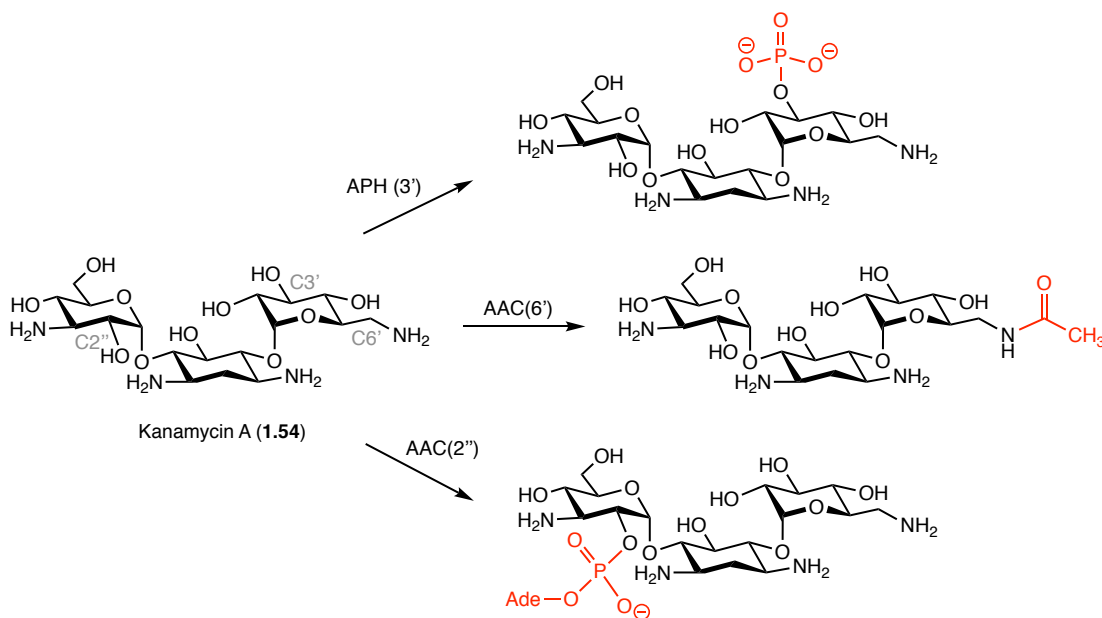


Figure 1.33. Mechanisms for structural modification of the aminoglycoside (AG) kanamycin A by select AG modifying enzymes (AMEs). Modification sites are denoted by the number in parentheses following the AME abbreviation. AG *N*-acetyltransferases (AACs) acetylate AG amines; AAC(6') acetylates the amine at C6'. AG *O*-nucleotidyltransferases/adenylyltransferases (ANTs) adenylylates AG alcohols; ANT(3') adenylylates the alcohol at C3'. AG *O*-phosphotransferases (APHs) phosphorylate AG alcohols; APH(2'') phosphorylates the alcohol at C2''. Abbreviations: Ade, adenosine.

AMEs are a large family of enzymes consisting of the following subclasses: AG *N*-acetyltransferases (AACs), which catalyze acylation of AG amino functionalities; AG *O*-nucleotidyltransferases or -adenylyltransferases (ANTs), which catalyze adenylylation of AG hydroxyl functionalities; and AG *O*-phosphotransferases (APHs), which catalyze phosphorylation of AG hydroxyl functionalities (**Figure 1.33**).^{36, 74, 75} These structural modifications introduce unfavorable steric and/or electronic interactions between the drug and its ribosomal binding site which greatly reduces AG affinity for its target.

The prevalence and effectiveness of AMEs has prompted significant efforts to modify AG structure in an attempt to protect against the action of AMEs. For example, amikacin (**1.29**) is kanamycin-derived AG that is more resistant to the action of several AMEs than its parent kanamycin (**1.54**) (**Figure 1.34**).⁷⁴ This increased resistance is attributable to the introduction of a (*S*)-2-hydroxyaminobiutyric acid (HABA) sidechain, which likely sterically shields the AG core structure from modification by certain AMEs.

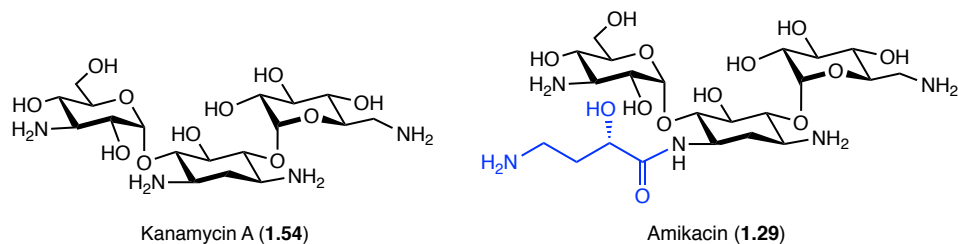


Figure 1.34. Structures of kanamycin A (**1.54**) and kanamycin A-derived amikacin (**1.29**). The (*S*)-2-hydroxyaminobiutyric acid (HABA) sidechain of amikacin is highlighted in blue. The kanamycin A core is shown in black.

Several additional classes of antibiotics such as the macrolides, rifamycins, and tetracyclines are subject to similar enzyme-mediated structural modifications that render the antibiotics inactive (**Table 1.3**).⁷⁶ These mechanisms are reviewed elsewhere.^{34, 76, 77}

Table 1.3. Enzymatic Strategies for Antibiotic Structural Modification and Inactivation

General Modification Strategy	Specific Type of Modification	Antibiotic Classes Affected
Hydrolysis	N/A	β -lactam Macrolide
Group Transfer	Acetylation	Aminoglycoside Fluoroquinolone
	Phosphorylation	Aminoglycoside Macrolide Rifamycin Peptide
	Thiolation	Fosfomycin
	Nucleotidylation	Aminoglycoside Lincosamide
	Glycosylation	Macrolide Rifamycin
Other	Redox	Tetracycline Rifamycin

1.3.4 Modification of Antibiotic Target

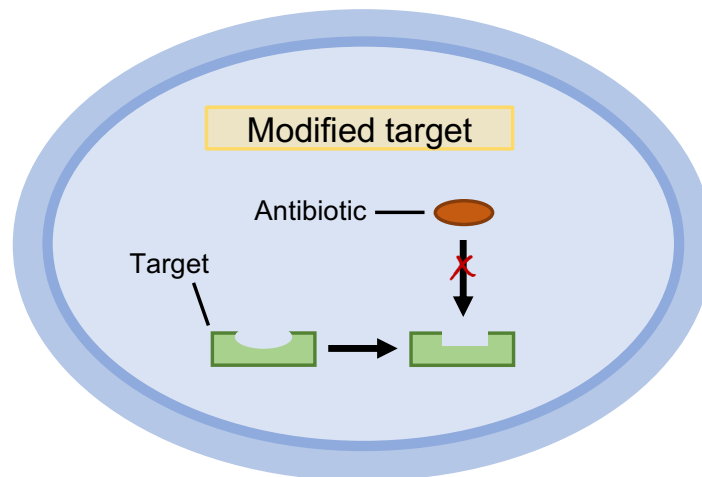


Figure 1.35. Modification of antibiotic cellular target as a resistance mechanism.

In addition to limiting intracellular concentrations of active antibiotics, bacteria also avoid the action of antibiotics by altering antibiotic cellular targets (**Figure 1.35**). This

highly specific strategy can take the form of structural modification(s) to the target itself that reduce(s) antibiotic affinity or protection of the target from engagement by an antibiotic. Notably, target site modification is one of the most common mechanisms used by bacteria to evade the action of antibiotics.⁵⁴ Common modifications include point mutations in genes that encode the antibiotic target site, enzymatic alteration of the target site, and replacement/bypass of the original target. Despite the variety of modification strategies, each strategy ultimately serves to decrease the affinity of an antibiotic for its intended cellular target.

A well-known example of mutation-mediated resistance is the development of rifamycin resistance. As previously described in section 1.2.5, rifamycins inhibit the initiation phase of transcription by binding DNA-bound, actively-transcribing RNAP with high affinity close to the RNAP active site.⁴⁴ More specifically, rifamycins bind in a highly conserved pocket located within the β subunit of RNAP (encoded by *rpoB*); the core RNAP enzyme has a subunit composition of $\beta\beta'\alpha_2\omega$ (**Figure 1.36**).^{46, 78} It has been shown that high-level rifamycin resistance can result from single amino acid substitutions in *rpoB*.^{46, 54} Amino acid deletions and insertions have also been reported. Importantly, although these modifications successfully reduce the affinity of rifamycins for RNAP, they spare RNAP activity and thus allow transcription to proceed.⁵⁴

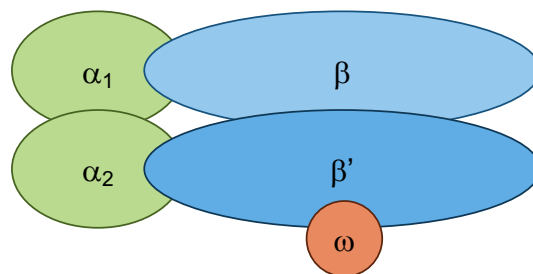


Figure 1.36. Bacterial RNA polymerase (RNAP) core enzyme subunit composition.

A similar form of resistance is observed against the quinolone class of antibiotic.⁴³
⁵⁴ As described in section 1.2.5, quinolones bind non-covalently to Topo II enzymes (DNA gyrase and Topo IV) at the DNA cleavage/ligation site. This binding stabilizes the Topo II-DNA cleavage complex, which leads to the formation of permanent double-stranded DNA breaks that can ultimately lead to cell death. Bacterial resistance to quinolones is most commonly associated with point mutations in DNA gyrase and/or Topo IV.⁴³ While multiple mutations have been identified, the most commonly mutated amino acid residue is the serine that interacts with the water-metal ion bridge that facilitates quinolone binding to Topo II enzymes (**Figure 1.37**). Although the acidic residues that interact with this bridge are also commonly mutated, mutations to these residues do result in a reduction of Topo II catalytic activity while mutations to the serine residue do not.

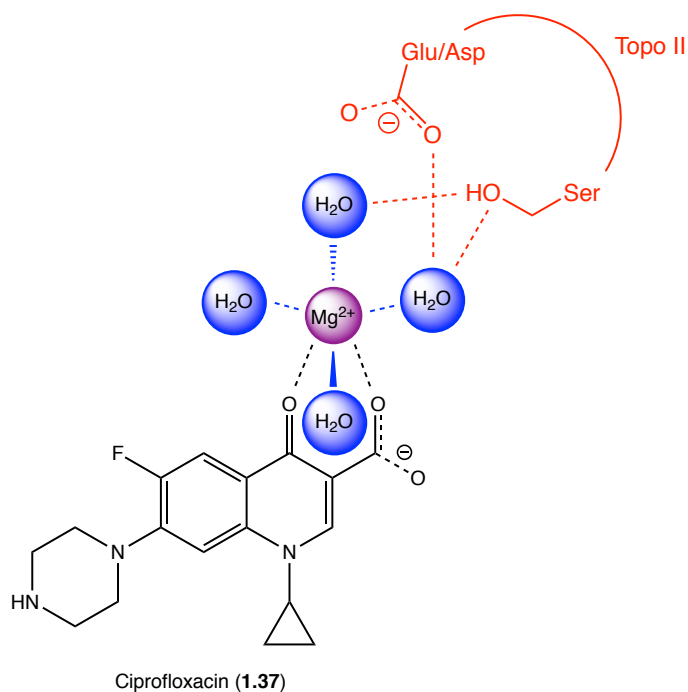


Figure 1.37. Schematic depiction of the water-ion bridge that facilitates quinolone (ex. ciprofloxacin (**1.37**)) binding to topoisomerase II (Topo II). Ciprofloxacin and its interactions with the Mg²⁺ ion (shown in purple) are shown in black. The participating serine and acidic amino acid residues of Topo II are and their interactions with the water molecules are shown in red. The water molecules and their interactions with the Mg²⁺ ion are shown in blue.

Methylation of antibiotic-binding site residue(s) is one of the most common enzyme-mediated target site modifications.⁵⁴ This form of resistance is particularly relevant for ribosome-targeting antibiotics. Indeed, various methylations of ribosomal RNA (rRNA) by rRNA methyltransferases (RMTs) can confer resistance against antibiotic classes including aminoglycosides, lincosamides, macrolides, and oxazolidinones.^{54, 79, 80}

A particularly well-characterized example is the antibiotic resistance that arises from mono- or dimethylation of an adenine residue in the 23rRNA of the 50S ribosomal subunit. Due to overlapping binding sites, this methylation confers resistance to macrolides, lincosamides, and streptogramin B (MLS_B) antibiotics. It is thought that methylation results in a ribosomal conformational shift that reduces antibiotic binding affinity.^{34, 79} Methylation of the adenine residue is catalyzed by enzymes encoded by the *erm* (erythromycin ribosomal methylation) genes.⁵⁴ To date, over 30 *erm* genes have been identified. Moreover, likely due to the fact that many of these genes are located on mobile genetic elements, *erm* genes have been found in over 30 different bacterial genera including *Escherichia*, *Mycobacterium*, *Staphylococcus*, *Streptomyces*, and *Streptococcus*.^{54, 79, 80} It is important to note, however, that there is a fitness cost associated with Erm-mediated resistance as the methylation associated with this resistance results in less efficient translation compared to wild-type ribosomes.^{34, 54} Thus, most *erm* genes are not constitutently expressed. Instead, their expression is induced when an antibiotic is present. Notably, erythromycin is typically the best inducer of *erm* expression.

In contrast to the fitness cost of Erm-mediated resistance, Cfr-mediated resistance has a low fitness cost.³⁴ Cfr monomethylates a different adenine residue of the 23rRNA;

erm genes methylate an adenine within the exit tunnel while *cfr* genes methylate an adenine in the PTC. Cfr-mediated methylation confers resistance against the oxazolidinone antibiotic linezolid as well as lincosamides and some macrolides. The *cfr* gene was first identified in *Staphylococcal* species and has since been found in *Enterococcus* species and some Gram-negative species.^{54, 81}

Another class of RMTs that are gaining clinical significance are those that facilitate resistance towards AGs by methylating residues in the 30S ribosomal subunit.^{36, 74, 82} These include ArmA and RmtA-D that methylate a guanine residue and NmpA that methylates an adenine residue. Each methylation serves to disfavor AG binding by introducing unfavorable steric and electronic interactions between the AG and its ribosome binding target. While originally an autoprotective mechanism in aminoglycoside-producing actinomycetes, this modification strategy has been identified in several pathogenic bacterial species such as *P. aeruginosa*, *K. pneumoniae*, and *A. baumannii*.⁸²⁻⁸⁵

The final strategy used by bacteria to directly modify antibiotic targets involves replacement or bypass of the original target. One of the most well-known and clinically-relevant examples of this strategy is the development of methicillin resistance in *S. aureus*.^{43, 68} In an attempt to combat penicillin resistance due to the production of β -lactamases, methicillin (**1.7**, see **Figure 1.8**) was introduced.^{64, 66, 68} Methicillin features a larger aryl moiety near the β -lactam ring which reduces the drug's affinity for *Staphylococcal* β -lactamases. However, shortly after methicillin's introduction, resistance to this β -lactam emerged. Contrary to penicillin resistance, the resistance to methicillin was not a result of drug inactivation, but rather a result of drug target bypass. Methicillin-

resistant *S. aureus* (MRSA) strains expressed an additional PBP known as PBP2a; PBP2a is encoded by the *mecA* gene that is hypothesized to have originated in *Staphylococcus sciuri*.^{54, 69} PBP2a is a PBP that has low affinity for all β -lactams and consequently renders most β -lactams ineffective against MRSA infections.

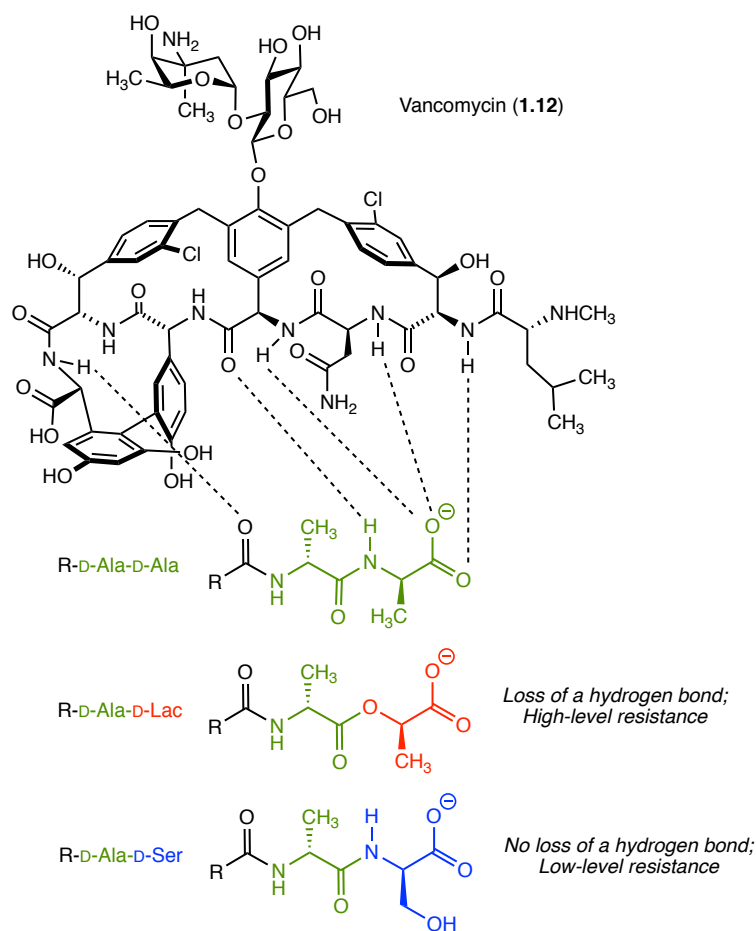


Figure 1.38. Alterations to terminal D-Ala-D-Ala dipeptide of peptidoglycan (PG) strands that confer resistance to vancomycin (1.12).

Another important example of target replacement/bypass is the development of vancomycin resistance. While vancomycin-resistant *S. aureus* (VRSA) strains have emerged, vancomycin resistance is particularly relevant in *Enterococcus* species such as *E. faecium* (VRE: vancomycin-resistant Enterococci).^{19, 54} Vancomycin resistance results from acquisition of genes that are responsible for remodeling PG synthesis. Specifically,

the *van* gene clusters encode a new pathway of enzymes that change the terminal D-Ala to D-Lactate (Lac) (high-level resistance) or D-Ser (low-level resistance) and destroys the original D-Ala-D-Ala ending precursors (prevents vancomycin binding to cell wall precursors). Exchange of the D-Ala for D-Lac removes a hydrogen bonding interaction between vancomycin and the terminal dipeptide of a PG strand (**Figure 1.38**). While exchange of D-Ala for D-Ser does not remove a hydrogen bonding interaction, the presence of the serine hydroxyl group nevertheless reduces the affinity of vancomycin for its target, albeit to a lesser extent that caused by replacement with D-Lac (**Figure 1.38**).

In addition to target modification that reduces antibiotic affinity, bacteria can also prevent antibiotics from engaging their desired targets via factor-associated protection of antibiotic cellular targets.^{9, 34, 54} For example, expression of the Tet(M) and Tet(O) proteins confers resistance to tetracycline antibiotics. Tet(M) and Tet(O) bind the ribosome and subsequently dislodge tetracyclines from their binding site. This action is facilitated by the structural homology of Tet(M) and Tet(O) to the elongation factors (EF-G and EF-Tu) used in protein synthesis. Moreover, the binding of these proteins to the ribosome results in a ribosomal conformational shift that prevents rebinding of the antibiotic.⁵⁴ Tet(M) and Tet(O), also termed ribosomal protection proteins (RPPs), were first identified in *C. jejuni* and *Streptococcal* species but are now widely distributed among numerous bacterial species.^{54, 86}

Target protection is also used to hinder the action of quinolone antibiotics.^{43, 54} This form of resistance involves the expression of Qnr (quinolone resistance protein). Qnr acts as a DNA mimic that competes for DNA binding to the Topo II enzymes, DNA gyrase and Topo IV. It is hypothesized that this competition decreases the interaction of DNA with

DNA-gyrase which in turn decreases the opportunity for quinolone antibiotics to form and stabilize lethal gyrase-cleaved DNA-quinolone complexes.

1.4 The ESKAPE Pathogens

The growing number of antimicrobial-resistant pathogens continues to challenge our ability to combat infectious diseases. As mentioned in section 1.1, although antimicrobial resistance (AMR) is a natural phenomenon, the modern age has seen an increase in the prevalence and diversity of resistant organisms.^{4, 10} Moreover, we have also seen the emergence of MDR pathogens; MDR is defined as resistance to two or more antimicrobials of different antimicrobial classes.⁸⁷ MDR pathogens pose one of the most significant threats to human health both in the hospital and the community. Indeed, several MDR pathogens are effectively untreatable with our current arsenal of antibiotics.⁴ A critically important class of MDR pathogens are the ESKAPE pathogens.

The ESKAPE pathogens (briefly introduced in section 1.1) are a cohort of microorganisms aptly named for their ability to “escape” the action of antibiotics.^{13, 14, 88,}
⁸⁹ This cohort consists of the following Gram-positive and Gram-negative species: *Enterococcus faecium*, *Staphylococcus aureus*, *Klebsiella pneumoniae*, *Acinetobacter baumannii*, *Pseudomonas aeruginosa*, and *Enterobacter* species (**Table 1.4**). Importantly, these pathogens are responsible for the majority of nosocomial infections and are common causes of life-threatening illnesses among immunocompromised or critically-ill patients.^{14, 89} While these pathogens are characterized by their MDR, exceptionally critical antibiotic resistances for each of the ESKAPE pathogens are noted in **Table 1.4**.

Table 1.4. The ESKAPE Pathogens

Pathogen	Gram Classification	Notable Resistance
<i>Enterococcus faecium</i>	Gram-positive	Vancomycin
<i>Staphylococcus aureus</i>	Gram-positive	Methicillin
<i>Klebsiella pneumoniae</i>	Gram-negative	Carbapenem
<i>Acinetobacter baumannii</i>	Gram-negative	MDR; Carbapenem
<i>Pseudomonas aeruginosa</i>	Gram-negative	MDR; Quinolone
<i>Enterobacter</i> species	Gram-negative	Carbapenem

E. faecium is a Gram-positive, facultative anaerobe frequently associated with hospital-acquired infections (HAI). *E. faecium* infections are particularly common among immunocompromised patients and include bloodstream, surgical site, and urinary tract infections.^{13, 89, 90} Enterococci species, like *E. faecium*, are also commonly associated with infections of indwelling medical devices due to their ability to colonize both skin and abiotic surfaces.¹³ In terms of resistance, there is an high prevalence of *E. faecium* resistance towards β -lactams. While this resistance is problematic, the increasing prevalence of vancomycin-resistant *E. faecium* (VRE) (first identified in the late 1980s) is particularly alarming as vancomycin is often an antibiotic of last resort; vancomycin resistance in *E. faecium* is conferred by expression of *van* gene clusters as described in section 1.3.4.^{13, 90}

S. aureus is a Gram-positive coccal bacterium that commonly colonizes the skin and moist areas like the mucous membranes of the nose.^{13, 89, 90} Indeed, approximately 60% of individuals are intermittent carriers of *S. aureus* (harbor the bacterium at irregular

intervals), while approximately 20% of people are persistent carriers (almost always colonized with *S. aureus*). *S. aureus* is the leading cause of skin and soft tissue infections and can also cause severe infections such as sepsis, pneumonia, bone and joint infections, and infective endocarditis. An especially important feature of *S. aureus* in terms of pathogenicity is its propensity for biofilm production.¹³ Biofilm will be discussed in more depth in Chapter 3, but briefly, biofilms are organized communities of cells surrounded by an extracellular matrix that serves as an extra source of protection against antimicrobial action.⁹¹⁻⁹³ Notably, *S. aureus* biofilms are the most common cause of device related infections (DRIs).

The majority of clinically- and community-acquired *S. aureus* isolates are resistant to penicillin due to the production of β -lactamases.^{13, 89} As described in section 1.3.4, attempts to overcome *S. aureus* penicillin resistance through the use of methicillin, which is resistant to the action of β -lactamases, has been met with the emergence of methicillin-resistant *S. aureus* (MRSA). Today, MRSA is a common hospital and community-acquired infection. For these infections, vancomycin, is generally the antibiotic of choice.¹³ However, the increased use of vancomycin to treat these infections has led to the emergence of vancomycin-intermediate and vancomycin-resistant *S. aureus* (VISA and VRSA). Importantly, vancomycin resistance in *S. aureus* has been traced to the interspecies transfer of vancomycin resistance determinants in VRE (i.e. *van* resistance genes).

Klebsiella pneumoniae is a Gram-negative, encapsulated bacillus that is a prominent member of the Enterobacteriaceae family.^{13, 94} *K. pneumoniae* is an intrinsically virulent species from the environment (e.g. soil and water surfaces) that readily colonizes

human mucosal surfaces, such as the gastrointestinal tract (GI) and oropharynx, and medical devices. From these initial colonization sites, *K. pneumoniae* gains access to other tissues and can cause a wide range of infections such as pneumonia, urinary tract infections (UTIs), bloodstream infections (BSIs), and meningitis. Notably, *K. pneumoniae* infections are prevalent in both hospital and community settings.

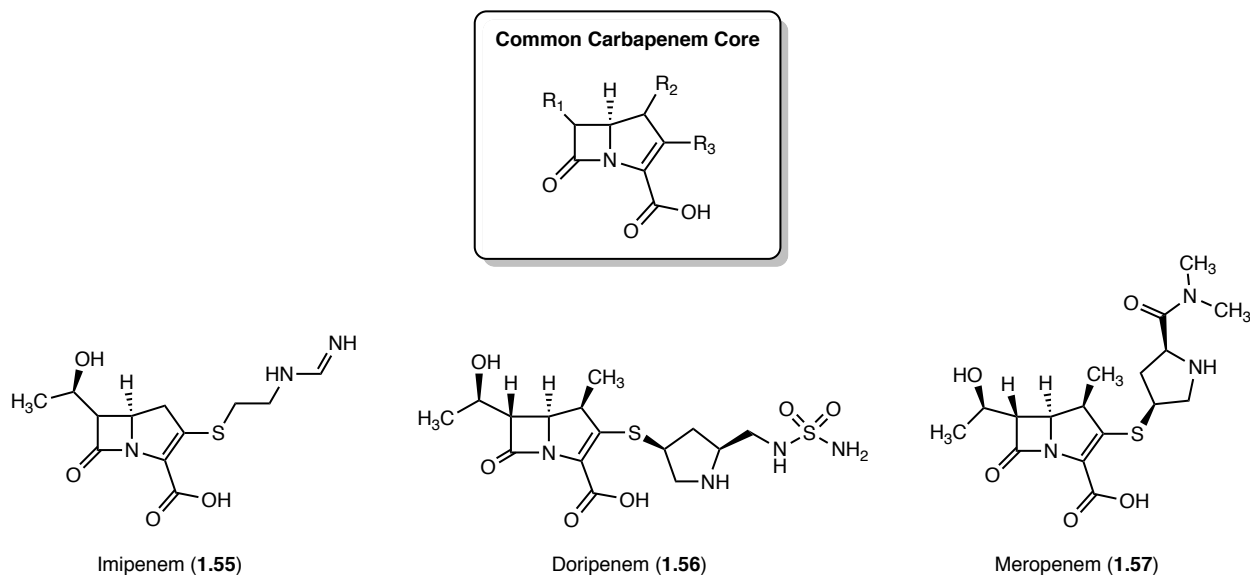


Table 1.39. Structure of the common carbapenem core and the carbapenem antibiotics imipenem (1.55), doripenem (1.56), and meropenem (1.57).

Another defining feature of this bacterial species is its notorious ability to rapidly accumulate and disseminate MDR determinates.^{13, 95} Indeed, recent times have seen *K. pneumoniae* strains acquire an extensive variety of β -lactamases capable of conferring resistance not only to penicillins and cephalosporins but also carbapenems (**Figures 1.39** and **1.8**). Moreover, *K. pneumoniae* is the pathogen most often associated with dissemination of ESBLs.⁹⁵ Because carbapenems are typically reserved for the treatment of difficult, persistent Gram-negative infections, the increasing occurrence of carbapenem-resistant *K. pneumoniae* (CRKP) poses a significant challenge.^{13, 89} To

compound this problem, a *K. pneumoniae* “super enzyme,” metallo- β -lactamase-1 (NDM-1), has emerged and has led to an increased number of CRKP isolates. Moreover, this enzyme is hypothesized to be a possible threat to the effectiveness of other antibiotic classes such as the AGs and quinolones.

Acinetobacter baumannii is a Gram-negative, opportunistic pathogen that has become a major source of nosocomial infections worldwide.^{13, 89, 96} While other *Acinetobacter* species are widely distributed in the environment (soil, water, and animals) *A. baumannii* is found almost exclusively in the hospital, especially in intensive care units (ICUs) and surgical wards.^{13, 97} Indeed, *A. baumannii* infection is most commonly associated with immunocompromised individuals or those who have undergone major surgery. *A. baumannii* can cause a variety of infections including skin, soft tissue, wound, and urinary tract infections. More severely and life-threateningly, *A. baumannii* can also cause ventilator-associated pneumonia and BSIs.⁹⁷ More recently, *A. baumannii* gained notoriety for its increased association with military personnel in combat regions.^{96, 97} The increasing prevalence of this species in the conflict in Iraq even garnered it colloquial names like “Iraqibacter” and “Iraqi-baumannii.”

A characteristic and notorious feature of *A. baumannii* is its ability to survive for long periods on human hands and hospital equipment.^{13, 96} This long lifetime is hypothesized to contribute to high-rates of cross-contamination in nosocomial infections. Another well-known feature of *A. baumannii* is its high level of MDR. In addition to being inherently resistant to numerous antibiotics due to the Gram-negative OM, *A. baumannii* expresses fewer and smaller OM porins compared to other Gram-negative species, which further decreases antibiotic penetration.^{13, 98} Moreover, *A. baumannii* is capable of

widening the periplasmic space in its cell wall in response to environmental conditions. An increasingly common resistance mechanism of *A. baumannii* is the production of β -lactamases. Perhaps most notably, *A. baumannii* has acquired numerous carbapenemases, such as imipenem metallo- β -lactamases and oxacillinase (OXA) serine β -lactamases, that confer widespread resistance to penicillins, cephalosporins, and carbapenems. Finally, *A. baumannii* has also been found to mutate DNA gyrase and Topo IV to reduce quinoline binding and to use efflux pumps to protect against the action of tetracyclines.^{99, 100}

Pseudomonas aeruginosa is a Gram-negative, facultative anaerobe that preferentially colonizes immunocompromised individuals (i.e. an opportunistic pathogen) in nosocomial settings.^{13, 101} Indicative of this preference, *P. aeruginosa* is the main pathogen associated with respiratory tract infections in cystic fibrosis (CF) patients and is also commonly associated with cancer patients and burn victims. Furthermore, due to its ability to metabolize a wide range of organic molecules, *P. aeruginosa* is able to survive in extreme environmental conditions.¹³

Similar to other Gram-negative pathogens, *P. aeruginosa* is inherently resistant to a range of antimicrobials due to its OM.^{13, 89} Moreover, most substances pass through the *P. aeruginosa* OM porin protein OprF which limits molecules to 500 Da or less. Antibiotic permeability can be further reduced in *P. aeruginosa* through decreased expression of another OM porin, OprD. This porin channel is the main route used by carbapenems to enter the cell. Thus, loss of this transmembrane channel confers resistance to several carbapenems. Resistance to carbapenems is also afforded by the production of broad-spectrum ESBLs and carbapenemases. Importantly, *P. aeruginosa* can simultaneously

up-regulate expression of the single efflux pump system MexAB-OprM which can increase resistance to a wide range of antibiotics including β -lactams, cephalosporins, fluoroquinolones, macrolides, tetracyclines, and sulfonamides.¹³ Finally, *P. aeruginosa* is also characterized by a resistance to quinolone antibiotics due to target mutations in DNA gyrase and/or Topo IV.

Enterobacter species are also Gram-negative opportunistic pathogens that are notorious for causing infections in immunocompromised individuals, particularly in hospital settings.^{13, 89} These species most commonly cause urinary and respiratory tract infections but have also been shown to cause BSIs. *Enterobacter* species are notable for their broad MDR mediated by numerous plasmid-encoded ESBLs and carbapenemases. Generally, only colistin and tigecycline are effective against *Enterobacter* species.

1.5 Alternative Approaches to Current Antibiotic Monotherapy

The increasing prevalence of MDR pathogens like the ESKAPE pathogens demonstrates the need for new treatment methods. While developing new antibiotics with novel structures and modes of actions is an obvious approach, in the last few decades, this approach has been largely unfruitful. Moreover, any new antibiotics that target essential cellular function(s) will ultimately be plagued by the development of resistance. With this in mind, several alternative approaches have been developed with the objective not only to combat infectious diseases but also to limit antibiotic resistance development. Examples of these alternative approaches include the use of multi-drug combination therapies, antibiotic and antibiotic adjuvant combinations, antibiotics that target virulence

factors, and antibiotics with narrow spectrums of activity. These approaches will be discussed briefly for the remainder of the chapter.

1.5.1 Multi-Antibiotic Combination Therapies

Treatments that rely on the use of two or more antibiotics are becoming increasingly common for the treatment of both bacterial and non-bacterial-associated diseased states.¹⁰²⁻¹⁰⁴ For example, drug combinations are standard for most cancer treatments and are routinely used in anti-HIV treatments. In terms of bacterial infections, a well-known example of multi-drug therapy is in the treatment of *Mycobacterium tuberculosis* infections.^{103, 105, 106} These treatments typically use a combination of at least four drugs (usually isoniazid (**1.58**), rifampicin (**1.41**), ethambutol (**1.59**), and pyrazinamide (**1.60**); **Figure 1.40**) and are often used to treat MDR and even extensively drug-resistant (XDR) *M. tuberculosis* infections. Treatments of MDR Gram-negative bacterial infections also commonly use a multi-drug approach. These treatments typically use colistin (**1.25**, **Figure 1.15**), an AMP that targets the Gram-negative OM and increases membrane permeability, and another non-OM targeting antibiotic.¹⁰³

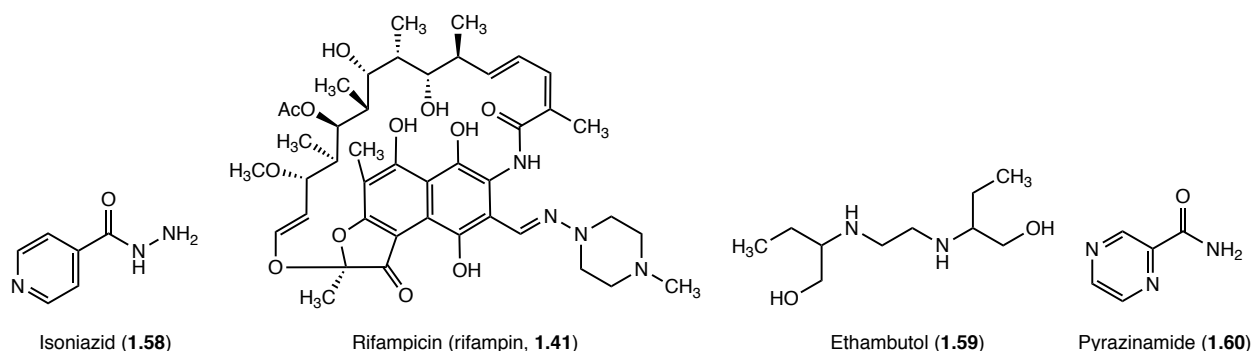


Figure 1.40. Structures of antibiotics typically used in multi-drug therapy for *Mycobacterium tuberculosis* infections.

The aforementioned combination therapies for bacterial infections are examples of multi-drug therapies that use antibiotics which target different pathways or different cellular targets. Another well-known example of this strategy is the combination of β -lactams, like penicillin and ampicillin (see **Figure 1.8**), and AGs, like gentamicin (see **Figure 1.7**).^{8, 107, 108} β -lactams target the cell wall and increase cell permeability which subsequently facilitates increased cellular uptake of AGs compared to treatment with AGs alone. This combination treatment has been used in the treatment of *Enterococci*-associated infections and is a common treatment for early-onset Group B *Streptococcus* disease in infants.¹⁰⁸⁻¹¹⁰

In addition to combination therapies that use antibiotics which target different pathways or cellular targets, combination therapies can also rely on combinations of antibiotics that inhibit different targets in the same pathway or the same target in different ways. A commonly used example of these first of these strategies is the combination of sulfamethoxazole (**1.61**) and trimethoprim (**1.51**) (**Figure 1.41**); this combination is marketed as co-trimoxazole.^{50, 52, 103} Sulfamethoxazole and trimethoprim both target folate synthesis (see section 1.2.6), but sulfamethoxazole inhibits dihydropteroate synthase (DHPS) while trimethoprim inhibits dihydrofolate reductase (DHFR) (see **Figure 1.26**). This antibiotic combination has been used to treat MRSA and *E. coli*-associated UTIs.⁵²

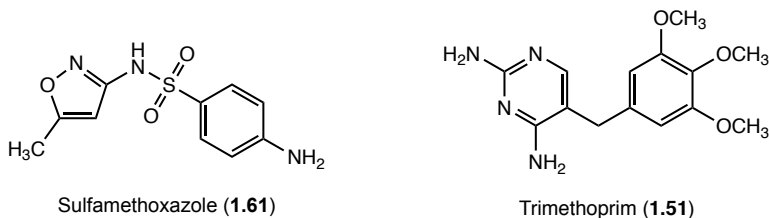


Figure 1.41. Structures of folate synthesis-targeting antibiotics typically used in combination therapies.

Combinations of streptogramins are prime examples of treatments using antibiotics that inhibit the same target but in different ways.¹⁰³ Streptogramins are depsipeptides that can be divided into two distinct categories: smaller type A streptogramins that block translation by binding the ribosomal P-site and the larger type B streptogramins that bind the 50S ribosome and block the peptide exit tunnel.¹¹¹⁻¹¹³ Importantly, binding by a type A streptogramin induces a ribosomal conformational shift that facilitates binding of a type B streptogramin.¹¹² Also importantly, when used alone, type A and B streptogramins exert only bacteriostatic effects as opposed to the bactericidal effect that results when these types are used in combination.^{111, 113} Synercid, a combination of dalfopristin (**1.62**, type A streptogramin) and quinupristin (**1.63**, type B streptogramin), has been used to treat MRSA and VRE (**Figure 1.42**).^{112, 113}

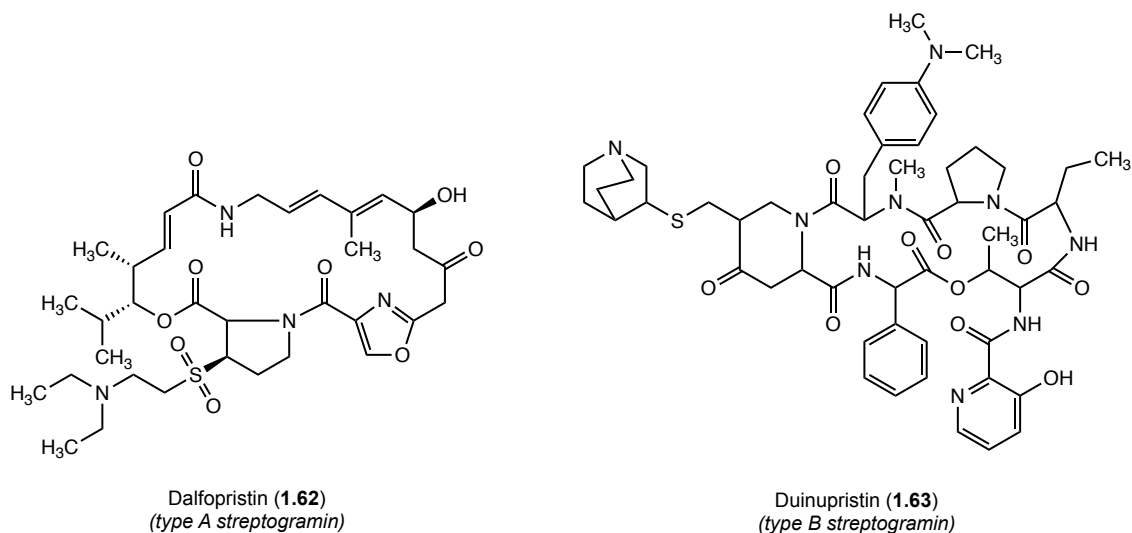


Figure 1.42. Structures of ribosome-targeting streptogramins used together in combination therapies.

1.5.2 Antibiotic and Antibiotic Adjuvant Combination Therapies

A common alternative to using a combination of two antibiotics is to use the combination of an antibiotic and an antibiotic adjuvant.^{103, 110, 114} An antibiotic adjuvant is

a compound that does not possess antimicrobial activity itself but rather potentiates the activity of an antibiotic. Notably, because adjuvants lack antimicrobial activity, it has been hypothesized that this antibiotic/adjuvant approach may decrease the development of antibiotic resistance.¹¹⁴ Adjuvants commonly potentiate antibiotic action by inhibiting a resistance mechanism against the antibiotic. These types of adjuvants are classified as class I adjuvants (**Figure 1.43**).¹¹⁰ Class I adjuvants can be further divided into class IA adjuvants that directly inhibit resistance mechanisms (ex. inactivating enzymes) and class IB adjuvants that indirectly inhibit resistance mechanisms by circumventing intrinsic resistance mechanisms (ex. perturbing proton motive force). In contrast to class I adjuvants, class II adjuvants do not directly impact bacteria but rather enhance host defense mechanisms (**Figure 1.43**).

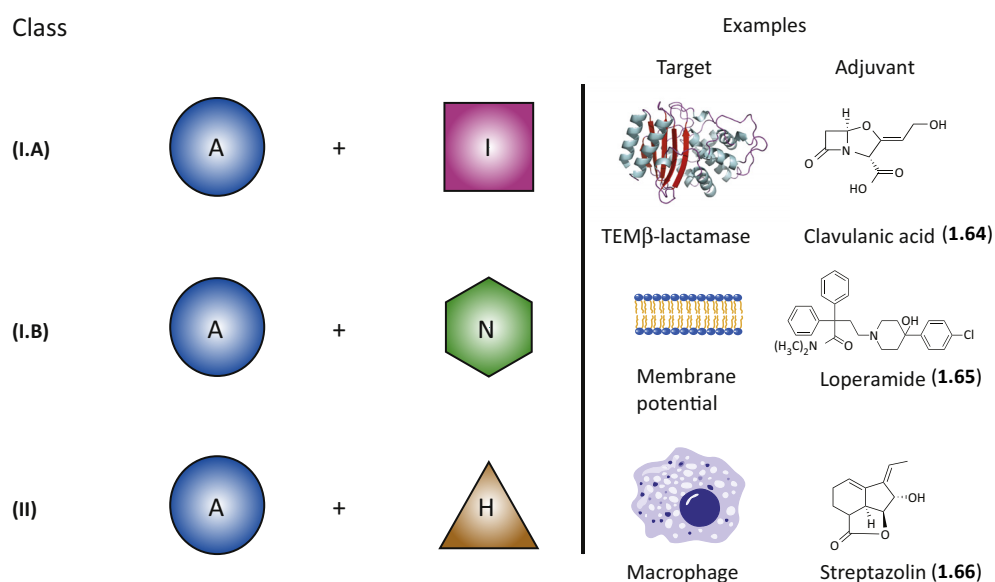


Figure 1.43. Classification of antibiotic adjuvants and corresponding examples from each adjuvant class (figure adapted from reference 110). Class I adjuvants potentiate antibiotic action by directly inhibiting active (class IA) or passive/intrinsic (class IB) resistance mechanisms, while class II potentiate antibiotic action by enhancing host defense mechanisms. Abbreviations: A, antibiotic; I, inhibitor; N, non-antibiotic; H, host defense mechanism.

The most well-known and clinically successful examples of antibiotic adjuvants are those that inhibit β -lactamase action (class IA adjuvants).^{103, 110, 114} A classic example is the combination drug Augmentin. Augmentin consists of the β -lactam antibiotic amoxicillin (**1.67**) and the β -lactamase inhibitor clavulanic acid (**1.64**) (**Figure 1.44**). While clavulanic acid alone has poor antimicrobial activity, it does exhibit potent and irreversible inactivation of β -lactamases. Thus, when used in combination with amoxicillin, clavulanic acid allows amoxicillin to escape the action of β -lactamases and inhibit cell wall biosynthesis. Despite the success of Augmentin, many β -lactamases, such as the carbapenem hydrolyzing oxacillinases (CHDLs) and the metallo- β -lactamases (MBLs) are not inhibited by clavulanic acid. To address the limitations of clavulanic acid, several other β -lactamase inhibitors have been developed. These compounds are reviewed elsewhere.^{103, 110}

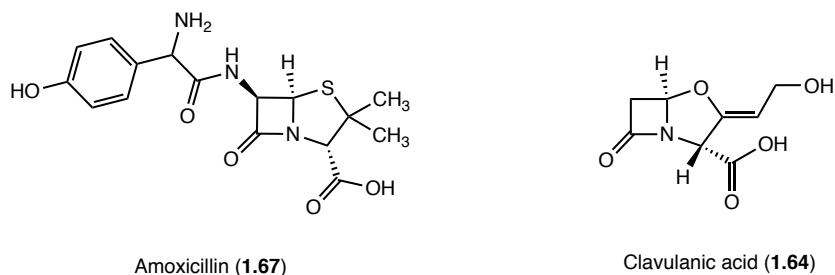


Figure 1.44. Structures of the components of Augmentin, amoxicillin (**1.67**) and clavulanic acid (**1.64**).

Compounds that inhibit efflux pumps (class IB adjuvants) have also been investigated as antibiotic adjuvants.^{103, 110} For example, Phe-Arg- β -naphthylamine (PA β N) was identified as an efflux pump inhibitor against a variety of species, including *P. aeruginosa*, and is able to enhance the activity of several antibiotics from a variety of antibiotic classes. As shown in **Figure 1.43**, loperamide (**1.65**) is another example of a class IB adjuvant. Loperamide operates by decreasing the electrical component of the

proton motive force in Gram-negative bacteria which ultimately results in increased uptake of tetracyclines.¹¹⁰

For the last class of adjuvant (class II), immunomodulatory peptides (ex. LL-37) that enhance that antimicrobial activity of the innate immune system represent attractive potential adjuvants.¹¹⁰ As illustrated in **Figure 1.43**, streptazolin (**1.66**) represents another example of a class II adjuvant. Streptazolin was shown to stimulate macrophage activity *in vitro* to increase bacterial killing.^{110, 115}

1.5.3 Antivirulence Antibiotics

Closely related to the development of antibiotic adjuvants is the development of antivirulence antibiotics. Unlike traditional antibiotics, antivirulence antibiotics do not target essential cellular processes like cell wall synthesis or DNA replication.^{116, 117} Rather, this class of compound targets and neutralizes virulence factors. Virulence factors are products produced by bacteria to promote pathogenesis via damaging the host or evading host immune system action. Examples of virulence factors include toxins, adhesions, siderophores, and factors that promote biofilm formation. Importantly, without these factors, bacteria are generally unable to cause infection in a host. Indeed, in the absence of virulence factors, the host immune system is more effective against pathogens, and commensal species within the host are also more likely to outcompete pathogenic species.

The strategy of targeting bacterial virulence factors has several attractive features.^{116, 117} First, because antivirulence agents do not target essential cellular processes or machinery, it is hypothesized that their use will be less likely to elicit the development of resistant phenotypes. Antivirulence drugs are also hypothesized to curb

resistance development due to the largely bacterium-specific nature of virulence factors. Thus, should one species develop resistance to an antivirulence drug, horizontal transfer of the relevant resistance genes to another species is unlikely to confer resistance to the recipient species. Another attractive feature of antivirulence agents is that they are unlikely to affect commensal species of the normal human flora as these species generally lack virulence factors. Collateral damage to commensal species is a common pitfall of typical antibiotic treatment, i.e. treatment with essential cell process-targeting antibiotics.¹¹⁷⁻¹¹⁹

Common antivirulence drug targets include but are not limited to bacterial toxins, quorum sensing (important for biofilm formation; see section 3.14 of Chapter 3), other biofilm-promoting factors, and secretion systems (molecule transport systems).^{116, 117} Bacterial toxins are perhaps the most clinically relevant targets as multiple bacterial toxin-targeting antivirulence drugs have been approved by the FDA.¹¹⁷ For example, immunoglobulins purified from donor plasma are used to neutralize botulinum neurotoxins (BoNTs) secreted by *Clostridium botulinum*. Similarly, bezlotoxumab, a human monoclonal antibody, targets the TcdB toxin produced by *Clostridium difficile* and has been shown to reduce the recurrence of *C. difficile* infections (CDIs) in patients at high risk of recurrence. Additional approved antivirulence drugs and antivirulence drugs still in development are reviewed elsewhere.^{117, 120}

1.5.4 Narrow-Spectrum Antibiotics

To date, antibiotic development has largely been focused on uncovering antibiotics that feature potent activity against a wide range of bacterial pathogens.^{118, 121, 122} This is

due in large part to the economic benefit associated with developing a drug with wide-reaching effects. Broad-spectrum antibiotics offer a better return on investment than antibiotics that are only effective against a narrow range of bacterial pathogens. While narrow-spectrum antibiotics have not been a primary focus of antibiotic development thus far, this class of antibiotic may prove key in the fight against antimicrobial resistance. Before continuing on in a discussion about narrow-spectrum antibiotics, it is important to note that the definition of narrow-spectrum has evolved over time.¹¹⁸ Originally, this term was developed to describe antibiotics that were only effective against one type of Gram stain group. However, for the present discussion, narrow-spectrum refers to antibiotics that are active against only one or a small cohort of bacterial species.

While broad-spectrum antibiotics have been and continue to be paramount for the treatment of infectious diseases, as previously discussed, their success is also their undoing. First, because the cellular targets of broad-spectrum antibiotics are highly conserved across bacterial species, continued use of these antibiotics is associated with an increased risk of resistance development and dissemination.¹²³⁻¹²⁶ Indeed, broad-spectrum antibiotics impose high selective pressure on numerous bacterial species and HGT among different species has contributed significantly to the rise of antibiotic resistance. Second, due to their lack of specificity in bacterial species they target, broad-spectrum antibiotics are prone to adverse effects such as damage to the host microbiome.^{125, 127} Importantly, antibiotic-associated damage to the microbiome can persist long after treatment has ceased. Additionally, damage to the normal gut flora can increase a patient's risk of developing secondary infections. For example, CDIs have

been directly linked to prior treatment with broadly-active antibiotics such as cephalosporins and quinolones.^{118, 127, 128}

In contrast to broad-spectrum antibiotics, narrow-spectrum antibiotics have been postulated to slow resistance development and dissemination, decrease the risk of damage to the microbiome, and help control the misuse and overuse of antibiotics^{129, 130} Because narrow-spectrum antibiotics fail to elicit the development of cross-resistance in pathogenic species not targeted by the antibiotics, this class of antibiotic represents an attractive approach to combat MDR bacterial infections. An example of a recently FDA-approved narrow-spectrum antibiotic is fidaxomicin (**14.3**, see **Figure 1.25**). Fidaxomicin is a macrolide antibiotic with selective antimicrobial activity against Gram-positive anaerobes that has garnered use in the treatment of severe CDI.^{118, 130, 131} Fidaxomicin inhibits spore and toxin formation by *C. difficile* and has been shown to decrease the recurrence of CDI compared to treatment of CDI with vancomycin. The multi-drug combination therapy used to treat *M. tuberculosis* infections is another example of a treatment that employs narrow-spectrum drugs.^{118, 130} Three of the four first-line drugs typically used to treat these infections (isoniazid (**1.58**), ethambutol (**1.59**), and pyrazinamide (**1.60**); see **Figure 1.40**) possess little to no activity against non-mycobacterial species. Additional narrow-spectrum antibiotics are reviewed elsewhere.^{118, 124, 130}

1.6 Conclusions and Future Outlook

As the occurrence of antibiotic-resistant bacteria continues to rise, new treatments are needed to combat infectious diseases, particularly those attributed to Gram-negative

pathogens. Without new treatments, we are at risk of returning to a “pre-antibiotic” era where infections are no longer treatable. In addition to new treatments, it is also imperative that we be more judicious with the use of current drugs so as to minimize the development and dissemination of antimicrobial resistance. To address these needs, several alternative approaches to treatment with a single, broadly-active antibiotic have been developed. These approaches include the use of multi-drug combinations, antibiotic adjuvants, antivirulence antibiotics, and narrowly-effective antibiotics that are active against only a small group of pathogens. While these approaches have often found success, additional work is needed to keep pace with the continued development of resistance.

1.7 References

1. Bentley, R.; Bennett, J. W., What Is an Antibiotic? Revisited. *Adv. Appl. Microbiol.* **2003**, 52, 303-331.
2. Silver, L. L., Challenges of antibacterial discovery. *Clin. Microbiol. Rev.* **2011**, 24 (1), 71-109.
3. Winau, F.; Westphal, O.; Winau, R., Paul Ehrlich—in search of the magic bullet. *Microbes Infect.* **2004**, 6 (8), 786-9.
4. Wright, G. D., The antibiotic resistome: the nexus of chemical and genetic diversity. *Nat. Rev. Microbiol.* **2007**, 5 (3), 175-86.
5. Wainwright, M.; Kristiansen, J. E., On the 75th anniversary of Prontosil. *Dyes Pigments* **2011**, 88 (3), 231-234.
6. Bentley, R., Different roads to discovery; Prontosil (hence sulfa drugs) and penicillin (hence beta-lactams). *J. Ind. Microbiol. Biotechnol.* **2009**, 36 (6), 775-86.

7. Zaman, S. B.; Hussain, M. A.; Nye, R.; Mehta, V.; Mamun, K. T.; Hossain, N., A Review on Antibiotic Resistance: Alarm Bells are Ringing. *Cureus* **2017**, 9 (6), e1403.
8. Brown, E. D.; Wright, G. D., Antibacterial drug discovery in the resistance era. *Nature* **2016**, 529 (7586), 336-43.
9. Wright, G. D., Q&A- Antibiotic resistance—where does it come from and what can we do about it? *BMC Biology* **2010**, 8.
10. Craft, K. M.; Townsend, S. D., The Human Milk Glycome as a Defense Against Infectious Diseases: Rationale, Challenges, and Opportunities. *ACS Infect. Dis.* **2017**, 4 (2), 77-83.
11. Clatworthy, A. E.; Pierson, E.; Hung, D. T., Targeting virulence: a new paradigm for antimicrobial therapy. *Nat. Chem. Biol.* **2007**, 3 (9), 541-8.
12. Global Priority List of Antibiotic-Resistant Bacteria to Guide Research, Discover, and Development of New Antibiotics. World Health Organization, **2017**.
13. Pendleton, J. N.; Gorman, S. P.; Gilmore, B. F., Clinical relevance of the ESKAPE pathogens. *Expert Rev. Anti. Infect. Ther.* **2013**, 11 (3), 297-308.
14. Boucher, H. W.; Talbot, G. H.; Bradley, J. S.; Edwards, J. E.; Gilbert, D.; Rice, L. B.; Scheld, M.; Spellberg, B.; Bartlett, J., Bad bugs, no drugs: no ESKAPE! An update from the Infectious Diseases Society of America. *Clin. Infect. Dis.* **2009**, 48 (1), 1-12.
15. Craft, K. M.; Gaddy, J. A.; Townsend, S. D., Human Milk Oligosaccharides (HMOs) Sensitize Group B *Streptococcus* to Clindamycin, Erythromycin, Gentamicin, and Minocycline on a Strain Specific Basis. *ACS Chem. Biol.* **2018**, 13 (8), 2020-2026.
16. Kohanski, M. A.; Dwyer, D. J.; Collins, J. J., How antibiotics kill bacteria: from targets to networks. *Nat. Rev. Microbiol.* **2010**, 8 (6), 423-35.
17. Silhavy, T. J.; Kahne, D.; Walker, S., The bacterial cell envelope. *Cold Spring Harb. Perspect. Biol.* **2010**, 2 (5), 1-16.
18. Vollmer, W.; Blanot, D.; de Pedro, M. A., Peptidoglycan structure and architecture. *FEMS Microbiol. Rev.* **2008**, 32 (2), 149-67.

19. Walsh, C., Molecular mechanisms that confer antibacterial drug resistance. *Nature* **2000**, *406* (6797), 775-781.
20. Macheboeuf, P.; Contreras-Martel, C.; Job, V.; Dideberg, O.; Dessen, A., Penicillin Binding Proteins: key players in bacterial cell cycle and drug resistance processes. *FEMS Microbiol. Rev.* **2006**, *30* (5), 673-691.
21. Bush, K., Antimicrobial agents targeting bacterial cell walls and cell membranes. *Rev. Sci. Tech.* **2012**, *31* (1), 43-56.
22. Falagas, M. E.; Vouloumanou, E. K.; Samonis, G.; Vardakas, K. Z., Fosfomycin. *Clin. Microbiol. Rev.* **2016**, *29* (2), 321-47.
23. Stone, K. J.; Strominger, J. L., Mechanism of Action of Bacitracin-Complexation with Metal Ion and C55-Isoprenyl Pyrophosphate. *PNAS* **1971**, *68* (12), 3223-3227.
24. Epand, R. M.; Walker, C.; Epand, R. F.; Magarvey, N. A., Molecular mechanisms of membrane targeting antibiotics. *Biochim. Biophys. Acta.* **2016**, *1858* (5), 980-7.
25. Erridge, C.; Bennett-Guerrero, E.; Poxton, I. R., Structure and function of lipopolysaccharides. *Microbes Infect.* **2002**, *4* (8), 837-51.
26. Raetz, C. R.; Whitfield, C., Lipopolysaccharide endotoxins. *Annu. Rev. Biochem.* **2002**, *71*, 635-700.
27. Alves, D.; Olivia Pereira, M., Mini-review: Antimicrobial peptides and enzymes as promising candidates to functionalize biomaterial surfaces. *Biofouling* **2014**, *30* (4), 483-99.
28. Fjell, C. D.; Hiss, J. A.; Hancock, R. E. W.; Schneider, G., Designing antimicrobial peptides: form follows function. *Nat. Rev. Drug Discov.* **2011**, *11* (1), 37-51.
29. Falagas, M. E.; Rafailidis, P. I.; Matthaiou, D. K., Resistance to polymyxins: Mechanisms, frequency and treatment options. *Drug Resist. Updat.* **2010**, *13* (4-5), 132-8.
30. Yu, Z.; Qin, W.; Lin, J.; Fang, S.; Qiu, J., Antibacterial mechanisms of polymyxin and bacterial resistance. *Biomed. Res. Int.* **2015**, *2015*, 679109.

31. Srinivas, P.; Rivard, K., Polymyxin Resistance in Gram-negative Pathogens. *Curr. Infect. Dis. Rep.* **2017**, *19* (11), 38.
32. Steenbergen, J. N.; Alder, J.; Thorne, G. M.; Tally, F. P., Daptomycin: a lipopeptide antibiotic for the treatment of serious Gram-positive infections. *J. Antimicrob. Chemother.* **2005**, *55* (3), 283-8.
33. Miller, W. R.; Bayer, A. S.; Arias, C. A., Mechanism of Action and Resistance to Daptomycin in *Staphylococcus aureus* and *Enterococci*. *Cold Spring Harb. Perspect. Med.* **2016**, *6* (11), 1-16.
34. Wilson, D. N., Ribosome-targeting antibiotics and mechanisms of bacterial resistance. *Nat Rev Microbiol* **2014**, *12* (1), 35-48.
35. Beringer, M.; Rodnina, M. V., The ribosomal peptidyl transferase. *Mol. Cell.* **2007**, *26* (3), 311-21.
36. Magnet, S.; Blanchard, J. S., Molecular insights into aminoglycoside action and resistance. *Chem. Rev.* **2005**, *105* (2), 477-497.
37. Livermore, D. M., Linezolid in vitro: mechanism and antibacterial spectrum. *J. Antimicrob. Chemother.* **2003**, *51 Suppl 2*, ii9-16.
38. Cruz-Vera, L. R.; Magos-Castro, M. A.; Zamora-Romo, E.; Guarneros, G., Ribosome stalling and peptidyl-tRNA drop-off during translational delay at AGA codons. *Nucleic Acids Res.* **2004**, *32* (15), 4462-8.
39. Polikanov, Y. S.; Aleksashin, N. A.; Beckert, B.; Wilson, D. N., The Mechanisms of Action of Ribosome-Targeting Peptide Antibiotics. *Front. Mol. Biosci.* **2018**, *5*, 48.
40. Arenz, S.; Wilson, D. N., Bacterial Protein Synthesis as a Target for Antibiotic Inhibition. *Cold Spring Harb Perspect Med* **2016**, *6* (9), 1-16.
41. van Eijk, E.; Wittekoek, B.; Kuijper, E. J.; Smits, W. K., DNA replication proteins as potential targets for antimicrobials in drug-resistant bacterial pathogens. *J. Antimicrob. Chemother.* **2017**, *72* (5), 1275-1284.
42. Sanyal, G.; Doig, P., Bacterial DNA replication enzymes as targets for antibacterial drug discovery. *Expert Opin. Drug. Discov.* **2012**, *7* (4), 327-39.

43. Aldred, K. J.; Kerns, R. J.; Osheroﬀ, N., Mechanism of quinolone action and resistance. *Biochemistry* **2014**, *53* (10), 1565-74.
44. Browning, D. F.; Busby, S. J., The regulation of bacterial transcription initiation. *Nat. Rev. Microbiol.* **2004**, *2* (1), 57-65.
45. Ma, C.; Yang, X.; Lewis, P. J., Bacterial Transcription as a Target for Antibacterial Drug Development. *Microbiol. Mol. Biol. Rev.* **2016**, *80* (1), 139-60.
46. Floss, H. G.; Yu, T.-W., Rifamycins Mode of Action, Resistance, and Biosynthesis. *Chem. Rev.* **2005**, *105*, 621-632.
47. Venugopal, A. A.; Johnson, S., Fidaxomicin: a novel macrocyclic antibiotic approved for treatment of *Clostridium difficile* infection. *Clin. Infect. Dis.* **2012**, *54* (4), 568-74.
48. Zhanel, G. G.; Walkty, A. J.; Karlowsky, J. A., Fidaxomicin: A novel agent for the treatment of *Clostridium difficile* infection. *Can. J. Infect. Dis. Med. Microbiol.* **2015**, *26* (6), 305-12.
49. Bermingham, A.; Derrick, J. P., The folic acid biosynthesis pathway in bacteria: evaluation of potential for antibacterial drug discovery. *Bioessays* **2002**, *24* (7), 637-48.
50. Ducker, G. S.; Rabinowitz, J. D., One-Carbon Metabolism in Health and Disease. *Cell Metab.* **2017**, *25* (1), 27-42.
51. Dawadi, S.; Kordus, S. L.; Baughn, A. D.; Aldrich, C. C., Synthesis and Analysis of Bacterial Folate Metabolism Intermediates and Antifolates. *Org. Lett.* **2017**, *19* (19), 5220-5223.
52. Wright, D. L.; Anderson, A. C., Antifolate agents: a patent review (2006 - 2010). *Expert Opin. Ther. Pat.* **2011**, *21* (9), 1293-308.
53. Then, R. L., History and future of antimicrobial diaminopyrimidines. *J. Chemother.* **1993**, *5* (6), 361-8.
54. Munita, J. M.; Arias, C. A., Mechanisms of Antibiotic Resistance. *Microbiol. Spectr.* **2016**, *4* (2).

55. Delcour, A. H., Outer membrane permeability and antibiotic resistance. *Biochim. Biophys. Acta.* **2009**, 1794 (5), 808-16.
56. Galdiero, S.; Falanga, A.; Cantisani, M.; Tarallo, R.; Della Pepa, M. E.; D'Orlando, V.; Galdiero, M., Microbe-host interactions: structure and role of Gram-negative bacterial porins. *Curr. Protein Pept. Sci.* **2012**, 13 (8), 843-54.
57. Sun, J.; Deng, Z.; Yan, A., Bacterial multidrug efflux pumps: mechanisms, physiology and pharmacological exploitations. *Biochem. Biophys. Res. Commun.* **2014**, 453 (2), 254-67.
58. Borges-Walmsley, M. I.; McKeegan, K. S.; Walmsley, A. R., Structure and function of efflux pumps that confer resistance to drugs. *Biochem. J.* **2003**, 376, 313-338.
59. Soto, S. M., Role of efflux pumps in the antibiotic resistance of bacteria embedded in a biofilm. *Virulence* **2013**, 4 (3), 223-9.
60. Martinez, J. L.; Sánchez, M. B.; Martínez-Solano, L.; Hernandez, A.; Garmendia, L.; Fajardo, A.; Alvarez-Ortega, C., Functional role of bacterial multidrug efflux pumps in microbial natural ecosystems. *FEMS Microbiol. Rev.* **2009**, 33 (2), 430-449.
61. McMurry, L.; Petrucci, R. E., Jr.; Levy, S. B., Active efflux of tetracycline encoded by four genetically different tetracycline resistance determinants in *Escherichia coli*. *PNAS* **1980**, 77 (7), 3974-7.
62. George, A. M.; Levy, S. B., Amplifiable resistance to tetracycline, chloramphenicol, and other antibiotics in *Escherichia coli*: involvement of a non-plasmid-determined efflux of tetracycline. *J. Bacteriol.* **1983**, 155 (2), 531-40.
63. Abraham, E. P.; Chain, E., An enzyme from bacteria able to destroy penicillin. 1940. *Rev. Infect. Dis.* **1988**, 10 (4), 677-8.
64. Kong, K. F.; Schnepfer, L.; Mathee, K., Beta-lactam antibiotics: from antibiosis to resistance and bacteriology. *APMIS* **2010**, 118 (1), 1-36.
65. Kirby, W. M., Extraction of a Highly Potent Penicillin Inactivator from Penicillin Resistant *Staphylococci*. *Science* **1944**, 99 (2579), 452-3.
66. Bush, K.; Bradford, P. A., Beta-Lactams and Beta-Lactamase Inhibitors: An Overview. *Cold Spring Harb. Perspect. Med.* **2016**, 6 (8), 1-16.

67. Kirby, W. M., Bacteriostatic and Lytic Actions of Penicillin on Sensitive and Resistant *Staphylococci*. *J. Clin. Invest.* **1945**, 24 (2), 165-9.
68. Chambers, H. F.; Deleo, F. R., Waves of resistance: *Staphylococcus aureus* in the antibiotic era. *Nat. Rev. Microbiol.* **2009**, 7 (9), 629-41.
69. Lowy, F. D., Antimicrobial resistance: the example of *Staphylococcus aureus*. *J. Clin. Invest.* **2003**, 111 (9), 1265-1273.
70. Paterson, D. L.; Bonomo, R. A., Extended-spectrum beta-lactamases: a clinical update. *Clin. Microbiol. Rev.* **2005**, 18 (4), 657-86.
71. Rupp, M. E.; Fey, P. D., Extended spectrum beta-lactamase (ESBL)-producing Enterobacteriaceae: considerations for diagnosis, prevention and drug treatment. *Drugs* **2003**, 63 (4), 353-65.
72. Knothe, H.; Shah, P.; Krcmery, V.; Antal, M.; Mitsuhashi, S., Transferable resistance to cefotaxime, cefoxitin, cefamandole and cefuroxime in clinical isolates of *Klebsiella pneumoniae* and *Serratia marcescens*. *Infection* **1983**, 11 (6), 315-7.
73. Rawat, D.; Nair, D., Extended-spectrum beta-lactamases in Gram-Negative Bacteria. *J. Glob. Infect. Dis.* **2010**, 2 (3), 263-74.
74. Garneau-Tsodikova, S.; Labby, K. J., Mechanisms of Resistance to Aminoglycoside Antibiotics: Overview and Perspectives. *Medchemcomm* **2016**, 7 (1), 11-27.
75. Becker, B.; Cooper, M. A., Aminoglycoside antibiotics in the 21st century. *ACS Chem. Biol.* **2013**, 8 (1), 105-15.
76. Wright, G. D., Bacterial resistance to antibiotics: enzymatic degradation and modification. *Adv. Drug Deliv. Rev.* **2005**, 57 (10), 1451-70.
77. Robicsek, A.; Strahilevitz, J.; Jacoby, G. A.; Macielag, M.; Abbanat, D.; Park, C. H.; Bush, K.; Hooper, D. C., Fluoroquinolone-modifying enzyme: a new adaptation of a common aminoglycoside acetyltransferase. *Nat. Med.* **2006**, 12 (1), 83-8.
78. Mathew, R.; Chatterji, D., The evolving story of the omega subunit of bacterial RNA polymerase. *Trends Microbiol.* **2006**, 14 (10), 450-5.

79. Seppala, H.; Skurnik, M.; Soini, H.; Roberts, M. C.; Huovinen, P., A novel erythromycin resistance methylase gene (ermTR) in *Streptococcus pyogenes*. *Antimicrob. Agents Chemother.* **1998**, 42 (2), 257-62.
80. Roberts, M. C., Update on macrolide-lincosamide-streptogramin, ketolide, and oxazolidinone resistance genes. *FEMS Microbiol. Lett.* **2008**, 282 (2), 147-59.
81. Morales, G.; Picazo, J. J.; Baos, E.; Candel, F. J.; Arribi, A.; Pelaez, B.; Andrade, R.; de la Torre, M. A.; Fereres, J.; Sanchez-Garcia, M., Resistance to linezolid is mediated by the cfr gene in the first report of an outbreak of linezolid-resistant *Staphylococcus aureus*. *Clin. Infect. Dis.* **2010**, 50 (6), 821-5.
82. Zarubica, T.; Baker, M. R.; Wright, H. T.; Rife, J. P., The aminoglycoside resistance methyltransferases from the ArmA/Rmt family operate late in the 30S ribosomal biogenesis pathway. *RNA* **2011**, 17 (2), 346-55.
83. Yokoyama, K.; Doi, Y.; Yamane, K.; Kurokawa, H.; Shibata, N.; Shibayama, K.; Yagi, T.; Kato, H.; Arakawa, Y., Acquisition of 16S rRNA methylase gene in *Pseudomonas aeruginosa*. *Lancet* **2003**, 362 (9399), 1888-93.
84. Galimand, M.; Courvalin, P.; Lambert, T., Plasmid-Mediated High-Level Resistance to Aminoglycosides in Enterobacteriaceae Due to 16S rRNA Methylation. *Antimicrob. Agents Chemother.* **2003**, 47 (8), 2565-2571.
85. Karthikeyan, K.; Thirunarayan, M. A.; Krishnan, P., Coexistence of blaOXA-23 with blaNDM-1 and armA in clinical isolates of *Acinetobacter baumannii* from India. *J. Antimicrob. Chemother.* **2010**, 65 (10), 2253-4.
86. Connell, S. R.; Tracz, D. M.; Nierhaus, K. H.; Taylor, D. E., Ribosomal Protection Proteins and Their Mechanism of Tetracycline Resistance. *Antimicrob. Agents Chemother.* **2003**, 47 (12), 3675-3681.
87. Augusta, B. M. M. T. C. A., New antibiotics for bad bugs: where are we? *Ann. Clin. Microbiol. Antimicrob.* **2013**, 12 (22).
88. Rice, Louis B., Federal Funding for the Study of Antimicrobial Resistance in Nosocomial Pathogens: No ESKAPE. *J. Infect. Dis.* **2008**, 197 (8), 1079-1081.
89. Santajit, S.; Indrawattana, N., Mechanisms of Antimicrobial Resistance in ESKAPE Pathogens. *Biomed. Res. Int.* **2016**, 2016, 2475067.

90. Antibiotic Resistance Threats in the United States Report, Centers for Disease Control. **2013**.
91. Costerton, J. W.; Stewart, P. S.; Greenberg, E. P., Bacterial biofilms: a common cause of persistent infections. *Science* **1999**, *284* (5418), 1318-22.
92. Davies, D., Understanding biofilm resistance to antibacterial agents. *Nat. Rev. Drug. Discov.* **2003**, *2* (2), 114-22.
93. Hoiby, N.; Ciofu, O.; Johansen, H. K.; Song, Z. J.; Moser, C.; Jensen, P. O.; Molin, S.; Givskov, M.; Tolker-Nielsen, T.; Bjarnsholt, T., The clinical impact of bacterial biofilms. *Int. J. Oral. Sci.* **2011**, *3* (2), 55-65.
94. Paczosa, M. K.; Meccas, J., *Klebsiella pneumoniae*: Going on the Offense with a Strong Defense. *Microbiol. Mol. Biol. Rev.* **2016**, *80* (3), 629-61.
95. Vading, M.; Naucner, P.; Kalin, M.; Giske, C. G., Invasive infection caused by *Klebsiella pneumoniae* is a disease affecting patients with high comorbidity and associated with high long-term mortality. *PLoS One* **2018**, *13* (4), e0195258.
96. Ackerman, D. L.; Craft, K. M.; Doster, R. S.; Weitkamp, J. H.; Aronoff, D. M.; Gaddy, J. A.; Townsend, S. D., Antimicrobial and Antibiofilm Activity of Human Milk Oligosaccharides against *Streptococcus agalactiae*, *Staphylococcus aureus*, and *Acinetobacter baumannii*. *ACS Infect. Dis.* **2018**, *4* (3), 315-324.
97. Antunes, L. C.; Visca, P.; Towner, K. J., *Acinetobacter baumannii*: evolution of a global pathogen. *Pathog. Dis.* **2014**, *71* (3), 292-301.
98. Singh, H.; Thangaraj, P.; Chakrabarti, A., *Acinetobacter baumannii*: A Brief Account of Mechanisms of Multidrug Resistance and Current and Future Therapeutic Management. *J. Clin. Diagn. Res.* **2013**, *7* (11), 2602-5.
99. Karageorgopoulos, D. E.; Falagas, M. E., Current control and treatment of multidrug-resistant *Acinetobacter baumannii* infections. *Lancet Infect. Dis.* **2008**, *8* (12), 751-62.
100. Peleg, A. Y.; Seifert, H.; Paterson, D. L., *Acinetobacter baumannii*: emergence of a successful pathogen. *Clin. Microbiol. Rev.* **2008**, *21* (3), 538-82.

101. Sadikot, R. T.; Blackwell, T. S.; Christman, J. W.; Prince, A. S., Pathogen-host interactions in *Pseudomonas aeruginosa* pneumonia. *Am. J. Respir. Crit. Care Med.* **2005**, *171* (11), 1209-23.
102. Walsh, C., Where will new antibiotics come from? *Nat. Rev. Microbiol.* **2003**, *1* (1), 65-70.
103. Worthington, R. J.; Melander, C., Combination approaches to combat multidrug-resistant bacteria. *Trends Biotechnol.* **2013**, *31* (3), 177-84.
104. Bollenbach, T., Antimicrobial interactions: mechanisms and implications for drug discovery and resistance evolution. *Curr. Opin. Microbiol.* **2015**, *27*, 1-9.
105. Caminero, J. A.; Sotgiu, G.; Zumla, A.; Migliori, G. B., Best drug treatment for multidrug-resistant and extensively drug-resistant tuberculosis. *Lancet Infect. Dis.* **2010**, *10* (9), 621-9.
106. Mitchison, D.; Davies, G., The chemotherapy of tuberculosis: past, present and future. *Int. J. Tuberc. Lung Dis.* **2012**, *16* (6), 724-32.
107. Barnes, A. I.; Herrero, I. L.; Albesa, I., New aspect of the synergistic antibacterial action of ampicillin and gentamicin. *Int. J. Antimicrob. Agents* **2005**, *26* (2), 146-51.
108. Le, T.; Bayer, A. S., Combination antibiotic therapy for infective endocarditis. *Clin. Infect Dis.* **2003**, *36* (5), 615-21.
109. Sass, L., Group B Streptococcal Infections. *Pediatr. Rev.* **2012**, *33* (5).
110. Wright, G. D., Antibiotic Adjuvants: Rescuing Antibiotics from Resistance. *Trends Microbiol.* **2016**, *24* (11), 862-871.
111. Vazquez, D., Studies on the mode of action of the streptogramin antibiotics. *J. Gen. Microbiol.* **1966**, *42* (1), 93-106.
112. Korczynska, M.; Mukhtar, T. A.; Wright, G. D.; Berghuis, A. M., Structural basis for streptogramin B resistance in *Staphylococcus aureus* by virginiamycin B lyase. *PNAS* **2007**, *104* (25), 10388-93.

113. Noeske, J.; Huang, J.; Olivier, N. B.; Giacobbe, R. A.; Zambrowski, M.; Cate, J. H., Synergy of streptogramin antibiotics occurs independently of their effects on translation. *Antimicrob. Agents Chemother.* **2014**, *58* (9), 5269-79.
114. Melander, R. J.; Melander, C., The Challenge of Overcoming Antibiotic Resistance: An Adjuvant Approach? *ACS Infect. Dis.* **2017**, *3* (8), 559-563.
115. Perry, J. A.; Koteva, K.; Verschoor, C. P.; Wang, W.; Bowdish, D. M. E.; Wright, G. D., A macrophage-stimulating compound from a screen of microbial natural products. *J. Antibiot.* **2014**, *68* (1), 40-46.
116. Gill, E. E.; Franco, O. L.; Hancock, R. E., Antibiotic adjuvants: diverse strategies for controlling drug-resistant pathogens. *Chem. Biol. Drug Des.* **2015**, *85* (1), 56-78.
117. Dickey, S. W.; Cheung, G. Y. C.; Otto, M., Different drugs for bad bugs: antivirulence strategies in the age of antibiotic resistance. *Nat. Rev. Drug. Discov.* **2017**, *16* (7), 457-471.
118. Maxson, T.; Mitchell, D. A., Targeted Treatment for Bacterial Infections: Prospects for Pathogen-Specific Antibiotics Coupled with Rapid Diagnostics. *Tetrahedron* **2016**, *72* (25), 3609-3624.
119. Tanaka, S.; Kobayashi, T.; Songjinda, P.; Tateyama, A.; Tsubouchi, M.; Kiyohara, C.; Shirakawa, T.; Sonomoto, K.; Nakayama, J., Influence of antibiotic exposure in the early postnatal period on the development of intestinal microbiota. *FEMS Immunol. Med. Microbiol.* **2009**, *56* (1), 80-7.
120. Leite, B.; Gomes, F.; Melo, P.; Souza, C.; Teixeira, P.; Oliveira, R.; Pizzolitto, E., *N*-acetylcysteine and vancomycin alone and in combination against staphylococci biofilm. *Rev. Bras. Eng. Bioméd.* **2013**, *29* (2), 184-192.
121. Koehn, F. E., New strategies and methods in the discovery of natural product anti-infective agents: the mannopeptimycins. *J. Med. Chem.* **2008**, *51* (9), 2613-7.
122. Payne, D. J., Microbiology. Desperately seeking new antibiotics. *Science* **2008**, *321* (5896), 1644-5.
123. May, A. K.; Fleming, S. B.; Carpenter, R. O.; Diaz, J. J.; Guillaumondegui, O. D.; Deppen, S. A.; Miller, R. S.; Talbot, T. R.; Morris, J. A., Influence of broad-spectrum antibiotic prophylaxis on intracranial pressure monitor infections and subsequent

- infectious complications in head-injured patients. *Surg Infect. (Larchmt)* **2006**, 7 (5), 409-17.
124. Molohon, K. J.; Blair, P. M.; Park, S.; Doroghazi, J. R.; Maxson, T.; Hershfield, J. R.; Flatt, K. M.; Schroeder, N. E.; Ha, T.; Mitchell, D. A., Plantazolicin is an ultra-narrow spectrum antibiotic that targets the *Bacillus anthracis* membrane. *ACS Infect. Dis.* **2016**, 2 (3), 207-220.
125. Gerber, J. S.; Ross, R. K.; Bryan, M.; Localio, A. R.; Szymczak, J. E.; Wasserman, R.; Barkman, D.; Odeniyi, F.; Conaboy, K.; Bell, L.; Zaoutis, T. E.; Fiks, A. G., Association of Broad- vs Narrow-Spectrum Antibiotics With Treatment Failure, Adverse Events, and Quality of Life in Children With Acute Respiratory Tract Infections. *JAMA* **2017**, 318 (23), 2325-2336.
126. de Man, P.; Verhoeven, B. A.; Verbrugh, H. A.; Vos, M. C.; van den Anker, J. N., An antibiotic policy to prevent emergence of resistant bacilli. *Lancet* **2000**, 355 (9208), 973-8.
127. Dethlefsen, L.; Relman, D. A., Incomplete recovery and individualized responses of the human distal gut microbiota to repeated antibiotic perturbation. *PNAS* **2010**, 108 (1), 4554-4561.
128. Koenigsnecht, M. J.; Young, V. B., Faecal microbiota transplantation for the treatment of recurrent *Clostridium difficile* infection: current promise and future needs. *Curr. Opin. Gastroenterol.* **2013**, 29 (6), 628-32.
129. Spellberg, B.; Bartlett, J.; Wunderink, R.; Gilbert, D. N., Novel approaches are needed to develop tomorrow's antibacterial therapies. *Am. J. Respir. Crit. Care Med.* **2015**, 191 (2), 135-40.
130. Melander, R. J.; Zurawski, D. V.; Melander, C., Narrow-Spectrum Antibacterial Agents. *Medchemcomm* **2018**, 9, 12-21.
131. Shah, D. N.; Chan, F. S.; Kachru, N.; Garcia, K. P.; Balcer, H. E.; Dyer, A. P.; Emanuel, J. E.; Jordan, M. D.; Lusardi, K. T.; Naymick, G.; Polisetty, R. S.; Sieman, L.; Tyler, A. M.; Johnson, M. L.; Garey, K. W., A multi-center study of fidaxomicin use for *Clostridium difficile* infection. *Springerplus* **2016**, 5 (1), 1224.

CHAPTER 2

Human Milk Oligosaccharides: A Source of Protection Against Infectious Diseases

2.1 *Infant Feeding: A Brief History*

Throughout history, breastmilk was considered the golden standard for infant nutrition.¹⁻³ Moreover, breastfeeding was judged by some to be a religious obligation.² While evidence suggests that animal milk was used as far back as ancient times as an alternative to human milk, wet nursing, a practice wherein a woman breastfeeds another's child, was long considered the best alternative for infants of mothers who could not breastfeed.^{2, 4} It was not until the 19th century with the introduction of the feeding bottle, increased availability of animal milk, and advancements in food preservation that animal milk and infant formula became popular alternative feeding methods.^{2, 4, 5}

As early as the mid 1700s, scientists began comparing the composition of human milk to that of animal milk. In 1760, Dr. Jean Charles Desessartz published the *Treatise of Physical Upbringing of Children* in which he concluded that based on their compositions, human milk was a superior source of infant nutrition than the milk of other animals including cows, goats, and sheep.² Around a century later, the first modern infant formula, composed of cow's milk, wheat flour, malt flour, and potassium bicarbonate (K_2CO_3), was developed by Justus von Liebig. By the 1880s, there were approximately 30 patented brands of infant food consisting of carbohydrates to be added to milk.^{2, 6}

Infant formula continued to rise in popularity and, by the 1950s, was considered by physicians and consumers alike to be a popular and safe alternative for human milk. These sentiments, accompanied by aggressive marketing campaigns for formula, contributed to a global decline in breastfeeding rates in the 21st century.^{2, 3} Interestingly, declining rates were seen despite several known and acknowledged advantages of human milk over formula. For example, formula manufacturers publicly acknowledged that human milk remained the ideal form of nourishment for infants. Moreover, there were observations dating back as far as the late 19th century that breastfed infants had higher survival rates and lower instances of diarrhea than bottle-fed infants.²

Today, it is well-known that infants who are breastfed experience decreased instances of diarrhea, ear and urinary tract infections (UTIs), necrotizing enterocolitis (NEC), and sudden infant death syndrome (SIDS) compared to formula-fed infants.^{1, 7} Additionally, it is well-known that breastfeeding promotes the development of a healthy infant intestinal microbiome as the intestinal microbiome of breastfed infants are consistently shown to be dominated to a much greater extent by symbiotes such as *Bifidobacteria* compared to their formula-fed counterparts. In accordance with these findings, the World Health Organization (WHO) and the American Academy of Pediatrics (AAP) both recommend exclusive breastfeeding for the first 6 months of life followed by continued breastfeeding in addition to complementary foods for 1 year or more.^{8, 9}

While the superiority of human milk for infant development was attributed to differences in milk composition over 200 years ago, today we have a much more thorough understanding of the molecular components of human milk and the benefits these components impart on infant health.^{1, 7, 10-12}

2.2 Human Milk Composition

Human milk, with its numerous nutritive and non-nutritive components, is well-tailored to promote infant survival and proper development. Indeed, human milk is a dynamic mixture whose composition varies over time to meet the evolving needs of an infant. For instance, colostrum, the first milk produced, features higher concentrations of secretory immunoglobulins and human milk oligosaccharides (HMOs) and lower concentrations of lactose and fat compared to mature milk.^{10, 12} As immunoglobulins and HMOs are non-nutritive protective components while lactose and fat are nutritional components, the composition of colostrum suggests that its primary role is immunologic rather than nutritional.¹² Conversely, the milk of mothers who give birth prematurely tends towards higher levels of protein and fat as a means to supplement the additional nutritional requirements of premature infants.

Broadly speaking, the macromolecular components of human milk can be broken down into three categories: fat, protein, and carbohydrate; the carbohydrate fraction can be further broken down into lactose and oligosaccharides. On average, mature milk, i.e. milk after 4-6 weeks postpartum, contains 8-12 g/L protein, 32-41 g/L fat, 67-78 g/L lactose, and 5-15 g/L oligosaccharides (**Figure 2.1**).^{7, 12} In contrast to the shifting concentrations of fat, protein, and carbohydrate during the first month of life, after 4-6 weeks postpartum, human milk composition remains largely consistent with only subtle changes observed over the remainder of lactation.¹² In addition to macromolecules, human milk also contains micronutrients such as vitamins A, B1, B2, B3, B6, B12, C, and D as well as iodine. Concentrations of several of these components can, however, vary greatly with maternal diet.^{12, 13}

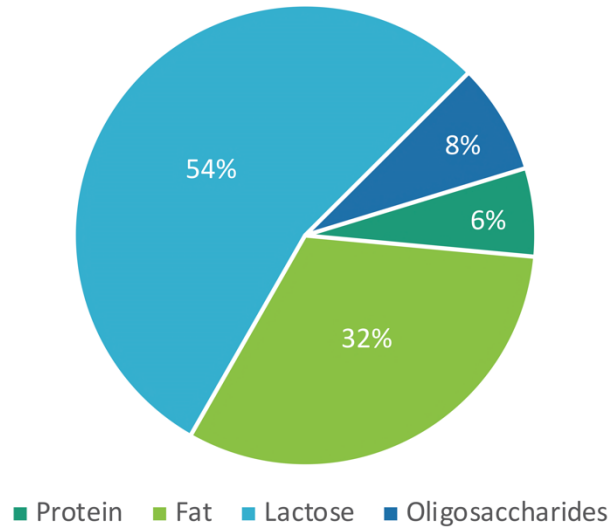


Figure 2.1. Human milk macromolecular composition.

2.2.1 Fats

Fats, or lipids, are the largest source of energy in human milk. Indeed, this class of macromolecule is estimated to account for 40-55% of the total energy derived from human milk. Fats also represent the most highly variable macronutrient in human milk.^{10, 14, 15} In addition to varying fat concentrations in preterm, colostrum, transitional, and mature milk, fat content can also vary over the course of a single feeding. Indeed, hindmilk, i.e. the last milk of a feed, can have two to three times the amount of fat as that of foremilk, i.e. the initial milk of a feed.^{12, 14} In terms of composition, triglycerides comprise the vast majority of lipids in human milk and account for around 98% of human milk fat. The remainder are predominately diglycerides, monoglycerides, and free fatty acids as well as phospholipids and cholesterol.^{10, 14} Lipid components are presented as milk fat globules wherein the nonpolar triglycerides constituent the majority of the core and phospholipids constitute the bulk of the outer membrane (**Figure 2.2**).¹⁵ In addition to phospholipids, the milk fat globule membrane (MFGM) contains sphingomyelin,

gangliosides, and cholesterol which are important for proper brain and central nervous system development.^{10, 16, 17}

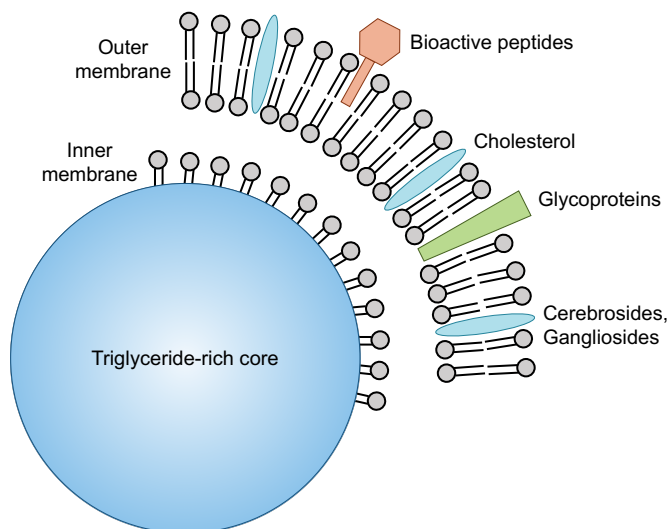


Figure 2.2. Structure and composition of human milk fat globules (figure adapted from reference 15).

While breast milk contains over 200 different types of fatty acids, oleic, palmitic, and linoleic acids are found in the highest concentrations with palmitic acid alone accounting for 25% of all milk fatty acids.^{10, 15} Through the action of gastric or lingual lipases, fatty acids are released from the glycerol backbone and can subsequently serve as energy sources and/or protective molecules.¹⁶ Interestingly, the position of fatty acids on the glycerol backbone influences their bioavailability. For example, in human milk, palmitic acid is most commonly found at the 2-position (sn-2) of triglycerides as this location assists in palmitic acid absorption.^{10, 12} During digestion, infant lipases primarily hydrolyze the fatty acids and the sn-1 and -3 positions while the fatty acid at the sn-2 position is left as the monoglyceride. While free palmitic acid is poorly water soluble and poorly absorbed, palmitoyl-monoglycerol is highly water soluble and consequently more readily absorbed.¹⁵ In addition to larger fatty acids like oleic, palmitic, and linoleic acids,

short-chain fatty acids (SCFAs) like acetate, butyrate, and propionate serve as important sources of energy. Moreover, SCFAs are important for the development of a healthy microbiome.¹⁰

2.2.2 Proteins

Milk proteins can be divided into three classes: mucin, casein, and whey. Casein and whey account for the vast majority of milk proteins while mucins contribute only minorly to total milk protein content.^{10, 18} An important distinguishing factor amongst these protein subclasses is the environment in which each protein type is found. Whey proteins are soluble and are consequently found in solution whereas casein proteins are not soluble and are instead found in casein micelles suspended in solution.¹⁰ Mucins, also termed MFGM proteins, are found in the outer membrane of milk fat globules (**Figure 2.2**).^{10, 15}

Generally speaking, protein levels decrease significantly over the first 4 to 6 weeks of lactation regardless of timing of delivery (term or preterm) then decrease at a much slower rate after that.^{18, 19} In line with this broad trend, the whey protein portion decreases in concentration over time. Conversely, the casein fraction increases over lactation. For example, ratios of whey to casein can range from around 80:20 early in lactation to closer to 50:50 at the late stages of lactation. Thus, the commonly cited 60:40 ratio of whey to casein proteins is simply an approximation or average of the dynamic ratio between these protein components.

While human milk proteins serve as direct sources of nutrition as they are major sources of amino acids, they also serve as nutrient absorption aids.¹⁸ For example, bile

salt-stimulating lipase (BSSL), which is found in human milk, is an enzyme that aids in the break-down of lipids. Importantly, BSSL can digest a wide range of substrates including mono-, di-, and triacylglycerols as well as cholesterol esters and diacylphosphatidylglycerols. Additionally, BSSL is capable of acting on both micellar and water-soluble substrates. Milk also contains several proteins which are important for mineral and ion absorption. The highly phosphorylated β -casein complexes Ca^{2+} ions and keeps them in solution (thus increasing their absorption), which likely contributes to the elevated bioavailability of calcium in human milk.¹⁸ α -lactalbumin, one of the most abundant milk proteins, also binds Ca^{2+} and Zn^{2+} ions, though to a lesser extent than β -casein, and is also thought to aid in mineral absorption. It remains, however, that a major benefit of α -lactalbumin is derived from its high levels of tryptophan, lysine, and cysteine which are released during α -lactalbumin digestion.^{17, 18}

Another major milk protein known for its absorption properties is lactoferrin. Lactoferrin accounts for around 15% of total protein content and is an iron-binding protein that facilitates iron uptake by intestinal cells.^{17, 18} Importantly, lactoferrin's ability to bind ferric iron also helps to protect infants from infection as it sequesters iron from iron-requiring bacteria. Interestingly, it has also been shown that lactoferrin possess strong bactericidal activity against numerous pathogens and that this activity is not dependent on the level of iron saturation of lactoferrin.¹⁸ Moreover, lactoferrin has been found to work synergistically with lysozyme, a major component of the whey fraction of human milk, to kill Gram-negative bacteria. Lysozyme is an enzyme that can degrade bacterial cell walls by hydrolyzing the β -1,4 linkages between *N*-acetylmuramic acid and *N*-acetylglucosamine in the peptidoglycan layer. Against Gram-negative bacteria, lactoferrin

first binds to and removes the lipopolysaccharide (LPS) outer layer. This then allows lysozyme to access and subsequently break down the peptidoglycan layer of the cell wall which leads to cell death.¹⁸ Lastly, lactoferrin has also been shown to promote the production and release of the pro-inflammatory cytokines interleukin (IL)-1 β , IL-8, and tumor necrosis factor (TNF)- α as well as transforming growth factor (TGF)- β . These actions promote immune system development and cell development and proliferation, respectively.^{17, 18}

Impressively, human milk is enriched with numerous immune factors including immune cells, cytokines, chemokines, and antibodies.¹² For example, macrophages, T cells, stem cells, and lymphocytes have all been found in human milk. Macrophages represent the largest cellular component in early milk with around 80% of cells being macrophages. These cells can then go on to differentiate into dendritic cells capable of stimulating T-cell activity. In terms of cytokine composition, TGF- β is the most abundant cytokine in human milk and is important for inflammation regulation and wound repair as well as the prevention of allergic diseases. While human milk also contains TNF- α , IL-6, IL-8, and interferon gamma (INF γ) cytokines, these are generally found at low levels and decrease in concentration over the course of lactation.

Maternal antibodies are extremely important for the proper development of an infant's immune system.¹⁰ As infants are born with immature acquired immunity, they are largely reliant on antibodies from their mother to protect them from infection. In light of this reality, it is unsurprising that antibodies, or immunoglobulins, are found in particularly high concentrations early in lactation. The most predominant of the human milk immunoglobulins is secretory IgA (SIgA). In colostrum, SIgA is generally found at

concentrations around 12 mg/mL as opposed to around 1 mg/mL in mature milk.^{10, 20} SIgA protects against mucosal pathogens by immobilizing them and consequently preventing their adherence to epithelial cell surfaces. Moreover, SIgA can neutralize toxins and virulence factors of these pathogens. In accordance with these findings, SIgA antibodies are found in high concentrations in mucous membranes.^{10, 20} Additionally, human milk contains SIgA antibodies against a number of enteric and respiratory pathogens such as *Vibrio cholerae*, *Campylobacter*, and *Shingella*. Also important is the increased resistance of SIgA towards proteolysis compared to other immunoglobulins. This allows SIgA to function in the gastrointestinal (GI) tract. Given the diverse array of protection it affords, SIgA is hypothesized to serve as the primary protective agent of human milk.

In addition to SIgA, human milk also contains IgM and IgG though to a lesser extent than SIgA.¹² IgM is the type of antibody that appears when an individual is exposed to a particular antigen for the first time and characteristically possesses lower antigen specificity and thus lower potency in defeating an infection.²¹ IgG on the other hand is involved in antigen uptake and is present in all body fluids. While SIgA and IgM are found in higher concentrations early in lactation, IgG is found in higher abundances in mature milk. Given the roles of SIgA and IgG, it is thought that the transition from higher SIgA levels to higher IgG levels as milk matures is suggestive of shift in milk function from directly protecting against pathogens via the action of maternal SIgA to indirectly aiding in the development of an infant's immune system via increased antigen intake through the action of IgG.²²

As previously mentioned, while whey and casein represent the largest protein classes in human milk, human milk also contains proteins that are integral components

of the outer membrane of fat globules called MFGM proteins.¹⁶ This class of proteins include mucin (MUC1), lactadherin, and lactoferrin. Many of these outer membrane integrated proteins serve as antimicrobial agents.¹⁷ For example, MUC1, a highly glycosylated glycoprotein, binds fimbriated *Escherichia coli* while lactadherin, also referred to as milk fat globule epidermal growth factor VIII (MFGE8), is a glycoprotein that protects against rotavirus, which is a major cause of diarrheal disease in infants. As is the general trend with many immunomodulatory and antimicrobial proteins in human milk, concentrations of MFGM proteins like MUC1 and lactadherin are highest earlier in lactation.

As a final note on human milk protein composition, human milk also contains several growth factors such as epidermal growth factor (EGF), vascular endothelial growth factor (VEGF), brain-derived neurotrophic factor (BDNF), insulin-like growth factor (IGF), erythropoietin (Epo), and adiponectin.¹² Many of these growth factors, such as EGF, are present in higher concentrations in early milk and decrease over the course of lactation. Epo in particular is found in significant quantities in milk. It is the primary hormone responsible for increasing the concentration of red blood cells (RBCs). Epo is also an important trophic factor (helps neurons to develop and maintain connections with surrounding neurons). Additionally, Epo tightens intestinal junctions and some evidence suggests it may help to reduce the risk of NEC as well as the transfer of human immunodeficiency virus (HIV) from mother to infant. EGF is vital to the maturation and healing of intestinal mucosa as it plays a role in stimulating cell division, absorption of glucose and water, and protein synthesis. Finally, adiponectin is important for the regulation of infant metabolism. Because levels of this growth factor are inversely

correlated with infant weight and BMI when an infant is exclusively breastfed, it is hypothesized that adiponectin may reduce the incidence of obesity later in life.

2.2.3 Carbohydrates

The carbohydrate portion of human milk is composed primarily of lactose. Lactose (2.1) is a disaccharide featuring a β -1,4 linkage between galactose (1.22) and glucose (1.21), wherein glucose is at the reducing end (Figure 2.3). For a more detailed description of carbohydrate structure and nomenclature, see section 4.3.1 of Chapter 3. Interestingly, human milk features some of the highest concentrations of lactose when compared to the milk of other species.¹⁰ Additionally, lactose concentrations in human milk are the least variable of all the macronutrient concentrations, though it has been found that mothers who produce larger quantities of milk have milk with higher lactose concentrations.¹²

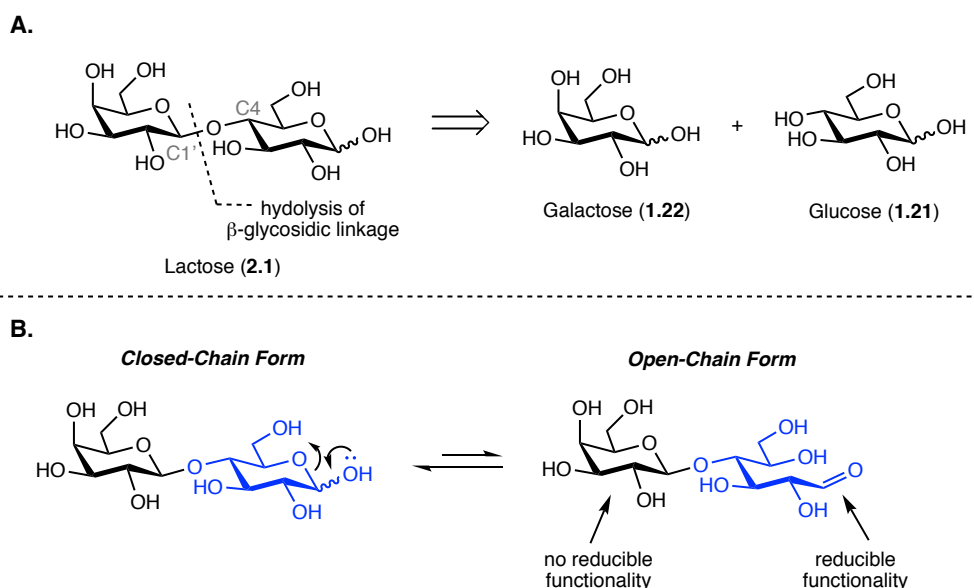
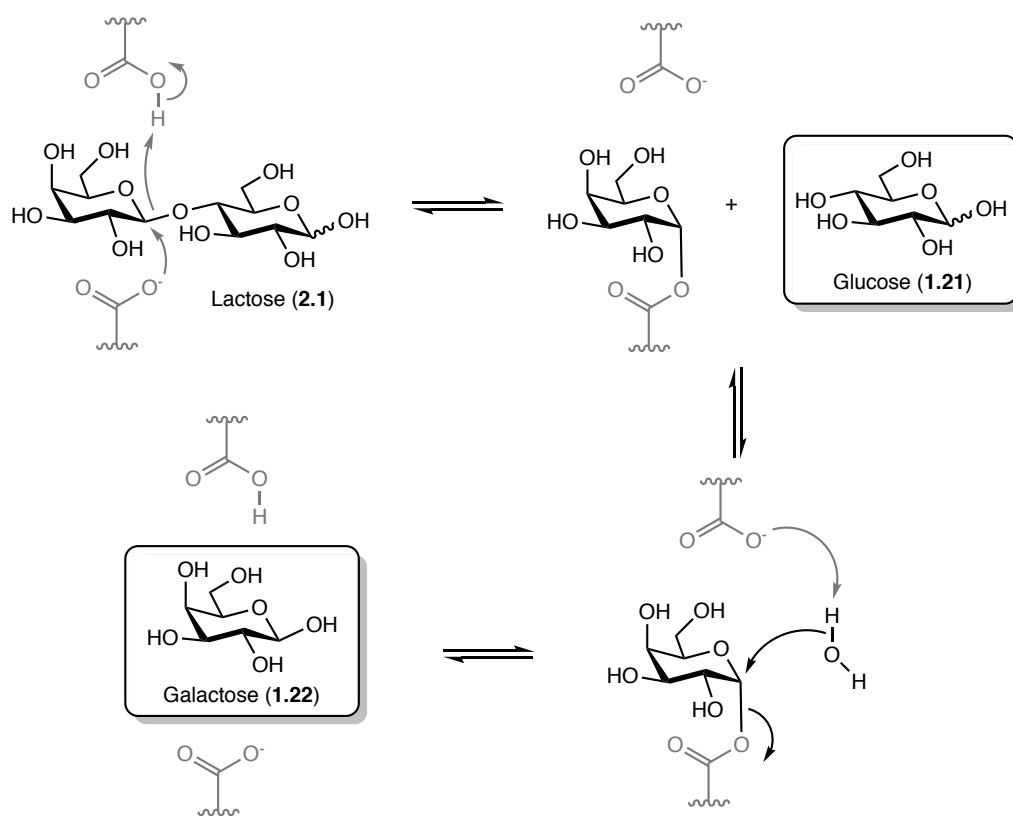


Figure 2.3. Structure of lactose (2.1). (A) Hydrolysis of the β 1-4 glycosidic linkage of lactose yields the monosaccharides galactose (1.22), and glucose (1.21). (B) The reducing end of lactose is highlighted in blue. The reducing end of any carbohydrate is the end that possesses a reducible aldehyde functionality when the carbohydrate converts from the closed-chain to open-chain form.

The primary function of human milk lactose is a nutritive one.²³ Most lactose is digested in the small intestine, and this digestion provides around 4 kcal/g of energy. If, however, lactose escapes digestion in the small intestine, it can be fermented by saccharolytic colonic bacteria into SCFAs which yields around 2 kcal/g of energy.^{23, 24} It is important to note that lactose itself cannot be directly absorbed in the small intestine. Rather, lactose must first be broken down into its monosaccharide constituents, galactose and glucose by β -galactosidase (β -Gal) (**Scheme 2.1**).²⁵⁻²⁸



Scheme 2.1. Enzymatic hydrolysis of lactose into glucose and galactose by β -galactosidase (β -Gal). Human β -Gal is a retaining glycosidase (stereochemistry of the starting material is retained in the product) that hydrolyzes the β -glycosidic bond of lactose via a double-displacement reaction mechanism. First, an acidic amino acid residue protonates the glycosidic oxygen and a nucleophilic, basic amino acid residue attacks the anomeric center to facilitate departure of glucose. The resulting galactosyl-enzyme construct is hydrolyzed by a water molecule, with the aid of a basic amino acid residue, to yield galactose and to regenerate the original acidic and basic amino acid residues.

After hydrolysis of the glycosidic bond, glucose enters into circulation where it can be used as an energy source.²⁹ Conversely, galactose must first be converted to glucose in the liver before it can serve as a source of energy. Interestingly, lactose has also been shown to enhance calcium, magnesium, and manganese absorption and retention when compared to other carbohydrate sources such as sucrose, corn starch hydrolysate, and glucose polymers.³⁰⁻³²

Oligosaccharides constitute the other significant carbohydrate component of milk. While the biosynthesis of human milk oligosaccharides (HMOs) will be discussed in depth in section 2.4, a brief description is provided here (**Figure 2.4**).

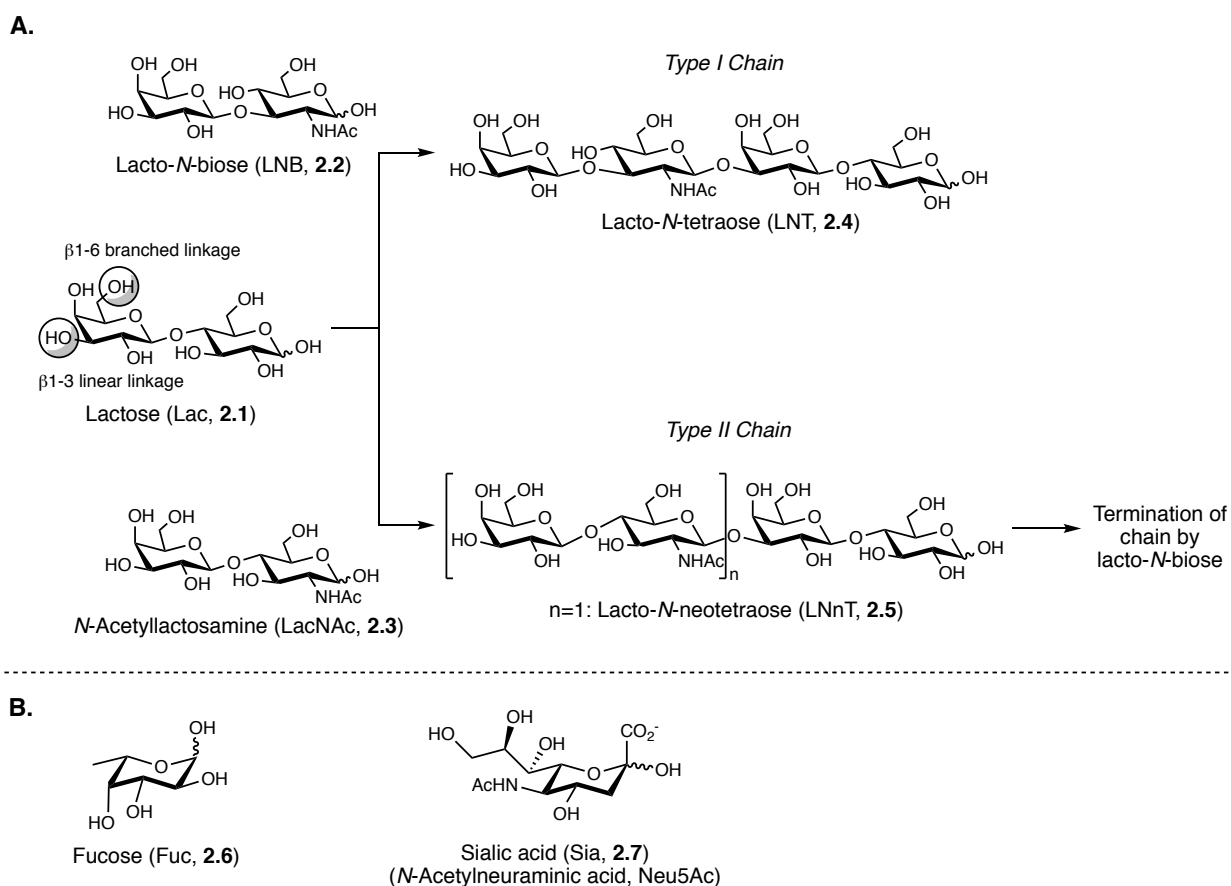


Figure 2.4. HMO structure and biosynthesis. **(A)** General HMO biosynthetic blueprint. **(B)** Structures of fucose (Fuc, **2.6**) and sialic acid (Sia, **2.7**). The growing HMO chains illustrated in **(A)** can be fucosylated and/or sialylated to yield additional HMOs.

All HMOs feature lactose at the reducing end. Lactose (Lac, **2.1**) can be elongated with lacto-*N*-biose (LNB, **2.2**) or *N*-acetyllactosamine (LacNAc, **2.3**) via β 1-3 linear or β 1-6 branched linkages. Elongation via a β 1-3 linkage with one LNB residue yields lacto-*N*-tetraose (LNT, **2.4**), while elongation via a β 1-3 linkage with one LacNAc residue yields lacto-*N*-neotetraose (LNnT, **2.5**). HMO chains can continue to be elongated with LacNAc residues until they are eventually terminated with an LNB residue. Finally, fucose (**2.6**) and/or sialic acid (**2.7**) can be added to the growing HMO chain to generate additional compounds (**Figure 2.4**).

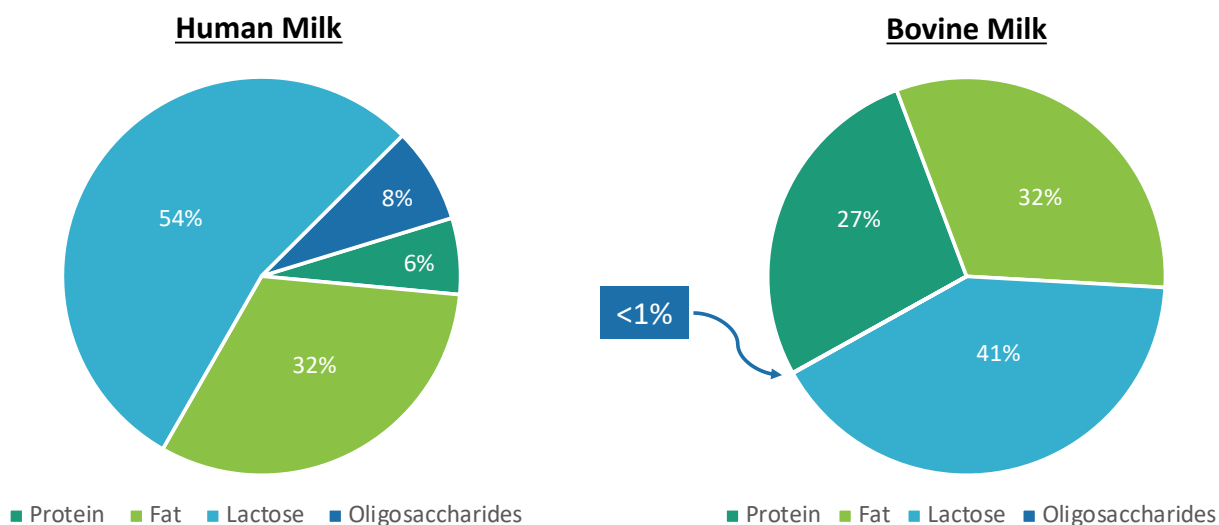


Figure 2.5. Human milk versus bovine milk macromolecular compositions.

Although oligosaccharides are the third largest macromolecular component of human milk, they are largely absent from bovine milk (**Figure 2.5**).^{7, 33, 34} The comparison between HMOs and bovine milk oligosaccharides (BMOs) is an important one to make as bovine milk serves as the basis for most types of infant formula. In addition to differences in concentration, HMOs and BMOs are significantly different in composition. For instance, while the majority of HMOs are fucosylated (50-80%) and the minority

sialylated (10-20%), this trend is reversed for BMOs; around 70% of BMOs are sialylated while only around 1% are fucosylated. Moreover, in contrast to the more than 200 different HMOs that have been identified, only around 40 BMOs have been identified. While HMOs are the focus of this dissertation and will be discussed in depth in the remaining sections of this chapter, a brief introduction is provided here.

HMOs are typically found in mature milk between 5 and 15 g/L. In colostrum, HMO concentration is typically higher at around 20-25 g/L.^{7, 35, 36} As mentioned, over 200 HMOs have been identified in milk, and the prevalence of specific compounds has been found to vary over the course of lactation. For example, fucosylated HMOs are typically found in higher concentrations in colostrum.³⁷ HMO composition is also known to vary from mother to mother on the basis of maternal blood type. Moreover, HMOs differ in composition from those of any other mammal.¹²

Unlike lactose, HMOs cannot be digested by the infant.^{1, 38} Rather, HMOs reach the small intestine intact where they can be broken down into SCFA by saccharolytic colonic bacteria. This accounts for the prebiotic activity of HMOs; a prebiotic is a nondigestible compound in food that promotes the growth or activity of beneficial microorganisms in the intestines. In addition to serving as important prebiotics, HMOs are known for their ability to serve as antiadhesive antimicrobials by serving as soluble decoy receptors for pathogens or pathogenic virulence agents (ex. toxins). This ability is made possible by the resemblance of HMOs to various cell surface glycan receptors. Finally, HMOs have also been shown to modulate host immune and intestinal epithelial cell responses, protect against necrotizing enterocolitis (NEC), and serve as important brain development nutrients. A more detailed explanation of the health benefits of HMOs will

be provided in the proceeding sections of this chapter. As a final note, the numerous health benefits attributed to HMOs coupled with the general lack of analogous BMOs has led to the development of numerous carbohydrate infant formula additives.²³ These additives are designed to mimic the protective properties of HMOs and thus confer similar protections to formula-fed infants as are afforded to breastfed infants.

2.3 Human Milk Oligosaccharides: Discovery and Early Research

In his *Treatise of Physical Upbringing of Children* published in 1760, Desessartz offered some of the first analyses of human milk composition.² In this work, Desessartz compared the composition of human milk to that of cow, goat, sheep, ass, and mare and subsequently concluded that human milk was the best source of infant nutrition. In light of the proposed superiority of human milk, many scientists began trying to develop animal milk-based infant formulas that more closely resembled human milk. By 1883, there were 27 patented brands of infant food.⁴ Despite these attempts, at the end of the 19th century when infant first-year mortality rates reached as high as 30%, it was observed that breastfed infants had significantly lower mortality rates and incidences of diarrhea and other infections than their formula-fed counterparts.^{6, 7} Indeed, breastfed infants were reported to have mortality rates up to 7 times lower than formula-fed infants.⁶

Around this time, Theodor Escherich, a respected pediatrician and microbiologist in Europe, discovered a relationship between intestinal bacteria and the physiology of digestion in infants.^{6, 39} Inspired by this finding as well as the observation that breastfed infants had higher survival rates, in 1900, Ernst Moro, a former student of Escherich's, discovered that fecal bacterial composition varied between breastfed and formula-fed

infants. At the same time and independent of Moro's studies, Henry Tissier, a graduate student at the University of Paris, noted similar compositional differences and is credited with the first isolation of bifidobacteria from the feces of breastfed infants (termed by Tissier in 1899 as *Bacillus bifidus*).⁷ After this discovery, Tissier went on to suggest that the increased levels of bifidobacteria in the feces of breastfed infants was likely the reason for the lower incidences of diarrhea seen in these infants.⁴⁰ It would not be until the collaborative efforts of Paul György, a pediatrician and former student of Moro's, and Richard Kuhn, an accomplished chemist, in the 1950's, however, that HMOs would be identified as the milk component responsible for determining bacterial composition in the infant gut and, by extension, infant feces.

While HMOs would not begin to be isolated cleanly and described clearly until the 1950s, in 1888, the chemist Eschbach noted that human milk contained a "different type of lactose" than bovine milk. Shortly after this assertion, another chemist, Deniges, found that human milk did not in fact contain a "different type of lactose" but rather possessed an additional unknown carbohydrate component.^{6,7} However, the composition of this non-lactose carbohydrate component remained uncharacterized until the work of Michel Polonowski and Albert Lespagnol in the 1930s. Polonowski and Lespagnol established a method to characterize the carbohydrate fraction they termed "gynolactose." They noted that the "gynolactose" component, which was weakly soluble in methanol, was not homogenous but rather consisted of numerous components that contained nitrogen and hexosamines.⁴¹⁻⁴⁴ Around 20 years later in 1954, Polonowski and Jean Montreuil, a pioneer in the field of carbohydrates and glycoconjugates, applied 2-dimensional paper chromatography to separate "gynolactose" into individual compounds.⁴⁵ This work

resulted in isolation of the first individual HMOs, 2'-fucosyllactose (2'-FL, **2.8**) and 3-fucosyllactose (3-FL, **2.9**), though the exact structures and potential functions of these HMOs were unknown at the time of initial discovery (**Figure 2.6**).^{6, 7}

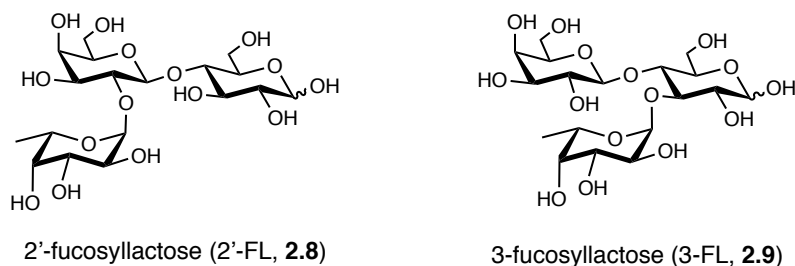


Figure 2.6. Structures of 2'-fucosyllactose (2'-FL, **2.8**) and 3-fucosyllactose (3-FL, **2.9**).

In the years following the initial finding by Moro and Tissier that the feces of breastfed infants featured unique bacterial compositions, there was an intense drive to identify the growth factors in human milk that were responsible. Due to the unique prominence of bifidobacteria in the feces of breastfed infants, the elusive growth factor was termed simply as the “bifidus factor.” In 1926, Herbert Schönfeld made a significant contribution to the search when he reported that the growth-promoting factor for *Bifidobacterium bifidus* (classified as *Lactobacillus bifidus* at the time of Schönfeld’s discovery) was in the nonprotein fraction of milk and was thermoresistant.^{6, 46} While Schönfeld hypothesized that the bifidus factor was a vitamin, less than 30 years later, György and Kuhn provided proof that HMOs were the true bifidus factors.^{6, 47-51} Specifically, they showed that the growth-promoting abilities were unique to the *N*-acetylglucosamine-containing carbohydrate fraction; the nitrogen-free carbohydrate fraction had no bifidogenic effect and neither did the carbohydrates wherein the amine of the *N*-acetylglucosamine component had been liberated via treatment with barium hydroxide.⁵⁰

In the years following György and Kuhn's groundbreaking studies, numerous individual HMOs were discovered and characterized by the groups of Kuhn and Montreuil^{52, 53} including 2'-FL (previously isolated by Polonowski and Montreuil without accompanying structural characterization),⁵⁴ lacto-*N*-tetraose (LNT, **2.4**)⁵⁵, lacto-*N*-fucopentaose I (LNFP I, **2.10**),⁵⁶ lacto-*N*-fucopentaose II (LNFP II, **2.11**),⁵⁷ and difucosyllactose (DFL, **2.12**) (also referred to as lacto-difucosyltetraose: LDFH) (**Figure 2.7**).⁵⁸

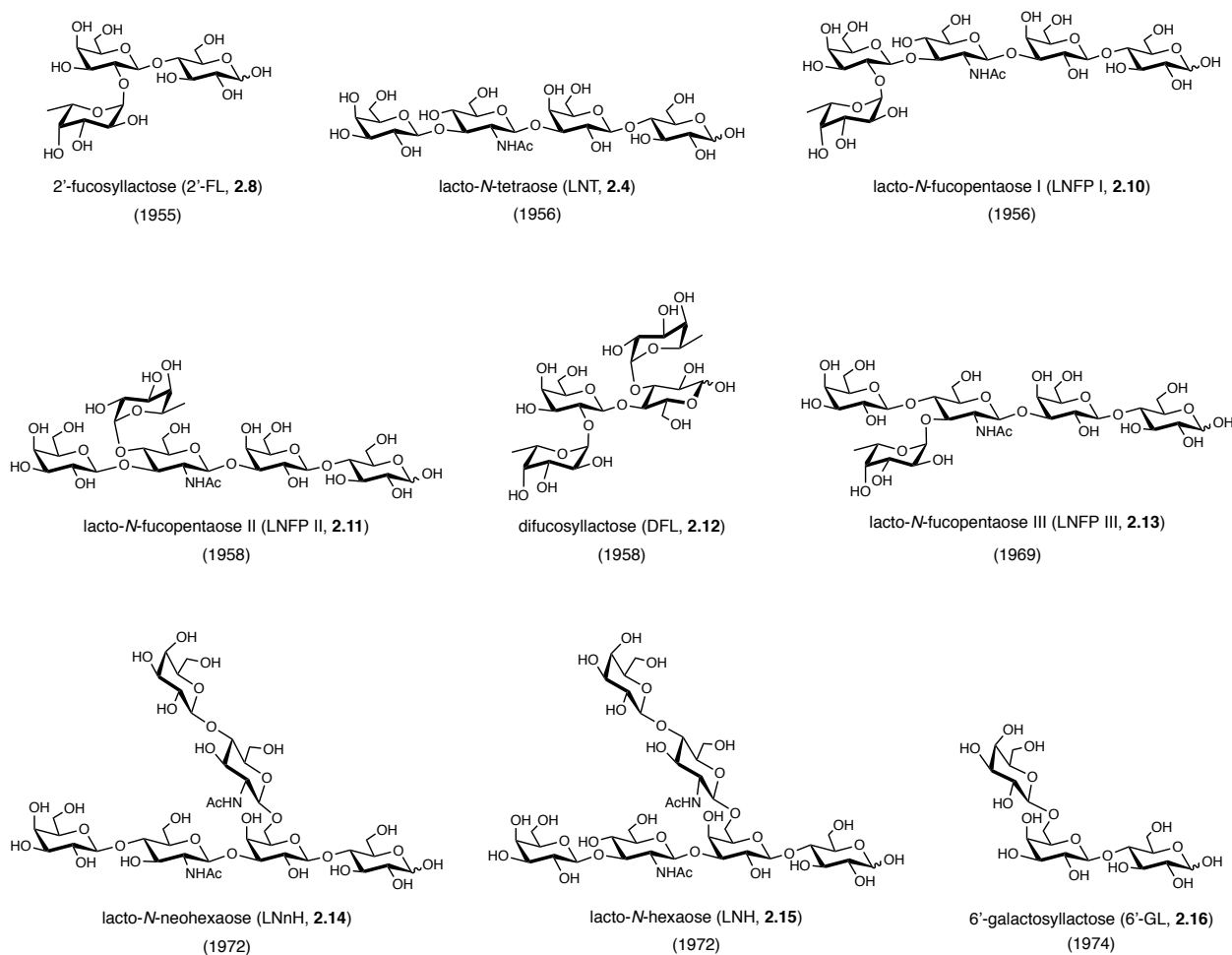


Figure 2.7. Selected HMO structures. Dates in parenthesis indicate year of isolation and characterization.

Shortly after, Akria Kobata and Victor Ginsburg developed a new method to determine oligosaccharide patterns in milk which involved a combination of Sephadex gel filtration and paper chromatography. Using this method in combination with various structural elucidation techniques, Akria and Ginsburg would go on to discover and characterize several new HMOs including lacto-*N*-fucopentaose III (LNFP III, **2.13**),⁵⁹ lacto-*N*-neohexaose (LNnH, **2.14**),⁶⁰ lacto-*N*-hexaose (LNH, **2.15**),⁶¹ and 6'-galactosyllactose (6'-GL, **2.16**) (**Figure 2.7**).⁶²

Importantly, Kobata and Ginsburg's work towards the elucidation of additional HMO structures was driven by previous work from the Ginsburg laboratory that detailed the relationship between oligosaccharide patterns in milk and human blood groups. Throughout the 1960's, Winfred Watkins worked to elucidate the structures of the blood group determinants in the ABO, Lewis (Le), and Secretor (Se) genetic systems,⁶³ see section 2.4 for a more detailed description of these blood group determinants and accompanying structures. Armed with the knowledge of specific structures, Ginsburg and his colleagues demonstrated that oligosaccharide patterns in milk varied with maternal blood type because the enzymes involved in the synthesis of blood group determinants were also involved in the synthesis of HMOs.^{64, 65} For instance, Grollman and Ginsburg reported that while the presence of 2'-FL was independent of the ABO blood group system, there was a direct correlation between the presence of 2'-FL in a particular sample and the Se status of the mother; no 2'-FL was found in the milk or colostrum of non-Secretors.⁶⁶

At the time of this discovery, the structural determinants for other blood types such as M, N, P, and Rh were not as well understood as those for the ABO and Lewis groups.^{64,}

⁶⁷ There was, however, some evidence that carbohydrates were related to specificities for the M, N, P, and Rh blood groups. As a result, Ginsburg and colleagues hypothesized that the presence or absence of certain HMOs might be related to these blood types.⁶⁴ Thus, elucidation of new HMO structures could provide information regarding the structural determinants of additional blood groups. This prospect ultimately led Ginsburg's group to develop new methods to discover previously uncharacterized HMOs.

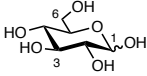
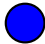
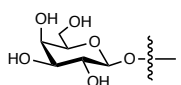

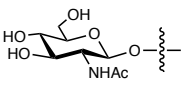

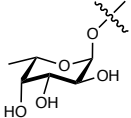

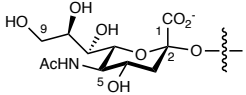

To date, more than 200 HMO structures have been identified.^{34, 68} Moreover, detailed descriptions of the relative concentrations of a long list of HMOs over the course of lactation are now available.^{33, 34, 69} This extensive characterization would not have been possible without the development of numerous, more advanced methods for HMO characterization than those used in the 1960s. Some of the first major advances in HMO characterization came courtesy of Heinz Egge, one of Richard Kuhn's former students. Egge was one of the first to use field desorption or fast atom bombardment (FAB)-mass spectrometry (MS) to characterize HMO structure.^{6, 70} This technique proved highly reliable and allowed for exact determination of molecular composition. Moreover, it facilitated analyses of oligosaccharide mixtures that were not resolved purely by chromatographic methods.⁶

Additional techniques that have been used for structural characterization and quantitation include high performance liquid chromatography (HPLC), high pH anion-exchange chromatography (HPEAC), capillary electrophoresis (CE), nuclear magnetic resonance (NMR), and additional MS techniques including matrix-assisted laser desorption/ionization MS (MALDI-MS).⁷¹⁻⁷⁴ Indeed, MALDI-MS has greatly increased the utility of MS analysis of HMOs.^{33, 75} Nevertheless, even with advanced characterization

techniques, it remains that analysis of HMO composition is challenging due to the number and complexity of HMO structures as well as the variations in HMO patterns seen from mother to mother and over the course of lactation.

2.4 Human Milk Oligosaccharides: Structure and Biosynthesis

Table 2.1. HMO Monosaccharide Building Blocks

Monosaccharides	Abbreviation	Structure	Symbol	Glycosidic linkages in HMOs
Glucose (1.21)	Glc			None*
Galactose (1.22)	Gal			β -linkages
<i>N</i> -Acetylglucosamine (1.4)	GlcNAc			β -linkages
Fucose (2.6)	Fuc			α -linkages
<i>N</i> -Acetylneuraminic acid (2.7) (Sialic acid)	Neu5Ac (Sia)			α -linkages

*Glc is found only at the reducing end of HMOs and consequently exists as a mixture of α and β anomers

Despite the vast array of HMO structures, all HMOs are composed of just five monosaccharide building blocks: glucose (Glc), galactose (Gal), *N*-acetylglucosamine (GlcNAc), fucose (Fuc), and *N*-acetylneuraminic acid (Neu5Ac) (**Table 2.1**).^{7, 34, 76} Neu5Ac is a form of sialic acid (Sia) and is thus far the only form to have been identified in HMOs. Thus, when describing HMO structure, Neu5Ac residues are termed Sia for simplicity. In addition to the simplicity of the building blocks, while HMOs can range

anywhere in size from 3 to 50 monosaccharide residues, all HMO biosyntheses follow the same basic blueprint (**Figure 2.4** and **2.8**).

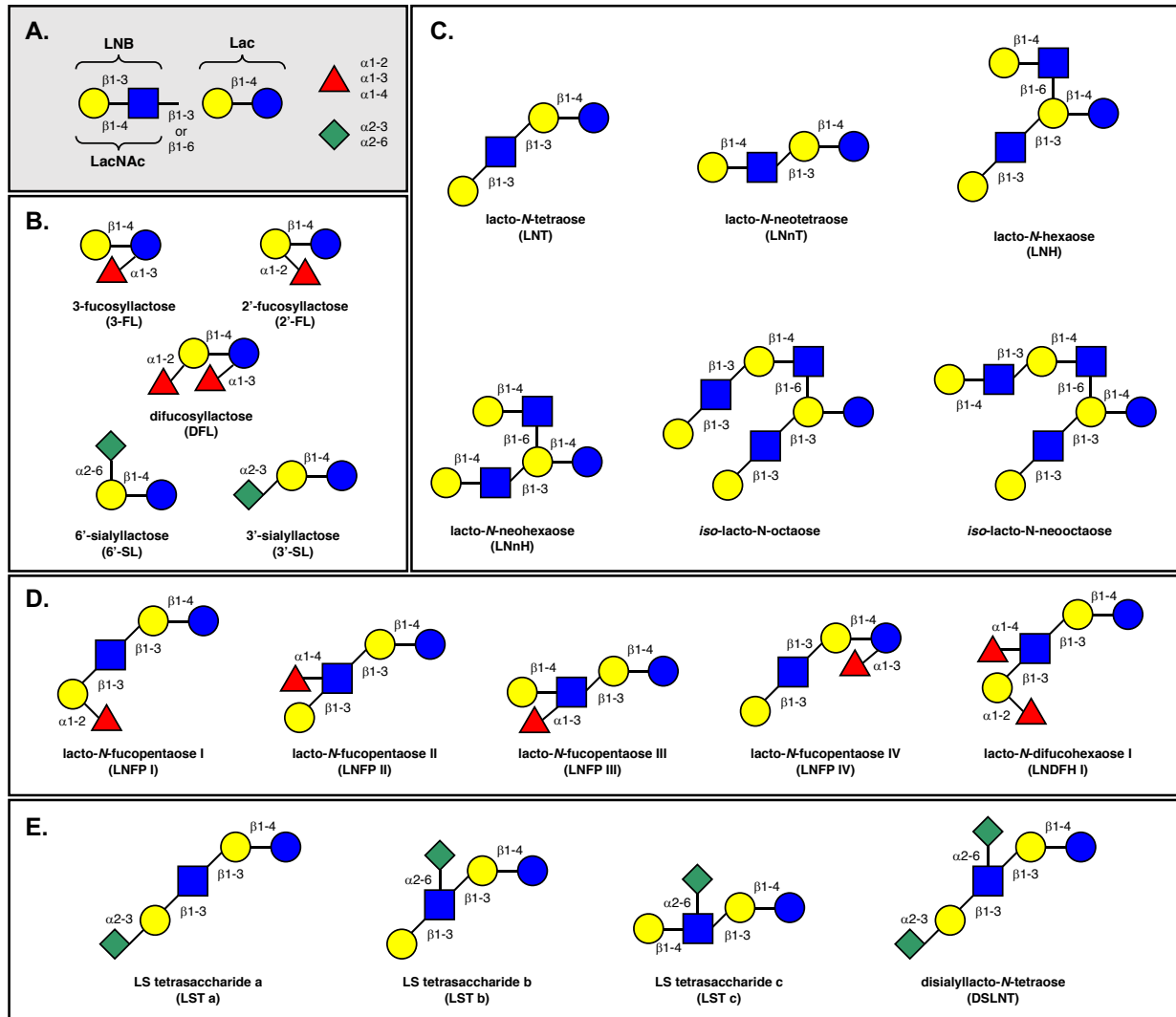


Figure 2.8. HMO biosynthetic blueprint and selected HMO structures. **(A)** General blueprint for HMO biosynthesis (monosaccharides are designated as specified in **Table 2.1**). Lactose can be elongated with lacto-*N*-biose (LNB) or *N*-acetyllactosamine (LacNAc) via a β 1-3 linkage to yield type I and II chains, respectively. Alternatively, lactose can be elongated with LNB or LacNAc via a β 1-6 linkage to introduce branching. Lactose or the growing HMO chain can be fucosylated via α 1-2, 3, or 4 linkages or sialylated via α 2-3 or 6 linkages. **(B)** Selected fucosylated or sialylated lactose HMOs. **(C)** Selected HMO chain structures. **(D)** Selected fucosylated type I and II chains. **(E)** Selected sialylated type I and II chains.

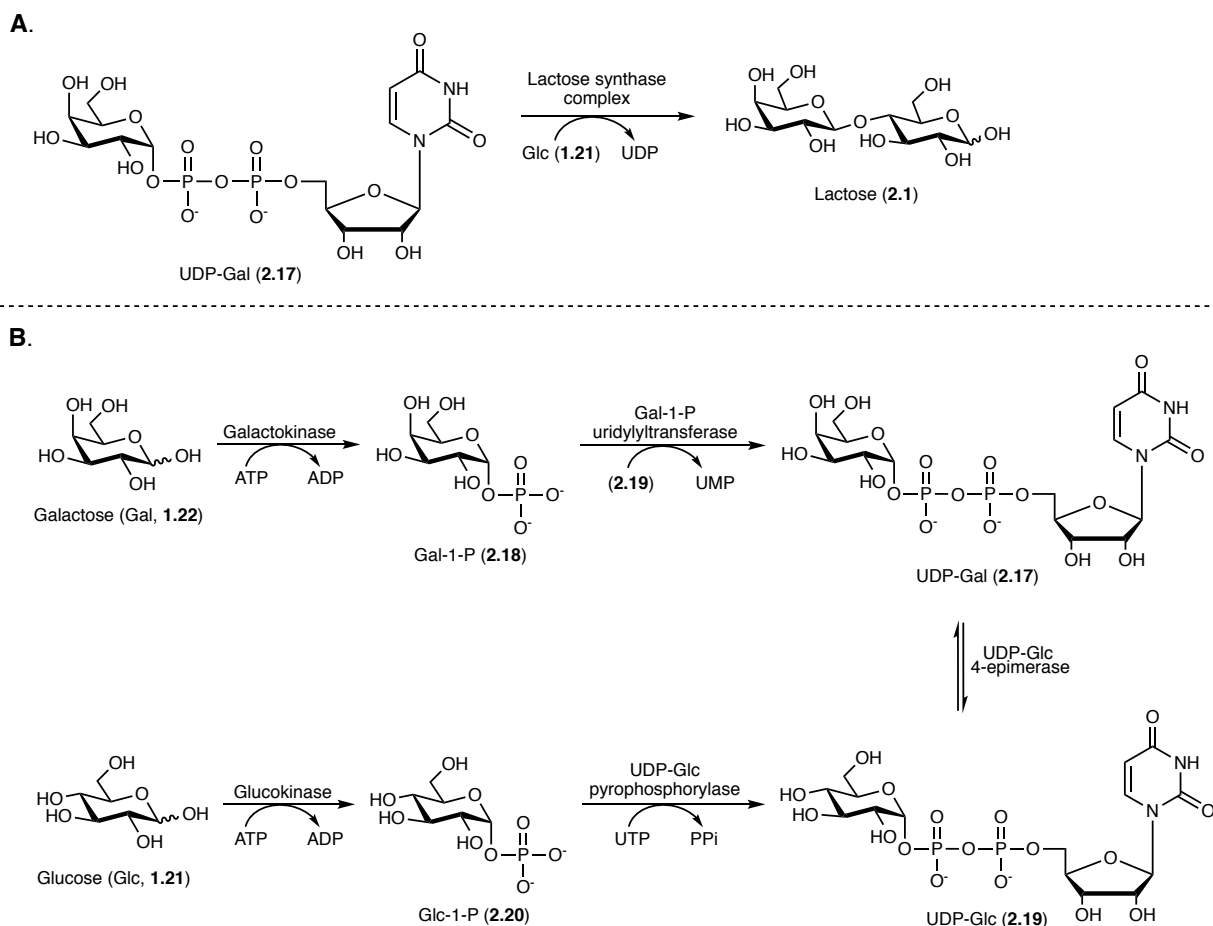
First, all HMOs contain lactose (Lac, Gal β 1-4Glc, **2.1**) at the reducing end. Lactose can then be elongated with either lacto-*N*-biose (LNB, Gal β 1-3GlcNAc, **2.2**) or *N*-acetyllactosamine (LacNAc, Gal β 1-4GlcNAc, **2.3**) via a linear β 1-3 glycosidic linkage to yield type I and II chains, respectively. Alternatively, lactose can be elongated with LNB or LacNAc via a β 1-6 linkage which introduces chain branching. Linear chains are termed *para*-HMOs while branched structures are termed *iso*-HMOs. While lactose can be elongated with multiple LacNAc residues, incorporation of an LNB residue appears to terminate the chain (**Figure 2.8A and C**).

Lactose and/or an elongated oligosaccharide chain can be further elaborated via fucosylation or sialylation (**Figure 2.8B, D, and E**). Specifically, fucose (**2.6**) can be incorporated via α 1-2, α 1-3, or α 1-4 linkages while sialic acid (**2.7**) can be incorporated via α 2-3 or α 2-6 linkages. Due to the various potential sites for fucosylation and sialylation, some HMOs exist in multiple isomeric forms. For example, lacto-*N*-fucopentaose (LNFP) exists in three forms: LNFP I, II, and III. Similarly, sialyllacto-*N*-tetraose (LST) exists in two forms: LST a and LST b.

While the general blueprints for HMO biosynthesis are known, our understanding of the exact biomechanical machinery involved in HMO biosynthesis remains limited.^{7,77} Additionally, the order of operations is not clearly understood. As all HMOs feature lactose at the reducing end, it is hypothesized that HMO biosynthesis is simply an extension of lactose biosynthesis catalyzed by glycosyltransferases in the mammary gland. However, most of the proposed glycosyltransferases have yet to be identified.⁷⁷

Lactose itself is synthesized in the mammary gland by the lactose synthase complex through the transfer of uridine 5'-diphosphate galactose (UDP-Gal, **2.17**) to

glucose (**1.21**) (**Scheme 2.2A**).^{23, 78} While plasma glucose is the main carbon source for lactose biosynthesis, glucose and galactose can also be synthesized in the mammary gland through a process known as hexoneogenesis. In this process, glycerol serves as a precursor for a large amount of galactose and a minor amount of glucose.^{79, 80} Other studies have shown by orally administering ¹³C-labeled galactose to lactating mothers that a portion of dietary galactose may be used directly in lactose biosynthesis.⁸¹



Scheme 2.2. Lactose biosynthesis. **(A)** Lactose biosynthesis from UDP-Gal and glucose. **(B)** Generation of uridine 5'-diphosphate galactose (UDP-Gal) starting from galactose and glucose. Abbreviations: ATP, adenosine triphosphate; ADP, adenosine diphosphate; UTP, uridine triphosphate; UDP, uridine diphosphate; PPi, pyrophosphate.

UDP-galactose can be synthesized directly from galactose in two steps: phosphorylation of galactose (**1.22**) by galactokinase to yield galactose 1-phosphate

(**2.18**) followed by transfer of uridine 5'-monophosphate (UMP) from UDP-glucose (**2.19**) by galactose 1-phosphate uridylyltransferase.^{23, 78} Alternatively, UDP-galactose can be synthesized from glucose in three steps: phosphorylation of glucose by glucokinase to yield glucose 1-phosphate (**2.20**), conversion of glucose 1-phosphate to UDP-glucose (**2.19**) by UDP-glucose pyrophosphorylase, and epimerization of the C4 center of UDP-glucose by UDP-glucose 4-epimerase (**Scheme 2.2B**).^{23, 78}

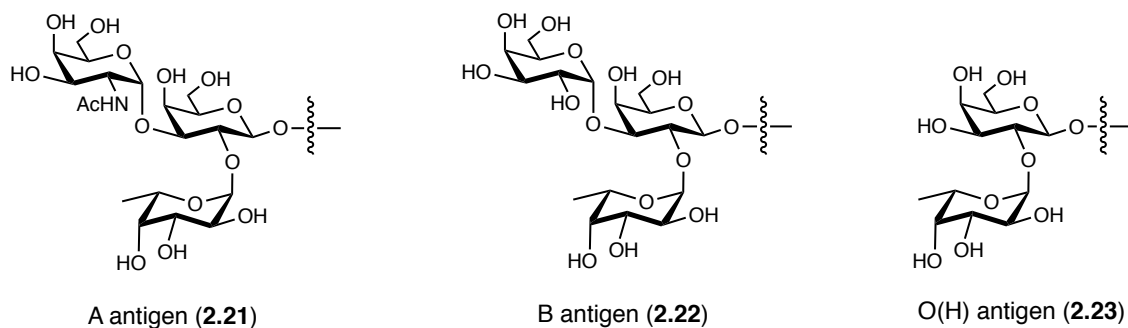
The lactose synthase complex consists of two proteins: galactosyltransferase and α -lactalbumin. Although galactosyltransferase is found outside the mammary gland, α -lactalbumin is expressed solely in the mammary gland and is key to lactose production.^{82, 83} Specifically, α -lactalbumin, whose expression is controlled by lactation hormones, promotes the preferential selection of glucose by galactosyltransferase.^{7, 23} In the absence of α -lactalbumin, glucose is a poor substrate, and galactosyltransferase will instead catalyze the transfer of UDP-galactose to GlcNAc. In the presence of α -lactalbumin, however, the K_m of galactosyltransferase for glucose is reduced by three orders of magnitude which resultantly allows for lactose synthesis at physiological glucose concentrations.^{23, 83}

While lactose synthesis is fairly well understood, the ways in which lactose is elongated is much less understood.⁷ This lack of understanding is at least partly attributable to the vastly different oligosaccharide compositions and concentrations in human milk versus animal milk. Indeed, these differences complicate any attempt to study HMO biosynthesis in animal models. For example, while mice models would be readily available, mice only produce 3'- and 6'-sialyllactose (3'-SL and 6'-SL, respectively) and thus are not suitable to study the biosynthesis of elongated or fucosylated

oligosaccharides.⁸⁴ Another roadblock is the limited success researchers have had using immortalized or transformed human mammary gland epithelial cells to study HMO biosynthesis.⁷

In contrast to lactose elongation, HMO fucosylation is a fairly well-understood process due to its direct link to maternal Secretor (Se) and Lewis (Le) blood groupings.⁷ To understand this linkage, it is important to digress momentarily into a discussion of ABO(H), Secretor, and Lewis blood group antigen determinants. The ABO system is characterized by the presence or absence of the A, B, and/or H antigens (**2.21**, **2.22**, and **2.23**, respectively) on red blood cell membranes (**Figure 2.9**).

A.



B.

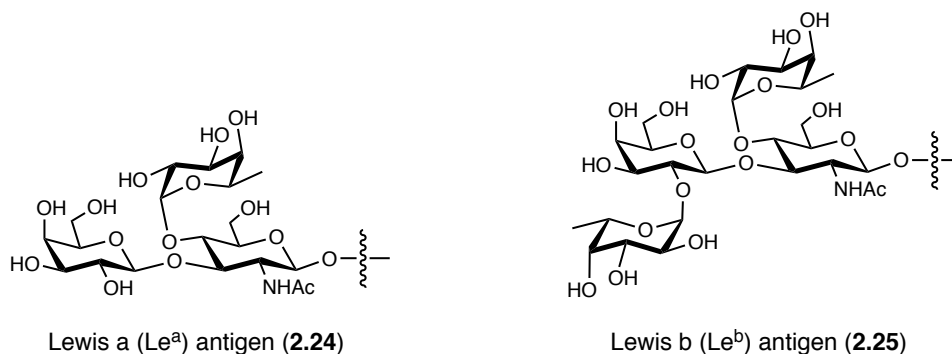
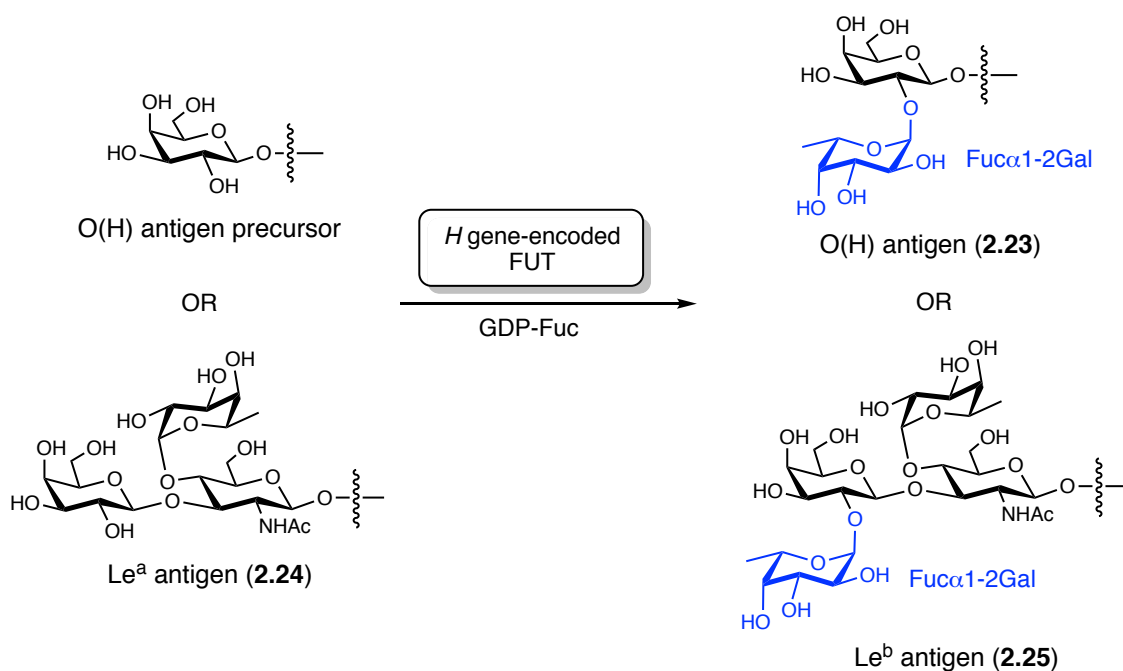


Figure 2.9. Structures of blood group antigens. **(A)** Structures of the A, B, and H antigens of the ABO blood group. **(B)** Structures of the Lewis a (Le^a) and Lewis b (Le^b) antigens of the Lewis (Le) blood group. Antigens are bound to various carbohydrate cores of glycoproteins and glycolipids that are not characteristic of a specific blood group.

Type A blood has only A antigens on red blood cells, type B has only B antigens, and type AB has both antigens. Type O blood is characterized by the absence of both the A and B antigens and the presence of the H antigen; the H antigen is a truncated form of the A and B antigens. In addition to expressing A, B, and/or H antigens on the surfaces of red blood cells, Secretors express these antigens in exocrine secretions corresponding to their individual blood type. Conversely, non-Secretors only express these antigens on red blood cell membranes. Finally, Lewis blood types are defined by the presence or absence of the Le^a and Le^b antigens (2.24 and 2.25, respectively) (Figure 2.9); Le(a +) blood types have only the Le^a antigen, Le(b +) have only the Le^b antigen, and Le(a-b-) have neither antigen.



Scheme 2.3. Activity of a hypothesized *H* gene-encoded fucosyltransferase (FUT). Watkins and Morgan hypothesized that an *H* gene encoded a FUT that was responsible for formation of the Fuc α 1-2Gal bonds in the H and Le^b blood group antigens. The added fucose residue is highlighted in blue. Abbreviations: GDP-Fuc, guanosine 5'-diphosphofucose.

Given these antigen determinant structures, it was proposed by Watkins and Morgan that variations in blood groups resulted from a genetically determined presence or absence of particular glycosyltransferases.^{85, 86} They hypothesized that the “*H* gene” was responsible for the fucosyltransferase (FUT) that catalyzes, one, the addition of fucose to galactose via an α 1-2 glycosidic linkage to generate the H antigen, and, two, the addition of fucose to the Le^a antigen, again via α 1-2 glycosidic linkage, to generate the Le^b antigen (**Scheme 2.3**). Furthermore, they noted that absence of this *H* gene-encoded FUT in the secretory organs of non-Secretors would result in the inability of non-Secretors to synthesize A, B, or H antigens; they could, however, still secrete the Le^a antigen as this antigen lacks the Fuc α 1-2Gal moiety. They thus also hypothesized that expression of the *H* gene in secretory organs would be controlled by the *Se* gene.

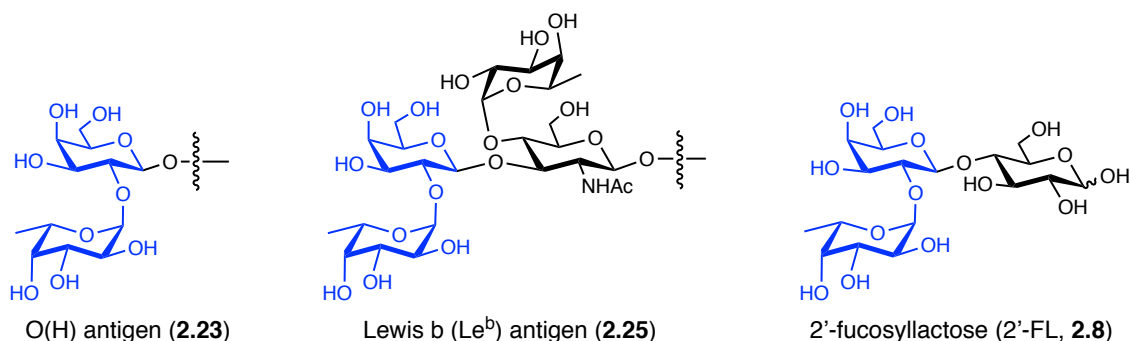
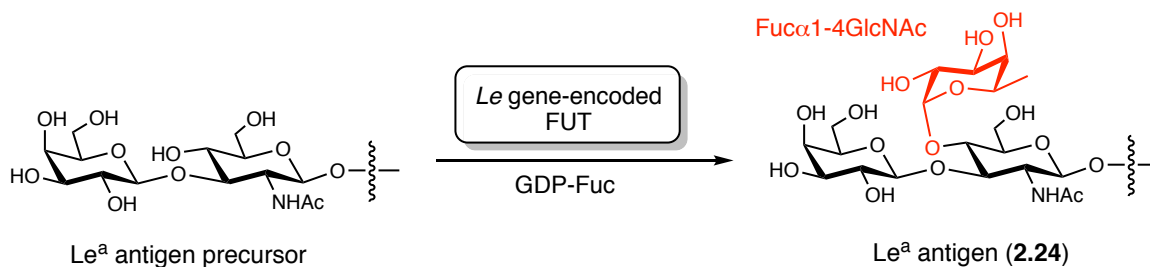


Figure 2.10. Structural similarities between blood group antigens H (**2.23**) and Le^b (**2.25**) and human milk-derived oligosaccharide 2'-fucosyllactose (2'-FL, **2.8**). The Fuc α 1-2Gal linkage moiety common to all structures is highlighted in blue.

These hypotheses were supported by Grollman and Ginsburg when they found that 2'-FL, an HMO that contains a Fuc α 1-2Gal linkage, was found only in the milk of Secretors (**Figure 2.10**).⁶⁶ This suggested that the FUT involved in the synthesis of 2'-FL was also involved in the synthesis of secreted blood group antigens, and that the presence or absence of this FUT determined maternal Secretor status.⁸⁷ Because FUTs

are found in human milk in soluble form, Grollman and Ginsburg were able to confirm a relationship between this FUT and Secretor status by comparing the ability of milk samples from Secretors and non-Secretors to transfer fucose, derived from GDP-fucose (guanosine 5'-phosphate fucose), to the C2-position of galactose. Only the milk of Secretors was able to catalyze this transfer. Importantly, this suggested that as originally hypothesized by Watkins and Morgan, Secretor status was characterized by the presence or absence of a specific FUT termed by Ginsburg and colleagues as GDP-L-fucose: β -D-galactosylsaccharide α -2-L-fucosyltransferase.⁸⁷

In addition to an *H* gene-encoded FUT, Watkins and Morgan also proposed that the *Le* gene encoded for a FUT that catalyzed the addition of fucose to GlcNAc via an α 1-4 linkage in the synthesis of the Le^a and Le^b antigens (**Scheme 2.4**).⁸⁶ Thus, individuals lacking this enzyme would not be able to synthesize either antigen, and their blood type would resultantly be $Le(a-b-)$. Based on their earlier work which demonstrated that the $Fuc\alpha$ 1-2Gal linkages of HMOs and blood group antigens were formed by the same FUT, Ginsburg and colleagues hypothesized that the $Fuc\alpha$ 1-4Gal linkages of HMOs and the Lewis antigens were similarly formed by the same FUT.



Scheme 2.4. Activity of a hypothesized *Le* gene-encoded fucosyltransferase (FUT). Watkins and Morgan hypothesized that an *Le* gene encoded a FUT that was responsible for formation of the $Fuc\alpha$ 1-4GlcNAc bonds in the Le^a and, by extension, the Le^b blood group antigens. The added fucose residue is highlighted in red. Abbreviations: GDP-Fuc, guanosine 5'-diphospho-fucose.

At the time of their hypothesis, two HMOs were known which featured Fuc α 1-4GlcNAc linkages: LNFP II (**2.11**) and LNDFH I (**2.26**) (**Figure 2.11**). If their hypothesis was correct, these HMOs should be present in the milk of Le(a+) and Le(b+) mothers but absent in Le(a-b-) mothers. Indeed, this is precisely what they observed.⁶⁵ Moreover, they found heightened levels of LNFP I (**2.10**, **Figure 2.11**), the precursor to LNDFH I, in the milk of Le(a-b-) mothers compared to the milk of Le(b+) mothers. To further support these findings, Ginsburg et al. also tested milk samples from the three Lewis blood types for the ability to catalyze the transfer of fucose from GDP-fucose to LNFP I to form LNDFH I. Consistent with previous results, only the milk from Le(a+) and Le(b+) mothers possessed the enzyme capable of completing this transformation.

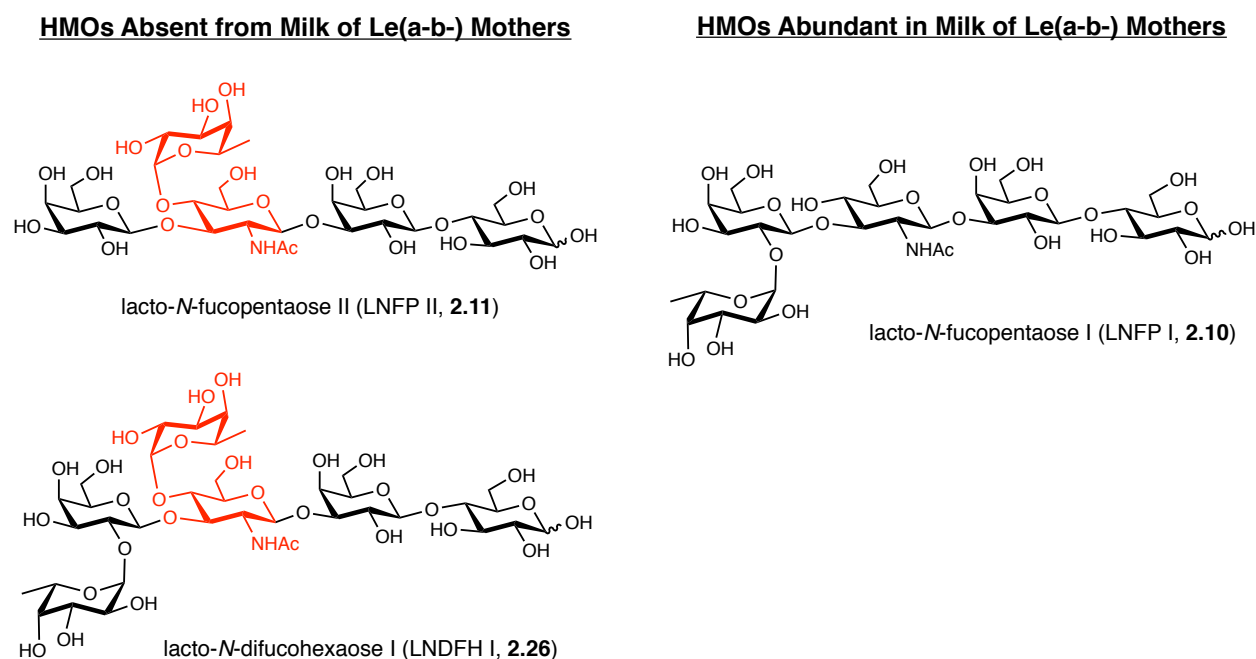
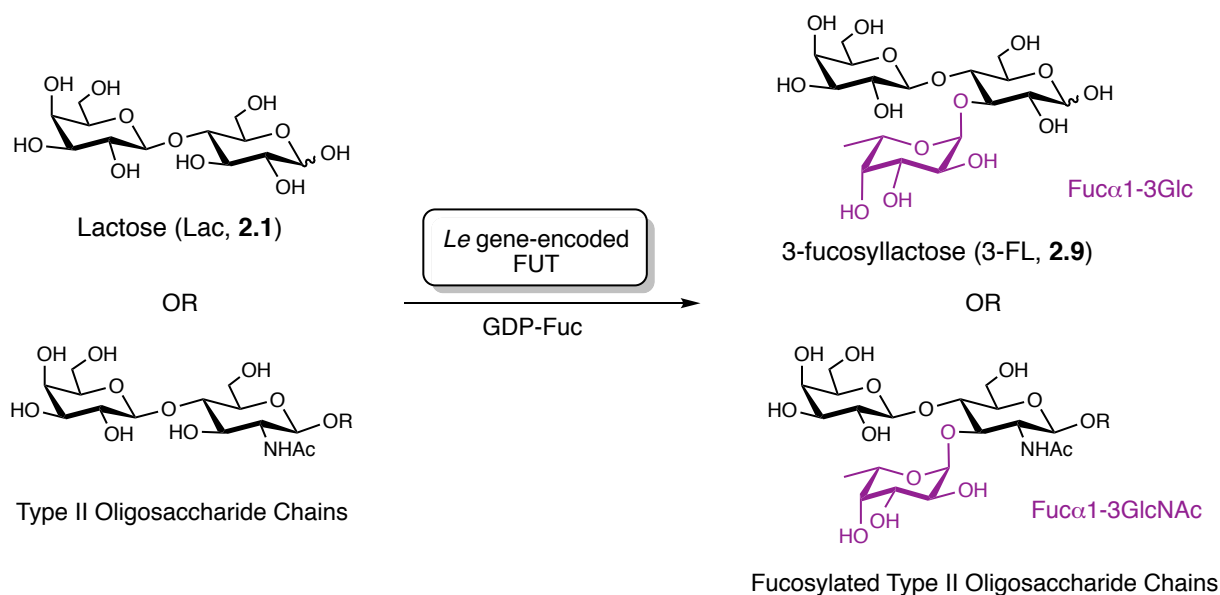


Figure 2.11. Experimental evidence that the fucosyltransferase (FUT) responsible for formation of the Fuc α 1-4GlcNAc bond of Lewis blood group antigens is also responsible for formation of the Fuc α 1-4GlcNAc bond of HMOs like LNFP II (**2.11**) and LNDFH I (**2.26**). Milk of Lewis negative mothers did not have LNFP II or LNDFH I, but did have heightened levels of LNFP I (**2.10**), the precursor to LNDFH I. The Fuc α 1-4GlcNAc moiety common to the Lewis blood group antigens, LNFP II, and LNDFH I is highlighted in red.

In a separate study which detailed the isolation and characterization of LNFP III (2.13, Figure 2.12), Kobata and Ginsburg provided evidence that the *Le* gene-encoded FUT might also be responsible for adding fucose to GlcNAc of type II chains and the glucose moiety of lactose via α 1-3 linkages (Scheme 2.5).⁵⁹



Scheme 2.5. Additional hypothesized activity of an *Le* gene-encoded fucosyltransferase (FUT). Kobata and Ginsburg hypothesized that the *Le* gene-encoded FUT was also responsible for formation of the $\text{Fuc}\alpha$ 1-3Glc bond of fucosylated lactose derivatives as well as the $\text{Fuc}\alpha$ 1-3GlcNAc bond in type II oligosaccharide chains. The added fucose residue is highlighted in purple. Abbreviations: GDP-Fuc, guanosine 5'-diphospho-fucose.

In the course of their characterizations, Kobata and Ginsburg found that LNFP III was present in 3 out of 4 milk samples from *Le*(a-b-) donors.⁵⁹ Importantly, the sample that lacked LNFP III also lacked all HMOs with $\text{Fuc}\alpha$ 1-3Glc linkages, such as 3-FL and DFL (Figure 2.12). Based on this result, they hypothesized that the FUT responsible for formation of the $\text{Fuc}\alpha$ 1-3GlcNAc bond in LNFP III was also responsible for formation of the $\text{Fuc}\alpha$ 1-3Glc bond in other oligosaccharides like 3-FL and DFL.

HMOs Absent from Milk of an Le(a-b-) Mother

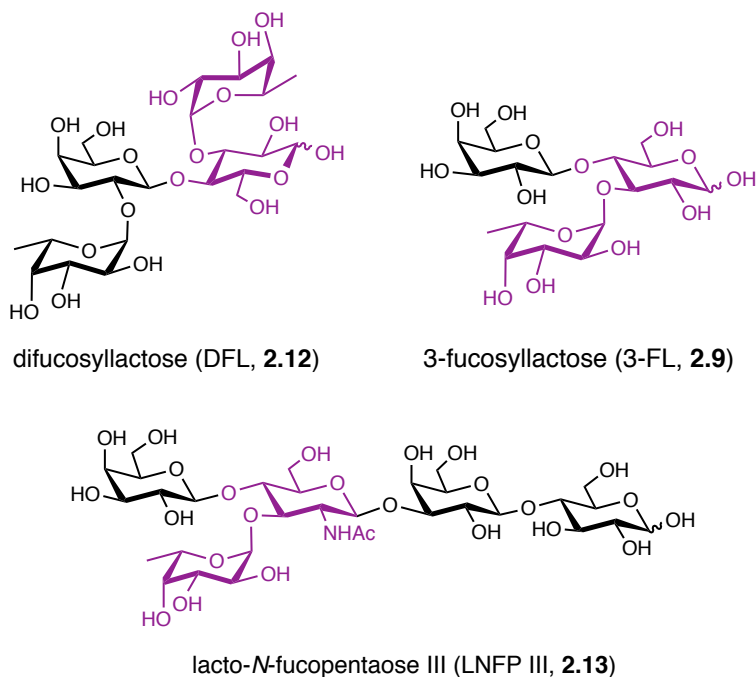


Figure 2.12. Experimental evidence that the fucosyltransferase (FUT) responsible for formation of the $\text{Fuc}\alpha 1\text{-4GlcNAc}$ bond of Lewis blood group antigens might also be responsible for formation of the $\text{Fuc}\alpha 1\text{-3GlcNAc}$ bond of HMOs like DFL (**2.12**), 3-FL (**2.9**), and LNFP III (**2.12**). The milk of a Lewis negative mother did not have DFL, 3-FL, or LNFP III all of which possess a $\text{Fuc}\alpha 1\text{-3GlcNAc}$ bond. The common $\text{Fuc}\alpha 1\text{-3GlcNAc}$ moiety is highlighted in purple.

In a later report by Watkins et al. investigating the occurrence of FUT activity in the saliva of individuals of differing Lewis blood types, it was observed that $\text{Fuc}\alpha 1\text{-3GlcNAc}$ FUT activity was independent of Lewis blood group while $\text{Fuc}\alpha 1\text{-3Glc}$ FUT activity was unique to donors expressing the *Le* gene.⁸⁸ Indeed, only the FUT dependent on *Le* gene expression was able to catalyze the transfer of fucose to the C3 position of glucose. This work demonstrated that the *Le* gene-encoded FUT was indeed an $\alpha 1\text{-3/4}$ FUT, not just an $\alpha 1\text{-3}$ FUT. However, there have been conflicting reports about the ability of this FUT to also catalyze the transfer of fucose to the C3 position of GlcNAc in type II chains.⁸⁹⁻⁹¹

Today, the *Le* gene-encoded enzyme is referred to as the α 1-3/4 fucosyltransferase FUT3.⁷ The enzyme originally termed by Ginsburg et al. as GDP-L-fucose: β -D-galactosylsaccharide α -2-L-fucosyltransferase is known today as the *Se* gene-encoded α 1-2 fucosyltransferase FUT2 (**Table 2.2**). Contrary to the original hypothesis of Watkins, however, it has been demonstrated that the *Se* gene does not regulate expression of the *H* gene, and by extension the α 1-2 FUT that synthesizes the blood group H antigen, in secretory tissues.^{86, 92} Indeed, it was found that the *H* and *Se* genes are both structural genes that encode distinct FUTs in different tissues (FUT1 and FUT2 for the *H* and *Se* genes, respectively).^{92, 93}

Table 2.2. *Le* and *Se* Gene-Encoded Fucosyltransferases

Gene	Fucosyltransferase (FUT) Encoded	HMO Glycosidic Bond Formed
<i>Se</i> (Secretor)	FUT2	Fuc α 1-2Gal
<i>Le</i> (Lewis)	FUT3	Fuc α 1-3GlcNAc

Based on the expression of FUT3 and FUT2 (corresponding to *Le* and *Se* blood types, respectively), human milk can be divided into four groups with each group corresponding to a particular Lewis blood group: *Le*-positive Secretors (*Se+Le+*), *Le*-positive non-Secretors (*Se-Le+*), *Le*-negative Secretors (*Se+Le-*), and *Le*-negative non-Secretors (*Se-Le-*).⁷ A schematic showing the HMO fucosylation patterns characteristic of these four groups is provided (**Figure 2.13**). It is important to note, however, that this classification system is an oversimplification of HMO expression. For example, in one study, Newburg and colleagues found α 1-2 fucosylated HMOs in the milk of both Secretors and non-Secretors, though these HMOs were not found in the milk of non-

Secretors until late in lactation.⁹⁴ Additionally, it has also been found that the milk of Le negative non-Secretors, i.e. mothers who lack both FUT2 and FUT3, is not completely devoid of fucosylated HMOs like 3-FL and LNFP III.⁷

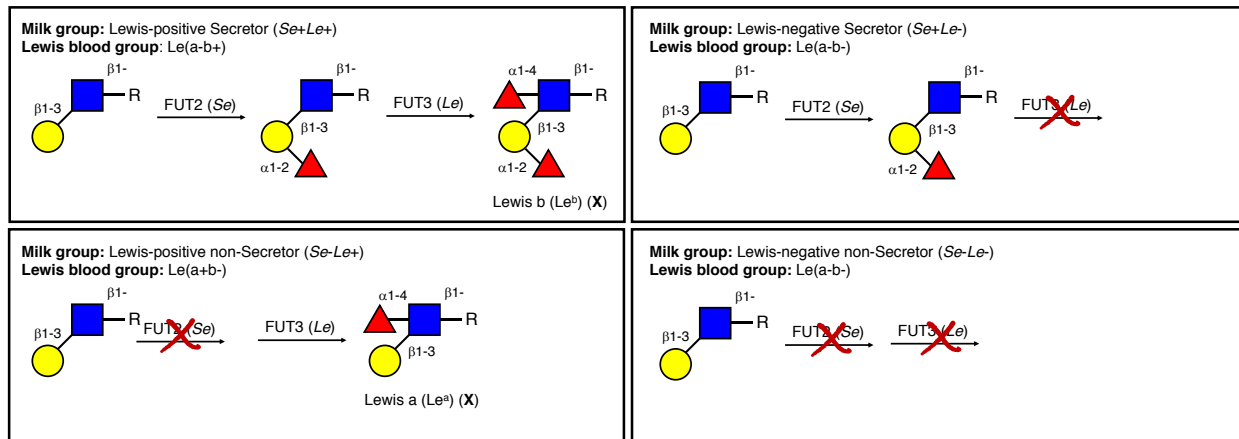
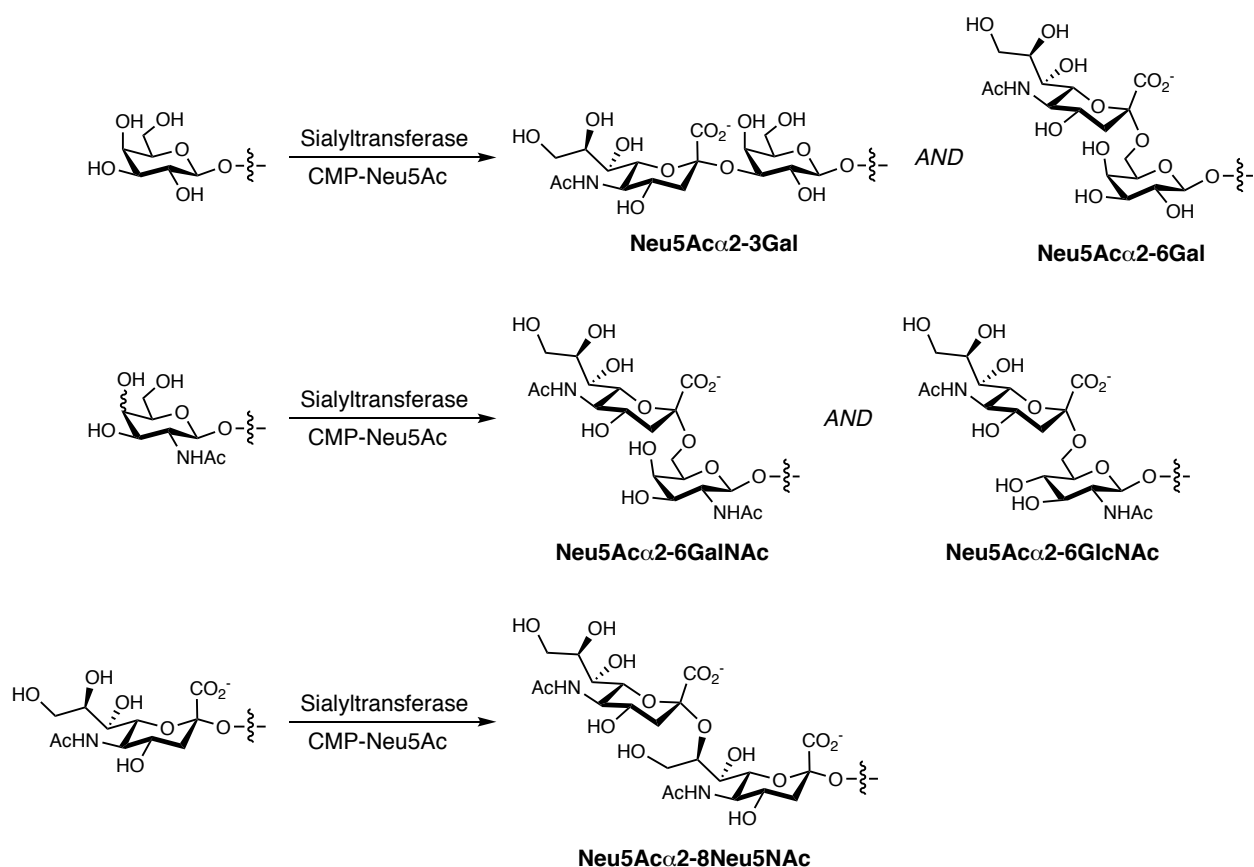


Figure 2.13. Human milk groups based on HMO fucosylation patterns. HMO fucosylation patterns are highly dependent on maternal Se- and Le-blood group status: the Se gene encodes FUT2 which adds Fuc to terminal Gal residues via an α 1-2 linkage; the Le gene encodes FUT3 which adds Fuc to subterminal GlcNAc residues of type I HMO chains via an α 1-4 linkage. When both FUT2 and FUT3 are both expressed, milk contains HMOs with the Le^b antigen moiety. When only FUT3 is expressed, milk contains HMOs with the Le^a antigen moiety. When FUT3 is not expressed, milk does not contain HMOs with the Le^a or Le^b antigen moieties.

Deviations from “typical” HMO fucosylation patterns based on Se and Le blood groups suggest the involvement of additional FUTs not expressed by either the Se or Le genes. To date, thirteen FUTs have been identified in the human genome.⁹³ Of these, FUT1 is an α 1-2 FUT and has been postulated to be involved in the production of α 1-2 fucosylated HMOs at certain stages in lactation. FUT4-7 and 9 are FUTs belonging to the α 1-3 FUT family and have been suggested to be involved in the synthesis of α 1-3 fucosylated HMOs.⁹³⁻⁹⁵

Unlike HMO fucosylation, HMO sialylation is not well-understood. To date, twenty human sialyltransferases (ST) have been identified, and these enzymes are responsible

for the transfer of sialic acid from cytidine 5'-monophospho-*N*-acetylneuraminic acid (CMP-Neu5Ac) to oligosaccharide chains of glycoproteins and glycolipids.⁹⁶ STs can add sialic acid via α 2-3 or -6 linkages to galactose, an α 2-6 linkage to *N*-acetylgalactosamine (GalNAc, **1.23**) or GlcNAc, or an α 2-8 linkage to another sialic acid residue (polysialic acid) (**Scheme 2.6**). Based on these regioselectivities and acceptor specificities, human STs can be grouped into four subfamilies: ST3Gal (1-6), ST6Gal (1 and 2), ST6GalNAc (1-6), and ST8Sia(1-6).^{97, 98}



Scheme 2.6. Patterns of sialyltransferase (ST)-catalyzed addition of *N*-acetylneuraminic acid (Neu5Ac) to oligosaccharide chains. Abbreviations: CMP-Neu5Ac, cytidine 5'-monophospho-*N*-acetylneuraminic acid.

Of the twenty human STs, ST3Gal4 and ST6Gal1, which add sialic acid via α 2-3 and -6 linkages to galactose, respectively, are thought to be involved in HMO sialylation.

Using a mouse model, Fuhrer et al. discovered that these STs had heightened expression levels and were two of the three most abundant ST transcripts in the lactating mammary gland.⁸⁴ The involvement of ST3Gal4 and ST6Gal1 in milk oligosaccharide biosynthesis was then confirmed by analyzing milk oligosaccharide content of *St3gal4* and *St6gal1* knockout mice; the milk of *St3gal4* knockout mice showed significant decreases in 3'-SL concentrations, and the milk of *St6gal1* knockout mice was devoid of 6'-SL. Nevertheless, it remains unknown if these STs are able to sialylate the terminal galactose residues of more structurally complex HMOs. A more recent study using recombinant human ST3Gal4 and ST6Gal1 (expressed in *Escherichia coli*) provided additional evidence that ST3Gal4 and ST6Gal1 are at least partly responsible for the sialylation of lactose to yield 3'- and 6'-SL, respectively.⁹⁸

Interestingly, although HMOs contain Sia α 2-6GlcNAc linkages, to date, no ST6GlcNAc sialyltransferases have been found in humans. Conversely, six ST6GalNAc human sialyltransferases have been identified.^{96, 99} There is some evidence that ST6GalNAc5 could be partially involved in HMO biosynthesis. In certain colon cancer lines, ST6GalNAc5 was found to add sialic acid to subterminal GlcNAc residues through an α 2-6 linkage to yield disialyl lactotetraosylceramide (disialyl Lc4). Sialylation of the terminal galactose residue of disialyl Lc4 through an α 2-3 linkage was, however, found to be a prerequisite for this enzymatic action.¹⁰⁰ Given this requirement, ST6GalNAc5 could potentially be involved in the synthesis of HMOs like DSLNT (see **Figure 2.7E**) which feature both terminal Sia α 2-3Gal and subterminal Sia α 2-6GlcNAc moieties.

2.5 Human Milk Oligosaccharides: Health Benefits

Since their debut in the mid-20th century as the *Bifidobacterium bifidus* growth-promoting factor of human milk (i.e. the “bifidus factor”), the benefits of HMOs have been shown to extend well beyond this prebiotic function. Indeed, it well-established that breastfed infants experience decreased instances of diarrhea, respiratory infection, urinary tract infection, ear infection, necrotizing enterocolitis (NEC), and sudden infant death syndrome (SIDS).¹ While the prebiotic role of HMOs can help to protect infants against disease (discussed in more detail below), protection from disease is largely attributable to the ability of HMOs to serve as antiadhesive antimicrobials. Due to their importance in the HMO-fostered protection against infectious disease, the prebiotic and antiadhesive roles of HMOs will be discussed in further detail in the remainder of this chapter. While the following functions will not be discussed in further detail, it is important to note that HMOs also serve as modulators of intestinal epithelial cell responses, modulators of immune responses, and brain development nutrients.^{7, 69, 76, 77}

2.5.1 Prebiotics

A prebiotic is broadly-defined as a non-digestible food substance that, when consumed, selectively stimulates the growth of colonic bacteria to improve host health.¹⁰¹ For the first of these criteria, i.e. non-digestible, a compound must resist gastric acidity, hydrolysis by host enzymes, and intestinal absorption. HMOs fulfill these criteria as the overwhelming majority reach the distal intestine in-tact; only ~1% are absorbed into circulation.^{1, 102, 103} Moreover, a portion of HMOs pass through the distal intestine in-tact and are excreted in urine and feces.^{7, 77, 104, 105}

It is well-established that HMOs also fulfill the second criteria of a prebiotic. As previously described, HMOs were first touted for their ability to promote the growth of the symbiotic colonic bacterial species *Bifidobacterium bifidus* back in the 1950s.⁴⁷⁻⁵⁰ Since the 1950s, HMOs have also been shown to promote the growth of other bifidobacteria species including *B. longum* subsp. *infantis* and *B. longum* subsp. *longum*.¹ Moreover, the growth of several species of *Bacteroides*, another class of intestinal symbiote, have been found to be promoted by HMOs such as 2'-FL, 3-FL, 3'-SL, and 6'-SL (**Figure 2.14**). Unlike bifidobacteria and *Bacteroides*, lactobacilli, a third class of intestinal symbiote, are largely unable to catabolize HMOs.^{1, 106, 107} A summary of HMO prebiotic activity is provided in **Table 2.3**.¹

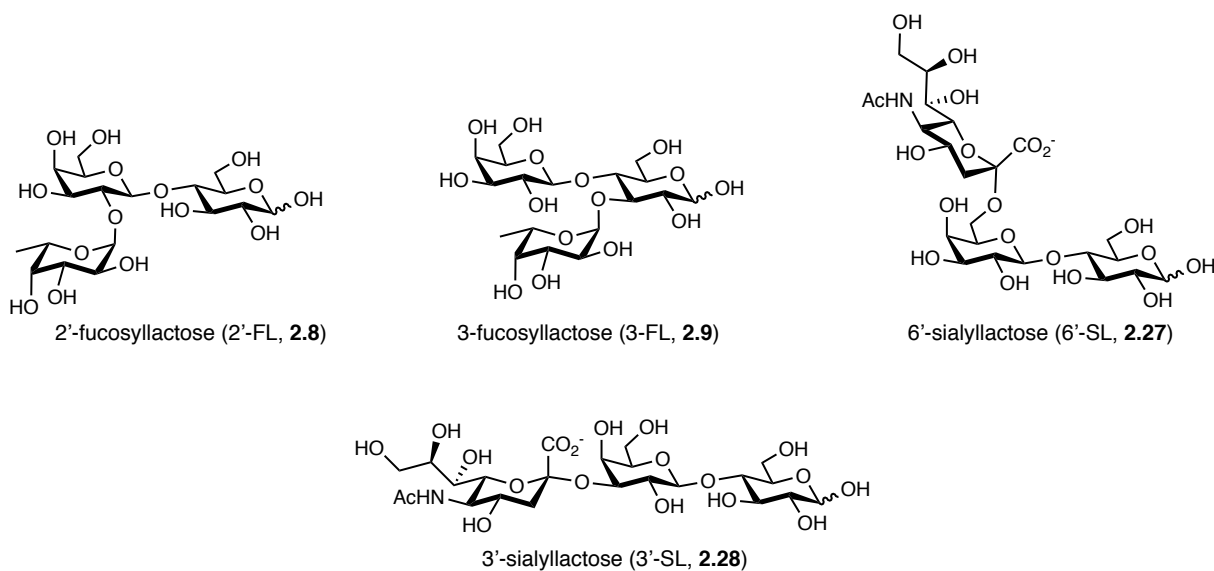


Figure 2.14. Structures of selected HMOs previously shown to promote the growth of several species of *Bacteroides*.

While various species of *Bacteroides* and *Lactobacillus* exist in the infant gut, bifidobacteria constitute the vast majority of the gut microbiota, particularly in breastfed infants. Indeed, bifidobacteria are often found to comprise over 75% of the gut microbiota in breastfed infants with *B. breve*, *B. longum* subsp. *infantis*, and *B. longum* subsp.

longum being among the most common species. Conversely, bifidobacteria are significantly less dominant in the guts of formula-fed infants. As a result, the gut microbiota of formula-fed infants features a more diverse array of species compared to breastfed infants.^{1, 38, 107, 108} Due to the prominence of bifidobacteria in the guts of breastfed infants, HMO utilization by this class of commensal will be discussed in more detail.

Table 2.3. HMO-Promoted Growth of Symbiotic Bacteria

Symbiote	Action	Ref.
<i>B. bifidum</i> , <i>B. longum</i>	Major strains found in breastfed infant feces Can grow using HMOs as the sole carbon source Metabolize “small” oligosaccharides in human milk	106
<i>B. breve</i> , <i>B. adolescentis</i>	Major strains associated with adult gut flora Do not grow efficiently on HMOs	106
<i>B. fragilis</i> , <i>B. thetaiotaomicron</i>	HMO use coupled to up-regulation of mucin degradation pathways	109, 110
<i>B. ovatus</i> , <i>B. stericoris</i>	Do not exhibit growth in the presence of HMO	109, 110
<i>L. plantarum</i> , <i>L. acidophilus</i>	Do not digest complex HMOs Metabolize neutral HMOs Ferment Lac, Glc, GlcNAc, and Fuc	111, 112
<i>L. reuteri</i> , <i>L. fermentum</i> , <i>L. mesenteroides</i> subsp. <i>cremoris</i> and <i>S. thermophilus</i>	Do not metabolize HMOs	111, 112

It has consistently been found that different species of infant-associated bifidobacteria possess varying levels of HMO metabolism.^{107, 113-115} For instance, *B. longum* subsp. *infantis* and *B. bifidum* have been shown to grow better with HMOs as the sole carbon source than *B. longum* subsp. *longum* and *B. breve*.^{107, 116-119} Concurrent with this variation, different species have also been found to possess different preferences for the HMO structures they consume.^{107, 113-115} For example, *B. longum* subsp. *infantis* has been found to consume preferentially HMOs containing eight or fewer monosaccharides,

corresponding to a degree of polymerization (DP) of ≥ 8 , with a mass of < 1400 Da.^{107, 114, 117} Examples of HMOs that are consumed by *B. longum* subsp. *infantis* include LNT, LNnH, isomeric fucosylated LNH, and DFL. While not preferred, it is important to note that this bifidobacterial species is capable of metabolizing other classes of HMOs.¹¹⁷

In contrast to *B. longum* subsp. *infantis*, *B. longum* subsp. *longum* and *B. breve* have been found to metabolize preferentially LNT and LNnT.^{7, 114, 117} Indeed, these strains were found to be devoid of fucosidase activity and possess lower sialidase activity than *B. longum* subsp. *infantis*.¹¹⁷ *B. breve* is, however, able to metabolize smaller HMO components including fucose, isomeric fucosyllactose, LNB, and sialic acid, all of which are released through the extracellular hydrolysis of larger HMOs by other species of bifidobacteria. *B. bifidum*, for example, is capable of degrading HMOs, but it often leaves behind portions of the hydrolyzed product which can subsequently be taken up by the scavenging *B. breve*.^{7, 114, 120}

While HMOs have long been deemed the “bifidus factor,” the unique molecular mechanisms that allow bifidobacteria to metabolize HMOs have only recently been described.¹¹⁸ Investigations into bifidobacteria genomes have not only revealed how this class of symbiote are able to use HMOs, it has also revealed reasons for variations in HMO metabolism seen among different bifidobacteria species. *B. longum* subsp. *infantis*, considered to be the archetypical HMO consumer, has been shown to possess a unique 43-kb gene cluster dedicated to HMO import into cells and subsequent degradation and processing (**Figure 2.15**).

Within this cluster are four glycosidases (β -galactosidase, fucosidase, sialidase, and β -hexosaminidase; **Figure 2.16**) multiple ABC transporters, and several extracellular

soluble binding proteins (SBP) that are predicted to bind oligosaccharides and facilitate their cellular uptake.^{115, 118} Importantly, these glycosidases have been found to be intracellular based on their lack of secretion signals.

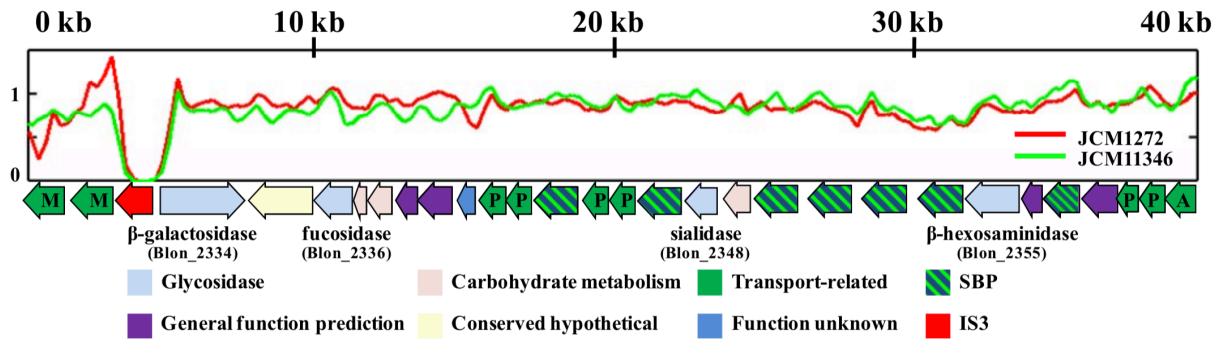


Figure 2.15. Glycosidases and transport-related genes located in the HMO utilization cluster (figure from reference 118). The 43 kbp HMO cluster possesses four glycosidases which are active on HMO glycosidic linkages. Family 1 (oligosaccharide-binding) solute binding proteins (SBP) associated with ABC transporters are found in high density in the cluster. HMO cluster sequence depth in JCM1272 and JCM11346 is normalized to *Bifidobacterium longum* subsp. *infantis* ATCC15697 in arbitrary units. With the exception of the IS3 insertion sequence, the entire locus is found to be present in both *B. longum* subsp. *infantis* genomes. Transport-related genes are denoted as M: major facilitator superfamily, P: ABC transporter permease component, and A: ABC transporter ATPase

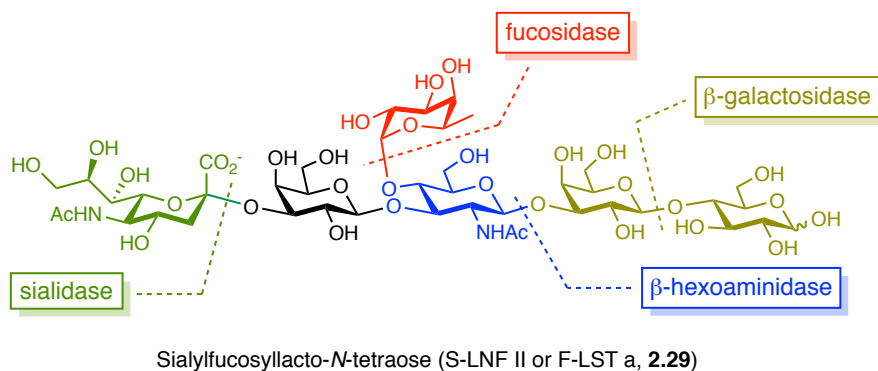


Figure 2.16. Example cleavage sites of the glycosidases in the HMO utilization gene cluster of *Bifidobacterium longum* subsp. *infantis* on the HMO sialylfucosyllacto-*N*-tetraose (S-LNF II or F-LST a, 2.29).

This finding highlights the importance of the ABC transporters in HMO utilization and may explain the preference of *B. longum* subsp. *infantis* for small-mass HMOs;

transporter specificity or steric constraints may limit the transfer of larger HMOs through the transporters and into the cell.^{113, 115} Although it possesses different molecular machinery, HMO degradation in *B. breve* follows the same general pattern as *B. longum* subsp. *infantis*; *B. breve* uses ABC transporters to get LNT and LNnT into cells where they are then degraded through intracellular processes.¹¹⁴

In contrast to the intracellular glycosidases of *B. longum* subsp. *infantis* and *B. breve*, *B. bifidum* possesses extracellular fucosidases and sialidases as well as a membrane-anchored lacto-*N*-biosidase which liberate fucose, sialic acid, and LNB, respectively. The simplified LNB is then transported into the cell by an ABC transporter in association with an LNB-specific SBP.^{113, 115, 120} While type I oligosaccharide chains predominate in human milk, *B. bifidum* is also equipped to degrade type II chains extracellularly which ultimately results in the formation of GlcNAc, Gal, and Glc. These monosaccharides can then be transferred into the cell and subsequently metabolized.¹¹⁴ It is hypothesized that the extracellular HMO degradation strategy used by *B. bifidum* allows it to use a wide range of HMO structures thus conferring a competitive advantage for this species.^{113, 115, 120} The differences between *B. longum* subsp. *infantis* and *B. bifidum* HMO metabolic pathways are depicted in **Figure 2.17**.

Despite numerous genetic differences among the various infant-associated bifidobacteria species, there is an HMO catabolic pathway that is conserved across *B. bifidum*, *B. breve*, *B. longum* subsp. *infantis*, and *B. longum* subsp. *longum*: the LNB/GNB pathway for the catabolism of LNB. The LNB/GNB gene cluster encodes for an ABC transporter responsible for the import of LNB and GNB (galacto-*N*-biose, the building block of mucin sugars), an LNB phosphorylase that cleaves LNB, and two enzymes of

the Leloir pathway to further metabolize the liberated galactose.^{107, 115, 118} Consistent with its inability to use HMOs, the adult-associated *B. adolescentis* lacks this LNB/GNB gene cluster.¹¹⁸

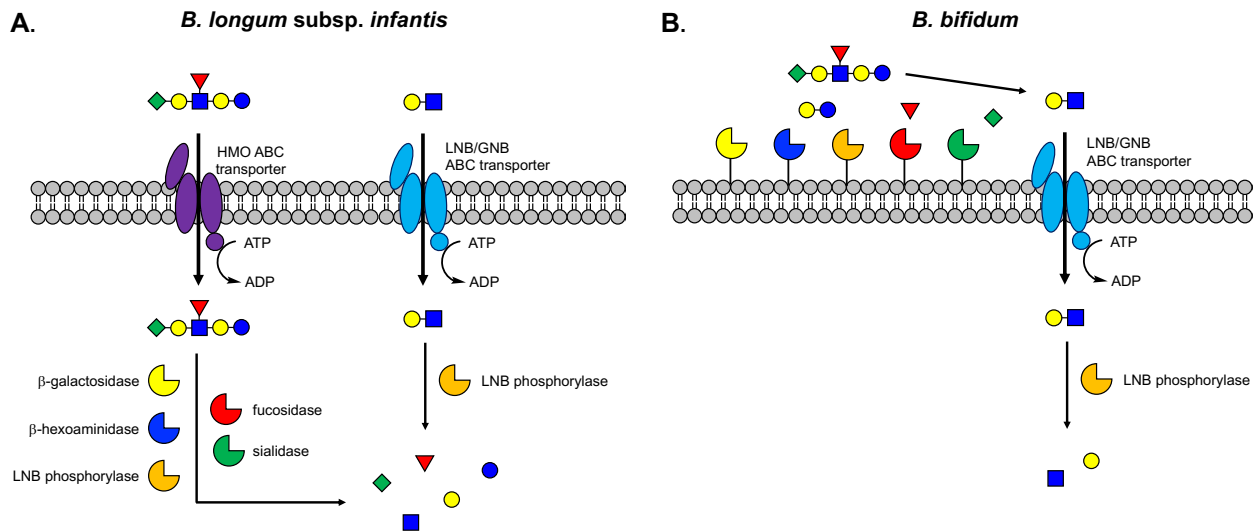


Figure 2.17. HMO metabolic pathways in *B. longum* subsp. *infantis* and *B. bifidum*. **(A)** In *B. longum* subsp. *infantis*, intact HMOs and LNB traverse the cell membrane through an HMO ABC transporter and an LNB/GNB ABC transporter, respectively. Once in the cell, HMOs are hydrolyzed by various cytoplasmic glycosidases to yield the constituent monosaccharides. **(B)** In *B. bifidum*, HMOs are hydrolyzed extracellularly by various cell membrane-bound glycosidases to generate LNB. LNB then traverses the cell membrane through the LNB/GNB ABC transporter. Once in the cell, LNB is further degraded by LNB phosphorylase to yield the constituent monosaccharides. Abbreviations: ABC, ATP-dependent binding cassette; ATP, adenosine triphosphate; ADP, adenosine diphosphate; HMO, human milk oligosaccharide; LNB, lacto-*N*-biose; GNB, galacto-*N*-biose.

Once HMOs have been broken down into their constituent monosaccharides, the monosaccharides can be further degraded by the appropriate catabolic pathways all of which feed into the bifid shunt. The bifid shunt is a *Bifidobacteriaceae*-specific metabolic pathway for the fermentation of hexaoses.^{118, 121} Ultimately, this pathway generates 1.5 and 1 mole of acetate and lactate, respectively, for every mole of hexose that enters the pathway.¹¹⁸ The acetate can subsequently be secreted or incorporated into *de novo* fatty acid synthesis (**Figure 2.18**). Importantly, the secreted acetate and lactate are beneficial

for the host. These SCFAs prevent the growth of pathogenic bacteria by lowering intestinal pH, serve as an energy source for intestinal epithelial cells, and modulate intestinal immune and inflammatory responses through G-protein-coupled receptors.^{118,}

121

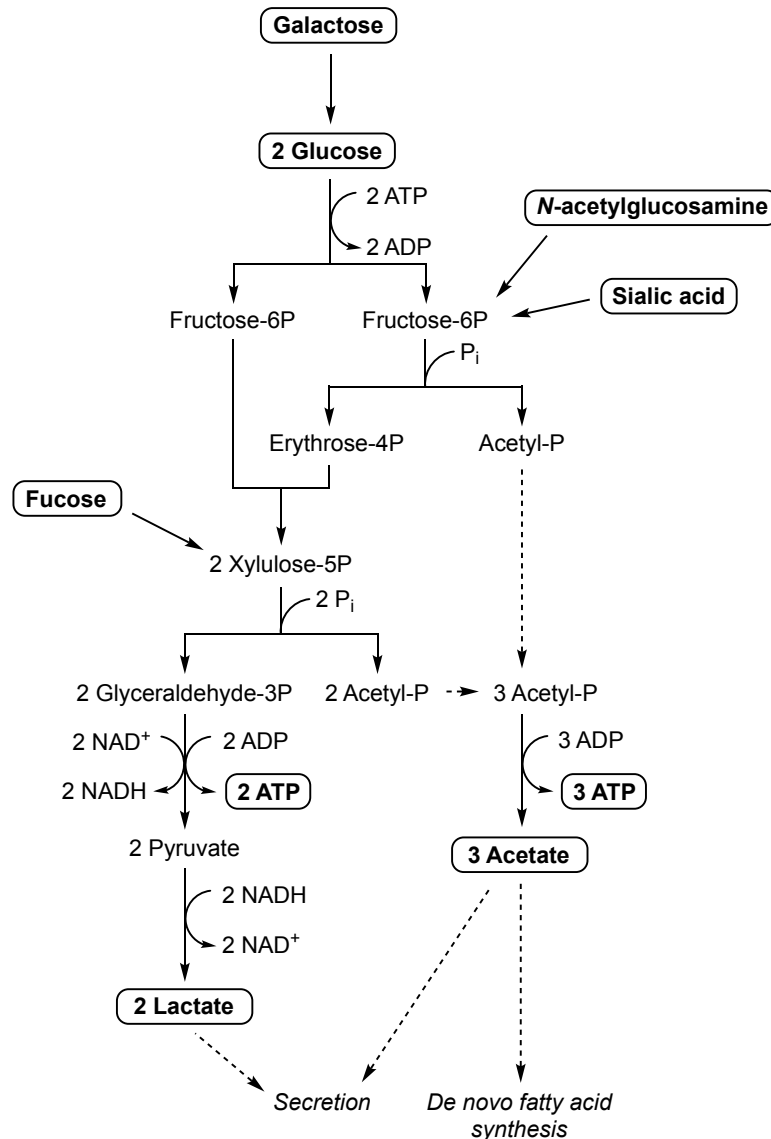


Figure 2.18. The bifid shunt hexose fermentative pathway. Bifidobacteria ferment carbohydrates through the bifid shunt pathway. Monosaccharides are degraded through this pathway to yield 3 acetate, 2 lactate, and 2 ATP per 2 glucose. The acetate produced through this pathway can be secreted into the extracellular environment or incorporated into *de novo* fatty acid synthesis. The lactate produced through this pathway is secreted into the extracellular environment. Abbreviations: ATP, adenosine triphosphate; ADP, adenosine diphosphate; P, phosphate; P_i, inorganic phosphate; NAD⁺, oxidized nicotinamide adenine dinucleotide; NADH, reduced nicotinamide adenine dinucleotide.

The prebiotic capacities of HMOs serve as a key source of indirect protection from pathogens. Not only does the selective metabolism of HMOs by infant-associated gut symbiotes like bifidobacteria confer a competitive growth advantage for these species over pathogenic species, the final products of HMO catabolism lower the pH of the gut which creates an environment which is further prohibitive of pathogenic growth. In contrast to this indirect form of protection, HMOs can also serve as direct sources of protection via their roles as antiadhesive antimicrobials.

2.5.2 Antiadhesive Antimicrobials

Central to the infectious disease process is the sequential invasion, colonization, and proliferation of a pathogen inside a host organism.^{122, 123} Initial host-pathogen interactions occur through pathogen adherence to an epithelial surface. The pathogen then colonizes the contact surface and surrounding tissues to establish a site of infection. Once a site of infection has been successfully established, the pathogen can spread and proliferate in other parts of the body and cause disease. Concurrent with this road to infection, the ability to inhibit initial binding of a pathogen to an epithelial surface effectively halts infection before it begins. Impressively, HMOs are well-known to prevent this initial attachment by serving as soluble decoy receptors for pathogens or pathogenic virulence agents such as toxins. An example of this mode of inhibition is illustrated in **Figure 2.19**. In this regard, HMOs serve as antiadhesive antimicrobials. A summary of HMO antiadhesive antimicrobial activities is provided in **Table 2.4**.

Table 2.4. Protection Against Infectious Disease Derived from Antiadhesive Antimicrobial Functions of HMOs

Bacterial Species	Action	HMOs	Ref.
<i>Campylobacter jejuni</i>	Inhibition of adhesion to epithelial cells Inhibition of inflammatory signaling	2'-FL Other α 1-2 fucosylated oligosaccharides	124-126
<i>Candida albicans</i>	Inhibition of adhesion to epithelial cells Interference with hyphal morphogenesis	Pooled HMOs	127
<i>Clostridium difficile</i>	Binding to exotoxins A (TcdA) and B (TcdB) (prevents interactions of toxin with cellular receptors)	Fucosylated HMOs (e.g. LNFP I, LNFP III) Acidic HMOs (e.g. LST b and c) LNT, LNnH	128, 129
<i>Enterococcus faecium</i>	Faster vancomycin-resistant <i>E. faecium</i> (VRE) colonization reduction compared to non-HMO treatment	Mixtures of fucosylated HMOs	130
<i>Escherichia coli</i>	Interference with intracellular signals used by UPEC to cause cell damage Inhibition of UPEC adhesion to epithelial cells Inhibition of EPEC adhesion to epithelial cells Binding to heat-labile enterotoxin type 1 (HLT)	Acidic and neutral HMO mixtures Neutral and acidic HMOs (e.g. 2'-FL, 6'-SL, LNFP I and II)	131-135
<i>Haemophilus influenzae</i>	Inhibition of adhesion to epithelial cells	High molecular weight fraction of milk	136
<i>Helicobacter pylori</i>	Inhibition of adhesion to epithelial cells	Acidic HMOs (e.g. 3'-SL and 6'-SL)	137
<i>Pseudomonas aeruginosa</i>	Inhibition of adhesion to epithelial cells Reduction of adhesion to and internalization in pneumocytes	2'-FL and 3-FL 3'-SL and 6'-SL	138, 139
<i>Streptococcus pneumoniae</i>	Inhibition of adhesion to epithelial cells	Low and high molecular weight milk fractions LNT	136
<i>Shigella dysenteriae</i>	Binding to Shiga toxins Stx2 and Stx1B ₅	Acidic and neutral HMOs (e.g. 2'-FL, 6'-SL, LNDFH I, LNFP III)	135
<i>Salmonella fytis</i>	Inhibition of adhesion to epithelial cells	Acidic and neutral low molecular weight HMOs (e.g. 3-FL and 6'-FL)	132
Noroviruses and Rotaviruses	Inhibition of binding to HBGAs (Norovirus) Inhibition of adhesion to epithelial cells (Rotavirus)	2'-FL and 3-FL Sialylated HMOs (e.g. 3'-SL and 6'-FL)	140-142

The propensity of HMOs to serve as decoy receptors for pathogens is made possible by their resemblance to various cell surface glycan receptors. For instance, the potential of HMOs to protect against norovirus infection is hypothesized to be due to commonalities between HMO and histo-blood group antigen (HBGA) fucosylation patterns (see **Figures 2.9** and **2.13**).^{140, 141} These structural similarities allow HMOs to act as natural decoys for the HBGA binding pocket of noroviruses. Noroviruses are a group of related viruses that are highly contagious and are collectively one of the dominant causes of gastroenteritis; gastroenteritis, also known as the stomach flu or stomach bug, is an intestinal infection characterized by stomach pain, nausea, vomiting, and diarrhea.¹⁴¹

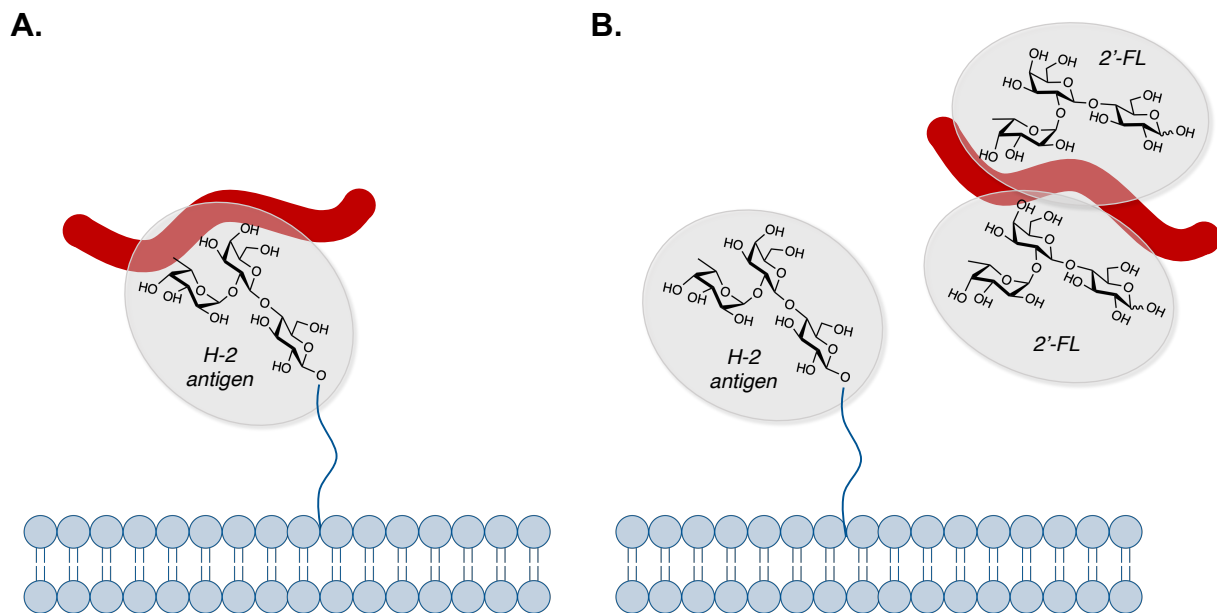


Figure 2.19. Antiadhesive antimicrobial activity of 2'-fucosyllactose (2'-FL) against *Campylobacter jejuni*. **(A)** *C. jejuni* binds the H-2 antigen on cell surfaces to initiate infection. **(B)** The binding of *C. jejuni* to its target H-2 cell surface antigen is inhibited in the presence of 2'-FL via competitive binding. *C. jejuni* is depicted in red.

Fucosylated HMOs, namely α -1,2 fucosylated HMOs like 2'-FL, have also been shown to prevent the binding of *Campylobacter jejuni* to host cell receptors.¹²⁴⁻¹²⁶ In a

study by Ruiz-Palacios, Newburg, et al. *C. jejuni* was first found to bind cells expressing the H-2 antigen, i.e. the H antigen (**Figure 2.9**) presented on a type II oligosaccharide chain. It was subsequently shown that this binding was inhibited by the addition of soluble α -1,2 fucosylated HMOs (**Figure 2.19**).¹²⁶ Like noroviruses, *C. jejuni* is leading cause of intestinal infection, and is the most common cause of bacterial diarrhea. As diarrheal disease is one of the most common causes of infant mortality, protection against pathogens such as the noroviruses and *C. jejuni* is extremely important to infant health and well-being.^{124, 126, 143} In addition to being directly relevant to infant health, this study also provided information about the host cell receptors for *C. jejuni* as our knowledge about these receptors and mechanisms for the entry of this pathogen into cells remains limited.^{126, 144, 145}

In addition to serving as antiadhesive antimicrobials against intestinal (enteric) infections, HMOs have also been shown to similarly protect against upper respiratory infections caused by pathogens such as *Pseudomonas aeruginosa*, *Streptococcus pneumoniae*, and *Haemophilus influenzae*. A summary of these protections is provided in **Table 2.4**.¹ HMOs can come into direct contact with mucosal pathogens as human milk often covers the mucosal surfaces of an infant's nasopharynx (upper part of the pharynx that connects the pharynx to the nasal cavity) and can also reach parts of the upper respiratory tract during bouts of aspiration.⁷ It is hypothesized that the presence of human milk in the naso- and oropharynx may similarly protect infants from infections caused by *Streptococcus agalactiae* (Group B *Streptococcus*, GBS); GBS is a leading cause of neonatal morbidity and mortality and will be discussed in detail in Chapter 3. GBS is

thought to initially colonize an infant's oropharyngeal mucosa through contact of this region with vaginal secretions during birth.²⁰

Finally, HMOs have also been shown to prevent the binding of uropathogenic *Escherichia coli* (UPEC); UPEC is a major cause of urinary tract infections (UTIs) (**Table 2.4**).^{131, 134} As previously discussed, HMOs are not metabolized by the infant and a portion pass intact through the colon and are excreted in feces and urine.^{7, 77, 104, 105} This source of HMO/pathogen contact helps to explain how HMOs may also help to lessen the occurrence of UTIs in infants.

2.6 Conclusion and Future Outlook

Human milk is uniquely tailored to promote infant health and well-being. Even under the harshest of scenarios and even when the mother's own nutrition is compromised, human milk provides infants will all the necessary nutrients, vitamins, and protective bioactive macromolecules that are essential to proper growth and development. Moreover, human milk composition changes over the course of lactation to adapt to the developing needs of a child. While human milk contains a plethora of protective immunogenic components such as immune cells, cytokines, chemokines, and antibodies, HMOs represent a unique and important source of protection against infectious agents. This class of structurally complex and diverse carbohydrates, which are absent from bovine milk and by extension absent from formula, are key to the lowered incidences of diarrhea, respiratory infection, urinary tract infection, ear infection, necrotizing enterocolitis (NEC), and sudden infant death syndrome (SIDS) seen in breastfed infants compared to their formula-fed counterparts. More specifically, HMOs serve as prebiotics

and antiadhesive antimicrobials to promote the growth of important intestinal symbiotes, including numerous bifidobacteria species, and to protect infants from colonization by infectious agents such as *Escherichia coli*, *Clostridium difficile*, and *Campylobacter jejuni*.¹

Although numerous prebiotic HMO mimics have been developed as formula additives, these compounds lack the structural complexity and diversity of HMOs and thus are not able to offer a comparable range of infant benefits.²³ Additionally, this class of additive does not address the antiadhesive antimicrobial properties of HMOs. While 2'-fucosyllactose, an important antiadhesive antimicrobial HMO, has more recently been developed as a formula additive, this single HMO is unlikely to yield comparable benefits to the actions of heterogenous HMO extracts. Thus, it is important to identify additional single-entity HMOs that are key to infection prevention. Closely related to this need is the need to continue to elucidate the protections HMOs afford against infectious disease, i.e. expanding our knowledge about the specific pathogens that HMOs protect against and the mechanisms by which these protections occur.

The greatest barrier to HMO research is the limited availability of these compounds. At a basic level, there is a limited supply of donor milk accessible to researchers as donor milk is rightfully prioritized for sick neonates who are most likely to benefit from exclusive consumption of human milk. Even if researchers have access to donor milk, however, the high variation in HMO composition and the difficulties associated with isolating homogeneous HMOs from heterogenous extracts makes determining specific HMO structure activity relationships difficult. To compound this problem, single-entity HMOs are by in large cost and/or synthetically prohibitive.¹ Regardless of the challenges,

continued research on the biological impact of HMOs, particularly with regard to infectious disease prevention, is paramount to human health.

In line with this need, the focus of my doctoral work was to investigate the extent to which HMOs can serve as sources of protection against infectious disease. The work completed in this regard is detailed in subsequent chapters and begins with a description of our investigations into the antibacterial properties of heterogenous HMOs against several clinically relevant pathogens (Chapter 3). Guided by these findings, we next moved to evaluate the antibacterial properties of single-entity compounds. As previously mentioned, single-entity HMOs are prohibitively expensive. Thus, I developed a scalable chemical synthesis of the ubiquitous HMO lacto-*N*-tetraose (LNT) (Chapter 4). In the final chapter of this dissertation, the antibacterial properties of LNT as well as several additional homogenous HMOs are presented (Chapter 5).

2.7 References

1. Craft, K. M.; Townsend, S. D., The Human Milk Glycome as a Defense Against Infectious Diseases: Rationale, Challenges, and Opportunities. *ACS Infect. Dis.* **2017**, *4* (2), 77-83.
2. Stevens, E. E.; Patrick, T. E.; Pickler, R., A history of infant feeding. *J. Perinat. Educ.* **2009**, *18* (2), 32-9.
3. Eglash, A.; Montgomery, A.; Wood, J., Breastfeeding. *DM* **2008**, *54* (6), 343-411.
4. Radbill, S. X., Infant-Feeding through the Ages. *Clin. Pediatr.* **1981**, *20* (10), 613-621.
5. Fomon, S., Infant feeding in the 20th century: formula and beikost. *J. Nutr.* **2001**, *131* (2), 409S-20S.
6. Kunz, C., Historical aspects of human milk oligosaccharides. *Adv. Nutr.* **2012**, *3* (3), 430S-9S.

7. Bode, L., Human milk oligosaccharides: every baby needs a sugar mama. *Glycobiology* **2012**, 22 (9), 1147-62.
8. Section on, B., Breastfeeding and the use of human milk. *Pediatrics* **2012**, 129 (3), e827-41.
9. Kramer, M. S.; Kakuma, R., Optimal duration of exclusive breastfeeding. *Cochrane Database Syst. Rev.* **2012**, (8), CD003517.
10. Andreas, N. J.; Kampmann, B.; Mehring Le-Doare, K., Human breast milk: A review on its composition and bioactivity. *Early Hum. Dev.* **2015**, 91 (11), 629-35.
11. Petherick, A., Development: Mother's milk: A rich opportunity. *Nature* **2010**, 468 (7327), S5-7.
12. Ballard, O.; Morrow, A. L., Human milk composition: nutrients and bioactive factors. *Pediatr. Clin. North Am.* **2013**, 60 (1), 49-74.
13. Valentine, C. J.; Wagner, C. L., Nutritional management of the breastfeeding dyad. *Pediatr. Clin. North. Am.* **2013**, 60 (1), 261-74.
14. Demmelmair, H.; Koletzko, B., Lipids in human milk. *Best Pract. Res. Clin. Endocrinol. Metab.* **2018**, 32 (1), 57-68.
15. Koletzko, B., Human Milk Lipids. *Ann. Nutr. Metab.* **2016**, 69 (Suppl 2), 28-40.
16. Hamosh, M.; Peterson, J. A.; Henderson, T. R.; Scallan, C. D.; Kiwan, R.; Ceriani, R. L.; Armand, M.; Mehta, N. R.; Hamosh, P., Protective function of human milk: the milk fat globule. *Semin. Perinatol.* **1999**, 23 (3), 242-9.
17. Lonnerdal, B., Infant formula and infant nutrition: bioactive proteins of human milk and implications for composition of infant formulas. *Am. J. Clin. Nutr.* **2014**, 99 (3), 712S-7S.
18. Lonnerdal, B., Nutritional and physiologic significance of human milk proteins. *Am. J. Clin. Nutr.* **2003**, 77 (6), 1537S-1543S.
19. Le Huerou-Luron, I.; Blat, S.; Boudry, G., Breast- v. formula-feeding: impacts on the digestive tract and immediate and long-term health effects. *Nutr. Res. Rev.* **2010**, 23 (1), 23-36.
20. Le Doare, K.; Kampmann, B., Breast milk and Group B streptococcal infection: vector of transmission or vehicle for protection? *Vaccine* **2014**, 32 (26), 3128-32.
21. Hurley, W. L.; Theil, P. K., Perspectives on immunoglobulins in colostrum and milk. *Nutrients* **2011**, 3 (4), 442-74.

22. Gao, X.; McMahon, R. J.; Woo, J. G.; Davidson, B. S.; Morrow, A. L.; Zhang, Q., Temporal changes in milk proteomes reveal developing milk functions. *J. Proteome Res.* **2012**, *11* (7), 3897-907.
23. Ackerman, D. L.; Craft, K. M.; Townsend, S. D., Infant food applications of complex carbohydrates: Structure, synthesis, and function. *Carbohydr. Res.* **2017**, *437*, 16-27.
24. Schaafsma, G., Lactose and lactose derivatives as bioactive ingredients in human nutrition. *International Dairy Journal* **2008**, *18* (5), 458-465.
25. Skovbjerg, H.; Sjostrom, H.; Noren, O., Purification and characterisation of amphiphilic lactase/phlorizin hydrolase from human small intestine. *Eur. J. Biochem.* **1981**, *114* (3), 653-61.
26. Ohto, U.; Usui, K.; Ochi, T.; Yuki, K.; Satow, Y.; Shimizu, T., Crystal structure of human beta-galactosidase: structural basis of Gm1 gangliosidosis and morquio B diseases. *J. Biol. Chem.* **2012**, *287* (3), 1801-12.
27. Davies, G.; Henrissat, B., Structures and mechanisms of glycosyl hydrolases. *Structure* **1995**, *3* (9), 853-9.
28. Zhang, S.; McCarter, J. D.; O'kamura-Oho, Y.; Yaghi, F.; Hinek, A.; Withers, S. G.; Callahan, J. W., Kinetic mechanism and characterization of human beta-galactosidase precursor secreted by permanently transfected Chinese hamster ovary cels. *Biochem. J.* **1994**, *304*, 281-288.
29. Urashima, T.; Fukuda, K.; Messer, M., Evolution of milk oligosaccharides and lactose: a hypothesis. *Animal* **2012**, *6* (3), 369-74.
30. Ziegler, E. E.; Fomon, S. J., Lactose enhances mineral absorption in infancy. *J. Pediatr. Gastroenterol. Nutr.* **1983**, *2* (2), 288-94.
31. Abrams, S. A.; Griffin, I. J.; Davila, P. M., Calcium and zinc absorption from lactose-containing and lactose-free infant formulas. *Am. J. Clin. Nutr.* **2002**, *76* (2), 442-6.
32. Moya, M. e. a., Short-Term polysucrose substitution for Lactose Reduces Calcium Absorption in Healthy Term Babies. *J. Pediatr. Gastroenterol. Nutr.* **1992**, *14*, 57-61.
33. Nijman, R. M.; Liu, Y.; Bunyatrchata, A.; Smilowitz, J. T.; Stahl, B.; Barile, D., Characterization and Quantification of Oligosaccharides in Human Milk and Infant Formula. *J. Agric. Food Chem.* **2018**, *66* (26), 6851-6859.
34. Ninonuevo, M. R.; Park, Y.; Yin, H.; Zhang, J.; Ward, R. E.; Clowers, B. H.; German, J. B.; Freeman, S. L.; Killeen, K.; Grimm, R.; Lebrilla, C. B., A strategy for annotating the human milk glycome. *J. Agric. Food Chem.* **2006**, *54* (20), 7471-80.

35. Vandenplas, Y.; Berger, B.; Carnielli, V. P.; Ksiazek, J.; Lagstrom, H.; Sanchez Luna, M.; Migacheva, N.; Mosselmans, J. M.; Picaud, J. C.; Possner, M.; Singhal, A.; Wabitsch, M., Human Milk Oligosaccharides: 2'-Fucosyllactose (2'-FL) and Lacto-N-Neotetraose (LNnT) in Infant Formula. *Nutrients* **2018**, *10* (9).
36. Urashima, T.; Saito, T.; Nakamura, T.; Messer, M., Oligosaccharides of milk and colostrum in non-human mammals. *Glycoconj. J.* **2001**, *18* (5), 357-71.
37. Chaturvedi, P.; Warren, C. D.; Altaye, M.; Morrow, A. L.; Ruiz-Palacios, G.; Pickering, L. K.; Newburg, D. S., Fucosylated human milk oligosaccharides vary between individuals and over the course of lactation. *Glycobiology* **2001**, *11* (5), 365-372.
38. Bode, L., Human milk oligosaccharides: prebiotics and beyond. *Nutr. Rev.* **2009**, *67 Suppl 2*, S183-91.
39. Escherich, T., Die Darmbakterien des Säuglings und ihre Beziehungen zur Physiologie der Verdauung. *Enke Verlag: Stuttgart* **1886**.
40. Lee, J. H.; O'Sullivan, D. J., Genomic insights into bifidobacteria. *Microbiol. Mol. Biol. Rev.* **2010**, *74* (3), 378-416.
41. Polonowski, M.; Lespagnol, A., Sur la nature glucidique de la substance lévogyre du lait de femme. *Bull. Soc. Biol.* **1929**, *101*, 61-63.
42. Polonowski, M.; Lespagnol, A., Sur l'existence de plusieurs glucides dans le lactoserum de femme. *C. R. Soc. Biol. (Paris)* **1930**, *104*, 555-557.
43. Polonowski, M.; Lespagnol, A., Sur deux nouveaux sucres du lait de femme, le gynolactose et l'allolactose. *C. R. Acad. Sci.* **1931**, *192*, 1319.
44. Polonowski, M.; Lespagnol, A., Nouvelles acquisitions sur les composés glucidiques du lai de femme. *Bull. Soc. Chim. Biol.* **1933**, *15*, 320-349.
45. Polonowski, M.; Montreuil, J., Etude chromatographique des polyosides du lait de femme. *C. R. Acad. Sci. Paris* **1954**, *238*, 2263-2264.
46. Schönfeld, H., Über die Beziehung der einzelnen Bestandteile der Frauenmilch zur Bifidusflora. *Jahrbuch Kinderh* **1926**, *113*, 19-60.
47. György, P.; Norris, R. F.; Rose, C. S., Bifidus Factor I. A Variant of *Latobucillus bifidus* Requiring a Special Growth Factor. *Arch. Biochem. Biophys.* **1954**, *48*, 193-201.

48. György, P.; Kuhn, R.; Rose, C. S.; Zilliken, F., Bifidus Factor. II. Its Occurrence in Milk from Different Species and in Other Natural Products. *Arch. Biochem. Biophys.* **1954**, *48*, 202-208.
49. György, P.; Hoover, J. R. E.; Kuhn, R.; Rose, C. S., Bifidus Factor. III. The Rate of Dialysis. *Arch. Biochem. Biophys.* **1954**, *48*, 209-213.
50. Gauhe, A.; György, P.; Hoover, J. R. E.; Kuhn, R.; Rose, C. S.; Ruelius, H. W.; Zilliken, F., Bifidus Factor. IV. Preparations Obtained from Human Milk. *Arch. Biochem. Biophys.* **1954**, *48* (1), 214-224.
51. György, P., A Hitherto Unrecognized Biochemical Difference Between Human Milk and Cow's Milk. *Pediatrics* **1953**, *11* (2), 98-108.
52. Montreuil, J., Les glucides du lait. *Bull. Soc. Chim. Biol.* **1960**, *42*, 1399-1427.
53. Kuhn, R.; Baer, H. H.; Bister, W.; Brossmer, R.; Gauhe, A.; Haas, H. J.; Haber, F.; Kruger, G.; Tiedmann, H.; Weiser, D., Aminosucker. *Angew. Chem.* **1957**, *69* (1-2), 23-33.
54. Kuhn, R.; Baer, H. H.; Gauhe, A., Fucosido-Lactose, Das Trisaccharid Der Frauenmilch. *Chem. Ber. -Recueil* **1955**, *88* (8), 1135-1146.
55. Kuhn, R.; Baer, H. H., Die Konstitution Der Lacto-N-Tetraose. *Chem. Ber.-Recueil* **1956**, *89* (2), 504-511.
56. Kuhn, R.; Baer, H. H.; Gauhe, A., Kristallisation und Konstitutionsermittlung der Lacto-N-fucopentaose I. *Chem. Ber.* **1956**, *89* (11), 2514-2523.
57. Kuhn, R.; Baer, H. H.; Gauhe, A., Die Konstitution Der Lacto-N-Fucopentaose II - Ein Beitrag Zur Spezifität Der Blutgruppensubstanz Lea. *Chem. Ber.-Recueil* **1958**, *91* (2), 364-374.
58. Kuhn, R.; Gauhe, A., Über Die Lacto-Difuco-Tetraose Der Frauenmilch - Ein Beitrag Zur Strukturspezifität Der Blutgruppensubstanz Leb. *Justus Liebigs Ann. Chem.* **1958**, *611* (1-3), 249-253.
59. Kobata, A.; Ginsburg, V., Oligosaccharides of Human Milk. II. Isolation and Characterization of a New Pentasaccharide, Lacto-N-fucopentaose III. *J. Biol. Chem.* **1969**, *244* (20), 5496-5502.
60. Kobata, A.; Ginsburg, V., Oligosaccharides of human milk. IV. Isolation and characterization of a new hexasaccharide, lacto-N-neohexaose. *Arch. Biochem. Biophys.* **1972**, *150* (1), 273-81.

61. Kobata, A.; Ginsburg, V., Oligosaccharides of human milk. III. Isolation and characterization of a new hexasaccharide, lacto-*N*-hexaose. *J. Biol. Chem.* **1972**, *247* (5), 1525-1529.
62. Yamashita, K.; Kobata, A., Oligosaccharides of Human Milk V. Isolation and Characterization of a New Trisaccharide, 6'-Galactosyllactose. *Arch. Biochem. Biophys.* **1974**, *161*, 164-170.
63. Morgan, W. T. J.; Watkins, W. M., Genetic and Biochemical Aspects of Human Blood-Group A-, B-, H-, Le^a- and Le^b-Specificity. *Br. Med. Bull.* **1969**, *25* (1), 30-34.
64. Kobata, A.; Ginsburg, V., Oligosaccharides of Human Milk I. Isolation and Characterization. *Arch. Biochem. Biophys.* **1969**, *130*, 509-513.
65. Grollman, E. F.; Kobata, A.; Ginsburg, V., An enzymatic basis for Lewis blood types in man. *J. Clin. Invest.* **1969**, *48* (8), 1489-94.
66. Grollman, E. F.; Ginsburg, V., Correlation Between Secretor Status and the Occurrence of 2'-Fucosyllactose in Human Milk. *Biochem. Biophys. Res. Commun.* **1967**, *28* (1), 50-53.
67. Grollman, E. F.; Kobata, A.; Ginsburg, V., Enzymatic Basis of Blood Types in Man. *Ann. N. Y. Acad. Sci.* **1970**, *169* (1), 153-158.
68. Urashima, T.; Asakuma, S.; Leo, F.; Fukuda, K.; Messer, M.; Oftedal, O. T., The predominance of type I oligosaccharides is a feature specific to human breast milk. *Adv. Nutr.* **2012**, *3* (3), 473S-82S.
69. Kunz, C.; Rudloff, S.; Baier, W.; Klein, N.; Strobel, S., Oligosaccharides in human milk: structural, functional, and metabolic aspects. *Ann. Rev. Nutr.* **2000**, *20*, 699-722.
70. Egge, H.; Dell, A.; Von Nicolai, H., Fucose containing oligosaccharides from human milk. I. Separation and identification of new constituents. *Arch. Biochem. Biophys.* **1983**, *224* (1), 235-53.
71. Charlwood, J.; Tolson, D.; Dwek, M.; Camilleri, P., A detailed analysis of neutral and acidic carbohydrates in human milk. *Anal. Biochem.* **1999**, *273* (2), 261-77.
72. Shen, Z.; Warren, C. D.; Newburg, D. S., High-performance capillary electrophoresis of sialylated oligosaccharides of human milk. *Anal. Biochem.* **2000**, *279* (1), 37-45.
73. Thurl, S.; MullerWerner, B.; Sawatzki, G., Quantification of individual oligosaccharide compounds from human milk using high-pH anion-exchange chromatography. *Anal. Biochem.* **1996**, *235* (2), 202-206.

74. Pfenninger, A.; Karas, M.; Finke, B.; Stahl, B.; Sawatzki, G., Matrix optimization for matrix-assisted laser desorption/ionization mass spectrometry of oligosaccharides from human milk. *J. Mass Spectrom.* **1999**, *34* (2), 98-104.
75. Blank, D.; Gebhardt, S.; Maass, K.; Lochnit, G.; Dotz, V.; Blank, J.; Geyer, R.; Kunz, C., High-throughput mass finger printing and Lewis blood group assignment of human milk oligosaccharides. *Anal. Bioanal. Chem.* **2011**, *401* (8), 2495-510.
76. Newburg, D. S., Glycobiology of human milk. *Biochemistry (Mosc)* **2013**, *78* (7), 771-85.
77. Chen, X., Human Milk Oligosaccharides (HMOS): Structure, Function, and Enzyme-Catalyzed Synthesis. *Adv. Carbohydr. Chem. Biochem.* **2015**, *72*, 113-90.
78. Holden, H. M.; Rayment, I.; Thoden, J. B., Structure and function of enzymes of the Leloir pathway for galactose metabolism. *J. Biol. Chem.* **2003**, *278* (45), 43885-8.
79. Sunehag, A. L.; Louie, K.; Bier, J. L.; Tigas, S.; Haymond, M. W., Hexoneogenesis in the human breast during lactation. *J. Clin. Endocrinol. Metab.* **2002**, *87* (1), 297-301.
80. Mohammad, M. A.; Maningat, P.; Sunehag, A. L.; Haymond, M. W., Precursors of hexoneogenesis within the human mammary gland. *Am. J. Physiol. Endocrinol. Metab.* **2015**, *308* (8), E680-7.
81. Rudloff, S.; Obermeier, S.; Borsch, C.; Pohlentz, G.; Hartmann, R.; Brosicke, H.; Lentze, M. J.; Kunz, C., Incorporation of orally applied (13)C-galactose into milk lactose and oligosaccharides. *Glycobiology* **2006**, *16* (6), 477-87.
82. Willi E. Heine, P. D. K., and Peter J. Reeds, The Importance of alpha-Lactalbumin in Infant Nutrition. *J. Nutr.* **1990**, *121* (3), 277-283.
83. Brew, K., Secretion of alpha-lactalbumin into Milk and Its Relevance to the Organization and Control of Lactose Synthetase. *Nature* **1969**, *222*, 671-672.
84. Fuhrer, A.; Sprenger, N.; Kurakevich, E.; Borsig, L.; Chassard, C.; Hennet, T., Milk sialyllactose influences colitis in mice through selective intestinal bacterial colonization. *J. Exp. Med.* **2010**, *207* (13), 2843-54.
85. Watkins, W. M., Blood Group Substances. *Science* **1966**, *152* (3719), 172-181.
86. Watkins, W. M.; Morgan, W. T. J., Possible Genetical Pathways for the Biosynthesis of Blood Group Mucopolysaccharides. *Vox Sang* **1959**, *4*, 97-119.
87. SHen, L.; Grollman, E. F.; Ginsburg, V., An Enzymatic Basis for Secretor Status and Blood Group Substance Specificity in Humans. *Biochem.* **1968**, *59*, 224-230.

88. Johnson, P. H.; Yates, A. D.; Watkins, W. M., Human Salivary Fucosyltransferases-Evidence for Two Distinct α -3-L-Fucosyltransferase Activities One of Which is Associated with the Lewis Blood Group Le Gene. *Biochem. Biophys. Res. Commun.* **1981**, *100* (4), 1611-1618.
89. Johnson, P. H.; Watkins, W. M., Purification of the Lewis blood-group gene associated alpha-3/4-fucosyltransferase from human milk: an enzyme transferring fucose primarily to type 1 and lactose-based oligosaccharide chains. *Glycoconj. J.* **1992**, *9* (5), 241-9.
90. Prieels, J.-P.; Monnom, D.; M., D., Co-purification of the Lewis Blood Group *N*-Acetylglucosaminide α 1 -4 Fucosyltransferase and an *N*-Acetylglucosaminide α 1 -3 Fucosyltransferase from Human Milk. *J. Biol. Chem.* **1981**, *256*, 10456-10463.
91. Johnson, P. H.; Donald, A. S.; Feeney, J.; Watkins, W. M., Reassessment of the acceptor specificity and general properties of the Lewis blood-group gene associated α -3/4-fucosyltransferase purified from human milk. *Glycoconj. J.* **1992**, *9* (5), 251-64.
92. Kumazaki, T.; Yoshida, A., Biochemical evidence that secretor gene, Se, is a structural gene encoding a specific fucosyltransferase. *PNAS* **1984**, *81*, 4193-4197.
93. Becker, D. J.; Lowe, J. B., Fucose: biosynthesis and biological function in mammals. *Glycobiology* **2003**, *13* (7), 41R-53R.
94. Newburg, D. S.; Ruiz-Palacios, G. M.; Morrow, A. L., Human milk glycans protect infants against enteric pathogens. *Ann. Rev. Nutr.* **2005**, *25*, 37-58.
95. Newburg, D. S.; Ruiz-Palacios, G. M.; Altaye, M.; Chaturvedi, P.; Meinzen-Derr, J.; Guerrero Mde, L.; Morrow, A. L., Innate protection conferred by fucosylated oligosaccharides of human milk against diarrhea in breastfed infants. *Glycobiology* **2004**, *14* (3), 253-63.
96. Harduin-Lepers, A.; Vallejo-Ruiz, V.; Krzewinski-Recchi, M. A.; Samyn-Petit, B.; Julien, S.; Delannoy, P., The human sialyltransferase family. *Biochimie* **2001**, *83* (8), 727-37.
97. Audry, M.; Jeanneau, C.; Imberty, A.; Harduin-Lepers, A.; Delannoy, P.; Breton, C., Current trends in the structure-activity relationships of sialyltransferases. *Glycobiology* **2011**, *21* (6), 716-26.
98. Ortiz-Soto, M. E.; Seibel, J., Expression of Functional Human Sialyltransferases ST3Gal1 and ST6Gal1 in *Escherichia coli*. *PLoS One* **2016**, *11* (5), e0155410.
99. Harduin-Lepers, A.; Krzewinski-Recchi, M. A.; Colomb, F.; Foulquier, F.; Groux-Degroote, S.; Delannoy, P., Sialyltransferases functions in cancers. *Front. Biosci. (Elite Ed)* **2012**, *4*, 499-515.

100. Tsuchida, A.; Okajima, T.; Furukawa, K.; Ando, T.; Ishida, H.; Yoshida, A.; Nakamura, Y.; Kannagi, R.; Kiso, M.; Furukawa, K., Synthesis of disialyl Lewis a (Le(a)) structure in colon cancer cell lines by a sialyltransferase, ST6GalNAc VI, responsible for the synthesis of alpha-series gangliosides. *J. Biol. Chem.* **2003**, *278* (25), 22787-94.
101. Hutkins, R. W.; Krumbeck, J. A.; Bindels, L. B.; Cani, P. D.; Fahey, G., Jr.; Goh, Y. J.; Hamaker, B.; Martens, E. C.; Mills, D. A.; Rastal, R. A.; Vaughan, E.; Sanders, M. E., Prebiotics: why definitions matter. *Curr. Opin. Biotechnol.* **2016**, *37*, 1-7.
102. Gnoth, M. J.; Kunz, C.; Kinne-Saffran, E.; Rudloff, S., Human milk oligosaccharides are minimally digested in vitro. *J. Nutr.* **2000**, *130* (12), 3014-20.
103. Engfer, M. B.; Stahl, B.; Finke, B.; Sawatzki, G.; Daniel, H., Human milk oligosaccharides are resistant to enzymatic hydrolysis in the upper gastrointestinal tract. *Am. J. Clin. Nutr.* **2000**, *71* (6), 1589-96.
104. De Leoz, M. L.; Wu, S.; Strum, J. S.; Ninonuevo, M. R.; Gaerlan, S. C.; Mirmiran, M.; German, J. B.; Mills, D. A.; Lebrilla, C. B.; Underwood, M. A., A quantitative and comprehensive method to analyze human milk oligosaccharide structures in the urine and feces of infants. *Anal. Bioanal. Chem.* **2013**, *405* (12), 4089-105.
105. Rudloff, S.; Pohlentz, G.; Diekmann, L.; Egge, H.; Kunz, C., Urinary excretion of lactose and oligosaccharides in preterm infants fed human milk or infant formula. *Acta Paediatr.* **1996**, *85* (5), 598-603.
106. Yu, Z. T.; Chen, C.; Newburg, D. S., Utilization of major fucosylated and sialylated human milk oligosaccharides by isolated human gut microbes. *Glycobiology* **2013**, *23* (11), 1281-92.
107. Garrido, D.; Dallas, D. C.; Mills, D. A., Consumption of human milk glycoconjugates by infant-associated bifidobacteria: mechanisms and implications. *Microbiology* **2013**, *159* (Pt 4), 649-64.
108. Sela, D. A.; Li, Y.; Lerno, L.; Wu, S.; Marcobal, A. M.; German, J. B.; Chen, X.; Lebrilla, C. B.; Mills, D. A., An infant-associated bacterial commensal utilizes breast milk sialyloligosaccharides. *J. Biol. Chem.* **2011**, *286* (14), 11909-18.
109. Marcobal, A.; Barboza, M.; Froehlich, J. W.; Block, D. E.; German, J. B.; Lebrilla, C. B.; Mills, D. A., Consumption of human milk oligosaccharides by gut-related microbes. *J. Agric. Food Chem.* **2010**, *58* (9), 5334-40.
110. Marcobal, A.; Barboza, M.; Sonnenburg, E. D.; Pudlo, N.; Martens, E. C.; Desai, P.; Lebrilla, C. B.; Weimer, B. C.; Mills, D. A.; German, J. B.; Sonnenburg, J. L.,

- Bacteroides in the infant gut consume milk oligosaccharides via mucus-utilization pathways. *Cell Host Microbe* **2011**, 10 (5), 507-14.
111. Schwab, C.; Ganzle, M., Lactic acid bacteria fermentation of human milk oligosaccharide components, human milk oligosaccharides and galactooligosaccharides. *FEMS Microbiol. Lett.* **2011**, 315 (2), 141-8.
 112. Ganzle, M. G.; Follador, R., Metabolism of oligosaccharides and starch in lactobacilli: a review. *Front Microbiol.* **2012**, 3, 340.
 113. Sela, D. A., Bifidobacterial utilization of human milk oligosaccharides. *Int. J. Food Microbiol.* **2011**, 149 (1), 58-64.
 114. James, K.; Motherway, M. O.; Bottacini, F.; van Sinderen, D., *Bifidobacterium breve* UCC2003 metabolises the human milk oligosaccharides lacto-*N*-tetraose and lacto-*N*-neo-tetraose through overlapping, yet distinct pathways. *Sci. Rep.* **2016**, 6, 1-16.
 115. Goh, Y. J.; Klaenhammer, T. R., Genetic mechanisms of prebiotic oligosaccharide metabolism in probiotic microbes. *Annu. Rev. Food Sci. Technol.* **2015**, 6, 137-56.
 116. Ward, R. E.; Ninonuevo, M.; Mills, D. A.; Lebrilla, C. B.; German, J. B., In vitro fermentation of breast milk oligosaccharides by *Bifidobacterium infantis* and *Lactobacillus gasseri*. *Appl. Environ. Microbiol.* **2006**, 72 (6), 4497-9.
 117. LoCascio, R. G.; Ninonuevo, M. R.; Freeman, S. L.; Sela, D. A.; Grimm, R.; Lebrilla, C. B.; Mills, D. A.; German, J. B., Glycoprofiling of bifidobacterial consumption of human milk oligosaccharides demonstrates strain specific, preferential consumption of small chain glycans secreted in early human lactation. *J. Agric. Food Chem.* **2007**, 55 (22), 8914-9.
 118. Sela, D. A.; Chapman, J.; Adeuya, A.; Kim, J. H.; Chen, F.; Whitehead, T. R.; Lapidus, A.; Rokhsar, D. S.; Lebrilla, C. B.; German, J. B.; Price, N. P.; Richardson, P. M.; Mills, D. A., The genome sequence of *Bifidobacterium longum* subsp. *infantis* reveals adaptations for milk utilization within the infant microbiome. *PNAS* **2008**, 105 (48), 18964-9.
 119. Ward, R. E.; Ninonuevo, M.; Mills, D. A.; Lebrilla, C. B.; German, J. B., In vitro fermentability of human milk oligosaccharides by several strains of bifidobacteria. *Mol. Nutr. Food Res.* **2007**, 51 (11), 1398-405.
 120. Sela, D. A.; Mills, D. A., Nursing our microbiota: molecular linkages between bifidobacteria and milk oligosaccharides. *Trends Microbiol.* **2010**, 18 (7), 298-307.
 121. Fushinobu, S., Unique sugar metabolic pathways of bifidobacteria. *Biosci. Biotechnol. Biochem.* **2010**, 74 (12), 2374-84.

122. Craft, K. M.; Thomas, H. C.; Townsend, S. D., Sialylated variants of lacto-*N*-tetraose exhibit antimicrobial activity against Group B *Streptococcus*. *Org. Biomol. Chem.* **2018**, *17* (7), 1893-1900.
123. Janeway, C. A. J.; Travers, P.; Walport, M.; Shlomchik, M. J., Immunobiology: The Immune System in Health and Disease, 5th edition. **2001**.
124. Yu, Z. T.; Nanthakumar, N. N.; Newburg, D. S., The Human Milk Oligosaccharide 2'-Fucosyllactose Quenches *Campylobacter jejuni*-Induced Inflammation in Human Epithelial Cells HEP-2 and HT-29 and in Mouse Intestinal Mucosa. *J. Nutr.* **2016**, *146* (10), 1980-1990.
125. Morrow, A. L.; Ruiz-Palacios, G. M.; Altaye, M.; Jiang, X.; Guerrero, M. L.; Meinen-Derr, J. K.; Farkas, T.; Chaturvedi, P.; Pickering, L. K.; Newburg, D. S., Human milk oligosaccharides are associated with protection against diarrhea in breast-fed infants. *J. Pediatr.* **2004**, *145* (3), 297-303.
126. Ruiz-Palacios, G. M.; Cervantes, L. E.; Ramos, P.; Chavez-Munguia, B.; Newburg, D. S., *Campylobacter jejuni* binds intestinal H(O) antigen (Fuc α 1, 2Gal β 1, 4GlcNAc), and fucosyloligosaccharides of human milk inhibit its binding and infection. *J. Biol. Chem.* **2003**, *278* (16), 14112-20.
127. Gonia, S.; Tuepker, M.; Heisel, T.; Autran, C.; Bode, L.; Gale, C. A., Human Milk Oligosaccharides Inhibit *Candida albicans* Invasion of Human Premature Intestinal Epithelial Cells. *J. Nutr.* **2015**, *145* (9), 1992-8.
128. El-Hawiet, A.; Kitova, E. N.; Kitov, P. I.; Eugenio, L.; Ng, K. K.; Mulvey, G. L.; Dingle, T. C.; Szpacenko, A.; Armstrong, G. D.; Klassen, J. S., Binding of *Clostridium difficile* toxins to human milk oligosaccharides. *Glycobiology* **2011**, *21* (9), 1217-27.
129. Nguyen, T. T.; Kim, J. W.; Park, J. S.; Hwang, K. H.; Jang, T. S.; Kim, C. H.; Kim, D., Identification of Oligosaccharides in Human Milk Bound onto the Toxin A Carbohydrate Binding Site of *Clostridium difficile*. *J. Microbiol. Biotechnol.* **2016**, *26* (4), 659-65.
130. Champion, E. M., Bruce; Dekany, Gyula, Mixtures of human milk oligosaccharides for treatment of bacterial infections. *U.S. Patent WO2016063262 A1*.
131. Lin, A. E.; Autran, C. A.; Espanola, S. D.; Bode, L.; Nizet, V., Human milk oligosaccharides protect bladder epithelial cells against uropathogenic *Escherichia coli* invasion and cytotoxicity. *J. Infect. Dis.* **2014**, *209* (3), 389-98.
132. Coppa, G. V.; Zampini, L.; Galeazzi, T.; Facinelli, B.; Ferrante, L.; Capretti, R.; Orazio, G., Human milk oligosaccharides inhibit the adhesion to Caco-2 cells of

diarrheal pathogens: *Escherichia coli*, *Vibrio cholerae*, and *Salmonella typhi*. *Pediatr. Res.* **2006**, 59 (3), 377-82.

133. Cravioto, A.; Tello, A.; Villafan, H.; Ruiz, J.; del Vedovo, S.; Neeser, J. R., Inhibition of localized adhesion of enteropathogenic *Escherichia coli* to HEp-2 cells by immunoglobulin and oligosaccharide fractions of human colostrum and breast milk. *J. Infect. Dis.* **1991**, 163 (6), 1247-55.
134. Coppa, G. V.; Gabrielli, O.; Giorgi, P.; Catassi, C.; Montanari, M. P.; Varaldo, P. E.; Nichols, B. L., Preliminary study of breastfeeding and bacterial adhesion to uroepithelial cells. *Lancet* **1990**, 335 (8689), 569-71.
135. El-Hawiet, A.; Kitova, E. N.; Klassen, J. S., Recognition of human milk oligosaccharides by bacterial exotoxins. *Glycobiology* **2015**, 25 (8), 845-54.
136. Andersson, B.; Porras, O.; Hanson, L. A.; Lagergard, T.; Svanborg-Eden, C., Inhibition of attachment of *Streptococcus pneumoniae* and *Haemophilus influenzae* by human milk and receptor oligosaccharides. *J. Infect. Dis.* **1986**, 153 (2), 232-7.
137. Simon, P. M.; Goode, P. L.; Mobasser, A.; Zopf, D., Inhibition of *Helicobacter pylori* binding to gastrointestinal epithelial cells by sialic acid-containing oligosaccharides. *Infect. Immun.* **1997**, 65 (2), 750-7.
138. Weichert, S.; Jennewein, S.; Hufner, E.; Weiss, C.; Borkowski, J.; Putze, J.; Schroten, H., Bioengineered 2'-fucosyllactose and 3-fucosyllactose inhibit the adhesion of *Pseudomonas aeruginosa* and enteric pathogens to human intestinal and respiratory cell lines. *Nutr. Res.* **2013**, 33 (10), 831-8.
139. Marotta, M.; Ryan, J. T.; Hickey, R. M., The predominant milk oligosaccharide 6'-sialyllactose reduces the internalisation of *Pseudomonas aeruginosa* in human pneumocytes. *J. Funct. Foods* **2014**, 6, 367-373.
140. Koromyslova, A.; Tripathi, S.; Morozov, V.; Schroten, H.; Hansman, G. S., Human norovirus inhibition by a human milk oligosaccharide. *Virology* **2017**, 508, 81-89.
141. Schroten, H.; Hanisch, F. G.; Hansman, G. S., Human Norovirus Interactions with Histo-Blood Group Antigens and Human Milk Oligosaccharides. *J. Virol.* **2016**, 90 (13), 5855-9.
142. Hester, S. N.; Chen, X.; Li, M.; Monaco, M. H.; Comstock, S. S.; Kuhlenschmidt, T. B.; Kuhlenschmidt, M. S.; Donovan, S. M., Human milk oligosaccharides inhibit rotavirus infectivity in vitro and in acutely infected piglets. *Br. J. Nutr.* **2013**, 110 (7), 1233-42.
143. Diarrhoeal disease. World Health Organization. **2017**.

144. Freitag, C. M.; Strijbis, K.; van Putten, J. P. M., Host cell binding of the flagellar tip protein of *Campylobacter jejuni*. *Cell Microbiol.* **2017**, 19 (6), e12714.
145. Cróinín, T. Ó.; Backert, S., Host epithelial cell invasion by *Campylobacter jejuni*: trigger or zipper mechanism? *Front. Cell Infect. Microbiol.* **2012**, 2, 25.

CHAPTER 3

Evaluation of the Antibacterial Properties of Heterogenous Human Milk Oligosaccharides Against *Streptococcus agalactiae*, *Staphylococcus aureus*, and *Acinetobacter baumannii*

3.1 *Group B Streptococcus*

3.1.1 *Group B Streptococcus: An Introduction*

Streptococcus agalactiae (Group B *Streptococcus*, Group B Strep, GBS) is an encapsulated Gram-positive diplococcus that colonizes the gastrointestinal (GI) and genital tracts of around 50% of women at some point during their pregnancy.^{1, 2} While GBS colonization is typically asymptomatic in healthy adults, it can pose a real threat to elderly, infant, and/or immunocompromised populations. Indicative of this reality, since the 1970s, GBS has been a leading cause of neonatal morbidity and mortality.^{1, 2, 3}

3.1.2 *Clinical Manifestations and Modes of Transmission*

Neonatal GBS infections most commonly present as pneumonia, sepsis, and meningitis.^{1, 2, 4, 5} Importantly, GBS is one of the most common causes of neonatal sepsis and is responsible for around 12% of stillbirths worldwide.^{6, 7} Though less frequently, GBS can also present as cellulitis, septic arthritis, adenitis, and osteomyelitis.^{1, 2}

GBS is most commonly transmitted from a GBS-colonized mother to her infant during labor and delivery as the infant passes through a colonized birth canal or *in utero* via bacterial ascension into the amniotic sac.¹ These modes of transmission are known

as vertical transmission. In women, the primary reservoirs for GBS are the GI and genital tracts. In infants, while the GI tract is similarly a frequent site of colonization, the throat is also a common GBS reservoir; the throats of infants are more commonly colonized than the throats of adults.^{1, 3, 8} It has been hypothesized that GBS initially colonizes the infant throat when it comes into contact with vaginal secretions during an infant's passage through the birth canal.³ Though much less common, GBS can also colonize infants via horizontal transmission from hospital or community sources; this transmission is likely fecal to oral.¹

In addition to these modes of transmission, there is also evidence that GBS may be transmitted through infected breastmilk. It is well-known that breastmilk is not sterile but rather contains hundreds of bacterial species.⁹⁻¹¹ Furthermore, it has been shown that the milk of healthy women contains around 10^3 - 10^4 cfu/mL of bacteria. The prevalence and diversity of bacteria in human milk has given rise to the term "the human milk microbiome" Some of the most commonly isolated species from breastmilk include various *Bifidobacterium*, *Lactobacillus*, *Staphylococcus*, and *Streptococcus* species.¹⁰

Despite the clear potential for the transmission of bacteria through breastmilk, studies detailing the prevalence of GBS in breastmilk are few in number and the methods for identification of GBS in these studies can be highly variable.³ Regardless, while numerous studies have found GBS in breastmilk, the manner in which breastmilk becomes colonized remains unclear.^{3, 10, 12-14} One proposed mechanism is through retrograde transmission from the infant. In this mode of transmission, GBS found in the throat and oral cavity of an infant who became colonized with GBS during labor and delivery contaminates the mother's milk ducts due to retrograde flow of milk during

suckling. Once introduced into the mammary ducts, GBS can then multiply and persistently infect the mother and infant.^{3, 10, 13} This can occur with or without mastitis.³

Another potential mechanism by which breastmilk may become contaminated is via translocation of GBS from the maternal gut and GI through lymphatics to the mammary glands.^{3, 13} However, the exact manner in which bacteria could cross the intestinal epithelium and reach the mammary gland whilst evading the immune system remains unknown.¹⁰ Regardless, there are several discoveries which lend credence to this mechanism of transmission. First, the presence of strict anaerobes like bifidobacteria in breastmilk suggests that there is mechanism of transmission other than via infant mouth to maternal skin. Second, bacteria can be isolated from colostrum even prior to an infant's birth.¹⁰ Third, the presence of orally administered bacteria, such as lactobacilli, in breastmilk suggests that bacteria from the maternal gut can in fact colonize the mammary gland and, by extension, breastmilk.^{3, 10}

As a final note, even in the absence of preventative treatments to stop vertical GBS transmission, not all infants born to GBS colonized mothers will be colonized with GBS themselves.^{1, 3, 7} Indeed, only around 50% of infants born to GBS colonized mothers will be colonized with GBS at birth, and only around 1-2% of these infants will go on to develop invasive GBS disease.

3.1.3 Types of GBS Disease and Methods for Prevention and Treatment

There are two main types of GBS disease: early-onset disease (EOD) and late-onset disease (LOD) (**Table 3.1**). EOD accounts for around 70% of all GBS cases and typically occurs within the first 24 hours of life.^{1, 3} EOD can also occur up to one week

after delivery and can present as a range of illnesses including asymptomatic bacteremia and septic shock. While maternal GBS colonization status is the most significant risk factor for EOD, other common risk factors include maternal intrapartum fever (>99 °F; 38 °C), prolonged rupture of membranes (>18 h before delivery), chorioamnionitis, and having had a previous infant with invasive GBS disease.^{1, 7}

LOD is less common than EOD and occurs after the first week of life and up to the first three months of life, though most cases of LOD present within the first month to month and a half after birth.¹ Similar to EOD, bacteremia without a defined focus is an exceedingly common manifestation of LOD. Meningitis is, however, more common in LOD than EOD.^{1, 3} Other manifestations of LOD include pneumonia, cellulitis, and osteoarticular infections.¹ Furthermore, up to 50% of infants who survive LOD suffer from severe neurological sequelae.³ Unlike EOD, LOD usually occurs with a lack of maternal obstetric and/or nursery complications.¹ Additionally, the risk factors for LOD are different than those for EOD. LOD can result from late onset presentation following early GBS colonization of the infant or from horizontal transmission. Importantly, horizontal transmission is a more common mode of acquisition for LOD than EOD. Moreover, reports of infants infected with GBS due to contaminated breast milk are generally associated with LOD.^{3, 13}

The last type of GBS disease is late-late onset disease, though this type of invasive disease is much less common than EOD or LOD (**Table 3.1**).¹ Late-late-onset infection occurs after the first three months. This type of infection most commonly presents as bacteremia without a focus and most commonly occurs in infants who were born before 35 weeks gestation who had prolonged stays in neonatal hospital units.

Table 3.1. Types of GBS Disease

	Early-Onset	Late-Onset	Late-Late-Onset
% of GBS Cases	~70%	<30%	Rare
Time Frame	1 st week of life	1 st week – 3 months	After 3 months
Common Mode of Transmission	Vertical from GBS positive mother	Late presentation of early colonization; horizontal from community; contaminated breast milk	Horizontal; common in premature babies with prolonged stay in neonatal units
Typical Presentation	Asymptomatic bacteremia	Bacteremia without a focus; meningitis	Bacteremia without a focus
Preventative Treatment	Intrapartum antibiotic prophylaxis (IAP)	None	None

In the United States alone, a 2014 report from the Centers for Disease Control (CDC) estimated that EOD and LOD affected around 1 in 4000 and 1 in 3000 newborns, respectively.¹⁵ Importantly, while the rates of EOD have decreased dramatically since the 1990s, the rates of LOD have remained largely stagnant in that time frame. The drop in EOD rates is attributed mainly to the introduction and implementation of intrapartum antibiotic prophylaxis (IAP). In the 1980s and '90s, studies emerged that demonstrated the ability of antenatal GBS screening combined with administration of IAP for GBS positive mothers to prevent EOD.¹⁶⁻¹⁸ As a result, in 1996, the CDC introduced the first

guidelines for the prevention of GBS disease which included GBS screening and IAP administration.^{1, 7}

Current CDC guidelines (also recommended by the American Academy of Pediatrics, AAP) recommend universal culture-based screening late in a woman's third trimester (between 35 and 37 weeks gestation) and implementation of IAP for mothers who test positive for GBS; screening late in pregnancy is recommended because GBS colonization status can vary over the course of pregnancy, so colonization status early in pregnancy is not a predictive factor for EOD.¹⁸ For the implementation of IAP, the CDC guidelines include a recommended regimen for antibiotic selection (**Figure 3.1**).

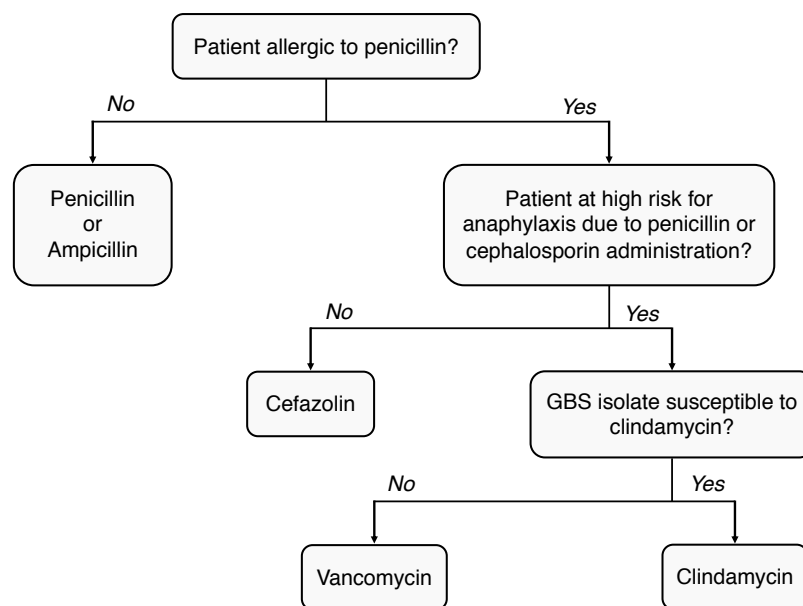


Figure 3.1. Current CDC antibiotic selection guidelines for intrapartum antibiotic prophylaxis (IAP) against early-onset GBS disease (EOD).

Broadly speaking, GBS is susceptible to penicillins, extended-spectrum penicillins, cephalosporins, and vancomycin.¹⁸ However, because penicillin has a narrow spectrum of antimicrobial activity and a well-understood safety profile for both mother and child, penicillin is the first antibiotic recommended for IAP with ampicillin being considered as

an acceptable alternative; β -lactam antibiotics for prophylaxis are typically administered every 4 hours until delivery. Unfortunately, maternal β -lactam allergies preclude the use of penicillin or ampicillin. Thus, for β -lactam allergic mothers, appropriate alternatives must be identified.

For women who do not have a history of anaphylaxis, angioedema, respiratory distress, or urticaria following administration of a β -lactam or cephalosporin, cefazolin is the recommended antibiotic.¹⁸ For women who do have a history of these reactions to β -lactams or cephalosporins and are at a high risk for anaphylaxis, GBS antimicrobial susceptibility testing is ordered to determine susceptibility of the GBS isolate to clindamycin. Earlier versions of guidelines instructed that susceptibility of GBS to erythromycin be tested. Due to increasing instances of GBS resistance to erythromycin (ca. 30% of isolates are erythromycin-resistant), however, erythromycin is no longer recommended as a potential antibiotic for IAP. Thus, if a woman is at high risk for β -lactam-induced anaphylaxis and her GBS isolate is sensitive to clindamycin, clindamycin is the recommended antibiotic. If her isolate is resistant to clindamycin, vancomycin is recommended.

While IAP has been largely effective at preventing EOD, it is not an effective preventative measure for LOD.¹⁸ It is important to note, however, that the antibiotics used for IAP are appropriate for treating LOD once it has manifested. The ineffectiveness of IAP and the current lack of any alternative preventative treatment for LOD is responsible for the multi-decade long stagnation in LOD rates. Moreover, IAP is also ineffective against prenatal-onset disease (includes stillbirths and miscarriages). It is also important to note that rates of GBS infections in developing and resource-poor settings have been

shown to be higher than those reported for the United States.¹⁹ This, at least with regard to EOD, is likely due in part to a lack of adequate facilities and resources for GBS screening and IAP administration.

As a final note, while IAP has dramatically reduced the GBS disease burden, concerns remain about the effects of antibiotic treatment on the developing flora of the infant and the established flora of the mother. Indeed, collateral damage to host symbiotes is a common problem with antibiotic treatments, and the extent of this damage due to IAP is currently unclear.^{2, 13, 20, 21} Additionally, continued antibiotic usage is most often accompanied with concerns about increasing antibiotic resistance. The reality that ca. 30% of clinical GBS isolates are resistant to erythromycin and around 20% are resistant to clindamycin highlights the validity of this concern with respect to IAP.¹⁸

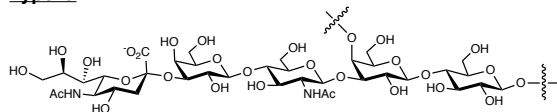
3.1.4 GBS Virulence Factors

GBS is an opportunistic pathogen that employs numerous virulence factors to help it persist in a hostile host environment and cause disease.²² These include factors to promote entry into host cells, intracellular survival and systemic circulation, immune evasion, resistance to host antimicrobial peptides (AMPs), and adherence and subsequent invasion of host-cell surfaces. For example, GBS produces pore-forming toxins that facilitate entry into host cells and possesses cell-surface pili which facilitate adherence and attachment to host cells. Moreover, GBS can decrease the net negative charge on its cell surface to decrease its affinity towards positively charged AMPs.²²

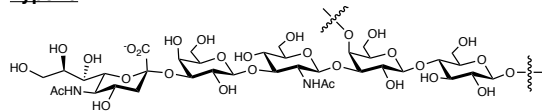
One GBS virulence factor that has been extensively studied and well-characterized are the capsular polysaccharides (CPS). These oligosaccharides are particularly

important for evasion of detection by the host immune system.²²⁻³² Based on their structures, GBS CPS can be divided into ten serotypes (Ia, Ib, II-IX) (Figure 3.2).^{25, 33}

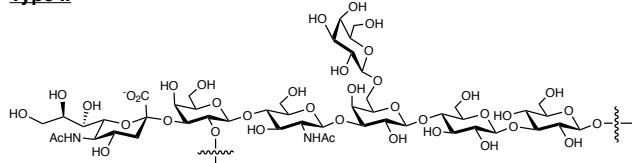
Type Ia



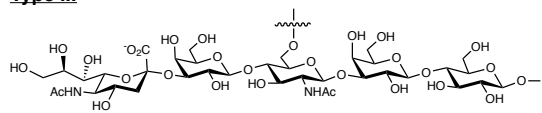
Type Ib



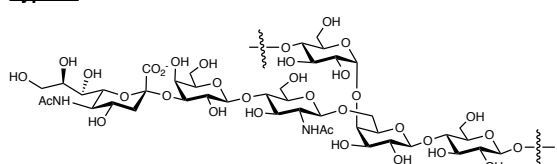
Type II



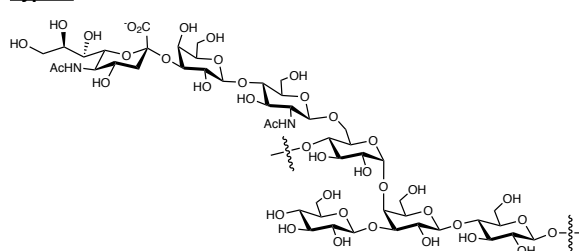
Type III



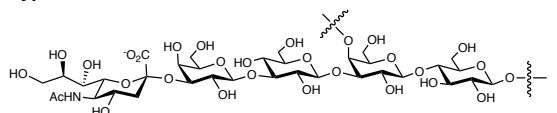
Type IV



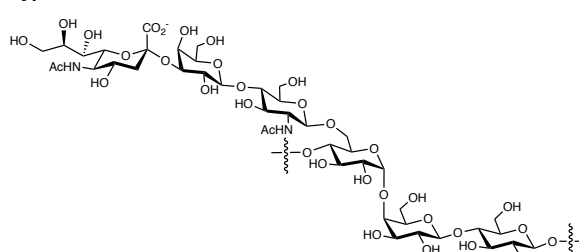
Type V



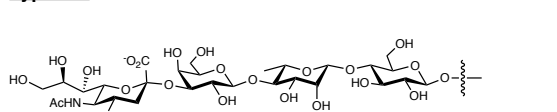
Type VI



Type VII



Type VIII



Type IX

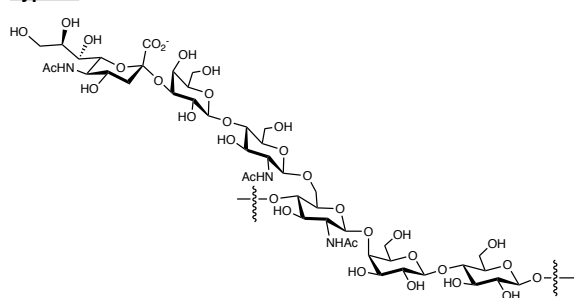


Figure 3.2. Structures of the repeating units of the Group B *Streptococcus* (GBS) capsular polysaccharides (CPS) for serotypes Ia, Ib, and II-XI.

Serotypes Ia, Ib, II, III, and IV account for over 85% of the global invasive GBS disease burden with serotype III alone accounting for around 25%.^{34, 35} Despite their structural differences, all GBS CPS repeating units feature a terminal sialic acid residue (the Neu5Ac form of sialic acid).^{25, 28, 35} This shared feature has been shown to be critical to GBS virulence. As glycoconjugates terminated with Neu5Ac are common host antigens, the terminal Neu5Ac moiety of GBS CPS is an example of molecular mimicry.^{22, 27, 32} As a result of this mimicry, the host fails to recognize GBS as a foreign antigen and thus does not initiate the necessary immune response.^{22, 26, 30}

Another method GBS uses to increase its pathogenicity is biofilm formation. To understand the relationship between biofilm production and GBS pathogenicity, it is important to digress briefly into a general description about biofilm production, structure, and function. Biofilms are structured, organized communities of cells encapsulated by a self-produced extracellular polymeric matrix (EPS) which can adhere to biotic or abiotic surfaces.³⁶⁻³⁸ The EPS consists primarily of oligosaccharides, DNA, and proteins and is important both to the structural integrity of the biofilm matrix and the ability of bacteria to adhere to and communicate with one another.³⁹ Importantly, within the matrix are open water channels to facilitate nutrient delivery and waste removal.³⁷ The stages of biofilm production are illustrated in **Figure 3.3**.³⁸ Following initial attachment (initiation), bacteria begin to multiply and excrete EPS (maturation). Once the biofilm has reached a mature stage, bacterial cells can be liberated from the biofilm matrix (detachment) and spread to new locations to form new biofilm communities.

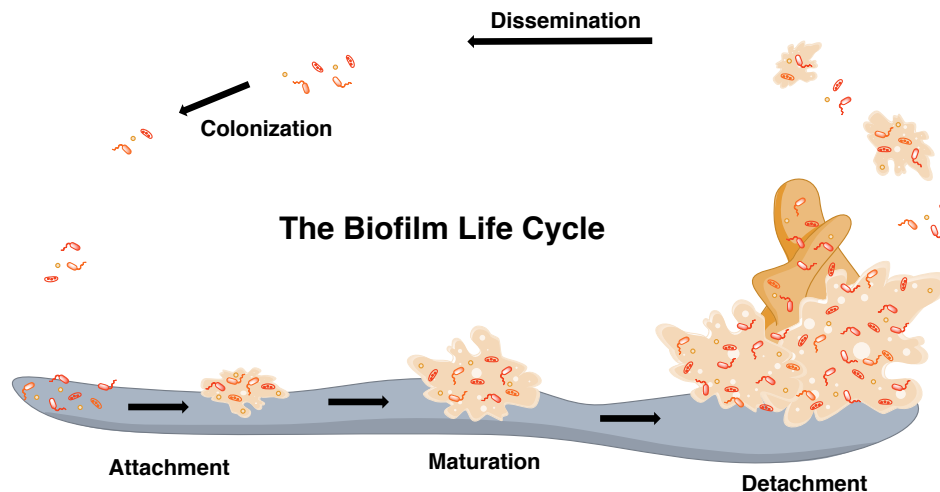


Figure 3.3. The biofilm life cycle.

For several species including *Pseudomonas aeruginosa*, *Staphylococcus aureus*, and *Streptococcus mutans*, it has been shown that quorum sensing (QS), a method of intercellular signaling and communication, is an important factor in the maturation and/or dissolution of biofilm bacterial communities.⁴⁰⁻⁴³ QS is a method of cell-to-cell communication that allows bacterial cells to evaluate their surrounding population density and respond accordingly with changes in gene expression once a threshold number of cells, also known as a “quorum,” has been reached.⁴³⁻⁴⁵ As cells within a biofilm encounter much higher local cell densities than planktonic, free-floating cells, it has been argued that biofilms represent a particularly environmentally relevant context for this intercellular communication.⁴⁰

QS is facilitated by the production of diffusible, low-molecular weight signaling molecules known as autoinducers (AIs); AI concentration in the local environment is proportional to cell density.^{44, 45} AIs differ among species with Gram-positive species typically using peptide signaling molecules, Gram-negative typically using *N*-acyl L-homoserine lactone (AHL) derivatives, and numerous Gram-positive and Gram-negative

species using the interspecies signal AI-2. Once a sufficient amount of environmental AI has accumulated signaling that a “quorum” of cells has been reached, the AI is able to bind its target receptor (intracellular or membrane-bound) and initiate changes in gene expression required for the QS phenotype. For example, in *S. aureus*, when a quorum is reached and the autoinducing peptide (AIP) binds its target receptor, this binding activates a regulatory cascade that leads to increased expression of invasive factors such as toxins, hemolysins, proteases, and other tissue-degrading enzymes.^{42, 46} Moreover, these factors alter the metabolic status of the bacteria which subsequently changes their biofilm-forming capacity.

A notable feature of bacteria in a biofilm matrix is the significantly higher resistance to environmental stressors seen for this population compared to their planktonic counterparts.³⁸ Indeed, bacteria growing in the biofilm have increased tolerance toward antibiotics and disinfectants as well as toward the actions of the host immune response. For example, the minimum inhibitory concentration (MIC) of antibiotics against biofilm-dwelling bacteria can be up to 1000-fold higher than that of planktonic bacteria.^{36, 37, 47} The observation that the ESKAPE pathogens (discussed in Chapter 1), which are notorious for their abilities to evade antimicrobial action, are also prolific biofilm producers speaks to the protective nature of biofilms.⁴⁸ Moreover, the reality that biofilms are involved in an estimated 80% of microbial infections in the body highlights the importance of biofilm production to bacterial pathogenesis.³⁷

The unique protection the biofilm matrix affords bacteria is multi-faceted. Perhaps the most obvious protection afforded by the biofilm is a physical one. The EPS creates a physical barrier between bacterial cells and the hostile host environment. This added

barrier can make it increasingly difficult for antimicrobial agents and host defense mechanisms to fully penetrate the biofilm.^{36, 38, 49} Perhaps paradoxically, while the EPS shields bacteria from harsh external conditions, bacteria within the EPS actual encounter harsh internal conditions including, but not limited to, decreased oxygen and nutrient levels.^{36, 37, 50, 51 51}

As a result of the harsh conditions inside the biofilm, it is largely accepted that some cells in the biofilm, particularly those deep within the matrix, exist in a slow-growing state.³⁸ This decreased metabolic growth rate is also postulated to play a critical role in the ability of bacteria in the biofilm to resist the action of antibiotics that target-specific growth factors. For example, β -lactams, which target cell wall synthesis, are ineffective against non-dividing cells.^{36, 37, 47, 49} Moreover, these persistent cells, i.e. dormant versions of regularly growing cells, are critical to the restoration of biofilm communities following antimicrobial treatment.⁴⁹ In sum, the physical barrier the biofilm provides as well as the phenotypic shift in metabolic rates and gene expression it causes for the bacteria enclosed within the matrix account for the increased resistance of bacteria in the biofilm state.

The first evidence that GBS could form biofilms came from a study by Marrie and Costerton wherein they isolated GBS from biofilms on intrauterine devices.⁵² Importantly, the isolated GBS strains were found in association with other known biofilm formers like *S. aureus*. Since this initial study, additional studies have demonstrated the ability of GBS to form biofilms on biotic and abiotic surfaces.^{5, 53-56} These studies have also shown that GBS pili and CPS are key to biofilm formation.^{53, 56, 57} Moreover, it has been found that environmental conditions including pH and media nutrient levels can have a strong

influence on biofilm formation.^{5, 55, 58} For example, it has been reported that acidic pH stimulates the production of biofilm in GBS. This finding subsequently led to the hypothesis that the acidic environment of the vagina signals the bacteria to produce biofilm thus allowing them to persist in a hostile environment.^{55, 58} While it has been shown that GBS can persist in the female genital tract, it is not yet well-understood how the bacteria accomplish this long-term.^{55, 59} Similarly, while there is evidence of the importance of biofilm formation to GBS survival, more research is needed to confirm the relevance of GBS biofilm formation *in vivo*.⁵⁵

3.1.5 Maternal-Derived Sources of Protection Against GBS

As noted earlier, of the infants born to GBS colonized mothers, only around 50% will become colonized with GBS themselves. Of that population, approximately 1-2% will develop invasive GBS disease. This apparent disconnect between maternal GBS colonization and infant GBS disease development led researchers to investigate potential maternal-derived sources of protection against GBS. Thus far, two major sources of protection have been identified: maternal antibodies and human milk oligosaccharides (HMOs).

As discussed in Chapter 2, human milk contains numerous immune-modulating components, such as SIgA, that serve to protect infants from infection. Indeed, high levels of breast milk SIgA could prevent the carbohydrate-mediated attachment of GBS to the epithelial cells of the nose and throat thus protecting infants from developing invasive GBS disease.³ The association between maternal type-specific anti-CPS antibody concentrations and the occurrence of GBS disease in newborns was initially reported by

Baker and Kasper in the late 1970s. In the original study, Baker and Kaper identified an antibody in maternal serum which bound a purified polysaccharide antigen extracted from a type III serotype GBS strain.⁶⁰ Moreover, they found that women who were deficient in this antibody were more likely to give birth to infants who developed invasive GBS disease. The presence of type III CPS-specific antibodies is also notable as type III serotype GBS strains are responsible for the majority of LOD cases. Subsequent studies reaffirmed an association between low maternal serotype-specific antibodies against type III CPS antigens and an increased risk of newborns developing invasive GBS disease.⁶¹⁻⁶⁴ Additional studies have also shown the presence of type Ia, II, and V CPS-specific antibodies in maternal serum and their link to lowered incidences of invasive GBS disease.^{3, 62, 64, 65}

In addition to antibodies, HMOs have shown to be important sources of protection for infants against several pathogens. While a more exhaustive description of these protections is provided in Chapter 2, briefly, HMOs offer direct protection against pathogens by serving as antiadhesive antimicrobials. By resembling glycan cell surface receptors, HMOs can serve as decoy receptors to prevent the adhesion of pathogens, such as *C. jejuni* and *E. coli*, to epithelial cells; adhesion is the first step in a pathogen's progression towards invasive disease.⁹ These results demonstrate the possibility that HMOs offer protection against GBS through a similar mechanism. Additionally, the structural similarities between HMOs and GBS CPS (see **Figure 3.2**), especially the serotype Ia and Ib, creates a unique link between HMOs and GBS. Indeed, murine monoclonal antibodies to type Ib GBS CPS have been shown to also bind to LST a (**3.1**) and LNT (**2.4**) (**Figure 3.4**).⁶⁶

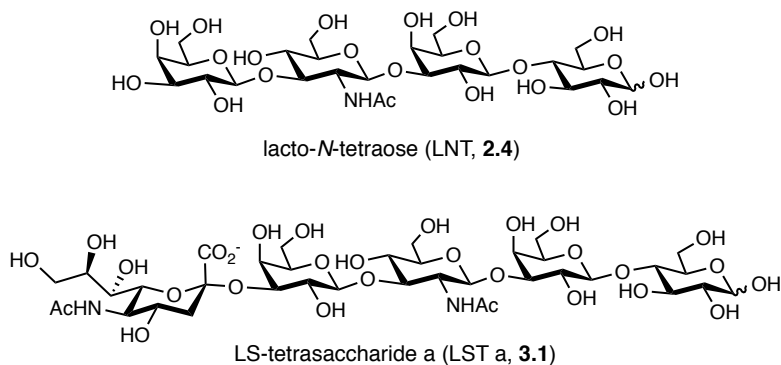


Figure 3.4. Structures of LS-tetrasaccharide a (LST a, **3.31**) and lacto-*N*-tetraose (LNT, **2.4**).

3.1.6 HMOs as a Source of Protection Against GBS: Previous Work

Recently, researchers began to investigate the roles HMOs have in GBS disease prevention. In a study from 2016 by Le Doare and coworkers, it was found that infants born to Lewis-positive mothers were significantly less likely to be colonized with GBS themselves at birth and were also more likely to clear colonization within ninety days than infants born to Lewis-negative mothers.⁴ There was, however, no association found between Secretor status and GBS colonization levels. Finally, they found that the presence of LNDFH I (**2.26**, see **Figure 2.10** in Chapter 2) and other similarly branched HMOs in milk was associated with significantly reduced levels of GBS growth.

In 2017, the Bode laboratory published a report that similarly demonstrated the ability of HMOs to inhibit GBS growth.⁶⁷ Using pooled HMO extracts (pHMO), Bode et al. found that HMOs possessed dose-dependent bacteriostatic activity against GBS strains of serotypes Ia, III, and V. Additionally, they showed that this activity did not extend to uropathogenic *E. coli* (UPEC), *P. aeruginosa*, or *S. aureus*. In an attempt to more narrowly define the active HMOs, they next separated pHMOs into sialylated, acidic HMOs (aHMOs) and non-sialylated, neutral HMOs (nHMOs). This separation facilitated

the discovery that the acidic fraction of HMOs did not inhibit GBS growth. Armed with the knowledge that the neutral portion of pHMOs were more active, Bode and coworkers next tested various single-entity neutral, fucosylated and non-fucosylated HMOs for activity against GBS. At 5 mg/mL, they found that LNT (**2.4**) and its fucosylated variant LNFP I (**2.10**, see **Figure 2.10** in Chapter 2) possessed the strongest antimicrobial activity.

Intrigued by these studies as well as the potential link between breastfeeding and GBS transmission, especially with regard to LOD, the Townsend lab began a program aimed at identifying and describing the protective effects of HMOs against GBS. To test the original hypothesis that HMOs possess antimicrobial and antivirulence activities, Townsend et al. assessed the antimicrobial and antibiofilm activities of whole HMO extracts from five different donors against a serotype V GBS strain (CNCTC 10/84).⁶⁸ Importantly, prior to biological evaluation, the Secretor and Lewis blood group status of each sample was determined using a high throughput mass spectrometry technique developed by Kunz and coworkers. This technique uses matrix assisted laser desorption ionization-time of flight (MALDI-TOF) MS and MS/MS to produce a mass fingerprint whose MS and MS/MS fragmentation peaks and intensities can be used to characterize fucosyl linkages in the HMOs present.⁶⁹ Due to the relationship between HMO fucosylation patterns and blood group status (detailed in Chapter 2), the corresponding Secretor and Lewis blood groups can be assigned based on HMO fucosylation patterns. The results of these experiments are summarized in **Table 3.2**; donor numbers correspond to the numbers previously assigned to each donor by the Vanderbilt Department of Pediatrics.

Table 3.2. Secretor and Lewis Blood Group Assignments of Five Donor Milk Samples

Donor	Lewis Blood Group	Milk Group
43	a+b-	Se-Le+
42	a-b+	Se+Le+
38	a-b-	Se+Le-
20	a-b+	Se+Le+
16	a-b-	Se+Le-

Following blood group assignments, HMO extracts were tested for their ability to alter GBS growth and viability over 24 h using a plate-based assay (**Figures 3.5 and 3.6**).⁶⁸ These evaluations were performed in both Todd-Hewitt Broth (THB) and THB supplemented with 1% glucose with HMOs dosed at 5 mg/mL.

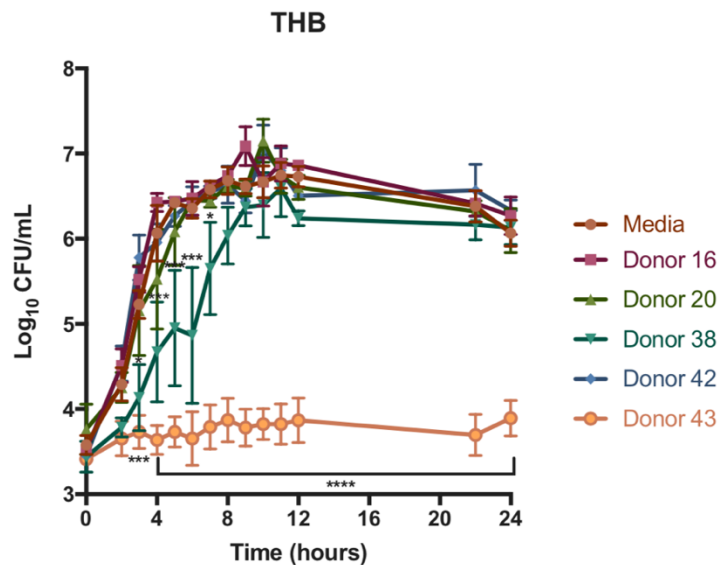


Figure 3.5. Effect of heterogeneous HMOs dosed at ca. 5 mg/mL on viability of GBS CNCTC 10/84 in THB. Enumeration of CFU/mL was performed at 0, 2, 4, 6, 8, 10, 12, 22, and 24 h. Mean \log_{10} CFU/mL for each HMO source and time point is indicated by the respective symbols. Data displayed represent the mean \log_{10} CFU/mL \pm SEM, of three independent experiments each with three technical replicates. * represents $p < 0.05$, ** represents $p < 0.01$, *** represents $p < 0.001$, and **** represents $p < 0.0001$ by two-way ANOVA with *posthoc* Dunnett's multiple comparison test comparing the viability of GBS CNCTC 10/84 in each HMO supplementation condition to the viability of GBS CNCTC 10/84 in media alone.

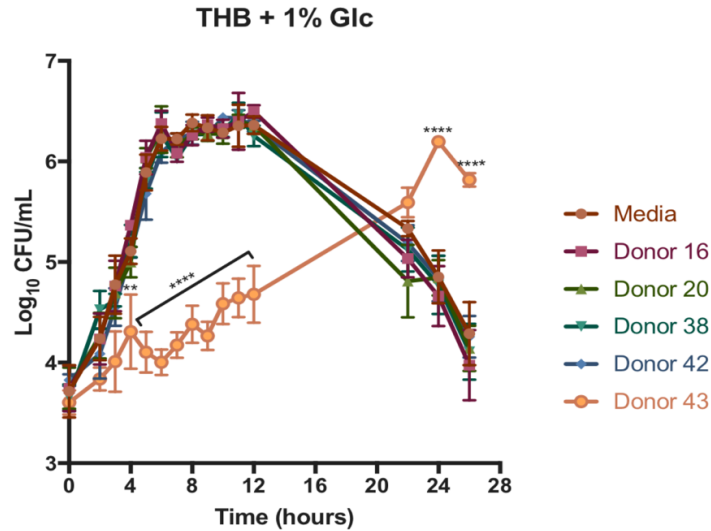


Figure 3.6. Effect of heterogeneous HMOs dosed at ca. 5 mg/mL on viability of GBS CNCTC 10/84 in THB + 1% glucose (glc). Enumeration of CFU/mL was performed at 0, 2, 4, 6, 8, 10, 12, 22, and 24 h. Mean log₁₀CFU/mL for each HMO source and time point is indicated by the respective symbols. Data displayed represent the mean log₁₀CFU/mL ± SEM, of three independent experiments each with three technical replicates. * represents $p < 0.05$, ** represents $p < 0.01$, *** represents $p < 0.001$, and **** represents $p < 0.0001$ by two -way ANOVA with *posthoc* Dunnett's multiple comparison test comparing the viability of GBS CNCTC 10/84 in each HMO supplementation condition to the viability of GBS CNCTC 10/84 in media alone.

In both growth conditions, HMOs from Donor 43 demonstrated significant antimicrobial activity; GBS growth was decreased by around 40%. It is important to note though, that GBS growth did begin to rebound before the end of the 24 h growth period. This demonstrates the bacteriostatic rather than bactericidal activity of HMOs, which agreed with previous studies.^{67,70} In THB, HMOs from Donor 38 also showed significant antimicrobial activity though to a lesser extent than those from Donor 43. In THB + 1% glucose, however, HMOs from Donor 38 did not cause any significant alternations to GBS growth. HMOs from the remaining donors showed no significant antimicrobial activity in either growth condition.

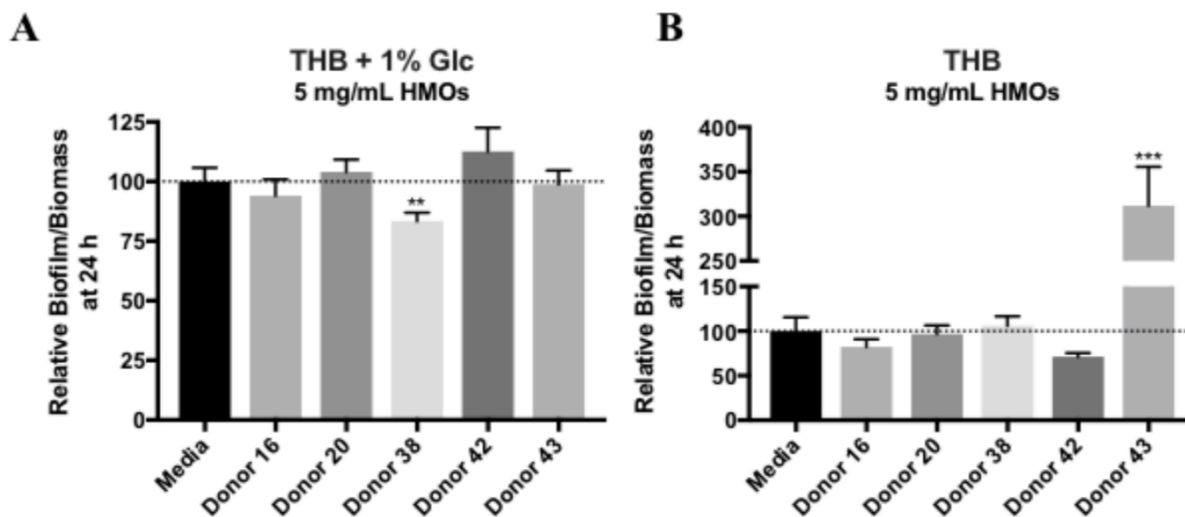


Figure 3.7. Effects of heterogeneous HMOs dosed at ca. 5 mg/mL on GBS CNCTC 10/84 biofilm production after 24 h of growth. **(A)** Biofilm production in THB, denoted by the ratio of biofilm/biomass (OD_{560}/OD_{600}), in the presence of heterogenous HMOs relative to biofilm production in media alone. Data displayed represent the relative mean biofilm/biomass ratio \pm SEM of at least three independent experiments, each with 3 technical replicates, wherein biofilm production in media alone is assigned a value of 100%. *** represents $p = 0.0008$ by one-way ANOVA, $F = 23.35$ with *posthoc* Dunnett's multiple comparison test comparing biofilm production in the presence of HMOs to biofilm production in media alone. **(B)** Biofilm production in THB + 1% glc, denoted by the ratio of biofilm/biomass (OD_{560}/OD_{600}), in the presence of heterogeneous HMOs relative to biofilm production in media alone. Data displayed represent the relative mean biofilm/biomass ratio \pm SEM of at least three independent experiments, each with 3 technical replicates, wherein biofilm production in media alone is assigned a value of 100%. ** represents $p = 0.0018$ by one-way ANOVA, $F = 3.449$ with *posthoc* Dunnett's multiple comparison test comparing biofilm production in the presence of HMOs to biofilm production in media alone. Mean GBS biofilm production levels in media alone are marked with a dotted line.

Using the same-plate based assay, antibiofilm activity of the HMO extracts at 5 mg/mL was evaluated at 24 h of growth (**Figure 3.7**).⁶⁸ To account for any accompanying antimicrobial activity, the biofilm results were expressed as a ratio of biofilm produced to the number of bacterial cells present (biomass); this essentially provides a measurement of biofilm produced per bacterial cell. While in THB no HMO extracts inhibited biofilm

formation, in THB + 1% glucose (which has been shown to promote biofilm production),⁵⁵ HMOs from Donor 38 did significantly decrease biofilm formation.

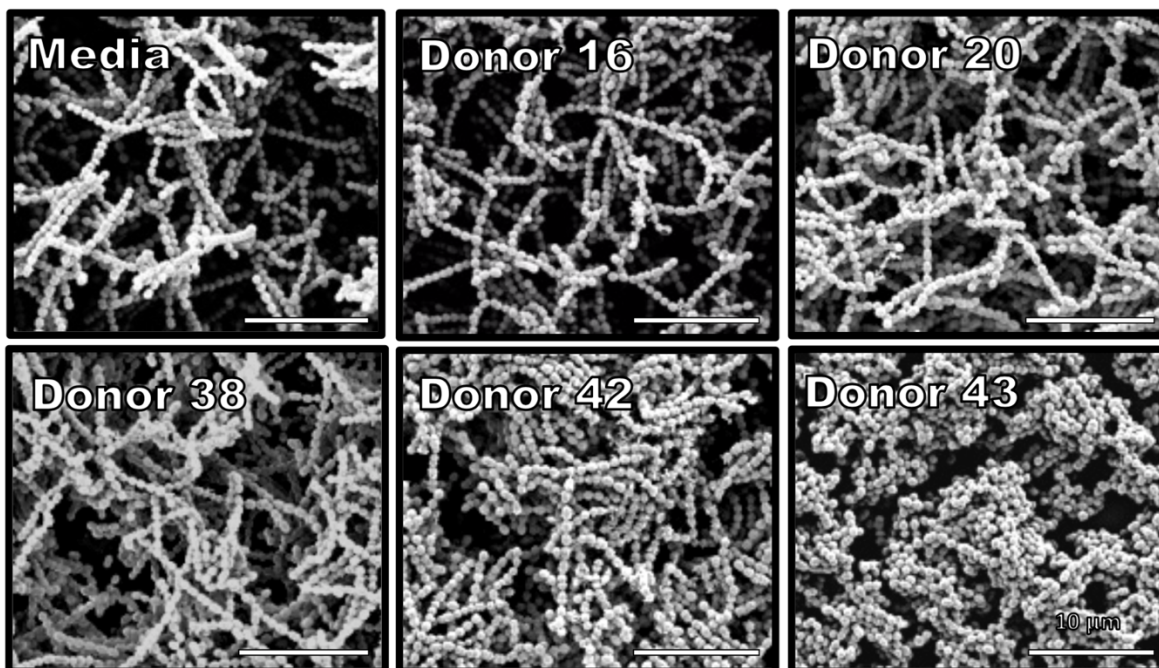


Figure 3.8. SEM micrographs of GBS CNCTC 10/84 biofilm formation after 24 h. GBS CNCTC 10/84 was cultured in THB + 1% glucose supplemented with HMOs from individual donor samples for 24 h at 37 °C. Images are shown at 1000x magnification.

As a final evaluation of HMO antibiofilm activity, Townsend et al. used scanning electron microscopy (SEM) and confocal laser scanning microscopy (CSLM) to evaluate the qualitative effects of HMOs on GBS biofilm formation (ex. alterations in biofilm structure and architecture) (**Figure 3.8**).⁶⁸ Interestingly, treatment with HMOs from Donor 43 resulted in biofilms that were smaller and less diffuse. Moreover, HMOs from Donor 43 caused changes in GBS chaining morphology. As opposed to the typical long, organized chains of GBS, in the presence of Donor 43 HMOs, GBS organized into truncated chains that were more densely packed compared to the control grown in the absence of HMOs. Additionally, GBS grown in the presence of HMOs from Donors 38 and 16 appeared to have less prominent nutrient channels in the biofilm. HMOs from

Donor 38 were also shown using CSLM to decrease the overall thickness of GBS biofilm (results not shown). Moreover, carbohydrates were shown to be concentrated at the tops of the biofilm.

Encouragingly, the results of this preliminary study demonstrated that HMOs possess both antimicrobial (bacteriostatic) and antibiofilm activities against GBS. Additionally, this study represented the first report of HMOs serving as antibiofilm agents. While encouraging, this probing study was nevertheless somewhat narrow in scope using HMOs from only five donors and testing against only one GBS strain. To address these limitations, an accompanying study was completed that not only expanded the number of donors but also expanded the number of GBS strains tested from one to three. We hypothesized that this expanded study would allow for, one, investigation of a potential relationship between Lewis and Secretor status and HMO biological activity, and, two, determination of whether HMO biological activity against GBS was species- or strain-specific. The results of this work are presented herein.

3.2 Evaluation of Antimicrobial and Antibiofilm Properties of Heterogenous HMOs⁷¹

The work described herein was enabled by the generous donation of human milk from a number of women from across the United States. Milk samples were obtained through Dr. Jörn-Hendrik Weitkamp of the Vanderbilt Department of Pediatrics as well as Medolac. Evaluation of heterogenous HMO antibacterial activity against GBS was completed in partnership with Dr. Dorothy L. Ackerman.

3.2.1 HMO Isolation and Blood Group Characterization

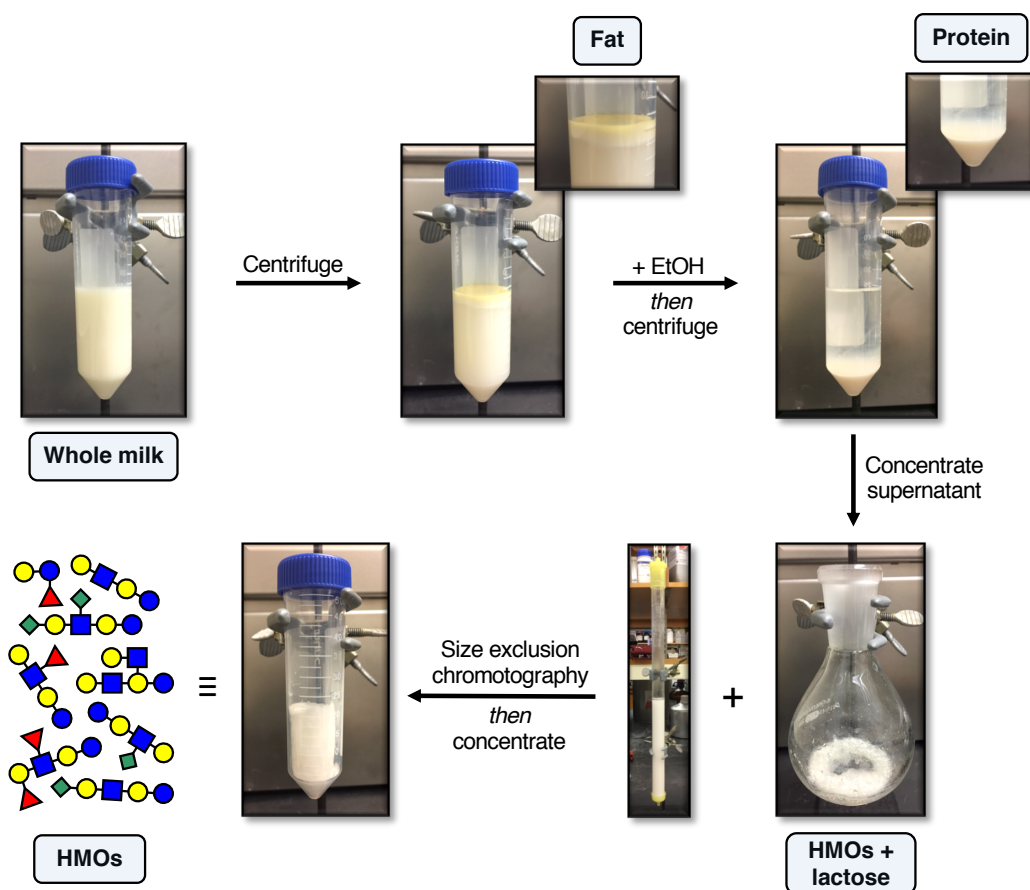


Figure 3.9. Isolation of HMOs from whole milk workflow.

HMOs from fourteen new donors were isolated using the four-step procedure illustrated in **Figure 3.9**. Briefly, fats are first removed via centrifugation. Proteins are then precipitated with ethanol and removed via centrifugation. Finally, HMOs can be de-salted (purified) using size exclusion chromatography. Following HMO isolation, the Lewis and Secretor status of each donor were assigned using the high throughput HMO mass fingerprinting technique developed by Kunz and co-workers (described previously); again, donor sample numbers correspond to the numbers previously assigned to each donor by the Vanderbilt Department of Pediatrics (**Table 3.3**). In total, blood groups for nineteen donors (five from previous study and fourteen from the presently described study) were

assigned. Importantly, the distribution of Lewis blood groups for these nineteen donors tracks well with distributions reported previously for larger populations (**Table 3.4**).⁷²⁻⁷⁴

Table 3.3. Secretor and Lewis Blood Group Assignments of Fourteen Donor Milk Samples

Donor	Lewis Blood Group	Milk Group
0	a-b+	Se+Le+
5	a-b+	Se+Le+
7	a-b+	Se+Le+
8	a-b+	Se+Le+
14	a-b+	Se+Le+
17	a+b-	Se-Le+
18	a+b-	Se-Le+
19	a-b+	Se+Le+
24	a-b+	Se+Le+
29	a+b-	Se-Le+
31	a+b-	Se-Le+
32	a-b+	Se+Le+
34	a-b+	Se+Le+
37	a-b+	Se+Le+

Table 3.4. Lewis Blood Group Distribution for Nineteen Donor Milk Samples

Lewis Blood Group	Distribution
a-b+	63%
a-b-	22%
a+b-	26%

3.2.2 Evaluation of Antimicrobial and Antibiofilm Activities of HMOs Against GBS⁷¹

After assigning blood groups to each HMO sample, we moved to test the antimicrobial and antibiofilm activities of HMOs from the fourteen new donors. To determine whether any observed activity was strain- or species-specific, we expanded the number of GBS strains from one to three. In addition to assaying against strain

CNCTC 10/84, we also assayed against the clinical isolate strains GB590 and GB2. Importantly, these strains are each of a differing serotype. CNCTC 10/84, GB590, and GB2 are serotypes V, III, and Ia strains, respectively. These particular strains and serotypes were chosen due to their relevance to the global GBS burden; of the ten identified serotypes, Ia, Ib, II, III, and V account for over 85% of cases of invasive GBS disease.^{34, 56, 75} Moreover, type III serotype strains are the most prevalent isolates associated with neonatal disease in the developed world.^{34, 76}

In addition to screening against multiple strains of GBS, we also elected to screen in two different media sources. For each HMO sample, activity was evaluated in both THB and THB + 1% glucose as supplementation with 1% glucose has been shown to increase bacterial biofilm production.^{53, 55} Finally, HMOs were screened for activity at a concentration of ca. 5 mg/mL as this concentration is at the low end of physiological levels; HMOs are typically found in milk at 5-25 mg/mL depending on the stage of lactation.⁷⁷

Antimicrobial and antibiofilm activity were assessed at 24 h of growth using a plate-based biofilm assay which allows for spectrophotometric quantification of both bacterial growth and biofilm formation. Growth (biomass) was first quantitated via spectrophotometric readings at an optical density of 600 nm (OD_{600}). Following the initial biomass reading, free-floating bacteria were gently removed and the remaining, adherent bacteria (i.e. bacteria in the biofilm) were stained with crystal violet. Bacteria in the biofilm could then be quantitated via spectrophotometric readings at OD_{560} . To account for any accompanying antimicrobial activity, biofilm results are expressed as a ratio of total biofilm produced (OD_{560} value) to the number of bacterial cells present (biomass, OD_{600} value).

This method allows for analysis of changes in biofilm production relative to the number of bacterial cells present.

Table 3.5. Antimicrobial Activity of Heterogeneous HMO Extracts Against Three Strains of *S. agalactiae* (GBS)^a

		Change in biomass from control (%) ± SEM					
		<i>S. agalactiae</i> CNCTC 10/84		<i>S. agalactiae</i> GB590		<i>S. agalactiae</i> GB2	
Lewis blood group	Donor	THB	THB + 1% glc	THB	THB + 1% glc	THB	THB + 1% glc
a-b+	0	-4 ± 2	+11 ± 2	+14 ± 3	+11 ± 3	+5 ± 2	+9 ± 2
	5	-26 ± 1	-12 ± 2	-31 ± 6	-9 ± 2	-22 ± 1	-5 ± 1
	7	-3 ± 1	+13 ± 4	+6 ± 3	+8 ± 2	-1 ± 2	-3 ± 2
	8	-80 ± 6	-5 ± 2	-75 ± 9	-8 ± 5	-89 ± 4	-6 ± 2
	14	+3 ± 1	+43 ± 1	+8 ± 4	+50 ± 2	+14 ± 2	+57 ± 1
	19	-8 ± 2	+7 ± 3	+13 ± 1	+28 ± 2	+11 ± 2	+14 ± 3
	24	-11 ± 3	+8 ± 1	+11 ± 3	+20 ± 2	+9 ± 3	-3 ± 1
	32	-14 ± 1	-16 ± 1	+10 ± 2	+15 ± 3	+14 ± 2	+6 ± 2
	34	+2 ± 1	+2 ± 3	+21 ± 3	+25 ± 4	+15 ± 2	+19 ± 5
	37	-1 ± 2	-17 ± 3	+23 ± 3	+24 ± 3	0 ± 2	+19 ± 3
a+b-	17	-2 ± 1	+4 ± 4	+7 ± 2	+17 ± 3	+7 ± 2	+17 ± 4
	18	-13 ± 3	+11 ± 1	-11 ± 3	+14 ± 2	-1 ± 2	-6 ± 2
	29	-42 ± 1	-17 ± 2	-35 ± 11	-22 ± 6	-15 ± 1	-6 ± 1
	31	-6 ± 2	+18 ± 2	+3 ± 2	+33 ± 4	+7 ± 2	+24 ± 3

^asignificant growth inhibition ($p \leq 0.05$, one-way ANOVA) compared to control is bolded and highlighted in blue.

To evaluate antimicrobial activity, we compared the biomass of bacteria grown in the presence of HMOs to that of bacteria grown in the absence of HMOs. Using this standard, several HMO samples were found to significantly inhibit bacterial growth for multiple GBS strains and both growth conditions ($p \leq 0.05$ by one-way ANOVA with *posthoc* Dunnett's multiple comparison test) (**Table 3.5**). The results presented in **Table 3.5** are shown as the average percent change \pm standard error of the mean (SEM) from the control (bacteria grown in media without HMOs) where negative numbers represent an overall decrease in growth and positive numbers represent an overall increase in growth.

The effects of HMOs from Donor 8 on GBS growth are particularly noteworthy. In THB, HMOs from Donor 8 decreased growth by more than 70% for all GBS strains. However, when 1% glucose was added to the growth medium, a drastic decrease in activity for Donor 8's HMOs was observed; in THB + 1% glucose, HMOs from Donor 8 decreased GBS growth by less than 10% for all three strains. It is possible that the profound antimicrobial activity of this sample, especially when compared to the activity of the other donors tested, may, in part, be a result of when in the lactation period the sample was collected. The time of collection can be important as HMO concentration and expression change over the course of lactation (detailed in Chapter 2). For example, HMO concentrations are highest early in lactation and numerous studies have reported higher concentrations of α 1-2 fucosylated HMOs, including 2'-FL, in early milk.⁷⁸⁻⁸⁰ Moreover, it has been suggested based on milk composition that the primary purpose of colostrum (the earliest milk) is protective rather than nutritive (see Chapter 2).⁸¹ Thus, it is possible that milk from Donor 8 was collected at a significantly earlier point in lactation

than the other samples and thus has larger quantities of HMOs that are especially protective against GBS. Due to milk sample deidentification, however, it is difficult to confidently assign an explanation for the marked activity of Donor 8.

To evaluate antibiofilm activity, we compared the biofilm/biomass ratios of bacteria grown in the presence of HMOs to bacteria grown in the absence of HMOs. Using this standard, all HMO samples were found to significantly reduce biofilm formation of at least one GBS strain ($p \leq 0.05$ by one-way ANOVA with *posthoc* Dunnett's multiple comparison test) (**Table 3.6**). In numerous cases, biofilm production was reduced by over 80% relative to the control. It is important to note that in order to determine significant reductions in GBS biofilm production in THB, the results from Donor 8 were omitted from analysis; results from Donor 8 were confirmed to be outliers by both ROUT ($Q = 1\%$) and Grubbs ($\alpha = 0.05$) outlier tests. It is likely that the exceptionally high biofilm/biomass ratios seen for Donor 8's HMOs are due to their extreme antimicrobial activity in THB (growth reductions were over 75% for each GBS strain). With the less dramatic antimicrobial activity seen for this sample in THB + 1% glucose, the biofilm/biomass ratios return to more reasonable, non-outlying values.

Overall, HMO antibiofilm activity appeared to be strongest against GB2 as eleven out of fourteen samples significantly reduced biofilm formation in at least one growth medium. While there also appeared to be strong antibiofilm activity against GB590, large fluctuations were observed in biofilm measurements for this strain, presumably due to variations in plate workup, and this variation precluded significant antibiofilm activity assignments for all HMOs. Interestingly, GB2 and GB590 were overall less susceptible than CNCTC 10/84 to growth reductions caused by HMO supplementation. The varying

susceptibilities of each strain to HMO supplementation demonstrated that HMO antimicrobial and antibiofilm activity can indeed be strain- rather than species-specific.

Table 3.6. Antibiofilm Activity of Heterogeneous HMO Extracts Against Three Strains of *S. agalactiae* (GBS)^a

		Change in biofilm/biomass from control (%) ± SEM					
		<i>S. agalactiae</i> CNCTC 10/84		<i>S. agalactiae</i> GB590		<i>S. agalactiae</i> GB2	
Lewis blood group	Donor	THB	THB + 1% glc	THB	THB + 1% glc	THB	THB + 1% glc
a-b+	0	-67 ± 11^b	-32 ± 13	-40 ± 28	-26 ± 6	-28 ± 14^b	-45 ± 3
	5	-80 ± 7	-1 ± 8	-17 ± 35	-19 ± 8	-51 ± 6^b	-45 ± 3
	7	-33 ± 13	-36 ± 11	-23 ± 22	-24 ± 5	+10 ± 37	-6 ± 4
	8	+346 ± 229	-5 ± 17	+178 ± 115	-21 ± 7	+273 ± 71	-49 ± 5
	14	-63 ± 13^b	-38 ± 11	-46 ± 18	-58 ± 5	-93 ± 4^b	-83 ± 1
	19	-71 ± 7^b	-23 ± 16	-10 ± 54	-28 ± 5	-40 ± 10^b	-51 ± 2
	24	-70 ± 8^b	-81 ± 3	0 ± 46	-42 ± 10	-70 ± 9^b	-33 ± 4
	32	-79 ± 6^b	-21 ± 12	-13 ± 44	-20 ± 6	+31 ± 25	-6 ± 3
	34	-37 ± 16	-20 ± 8	11 ± 32	5 ± 7	+8 ± 24	-13 ± 3
37	-53 ± 11^b	+34 ± 14	22 ± 35	-5 ± 3	+39 ± 28	-10 ± 3	
a+b-	17	-65 ± 7^b	-20 ± 8	-35 ± 17	-11 ± 3	+11 ± 24	-19 ± 3
	18	-38 ± 18	-40 ± 12	-18 ± 40	-18 ± 3	-53 ± 21^b	+7 ± 5
	29	-60 ± 8^b	-27 ± 12	-3 ± 52	+80 ± 31	-37 ± 12^b	-23 ± 5
	31	-33 ± 15	-43 ± 9	-23 ± 25	-54 ± 5	-43 ± 10^b	-69 ± 2

^asignificant biofilm inhibition ($p \leq 0.05$, one-way ANOVA) compared to control is bolded and highlighted in blue. ^bstatistically significant activity when results from Donor 8 were omitted; Donor 8 was determined to be an outlier by both ROUT and Grubbs tests.

As mentioned previously, another goal of the present study was to determine if there is a relationship between HMO activity and Lewis blood and Secretor status of the donor. Interestingly, the data presented herein (**Tables 3.5** and **3.6**) did not reveal any such relationship. Indeed, the data suggests that HMOs from Secretors and non-Secretors generally demonstrate comparable levels of biological activity.

3.2.3 Evaluation of Antimicrobial and Antibiofilm Activities of HMOs Against *Staphylococcus aureus* and *Acinetobacter baumannii*⁷¹

Encouraged by the strong antimicrobial and antibiofilm activities observed for HMOs against GBS, we next set out to determine if similar activities would be observed against other Gram-positive species. Moreover, we were interested to see if HMOs also possessed activity against a Gram-negative species. Ultimately, we elected to screen against two of the ESKAPE pathogens: *Staphylococcus aureus* (Gram-positive) and *Acinetobacter baumannii* (Gram-negative).

While the ESKAPE pathogens were discussed in detail in Chapter 1, briefly, the pathogens in this group (*Enterococcus faecium*, *Staphylococcus aureus*, *Klebsiella pneumoniae*, *Acinetobacter baumannii*, *Pseudomonas aeruginosa*, and *Enterobacter* species) are the leading causes of multidrug resistant (MDR) nosocomial infections worldwide and are characterized by their high levels of antimicrobial resistance.^{48, 82-84} While each ESKAPE pathogen is highly clinically relevant, *S. aureus* and *A. baumannii* were selected specifically due to their relevance to pediatric populations and the

corresponding urgent need to develop therapeutics to protect pediatric populations from infectious diseases (**Table 3.7**).⁸⁵⁻⁸⁸

Table 3.7. Important Pathogens Responsible for Infection During Pediatric Age Period

Age	Common Pathogens
< 2 days	Group B <i>Streptococcus</i>
2 days to 2 weeks	Group B <i>Streptococcus</i>
14 days to 60 days	Group B <i>Streptococcus</i> <i>Staphylococcus aureus</i> <i>Escherichia coli</i> <i>Klebsiella pneumoniae</i> <i>Enterobacteriaceae</i> <i>Listeria monocytogenes</i>
2 months to 5 years	Group B <i>Streptococcus</i> <i>Streptococcus pneumoniae</i> <i>Staphylococcus aureus</i> <i>Staphylococcus epidermidis</i> <i>Candida albicans</i> <i>Haemophilus influenzae</i> <i>Enterobacteriaceae</i> <i>Acinetobacter baumannii</i>
60 days to 5 years	<i>Haemophilus influenzae</i> <i>Streptococcus pneumoniae</i> <i>Acinetobacter baumannii</i>
5 years to 10 years	Group A <i>Streptococcus</i> <i>Streptococcus pneumoniae</i> <i>Acinetobacter baumannii</i>
10 years to 21 years	Group A <i>Streptococcus</i> <i>Haemophilus influenzae</i> <i>Streptococcus pneumoniae</i> <i>Mycoplasma pneumoniae</i> <i>Chlamydia pneumoniae</i>

Table 3.8. Antimicrobial Activity of Heterogeneous HMO Extracts Against *S. aureus* and *A. baumannii*^a

		Change in biomass from control (%) ± SEM			
		<i>S. aureus</i> USA300		<i>A. baumannii</i> ATCC 19606	
Lewis blood group	Donor	THB	THB + 1% glc	THB	THB + 1% glc
a-b+	0	+8 ± 2	+6 ± 3	+4 ± 2	-1 ± 2
	5	+9 ± 2	+44 ± 2	+5 ± 2	1 ± 1
	7	-2 ± 2	+0 ± 3	0 ± 2	-4 ± 1
	8	+2 ± 3	+22 ± 1	-5 ± 1	-10 ± 2
	14	+1 ± 2	-7 ± 2	+6 ± 4	-2 ± 2
	19	+10 ± 2	+11 ± 4	+2 ± 2	0 ± 1
	24	+4 ± 2	-3 ± 4	+2 ± 2	-6 ± 2
	32	+3 ± 2	-4 ± 4	+7 ± 1	0 ± 1
	34	+6 ± 2	+1 ± 3	+8 ± 2	+4 ± 2
	37	+8 ± 2	+5 ± 3	+8 ± 2	+2 ± 1
a+b-	17	+4 ± 2	-2 ± 3	+8 ± 2	1 ± 1
	18	-2 ± 2	-8 ± 5	-2 ± 2	-5 ± 1
	29	+5 ± 2	+12 ± 3	-7 ± 2	-11 ± 2
	31	+3 ± 3	-5 ± 3	-2 ± 1	-6 ± 1

^asignificant growth inhibition ($p \leq 0.05$, one-way ANOVA) compared to control is bolded and highlighted in blue.

Employing the previously described plate-based assay, the antimicrobial and antibiofilm activities of HMOs against *S. aureus* strain USA300 and *A. baumannii* strain ATCC 19606 were evaluated at 24 h of growth. Once again, for all screens, HMOs were dosed at ca. 5 mg/mL and activity was assessed in both THB and THB + 1% glucose. The results of these screens are shown in **Tables 3.8** and **3.9**. While no HMOs were found to inhibit *S. aureus* growth, HMOs from four samples (samples from both Secretor and non-Secretor donors) did significantly decrease the growth of *A. baumannii* in THB + 1% glucose with reductions ranging from 6-11%; in THB, no growth inhibition was seen against either pathogen. Intriguingly, this result reverses the trend observed for HMO antimicrobial activity against GBS. Against GBS, greater antimicrobial activity was seen in THB, whereas against *A. baumannii*, greater activity is seen in THB + 1% glucose (**Table 3.8**).

Carbohydrate catabolism has been implicated as a critical step in the pathogenesis of streptococcal disease as a number of mechanisms (ex. initiation of virulence factor production) are closely associated with the ability of streptococci to use glucose.⁸⁹ For example, it was shown by Manetti et al. that glucose supplementation enhanced biofilm production in *Streptococcus pyogenes* and that this enhancement was a direct result of environment acidification due to metabolism of glucose into organic acids.^{55, 90} Work from D'Urzo et al. provided evidence that this finding is also extendable to GBS biofilm formation. Concurrent with these reports, we hypothesize that, in the case of GBS, glucose supplementation assists the bacteria in averting exposure to HMOs.^{55, 58}

Conversely, *A. baumannii* is a member of the glucose non-fermenting class of bacteria which are not able to catabolize glucose and thus cannot use glucose

oxidatively.⁹¹ Although glucose catabolism is not possible, glucose does enhance *A. baumannii* anabolism. Interestingly, it has been demonstrated that glucose availability enhances lipopolysaccharide (LPS) production in *A. baumannii*.⁹² Theoretically, as LPS is a major component of the outer membrane of Gram-negative pathogens, one would anticipate the presence of glucose would enhance *A. baumannii* growth. Thus, more research is need to explain the observed reversal in selectivity.

While the limited antimicrobial activity of HMOs against the Gram-negative *A. baumannii* was not surprising, we were intrigued by the lack of activity seen against the Gram-positive *S. aureus*. It was also intriguing that not only did HMO supplementation not significantly decrease *S. aureus* growth, it also did not increase growth. Indeed, the HMOs appeared to have no effect on *S. aureus* growth. This led to the hypothesis that *S. aureus* does not, or perhaps cannot, catabolize HMOs. This hypothesis was supported by work from the McGuire and Bode laboratories which demonstrated that although HMO extracts stimulated the growth of *S. aureus* (isolated from human milk) over a 24 h period, this growth stimulation was not attributable to bacterial HMO catabolism.⁹³ Additionally, they found that the extent of HMO-fostered growth stimulation was dependent on the nutritional components of the growth medium.

In contrast to a lack of antimicrobial activity against *S. aureus*, HMOs from numerous donors did exhibit significant antibiofilm activity against *S. aureus* with reductions in biofilm production ranging from 30-60% (**Table 3.9**). This antibiofilm activity was, however, unique to the THB + 1% glucose growth condition and also to the Le(a+b-) blood group (Lewis positive Secretor milk group). Against *A. baumannii*, HMO supplementation led only to increases in biofilm formation (**Table 3.9**).

Table 3.9. Antibiofilm Activity of Heterogeneous HMO Extracts Against *S. aureus* and *A. baumannii*^a

		Change in biofilm/biomass from control (%) ± SEM			
		<i>S. aureus</i> USA300		<i>A. baumannii</i> ATCC 19606	
Lewis blood group	Donor	THB	THB + 1% glc	THB	THB + 1% glc
a-b+	0	+40 ± 7	-46 ± 7	+82 ± 8	+58 ± 12
	5	+446 ± 119	-25 ± 6	+197 ± 37	+79 ± 17
	7	+90 ± 19	-21 ± 11	+87 ± 51	+114 ± 20
	8	+325 ± 169	-33 ± 8	+153 ± 71	+117 ± 19
	14	+215 ± 81	-39 ± 9	+128 ± 6	+48 ± 7
	19	+59 ± 39	-40 ± 9	+96 ± 54	+83 ± 29
	24	+89 ± 56	-60 ± 11	+72 ± 55	+56 ± 14
	32	+113 ± 56	-22 ± 12	+111 ± 58	+73 ± 33
	34	+104 ± 57	-23 ± 12	+26 ± 33	+48 ± 23
	37	+80 ± 51	-35 ± 10	+80 ± 48	+71 ± 32
a+b-	17	+126 ± 51	-20 ± 11	+71 ± 48	+70 ± 22
	18	+160 ± 69	-8 ± 17	+90 ± 55	+95 ± 21
	29	+342 ± 139	5 ± 12	+321 ± 24	+114 ± 41
	31	+68 ± 42	-25 ± 9	+198 ± 29	+62 ± 21

^aSignificant biofilm inhibition ($p \leq 0.05$, one-way ANOVA) compared to control is bolded and highlighted in blue.

In addition to the lack of antimicrobial activity observed against *S. aureus*, the differing effects of HMOs on *S. aureus* biofilm production in THB versus THB + 1% glucose were striking. Moreover, the increase in biofilm production but not biomass due to HMO supplementation in glucose-free THB was particularly interesting. The potential of HMOs to serve as either stimulants or inhibitors of *S. aureus* biofilm formation depending on the nutritional content of growth medium was not, however, addressed in the McGuire and Bode study. As a result, we elected to investigate the effects of HMOs on *S. aureus* growth and biofilm production when the bacteria were exposed to a co-treatment of HMOs and a known *S. aureus* biofilm-inhibitor, *N*-acetylcysteine (Ac-CYS-OH; NAC).⁹⁴⁻⁹⁶

Initial screens were performed to determine the MIC of NAC against *S. aureus* as well as patterns of biofilm formation in the presence of sub-MIC concentrations of NAC. In both THB and THB + 1% glucose, the MIC was found to be 8 mg/mL (**Figure 3.10A** and **C**). For biofilm production in THB, the only significant effect was seen at 2 mg/mL NAC. Despite being a reported biofilm inhibitor, at this concentration (4-fold below the MIC), NAC was found to significantly increase biofilm production (**Figure 3.10B**). This result was not wholly surprising though as several reports have found increased biofilm production levels for bacterial species, including as *S. aureus*, when grown in the presence of sub-MIC antimicrobial compound concentrations.⁹⁷⁻⁹⁹ In contrast, no concentration of NAC was found to significantly increase biofilm production when THB + 1% glucose was used. Furthermore, at 4 mg/mL, NAC significantly decreased biofilm formation without completely inhibiting bacterial growth (**Figure 3.10D**).

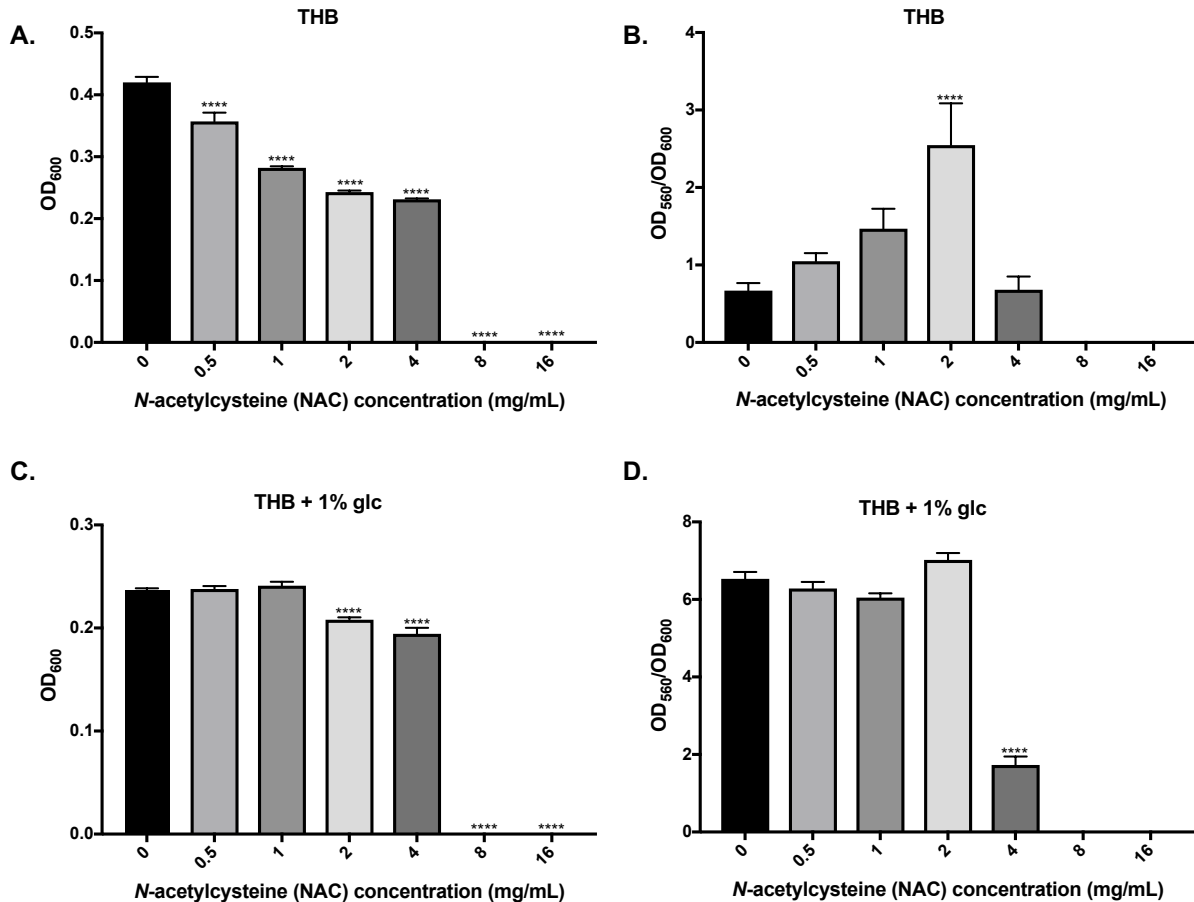


Figure 3.10. Effects of various concentrations of *N*-acetylcysteine (NAC) on *S. aureus* strain USA300 growth and biofilm formation after 24 h of growth. **(A)** Biomass in THB alone or in the presence of varying concentrations of NAC. **(B)** Biofilm to biomass ratio in THB alone or in the presence of varying concentrations of NAC. **(C)** Biomass in THB + 1% glucose (glc) alone or in the presence of varying concentrations of NAC. **(D)** Biofilm to biomass ratio in THB + 1% glucose (glc) alone or in the presence of varying concentrations of NAC. All data are expressed as mean biomass (OD₆₀₀) or biofilm/biomass (OD₅₆₀/OD₆₀₀) measurements ± SEM of 3 separate experiments, each with 3 technical replicates. **** represents $p < 0.0001$ by one-way ANOVA with *posthoc* Dunnett's multiple comparison test comparing biomass or biofilm/biomass at each NAC concentration to biomass and biofilm/biomass in media alone.

For the combined NAC and HMO treatment, we elected to assay HMOs from four different sources. The first two sources were samples from Donors 5 and 7. These samples were chosen due to their contrasting effects on *S. aureus* biofilm formation in THB (**Table 3.9**). For the remaining two samples, HMO cocktails were created based on

antimicrobial and antibiofilm activities against GBS. Pulling from the pool of nineteen donors, the antimicrobial cocktail (am-cocktail) consisted of five samples that most consistently exhibited significant antimicrobial activity but limited antibiofilm activity, and the antibiofilm cocktail (ab-cocktail) consisted of seven samples that consistently exhibited significant antibiofilm activity but limited antimicrobial activity. The am-cocktail was composed of equal contributions from Donors 5, 8, 32, 43; the ab-cocktail was composed of equal contributions from Donors 0, 7, 14, 18, 19, 24, and 31.

We observed that the combined treatment of HMOs (dosed at ca. 5 mg/mL) and NAC (dosed at various concentrations) generally did not result in greater growth inhibition than treatment with NAC alone for either growth condition (**Figure 3.11**). In THB, the combinations of 2 mg/mL NAC and HMOs from Donor 5, Donor 7, or the ab-cocktail resulted in a modestly significant reduction in bacterial growth compared to treatment with NAC alone (**Figure 3.11A**). However, no growth inhibition was observed for any other combination of HMO and NAC in either growth condition. Furthermore, several combinations actually increased growth compared to treatment with NAC alone (**Figure 3.11**).

For biofilm production at sub-MIC concentrations of NAC, only the combination of 2 mg/mL NAC and the am-cocktail in THB + 1% glucose caused a significant reduction in biofilm production compared to treatment with NAC alone (**Figure 3.12B**). Interestingly, this combined treatment did not reduce biofilm production levels to a greater extent than treatment with the am-cocktail alone. Moreover, multiple HMO samples were actually found to increase biofilm production relative to treatment with NAC alone in either THB or THB + 1% glucose (**Figures 3.12**). Taken together, the results of these combination

studies appear to further demonstrate that HMOs have the potential to act as both growth and biofilm production stimulants for *S. aureus*.

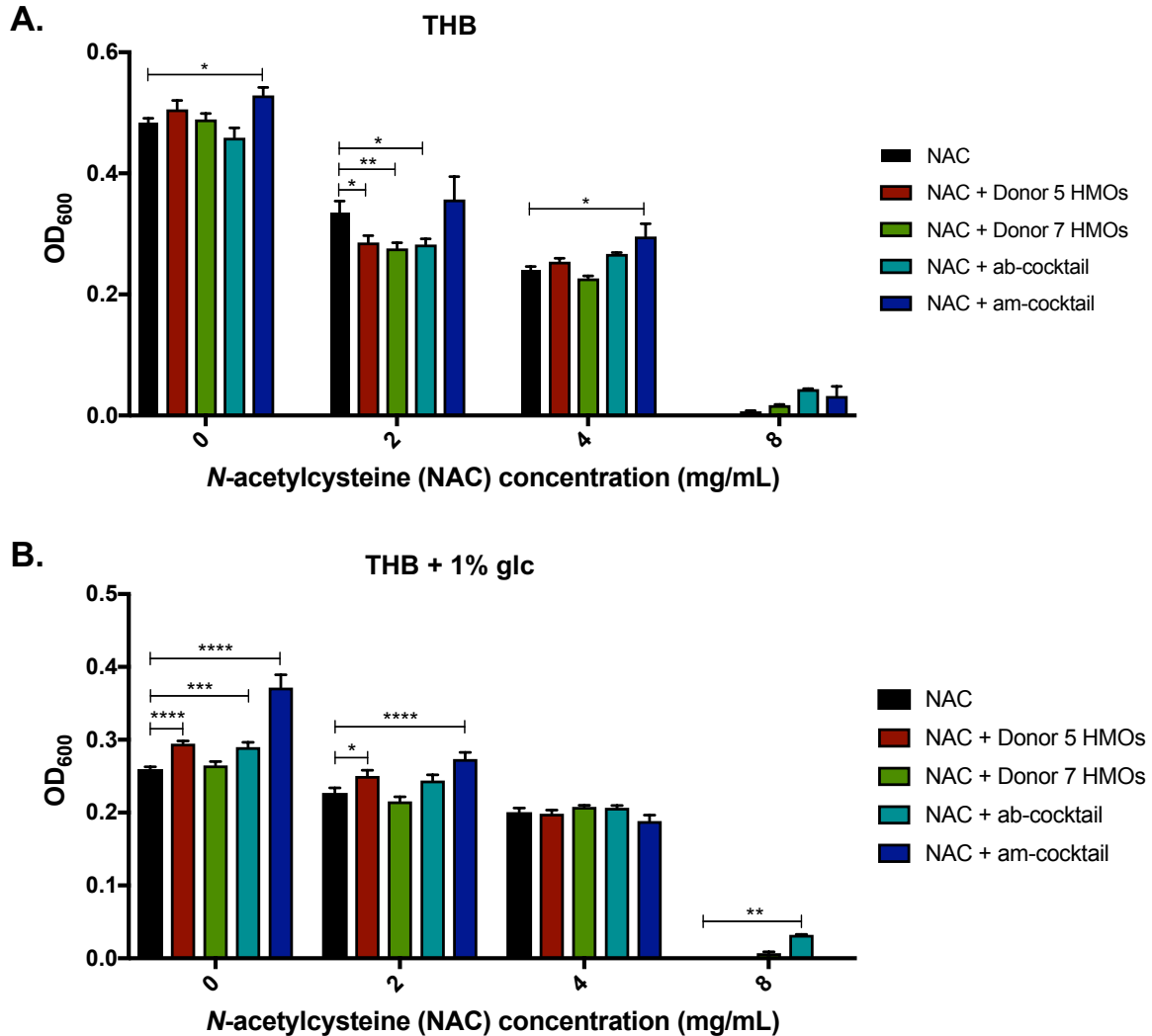


Figure 3.11. Effect of co-treatment of HMOs and varying concentrations of *N*-acetylcysteine (NAC) on *S. aureus* strain USA300 growth after 24 h. **(A)** Biomass in THB alone or in the presence of HMOs from various samples, varying concentrations of NAC, or combinations of NAC at various concentrations at ca. 5 mg/mL HMO. **(B)** Biomass in THB + 1% glucose (glc) alone or in the presence of HMOs from various samples, varying concentrations of NAC, or combinations of NAC at various concentrations at ca. 5 mg/mL HMO. Data are expressed as mean biomass measurements (OD_{600}) \pm SEM of 3 separate experiments, each with 3 technical replicates. ** represents $p = 0.0028$ and **** represents $p < 0.0001$ by two-way ANOVA with *posthoc* Dunnett's multiple comparison test comparing each NAC and HMO concentration at a given NAC concentration to NAC alone at the same NAC concentration. When NAC concentration is 0 mg/mL, growth in media alone is compared to growth in the presence of HMOs.

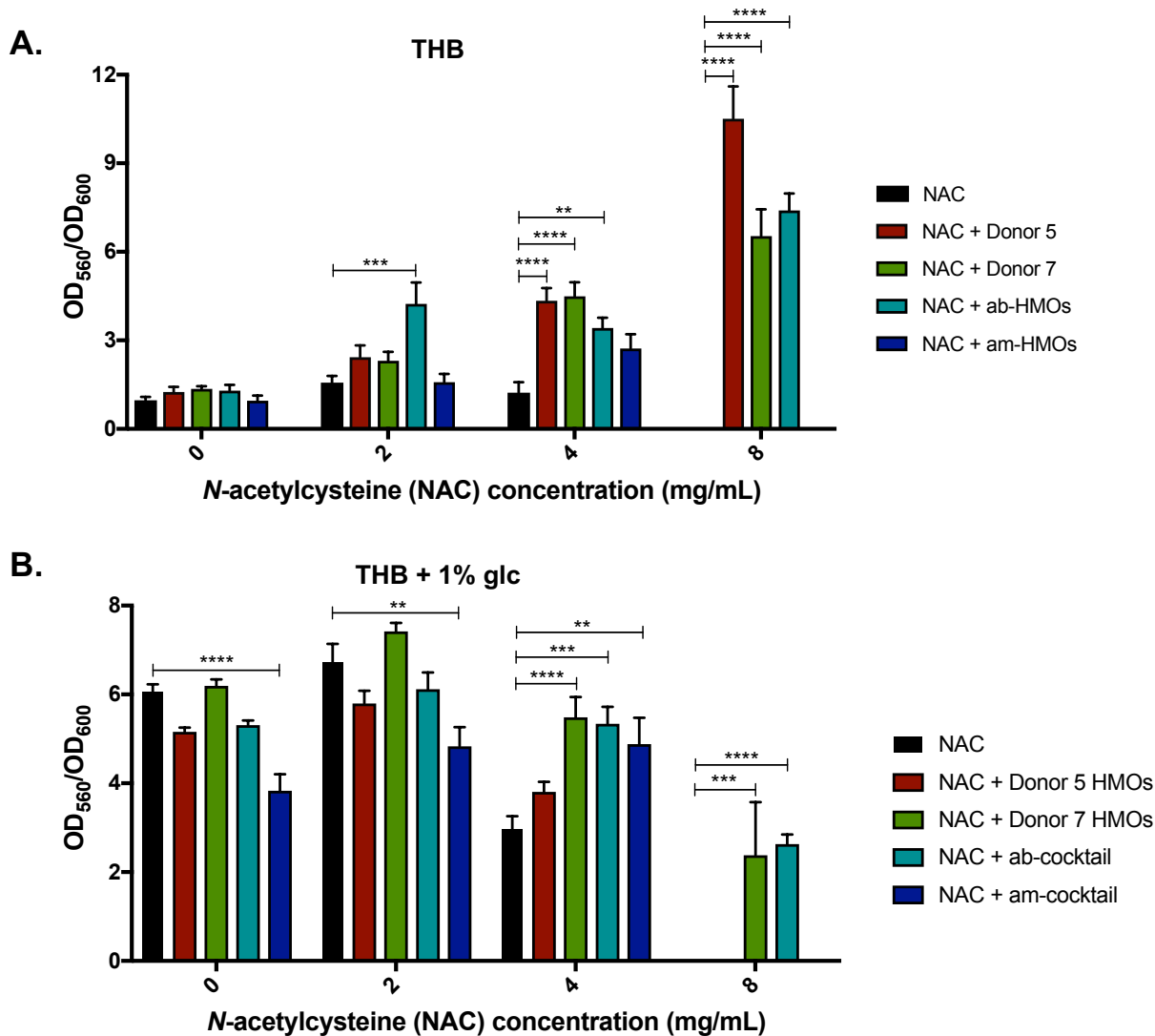


Figure 3.12. Effect of co-treatment of HMOs and varying concentrations of *N*-acetylcysteine (NAC) on *S. aureus* strain USA300 biofilm formation after 24 h. **(A)** Biofilm to biomass ratio in THB alone or in the presence of HMOs from various samples, varying concentrations of NAC, or combinations of NAC at various concentrations at ca. 5 mg/mL HMO. **(B)** Biofilm to biomass ratio in THB + 1% glucose (glc) alone or in the presence of HMOs from various samples, varying concentrations of NAC, or combinations of NAC at various concentrations at ca. 5 mg/mL HMO. Data are expressed as mean biofilm to biomass measurements (OD_{560}/OD_{600}) \pm SEM of 3 separate experiments, each with 3 technical replicates. **** represents $p < 0.0001$ by two-way ANOVA with *posthoc* Dunnett's multiple comparison test comparing each NAC and HMO concentration at a given NAC concentration to NAC alone at the same NAC concentration. When NAC concentration is 0 mg/mL, growth in media alone is compared to growth in the presence of HMOs.

In summary, while HMOs did not possess significant antimicrobial activity against *S. aureus*, they were active against *A. baumannii* which demonstrates that HMO antimicrobial activity is not limited to GBS or Gram-positive pathogens. That said, due to the severely lessened levels of antimicrobial activity seen for HMOs against *A. baumannii* compared to GBS, it does appear as though HMOs generally possess narrow-spectrum antimicrobial activity against GBS. In terms of antibiofilm activity, HMOs may possess broader-spectrum antibiofilm activity across Gram-positive species. Indeed, we observed maximum biofilm inhibitions of 93% and 60% compared to bacteria grown in the absence of HMOs for GBS and *S. aureus*, respectively. Although significant biofilm inhibition was observed against *S. aureus*, this was found to be dependent on the nutritional composition of the growth medium. Thus, the ability of HMOs to serve as antibiofilm agents as opposed to biofilm production stimulants for *S. aureus* will require further study.

While the results of this study support the therapeutic potential of HMOs in disease intervention, they did not reveal a mechanism behind the observed antimicrobial and antibiofilm activities and, concurrently, the cellular target(s) remained unknown. In the following study, we aimed to expand upon the therapeutic potential of HMOs while simultaneously providing evidence for a potential mechanism of action behind the observed HMO antibacterial activities. The results of this study are presented herein.

*3.3 Investigation of HMO Antimicrobial Mechanism of Action*¹⁰⁰

3.3.1 Evaluation of Heterogeneous HMOs in Antibiotic Combination Therapies

On the basis of our previous studies, we hypothesized that HMOs could sensitize GBS to small molecule antibiotics. Importantly, testing this hypothesis would not only

potentially broaden the therapeutic utility of HMOs but also assist in deciphering the mechanism(s) of action underlying HMO antibacterial activity. For the present study, we once again elected to use heterogenous HMO extracts as opposed to single compounds. Our reasoning was two-fold. First, the majority of single compounds are prohibitively expensive in the amounts required for this study. Second, several labs, including the Townsend lab, have shown that while there are several pharmacophoric units in human milk, individual HMOs are less effective against bacterial pathogens than heterogeneous mixtures. Indeed, studies from the Bode and Chen laboratories have found that while various disialylated HMOs can prevent necrotizing enterocolitis (NEC) in a neonatal rat model, these compounds are less effective than heterogenous HMO extracts.^{101, 102}

Unlike the previously described study, for the present study, lactose was rigorously removed from the heterogenous HMO extracts. As pathogens are largely capable of catabolizing lactose but not HMOs, we hypothesized that rigorous removal of lactose would furnish a more potent carbohydrate mixture and would result in more accurate HMO concentrations for biological assays. The second-generation workflow for HMO isolation is presented in **Figure 3.13**.

Briefly, fats and proteins are removed in an analogous fashion to that shown in **Figure 3.9**. After protein removal, rather than directly subjecting the carbohydrate fraction to size exclusion chromatography, this fraction is first treated with β -galactosidase (from *Kluyveromyces lactis*). β -galactosidase hydrolyses lactose into its constituent monosaccharide components, glucose and galactose, but is not able to hydrolyze the glycosidic bonds of HMOs. Thus, β -galactosidase treatment results in the formation of a new carbohydrate extract consisting of glucose, galactose, and HMOs. This mixture is

more desirable compared to a mixture of lactose and HMOs as the next purification step is size exclusion chromatography; the increased mass difference between the desired and undesired carbohydrate components greatly facilitates isolation of pure HMO fractions.

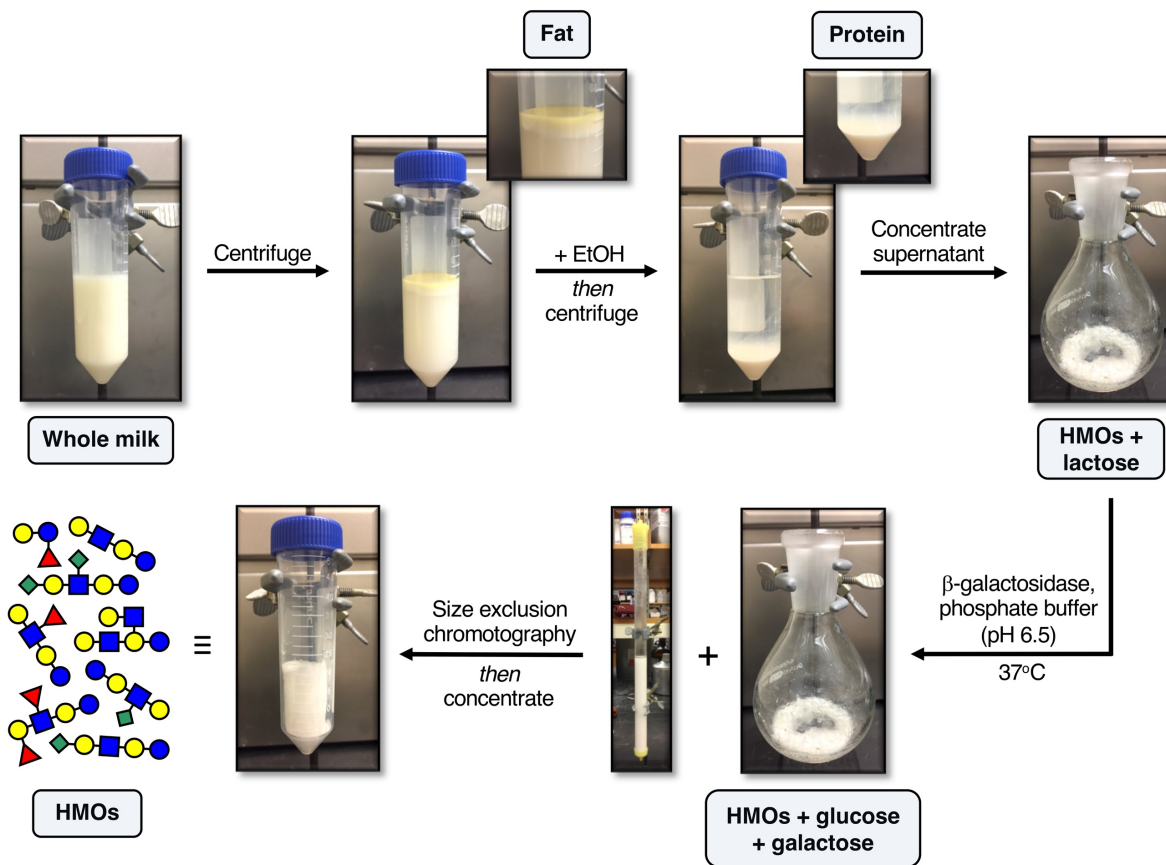


Figure 3.13. Second-generation isolation of HMOs from whole milk workflow.

Another deviation from the previously described study was our decision in the present study to pool HMO extracts from different donors to create one HMO cocktail. Again, our reasoning was two-fold. First, pooling samples from different donors helped to account for variations in HMO composition seen from mother to mother; variations in activity among donors was not a focus of our work moving forward and was thus a variable we wished to eliminate. Second, the mechanistic studies we wanted to undertake required

significantly more material than could be obtained from a single donor. Thus, pooling samples was a necessity.

Related to the need for more material, two additional donors were added to the donor pool for the present study. Donors are denoted with either the sample label/number or the sample label/number and collection date (month/year) assigned to them by the providing company, Medolac. HMOs from these donors were isolated with rigorous removal of lactose, and the HMO extracts were subsequently evaluated for antimicrobial and antibiofilm activity against GBS strains CNCTC 10/84, GB590, and GB2 (**Tables 3.10** and **3.11**, respectively); again, HMOs were dosed at 5 mg/mL. It is important to note that while there are three HMO sources presented in **Tables 3.10** and **3.11**, two of these are derived from the same donor (RGB) at different points. Interestingly, the two RGB samples, collected three months apart, possessed varying levels of activity. However, as HMO composition is known to change over the course of lactation, this result was not wholly unexpected.

Table 3.10. Antimicrobial Activity of Three Additional Heterogeneous HMO Extracts Against Three Strains of *S. agalactiae* (GBS)^a

	Change in biomass from control (%) ± SEM					
	<i>S. agalactiae</i> CNCTC 10/84		<i>S. agalactiae</i> GB590		<i>S. agalactiae</i> GB2	
Donor	THB	THB + 1% glc	THB	THB + 1% glc	THB	THB + 1% glc
1049	-64 ± 5	-15 ± 5	-24 ± 9	+34 ± 14	-56 ± 7	-56 ± 2
RGB 2/14	-12 ± 3	-35 ± 3	-12 ± 4	-11 ± 5	-11 ± 2	-17 ± 6
RGB 5/14	+20 ± 6	+30 ± 6	+34 ± 5	+42 ± 7	+44 ± 2	+11 ± 4

^asignificant growth inhibition ($p \leq 0.05$, one-way ANOVA) compared to control is bolded and highlighted in blue.

Table 3.11. Antibiofilm Activity of Three Additional Heterogeneous HMO Extracts Against Three Strains of *S. agalactiae* (GBS)^a

	Change in biofilm/biomass from control (%) ± SEM					
	<i>S. agalactiae</i> CNCTC 10/84		<i>S. agalactiae</i> GB590		<i>S. agalactiae</i> GB2	
Donor	THB	THB + 1% glc	THB	THB + 1% glc	THB	THB + 1% glc
1049	-2 ± 2	+7 ± 14	-45 ± 22	-36 ± 7	-63 ± 15	-50 ± 19
RGB 2/14	+16 ± 9	+174 ± 22	+44 ± 11	+43 ± 9	-25 ± 2	0 ± 7
RGB 5/14	+53 ± 9	34 ± 6	+13 ± 14	+4 ± 5	-53 ± 2	-8 ± 3

^asignificant biofilm inhibition ($p \leq 0.05$, one-way ANOVA) compared to control is bolded and highlighted in blue.

With HMO cocktail in hand, we once again elected to screen against three strains of GBS of varying serotypes to determine whether any HMO-fostered antibiotic potentiation was strain- or species- specific. As before, we selected GBS strains CNCTC 10/84 (serotype V), GB590 (serotype III), and GB2 (serotype Ia). For our antibiotic selection, the following antibiotics were selected due to their relevance to GBS prevention and treatment, i.e. the antibiotics suggested for IAP (**Figure 3.1**): penicillin (β -lactam), ampicillin (β -lactam), cefazolin (cephalosporin), clindamycin (lincosamide), and vancomycin (glycopeptide). We also elected to test erythromycin (macrolide), gentamicin (aminoglycoside), minocycline (tetracycline), and linezolid (oxazolidinone). Erythromycin, gentamicin, and minocycline, while not used for GBS treatments, were selected due to an increasing prevalence of GBS resistance to these antibiotics.¹⁰³⁻¹⁰⁵ Moreover, we hypothesized that their inclusion would assist in analyzing HMO mechanisms of action. Finally, linezolid was selected due to its overarching relevance to infectious disease

prevention; linezolid was included in the World Health Organization’s (WHO) list of essential medicines in 2017.¹⁰⁶

To begin our studies, we determined MICs for the HMO cocktail and each antibiotic in both THB and THB + 1% glucose using a microbroth dilution assay. Bacterial growth was assessed after 24 h via spectrophotometric reading at OD₆₀₀, and the MIC was assigned at the concentration where no bacterial growth was detected. In all cases, the HMO cocktail MIC was 10.25 mg/mL. Strain- and media-specific HMO IC₅₀ concentrations (half maximal inhibitory concentrations) are provided in **Table 3.12**. Interestingly, at concentrations below 5 mg/mL (the low end of physiological concentration), HMOs were generally observed to promote bacterial growth (**Figure 3.14**).

Table 3.12. HMO IC₅₀ Values Against Three Strains of *S. agalactiae* (GBS)^a

	<i>S. agalactiae</i> CNCTC 10/84	<i>S. agalactiae</i> GB590	<i>S. agalactiae</i> GB2
THB	7.25	7.24	5.04
THB + 1% glc	5.83	5.51	4.45

^aAll IC₅₀ values are given in mg/mL.

For the combination treatments, HMOs were dosed at their IC₅₀ values except for treatments against CNCTC 10/84 and GB590 in THB. For these trials, HMOs were dosed instead at 5 mg/mL as the HMO IC₅₀ curves for these strains in THB were not reflective of the biomass data (**Figure 3.14A and C**). Regardless, it is important to note that for all trials, HMOs were used at the low end of their typical physiological concentrations (5-25 mg/mL). Antibiotic MICs are provided in **Tables 3.13 and 3.14**. With the solo MIC values determined, we moved to test the effects of HMO and antibiotic combined treatments.

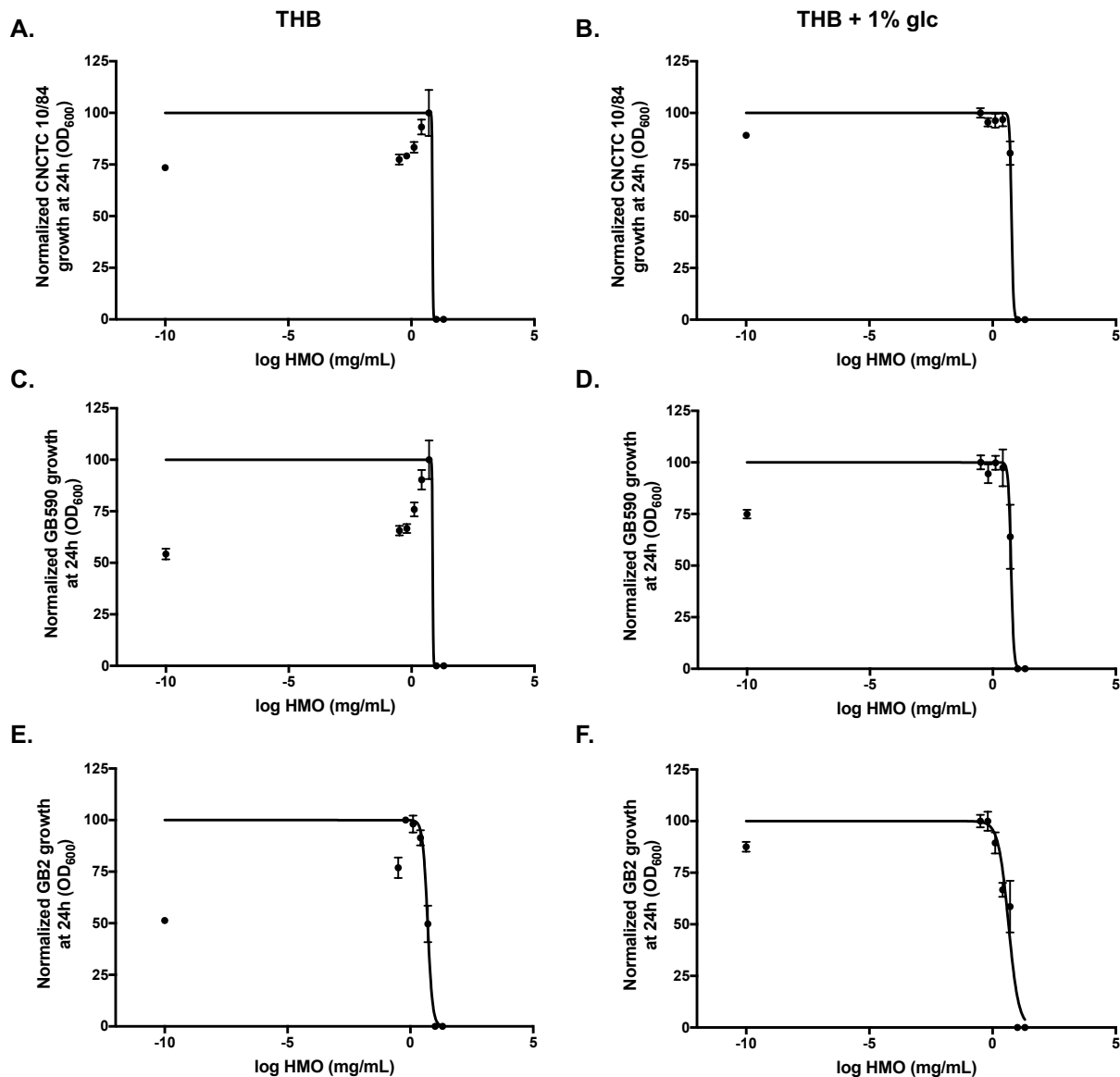


Figure 3.14. IC₅₀ curves for HMO cocktail against three GBS strains in THB (A, C, E) and THB + 1% glucose (glc) (B, D, F). Bacterial growth (OD₆₀₀) was recorded after 24 h of HMO treatment at 20.5; 10.25; 5.12; 2.56; 1.28; 0.64; 0.32; and 0 mg/mL. (A) HMO IC₅₀ curve against CNCTC 10/84 in THB. (B) HMO IC₅₀ curve against CNCTC 10/84 in THB + 1% glc. (C) HMO IC₅₀ curve against GB590 in THB. (D) HMO IC₅₀ curve against GB590 in THB + 1% glc. (E) HMO IC₅₀ curve against GB2 in THB. (F) HMO IC₅₀ curve against GB2 in THB + 1% glc. Data displayed represent the mean normalized growth (OD₆₀₀) ± SEM of at least three independent experiments, each with 3 technical replicates. Mean normalized growth (OD₆₀₀) for each time point is indicated by the respective symbols.

Table 3.13. Antibiotic Sensitization Data for HMOs Against Three Strains of *S. agalactiae* (GBS) in THB^{a,b}

Antibiotic	<i>S. agalactiae</i> CNCTC 10/84			<i>S. agalactiae</i> GB590			<i>S. agalactiae</i> GB2		
	MIC without HMO	MIC with HMO ^c	F.R. ^d	MIC without HMO	MIC with HMO ^c	F.R. ^d	MIC without HMO	MIC with HMO ^c	F.R. ^d
Penicillin	0.03	0.015	2	0.03	0.03	0	0.03	0.015	2
Ampicillin	0.0625	0.0312	2	0.0625	0.0625	0	0.125	0.0625	2
Cefazolin	0.125	0.0625	2	0.125	0.0625	2	0.125	0.0625	0
Vancomycin	2	1	2	1	0.5	2	1	0.5	2
Clindamycin	0.0325	0.0156	2	0.0312	0.0156	2	0.0312	0.0078	4
Gentamicin	16	2	8	16	1	16	16	2	8
Erythromycin	0.0156	0.002	8	0.0312	0.001	32	0.0156	0.001	16
Linezolid	2	1	2	2	1	2	2	1	2
Minocycline	0.0625	0.0019	32	4	0.5	8	2	0.25	8

^aall MIC values are given in µg/mL. ^bSignificant MIC fold reductions are bolded and highlighted in blue. ^cHMOs were dosed against CNCTC 10/84, GB590, and GB2 at 5 mg/mL. ^dF.R. denotes MIC fold reduction.

Table 3.14. Antibiotic Sensitization Data for HMOs Against Three Strains of *S. agalactiae* (GBS) in THB + 1% Glucose^{a,b}

Antibiotic	<i>S. agalactiae</i> CNCTC 10/84			<i>S. agalactiae</i> GB590			<i>S. agalactiae</i> GB2		
	MIC without HMO	MIC with HMO ^c	F.R. ^d	MIC without HMO	MIC with HMO ^c	F.R. ^d	MIC without HMO	MIC with HMO ^c	F.R. ^d
Penicillin	0.03	0.12	0	0.03	0.06	0	0.03	0.06	0
Ampicillin	0.125	0.125	0	0.0625	0.125	0	0.0625	0.125	0
Cefazolin	0.125	0.125	0	0.125	0.125	0	0.125	0.125	0
Clindamycin	0.0625	0.004	16	0.0625	0.0156	4	0.0312	0.0156	2
Gentamicin	32	2	16	32	4	8	32	16	2
Erythromycin	0.0312	0.0078	4	0.125	0.0156	8	0.0312	0.0156	2
Linezolid	2	1	2	2	1	2	2	2	0
Minocycline	0.03125	0.0156	2	4	1	4	0.25	0.125	2

^aall MIC values are given in µg/mL. ^bsignificant MIC fold reductions are bolded and highlighted in blue. ^cHMOs were dosed against CNCTC 10/84, GB590, and GB2 at 5.8; 5.5; and 4.5 mg/mL, respectively. ^dF.R. denotes MIC fold reduction.

While the extent of antibiotic activity potentiation in co-treatments varied among strains and growth conditions, overarching patterns of activity potentiation did emerge. First, no potentiation was observed against any strain in either growth condition for the β -lactams (including cephalosporins) or vancomycin (**Tables 3.13** and **3.14**). Second, aside from linezolid, which saw no significant MIC fold reduction in either growth condition, all other ribosome-targeting antibiotics saw significant fold reductions against at least one GBS strain; MIC fold reductions of 4 or higher were deemed significant. Most notable were gentamicin and erythromycin. These antibiotics saw the most consistent activity potentiation and the largest MIC reductions, which reached as high as 32-fold.

Strain-specific GBS susceptibility was found to be dependent on the nutritional content of the growth medium. For example, while GB2 was the strain most globally affected by HMO supplementation in THB, in THB + 1% glucose, HMO supplementation had no effect on the activity of any antibiotic against GB2. While HMOs sensitized CNCTC 10/84 and GB590 to a similar list of antibiotics as GB2, the magnitudes of the MIC fold reductions were highly variable. Perhaps the most striking example of this observation is clindamycin against CNCTC 10/84. In THB, HMO supplementation resulted in only a 2-fold reduction while in THB + 1% glucose, HMO supplementation caused a 16-fold reduction.

Encouraged by these results, we next investigated whether the patterns of antibiotic potentiation against GBS were extendable to *S. aureus* (another Gram-positive pathogen). For antibiotic sensitization trials against *S. aureus*, HMOs were dosed at ca. 5 mg/mL; the HMO cocktail did not completely inhibit bacterial growth even at 20 mg/mL (at the higher end of physiological concentration), so no IC₅₀ values could be determined.

Initial screens in THB and THB + 1% glucose revealed that the only significant antibiotic MIC fold reduction was for gentamicin in THB + 1% glucose (**Table 3.15** and Appendix A1). Additional trials confirmed an 8-fold reduction for gentamicin when dosed in combination with HMOs in THB + 1% glucose.

Table 3.15. Antibiotic Sensitization Data for HMOs Against *S. aureus* in THB + 1% Glucose^{a,b}

Antibiotic	MIC without HMO	MIC with HMO ^c	F.R. ^d
Cefazolin	8	8	0
Vancomycin	8	8	0
Clindamycin	0.25	0.25	0
Gentamicin	4	0.5	8
Erythromycin	32	32	0
Linezolid	1.7	3.4	0

^aall MIC values are given in $\mu\text{g/mL}$. ^bsignificant MIC fold reductions are bolded and highlighted in blue. ^cHMOs were dosed at 5 mg/mL. ^dF.R. denotes MIC fold reduction.

As a final point of study, we investigated whether HMOs could also sensitive *A. baumannii* (a Gram-negative pathogen) to small molecule antibiotics. The following antibiotics were used in combination treatments against *A. baumannii*: amikacin (aminoglycoside), tobramycin (aminoglycoside), minocycline (tetracycline), tigecycline (glycylcycline), and doripenem (β -lactam). An initial screen revealed similar patterns of antibiotic potentiation as were seen with the Gram-positive pathogens. Similar to GBS and *S. aureus*, no antibiotic activity potentiation was seen for antibiotics that inhibit cell wall synthesis (**Table 3.16** and Appendix A1). Furthermore, as with *S. aureus*, the only significant antibiotic MIC fold reductions against *A. baumannii* were seen with the aminoglycosides. Additional trials corroborated 4-fold reductions for amikacin and

tobramycin in THB. No significant fold reductions were seen for any antibiotic in THB + 1% glucose (see Appendix A1).

Table 3.16. Antibiotic Sensitization Data for HMOs Against *A. baumannii* in THB^{a,b}

Antibiotic	MIC without HMO	MIC with HMO ^c	F.R. ^d
Amikacin	16	4	4
Tobramycin	8	2	4
Imipenem	0.5	1	0
Meropenem	1	1	0
Minocycline	0.31	0.31	0
Tigecycline	0.0625	0.125	0
Doripenem	0.5	1	0

^aall MIC values are given in µg/mL. ^bsignificant MIC fold reductions are bolded and highlighted in blue. ^cHMOs were dosed at 5 mg/mL. ^dF.R. denotes MIC fold reduction.

In summary, we observed that HMOs potentiate the activity of four classes of antibiotics with intracellular targets (aminoglycosides, lincosamides, macrolides, and tetracyclines) across multiple bacterial strains but do not potentiate the activity of cell wall-targeting antibiotics (β-lactams, cephalosporins, glycopeptides, and carbapenems). This result is particularly noteworthy as HMOs have been shown to act as bacteriostatic agents, yet bacteriostatic agents are often observed to antagonize the actions of bactericidal antibiotics. Against GBS, HMO combination treatments resulted in up to a 16-fold MIC reduction for clindamycin and gentamicin and up to a 32-fold reduction for erythromycin and minocycline. Furthermore, HMO supplementation significantly reduced the MICs of aminoglycosides against two of the ESKAPE pathogens.

The consistent aminoglycoside activity potentiation seen across both Gram-positive and -negative species is particularly notable. While aminoglycosides are effective antibiotics and are classified by the WHO as a critically important class of antimicrobial,

the nephrotoxicity of this class limits their utility.¹⁰⁷⁻¹¹⁰ Thus, the ability of HMOs, which are nontoxic at any concentration, to lower the effective dosage of aminoglycosides holds real therapeutic promise. Furthermore, while HMOs generally potentiated clindamycin, gentamicin, erythromycin, and minocycline activity across multiple strains, it is important to highlight that in the context of GBS, activity potentiation was strain-specific. This result provides support for the potential of developing narrow-spectrum strain-specific chemotherapeutic regimens.

The HMO-fostered activity potentiation observed for clindamycin and erythromycin is especially promising for the prevention of GBS transmission as these two drugs remain relevant to IAP despite the fact that they continue to become less effective due to resistance development. Our findings, however, demonstrate the feasibility of sensitizing GBS to antibiotics that have failed or are struggling in the clinic thus offering new insights into the battle against antimicrobial resistance.¹¹¹

A final point of emphasis is that all HMO concentrations used in the combination treatments were at the low end of physiological concentrations. Additionally, while the millimolar HMO cocktail IC₅₀ values may appear high in comparison to typical micromolar antibiotic dosages, it is important to remember that HMOs are delivered to infants in multigram doses per day. Given this context, the millimolar HMO dosages used in this study are impressive, as is the fact that these molecules are themselves bactericidal at the high end of physiological concentration.⁶⁸

Finally, based on the observed patterns of antibiotic activity potentiation, we hypothesized that HMOs act by increasing bacterial membrane permeability. Notably, this mode of action is characteristic of the role of β -lactams in combination therapies with

aminoglycosides. This hypothesis was further supported by a previous study by Townsend et al. wherein it was demonstrated that HMOs could potentiate the activity of polymyxin B against GBS.⁶⁸ Polymyxins are antimicrobial peptides (AMPs) that are used in the treatment of Gram-negative bacterial infections but are generally inactive against Gram-positive species like GBS.¹¹²⁻¹¹⁵ Mechanistically, polymyxins are believed to target bacterial cellular membranes.¹¹⁶ In Gram-negative bacteria, the cell membrane is the outermost layer. In Gram-positive bacteria, however, the cell membrane is protected by a thick peptidoglycan layer. Thus, if HMOs damage the peptidoglycan layer, this action would theoretically provide greater access to the cellular membrane and account for the potentiation of polymyxin B activity.

3.3.2 Evaluation of HMO Antimicrobial Mechanism of Action¹⁰⁰

To determine if HMO inhibition of bacterial growth and viability was associated with cognate changes in bacterial cell membrane integrity, the LIVE/DEAD BacLight assay (Invitrogen, ThermoFisher) was used. Briefly, this assay employs two stains: SYTO 9, which passes through intact membranes to stain cells green, and propidium iodide (PI), which is a larger molecule that can only pass through membranes with breached integrity to stain cells red (associated with dead cells). As PI can quench the signal of SYTO 9, the ratio of SYTO to PI signal yields a measurement of live to dead cells or intact to nonintact cell membranes.

As expected, when grown in THB alone, GB590 exhibited a LIVE/DEAD cell ratio of $100 \pm \text{SEM } 2.2$. Gratifyingly, exposure to 2.56 mg/mL HMO resulted in a 33% decrease in the LIVE/DEAD cell ratio ($P = 0.00168$) (**Figure 3.17** and Appendix A1). Moreover,

exposure to 5.125 mg/mL HMO resulted in a 27% decrease, and exposure to 10.25 mg/mL and 20.5 mg/mL resulted in 28% decreases in the LIVE/DEAD cell ratio ($P = 0.0011$ and $P = 0.00044$, respectively). Similar results were observed with strains CNCTC 10/84 and GB2 as these strains also exhibited significant decreases in membrane integrity at 2.56; 5.125; 10.25; and 20.5 mg/mL HMO ($P < 0.05$). The addition of glucose to the growth medium inhibited this phenotype at 2.56 mg/mL HMO for all strains, but membrane integrity was significantly perturbed in THB + 1% glucose at 10.25 mg/mL HMO and higher ($P < 0.05$). These results indicated that HMOs are in fact altering GBS cell membrane integrity in a dose-dependent fashion and could be altering downstream processes such as proton motive force.

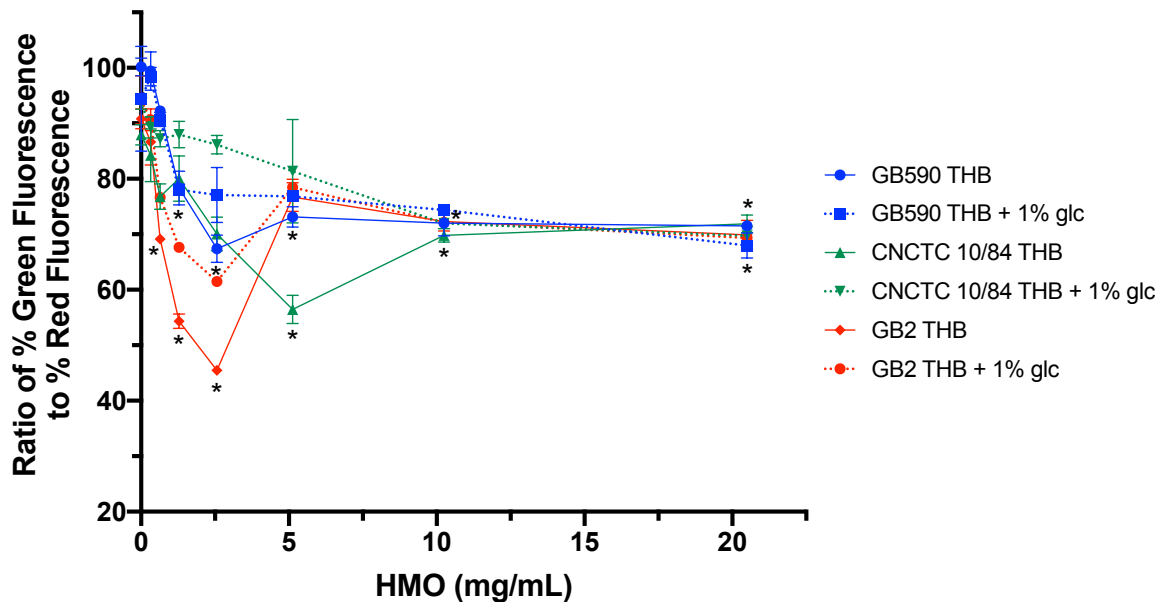


Figure 3.15. LIVE/DEAD BacLight assay to evaluate bacterial cell membrane integrity. Assay reveals that exposure to increasing concentrations of HMOs results in decreased cell integrity as determined by the ratio of green fluorescence (SYTO 9 stain of intact cells) to red fluorescence (PI stain of nonintact cells). * represents $P < 0.05$, Student's t test, $N = 3$ replicates.

It is noteworthy that the results of the BacLight assay compliment results presented in a previous study by Bode et al.⁶⁷ In this study, Bode and co-workers identified a GBS serotype III mutant that exhibited normal growth despite exposure to an HMO mixture. The observed resistance was attributed to inactivation of the gene *gbs0738* which encodes a glycosyltransferase (GT) of the carbohydrate-active enzymes (CAZY) GT-8 family that is conserved across numerous GBS subspecies of varying serotypes. They subsequently hypothesized that this GT could promiscuously incorporate HMOs into either the capsular polysaccharide structure or the peptidoglycan/glycan-binding proteins of the cell wall. The first of these hypotheses, however, was disproved when they observed that a GBS serotype III capsule-deficient mutant remained susceptible to HMO exposure. Thus, the results of their study in conjunction with the results of our study provide compelling evidence that HMOs are affecting cell wall integrity.

3.4 Conclusions and Future Outlook

The work with heterogenous HMO extracts discussed in this chapter demonstrates the protective potential of HMOs against the important neonate pathogen Group B *Streptococcus* (*Streptococcus agalactiae*, GBS) as well as the broadly clinically relevant ESKAPE pathogens *Staphylococcus aureus* and *Acinetobacter baumannii*. HMO extracts were shown to possess strong antimicrobial and antibiofilm activities against GBS, strong (albeit variably so) antibiofilm activity against *S. aureus*, and weak antimicrobial activity against *A. baumannii*. Importantly, both antimicrobial and antibiofilm activity against GBS were found to be largely strain-specific. This finding provides support for the development

of narrow-spectrum antimicrobials. Finally, HMO extracts from Secretors and non-Secretors were found to possess similar levels of antibacterial activity.

In addition to uncovering antibacterial properties of HMOs against various pathogens, we also demonstrated the therapeutic potential of HMOs in antibiotic combination therapies. HMOs were found to potentiate the function of aminoglycosides, lincosamides, macrolides, and tetracyclines against GBS, as well as aminoglycosides against *S. aureus* and *A. baumannii*, but not β -lactams or glycopeptides that inhibit cell wall synthesis. This pattern of activity potentiation led us to hypothesize that HMOs were increasing membrane permeability. This hypothesis was subsequently validated using a bacterial membrane permeability assay which revealed that HMOs increase membrane permeability toward propidium iodide.

Although these studies collectively show that HMOs possess antibacterial activity and that this activity results from alteration of bacterial membrane permeability, we still lacked knowledge about the activities of individual HMOs. Moreover, although a mechanism of action was identified, the specific cellular targets of HMOs remained unknown. To address these gaps in our understanding, subsequent studies relied on the use of single entity HMOs.

3.5 Experimental Methods

3.5.1 General Methods and Materials^{71, 100}

Bacterial Strains and Culture Conditions

Table 3.17. Bacterial Strains

Bacterial strains	Source
<i>S. agalactiae</i> strain CNCTC 10/84	ATCC
<i>S. agalactiae</i> strain GB590	Clinical isolate, Shannon Manning, Michigan State
<i>S. agalactiae</i> strain GB2	Clinical isolate, Shannon Manning, Michigan State
<i>S. aureus</i> strain USA300	The <i>S. aureus</i> strain used was USA300 JE2, ¹¹⁷ a laboratory-adapted strain derived from the parental USA300 strain isolated from a skin and soft tissue infection ¹¹⁸
<i>A. baumannii</i> strain 19606	ATCC

Bacterial strains are shown in **Table 3.17**. All strains were grown on tryptic soy agar plates supplemented with 5% sheep blood (blood agar plates) at 37 °C in ambient air overnight. Strains were subcultured from blood agar plates into 5 mL of Todd-Hewitt broth (THB) and incubated under shaking conditions at 180 rpm at 37 °C in ambient air overnight. Following overnight incubation, bacterial density was quantified through absorbance readings at 600 nm (OD_{600}) using a Promega GloMax-Multi Detection System plate reader. Bacterial numbers were determined using the predetermined coefficient of 1 $OD_{600} = 10^9$ CFU/mL (colony forming units/mL).

3.5.2 Evaluation of Antimicrobial and Antibiofilm Activities of HMOs Against GBS, Staphylococcus aureus, and Acinetobacter baumannii⁷¹

HMO Isolation

Human milk samples were obtained from 14 healthy, lactating women between 3 days and 3 months postnatal under a collection protocol approved by the Vanderbilt University Institutional Review Board (IRB#100897) and were stored at -20°C . The deidentified milk was provided by Dr. J.-H. Weitkamp from the Vanderbilt Department of Pediatrics under a collection protocol approved by the Vanderbilt University Institutional Review Board (IRB#100897). Milk samples were first thawed then centrifuged for 30 min at 4°C . Following centrifugation, the resultant top lipid layer was removed. The proteins were then removed by diluting the remaining sample with roughly 1:1 v/v 180 or 200 proof ethanol and centrifuging the samples for 30 min at 4°C followed by removal of the resulting HMO-containing supernatant. The supernatant was then concentrated in vacuo, and the remaining salts were removed by P-2 Gel (H_2O elutant). The oligosaccharides were then dried by lyophilization.

MS and MS/MS Analysis of HMO Samples

Dried HMO samples were prepared and processed for evaluation by reconstitution in water to approximately 1 mg/mL. These solutions were deposited on a matrix-assisted laser desorption/ionization (MALDI) target plate as follows: 1 μL of HMO was spotted followed by 0.2 μL of 10 mM NaCl and 1 μL of DHB matrix (60 mg/mL in 50% methanol). The spots were allowed to air-dry and then were analyzed in positive ion mode on a 9.4T Fourier transform ion cyclotron resonance (FT-ICR) mass spectrometer (MS) (Bruker

Solarix). Mass spectra were acquired in positive ion mode from m/z 300 to 2500. Sodium ion adducts of HMOs were detected with a mass accuracy of >2 ppm. MS/MS analysis was performed for selected ions with a linear ion trap mass spectrometer equipped with a MALDI source (LTQ XL, Thermo Scientific). Selected sodium adduct ions of interest were isolated with a 1 amu window and fragmented via CID using a collision energy of 35 eV.¹¹⁹

HMO Bacterial Biofilm Assays

All bacterial strains were grown overnight as described above and used to inoculate fresh THB or THB + 1% glucose at a multiplicity of infection (MOI) of 10^6 colony forming units per 200 μ L of growth medium in 96 well tissue culture treated, sterile polystyrene plates. HMOs isolated from the 14 human milk samples were then added to achieve a final carbohydrate concentration of ca. 5 mg/mL. Bacteria grown in THB or THB + 1% glucose in the absence of any HMOs served as the controls. Biofilm assays were conducted as previously described. Briefly, cultures were incubated under static conditions at 37 °C in ambient air for 24 h. Bacterial growth was quantified through absorbance readings at an optical density of 600 nm (OD_{600}). Results were analyzed compared to controls in the absence of HMOs and were expressed as the percent change in biomass with negative numbers indicating a net decrease in biomass and positive numbers indicating a net increase in biomass. Culture medium was then removed, and wells were washed gently with phosphate buffered saline (PBS, pH 7.4) to remove non-adherent cells; the remaining biofilms were stained with a 10% crystal violet solution for 5–10 min for Gram-positive bacteria and 15–20 min for Gram-negative bacteria. Following staining, wells

were washed with PBS and allowed to dry at room temperature for at least 30 min. After drying, the remaining crystal violet stain was solubilized via addition of 200 μ L of 80% ethanol/20% acetone solution. Biofilm formation was quantified through absorbance readings (OD_{560}). Results were analyzed compared to controls in the absence of HMOs and expressed as the percent change in biofilm/biomass ratio with negative numbers indicating a net decrease in biofilm production and positive numbers indicating a net increase in biofilm production.

Broth Microdilution Method for Determination of Minimum Inhibitory Concentrations and Biofilm Production Patterns of NAC Treatment Against S. aureus

S. aureus cultures were grown overnight as described above and used to inoculate fresh THB or THB + 1% glucose to achieve 5×10^5 CFU/mL. To 96 well tissue culture treated, sterile polystyrene plates was added the inoculated media in the presence of increasing concentrations of *N*-acetylcysteine (NAC) to achieve a final volume of 100 μ L per well. Bacteria grown in THB or THB + 1% glucose in the absence of NAC served as the controls. The plates were incubated under static conditions at 37 °C in ambient air for 24 h. Bacterial growth was quantified through absorbance readings (OD_{600}). The minimum inhibitory concentrations (MICs) were assigned at the lowest concentration of compound at which no visible growth of bacteria was observed. Biofilm production patterns were then determined using the procedure described above with the exception that the final step of solubilizing the remaining crystal violet stain was done via addition of 100 μ L of 80% ethanol/20% acetone.

HMO and NAC Combined Bacterial Biofilm Assays

S. aureus cultures were grown overnight as described above and used to inoculate fresh THB or THB + 1% glucose to achieve 5×10^5 CFU/mL. To the inoculated media was added HMOs from Donor 5, Donor 7, am-HMO cocktail, or ab-HMO cocktail to achieve an HMO concentration of ca. 5 mg/mL. To 96 well tissue culture treated, sterile polystyrene plates was added the HMO-containing inoculated media in the presence of increasing concentrations of N-acetylcysteine (NAC) to achieve a final volume of 100 μ L per well. MICs and biofilm production patterns were determined as previously described.

Statistical Analysis

The data shown represent at least 3 independent experiments. Data are expressed as the mean of three technical replicates \pm SEM. Statistical analyses were performed in GraphPad Prism Software v. 7.0c. Statistical significance for the individual HMO sample assays and the NAC treatment assays was determined using one-way ANOVA with posthoc Dunnett's multiple comparison test comparing growth and/or biofilm production in the presence of HMOs or NAC to growth and/or biofilm production in media alone. Statistical significance for the combined NAC and HMO treatment assays was determined using two-way ANOVA with posthoc Dunnett's multiple comparison test comparing growth and/or biofilm production for each NAC and HMO combination at a given NAC concentration to treatment with NAC alone at the same NAC concentration.

3.5.3 Investigation of HMO Antimicrobial Mechanism of Action¹⁰⁰

HMO Isolation

Human milk was obtained from 21 healthy, lactating women between 3 days and 3 months postnatal and stored between -80 and -20 °C. Deidentified milk was provided by Dr. Jörn-Hendrik Weitkamp from the Vanderbilt Department of Pediatrics, under a collection protocol approved by the Vanderbilt University Institutional Review Board (IRB#100897), and Medolac. Milk samples were thawed then centrifuged for 45 min. Following centrifugation, the resultant top lipid layer was removed. The proteins were then removed by diluting the remaining sample with roughly 1:1 v/v 180 or 200 proof ethanol, chilling the sample briefly, and centrifuging for 45 min followed by removal of the resulting HMO- containing supernatant. Following concentration of the supernatant in vacuo, the HMO-containing extract was dissolved in phosphate buffer (pH 6.5, 0.2 M) and heated to 37 °C. β -galactosidase from *Kluveromyces lactis* was added, and the reaction was stirred until lactose hydrolysis was complete.^{120, 121} The reaction mixture was diluted with roughly 1:0.5 v/v 180 or 200 proof ethanol, chilled briefly, then centrifuged for 30 min. The supernatant was removed and concentrated in vacuo, and the remaining salts, glucose, and galactose were separated from the oligosaccharides using P-2 Gel (H₂O elutant). The oligosaccharides were then dried by lyophilization.

HMO Bacterial Biofilm Assays

HMO antimicrobial and antibiofilm activities for three new donor samples were determined as previously described in section 3.6.2 of this chapter.

Broth Microdilution Method for Determination of Minimum Inhibitory Concentrations of HMO Cocktail and Antibiotics

All strains were grown overnight as described in section 3.6.1 of this chapter and used to inoculate fresh THB or THB + 1% glucose to achieve 5×10^5 CFU/mL. To 96 well tissue-culture- treated, sterile polystyrene plates was added the inoculated media in the presence of increasing concentrations of antibiotic or HMO cocktail to achieve a final volume of 100 μ L per well. Bacteria grown in media in the absence of any compounds served as the control. The plates were incubated under static conditions at 37 °C in ambient air for 24 h. Bacterial growth was quantified through absorbance readings (OD_{600}). The minimum inhibitory concentrations (MICs) were assigned at the lowest concentration of compound at which no bacterial growth was observed.

Broth Microdilution Method for Antibiotic Sensitization

All strains were grown overnight as described previously and the subcultures used to inoculate fresh THB or THB + 1% glucose to achieve 5×10^5 CFU/mL. The freshly inoculated media was then supplemented with HMOs. To 96 well tissue-culture-treated, sterile polystyrene plates was added the inoculated media supplemented with HMOs in the presence of increasing concentrations of antibiotic. Bacteria grown in media in the absence of any compounds served as one control. Bacteria grown in media supplemented with HMOs in the absence of any antibiotic served as a second control. MICs were determined as described in section 3.6.2 of this chapter.

Bacterial Membrane Permeabilization Assay

In order to assess bacterial cell membrane integrity after exposure to HMOs, a LIVE/DEAD BacLight assay (Invitrogen, ThermoFisher) was employed. All strains were grown overnight as described above and used to inoculate fresh THB or THB + 1% glucose to achieve 5×10^5 CFU/mL. To 96 well tissue-culture-treated, sterile polystyrene plates was added the inoculated media in the presence of the following HMO concentrations: 0, 0.32, 0.64, 1.28, 2.56, 5.125, 10.25, and 20.5 mg/mL. Following incubation under static conditions at 37 °C in ambient air for 24 h, cells were stained with propidium iodide (PI) and SYTO 9 (8 μ L/mL) for 15 min prior to reading with a Promega Glomax-Multi Detection System plate reader for excitation/emission 525 nm/580–640 nm (green, SYTO 9) and 625 nm/660–720 nm (red, PI). The percent ratio of green to red fluorescence was calculated ($\text{ratio}_{\text{green/red}} \times 100$). Three biological replicates were used, and statistical significance was calculated using a Student's t test comparison to bacteria grown in medium alone (*P < 0.05).

Statistical Analysis

The data for the HMO antimicrobial and antibiofilm screens represents three independent experiments each with three technical replicates. Data are expressed as the mean biomass and/or biofilm/biomass ratio \pm SEM. Statistical analyses were performed in GraphPad Prism Software v. 7.0c. Statistical significance was determined using one-way ANOVA with a posthoc Dunnett's multiple comparison test comparing growth and/or biofilm production in the presence of ca. 5 mg/mL HMOs to growth and/or biofilm production in media alone. All antibiotic-only and all antibiotic + HMO antibiotic MIC

values against GBS represent at least three independent trials each with three technical replicates. HMO IC₅₀ curves were generated in GraphPad Prism Software v. 7.0c. using an inhibition dose–response nonlinear regression curve fit for log(inhibitor) vs normalized response with a variable slope. All antibiotic-only MIC values against *S. aureus* and *A. baumannii* represent at least three independent trials each with three technical replicates. For *S. aureus*, the following antibiotic + HMO antibiotic MIC values represent one trial with three technical replicates: cefazolin, vancomycin, clindamycin, erythromycin, and linezolid. The gentamicin + HMO antibiotic MIC value represents at least three independent trials each with three technical replicates. For *A. baumannii*, the following antibiotic + HMO antibiotic MIC values represent one trial with three technical replicates: imipenem, meropenem, minocycline, tigecycline, and doripenem. The amikacin and tobramycin + HMO antibiotic MIC values represent at least three independent trials each with three technical replicates. Statistical analysis for the BacLight assay was performed in GraphPad Prism Software v. 7.0c. Statistical significance was determined using Student's *t* test, *N* = 3 replicates, comparing the LIVE/DEAD ratio of an HMO treatment at a given concentration to the LIVE/DEAD ratio of bacteria grown in media alone.

3.6 References

1. Sass, L., Group B Streptococcal Infections. *Pediatr. Rev.* **2012**, 33 (5).
2. Gibbs, R. S.; Schrag, S.; Schuchat, A., Perinatal infections due to group B streptococci. *Obstet. Gynecol.* **2004**, 104 (5 Pt 1), 1062-76.
3. Le Doare, K.; Kampmann, B., Breast milk and Group B streptococcal infection: vector of transmission or vehicle for protection? *Vaccine* **2014**, 32 (26), 3128-32.

4. Andreas, N. J.; Al-Khalidi, A.; Jaiteh, M.; Clarke, E.; Hyde, M. J.; Modi, N.; Holmes, E.; Kampmann, B.; Mehring Le Doare, K., Role of human milk oligosaccharides in Group B *Streptococcus* colonisation. *Clin. Transl. Immunology*. **2016**, 5 (8), e99.
5. Borges, S.; Silva, J.; Teixeira, P., Survival and biofilm formation by Group B streptococci in simulated vaginal fluid at different pHs. *Antonie Van Leeuwenhoek* **2012**, 101 (3), 677-82.
6. Nan, C.; Dangor, Z.; Cutland, C. L.; Edwards, M. S.; Madhi, S. A.; Cunnington, M. C., Maternal group B *Streptococcus*-related stillbirth: a systematic review. *BJOG* **2015**, 122 (11), 1437-45.
7. Pupolo, K. M., Epidemiology of Neonatal Early-onset Sepsis. *NeoReviews* **2008**, 9 (12), e571-579.
8. Butter, M. N. W.; De Moor, C. E., *Streptococcus agalactiae* as a cause of meningitis in the newborn, and of bacteraemia in adults. *Antonie van Leeuwenhoek* **1967**, 33, 439-450.
9. Craft, K. M.; Townsend, S. D., The Human Milk Glycome as a Defense Against Infectious Diseases: Rationale, Challenges, and Opportunities. *ACS Infect. Dis.* **2017**, 4 (2), 77-83.
10. Jeurink, P. V.; van Bergenhenegouwen, J.; Jimenez, E.; Knippels, L. M.; Fernandez, L.; Garsen, J.; Knol, J.; Rodriguez, J. M.; Martin, R., Human milk: a source of more life than we imagine. *Benef. Microbes* **2013**, 4 (1), 17-30.
11. Cabrera-Rubio, R.; Collado, M. C.; Laitinen, K.; Salminen, S.; Isolauri, E.; Mira, A., The human milk microbiome changes over lactation and is shaped by maternal weight and mode of delivery. *Am. J. Clin. Nutr.* **2012**, 96 (3), 544-51.
12. Bingen, E.; Denamur, E.; Lambert-Zechovsky, N.; Aujard, Y.; Brahimi, N.; Geslin, P.; Elion, J., Analysis of DNA restriction fragment length polymorphism extends the evidence for breast milk transmission in *Streptococcus agalactiae* late-onset neonatal infection. *J. Infect. Dis.* **1992**, 165 (3), 569-73.
13. Zimmermann, P.; Gwee, A.; Curtis, N., The controversial role of breast milk in GBS late-onset disease. *J. Infect.* **2017**, 74 Suppl 1, S34-S40.

14. Burianova, I.; Paulova, M.; Cermak, P.; Janota, J., Group B *streptococcus* colonization of breast milk of group B *streptococcus* positive mothers. *J. Hum. Lact.* **2013**, 29 (4), 586-90.
15. Active Bacterial Core Surveillance Report, Emerging Infections Program Network, Group B *Streptococcus*, 2014. Centers for Disease Control and Prevention. **2014**.
16. Boyer, K. M.; Gotoff, S. P., Prevention of early-onset neonatal group B streptococcal disease with selective intrapartum chemoprophylaxis. *N. Engl. J. Med.* **1986**, 314 (26), 1665-9.
17. Schrag, S. J.; Zell, E. R.; Lynfield, R.; Roome, A.; Arnold, K. E.; Craig, A. S.; Harrison, L. H.; Reingold, A.; Stefonek, K.; Smith, G.; Gamble, M.; Schuchat, A.; Active Bacterial Core Surveillance, T., A population-based comparison of strategies to prevent early-onset group B streptococcal disease in neonates. *N. Engl. J. Med.* **2002**, 347 (4), 233-9.
18. Cagno, C. K.; Pettit, J. M.; Weiss, B. D., Prevention of Perinatal Group B Streptococcal Disease Revised Guidelines from CDC, 2010. *Am. Fam. Physician* **2010**, 86, 59-65.
19. Dagnew, A. F.; Cunnington, M. C.; Dube, Q.; Edwards, M. S.; French, N.; Heyderman, R. S.; Madhi, S. A.; Slobod, K.; Clemens, S. A., Variation in reported neonatal group B streptococcal disease incidence in developing countries. *Clin. Infect. Dis.* **2012**, 55 (1), 91-102.
20. Bizzarro, M. J.; Dembry, L. M.; Baltimore, R. S.; Gallagher, P. G., Changing patterns in neonatal *Escherichia coli* sepsis and ampicillin resistance in the era of intrapartum antibiotic prophylaxis. *Pediatrics* **2008**, 121 (4), 689-96.
21. Phares, C. R.; Lynfield, R.; Farley, M. M.; Mohle-Boetani, J.; Harrison, L. H.; Petit, S.; Craig, A. S.; Schaffner, W.; Zansky, S. M.; Gershman, K.; Stefonek, K. R.; Albanese, B. A.; Zell, E. R.; Schuchat, A.; Schrag, S. J.; Active Bacterial Core surveillance/Emerging Infections Program, N., Epidemiology of invasive group B streptococcal disease in the United States, 1999-2005. *JAMA* **2008**, 299 (17), 2056-65.
22. Rajagopal, L., Understanding the regulation of Group B Streptococcal virulence factors. *Future Microbiol.* **2009**, 4 (2), 201-21.

23. Chang, Y. C.; Olson, J.; Beasley, F. C.; Tung, C.; Zhang, J.; Crocker, P. R.; Varki, A.; Nizet, V., Group B *Streptococcus* engages an inhibitory Siglec through sialic acid mimicry to blunt innate immune and inflammatory responses in vivo. *PLoS Pathog.* **2014**, *10* (1), e1003846.
24. Almeida, A.; Rosinski-Chupin, I.; Plainvert, C.; Douarre, P. E.; Borrego, M. J.; Poyart, C.; Glaser, P., Parallel Evolution of Group B *Streptococcus* Hypervirulent Clonal Complex 17 Unveils New Pathoadaptive Mutations. *mSystems* **2017**, *2* (5), e00074-17.
25. Cieslewicz, M. J.; Chaffin, D.; Glusman, G.; Kasper, D.; Madan, A.; Rodrigues, S.; Fahey, J.; Wessels, M. R.; Rubens, C. E., Structural and genetic diversity of group B *streptococcus* capsular polysaccharides. *Infect. Immun.* **2005**, *73* (5), 3096-103.
26. Marques, M. B.; Kasper, D. L.; Pangburn, M. K.; Wessels, M. R., Prevention of C3 Deposition by Capsular Polysaccharide Is a Virulence Mechanism of Type I Group B Streptococci. *Infect. Immun.* **1992**, *60* (10), 3986-3993.
27. Rubens, C. E.; Wessels, M. R.; Heggen, L. M.; kasper, D. L., Transposon mutagenesis of type III group B *Streptococcus*—Correlation of capsule expression with virulence. *PNAS* **1987**, *84*, 7208-7212.
28. Slotved, H. C.; Kong, F.; Lambertsen, L.; Sauer, S.; Gilbert, G. L., Serotype IX, a Proposed New *Streptococcus agalactiae* Serotype. *J. Clin. Microbiol.* **2007**, *45* (9), 2929-36.
29. Sorensen, U. B.; Poulsen, K.; Ghezzi, C.; Margarit, I.; Kilian, M., Emergence and global dissemination of host-specific *Streptococcus agalactiae* clones. *MBio.* **2010**, *1* (3), e00178-10.
30. Takahashi, S.; Aoyagi, Y.; Adderson, E. E.; Okuwaki, Y.; Bohnsack, J. F., Capsular sialic acid limits C5a production on type III group B streptococci. *Infect. Immun.* **1999**, *67* (4), 1866-70.
31. Teatero, S.; Ferrieri, P.; Martin, I.; Demczuk, W.; McGeer, A.; Fittipaldi, N., Serotype Distribution, Population Structure, and Antimicrobial Resistance of Group B *Streptococcus* Strains Recovered from Colonized Pregnant Women. *J. Clin. Microbiol.* **2017**, *55* (2), 412-422.

32. Wessels, M. R.; Rubens, C. E.; Benedi, V. J.; Kasper, D. L., Definition of a bacterial virulence factor: sialylation of the group B streptococcal capsule. *PNAS* **1989**, *86* (22), 8983-7.
33. Berti, F.; Campisi, E.; Toniolo, C.; Morelli, L.; Crotti, S.; Rosini, R.; Romano, M. R.; Pinto, V.; Brogioni, B.; Torricelli, G.; Janulczyk, R.; Grandi, G.; Margarit, I., Structure of the type IX group B *Streptococcus* capsular polysaccharide and its evolutionary relationship with types V and VII. *J. Biol. Chem.* **2014**, *289* (34), 23437-48.
34. Melin, P.; Efstratiou, A., Group B streptococcal epidemiology and vaccine needs in developed countries. *Vaccine* **2013**, *31 Suppl 4*, D31-42.
35. Russell, N. J.; Seale, A. C.; O'Driscoll, M.; O'Sullivan, C.; Bianchi-Jassir, F.; Gonzalez-Guarin, J.; Lawn, J. E.; Baker, C. J.; Bartlett, L.; Cutland, C.; Gravett, M. G.; Heath, P. T.; Le Doare, K.; Madhi, S. A.; Rubens, C. E.; Schrag, S.; Sobanjo-Ter Meulen, A.; Vekemans, J.; Saha, S. K.; Ip, M.; Group, G. B. S. M. C. I., Maternal Colonization With Group B *Streptococcus* and Serotype Distribution Worldwide: Systematic Review and Meta-analyses. *Clin. Infect. Dis.* **2017**, *65* (Suppl 2), S100-S111.
36. Costerton, J. W.; Stewart, P. S.; Greenberg, E. P., Bacterial biofilms: a common cause of persistent infections. *Science* **1999**, *284* (5418), 1318-22.
37. Davies, D., Understanding biofilm resistance to antibacterial agents. *Nat. Rev. Drug Discov.* **2003**, *2* (2), 114-22.
38. Craft, K. M.; Nguyen, J. M.; Berg, L. J.; Townsend, S. D., Methicillin-Resistant *Staphylococcus aureus* (MRSA): Antibiotic Resistance and the Biofilm Phenotype. *Medchemcomm* **2019**, *Ahead of print*.
39. Flemming, H.-C.; Wingender, J., The biofilm matrix. *Nat. Rev. Microbiol.* **2010**, *8* (9), 623-633.
40. Parsek, M. R.; Greenberg, E. P., Sociomicrobiology: the connections between quorum sensing and biofilms. *Trends Microbiol.* **2005**, *13* (1), 27-33.
41. Sauer, K.; Camper, A. K.; Ehrlich, G. D.; Costerton, J. W.; Davies, D. G., *Pseudomonas aeruginosa* Displays Multiple Phenotypes during Development as a Biofilm. *J. Bacteriol.* **2002**, *184* (4), 1140-1154.

42. Yarwood, J. M.; Bartels, D. J.; Volper, E. M.; Greenberg, E. P., Quorum Sensing in *Staphylococcus aureus* Biofilms. *J. Bacteriol.* **2004**, *186* (6), 1838-1850.
43. Fux, C. A.; Costerton, J. W.; Stewart, P. S.; Stoodley, P., Survival strategies of infectious biofilms. *Trends Microbiol.* **2005**, *13* (1), 34-40.
44. Welsh, M. A.; Blackwell, H. E., Chemical probes of quorum sensing: from compound development to biological discovery. *FEMS Microbiol. Rev.* **2016**, *40* (5), 774-94.
45. Praneenararat, T.; Palmer, A. G.; Blackwell, H. E., Chemical methods to interrogate bacterial quorum sensing pathways. *Org. Biomol. Chem.* **2012**, *10* (41), 8189-99.
46. Kong, K. F.; Vuong, C.; Otto, M., *Staphylococcus* quorum sensing in biofilm formation and infection. *Int. J. Med. Microbiol.* **2006**, *296* (2-3), 133-9.
47. Hoiby, N.; Ciofu, O.; Johansen, H. K.; Song, Z. J.; Moser, C.; Jensen, P. O.; Molin, S.; Givskov, M.; Tolker-Nielsen, T.; Bjarnsholt, T., The clinical impact of bacterial biofilms. *Int. J. Oral. Sci.* **2011**, *3* (2), 55-65.
48. Santajit, S.; Indrawattana, N., Mechanisms of Antimicrobial Resistance in ESKAPE Pathogens. *Biomed. Res. Int.* **2016**, *2016*, 2475067.
49. Hall-Stoodley, L.; Costerton, J. W.; Stoodley, P., Bacterial biofilms: from the natural environment to infectious diseases. *Nat. Rev. Microbiol.* **2004**, *2* (2), 95-108.
50. de Beer, D.; Stoodley, P.; Roe, F.; Lewandowski, Z., Effects of biofilm structures on oxygen distribution and mass transport. *Biotechnol. Bioeng.* **1994**, *43* (11), 1131-8.
51. Stewart, P. S.; Costerton, J. W., Antibiotic resistance of bacteria in biofilms. *Lancet* **2001**, *358* (9276), 135-8.
52. Marrie, T. J.; Costerton, J. W., A scanning and transmission electron microscopic study of the surfaces of intrauterine contraceptive devices. *Am. J. Obstet. Gynecol.* **1983**, *146* (4), 384-94.
53. Rinaudo, C. D.; Rosini, R.; Galeotti, C. L.; Berti, F.; Necchi, F.; Reguzzi, V.; Ghezzi, C.; Telford, J. L.; Grandi, G.; Maione, D., Specific involvement of pilus type 2a in biofilm formation in group B *Streptococcus*. *PLoS One* **2010**, *5* (2), e9216.

54. Kaur, H.; Kumar, P.; Ray, P.; Kaur, J.; Chakraborti, A., Biofilm formation in clinical isolates of group B streptococci from north India. *Microb. Pathog.* **2009**, *46* (6), 321-7.
55. Rosini, R.; Margarit, I., Biofilm formation by *Streptococcus agalactiae*: influence of environmental conditions and implicated virulence factors. *Front Cell. Infect. Microbiol.* **2015**, *5*, 6.
56. Xia, F. D.; Mallet, A.; Caliot, E.; Gao, C.; Trieu-Cuot, P.; Dramsi, S., Capsular polysaccharide of Group B *Streptococcus* mediates biofilm formation in the presence of human plasma. *Microbes Infect.* **2015**, *17* (1), 71-6.
57. Konto-Ghiorgi, Y.; Mairey, E.; Mallet, A.; Dumenil, G.; Caliot, E.; Trieu-Cuot, P.; Dramsi, S., Dual role for pilus in adherence to epithelial cells and biofilm formation in *Streptococcus agalactiae*. *PLoS Pathog.* **2009**, *5* (5), e1000422.
58. D'Urzo, N.; Martinelli, M.; Pezzicoli, A.; De Cesare, V.; Pinto, V.; Margarit, I.; Telford, J. L.; Maione, D.; Members of the, D. S. G., Acidic pH strongly enhances in vitro biofilm formation by a subset of hypervirulent ST-17 *Streptococcus agalactiae* strains. *Appl. Environ. Microbiol.* **2014**, *80* (7), 2176-85.
59. Carey, A. J.; Tan, C. K.; Mirza, S.; Irving-Rodgers, H.; Webb, R. I.; Lam, A.; Ulett, G. C., Infection and cellular defense dynamics in a novel 17beta-estradiol murine model of chronic human group B *streptococcus* genital tract colonization reveal a role for hemolysin in persistence and neutrophil accumulation. *J. Immunol.* **2014**, *192* (4), 1718-31.
60. Baker, C. J.; Kasper, D. L., Correlation of Maternal Antibody Deficiency with Susceptibility to Neonatal Group B Streptococcal Infection. *N. Engl. J. Med.* **1976**, *294*, 753-756.
61. Baker, C. J.; Edwards, M. S.; Kasper, D. L., Role of antibody to native type III polysaccharide of group B *Streptococcus* in infant infection. *Pediatrics* **1981**, *68* (4), 544-9.
62. Kwatra, G.; Adrian, P. V.; Shiri, T.; Buchmann, E. J.; Cutland, C. L.; Madhi, S. A., Natural acquired humoral immunity against serotype-specific group B *Streptococcus* rectovaginal colonization acquisition in pregnant women. *Clin. Microbiol. Infect.* **2015**, *21* (6), 568 e13-21.

63. Beachler, C. W.; Baker, C. J.; Kasper, D. L.; Fleming, D. K.; Webb, B. J.; Yow, M. D., Group B streptococcal colonization and antibody status in lower socioeconomic parturient women. *Am. J. Obstet. Gynecol.* **1979**, *133* (2), 171-3.
64. Baker, C. J.; Carey, V. J.; Rench, M. A.; Edwards, M. S.; Hillier, S. L.; Kasper, D. L.; Platt, R., Maternal antibody at delivery protects neonates from early onset group B streptococcal disease. *J. Infect. Dis.* **2014**, *209* (5), 781-8.
65. Heath, P. T.; Culley, F. J.; Jones, C. E.; Kampmann, B.; Le Doare, K.; Nunes, M. C.; Sadarangani, M.; Chaudhry, Z.; Baker, C. J.; Openshaw, P. J. M., Group B streptococcus and respiratory syncytial virus immunisation during pregnancy: a landscape analysis. *Lancet Infect. Dis.* **2017**, *17* (7), e223-e234.
66. Pritchard, D. G., Gray, B.M. Egan, M.L. , Murine Monoclonal Antibodies to Type Ib Polysaccharide of Group B Streptococci Bind to Human Milk Oligosaccharides. *Infect. Immun.* **1992**, *60* (4), 1598-1602.
67. Lin, A. E.; Autran, C. A.; Szyszka, A.; Escajadillo, T.; Huang, M.; Godula, K.; Prudden, A. R.; Boons, G. J.; Lewis, A. L.; Doran, K. S.; Nizet, V.; Bode, L., Human milk oligosaccharides inhibit growth of group B *Streptococcus*. *J. Biol. Chem.* **2017**, *292* (27), 11243-11249.
68. Ackerman, D. L.; Doster, R. S.; Weitkamp, J. H.; Aronoff, D. M.; Gaddy, J. A.; Townsend, S. D., Human Milk Oligosaccharides Exhibit Antimicrobial and Antibiofilm Properties against Group B *Streptococcus*. *ACS Infect. Dis.* **2017**, *3* (8), 595-605.
69. Blank, D.; Gebhardt, S.; Maass, K.; Lochnit, G.; Dotz, V.; Blank, J.; Geyer, R.; Kunz, C., High-throughput mass finger printing and Lewis blood group assignment of human milk oligosaccharides. *Anal. Bioanal. Chem.* **2011**, *401* (8), 2495-510.
70. Bode, L., The functional biology of human milk oligosaccharides. *Early Hum. Dev.* **2015**, *91* (11), 619-22.
71. Ackerman, D. L.; Craft, K. M.; Doster, R. S.; Weitkamp, J. H.; Aronoff, D. M.; Gaddy, J. A.; Townsend, S. D., Antimicrobial and Antibiofilm Activity of Human Milk Oligosaccharides against *Streptococcus agalactiae*, *Staphylococcus aureus*, and *Acinetobacter baumannii*. *ACS Infect. Dis.* **2018**, *4* (3), 315-324.
72. Arifuzzaman, M.; Ahmed, T.; Rahman, M. A.; Chowdhury, F.; Rashu, R.; Khan, A. I.; LaRocque, R. C.; Harris, J. B.; Bhuiyan, T. R.; Ryan, E. T.; Calderwood, S. B.;

- Qadri, F., Individuals with Le(a+b-) blood group have increased susceptibility to symptomatic vibrio cholerae O1 infection. *PLoS Negl. Trop. Dis.* **2011**, *5* (12), e1413.
73. Jaff, M. S., Higher frequency of secretor phenotype in O blood group - its benefits in prevention and/or treatment of some diseases. *Int. J. Nanomedicine* **2010**, *5*, 901-5.
74. Vague, P.; Melis, C.; Mercier, P.; Vialettes, B.; Lassmann, V., The increased frequency of the Lewis negative blood group in a diabetic population. *Diabetologia* **1978**, *15* (1), 33-6.
75. Lin, F. Y.; Clemens, J. D.; Azimi, P. H.; Regan, J. A.; Weisman, L. E.; Philips, J. B., 3rd; Rhoads, G. G.; Clark, P.; Brenner, R. A.; Ferrieri, P., Capsular polysaccharide types of group B streptococcal isolates from neonates with early-onset systemic infection. *J. Infect. Dis.* **1998**, *177* (3), 790-2.
76. Johri, A. K.; Lata, H.; Yadav, P.; Dua, M.; Yang, Y.; Xu, X.; Homma, A.; Barocchi, M. A.; Bottomley, M. J.; Saul, A.; Klugman, K. P.; Black, S., Epidemiology of Group B *Streptococcus* in developing countries. *Vaccine* **2013**, *31 Suppl 4*, D43-5.
77. Bode, L., Human milk oligosaccharides: every baby needs a sugar mama. *Glycobiology* **2012**, *22* (9), 1147-62.
78. Asakuma, S.; Urashima, T.; Akahori, M.; Obayashi, H.; Nakamura, T.; Kimura, K.; Watanabe, Y.; Arai, I.; Sanai, Y., Variation of major neutral oligosaccharides levels in human colostrum. *Eur. J. Clin. Nutr.* **2008**, *62* (4), 488-94.
79. Urashima, T.; Asakuma, S.; Leo, F.; Fukuda, K.; Messer, M.; Oftedal, O. T., The predominance of type I oligosaccharides is a feature specific to human breast milk. *Adv. Nutr.* **2012**, *3* (3), 473S-82S.
80. Kunz, C.; Meyer, C.; Collado, M. C.; Geiger, L.; Garcia-Mantrana, I.; Bertua-Rios, B.; Martinez-Costa, C.; Borsch, C.; Rudloff, S., Influence of Gestational Age, Secretor, and Lewis Blood Group Status on the Oligosaccharide Content of Human Milk. *J. Pediatr. Gastroenterol. Nutr.* **2017**, *64* (5), 789-798.
81. Ballard, O.; Morrow, A. L., Human milk composition: nutrients and bioactive factors. *Pediatr. Clin. North Am.* **2013**, *60* (1), 49-74.
82. Bassetti, M.; Merelli, M.; Temperoni, C.; Astilean, A. New antibiotics for bad bugs: where are we? *Ann. Clin. Microbiol. Antimicrob.* **2013**, *12* (22).

83. Boucher, H. W.; Talbot, G. H.; Bradley, J. S.; Edwards, J. E.; Gilbert, D.; Rice, L. B.; Scheld, M.; Spellberg, B.; Bartlett, J., Bad bugs, no drugs: no ESKAPE! An update from the Infectious Diseases Society of America. *Clin. Infect. Dis.* **2009**, *48* (1), 1-12.
84. Pendleton, J. N.; Gorman, S. P.; Gilmore, B. F., Clinical relevance of the ESKAPE pathogens. *Expert Rev. Anti. Infect. Ther.* **2013**, *11* (3), 297-308.
85. Alter, S. J.; Vidwan, N. K.; Sobande, P. O.; Omoloja, A.; Bennett, J. S., Common childhood bacterial infections. *Curr. Probl. Pediatr. Adolesc. Health Care* **2011**, *41* (10), 256-83.
86. Van den Bruel, A.; Bruyninckx, R.; Vermeire, E.; Aerssens, P.; Aertgeerts, B.; Buntinx, F., Signs and symptoms in children with a serious infection: a qualitative study. *BMC Fam. Pract.* **2005**, *6*, 36.
87. Rajaratnam, J. K.; Marcus, J. R.; Flaxman, A. D.; Wang, H.; Levin-Rector, A.; Dwyer, L.; Costa, M.; Lopez, A. D.; Murray, C. J., Neonatal, postneonatal, childhood, and under-5 mortality for 187 countries, 1970-2010: a systematic analysis of progress towards Millennium Development Goal 4. *Lancet* **2010**, *375* (9730), 1988-2008.
88. Galetto-Lacour, A.; Gervaix, A., Identifying severe bacterial infection in children with fever without source. *Expert Rev. Anti. Infect. Ther.* **2010**, *8* (11), 1231-7.
89. Almengor, A. C.; Kinkel, T. L.; Day, S. J.; McIver, K. S., The catabolite control protein CcpA binds to Pmga and influences expression of the virulence regulator Mga in the Group A streptococcus. *J. Bacteriol.* **2007**, *189* (23), 8405-16.
90. Manetti, A. G.; Zingaretti, C.; Falugi, F.; Capo, S.; Bombaci, M.; Bagnoli, F.; Gambellini, G.; Bensi, G.; Mora, M.; Edwards, A. M.; Musser, J. M.; Graviss, E. A.; Telford, J. L.; Grandi, G.; Margarit, I., *Streptococcus pyogenes* pili promote pharyngeal cell adhesion and biofilm formation. *Mol. Microbiol.* **2007**, *64* (4), 968-83.
91. Winn W Jr, A. S., Janda W, Koneman E, Procop G, Schreckenberger P, et al., editors, Nonfermenting Gram negative bacilli. *Koneman's Color Atlas and Textbook of Diagnostic Microbiology*, 6th ed. **2006**, 305-91.
92. Rossi, E.; Longo, F.; Barbagallo, M.; Peano, C.; Consolandi, C.; Pietrelli, A.; Jaillon, S.; Garlanda, C.; Landini, P., Glucose availability enhances

- lipopolysaccharide production and immunogenicity in the opportunistic pathogen *Acinetobacter baumannii*. *Future Microbiol.* **2016**, *11* (3), 335-49.
93. Hunt, K. M.; Preuss, J.; Nissan, C.; Davlin, C. A.; Williams, J. E.; Shafii, B.; Richardson, A. D.; McGuire, M. K.; Bode, L.; McGuire, M. A., Human milk oligosaccharides promote the growth of staphylococci. *Appl. Environ. Microbiol.* **2012**, *78* (14), 4763-70.
 94. Perez-Giraldo, C.; Rodriguez-Benito, A.; Moran, F. J.; Hurtado, C.; Blanco, M. T.; Gomez-Garcia, A. C., Influence of *N*-acetylcysteine on the formation of biofilm by *Staphylococcus epidermidis*. *J. Antimicrob. Chemother.* **1997**, *39* (5), 643-6.
 95. Leite, B.; Gomes, F.; Melo, P.; Souza, C.; Teixeira, P.; Oliveira, R.; Pizzolitto, E., *N*-acetylcysteine and vancomycin alone and in combination against staphylococci biofilm. *Rev. Bras. Eng. Bioméd.* **2013**, *29* (2), 184-192.
 96. Aslam, S.; Trautner, B. W.; Ramanathan, V.; Darouiche, R. O., Combination of tigecycline and *N*-acetylcysteine reduces biofilm-embedded bacteria on vascular catheters. *Antimicrob. Agents. Chemother.* **2007**, *51* (4), 1556-8.
 97. Charlebois, A.; Jacques, M.; Archambault, M., Biofilm formation of *Clostridium perfringens* and its exposure to low-dose antimicrobials. *Front Microbiol.* **2014**, *5*.
 98. Kaplan, J. B., Antibiotic-induced biofilm formation. *Int. J. Artif. Organs* **2011**, *34* (9), 737-51.
 99. Lazaro-Diez, M.; Remuzgo-Martinez, S.; Rodriguez-Mirones, C.; Acosta, F.; Icardo, J. M.; Martinez-Martinez, L.; Ramos-Vivas, J., Effects of Subinhibitory Concentrations of Ceftaroline on Methicillin-Resistant *Staphylococcus aureus* (MRSA) Biofilms. *PLoS One* **2016**, *11* (1), e0147569.
 100. Craft, K. M.; Gaddy, J. A.; Townsend, S. D., Human Milk Oligosaccharides (HMOs) Sensitize Group B *Streptococcus* to Clindamycin, Erythromycin, Gentamicin, and Minocycline on a Strain Specific Basis. *ACS Chem. Biol.* **2018**, *13* (8), 2020-2026.
 101. Jantscher-Krenn, E.; Zhrebtssov, M.; Nissan, C.; Goth, K.; Guner, Y. S.; Naidu, N.; Choudhury, B.; Grishin, A. V.; Ford, H. R.; Bode, L., The human milk oligosaccharide disialyllacto-*N*-tetraose prevents necrotising enterocolitis in neonatal rats. *Gut* **2012**, *61* (10), 1417-25.

102. Autran, C. A.; Schoterman, M. H.; Jantscher-Krenn, E.; Kamerling, J. P.; Bode, L., Sialylated galacto-oligosaccharides and 2'-fucosyllactose reduce necrotising enterocolitis in neonatal rats. *Br. J. Nutr.* **2016**, *116* (2), 294-9.
103. Shivekar, S.; Menon, T., Molecular Basis for Erythromycin Resistance in Group A *Streptococcus* Isolated From Skin and Soft Tissue Infections. *J. Clin. Diagn. Res.* **2015**, *9* (11), DC21-3.
104. Lo, H. H.; Nien, H. H.; Cheng, Y. Y.; Su, F. Y., Antibiotic susceptibility pattern and erythromycin resistance mechanisms in beta-hemolytic group G *Streptococcus dysgalactiae* subspecies *equisimilis* isolates from central Taiwan. *J. Microbiol. Immunol. Infect.* **2015**, *48* (6), 613-7.
105. Yook, J. H.; Kim, M. Y.; Kim, E. J.; Yang, J. H.; Ryu, H. M.; Oh, K. Y.; Shin, J. H.; Foxman, B.; Ki, M., Risk factors associated with group B *streptococcus* resistant to clindamycin and erythromycin in pregnant korean women. *Infect. Chemother.* **2013**, *45* (3), 299-307.
106. World Health Organization Model List of Essential Medicines, 2017. **2017**.
107. Begg, E. J.; Barclay, M. L., Aminoglycosides - 50 Years On. *Brit. J. Clin. Pharmacol.* **1995**, *39* (6), 597-603.
108. World Health Organization List of Critically Important Antimicrobials for Human Medicine (WHO CIA list). **2017**.
109. Mingeot-Leclercq, M. P.; Glupczynski, Y.; Tulkens, P. M., Aminoglycosides: activity and resistance. *Antimicrob. Agents Chemother.* **1999**, *43* (4), 727-37.
110. Mingeot-Leclercq, M. P.; Tulkens, P. M., Aminoglycosides: nephrotoxicity. *Antimicrob. Agents Chemother.* **1999**, *43* (5), 1003-12.
111. Melander, R. J.; Melander, C., The Challenge of Overcoming Antibiotic Resistance: An Adjuvant Approach? *ACS Infect. Dis.* **2017**, *3* (8), 559-563.
112. Srinivas, P.; Rivard, K., Polymyxin Resistance in Gram-negative Pathogens. *Curr. Infect. Dis. Rep.* **2017**, *19* (11), 38.
113. Garg, S. K.; Singh, O.; Juneja, D.; Tyagi, N.; Khurana, A. S.; Qamra, A.; Motlekar, S.; Barkate, H., Resurgence of Polymyxin B for MDR/XDR Gram-

- Negative Infections: An Overview of Current Evidence. *Crit. Care Res. Pract.* **2017**, 2017, 3635609.
114. Olaitan, A. O.; Li, J., Emergence of polymyxin resistance in Gram-negative bacteria. *Int. J. Antimicrob. Agents* **2016**, 48 (6), 581-582.
 115. Harm, S.; Gabor, F.; Hartmann, J., Low-dose polymyxin: an option for therapy of Gram-negative sepsis. *Innate Immun.* **2016**, 22 (4), 274-83.
 116. HsuChen, C. C.; Feingold, D. S., The mechanism of polymyxin B action and selectivity toward biologic membranes. *Biochemistry* **1973**, 12 (11), 2105-11.
 117. Fey, P. D.; Endres, J. L.; Yajjala, V. K.; Widhelm, T. J.; Boissy, R. J.; Bose, J. L.; Bayles, K. W., A genetic resource for rapid and comprehensive phenotype screening of nonessential *Staphylococcus aureus* genes. *MBio.* **2013**, 4 (1), e00537-12.
 118. Voyich, J. M.; Braughton, K. R.; Sturdevant, D. E.; Whitney, A. R.; Said-Salim, B.; Porcella, S. F.; Long, R. D.; Dorward, D. W.; Gardner, D. J.; Kreiswirth, B. N.; Musser, J. M.; DeLeo, F. R., Insights into Mechanisms Used by *Staphylococcus aureus* to Avoid Destruction by Human Neutrophils. *J. Immunol.* **2005**, 175 (6), 3907-3919.
 119. Ackerman, D. L.; Craft, K. M.; Townsend, S. D., Infant food applications of complex carbohydrates: Structure, synthesis, and function. *Carbohydr. Res.* **2017**, 437, 16-27.
 120. Ramirez-Macias, D.; Shaw, K.; Ward, R.; Galvan-Magana, F.; Vazquez-Juarez, R., Isolation and characterization of microsatellite loci in the whale shark (*Rhincodon typus*). *Mol. Ecol. Resour.* **2009**, 9 (3), 798-800.
 121. Santibáñez, L.; Fernández-Arrojo, L.; Guerrero, C.; Plou, F. J.; Illanes, A., Removal of lactose in crude galacto-oligosaccharides by β -galactosidase from *Kluyveromyces lactis*. *J. Mol. Cat. B: Enzym.* **2016**, 133, 85-91.
 122. Kjelleberg, S.; Molin, S., Is there a role for quorum sensing signals in bacterial biofilms? *Curr. Opin. Microbiol.* **2002**, 5 (3), 254-258.

Appendix A1:
Data and Spectra Relevant to Chapter 3

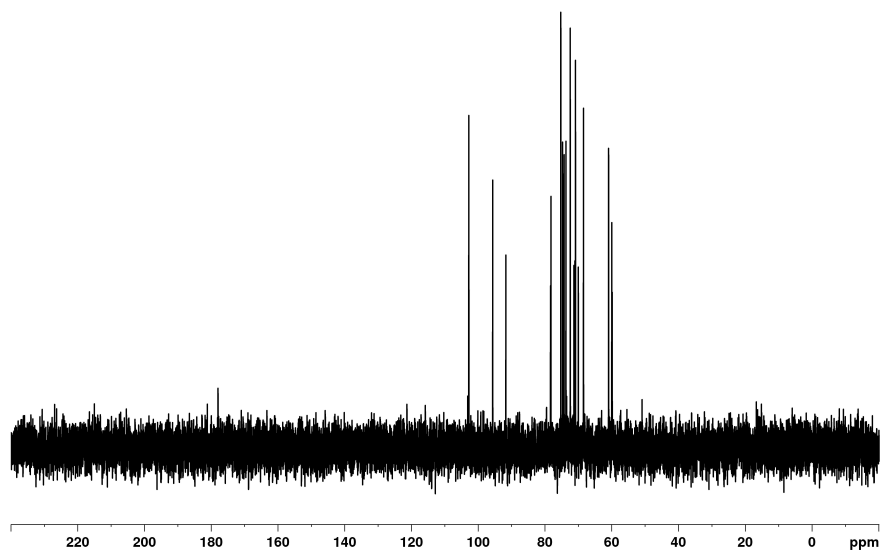
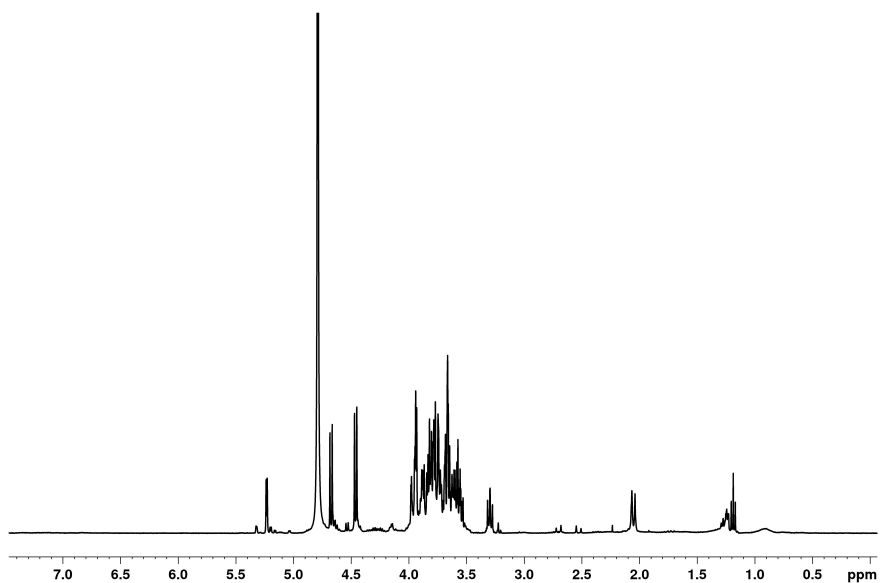


Figure A1.1. ^1H NMR (400 MHz, D_2O) and ^{13}C NMR (100 MHz, D_2O) spectra of HMOs isolated from Donor 14. The absence of saturated alkyl chain peaks characteristic of lipids in the lower ppm region of the ^1H NMR spectrum and the absence of amide bond peaks characteristic of proteins in the upper ppm region of the ^{13}C NMR preclude the presence of fat or protein in the sample. The peaks observed are characteristic of carbohydrates.

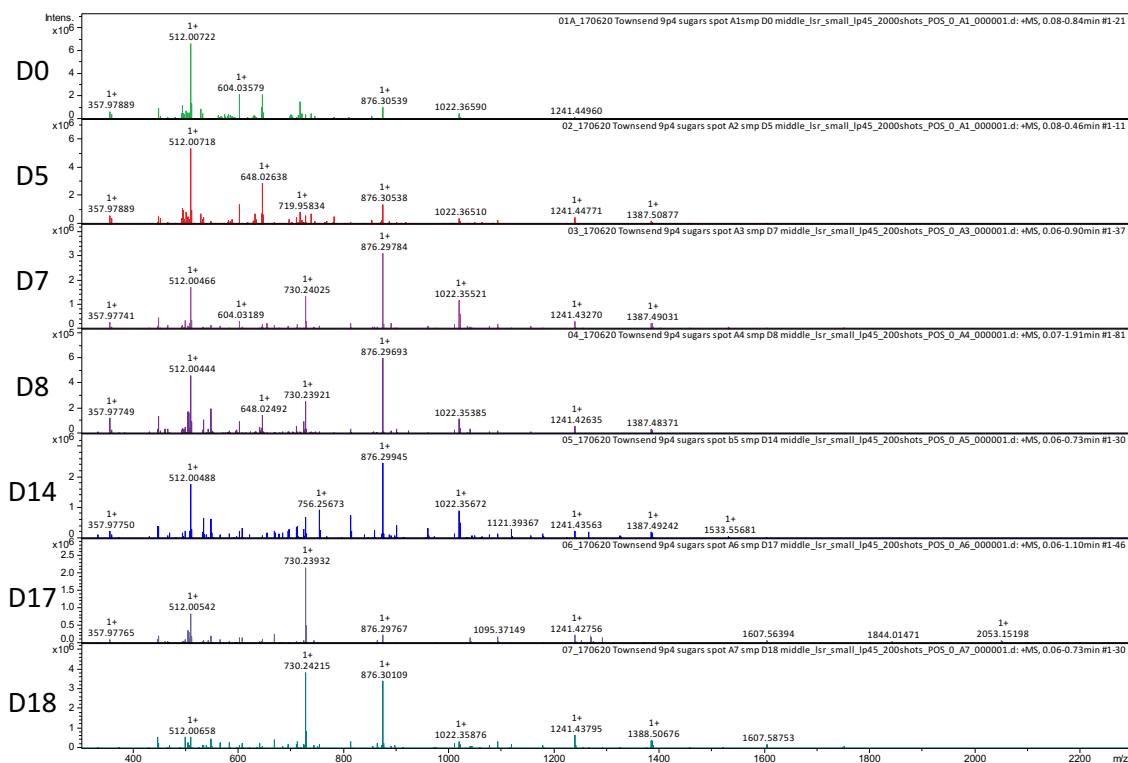


Figure A1.2. Matrix-assisted laser desorption/ionization (MALDI) full size MS spectra for HMO mixtures isolated from Donors 0, 5, 7, 8, 14, 17, and 18. Sample labels are listed to the left of each spectrum with a *D*# designation such that D0 corresponds to Donor 0, and so on. Samples were analyzed in positive ion mode on a 9.4T Fourier transform ion cyclotron resonance (FT-ICR) mass spectrometer (MS) (Bruker Solarix). Mass spectra were acquired in positive ion mode from *m/z* 300–2500. Sodium ion adducts of HMOs were detected with a mass accuracy of >2 ppm.

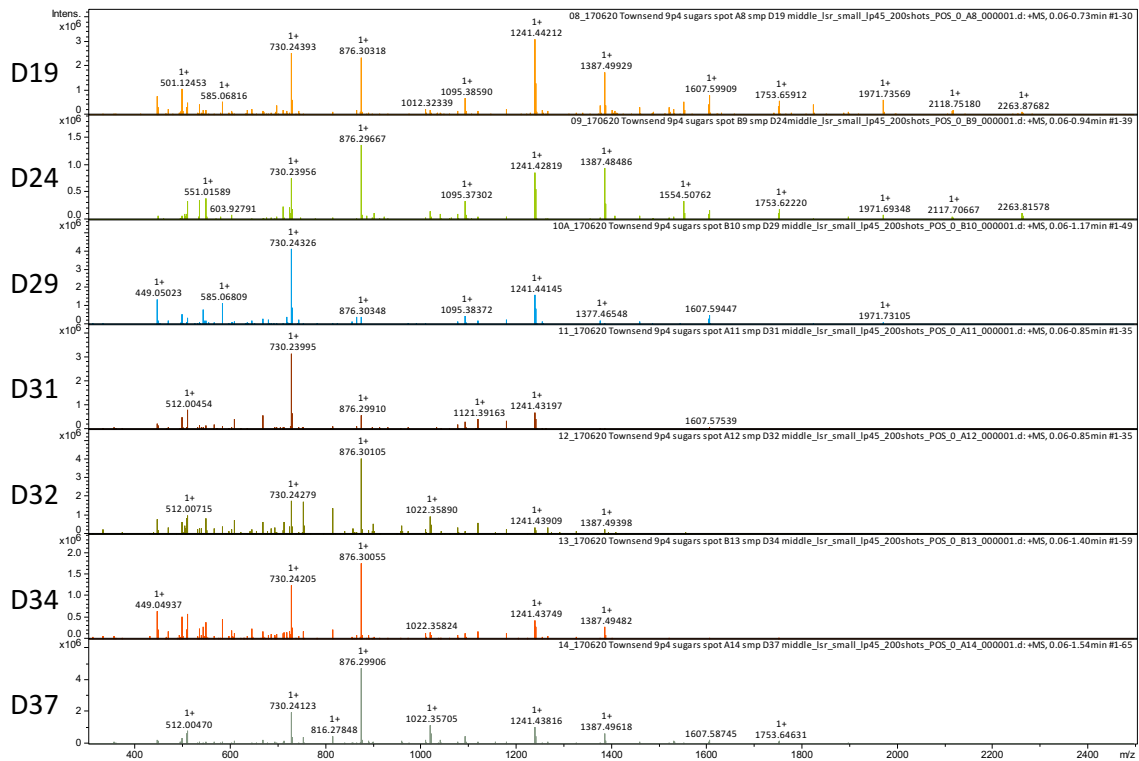


Figure A1.3. Matrix-assisted laser desorption/ionization (MALDI) full size MS spectra for HMO mixtures isolated from Donors 19, 24, 29, 31, 32, 34, and 37. Sample labels are listed to the left of each spectrum with a D# designation such that D19 corresponds to Donor 19, and so on. Samples were analyzed in positive ion mode on a 9.4T Fourier transform ion cyclotron resonance (FT-ICR) mass spectrometer (MS) (Bruker Solarix). Mass spectra were acquired in positive ion mode from m/z 300-2500. Sodium ion adducts of HMOs were detected with a mass accuracy of >2 ppm.

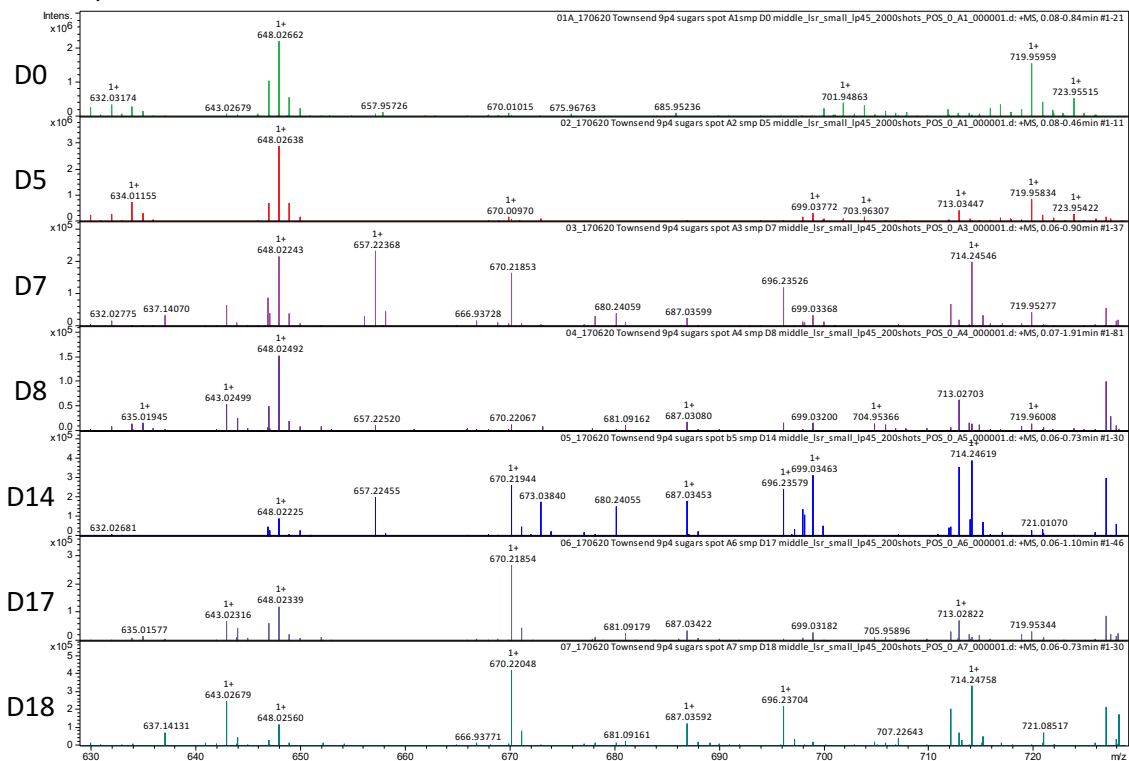


Figure A1.4. Matrix-assisted laser desorption/ionization (MALDI) partial MS spectra from m/z 630-730 for HMO mixtures isolated from Donors 0, 5, 7, 8, 14, 17, and 18. Sample labels are listed to the left of each spectrum with a D# designation such that D0 corresponds to Donor 0, and so on. Samples were analyzed in positive ion mode on a 9.4T Fourier transform ion cyclotron resonance (FT-ICR) mass spectrometer (MS) (Bruker Solarix). Mass spectra were acquired in positive ion mode from m/z 300-2500. Sodium ion adducts of HMOs were detected with a mass accuracy of >2 ppm.

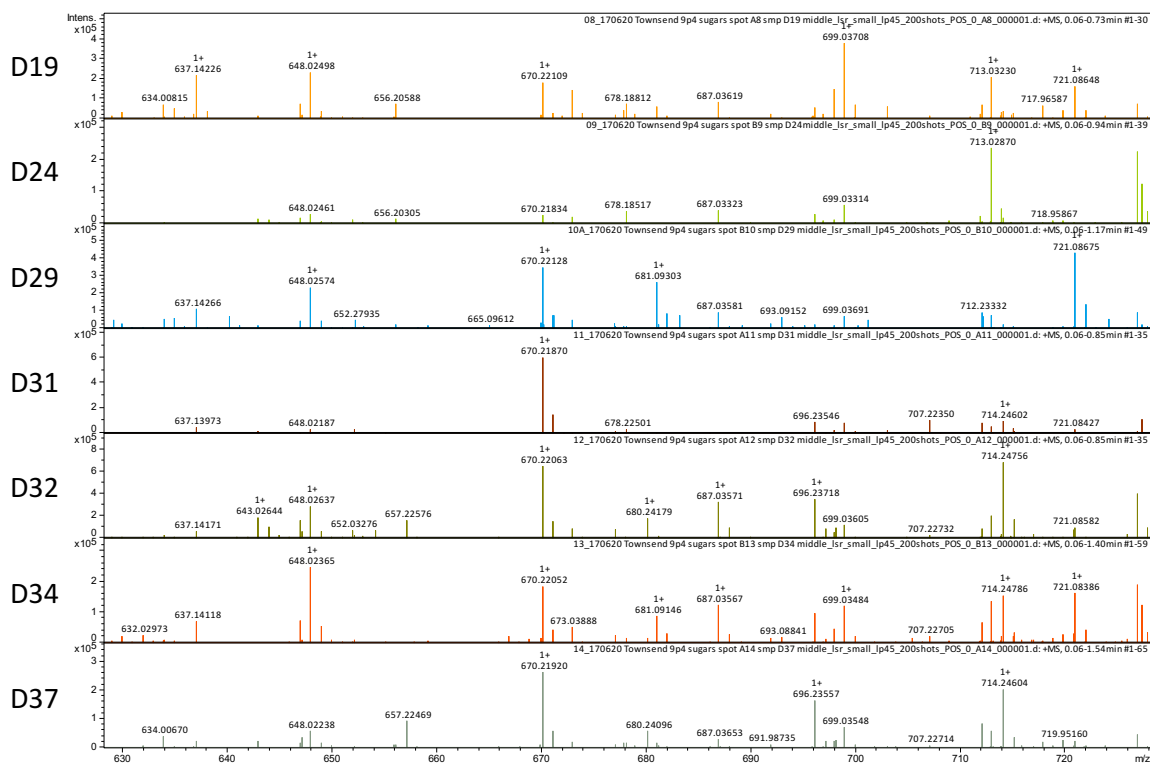


Figure A1.5. Matrix-assisted laser desorption/ionization (MALDI) partial MS spectra from m/z 630-730 for HMO mixtures isolated from Donors 19, 24, 29, 31, 32, 34, and 37. Sample labels are listed to the left of each spectrum with a $D\#$ designation such that D19 corresponds to Donor 19, and so on. Samples were analyzed in positive ion mode on a 9.4T Fourier transform ion cyclotron resonance (FT-ICR) mass spectrometer (MS) (Bruker Solarix). Mass spectra were acquired in positive ion mode from m/z 300-2500. Sodium ion adducts of HMOs were detected with a mass accuracy of >2 ppm.

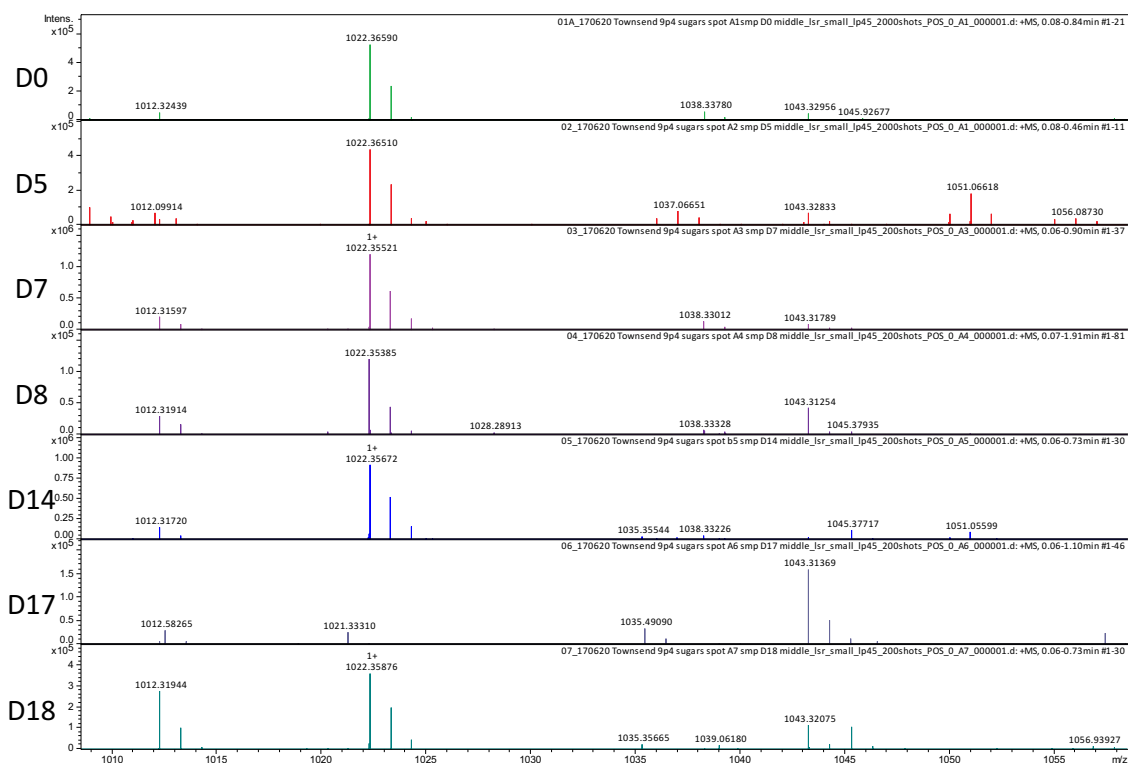


Figure A1.6. Matrix-assisted laser desorption/ionization (MALDI) partial MS spectra from m/z 1010-1060 for HMO mixtures isolated from Donors 0, 5, 7, 8, 14, 17, and 18. Sample labels are listed to the left of each spectrum with a D# designation such that D0 corresponds to Donor 0, and so on. Samples were analyzed in positive ion mode on a 9.4T Fourier transform ion cyclotron resonance (FT-ICR) mass spectrometer (MS) (Bruker Solarix). Mass spectra were acquired in positive ion mode from m/z 300-2500. Sodium ion adducts of HMOs were detected with a mass accuracy of >2 ppm.

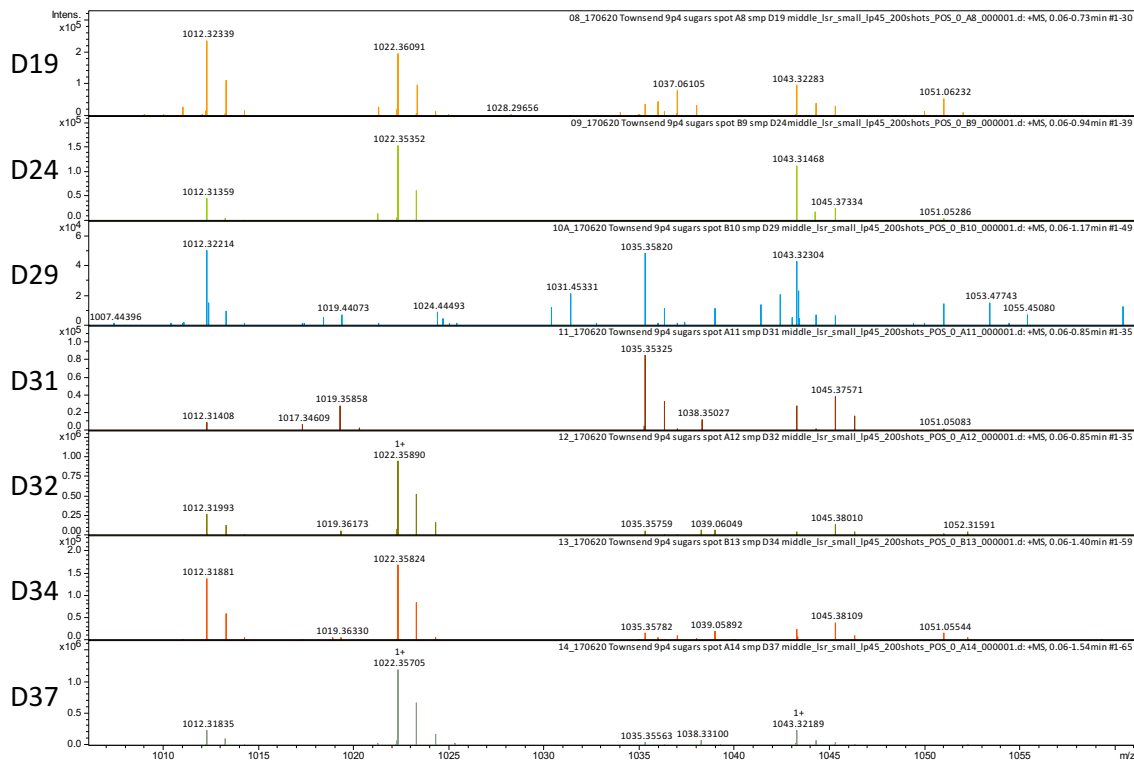


Figure A1.7. Matrix-assisted laser desorption/ionization (MALDI) partial MS spectra from m/z 1010-1060 for HMO mixtures isolated from Donors 19, 24, 29, 31, 32, 34, and 37. Sample labels are listed to the left of each spectrum with a D# designation such that D19 corresponds to Donor 19, and so on. Samples were analyzed in positive ion mode on a 9.4T Fourier transform ion cyclotron resonance (FT-ICR) mass spectrometer (MS) (Bruker Solarix). Mass spectra were acquired in positive ion mode from m/z 300-2500. Sodium ion adducts of HMOs were detected with a mass accuracy of >2 ppm.

MS/MS of m/z 657.2 →

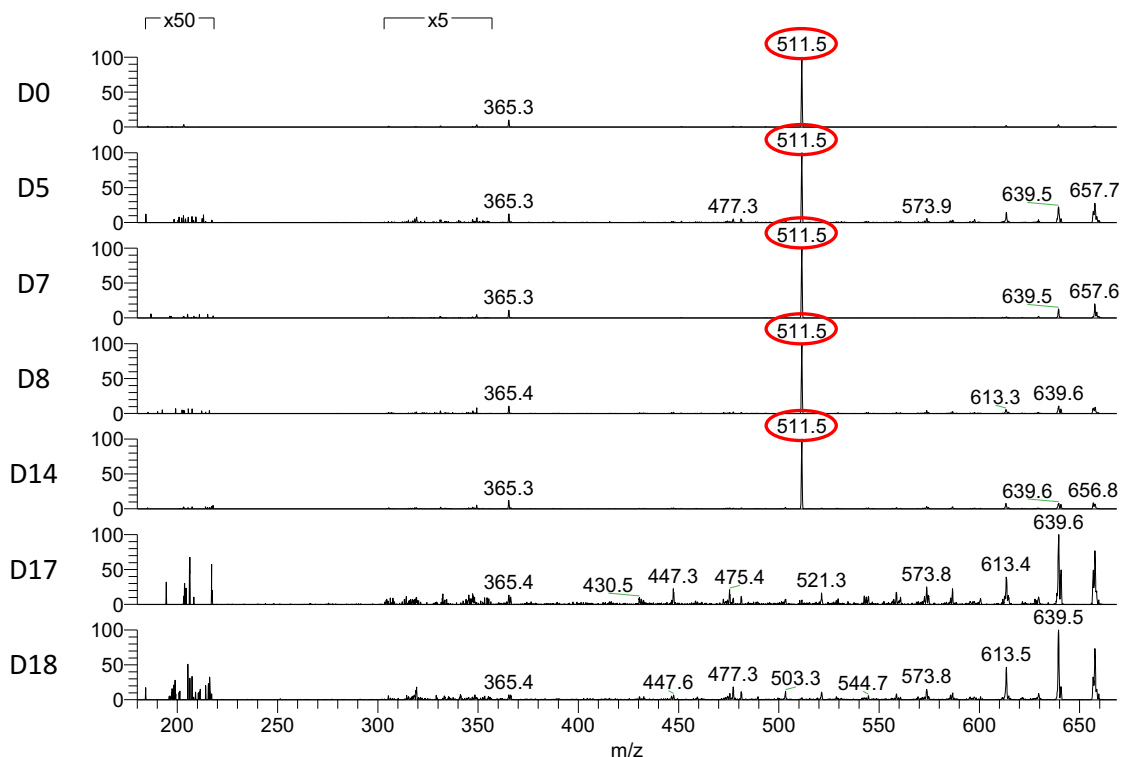


Figure A1.8. Matrix-assisted laser desorption/ionization (MALDI) MS/MS spectra of selected m/z 657.2 ion for HMO mixtures isolated from Donors 0, 5, 7, 8, 14, 17, and 18. Sample labels are listed to the left of each spectrum with a D# designation such that D0 corresponds to Donor 0, and so on. MS/MS analysis was performed with a linear ion trap mass spectrometer equipped with a MALDI source (LTQ XL, Thermo Scientific). Selected sodium adduct ions of interest were isolated with a 1 amu window and fragmented via CID using a collision energy of 35 eV. Ions circled in red are deterministic for Lewis blood group and secretor status assignment.

MS/MS of m/z 657.2 →

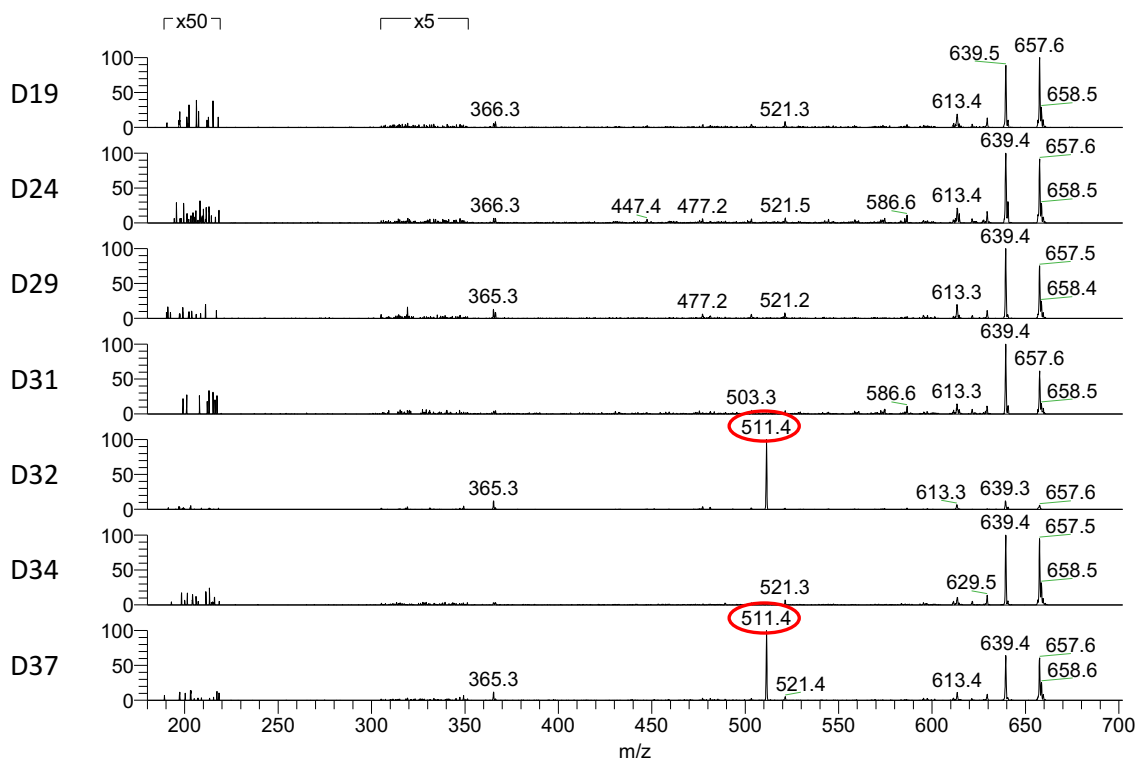


Figure A1.9. Matrix-assisted laser desorption/ionization (MALDI) MS/MS spectra of selected m/z 657.2 ion for HMO mixtures isolated from Donors 19, 24, 29, 31, 32, 34, and 37. Sample labels are listed to the left of each spectrum with a D# designation such that D19 corresponds to Donor 19, and so on. MS/MS analysis was performed with a linear ion trap mass spectrometer equipped with a MALDI source (LTQ XL, Thermo Scientific). Selected sodium adduct ions of interest were isolated with a 1 amu window and fragmented via CID using a collision energy of 35 eV. Ions circled in red are deterministic for Lewis blood group and secretor status assignment.

MS/MS of m/z 1022.2 →

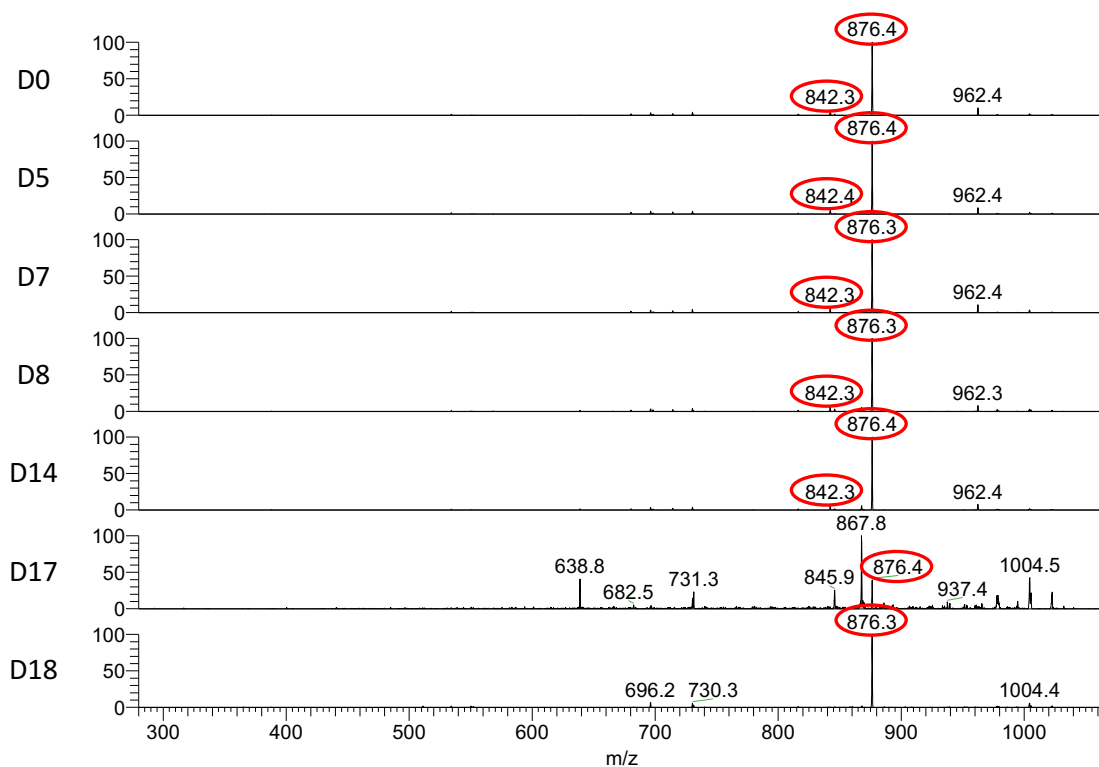


Figure A1.10. Matrix-assisted laser desorption/ionization (MALDI) MS/MS spectra of selected m/z 1022.2 ion for HMO mixtures isolated from Donors 0, 5, 7, 8, 14, 17, and 18. Sample labels are listed to the left of each spectrum with a D# designation such that D0 corresponds to Donor 0, and so on. MS/MS analysis was performed with a linear ion trap mass spectrometer equipped with a MALDI source (LTQ XL, Thermo Scientific). Selected sodium adduct ions of interest were isolated with a 1 amu window and fragmented via CID using a collision energy of 35 eV. Ions circled in red are deterministic for Lewis blood group and secretor status assignment.

MS/MS of m/z 1022.2 \rightarrow [fragments from m/z 700-900]

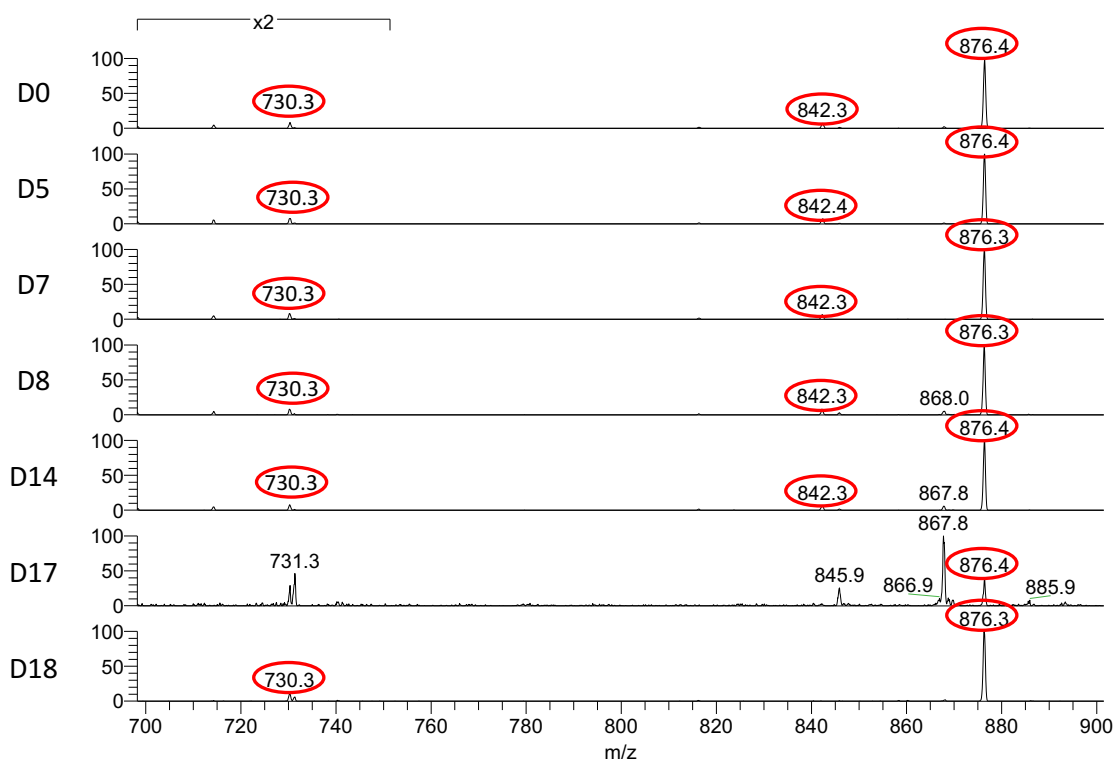


Figure A1.11. Matrix-assisted laser desorption/ionization (MALDI) MS/MS partial spectra of selected m/z 1022.2 ion (from m/z 700-900) for HMO mixtures isolated from Donors 0, 5, 7, 8, 14, 17, and 18. Sample labels are listed to the left of each spectrum with a D# designation such that D0 corresponds to Donor 0, and so on. MS/MS analysis was performed with a linear ion trap mass spectrometer equipped with a MALDI source (LTQ XL, Thermo Scientific). Selected sodium adduct ions of interest were isolated with a 1 amu window and fragmented via CID using a collision energy of 35 eV. Ions circled in red are deterministic for Lewis blood group and secretor status assignment.

MS/MS of m/z 1022.2 →

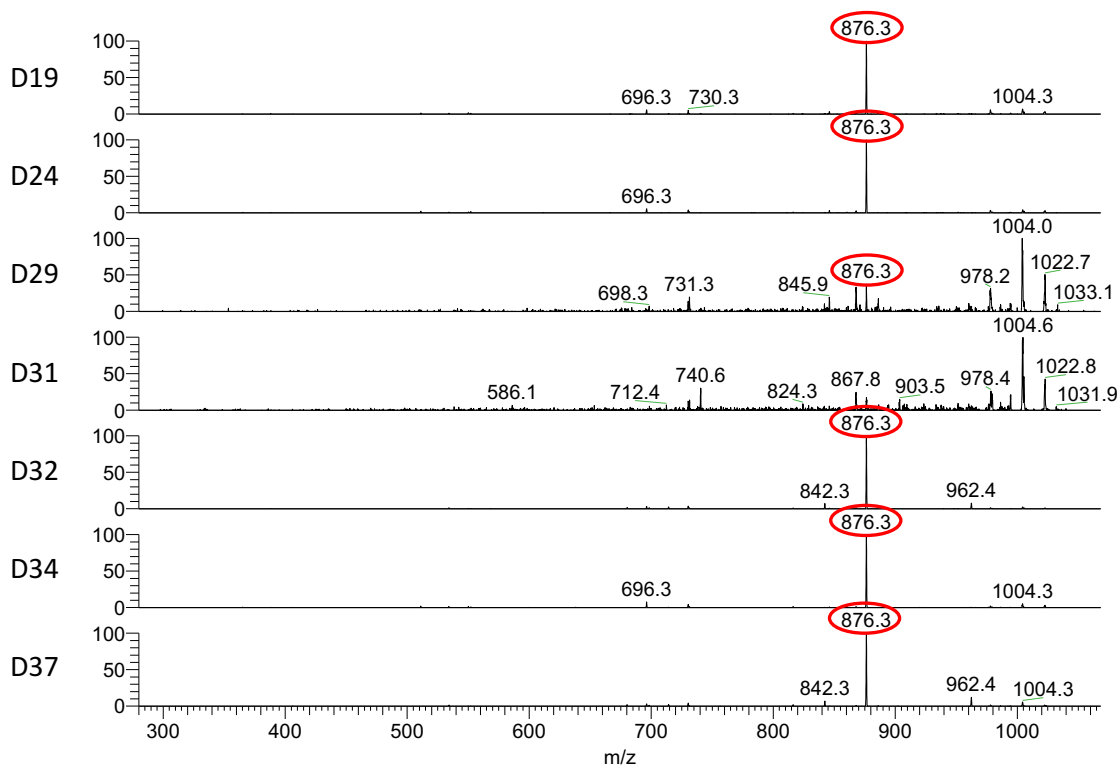


Figure A1.12. Matrix-assisted laser desorption/ionization (MALDI) MS/MS spectra of selected m/z 1022.2 ion for HMO mixtures isolated from Donors 19, 24, 29, 31, 32, 34, and 37. Sample labels are listed to the left of each spectrum with a D# designation such that D19 corresponds to Donor 19, and so on. MS/MS analysis was performed with a linear ion trap mass spectrometer equipped with a MALDI source (LTQ XL, Thermo Scientific). Selected sodium adduct ions of interest were isolated with a 1 amu window and fragmented via CID using a collision energy of 35 eV. Ions circled in red are deterministic for Lewis blood group and secretor status assignment.

MS/MS of m/z 1022.2 \rightarrow [fragments from m/z 700-900]

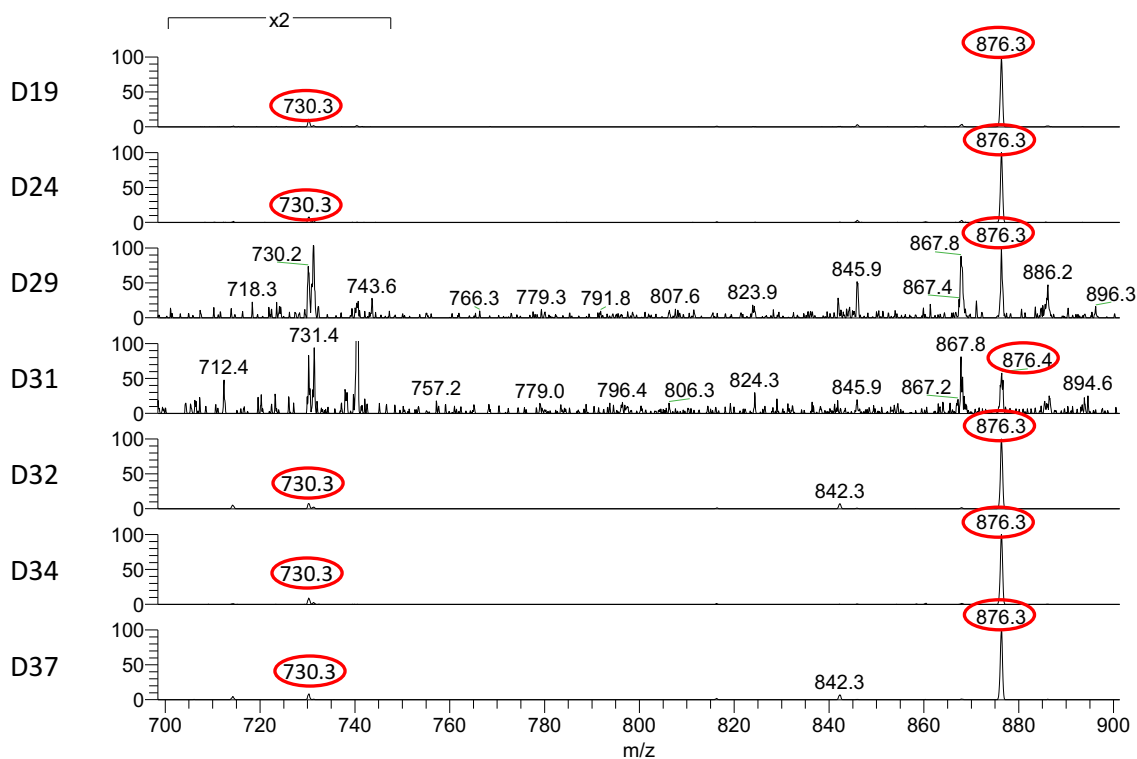


Figure A1.13. Matrix-assisted laser desorption/ionization (MALDI) MS/MS partial spectra of selected m/z 1022.2 ion (from m/z 700-900) for HMO mixtures isolated from Donors 19, 24, 29, 31, 32, 34, and 37. Sample labels are listed to the left of each spectrum with a D# designation such that D19 corresponds to Donor 19, and so on. MS/MS analysis was performed with a linear ion trap mass spectrometer equipped with a MALDI source (LTQ XL, Thermo Scientific). Selected sodium adduct ions of interest were isolated with a 1 amu window and fragmented via CID using a collision energy of 35 eV. Ions circled in red are deterministic for Lewis blood group and secretor status assignment.

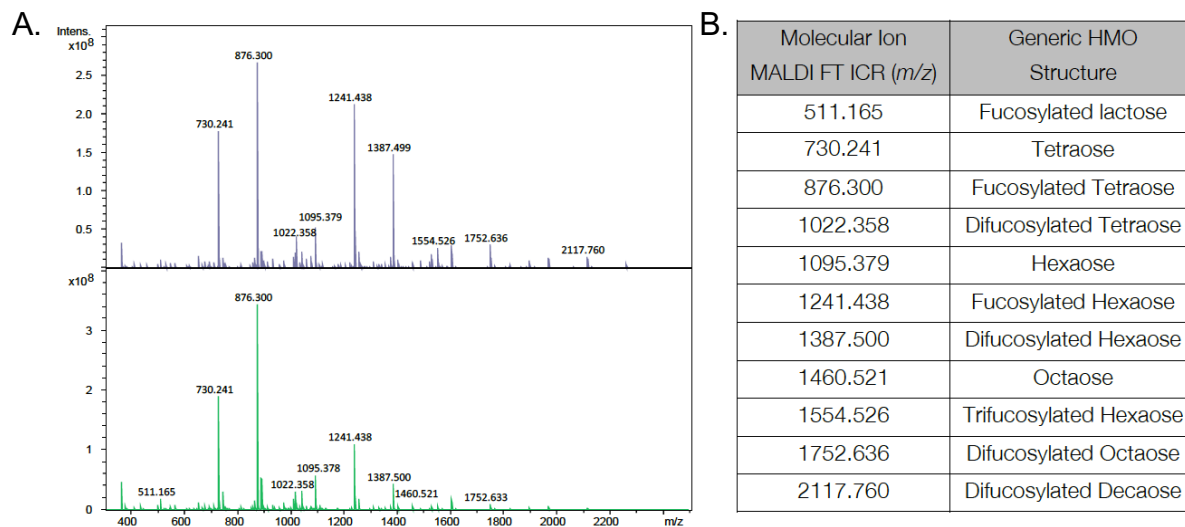


Figure A1.14. General HMO composition of two distinct donors. **(A)** Matrix-assisted laser desorption/ionization (MALDI) MS spectra for HMO mixtures isolated from two distinct donor samples. Samples were analyzed in positive ion mode on a 9.4T Fourier transform ion cyclotron resonance (FT-ICR) mass spectrometer (MS) (Bruker Solarix). Mass spectra were acquired in positive ion mode from *m/z* 300-2500. Sodium ion adducts of HMOs were detected with a mass accuracy of >2 ppm. **(B)** Generic structural descriptions for the molecular ions observed.

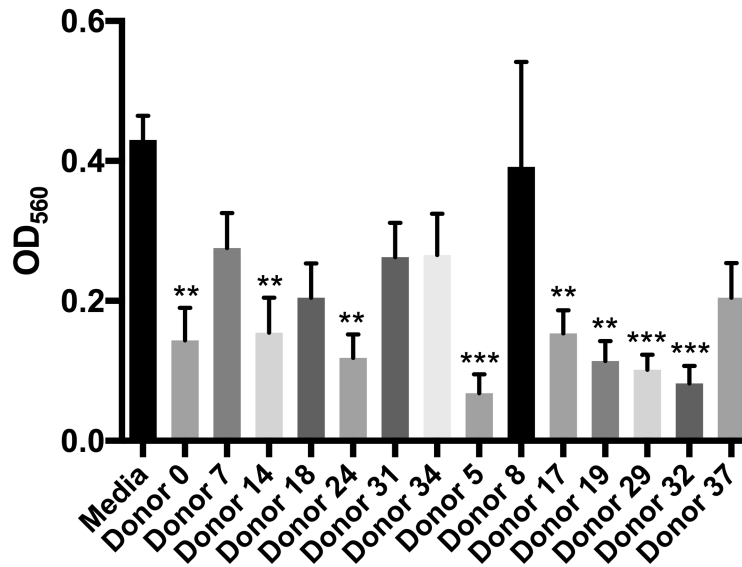


Figure A1.15. Biofilm formation for *S. agalactiae* strain CNCTC 10/84 after 24 H of growth in THB media alone or in the presence of ca. 5 mg/mL HMOs from various donors. Data expressed as mean biofilm measurements ($OD_{560} \pm SEM$) of 3 separate experiments, each with 3 technical replicates. **** represents $p < 0.0001$ by one-way ANOVA, $F = 3.843$ with *posthoc* Dunnett's multiple comparison test comparing each HMO sample against the control sample without HMOs.

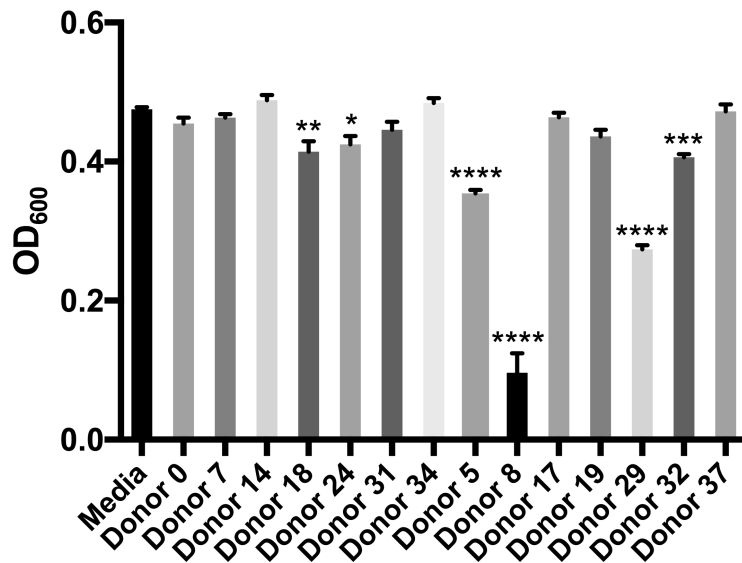


Figure A1.16. Biomass for *S. agalactiae* strain CNCTC 10/84 after 24 H of growth in THB media alone or in the presence of ca. 5 mg/mL HMOs from various donors. Data expressed as mean biomass measurements ($OD_{600} \pm SEM$) of 3 separate experiments, each with 3 technical replicates. **** represents $p < 0.0001$ by one-way ANOVA, $F = 88.34$ with *posthoc* Dunnett's multiple comparison test comparing each HMO sample against the control sample without HMOs.

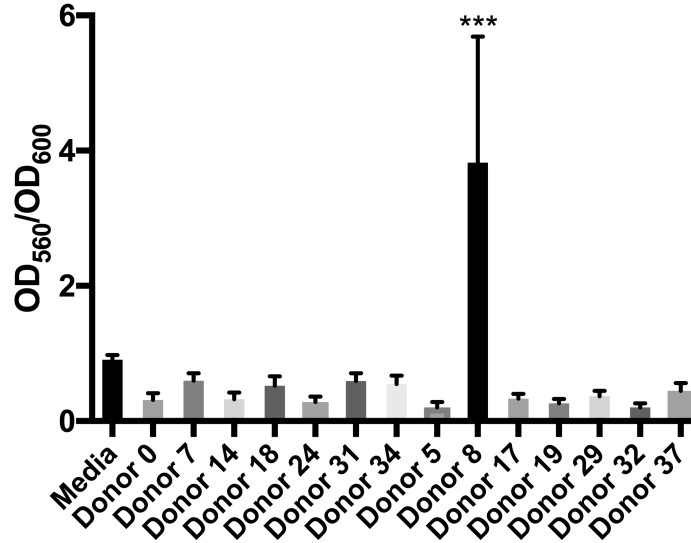


Figure A1.17. Biofilm to biomass ratio of *S. agalactiae* strain CNCTC 10/84 after 24 H of growth in THB media alone or in the presence of ca. 5 mg/mL HMOs from various donors. Data expressed as mean biofilm/biomass ratio measurements (OD₅₆₀/OD₆₀₀) ± SEM of 3 separate experiments, each with 3 technical replicates. *** represents p=0.0001 by one-way ANOVA, F=3.351 with *posthoc* Dunnett's multiple comparison test comparing each HMO sample against the control sample without HMOs.

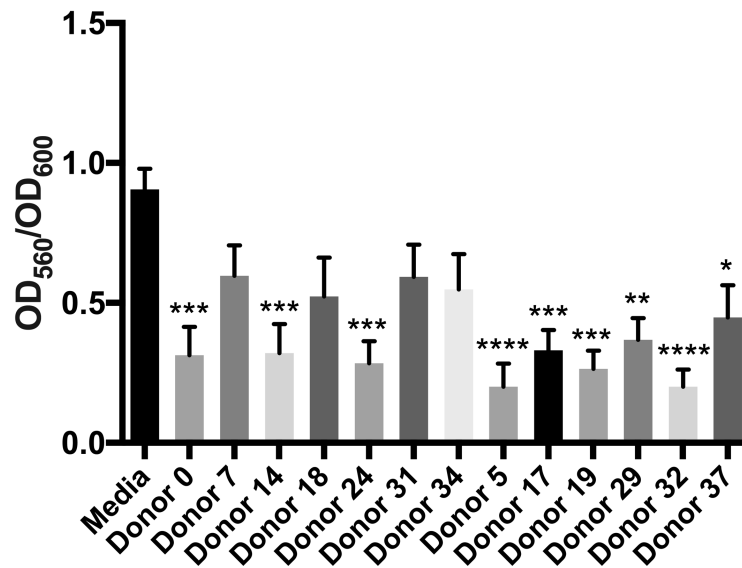


Figure A1.18. Biofilm to biomass ratio of *S. agalactiae* strain CNCTC 10/84 after 24 H of growth in THB media alone or in the presence of ca. 5 mg/mL HMOs from various donors excluding Donor 8. Data expressed as mean biofilm/biomass ratio measurements (OD₅₆₀/OD₆₀₀) ± SEM of 3 separate experiments, each with 3 technical replicates. **** represents p<0.0001 by one-way ANOVA, F=4.065 with *posthoc* Dunnett's multiple comparison test comparing each HMO sample against the control sample without HMOs. Results from Donor 8 were determined to be outliers using ROUT (Q=1) and Grubbs (alpha=0.05) outlier tests.

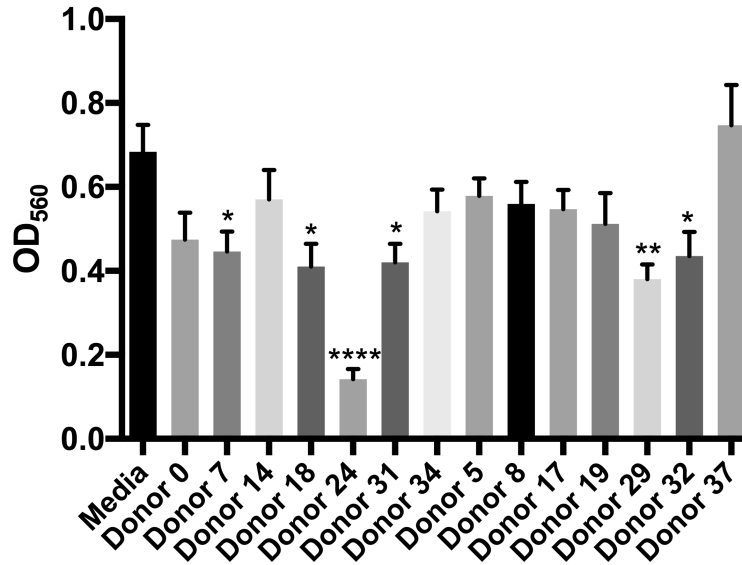


Figure A1.19. Biofilm for *S. agalactiae* strain CNCTC 10/84 after 24 H of growth in THB + 1% glucose media alone or in the presence of ca. 5 mg/mL HMOs from various donors. Data expressed as mean biofilm measurements (OD₅₆₀) ± SEM of 3 separate experiments, each with 3 technical replicates. **** represents p<0.0001 by one-way ANOVA, F=6.057 with *posthoc* Dunnett's multiple comparison test comparing each HMO sample against the control sample without HMOs.

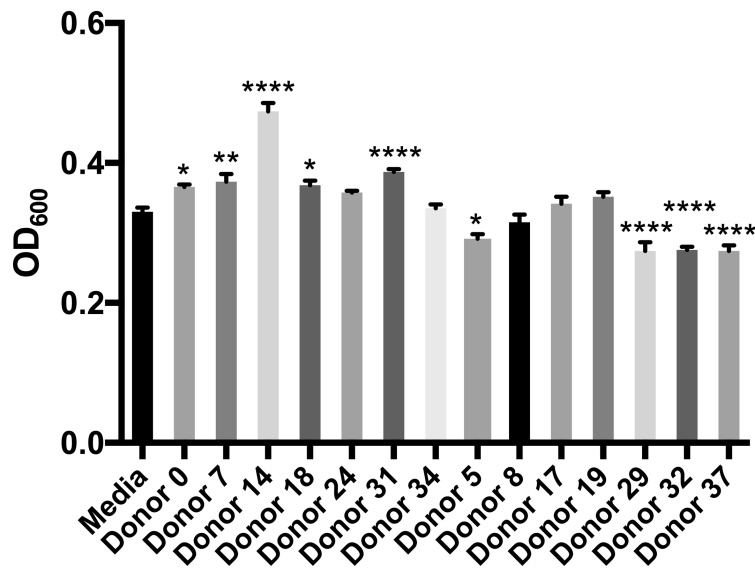


Figure A1.20. Biomass for *S. agalactiae* strain CNCTC 10/84 after 24 H of growth in THB + 1% glucose media alone or in the presence of ca. 5 mg/mL HMOs from various donors. Data expressed as mean biomass measurements (OD₆₀₀) ± SEM of 3 separate experiments, each with 3 technical replicates. **** represents p=<0.0001 by one-way ANOVA, F=43.21 with *posthoc* Dunnett's multiple comparison test comparing each HMO sample against the control sample without HMOs.

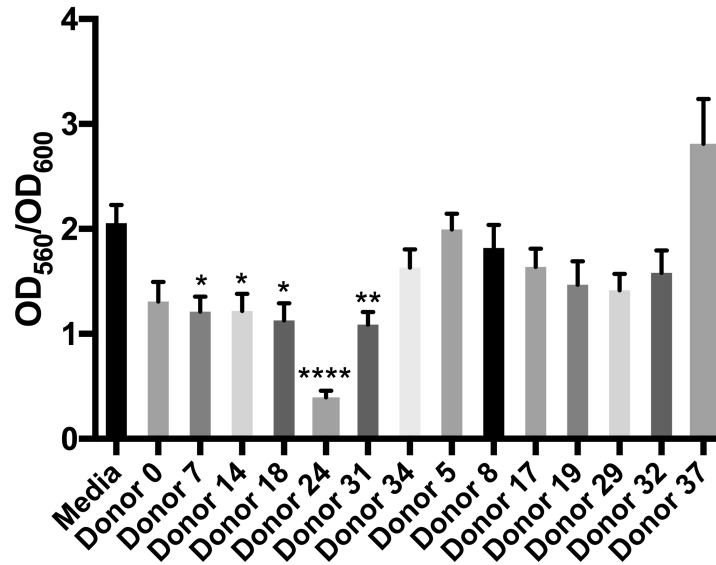


Figure A1.21. Biofilm to biomass ratio of *S. agalactiae* strain CNCTC 10/84 after 24 H of growth in THB + 1% glucose media alone or in the presence of ca. 5 mg/mL HMOs from various donors. Data expressed as mean biofilm/biomass ratio measurements (OD_{560}/OD_{600}) \pm SEM of 3 separate experiments, each with 3 technical replicates. **** represents $p < 0.0001$ by one-way ANOVA, $F = 7.579$ with *posthoc* Dunnett's multiple comparison test comparing each HMO sample against the control sample without HMOs.

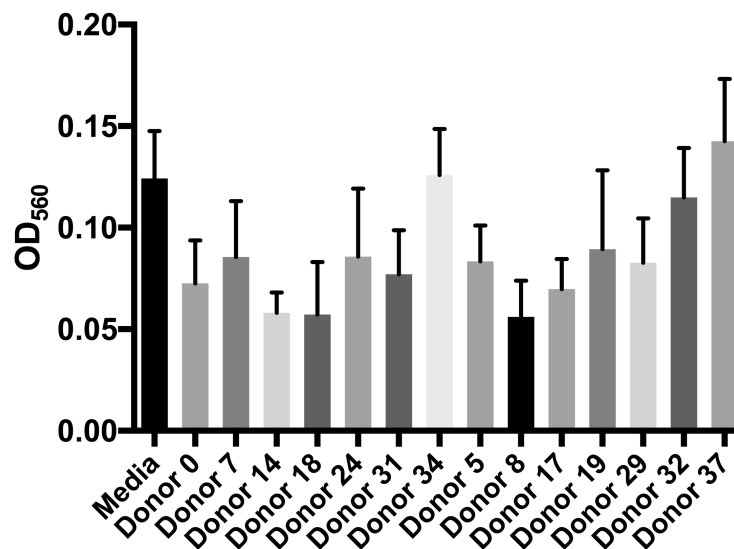


Figure A1.22. Biofilm for *S. agalactiae* strain GB590 after 24 H of growth in THB media alone or in the presence of ca. 5 mg/mL HMOs from various donors. Data expressed as mean biofilm measurements (OD_{560}) \pm SEM of 3 separate experiments, each with 3 technical replicates. No results were found to be significant by one-way ANOVA, $F = 1.197$ with *posthoc* Dunnett's multiple comparison test comparing each HMO sample against the control sample without HMOs.

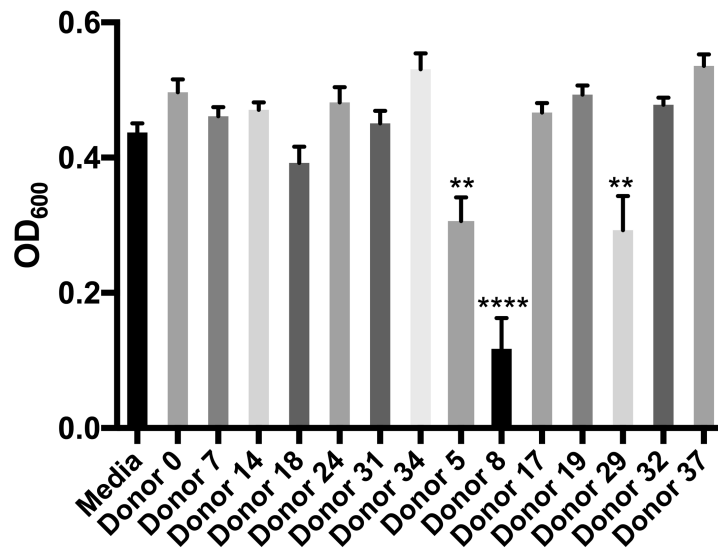


Figure A1.23. Biomass for *S. agalactiae* strain GB590 after 24 H of growth in THB media alone or in the presence of ca. 5 mg/mL HMOs from various donors. Data expressed as mean biomass measurements (OD₆₀₀) ± SEM of 3 separate experiments, each with 3 technical replicates. **** represents p<0.0001 by one-way ANOVA, F=19.55 with *posthoc* Dunnett's multiple comparison test comparing each HMO sample against the control sample without HMOs.

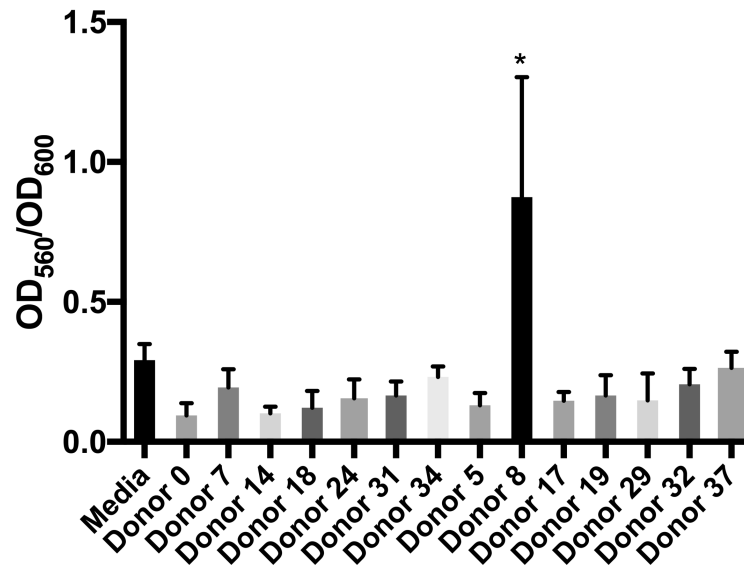


Figure A1.24. Biofilm to biomass ratio of *S. agalactiae* strain GB590 after 24 H of growth in THB media alone or in the presence of ca. 5 mg/mL HMOs from various donors. Data expressed as mean biofilm/biomass ratio measurements (OD₅₆₀/OD₆₀₀) ± SEM of 3 separate experiments, each with 3 technical replicates. ** represents p=0.0064 by one-way ANOVA, F=2.354 with *posthoc* Dunnett's multiple comparison test comparing each HMO sample against the control sample without HMOs.

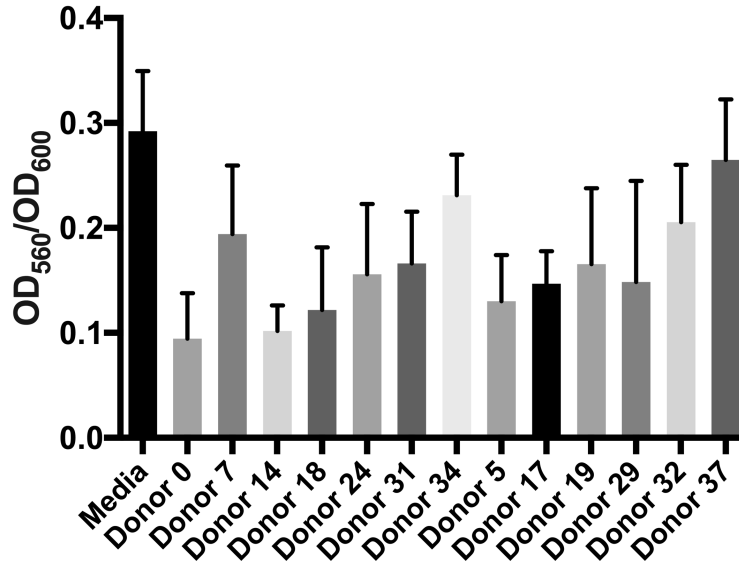


Figure A1.25. Biofilm to biomass ratio for *S. agalactiae* strain GB590 after 24 H of growth in THB media alone or in the presence of ca. 5 mg/mL HMOs from various donors excluding Donor 8. Data expressed as mean biofilm/biomass ratio measurements (OD_{560}/OD_{600}) \pm SEM of 3 separate experiments, each with 3 technical replicates. No results were found to be significant by one-way ANOVA, $F=1.061$ with *posthoc* Dunnett's multiple comparison test comparing each HMO sample against the control sample without HMOs. Results from Donor 8 were determined to be outliers using ROUT ($Q=1$) and Grubbs ($\alpha=0.05$) outlier tests.

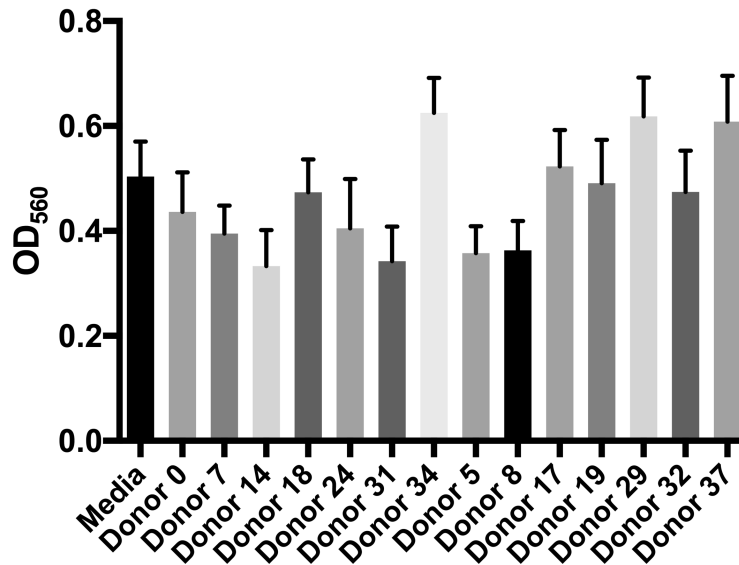


Figure A1.26. Biofilm for *S. agalactiae* strain GB590 after 24 H of growth in THB + 1% glucose media alone or in the presence of ca. 5 mg/mL HMOs from various donors. Data expressed as mean biofilm measurements (OD_{560}) \pm SEM of 3 separate experiments, each with 3 technical replicates. No results were found to be significant by one-way ANOVA, $F=1.961$ with *posthoc* Dunnett's multiple comparison test comparing each HMO sample against the control sample without HMOs.

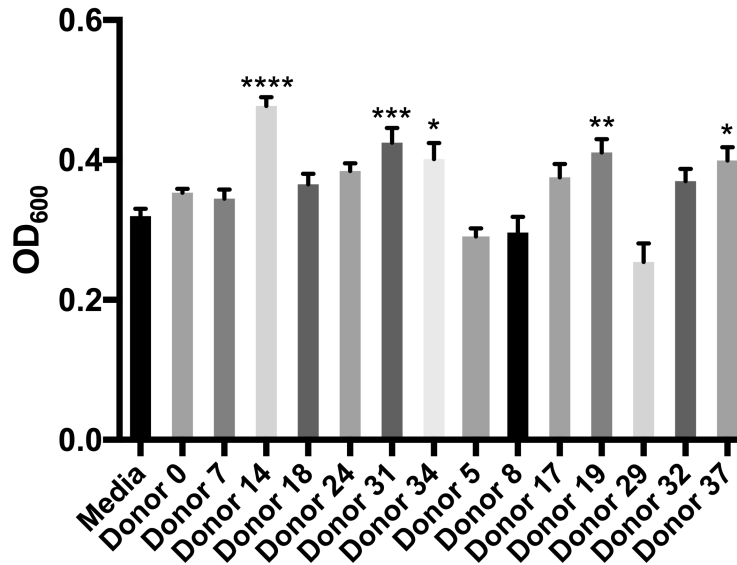


Figure A1.27. Biomass for *S. agalactiae* strain GB590 after 24 H of growth in THB + 1% glucose media alone or in the presence of ca. 5 mg/mL HMOs from various donors. Data expressed as mean biomass measurements (OD₆₀₀) ± SEM of 3 separate experiments, each with 3 technical replicates. **** represents p<0.0001 by one-way ANOVA, F=10.93 with *posthoc* Dunnett's multiple comparison test comparing each HMO sample against the control sample without HMOs.

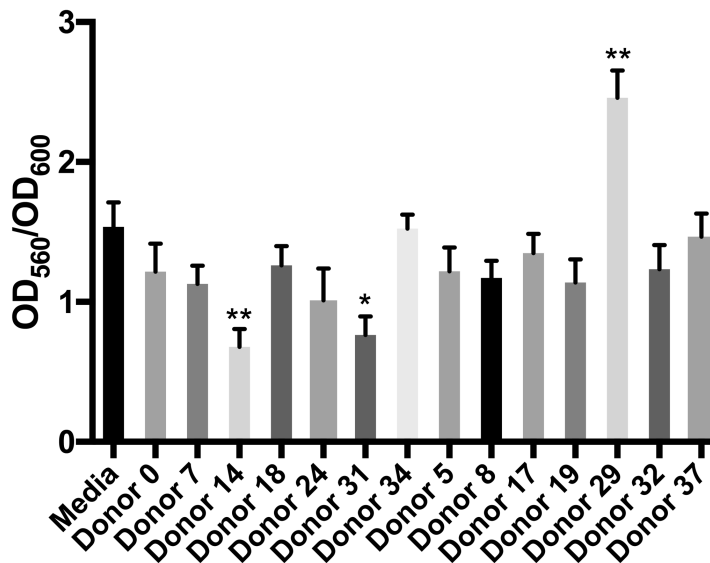


Figure A1.28. Biofilm to biomass ratio of *S. agalactiae* strain GB590 after 24 H of growth in THB + 1% glucose media alone or in the presence of ca. 5 mg/mL HMOs from various donors. Data expressed as mean biofilm/biomass ratio measurements (OD₅₆₀/OD₆₀₀) ± SEM of 3 separate experiments, each with 3 technical replicates. **** represents p<0.0001 by one-way ANOVA, F=6.423 with *posthoc* Dunnett's multiple comparison test comparing each HMO sample against the control sample without HMOs.

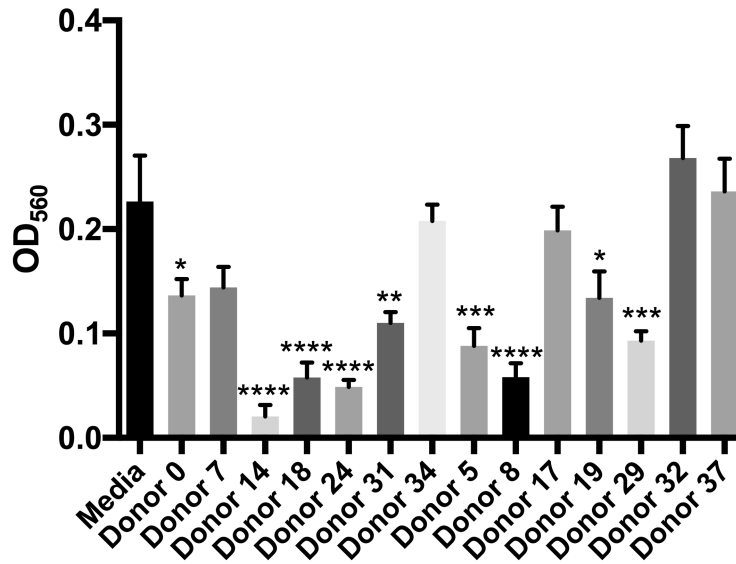


Figure A1.29. Biofilm for *S. agalactiae* strain GB2 after 24 H of growth in THB media alone or in the presence of ca. 5 mg/mL HMOs from various donors. Data expressed as mean biofilm measurements (OD₅₆₀) ± SEM of 3 separate experiments, each with 3 technical replicates. **** represents $p < 0.0001$ by one-way ANOVA, $F = 12.85$ with *posthoc* Dunnett's multiple comparison test comparing each HMO sample against the control sample without HMOs.

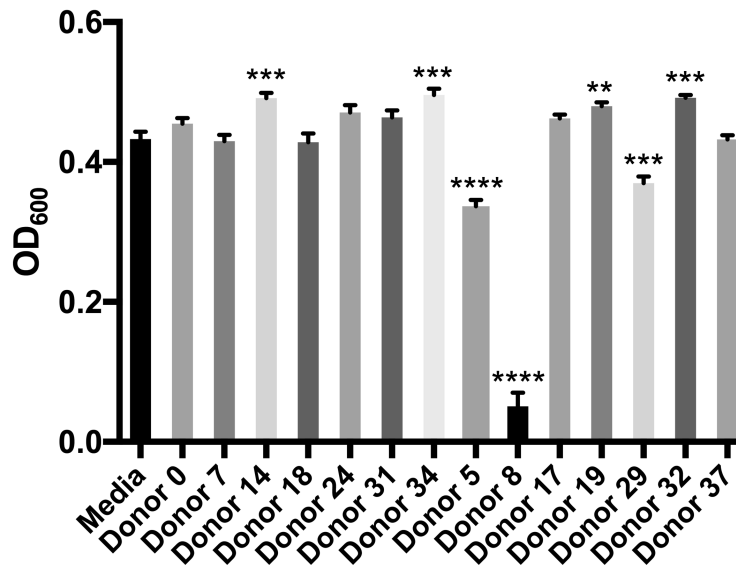


Figure A1.30. Biomass for *S. agalactiae* strain GB2 after 24 H of growth in THB media alone or in the presence of ca. 5 mg/mL HMOs from various donors. Data expressed as mean biomass measurements (OD₆₀₀) ± SEM of 3 separate experiments, each with 3 technical replicates. **** represents $p < 0.001$ by one-way ANOVA, $F = 132.3$ with *posthoc* Dunnett's multiple comparison test comparing each HMO sample against the control sample without HMOs.

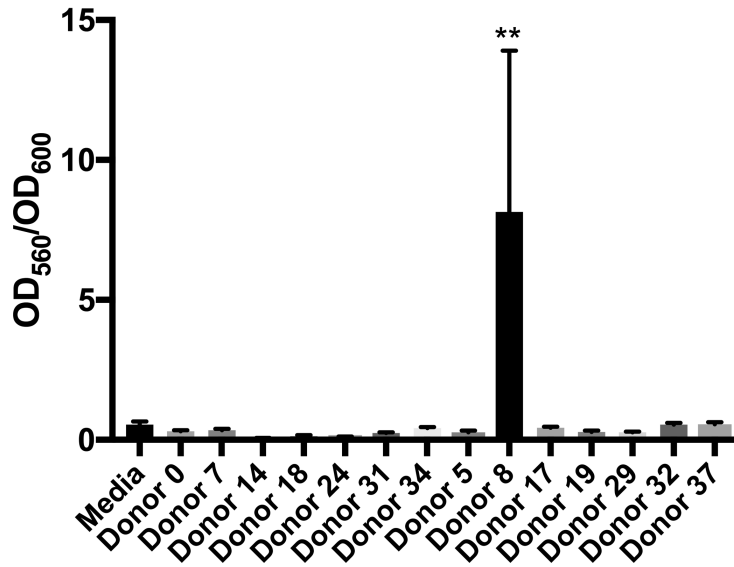


Figure A1.31. Biofilm to biomass ratio of *S. agalactiae* strain GB2 after 24 H of growth in THB media alone or in the presence of ca. 5 mg/mL HMOs from various donors. Data expressed as mean biofilm/biomass ratio measurements (OD₅₆₀/OD₆₀₀) ± SEM of 3 separate experiments, each with 3 technical replicates. * represents p=0.0382 by one-way ANOVA, F=1.855 with *posthoc* Dunnett's multiple comparison test comparing each HMO sample against the control sample without HMOs.

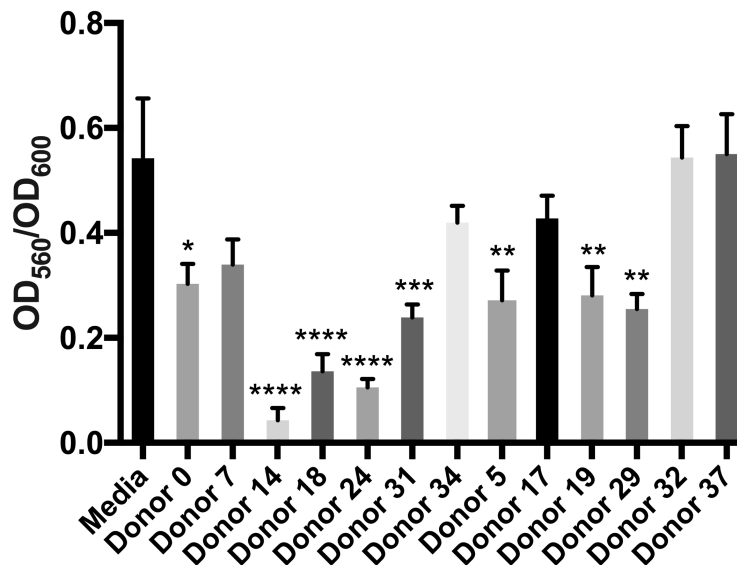


Figure A1.32. Biofilm to biomass ratio for *S. agalactiae* strain CNCTC 10/84 after 24 H of growth in THB media alone or in the presence of ca. 5 mg/mL HMOs from various donors excluding Donor 8. Data expressed as mean biofilm/biomass ratio measurements (OD₅₆₀/OD₆₀₀) ± SEM of 3 separate experiments, each with 3 technical replicates. **** represents p<0.0001 by one-way ANOVA, F=9.692 with *posthoc* Dunnett's multiple comparison test comparing each HMO sample against the control sample without HMOs. Results from Donor 8 were determined to be outliers using ROUT (Q=1) and Grubbs (alpha=0.05) outlier tests.

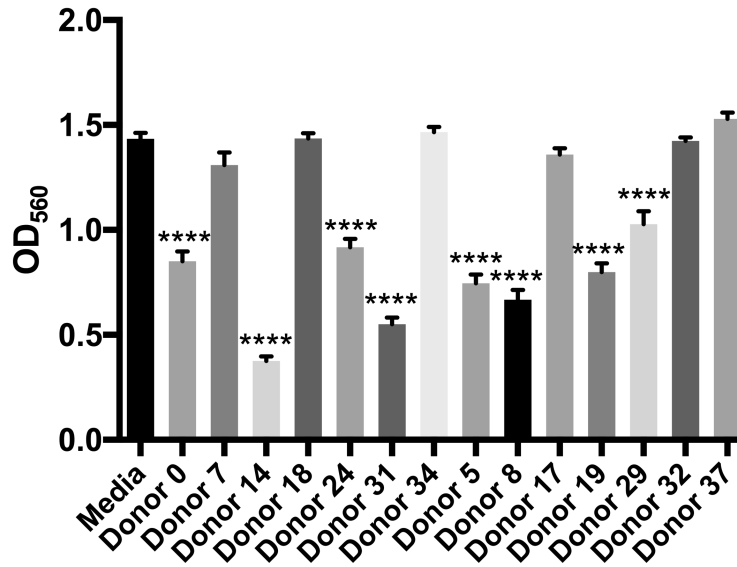


Figure A1.33. Biofilm for *S. agalactiae* strain GB2 after 24 H of growth in THB + 1% glucose media alone or in the presence of ca. 5 mg/mL HMOs from various donors. Data expressed as mean biofilm measurements (OD₅₆₀) ± SEM of 3 separate experiments, each with 3 technical replicates. **** represents p<0.0001 by one-way ANOVA, F=99.11 with *posthoc* Dunnett's multiple comparison test comparing each HMO sample against the control sample without HMOs.

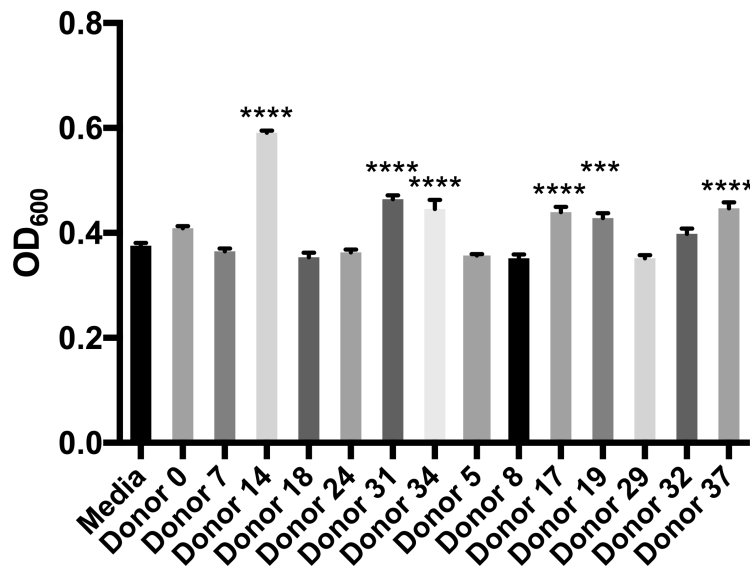


Figure A1.34. Biomass for *S. agalactiae* strain GB2 after 24 H of growth in THB + 1% glucose media alone or in the presence of ca. 5 mg/mL HMOs from various donors. Data expressed as mean biomass measurements (OD₆₀₀) ± SEM of 3 separate experiments, each with 3 technical replicates. **** represents p<0.0001 by one-way ANOVA, F=58.52 with *posthoc* Dunnett's multiple comparison test comparing each HMO sample against the control sample without HMOs.

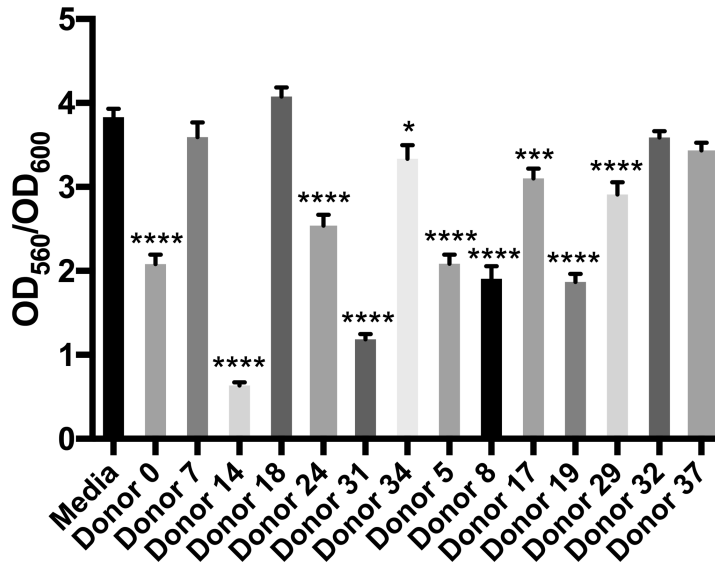


Figure A1.35. Biofilm to biomass ratio of *S. agalactiae* strain GB2 after 24 H of growth in THB + 1% glucose media alone or in the presence of ca. 5 mg/mL HMOs from various donors. Data expressed as mean biofilm/biomass ratio measurements (OD₅₆₀/OD₆₀₀) ± SEM of 3 separate experiments, each with 3 technical replicates. **** represents p<0.0001 by one-way ANOVA, F=8.55 with *posthoc* Dunnett's multiple comparison test comparing each HMO sample against the control sample without HMOs.

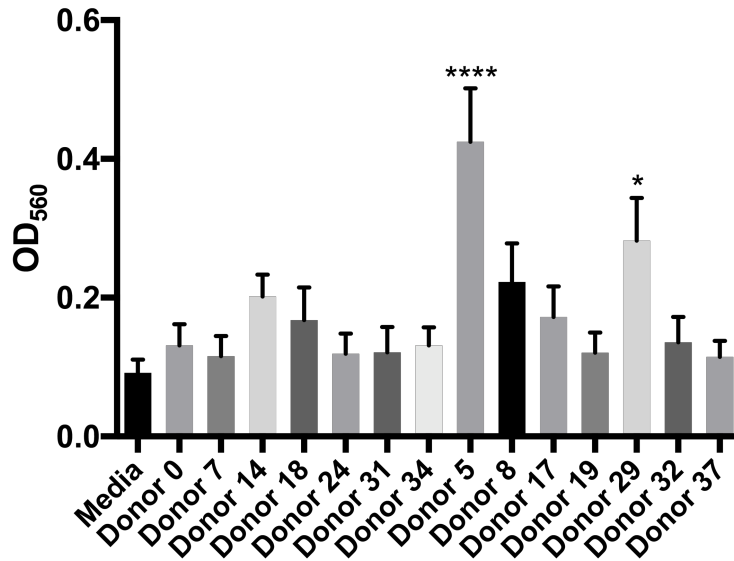


Figure A1.36. Biofilm formation for *S. aureus* USA300 after 24 H of growth in THB media alone or in the presence of ca. 5 mg/mL HMOs from various donors. Data expressed as mean biofilm measurements (OD₅₆₀) ± SEM of 3 separate experiments, each with 3 technical replicates. **** represents p<0.0001 by one-way ANOVA, F=4.364 with *posthoc* Dunnett's multiple comparison test comparing each HMO sample against the control sample without HMOs.

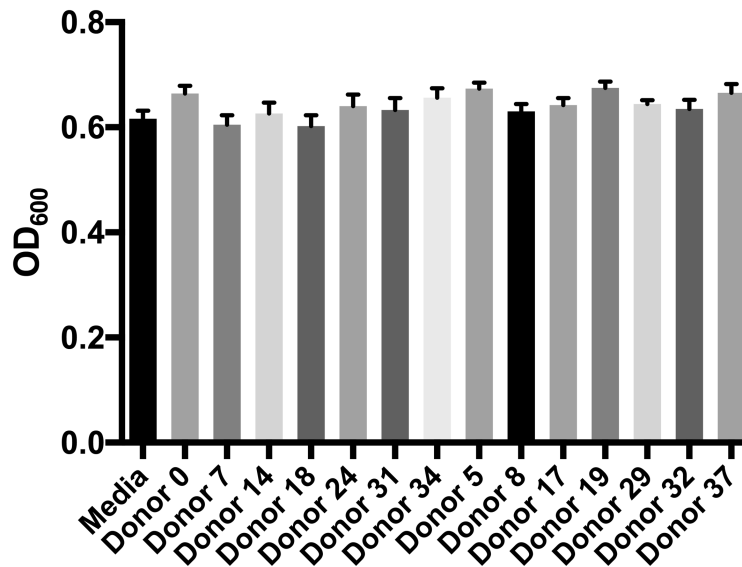


Figure A1.37. Biomass for *S. aureus* strain USA300 after 24 H of growth in THB media alone or in the presence of ca. 5 mg/mL HMOs from various donors. Data expressed as mean biomass measurements (OD₆₀₀) ± SEM of 3 separate experiments, each with 3 technical replicates. *** represents p=0.0001 by one-way ANOVA, F=1.884 with *posthoc* Dunnett's multiple comparison test comparing each HMO sample against the control sample without HMOs.

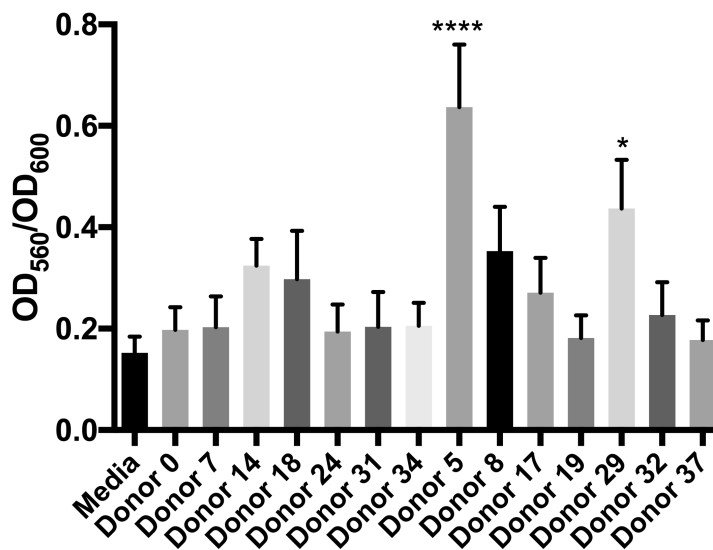


Figure A1.38. Biofilm to biomass ratio of *S. aureus* strain USA300 after 24 H of growth in THB media alone or in the presence of ca. 5 mg/mL HMOs from various donors. Data expressed as mean biofilm/biomass ratio measurements (OD₅₆₀/OD₆₀₀) ± SEM of 3 separate experiments, each with 3 technical replicates. *** represents p=0.0001 by one-way ANOVA, F=3.384 with *posthoc* Dunnett's multiple comparison test comparing each HMO sample against the control sample without HMOs.

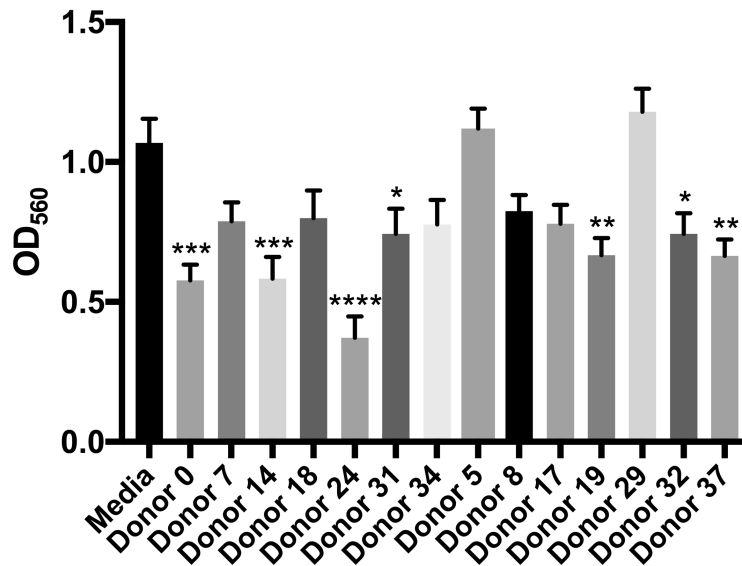


Figure A1.39. Biofilm formation for *S. aureus* strain USA300 after 24 H of growth in THB + 1% glucose media alone or in the presence of ca. 5 mg/mL HMOs from various donors. Data expressed as mean biofilm measurements (OD₅₆₀) ± SEM of 3 separate experiments, each with 3 technical replicates. **** represents p<0.0001 by one-way ANOVA, F=8.034 with *posthoc* Dunnett's multiple comparison test comparing each HMO sample against the control sample without HMOs.

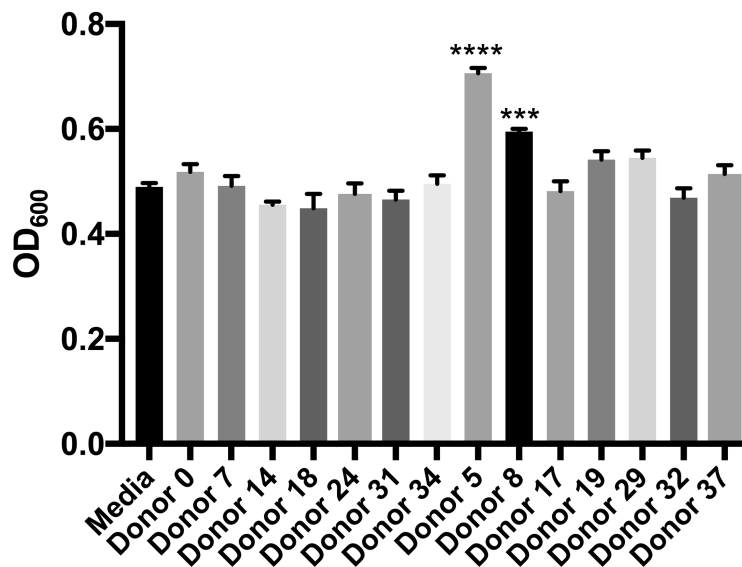


Figure A1.40. Biomass for *S. aureus* strain USA300 after 24 H of growth in THB + 1% glucose media alone or in the presence of ca. 5 mg/mL HMOs from various donors. Data expressed as mean biomass measurements (OD₆₀₀) ± SEM of 3 separate experiments, each with 3 technical replicates. **** represents p<0.0001 by one-way ANOVA, F=17.12 with *posthoc* Dunnett's multiple comparison test comparing each HMO sample against the control sample without HMOs.

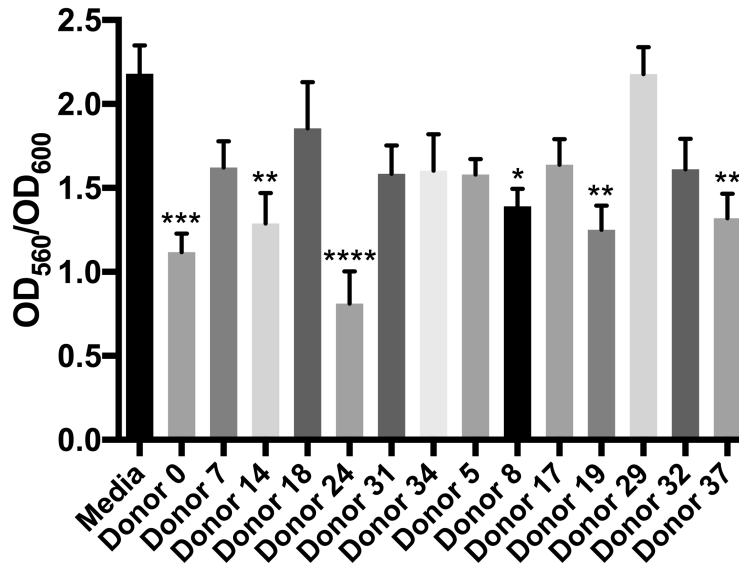


Figure A1.41. Biofilm to biomass ratio of *S. aureus* strain USA300 after 24 H of growth in THB + 1% glucose media alone or in the presence of ca. 5 mg/mL HMOs from various donors. Data expressed as mean biofilm/biomass ratio measurements (OD₅₆₀/OD₆₀₀) ± SEM of 3 separate experiments, each with 3 technical replicates. **** represents p<0.0001 by one-way ANOVA, F=4.694 with *posthoc* Dunnett's multiple comparison test comparing each HMO sample against the control sample without HMOs.

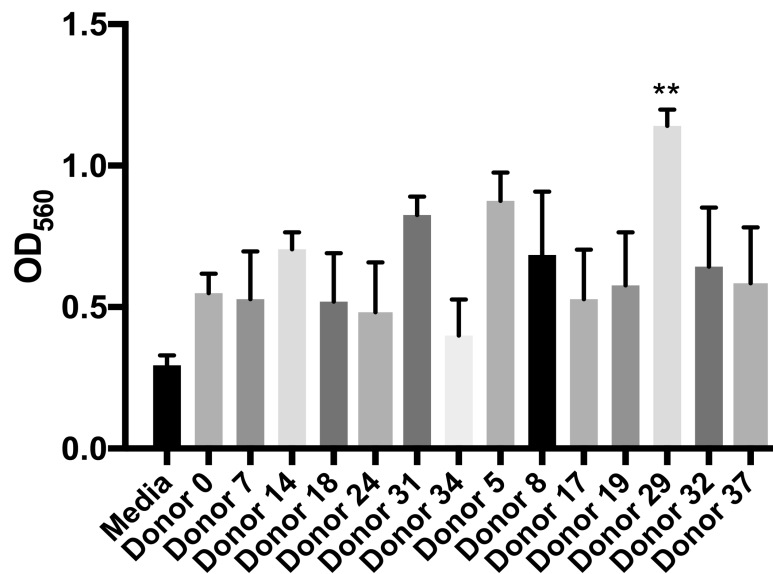


Figure A1.42. Biofilm formation for *A. baumannii* strain ATCC 19606 after 24 H of growth in THB media alone or in the presence of ca. 5 mg/mL HMOs from various donors. Data expressed as mean biofilm measurements (OD₅₆₀) ± SEM of 2 separate experiments, each with 3 technical replicates. * represents p=0.0347 by one-way ANOVA, F=1.943 with *posthoc* Dunnett's multiple comparison test comparing each HMO sample against the control sample without HMOs.

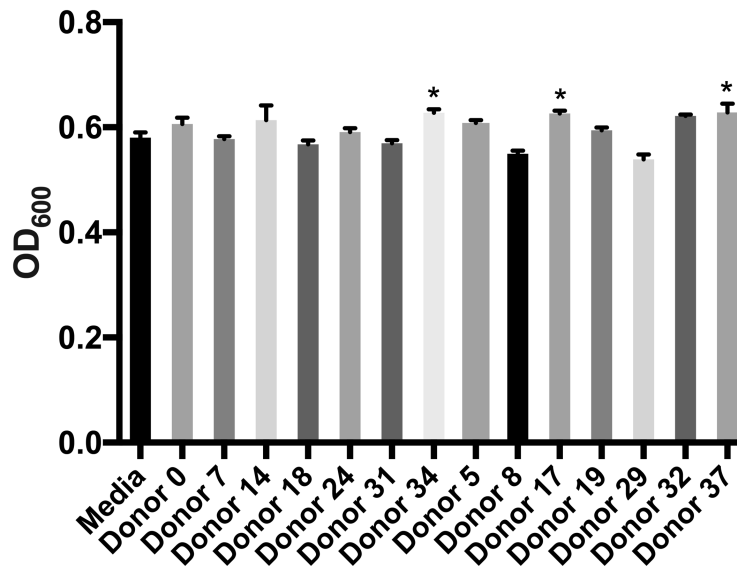


Figure A1.43. Biomass for *A. baumannii* strain ATCC 19606 after 24 H of growth in THB media alone or in the presence of ca. 5 mg/mL HMOs from various donors. Data expressed as mean biomass measurements (OD₆₀₀) ± SEM of 3 separate experiments, each with 3 technical replicates. **** represents p<0.0001 by one-way ANOVA, F=7.17 with *posthoc* Dunnett's multiple comparison test comparing each HMO sample against the control sample without HMOs.

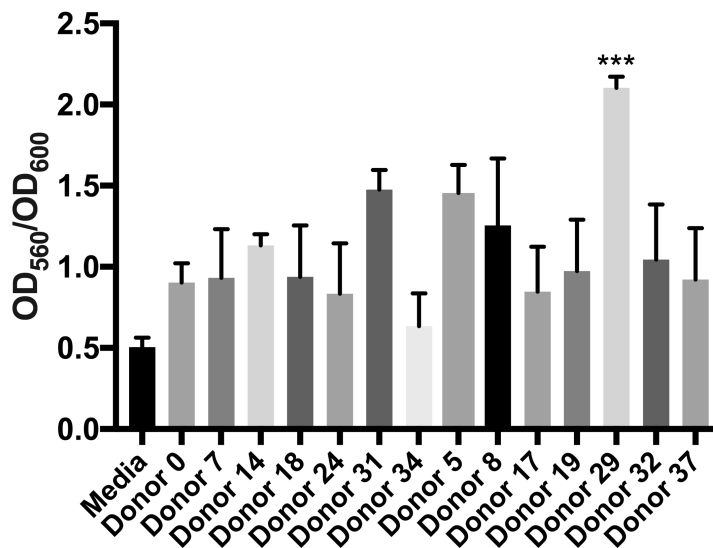


Figure A1.44. Biofilm to biomass ratio of *A. baumannii* strain ATCC 19606 after 24 H of growth in media alone or in the presence of ca. 5 mg/mL HMOs from various donors. Data expressed as mean biofilm/biomass ratio measurements (OD₅₆₀/OD₆₀₀) ± SEM of 2 separate experiments, each with 3 technical replicates. ** represents p=0.0088 by one-way ANOVA, F=2.369 with *posthoc* Dunnett's multiple comparison test comparing each HMO sample against the control sample without HMOs.

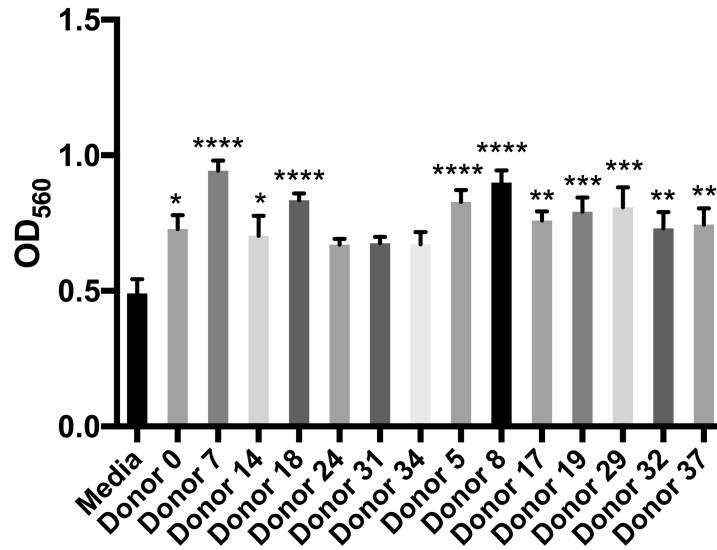


Figure A1.45. Biofilm formation for *A. baumannii* strain ATCC 19606 after 24 H of growth in THB + 1% glucose media alone or in the presence of ca. 5 mg/mL HMOs from various donors. Data expressed as mean biofilm measurements (OD₅₆₀) ± SEM of 2 separate experiments, each with 3 technical replicates. **** represents p<0.0001 by one-way ANOVA, F=4.853 with *posthoc* Dunnett's multiple comparison test comparing each HMO sample against the control sample without HMOs.

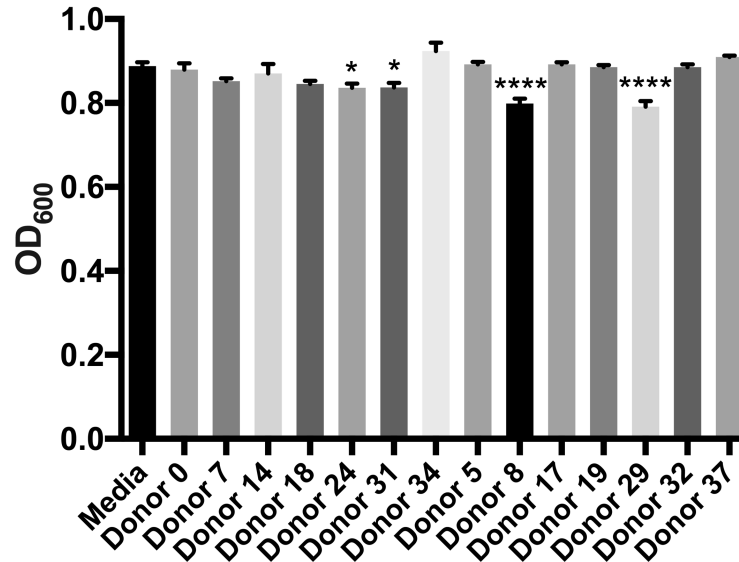


Figure A1.46. Biomass for *A. baumannii* strain ATCC 19606 after 24 H of growth in THB + 1% glucose media alone or in the presence of ca. 5 mg/mL HMOs from various donors. Data expressed as mean biomass measurements (OD₆₀₀) ± SEM of 3 separate experiments, each with 3 technical replicates. **** represents p<0.0001 by one-way ANOVA, F=11.23 with *posthoc* Dunnett's multiple comparison test comparing each HMO sample against the control sample without HMOs.

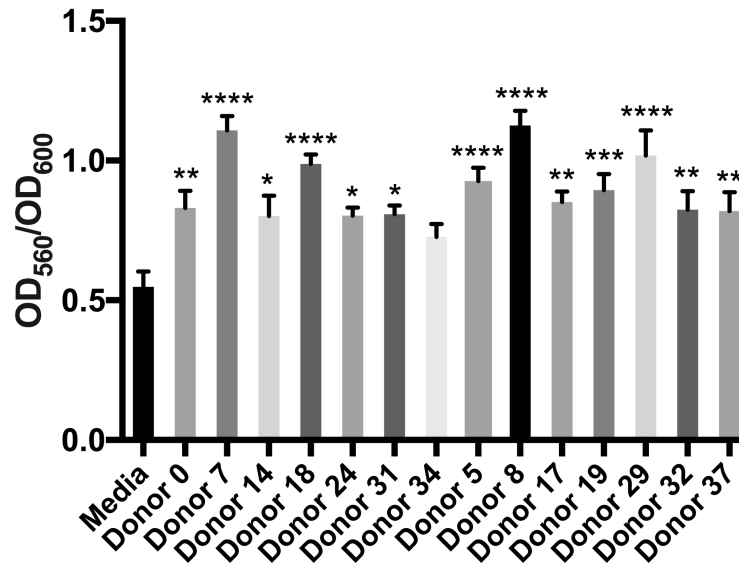


Figure A1.47. Biofilm to biomass ratio of *A. baumannii* strain ATCC 19606 after 24 H of growth in THB + 1% glucose media alone or in the presence of ca. 5 mg/mL HMOs from various donors. Data expressed as mean biofilm/biomass ratio measurements (OD₅₆₀/OD₆₀₀) ± SEM of 2 separate experiments, each with 3 technical replicates. **** represents $p < 0.0088$ by one-way ANOVA, $F = 7.029$ with *posthoc* Dunnett's multiple comparison test comparing each HMO sample against the control sample without HMOs.

Table A1.1. Antibiotic sensitization data for HMOs against *S. aureus* in THB^{a,b}

Antibiotics	MIC without HMO	MIC with HMO	Fold Reduction
Cefazolin	8	8	0
Vancomycin	8	8	0
Clindamycin	0.125	0.125	0
Gentamicin	1	1	0
Erythromycin	16	16	0
Linezolid	1.7	1.7	0

^aall MIC values given in µg/mL. ^bHMOs were dosed at ca. 5 mg/mL.

Table A1.2. Antibiotic sensitization data for HMOs against *A. baumannii* in THB + 1% glucose^{a,b}

Antibiotic	MIC without HMO	MIC with HMO	Fold Reduction
Amikacin	16	16	0
Tobramycin	16	8	2
Imipenem	0.25	1	0
Meropenem	0.5	0.5	0
Minocycline	0.0156	0.0312	0
Tigecycline	0.125	0.25	0
Doripenem	0.5	0.5	0

^aall MIC values given in µg/mL. ^bHMOs were dosed at ca. 5 mg/mL.^{40-46, 122}

Table A1.3. Results of LIVE/DEAD BacLight Assay for Treatment of Three Strains of GBS with Heterogenous HMO Extracts^{a, b, c}

	THB			THB + 1% glc		
	GB590	CNCTC 10/84	GB2	GB590	CNCTC 10/84	GB2
HMO Concentration (mg/mL)	Difference in LIVE/DEAD Ratio from control (%) ± SEM					
0 (control)	0.00 ± 2.23	0.00 ± 2.96	0.00 ± 2.78	0.00 ± 14.14	0.00 ± 1.56	0.00 ± 6.52
0.32	-0.72 ± 3.80	-4.23 ± 5.77	-4.57 ± 4.94	4.22 ± 10.57	-4.62 ± 2.32	-3.81 ± 4.89
0.64	-7.94 ± 1.63	-12.66 ± 3.18	-23.87 ± 1.58	-3.95 ± 9.69	-6.79 ± 1.86	-18.66 ± 3.79
1.28	-21.79 ± 3.23	-9.00 ± 5.01	-40.16 ± 1.85	-17.35 ± 8.33	-6.02 ± 2.73	-28.19 ± 3.33
2.56	-32.70 ± 2.68	-20.34 ± 3.83	-49.94 ± 1.46	-18.36 ± 9.71	-7.98 ± 2.04	-34.76 ± 3.08
5.12	-27.00 ± 2.18	-35.81 ± 3.17	-15.53 ± 3.29	-18.62 ± 8.16	-13.09 ± 10.02	-16.75 ± 4.14
10.25	-28.20 ± 2.57	-20.61 ± 2.18	-20.37 ± 2.46	-21.22 ± 7.94	-23.13 ± 0.96	-23.46 ± 3.60
20.5	-28.59 ± 1.35	-18.25 ± 2.48	-23.46 ± 3.60	-27.99 ± 7.58	-20.37 ± 2.46	-26.40 ± 3.43

^ameasurements taken at 24 h of growth. ^bHMOs dosed at ca. 5 mg/mL. ^csignificantly decreased LIVE/DEAD ratios are bolded and highlighted in blue ($P < 0.05$ by Student's t test, $N = 3$ replicates).

CHAPTER 4

Synthesis of Lacto-*N*-Tetraose

*4.1 Rationale for the Synthesis of Lacto-*N*-Tetraose*

Having described the antibacterial activities of heterogenous HMO extracts against various bacterial pathogens, our next aim was to more narrowly-define these activities, i.e. to uncover single compounds with biological activity. However, as there have been over 200 distinct HMOs recognized, identifying active single compounds is no trivial task.¹ First, it is essential to narrow down the list of possible active compounds as it is impractical to randomly select HMOs to evaluate. This research strategy is made even more impractical when one considers the nature of the compounds to be tested. As described in Chapter 2, HMOs vary in size and complexity from simple fucosylated lactose trisaccharides to HMOs that incorporate over 30 monosaccharide residues. While some of the simpler, smaller HMOs are commercially available, the vast majority are either not commercially available or are too costly to purchase in sufficient amounts.¹

In addition to the infeasibility of purchasing most HMOs in the quantities needed for thorough biological testing, it is also infeasible to isolate single compounds from human milk in purities and quantities sufficient for testing. Thus, in order to evaluate individual compounds, it becomes necessary for researchers to synthesize, chemically or enzymatically, the desired HMOs.^{1, 2} While synthesis is a viable route, it remains that carbohydrate synthesis is known for being time-consuming and challenging. Due to the need to dedicate significant time and resources for the synthesis of each compound, it

becomes even more imperative that researchers be judicious with their choice of synthetic target(s).

When selecting an HMO target, we considered the following criteria: concentrations in individual samples, prevalence across different samples, synthetic feasibility, and synthetic utility. Ultimately, we wanted to target a ubiquitous HMO that was one, at the time largely inaccessible to researchers, and, two, whose synthesis would yield not only a potentially active compound but also a compound whose synthesis could be easily altered to provide access to additional molecules. Given these criteria, lacto-*N*-tetraose (LNT, **2.4**) (**Figure 4.1**) stood out as an attractive target.

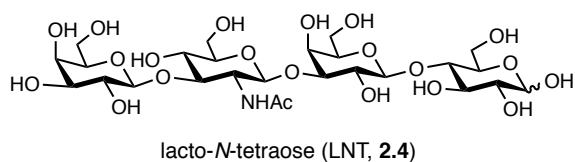


Figure 4.1. Structure of lacto-*N*-tetraose (LNT, **2.4**).

First and foremost, LNT is present in high concentrations in human milk and is common across donor samples regardless of donor blood group.³⁻⁶ Second, although several groups had previously completed chemical or enzymatic syntheses of LNT or LNT-derivatives,⁷⁻¹³ it remains that LNT is not currently available at large scale through chemical or enzymatic synthesis. Third, as described in Chapter 2, LNT serves as a core tetrasaccharide in type I chains which predominate over type II chains in human milk.⁵ Indeed, LNT is significantly more common in human milk than its type II chain isomer lacto-*N*-neotetraose (LNnT, **2.5**).^{5, 14} Thus, we envisioned that developing a scalable route to LNT would allow access both to large quantities of an important and ubiquitous HMO and to a number of additional HMOs with minimal effort. Access to larger quantities of

HMOs would then allow for studies aimed at investigating the biological importance of single-entity compounds.

4.2 Methods for Oligosaccharide Synthesis

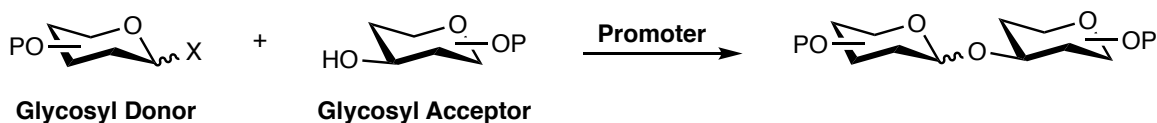
It is well-known that oligosaccharide synthesis is a challenging endeavor and one that is significantly more complicated than the synthesis of other biopolymers like nucleic acids and proteins. Simply put, the increased difficulty results from a greater number of possible combinations of polymeric building blocks, i.e. monosaccharides. First, there exist a vast array of monosaccharides which can vary in ring size, substitution pattern, modifications such as sulfonation and phosphorylation, and so on. Second, in contrast to amide and phosphodiester linkages, linkages between monosaccharide residues (a glycosidic bond) generates a new stereocenter (α or β linkages). Third, the location of the glycosidic bond can vary. For example, LNT and LNnT feature the same monosaccharide building blocks that are connected similarly through β -oriented glycosidic bonds, yet these structures differ in the location of glycosidic bonds: LNT features a β 1-3 bond between Gal and GlcNAc while LNnT features a β 1-4 bond. Thus, synthetic efforts must not only yield the correct building blocks, they must also link these building blocks together in a stereoselective and regioselective fashion.

Due to the complexity and diversity inherent to oligosaccharide synthesis, a variety of methods have been developed for the synthesis of this class of compound. These methods can be broadly classified as chemical or enzymatic, or a combination of the two. In the next section, the methods for and attributes of chemical carbohydrate synthesis will

be discussed. The corresponding information for enzymatic carbohydrate synthesis is reviewed elsewhere.¹⁵⁻¹⁹

4.3 Chemical Approaches for Oligosaccharide Synthesis

4.3.1 Glycoside Bond Formation: The Glycosylation Reaction²⁰⁻²²



Scheme 4.1. The chemical glycosylation reaction. A latent leaving group, X, at the anomeric center of a glycosyl donor is activated with a promoter in the presence of a protected glycosyl acceptor bearing a free alcohol. The alcohol of the acceptor effectively replaces the latent leaving group of the donor and “accepts” the “donor” monosaccharide to form a glycosidic bond. The newly formed bond can have an α or β orientation. Abbreviations: P, protecting group; X, latent leaving group.

At the heart of oligosaccharide synthesis is the glycosylation reaction. This reaction links building blocks and must be done with both regio- and stereoselectivity. Generally speaking, this reaction is characterized by the union of a suitably protected acceptor bearing a free alcohol at the position of the desired glycosidic bond and a suitably protected donor bearing a latent leaving group at the anomeric position (**Scheme 4.1**).

When a new glycosidic bond is formed, it can have either an α or β orientation. Carbohydrate α/β configuration is determined by the orientation of the non-hydrogen substituent at C1 in relation to the non-hydrogen substituent at C6. An α glycoside is one in which these substituents are trans to one another. In contrast, a β glycoside is one in which these substituents are cis to one another. In the case of a 6-deoxy sugar, such as fucose, α/β is determined by the orientation of the C1 substituent in relation to the C5 substituent. Additionally, glycosidic bonds can be termed 1,2-*cis* or 1,2-*trans* linkages; in

an 1,2-*cis* linkage, the C1 and C2 substituents are *cis* whereas in a 1,2-*trans* linkage these groups will be *trans* to one another (**Figure 4.2**).

By conventional carbohydrate carbon numbering, ring carbons of a monosaccharide are labeled clockwise in numerical order beginning with the anomeric carbon which is labeled C1; the anomeric center is the ring carbon directly adjacent to the in-ring oxygen (endocyclic) when moving around the ring in a clockwise fashion. With a disaccharide, the carbons in the ring furthest from the reducing end are still labeled clockwise in numerical order, but they are denoted with a prime, i.e. C1'. Additional rings are labeled as double prime and so on. Finally, when denoting a glycosidic bond, the designation of α/β is followed by the numbers of the ring carbons that are connected by the bond (**Figure 4.2**).

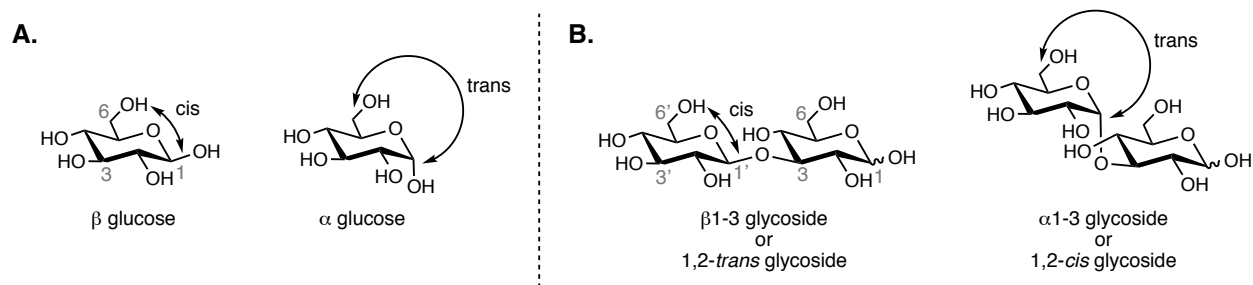
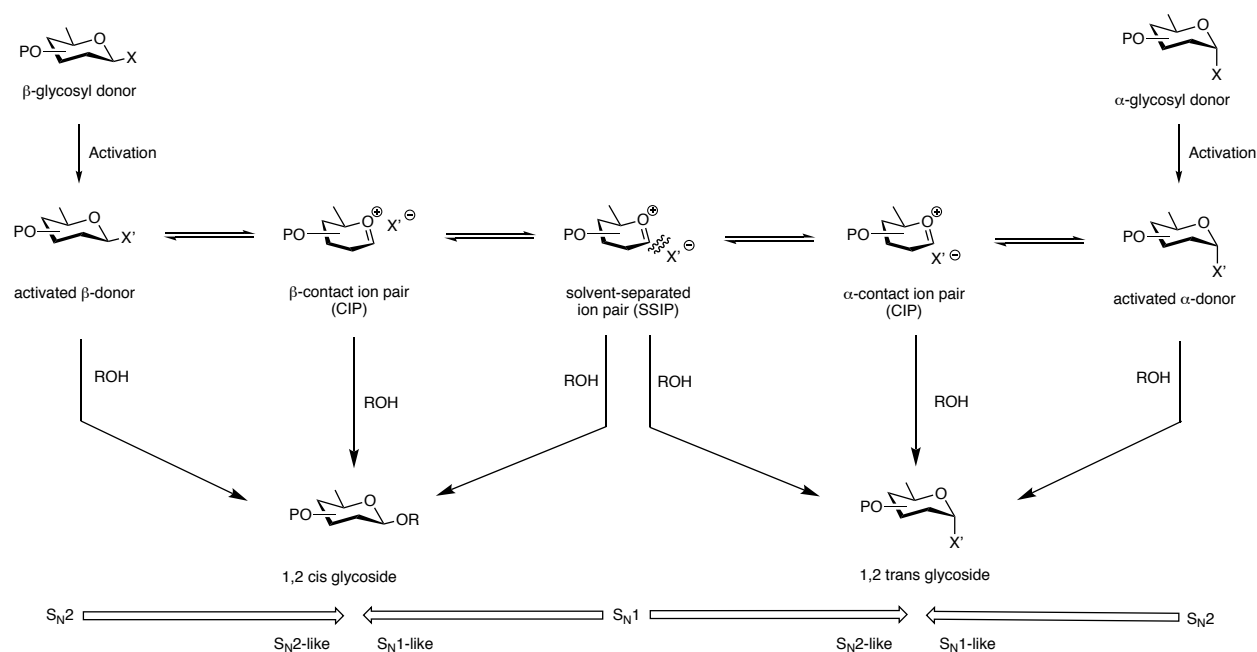


Figure 4.2. Conventional carbohydrate carbon numbering and α/β and *cis/trans* designations for monosaccharides (**A**) and larger (**B**).

While the glycosylation reaction may seem straight-forward, the mechanism of nucleophilic displacement at the sp^3 anomeric carbon can vary greatly from reaction to reaction. Indeed, the outcome of a glycosylation reaction can be affected by solvent, protecting group strategies, donor type, promoter systems, temperature, etc. Based on reaction conditions, glycosylation reaction mechanisms can span from a unimolecular, dissociative S_N1 process that proceeds through an oxocarbenium intermediate to a biomolecular associate S_N2 process that proceeds in a single step.^{22, 23} Consequently,

the glycosylation reaction mechanism is generally considered to be a continuum between purely S_N1 and purely S_N2 . Between these two ends of the mechanistic spectrum are ion-associated mechanisms where contact ion pair (CIP) mechanisms are more S_N2 -like and solvent-separated ion pair (SSIP) mechanisms are more S_N1 -like. Generally speaking, polar solvents will better stabilize a SSIP and consequently promote more S_N1 -type reactions while non-polar solvents are not as capable of stabilizing a SSIP and thus promote more S_N2 -type reactions proceeding through CIP (**Scheme 4.2**).



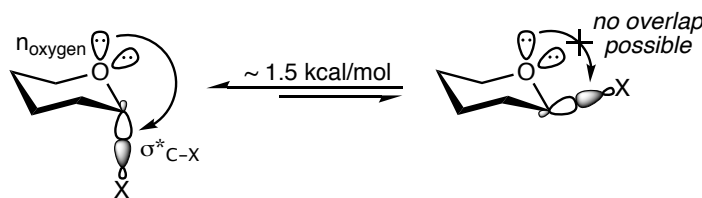
Scheme 4.2. Mechanistic continuum for a glycosylation reaction. Abbreviations: P, protecting group; X, latent leaving group; X', activated leaving group.

4.3.2 The Anomeric Effect^{20, 24}

Important to understanding any glycosylation mechanism is understanding the anomeric effect (**Scheme 4.3**). The anomeric effect, first described by Edward and later named by Lemieux and Chü, refers to the preferential axial orientation of electronegative substituents (halides, alkoxy groups, triflates, etc.) at the anomeric carbon.²⁵⁻²⁷ This

preference is attributed to stabilization that occurs through delocalization of a lone pair of electrons from the endocyclic oxygen to the periplanar antibonding σ orbital of the anomeric carbon to electronegative anomeric substituent bond (C-X bond). Indeed, this interaction is not possible in the non-periplanar C-X bond of the β -anomer. The stabilization uniquely experienced by the α -anomer is estimated to be around 1.5 kcal/mol.

While stabilization via hyperconjugation is not the only proposed explanation of the anomeric effect, it is the only one that explains the shortening of the C-X bond of the α -anomer compared to the β -anomer. Indeed, although reduction of unfavorable dipole-dipole or electron-pair-electron-pair interactions have similarly been offered as an explanation for the axial preference, these explanations do not explain the shorter bond length. As a final note, generally speaking, the stronger the electronegativity of an anomeric substituent, the stronger the axial preference. Moreover, in the case of alkoxy substituents, electronics dominate the orientation preference; the size of the alkoxy group has little effect.



Scheme 4.3. The anomeric effect. Electrons in a non-bonding orbital of the endocyclic oxygen (n_{oxygen}) can interact with the antibonding sigma orbital of an α -oriented anomeric C-X bond ($\sigma^*_{\text{C-X}}$). This interaction ($n \rightarrow \sigma^*$) imparts additional stabilization for the α anomer as this interaction is not possible with the β anomer.

4.3.3 Protecting Groups^{20, 28}

As previously mentioned, there are several factors that can influence the outcome of a glycosylation. One of the most important is the protecting group strategy used,

especially that used on the glycosyl donor. A list of commonly employed *O*- and *N*-protecting groups is provided in **Figure 4.3**. Protecting groups can influence the stereoselectivity of a glycosylation and can also tune donor reactivity. While the effects of protecting groups can be far reaching and can take many forms, two of the most well know effects are neighboring group participation (NGP) and donor arming/disarming.

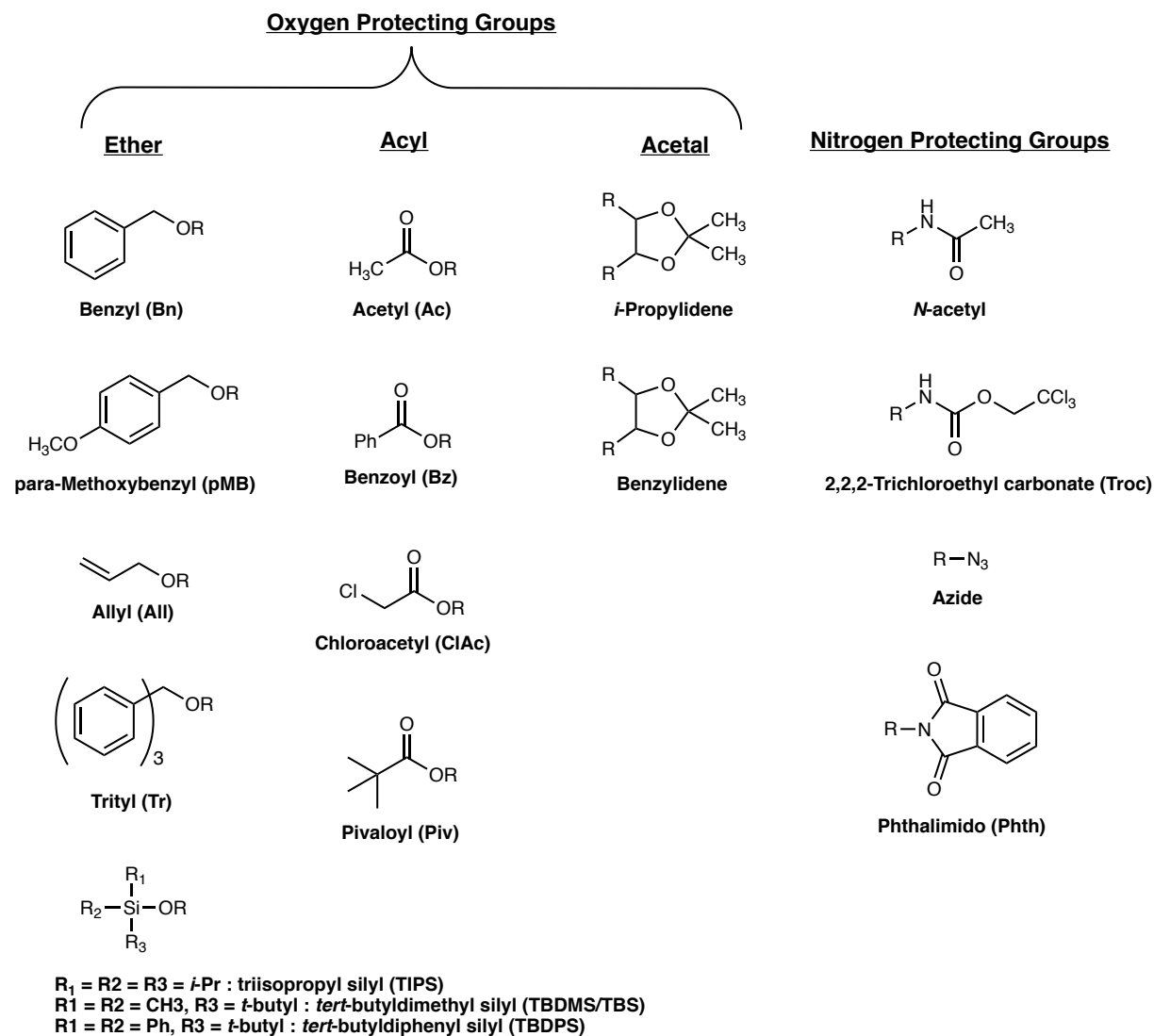
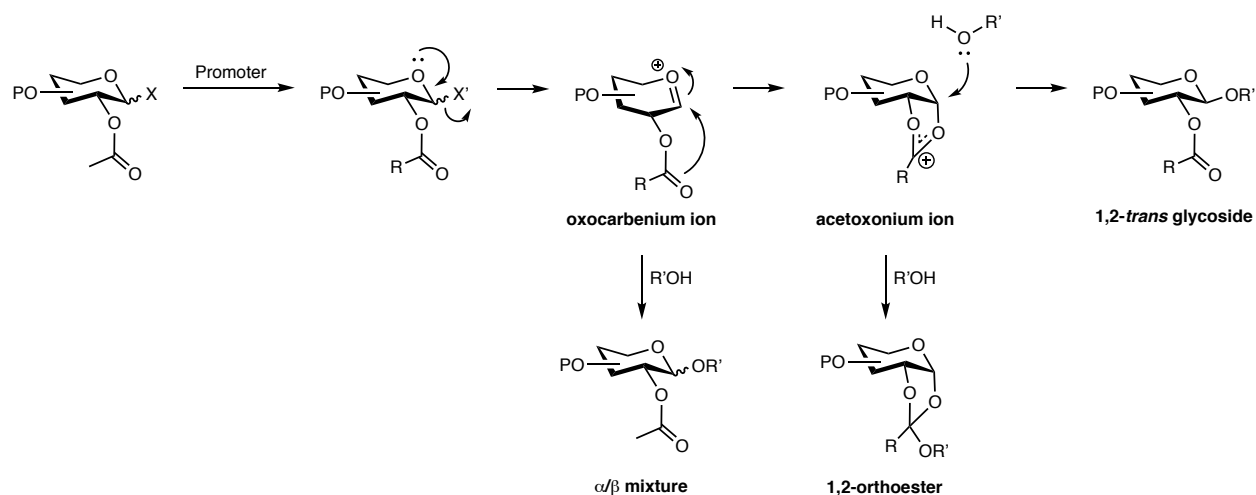


Figure 4.3. Common oxygen and nitrogen protecting groups in carbohydrate chemistry.

NGP, also termed anchimeric assistance, refers to the capability of 2-*O*- or -*N*-acyl protecting groups to generate 1,2-*trans* glycosides through their interaction with the

oxocarbenium ion intermediate. Indeed, this strategy is one of the most common and reliable methods for generating 1,2-*trans* glycosides. Briefly, a latent leaving group on a glycosyl donor is activated by a promoter to facilitate its departure. The departure of the leaving group generates an oxocarbenium ion intermediate which can interact with a C2 acyl substituent to generate a more stable acetoxonium ion (the positive charge is shared across two oxygen atoms as opposed isolated to one). Subsequent nucleophilic attack at the anomeric center will result in the 1,2-*trans* glycoside (**Scheme 4.4**). In the absence of a C2 participating group, nucleophilic attack at the anomeric center can occur from either face of the ring resulting in a mixture of α/β glycosides. Importantly, nucleophilic attack can also occur at the C2 position of the dioxolane ring of the acetoxonium ion to generate an undesired 1,2-orthoacetate (**Scheme 4.4**). While often unstable, these orthoacetates can sometimes rearrange to give the desired 1,2-*trans* product or even the 1,2-*cis* product. Generally, use of a bulky C2-acyl protecting group like a benzoyl or pivaloyl group disfavors formation of the orthoacetate.



Scheme 4.4. Neighboring group participation (NGP). C2-O-acetyl groups can participate in glycosylations by stabilizing the oxocarbenium ion intermediate that results from departure of an activated leaving group. The resulting acetoxonium ion facilitates formation of the 1,2-*trans* product.

The “armed/disarmed” effect, originally introduced by Fraser-Reid, refers to the ability of protecting groups to influence donor reactivity.^{21, 29-31} Specifically, donors protected with acyl groups are less reactive (“disarmed”) than donors protected with ether groups (“armed”) (**Figure 4.4**). While this effect was initially applied only to the protecting group at C2, the electronics of protecting groups at other positions have similarly been shown to affect donor reactivity.^{21, 32} The lessened reactivity of disarmed donors is due to the strong electron-withdrawing nature of the ester protecting groups. This serves not only to decrease the nucleophilicity of the latent leaving group but also to destabilize the oxocarbenium ion intermediate that forms in concert with the departure of this group. Contrarily, electron-donating ether groups increase nucleophilicity and stabilize the oxocarbenium ion intermediate which consequently increases reaction rate.

In addition to strongly electron-withdrawing substituents, cyclic protecting groups, such as a benzylidene acetal, can also create “disarmed” donors (**Figure 4.4**).^{33, 34} Rather than an electronic effect, these protecting groups disarm donors through torsional effects. More specifically, cyclic protecting groups constrict ring flexibility and effectively “lock” pyranoses into a chair confirmation. This imposed rigidity creates a higher energy oxocarbenium ion intermediate; the ideal C₅O₅-C₁C₂ dihedral angle (ω) of 0 °C for the oxocarbenium ion cannot be obtained with a cyclic protecting group.³³

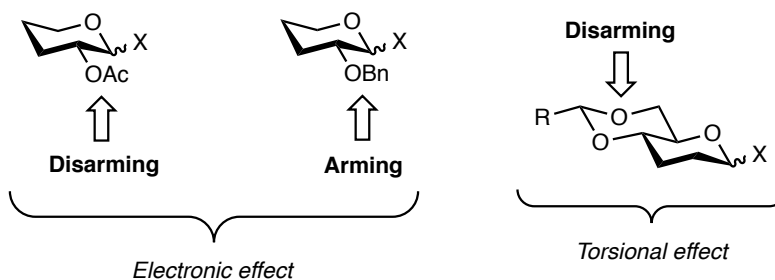
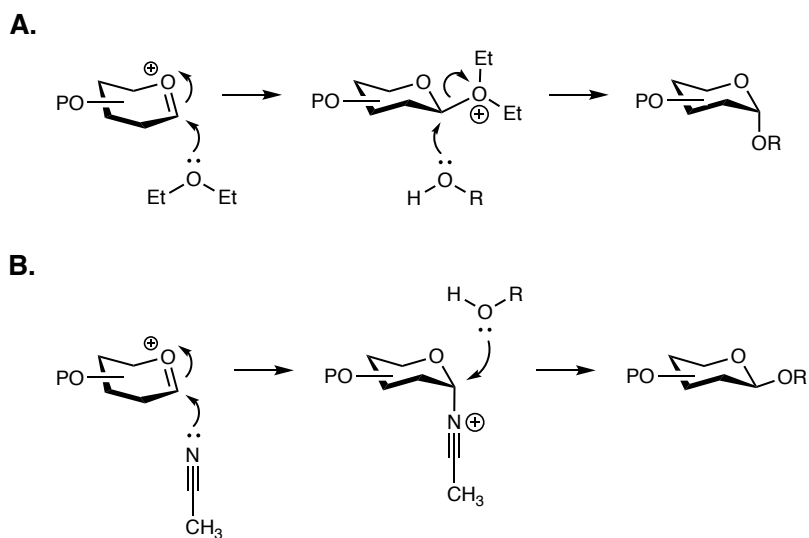


Figure 4.4. Arming and disarming effects of protecting groups.

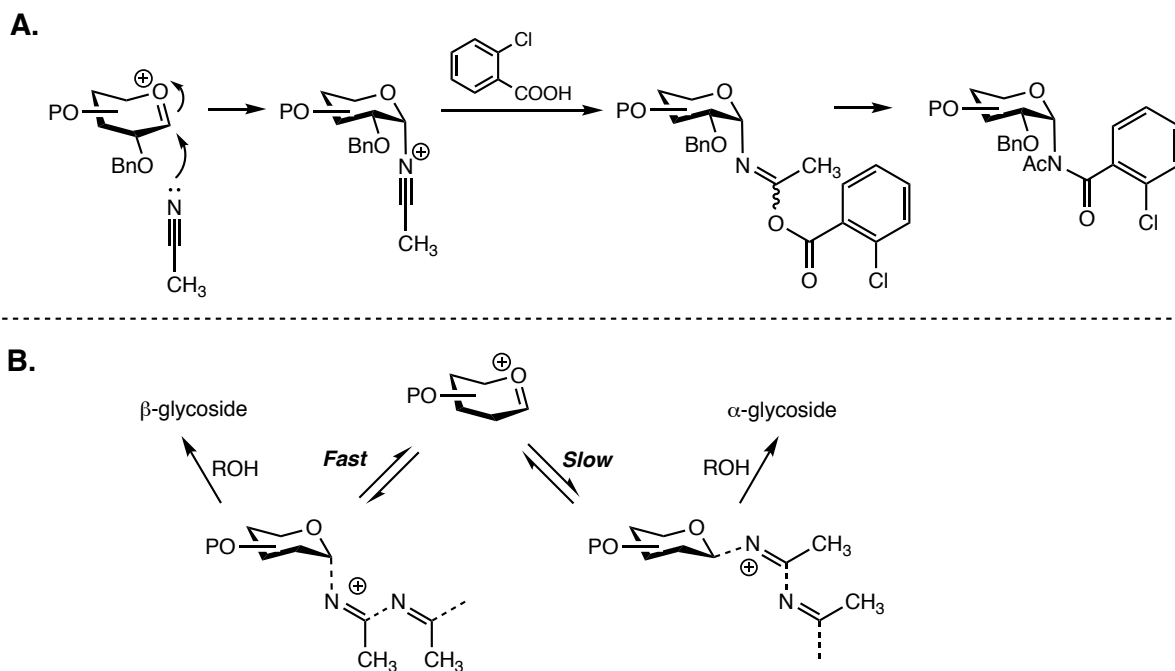
4.3.4 Solvent Effects^{20-22, 35, 36}

In addition to protecting group strategies, solvent can also have a significant effect on the outcome of a glycosylation. This effect is even greater when the glycosyl donor lacks a C2 participating group. For example, formation of 1,2-*cis* glycosides requires a non-participating C2 protecting group. Thus, solvent choice can be particularly important in the formation of this class of glycoside.³⁶ Generally speaking, solvents of low polarity are hypothesized to increase α -selectivity due to a combination of suppressing oxocarbenium ion formation and promoting *in situ* anomerization to the more reactive β -oriented leaving group (more reactive because less stabilized due to the anomeric effect).^{20, 22} The reaction then proceeds through a more S_N2-like mechanism to yield an α -glycoside. In contrast, solvents of moderate polarity are hypothesized to stabilize a positively charged oxocarbenium or acetoxonium intermediate. While useful when a glycosyl donor has a C2 participating group, in the absence of a C2 participating group, solvents of moderate stability are unlikely by themselves to yield highly stereoselective glycosylations.

Solvents can also influence stereoselectivity by forming complexes with the oxocarbenium ion intermediate.^{20, 22} For example, ethereal solvents, most commonly diethyl ether, are known to increase α selectivity (**Scheme 4.5A**). The increased α selectivity is best explained by preferential formation of a β -oriented diethyl oxonium ion followed by an S_N2-like displacement to yield the α glycoside. The β configuration of this intermediate is favored due to the reverse anomeric effect; the reverse anomeric effect refers to the preference of positively charged-electronegative substituents to adopt an equatorial, β orientation.



Scheme 4.5. Solvent participation in glycosylation reactions. **(A)** Etheral solvents, such as diethyl ether, increase α selectivity. **(B)** Acetonitrile increases β selectivity.



Scheme 4.6. Participation of acetonitrile solvent in glycosylations. **(A)** Trapping of the intermediate nitrilium ion with 2-chlorobenzoic acid yielded the corresponding α -imide which provided experimental evidence for the existence of an α -nitrilium species. **(B)** Mechanistic explanation for the preferential formation of β -glycosides when using acetonitrile as the reaction solvent.

Contrarily, acetonitrile has been shown to lead preferentially to equatorial, β -linked glycosides (**Scheme 4.5B**).^{20, 37} This result is best explained by formation of an α -nitrilium ion followed by S_N2 -like displacement to yield the β glycoside. While this result contrasts that predicted by the reverse anomeric effect, experimental evidence does support its existence. Through the combined efforts of Pougny and Sinjajä (1976) and Fraser-Reid and Ratcliffe (1990), it was shown that trapping of the intermediate nitrilium ion with 2-chlorobenzoic acid affords the corresponding α -imide, thus confirming existence of the α -nitrilium intermediate (**Scheme 4.6A**). Importantly, this outcome agreed with the explanation from Schmidt that fast α -nitrilium-nitrile-complex formation precedes formation of a more thermodynamically stable β -nitrilium-nitrile-complex (**Scheme 4.6B**).

4.3.5 Glycosyl Donors^{20, 36, 38}

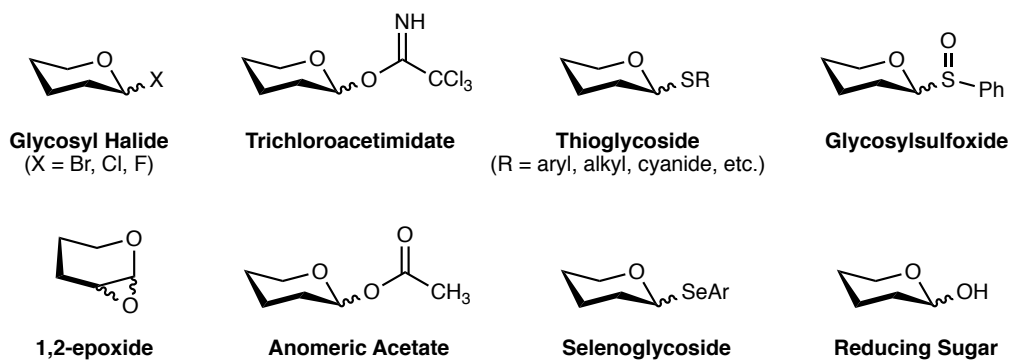
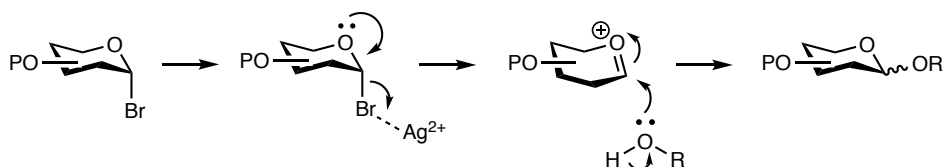


Figure 4.5. Common classes of glycosyl donor.

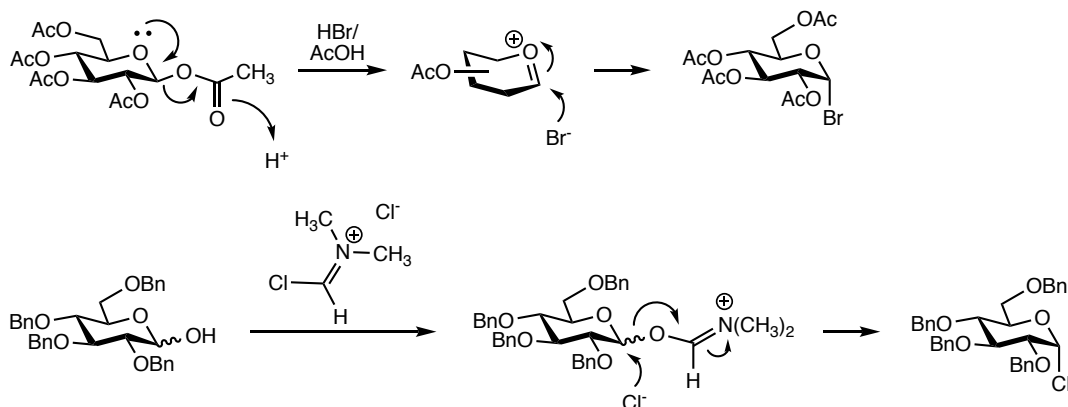
Another key factor for a glycosylation reaction is the type of donor employed. A list of commonly used donor types is provided in **Figure 4.5**. Glycosyl chlorides and bromides, introduced in 1901 by Koenigs and Knörr, served as the original glycosyl donors.^{20, 39} These donors, typically found as the α anomer due to the anomeric effect, can be

activated with heavy metal salts, mainly silver or mercury salts (**Scheme 4.7A**). Glycosyl bromides are commonly prepared via treatment of a per-*O*-acetylated glycoside with HBr in acetic acid (**Scheme 4.7B**). While glycosyl chlorides can similarly be prepared from a per-*O*-acetylated glycoside using aluminum chloride (AlCl₃) or phosphorus pentachloride (PCl₅), a milder method to generate the anomeric chloride is via treatment of a lactol with the Vilsmeier-Haack reagent (**Scheme 4.7B**).

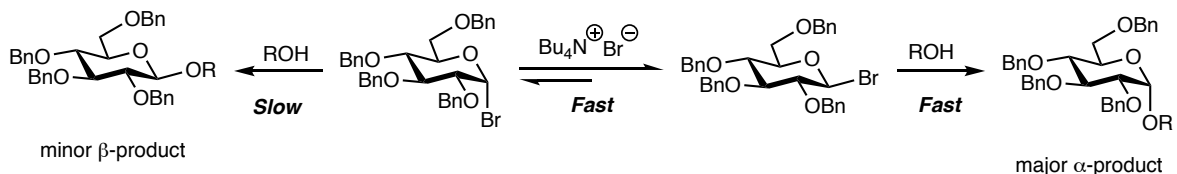
A.



B.



C.

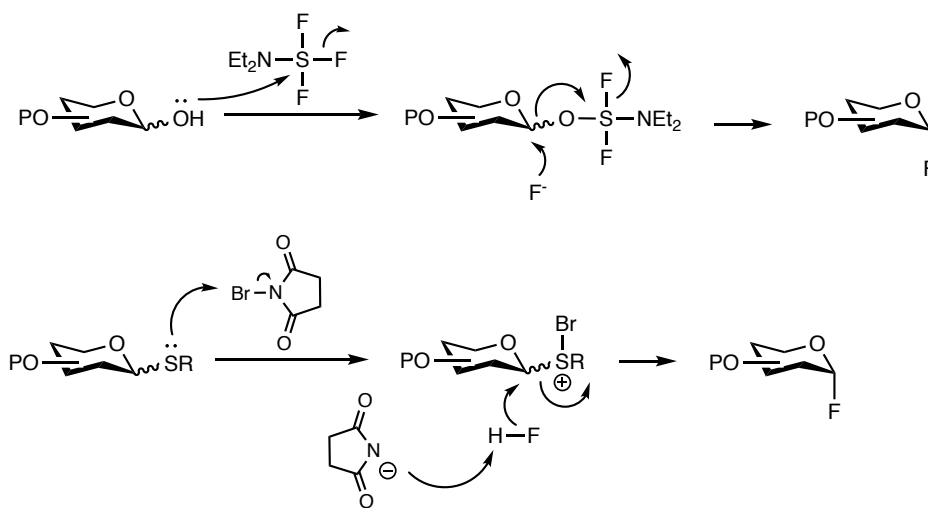


Scheme 4.7. Preparation and use of glycosyl bromides and chlorides. **(A)** Activation of glycosyl bromides. **(B)** Common methods to prepare glycosyl bromides and chlorides. **(C)** Method for *in situ* anomerization of glycosyl bromides for formation of α -glycosides.

Depending on the promoter system, glycosyl halides can be used to generate α - or β -glycosides selectively via direct displacement of the anomeric halide.²⁰ Synthesis of an α -glycoside requires *in situ* anomerization of the more stable α -halide to the much more reactive β -halide. In this procedure, developed by Lemieux and coworkers, tetra-*n*-butylammonium bromide (TBAB) is added to promote anomerization to the β -halide which subsequently undergoes nucleophilic attack in an S_N2 fashion to yield the α -glycoside; to facilitate S_N2 -type displacement, solvents of low polarity must be used to suppress formation of the oxocarbenium ion intermediate (**Scheme 4.7C**).^{40, 41} Conversely, to generate a β -glycoside, *in situ* anomerization to the β -halide must be suppressed. This can be achieved using an insoluble silver salt which sequesters halide nucleophiles from the reaction mixture.

Often more stable alternatives to glycosyl bromides are glycosyl fluorides. While these types of halide donors were originally believed to be too stable and unreactive, in 1981 Mukaiyama and co-workers found that glycosyl fluorides could be activated using $AgClO_4/SnCl_2$.⁴² Since this initial report, additional fluoride promoter systems have been developed such as $Cp_2HfCl_2-AgClO_4$, $Cp_2ZrCl_2-AgClO_4$, and $Cp_2HfCl_2-AgOTf$.^{20, 35} Glycosyl fluorides are most commonly prepared from a thioglycoside via treatment with *N*-bromosuccinimide (NBS) and (diethylamino)sulfur trifluoride (DAST) or from a lactol via treatment with DAST. Similarly, fluorides can be generated from the corresponding thioglycoside via treatment with NBS and hydrofluoric acid (HF) (**Scheme 4.8**). Due to the high stability of anomeric α -fluorides (arising from the anomeric effect), for glycosylation to proceed with this class of donor, *in situ* anomerization to the more reactive β -fluoride must occur. Direct displacement of the β -fluoride yields the α -glycoside (see

Scheme 4.7C for more detail). Consequently, glycosyl fluorides are particularly well-known for their highly α -selective glycosylations.^{20, 35, 36, 42}

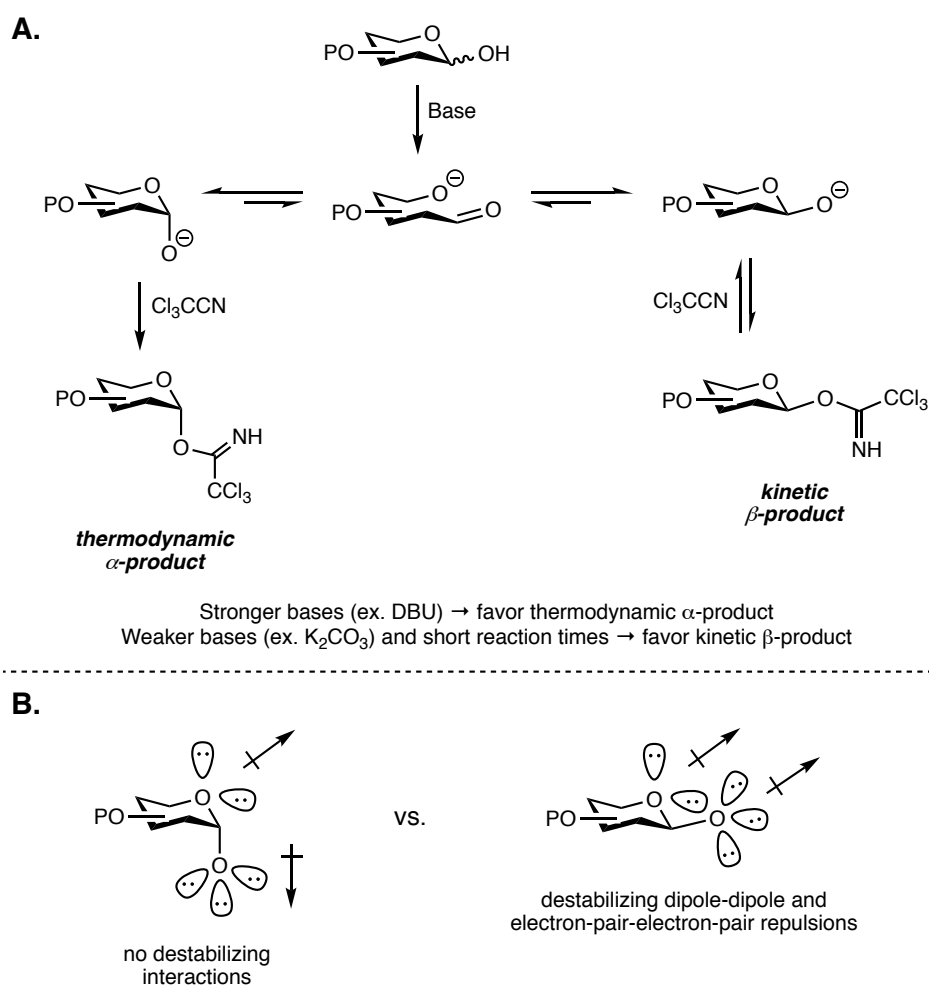


Scheme 4.8. Common methods for the synthesis of glycosyl fluorides.

In contrast to glycosyl fluorides, trichloroacetimidates are highly reactive and easily activated donors. Moreover, this class of donor does not require heavy metal salts for activation. Introduced by Schmidt and Michel in 1980, glycosyl trichloroacetimidates, also known as Schmidt imidates, have become the most widely used class of donor.^{36, 43} Their widespread use arises from their ease of preparation, high reactivity, methods for catalytic activation, and utility in forming α - or β -glycosides. As trichloroacetimidates were used extensively as glycosyl donors in our synthesis of LNT (see section 4.5 of this chapter), this class of donor will be discussed in more detail.

Trichloroacetimidates can be prepared readily via treatment of a lactol with base and trichloroacetonitrile.^{20, 23, 43, 44} Judicious choice of base and reaction time allows for selective generation of either the α - or β -imidate. For example, use of a mild base like potassium carbonate (K_2CO_3) and short reaction times yields the kinetic β -

trichloroacetimidate product. More specifically, using these conditions, the more reactive β -alkoxide is formed preferentially, and this alkoxide subsequently attacks the trichloroacetonitrile. Conversely, use of a strong base like sodium hydride (NaH) or 1,8-diazabicyclo[5.4.0]undec-7-ene (DBU) yields the thermodynamic α -trichloroacetimidate product. Strong bases facilitate alkoxide equilibration to the more stable α -alkoxide which subsequently attacks trichloroacetonitrile to yield the α -trichloroacetimidate (**Scheme 4.9**).



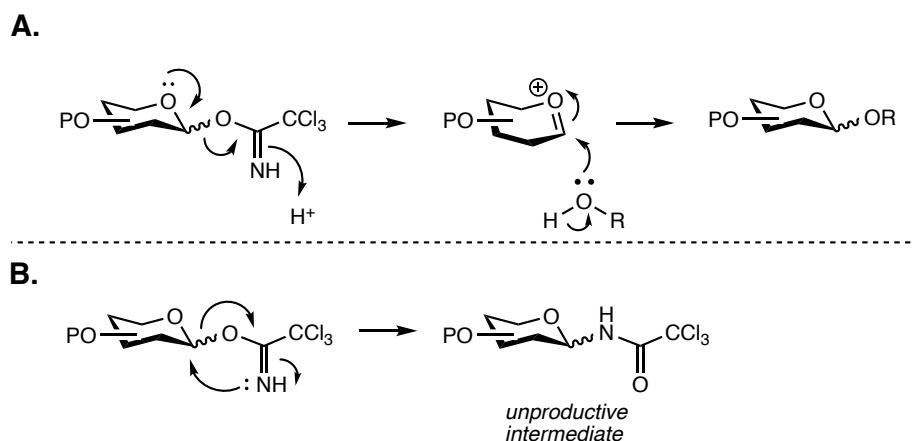
Scheme 4.9. Synthesis of trichloroacetimidate glycosyl donors. **(A)** Methods and corresponding mechanistic explanations for the generation of α - and β -trichloroacetimidates. **(B)** Mechanistic explanation for the increased reactivity of the β -alkoxide compared to the α -alkoxide.

In addition to their ease of preparation, trichloroacetimidates are readily activated via treatment with catalytic amounts of acid (**Scheme 4.10A**). The most commonly employed Lewis acids are trimethylsilyl trifluoromethanesulfonate/triflate (TMSOTf) and boron trifluoride diethyl etherate ($\text{BF}_3 \cdot \text{OEt}_2$) while trifluoromethanesulfonic acid (triflic acid, TfOH) is a commonly employed Brønsted acid.^{20, 23} In glycosylations where the trichloroacetimidate donor lacks a C2 participating group, the choice of acid promoter, as well as the starting trichloroacetimidate anomeric configuration and reaction solvent, can greatly influence the α/β ratio of the glycosylation product. For instance, use of strong catalysts like TMSOTf and TfOH with β -trichloroacetimidates has been shown to favor formation of the thermodynamic α -glycosides.^{23, 36} This preference can be enhanced by using ethereal solvents which, as previously described, promote α -glycoside formation.

In glycosylations using a donor with a C2 participating group, trichloroacetimidate donors generally yield the β -glycoside selectively and cleanly regardless of the starting donor anomeric configuration.²³ However, acyl protection does decrease donor reactivity (disarmed donors). Thus, for extensively acyl protected donors, strong catalysts like TMSOTf and TfOH are generally preferred over more mild catalysts like $\text{BF}_3 \cdot \text{OEt}_2$.²³ Interestingly, it has been observed that glycosylations with $\text{BF}_3 \cdot \text{OEt}_2$ and disarmed trichloroacetimidate donors can lead to formation of the corresponding glycosyl fluoride.⁴⁵

Although the reactive nature of trichloroacetimidates is often advantageous in glycosylations, this reactivity does restrict their formation to the last step in a donor's synthesis.^{20, 23} Additionally, trichloroacetimidates can undergo internal rearrangement to the corresponding trichloroacetamide, termed a Chapman rearrangement, especially

when activated in the presence of an unreactive acceptor; the trichloroacetamide is an unreactive intermediate (**Scheme 4.10B**).

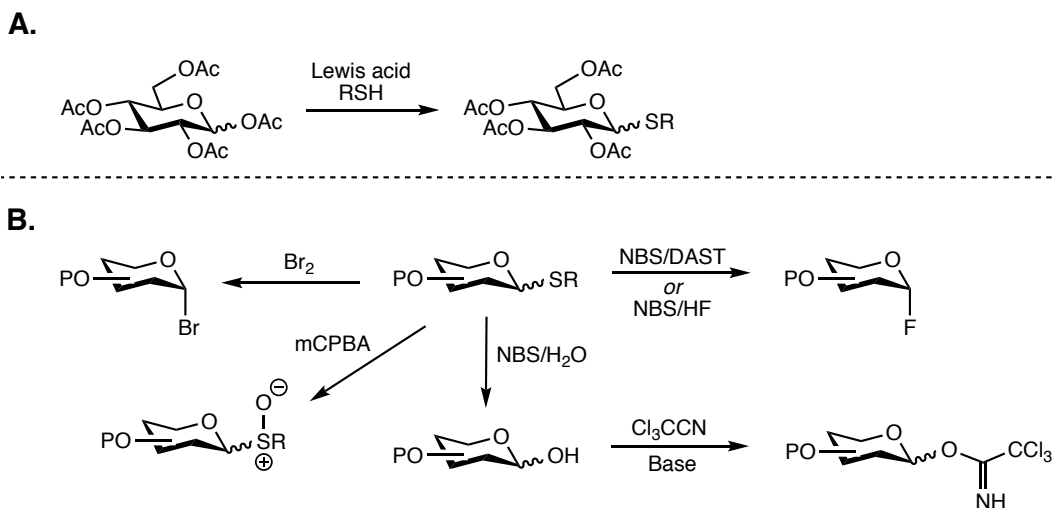


Scheme 4.10. Reactions of trichloroacetimidates. **(A)** Acid-mediated activation of trichloroacetimidate glycosyl donors. **(B)** Intramolecular Chapman rearrangement of trichloroacetimidate to the corresponding trichloroacetamide.

Thioglycosides, aryl or alkyl, are another common donor type.^{20, 36, 46} Unlike trichloroacetimidates, anomeric thiols have excellent stability and are consequently compatible with a wide range of reaction conditions typically used in carbohydrate chemistry. Thus, in addition to ultimately serving as a donor, thiols can be used as a temporary protecting group for an anomeric center. Another attractive feature of the thioglycoside donor is its general ease of preparation; alkyl and aryl thioglycosides can be prepared by Lewis-acid mediated reaction of an anomeric acetate with the appropriate starting thiol (**Figure 4.11A**). In a similar vein, thioglycosides can be converted readily into a number of different donor types (**Figure 4.11B**).

Thioglycosides can be selectively activated by fairly mild, soft electrophiles. Some of the most commonly used activators are *N*-iodosuccinimide/triflic acid (NIS/TfOH), methyl triflate (MeOTf), dimethyl(methylthio) sulfonium triflate (DMTST), iodonium dicollidine perchlorate (IDCP), and benzenesulfonyl triflate (PhSOTf) and related

variants.²⁰ Moreover, judicious selection of activator coupled with proper tuning of the electron-donating or -withdrawing nature of the anomeric thiol can allow for selective activation of one thioglycoside over another.⁴⁷ This approach is referred to as a “one-pot sequential glycosylation.”



Scheme 4.11. Thioglycoside preparation and donor interconversion. **(A)** Preparation of thioglycosides. **(B)** Methods for conversion of thioglycoside to other donor types.

Detailed descriptions of the remaining donor types presented in **Figure 4.5** as well as additional donor types not included in this figure are reviewed elsewhere.^{20, 36, 38, 44}

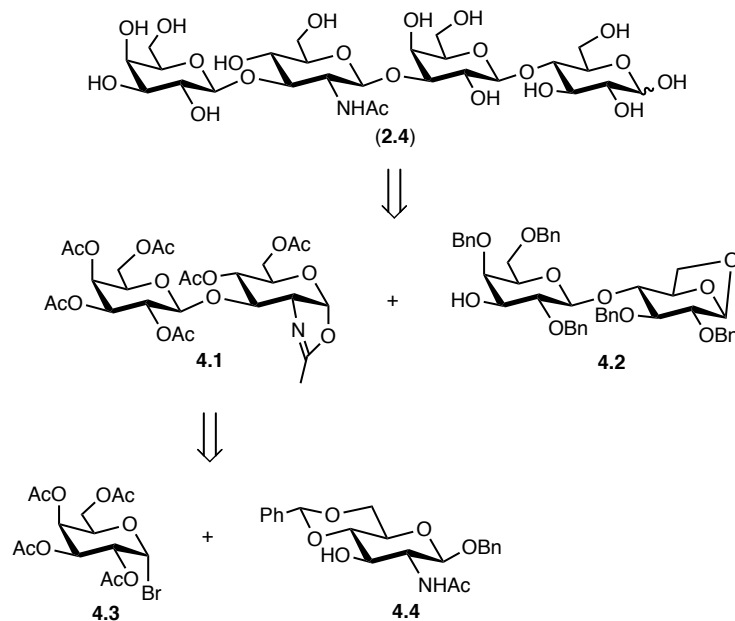
4.4 Previous Syntheses of Lacto-*N*-Tetraose and Derivatives

4.4.1 Introduction

LNT serves as a core structure not only for type I HMOs but also for numerous glycolipids, such as the lacto-series glycosphingolipids (GSLs) and sialylated lipooligosaccharide (LOS) structures of bacterial outer membranes. Due to its relevance as a core carbohydrate structure, LNT and LNT-derivatives featuring an anomeric amino linker have been the focus of numerous synthetic efforts. These efforts have ranged from

purely chemical^{7-11, 13} to purely enzymatic^{48, 49} to a combination of the two.¹² Several of these syntheses will now be presented.

4.4.2 Tejima et al. LNT Synthesis (Chemical)⁹

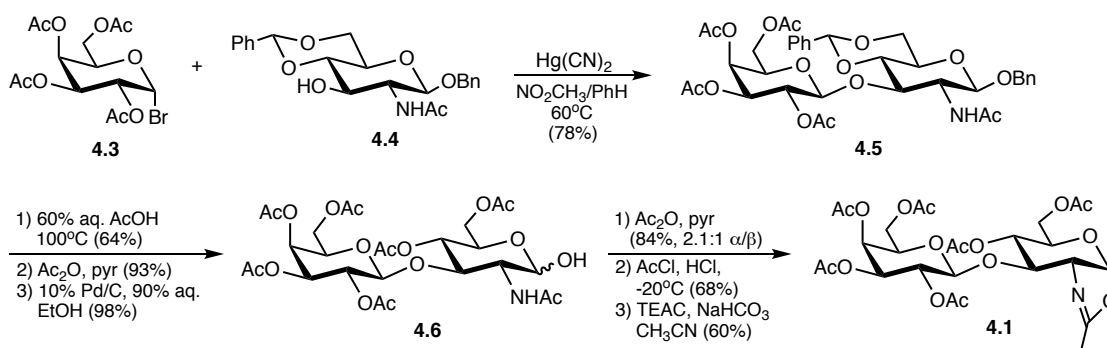


Scheme 4.12. Tejima's retrosynthetic analysis of LNT.

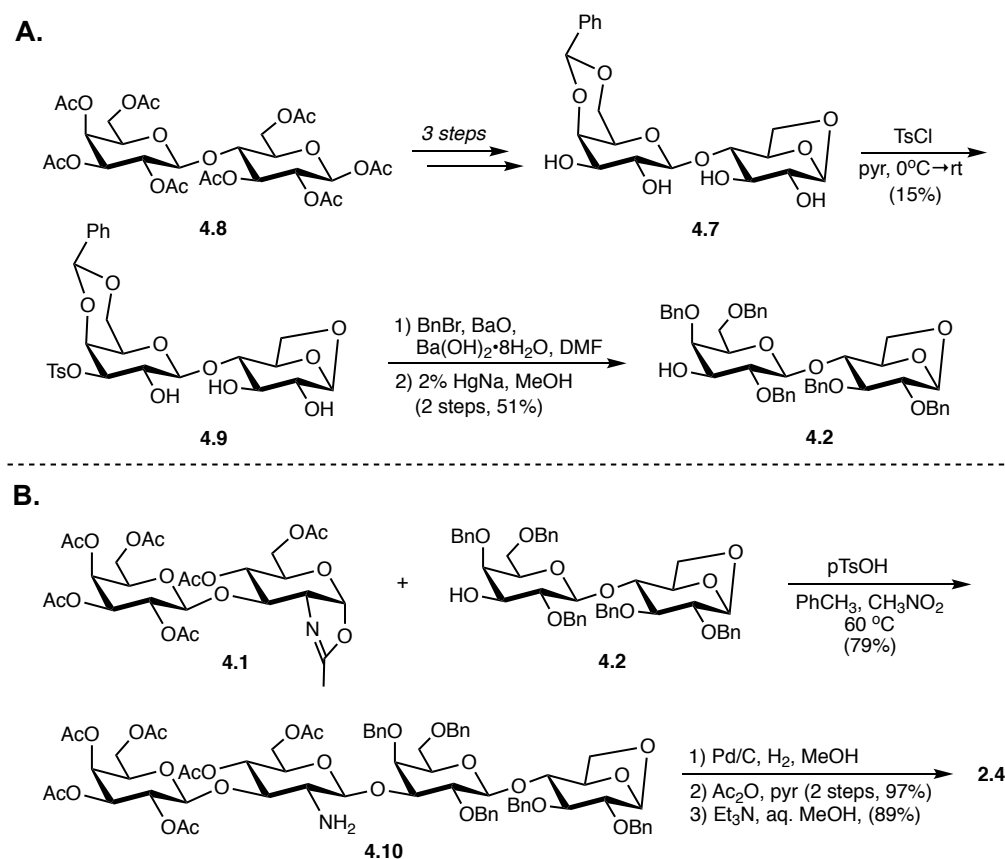
As part of a campaign to synthesize various oligosaccharides found in human milk, in 1980, Tejima and coworkers described the first reported synthesis of LNT (2.4). Their synthetic route relied on the union of known acetylated oxazoline lacto-*N*-biose (LNB) donor **4.1** with selectively benzylated lactose acceptor **4.2**;⁵⁰ LNB derivative **4.1** could be accessed from peracetylated galactosyl bromide **4.3** and orthogonally-protected glucosamine acceptor **4.4** (**Scheme 4.12**).

As described by Augé and Veyrières, mercuric cyanide-promoted glycosylation of galactosyl bromide **4.3** and glucosamine acceptor **4.4** furnished disaccharide **4.5** in 78% yield (**Scheme 4.13**). Subsequent acid-mediated hydrolysis of the benzylidene acetal and

acetylation of the resulting diol followed by hydrogenation of the anomeric benzyl ether yielded lactol **4.6**. Acetylation of **4.6** followed by treatment of the α -acetate with acetyl chloride and dry HCl furnished the anomeric chloride, which was subsequently treated with tetraethylammonium chloride (TEAC) to yield oxazoline donor **4.1** in 60% yield.



Scheme 4.13. Augé and Veyrières' synthesis of oxazoline LNB donor **4.1**.



Scheme 4.14. Tejima's synthesis of LNT (**2.4**). (A) Synthesis of lactose acceptor **4.2**. (B) Synthesis of LNT (**2.4**).

Synthesis of lactose acceptor **4.2** began with partial tosylation of known 1,6-anhydro-4', 6'-benzylidene lactose derivative **4.7**, accessible in three steps from lactose octaacetate (LOA) **4.8**, to yield 3'-tosylate **4.9** in 15% yield (**Scheme 4.14**).⁵¹⁻⁵⁴ Benzylation of **4.9** followed by tosyl group removal gave lactose acceptor **4.2** in 51% over two steps. Protected LNT derivative **4.10** was then synthesized via *para*-toluenesulfonic acid (pTsOH)-mediated glycosylation of **4.1** and **4.2** in 79% yield. Notably, this glycosylation required two days of stirring at 60 °C and upwards of three equivalents of oxazoline donor **4.1**. A three step deprotection sequence then gave LNT (**2.4**).

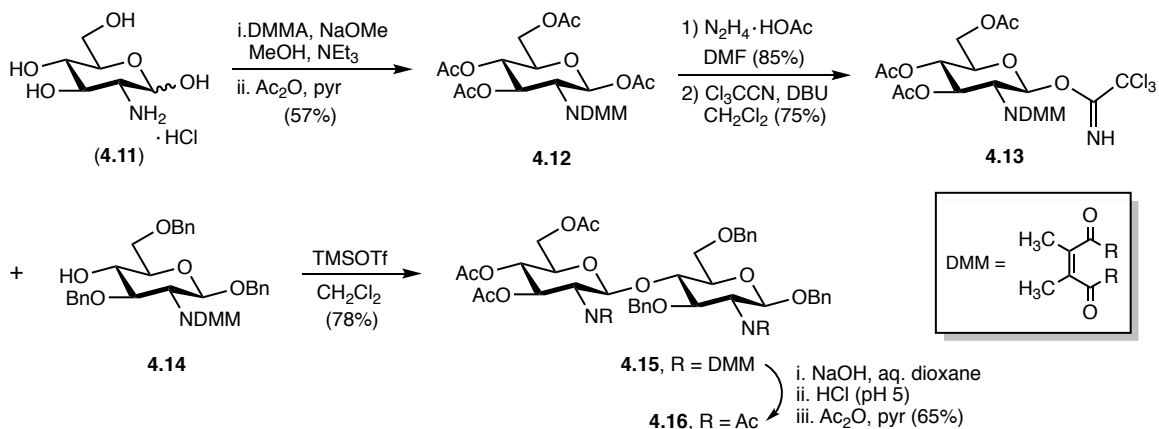
4.4.3 Schmidt et al. LNT Synthesis (Chemical)⁷

In 1998, the Schmidt laboratory introduced the dimethylmaleoyl (DMM) group as a novel amino protecting group for glucosamine (**Scheme 4.15**); while the DMM group had been reported previously, it had not yet been used in the protection of amino sugars.⁵⁵ Importantly, it was hypothesized that this new protecting group would increase donor reactivity compared to glucosamine donors wherein the amine was protected as the acetamide; the 1,3 oxazolinium intermediate (see **Scheme 4.4**) derived from neighboring group participation from the C2 acetamide possesses weak donor properties.

In their initial report, Schmidt and coworkers demonstrated that DMM-protected glucosamine, accessible via treatment of glucosamine hydrochloride (**4.11**) with dimethyl maleoyl anhydride (DMMA), could be transformed into numerous glycosyl donors and acceptors. This served to showcase the protecting group's stability toward acid and non-nucleophilic bases. Next, using TMSOTf as a promoter, various DMM-protected glucosamine trichloroacetimidate donors and DMM-protected glucosamine acceptors

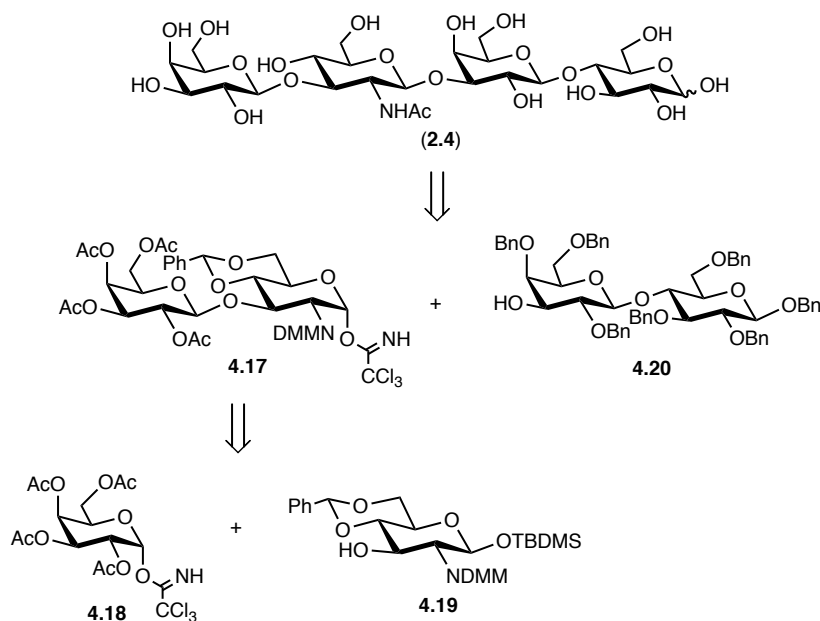
were glycosylated to yield β -glycosides in generally high yields. Finally, it was found that cleavage of the DMM and conversion to the acetamide worked reliably and in good yields

(Scheme 4.15).⁵⁵



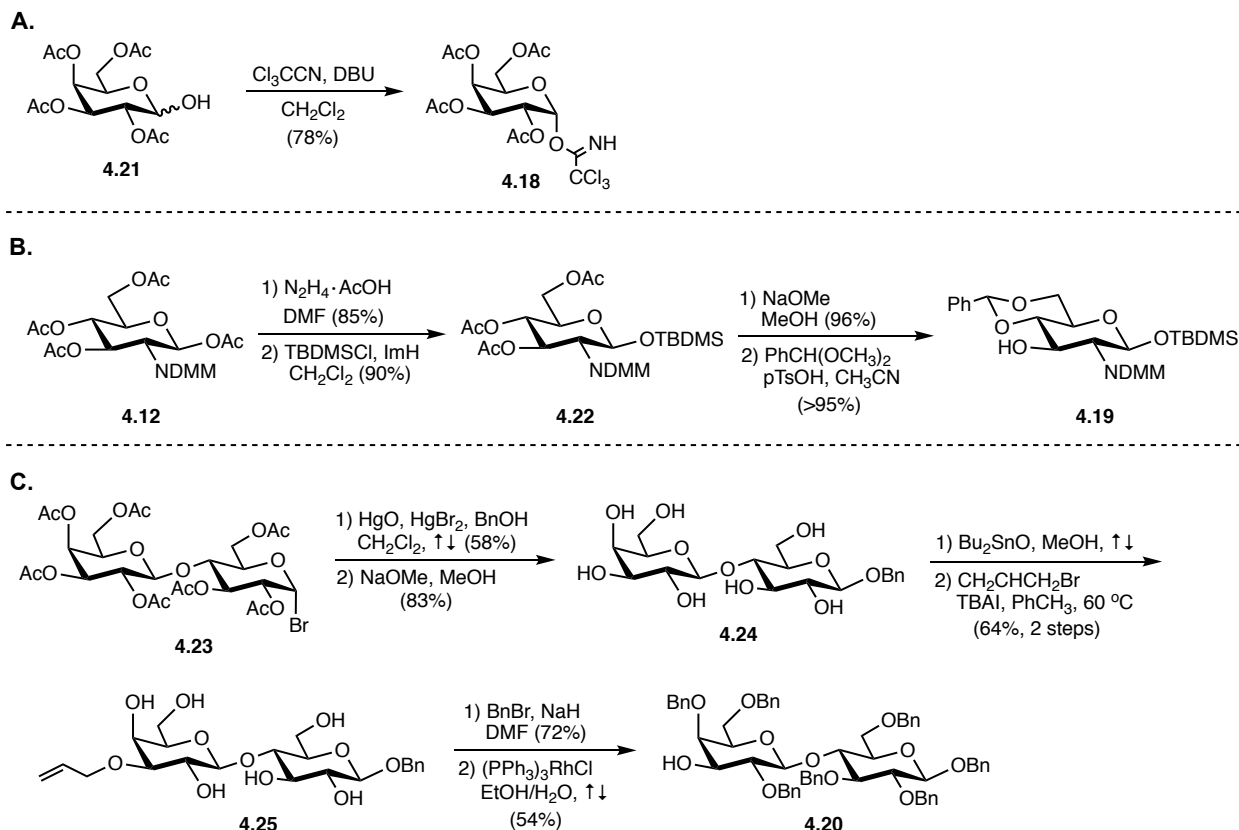
Scheme 4.15. Selected example of dimethylmaleoyl (DMM) amino protecting group in carbohydrate synthesis.

To further demonstrate the utility of this new amino sugar protecting group, Schmidt et al. developed a synthesis of LNT (as well as LNnT) featuring a DMM-protected glucosamine derivative (**Scheme 4.16**).



Scheme 4.16. Schmidt's retrosynthetic analysis of LNT (2.4).

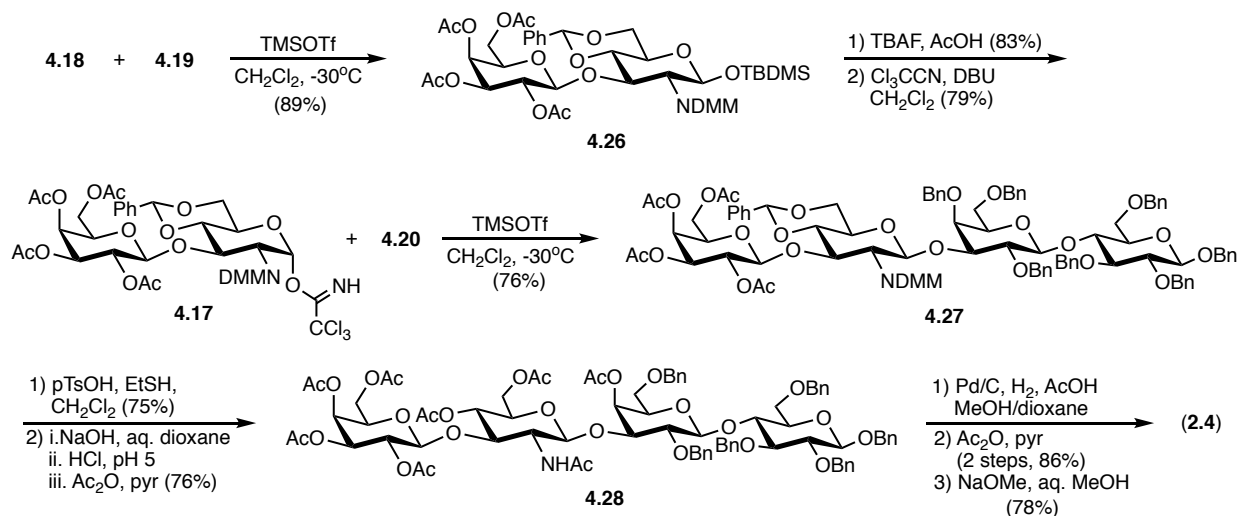
Similar to Tejima's synthesis, the Schmidt synthesis relied on union of an LNB donor, **4.17** (accessed via union of galactose donor **4.18**⁵⁶ and glucosamine acceptor **4.19**)⁵⁵ and a lactose acceptor, **4.20**;⁵⁷ importantly, galactose donor **4.18**, glucosamine acceptor **4.19**, and lactose acceptor **4.20** had all been previously synthesized in the Schmidt laboratory.



Scheme 4.17. LNT building block synthesis. **(A)** Synthesis of galactosyl imidate donor **4.18**. **(B)** Synthesis of DMM-protected glucosamine acceptor **4.19**. **(C)** Synthesis of benzylated lactose acceptor **4.20**.

Galactose donor **4.18** was prepared in one step from known acetylated galactosyl lactol **4.21** (**Scheme 4.17A**).⁵⁸ Glucosamine acceptor **4.19** was prepared beginning from known peracetylated, DMM-protected glucosamine derivative **4.12** (**Scheme 4.17B**). Selective anomeric deacetylation with hydrazine acetate furnished the lactol which was subsequently converted to anomeric *tert*-butyldimethyl silyl ether **4.22** in 90% yield.

Deacetylation of **4.22** followed by treatment with benzaldehyde dimethyl acetal (BDMA) yielded the 4,6-benzylidene acetal glucosamine acceptor **4.19**.⁵⁵ Lactose acceptor **4.20** was synthesized starting with a Koenigs-Knorr glycosylation of known peracetylated lactosyl bromide **4.23**, synthesized via treatment of LOA with HBr in acetic acid,⁵⁹ with benzyl alcohol to yield the β -benzyl lactoside (not pictured) in 58% yield. The benzyl lactoside was then deacetylated to yield polyol **4.24** (**Scheme 4.17C**). Treatment of polyol **4.24** with dibutyltin oxide furnished the stannylene complex which facilitated regioselective allylation of the C3' alcohol to yield **4.25**. Finally, perbenzylation of allyl ether **4.25** followed by tris(triphenylphosphine)rhodium(I) chloride-mediated cleavage of the allyl group furnished lactose acceptor **4.20**.⁵⁷



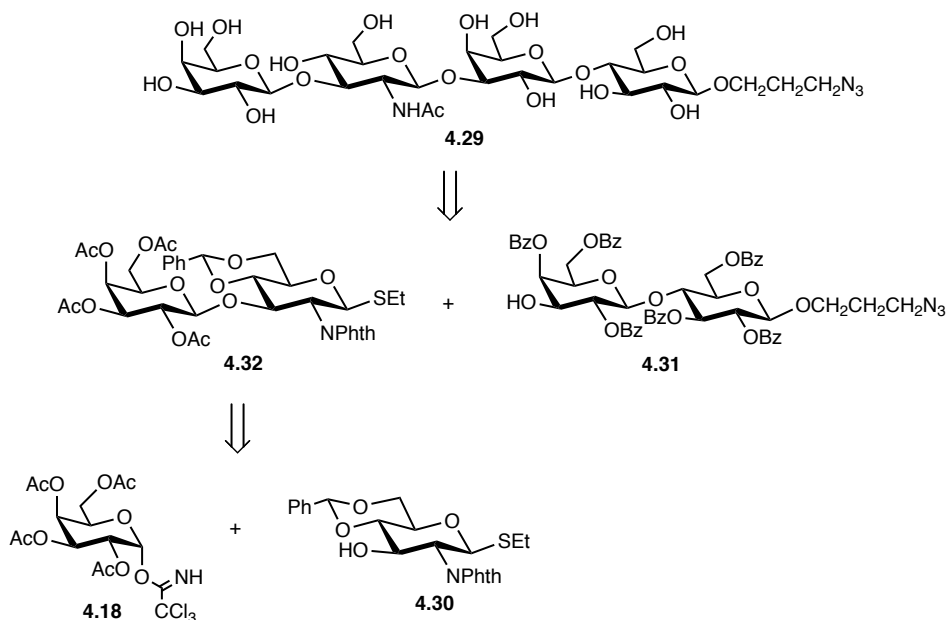
Scheme 4.18. Schmidt's synthesis of LNT (**2.4**).

As described in an earlier report by Schmidt et al., TMSOTf-promoted glycosylation of galactosyl trichloroacetimidate donor **4.18** and DMM-protected glucosamine acceptor **4.19** yielded disaccharide **4.26** in 89% yield (**Scheme 4.18**).⁵⁵ Treatment of **4.26** with tetra-*n*-butylammonium fluoride (TBAF) and acetic acid followed by treatment of the resulting lactol with DBU and trichloroacetonitrile gave LNB donor **4.17**. A second

TMSOTf-promoted glycosylation between LNB trichloroacetimidate donor **4.17** and lactose acceptor **4.20** furnished fully protected LNT derivative **4.27**.⁷ A five-step deprotection sequence then afforded LNT (**2.4**).

4.4.4 Chen et al. LNT-ProN₃ Synthesis (Chemical)¹¹

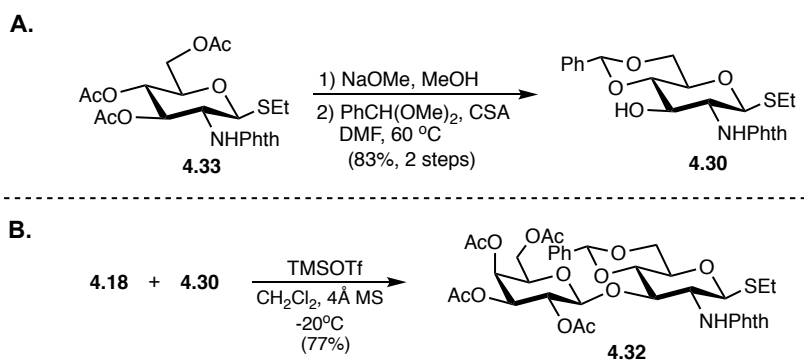
In 2011, the Chen group reported the chemoenzymatic syntheses of numerous α 2-3 sialylated carbohydrate epitopes. Importantly, each sialoside featured an anomeric propyl azide (ProN₃) functionality so that they could be used as probes to investigate the biological importance of this class of sialylated compound. To access the α 2-3 sialylated carbohydrates, neutral core carbohydrate structures with the ProN₃ feature, including LNT-Pro₃ **4.29** (Scheme 4.19), were chemically synthesized. The sialic acid moieties were then added enzymatically using a one-pot, three enzyme approach including an α 2-3 sialyltransferase from *Pasteurella multocida*.



Scheme 4.19. Chen's retrosynthetic analysis of LNT-ProN₃ **4.29**.

LNT-Pro₃ **4.29** was synthesized using a two-glycosylation approach with known galactose donor **4.18**,⁵⁶ glucosamine acceptor **4.30**, and benzoylated lactose acceptor **4.31** (**Scheme 4.19**). In contrast to previously described syntheses, the present synthesis relied heavily on thioglycoside donors and featured a benzoylated rather than benzylated lactose acceptor. The later was selected due to the increased ease of selective benzoyl deprotection compared to selective benzyl deprotection in the presence of an azide.

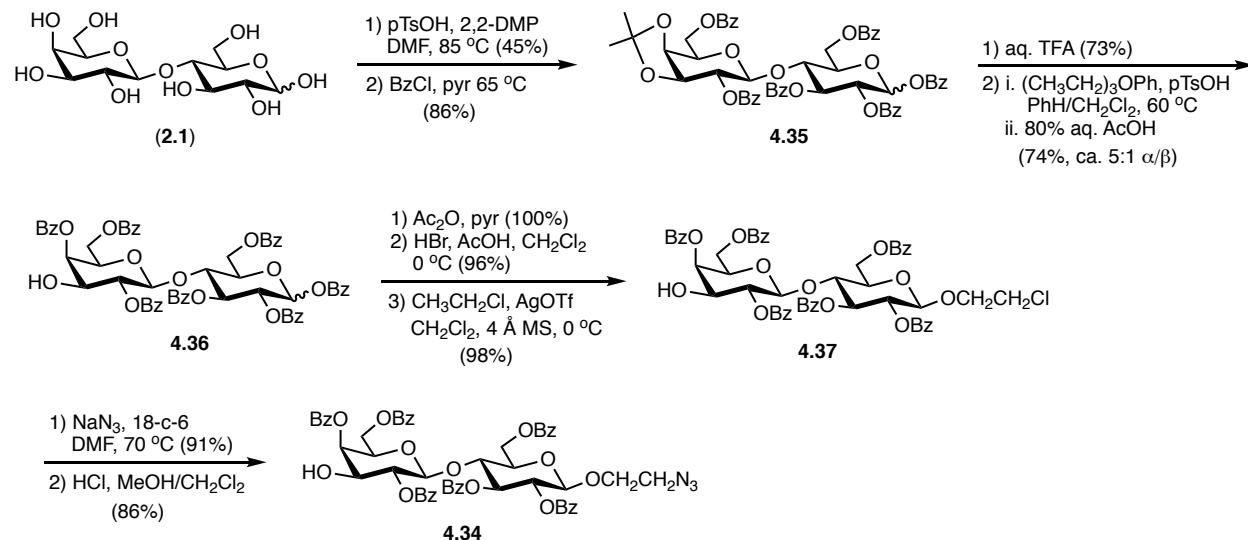
Glucosamine acceptor **4.30** was readily synthesized in 83% yield over 2 steps from known glucosamine thioglycoside **4.33** (**Scheme 4.20A**);⁶⁰ thioglycoside **4.33** can be accessed in two steps via phthalimide protection of glucosamine•HCl (**4.11**) followed a two-step, one-pot, BF₃•OEt₂-catalysed peracetylation and thioglycoside formation. TMSOTf-promoted glycosylation between glucosamine acceptor **4.30** galactose donor **4.18**⁵⁶ yielded disaccharide thioglycoside donor **4.32** in 77% yield (**Scheme 4.20B**).



Scheme 4.20. Synthesis of LNB donor **4.32**. **(A)** Synthesis of glucosamine acceptor **4.30**. **(B)** Glycosylation to yield LNB donor **4.32**.

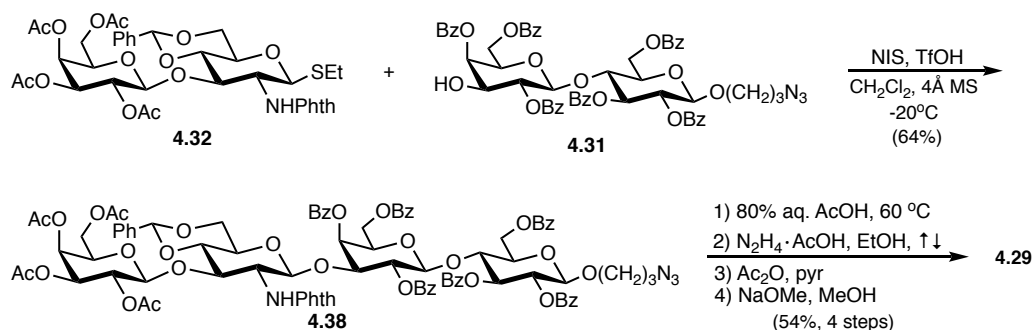
Benzoylated lactose acceptor **4.31** was synthesized in an analogous fashion to that of benzoylated lactose derivative **4.34** reported previously by the Abbas and Nifantiev laboratories (**Scheme 4.21**);^{61, 62} in the Chen synthesis, a 3-azido propyl appendage was used as opposed to a 2-azido ethyl appendage. First, treatment of lactose (**2.1**) with

pTsOH and 2,2-dimethoxypropane (2,2-DMP) gave the 3',4'-acetonide (not pictured) in 45% yield along with 21% of the 4',6'-acetonide (not pictured). Benzoylation of the 3',4'-acetonide then furnished **4.35**. Treatment of **4.35** with aqueous acid facilitated acetonide removal to reveal the 3',4'-diol (not pictured)⁶¹ which was subsequently treated with triethylortho-benzoate.⁶² The resulting 3',4'-ortho-benzoate was then opened regioselectively to furnish C4' O-benzoylated **4.36**. The free C3' alcohol of **4.36** was acetylated and the resulting glycoside was converted to the corresponding anomeric bromide and glycosylated with 2-chloroethanol to yield 2-chloroethyl lactoside **4.37**. Finally, chloride displacement with sodium azide (NaN₃) followed by deacetylation furnished lactose derivative **4.34**.⁶²



Scheme 4.21. Synthesis of lactose derivative **4.34**.

With LNB thioglycoside **4.32** and benzoylated lactose acceptor **4.31** in hand, NIS and TfOH-promoted glycosylation between **4.32** and **4.31** gave fully protected LNT-ProN₃ **4.38** in 64% yield (**Scheme 4.22**). A four-step deprotection sequence furnished the desired LNT-ProN₃ **4.29** in 54% over 4 steps.



4.4.5 Wong et al. Linker-Attached Lc₄ Synthesis (Chemical)¹³

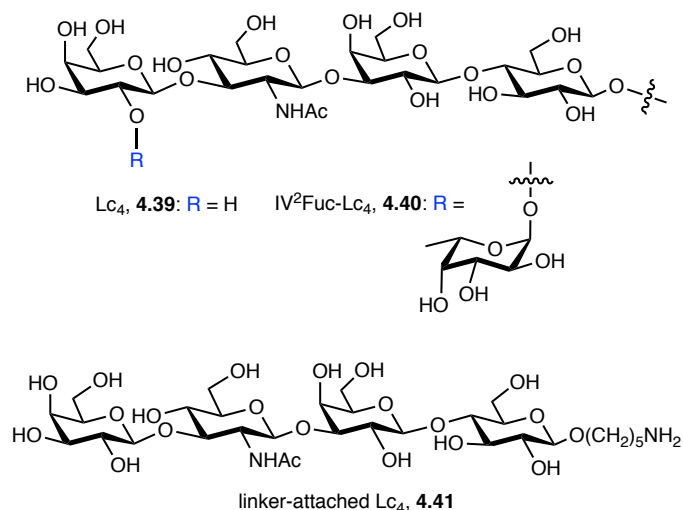
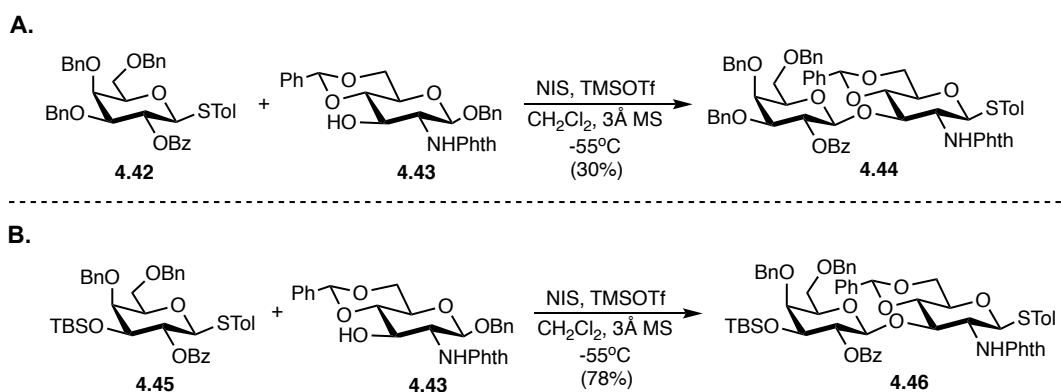


Figure 4.6. Structures of Lc₄ ceramide (**4.39**), IV²Fuc-Lc₄ ceramide (**4.40**), and linker-attached Lc₄, **4.41**.

In 2012, the Wong group synthesized linker-attached derivatives of the lacto-series GSLs lactosyltetraosyl (Lc₄) and 2'''-O-fucosyl Lc₄ (IV²Fuc-Lc₄) ceramide (**4.39**) and (**4.40**), respectively (**Figure 4.6**). Notably, these syntheses featured a one-pot, two-glycosylation reaction which showcased the influence of donor protecting group patterns on donor reactivity. In their initial attempt to synthesize linker-attached Lc₄ **4.41**, Wong et al. attempted an NIS/TMSOTf-promoted glycosylation between known thiogalactoside

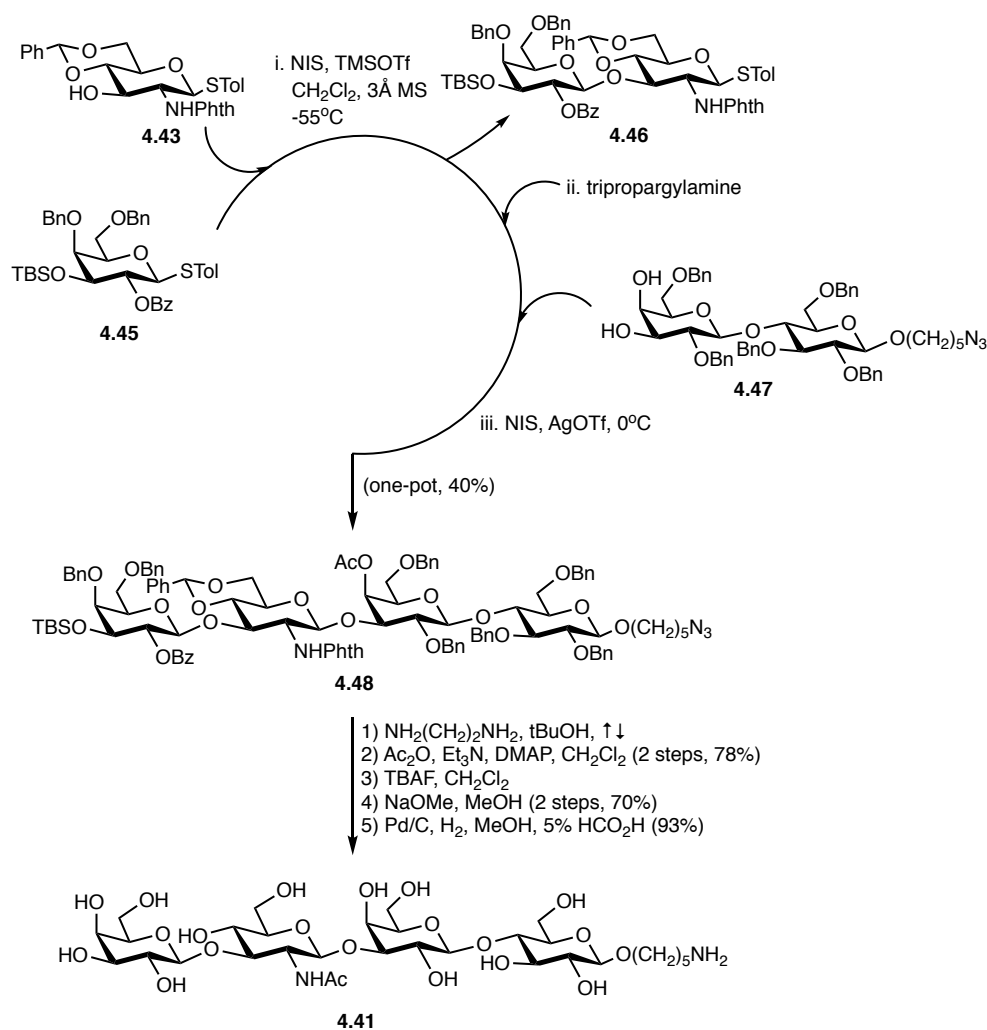
donor **4.42**,⁶³ and known glucosamine acceptor **4.43** (**Scheme 4.23A**).⁴⁷ However, these conditions resulted in a mere 30% yield of the desired disaccharide **4.44**. Moreover, a significant amount of unreacted acceptor was recovered. As an alternative, donor **4.42** was replaced with known 3-*O*-silylated thiogalactoside **4.45**; thiogalactoside **4.45** had previously been determined to be more reactive than **4.42** based on relative reactivity rate (RRV) calculations.⁶⁴ Substitution of the 3-*O*-benzyl for a 3-*O*-TBS ether did indeed provide a more reactive donor as glycosylation between sialylated donor **4.45** and acceptor **4.43** yielded disaccharide **4.46** in 78% yield (**Scheme 4.23B**).



Scheme 4.23. Synthesis of LNB donors **4.44** and **4.46**. (A) Synthesis of LNB donor **4.44**. (B) Synthesis of LNB donor **4.46**.

With the first glycosylation optimized, Wong et al. moved to implement the one-pot, two-glycosylation procedure using known lactose diol acceptor **4.47** (**Scheme 4.24**).⁶⁵ While initial attempts were unsuccessful, it was discovered that addition of tripropargylamine after completion of the first coupling followed by NIS/AgOTf-promoted glycosylation between newly formed LNB donor **4.46** and lactose acceptor **4.47** furnished tetrasaccharide **4.48** in 40% yield; conversely, glycosylation of LNB donor **4.44** with lactose acceptor **4.47** yielded only 18% of the corresponding tetrasaccharide (not

pictured). From **4.48**, a 5-step deprotection sequence afforded linker-attached Lc₄ **4.41** in 50% yield over 5 steps.

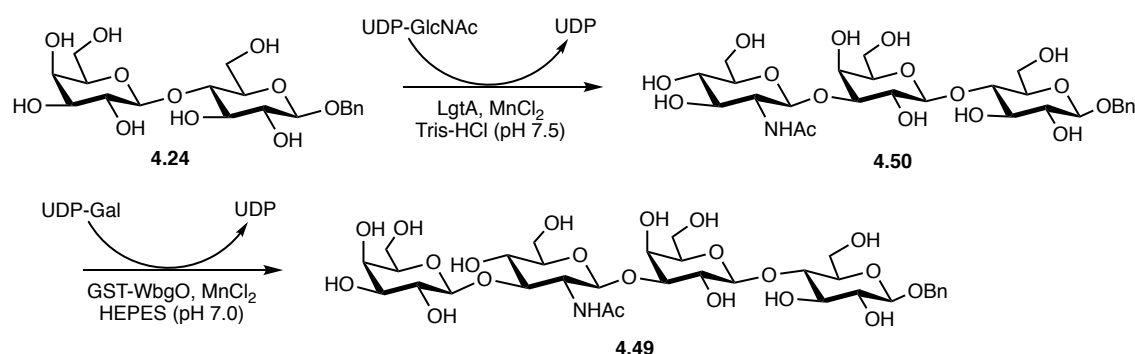


Scheme 4.24. Wong's one-pot, two-glycosylation approach to linker-attached Lc₄ **4.41**.

4.4.6 Albermann et al. LNT Synthesis (Enzymatic)⁴⁹

In 2014, the Albermann group developed a method for the enzymatic production of LNT using metabolically engineered, plasmid-free *E. coli*. Important to this method development was a 2009 report from the Wang laboratory wherein they identified and characterized a novel β 1-3-galactosyltransferase (β 1-3-GalT) in *E. coli* 055:H7.⁶⁶ This

GalT, termed WbgO, was capable of transferring galactose to GlcNAc and/or oligosaccharides with a non-reducing end GlcNAc. Moreover, Wang et al. used this enzyme, overexpressed in *E. coli* BL21, in the *in vitro* enzymatic synthesis of benzyl β -lacto-*N*-tetraoside (LNT- β -OBn) **4.49** (Scheme 4.25).

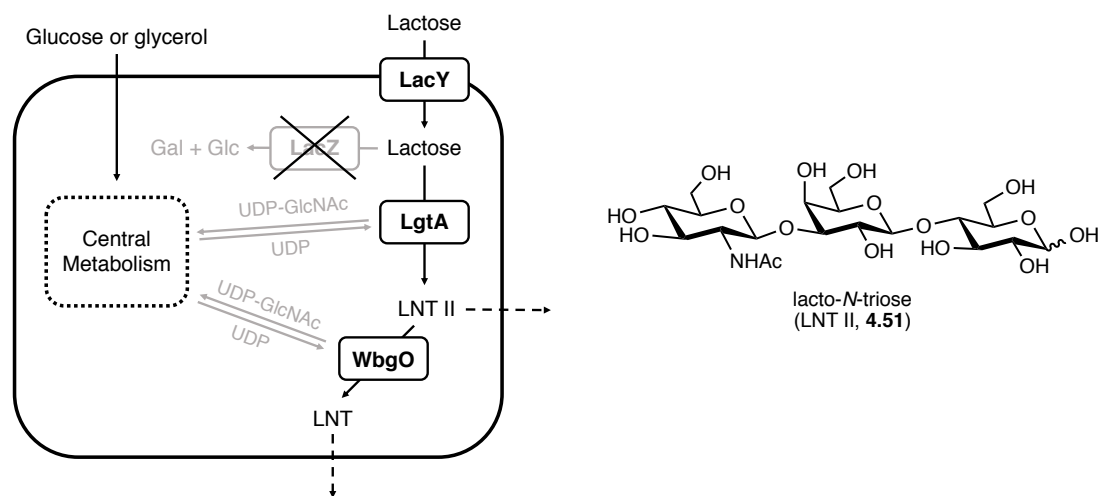


Scheme 4.25. Wang's enzymatic synthesis of benzyl β -lacto-*N*-tetraoside **4.49** using recombinant LgtA and WbgO. Abbreviations: UDP-GlcNAc, uridine 5'-diphosphate-*N*-acetylglucosamine; LgtA, β 1-3 GlcNAc-transferase from *Neisseria meningitidis*; MnCl₂, manganese(II) chloride; GST-WbgO, glutathione S-transferase-WbgO (β 1-3 galactosyltransferase in *E. coli* 055:H7) fused protein.

For their study, Albermann et al. selected *E. coli* strain K-12 LJ110 as the parent. To construct an LNT-producing strain, the *lacZ* gene, which encodes the LacZ β -galactosidase, was removed; LacZ β -galactosidase hydrolyzes lactose into glucose and galactose. The strain was next equipped with LgtA, the β 1-3-*N*-acetylglucosaminyltransferase from *N. meningitidis*. The resulting strain was supplemented with the *wbgO* gene, which encodes the β 1-3-Gal WbgO. Importantly, the modified strain, termed strain LJ-AYO-cat, retained the *lacY* gene, which encodes the lactose permease (LacY) transporter. This allowed for continued lactose uptake despite the lack of intracellular LacZ. Finally, the necessary nucleotide-sugars that serve as

donors for the glycosyltransferases were derived endogenously from the intracellular pool of nucleotide-activated sugars (produced for use by host Leloir glycosyltransferases).

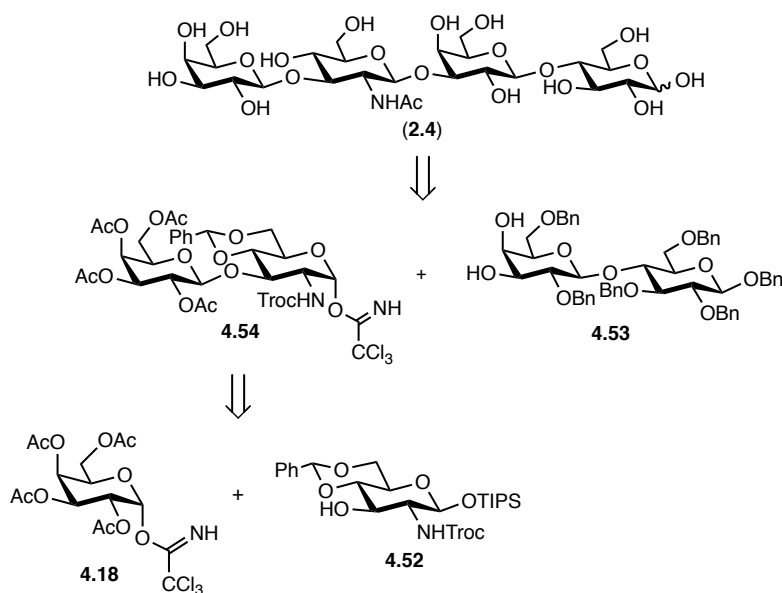
Starting with a combination of lactose and glucose or lactose and glycerol, strain LJ-AYO-cat was able to produce both lacto-*N*-triose (LNT II, **4.51**) and LNT (**2.4**) (**Scheme 4.26**). Notably, it was found that the use of glycerol resulted in higher yields of LNT II than LNT; the use of glucose reversed this trend. Specifically, medium with glucose had 219.1 ± 3.5 mg/L LNT 24 h after induction whereas medium with glycerol had only 162.1 ± 6.2 mg/L. These concentrations corresponded to LNT yields of 66.2 ± 1.6 mg/g_{CDW} (CDW, cell dry weight) for glucose-supplemented medium and 58.5 ± 2.0 mg/g_{CDW} for glycerol-supplemented medium. While LNT II was not fully converted to LNT by strain LJ-AYO-cat using either glycerol or glucose, this report nevertheless represents the first report of LNT being synthesized using recombinant *E. coli* cells.⁴⁹



Scheme 4.26. Albermann's *in vivo* synthesis of lacto-*N*-triose (LNT II, **4.51**) and lacto-*N*-tetraose (LNT, **2.4**) in recombinant *E. coli* cells using Leloir glycosyltransferases and intracellular nucleotide sugars. Dashed arrows indicate that the majority of these compounds are found in the extracellular environment (culture supernatant). Abbreviations: LacY, lactose permease from *E. coli* strain K-12; LacZ, β 1-3 galactosidase from *E. coli* strain K-12; LgtA, β 1-3 GlcNAc-transferase from *N. meningitidis*; WbgO, β 1-3-galactosyltransferase from *E. coli* O55:H7.

4.5 Synthesis of Lacto-*N*-Tetraose⁶⁷

4.5.1 Synthetic Strategy



Scheme 4.27. Retrosynthetic analysis of LNT (**2.4**).

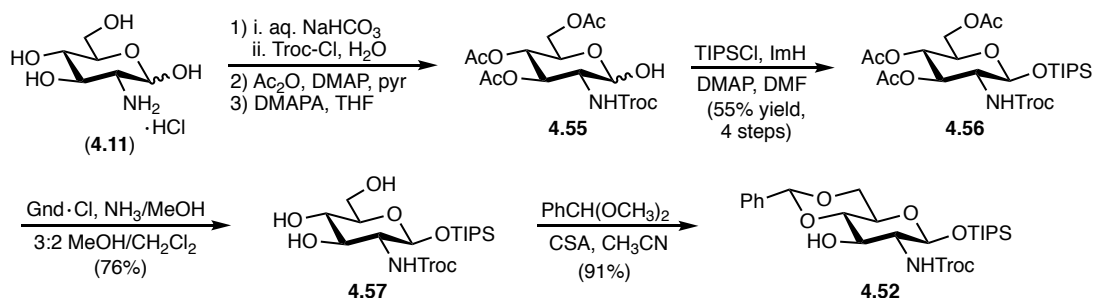
Similar to the previously described Tejima and Schmidt LNT syntheses, our approach to LNT (**2.4**) featured a two-glycosylation approach wherein the tetrasaccharide could be assembled from known galactose donor **4.18**,⁵⁶ glucosamine acceptor **4.52**, and known lactose acceptor **4.53** (**Scheme 4.27**).⁵⁷ Importantly, galactose donor **4.18** possessed a C2 functionality capable of neighboring group participation to facilitate β -glycoside formation. Similarly, the C2 amine of glucosamine acceptor **4.52** was protected as the trichloroethyl (Troc) carbamate which is also capable of neighboring group participation; this participation would be key in the second glycosylation between LNB donor **4.54** and lactose acceptor **4.53** to form the desired β -linkage. Finally, in addition to providing an expeditious route to LNT, use of building blocks **4.52** and **4.53** would allow for potential installation of branching or other modification at the C6 and/or C4 alcohols of glucosamine as well as the C4' of lactose, respectively.

4.5.2 Synthesis of Glucosamine Acceptor **4.52**

Synthesis of glucosamine acceptor **4.52** commenced with protection of the C2 amine as the Troc carbamate via treatment of glucosamine•HCl (**4.11**) with saturated aqueous NaHCO₃ solution followed by addition of 2,2,2-trichloroethyl chloroformate (Troc-Cl) (**Scheme 4.28**). Following peracetylation, selective removal of the anomeric acetate was accomplished using 3-(dimethylamino)-1-propylamine (DMAPA) to afford known lactol **4.55**.⁶⁸ Originally, this selective anomeric deacetylation was accomplished via treatment of the peracetylated compound with hydrazine acetate in DMF as reported by Schmidt et al.⁶⁸ During the course of the synthesis, however, the Jensen group introduced DMAPA as a cheaper and safer alternative to hydrazine acetate.⁶⁹ Moreover, the bifunctional nature of DMAPA allows it to be removed from the reaction by a simple acidic workup. Conversely, byproducts of hydrazine acetate-mediated deacetylation require chromatographic separation. As a final point of advantage, anomeric deacetylation with DMAPA can be performed in THF rather than DMF.

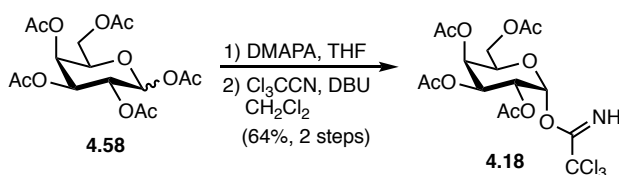
Lactol **4.55** was next converted to its triisopropylsilyl (TIPS) ether using standard Corey conditions (imidazole and DMF)⁷⁰ to yield β -silyl ether **4.56** as a single anomer in 54% yield for the 4-step sequence (**Scheme 4.28**). Deacetylation of **4.56** to furnish triol **4.57** was initially attempted using sodium methoxide in methanol. Unfortunately, NaOMe treatment proved incompatible with the Troc carbamate. NMR analysis of the reaction product suggested that deacetylation was accompanied by deprotonation of the Troc methylene and subsequent elimination of a chloride atom from the Troc trichloromethyl group (effectively elimination of HCl). Fortunately, previous reports had identified guanidine as a milder deacetylating agent capable of sparing the Troc functionality.⁷¹⁻⁷³

Consistent with these reports, deacetylation of **4.56** using guanidinium chloride in the presence of ammonia gave triol **4.57** cleanly in 76% yield. Finally, triol **4.57** was converted to the corresponding 4,6-benzylidene acetal upon treatment with BDMA and catalytic 10-camphorsulfonic acid (CSA) to yield glucosamine acceptor **4.52** in 91% yield (**Scheme 4.28**). Notably, acceptor **4.52** is closely related to a compound synthesized previously by the Boons laboratory; rather than converting lactol **4.55** to its β -TIPS ether, Boons et al. converted the lactol to the corresponding β -dimethylthexylsilyl (TDS) ether.⁷³



Scheme 4.28. Synthesis of glucosamine acceptor **4.52**.

4.5.3 Synthesis of Lacto-*N*-Biose Donor **4.54**

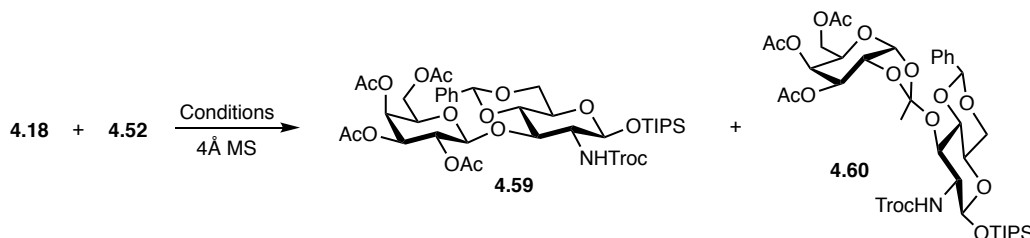


Scheme 4.29. Synthesis of galactose donor **4.18**.

Formation of LNB donor **4.54** first required union of glucosamine acceptor **4.52** with known galactose trichloroacetimidate donor **4.18**.⁵⁶ Donor **4.18** is accessible in two steps from galactose pentaacetate **4.58** via anomeric deacetylation followed by treatment of the resulting lactol with trichloroacetonitrile and DBU in acetonitrile.⁵⁶ For our synthesis of **4.18**, we once again elected to use DMAPA for selective anomeric deacetylation as

opposed to hydrazine acetate as was previously reported.^{56, 58} Subsequent treatment of the crude lactol with trichloroacetonitrile and DBU in acetonitrile furnished galactose donor **4.18** in 64% over 2 steps (**Scheme 4.29**).

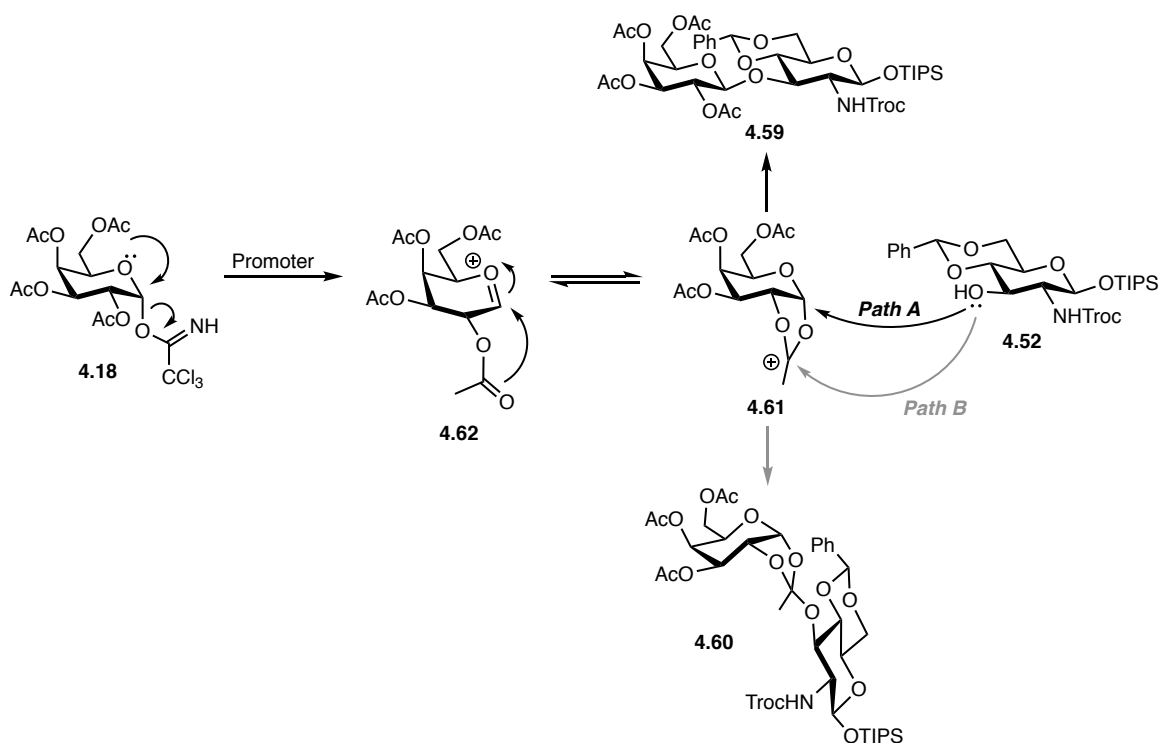
Table 4.1. Synthesis of Lacto-*N*-Biose Disaccharide **4.59** and Orthoacetate **4.60**



Entry	Promoter	Solvent	Temp (° C)	% Yield 4.59	% Yield 4.60
1	TMSOTf	CH ₃ CN	-40	18-60	0-50
2	BF ₃ •OEt ₂	CH ₃ CN	-40	0	23
3	TMSOTf	CH ₃ CN	-10	28-76	0-40
4	TMSOTf	CH ₃ CN	0	0-44	26-49
5	TMSOTf	CH ₃ CN	r.t	30-70	0
6	TMSOTf	CH ₂ Cl ₂	-78	0	22
7	TMSOTf	CH ₂ Cl ₂	-10 to 0	70-85	0

For glycosylation between donor **4.18** and acceptor **4.52**, although donor **4.18** possessed a C2 *O*-acetyl protecting group capable of NGP, we hypothesized we could further promote β -glycoside formation by using acetonitrile, a known β -director (as described in section 4.3.4 of this chapter), as the reaction solvent. In the initial attempt, TMSOTf was used as the promoter, acetonitrile as the solvent, and -40 °C as the reaction temperature. Under these conditions, the desired LNB disaccharide **4.59** was formed in 60% yield (**Table 4.1**). It should be noted though that glycoside **4.59** was co-isolated with around 6% of rearranged galactose donor **4.18** (rearrangement from the trichloroacetimidate to the trichloroacetamide). Interestingly, in a second attempt using

the same reaction conditions, disaccharide **4.59** was obtained in only 18% yield while orthoacetate disaccharide **4.60** was isolated as the major product in 50% yield.



Scheme 4.30. Mechanistic explanation for the formation of undesired orthoacetate **4.60** and desired β -linked disaccharide **4.59** glycosylation products.

Formation of orthoacetate **4.60** results from nucleophilic attack of acceptor **4.52** at the C2 position of the dioxolane ring of the acyloxonium ion intermediate **4.61** (Path B) rather than at the anomeric center of intermediate **4.61** (Path A) (**Scheme 4.30**). Importantly, not only was **4.60** the undesired product, but its formation complicated chromatographic isolation of the desired disaccharide as the desired and undesired disaccharide products were extremely close in polarity. In an attempt to alleviate orthoacetate formation, TMSOTf was substituted for the milder $\text{BF}_3 \cdot \text{OEt}_2$ while keeping all other reaction parameters consistent (**Table 4.1**). However, this change proved only

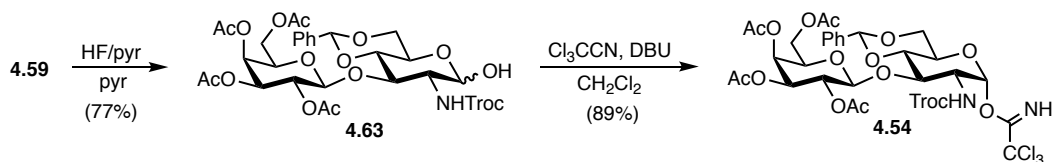
to promote orthoacetate isolation as under these conditions orthoacetate **4.60** was the sole glycosylation product isolated, albeit in a meager 23% yield.

We next hypothesized that orthoacetate formation could be mitigated by raising the temperature of the reaction and retaining TMSOTf as the promoter (**Table 4.1**). In the first attempt, raising the reaction temperature to -10 °C resulted in formation of the desired disaccharide **4.59** in 76% yield without any contaminant orthoacetate formation. Unfortunately, once again, this result was not reproducible in a second attempt. The second attempt at -10 °C yielded the disaccharide in only 28% yield while orthoacetate **4.60** was isolated as the major product in 40% yield. Similarly, inconsistent desired to undesired disaccharide product ratios were seen at 0 °C. Notably, it was found that orthoacetate **4.60** could be rearranged to the desired disaccharide via treatment with an equimolar quantity of acceptor **4.52** and catalytic TMSOTf in acetonitrile at 0 °C. However, the yield of disaccharide **4.59** was low. Finally, the reaction temperature was raised to room temperature. While at this temperature no orthoacetate product was isolated, the yield of disaccharide **4.59** was highly inconsistent and was accompanied by the formation of several unidentifiable by-products.

Due to significant quantities of orthoacetate formation as well as the consistent lack of any α -glycoside formation, it became clear that the C2 acetate of donor **4.18** was sufficient to promote β -glycoside formation, i.e. the use of β -directing acetonitrile was unnecessary. Thus, we elected to change the reaction solvent from acetonitrile to dichloromethane; dichloromethane is a non-participating solvent commonly used in glycosylation reactions. Moreover, it appeared that lower reaction temperatures and milder promoters facilitated preferential orthoacetate formation. Consequently, TMSOTf

was again selected as the promoter and the reaction temperature was raised to 0 °C. Satisfyingly, using these reaction parameters, the desired disaccharide was isolated consistently in yields exceeding 70% without the accompanying formation of any orthoacetate (**Table 4.1**). Moreover, this glycosylation was performed on gram scale without any decrease in yield. As expected, lowering of the reaction temperature to -78 °C resulted in exclusive orthoacetate formation (again, albeit in low yield) despite the use of TMSOTf and dichloromethane.

After obtaining gram quantities of disaccharide **4.59**, the β -silyl ether was removed via treatment with a 70% solution of HF in pyridine to yield lactol **4.63** in 77% yield (**Scheme 4.31**). It should be noted that silyl deprotection was also attempted using TBAF, both neat and with acetic acid, but this method resulted in low yields of the corresponding lactol. Finally, lactol **4.63** was treated with trichloroacetonitrile and DBU to afford α -imidate donor **4.54** in 89% yield.

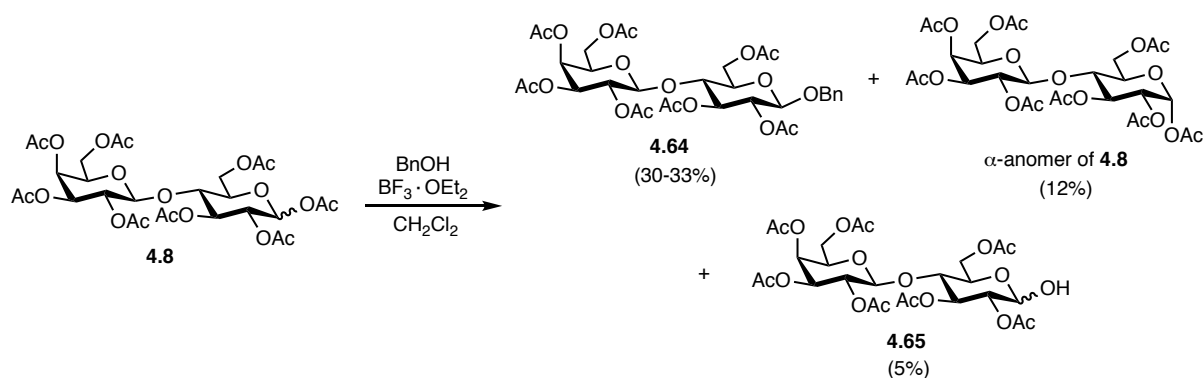


Scheme 4.31. Synthesis of lacto-*N*-biose donor **4.54**.

4.5.4 Synthesis of Lactose Acceptor **4.53**

Synthesis of acceptor **4.53** commenced with conversion of LOA **4.8** (in the form of an α/β mixture of the reducing end acetate) to the corresponding anomeric β -benzyl ether **4.64** (**Scheme 4.32**). In a first-generation approach, this transformation was accomplished by activating the anomeric acetate of **4.8** with $\text{BF}_3 \cdot \text{OEt}_2$ followed by treatment with benzyl alcohol. However, this approach proved problematic. First, the α -

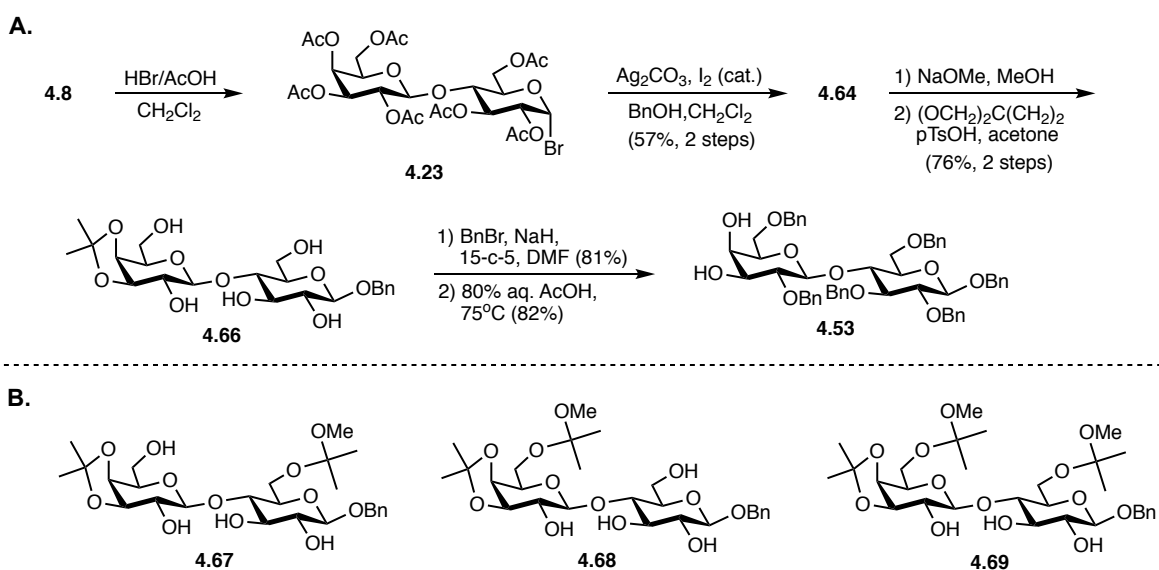
acetate of **4.8** was found to be unreactive towards activation with $\text{BF}_3 \cdot \text{OEt}_2$ and subsequent displacement by benzyl alcohol. This lack of reactivity was largely accountable for the low yields of benzyl ether **4.64**. Second, chromatographic separation of the desired benzyl ether from unreacted α -acetate starting material proved to be extremely difficult. Third, formation of the desired benzyl glycoside was accompanied by formation of the undesired lactol **4.65**, which also proved difficult to separate from the desired product.



Scheme 4.32. First-generation approach to acetylated β -benzyl lactoside **4.64**.

In the second-generation approach, acetylated β -benzyl lactoside **4.64** was synthesized via Koenigs-Knorr glycosylation of known acetylated lactosyl bromide **4.23** with benzyl alcohol (**Scheme 4.33A**).⁵⁹ Bromide **4.23** was synthesized in one step from LOA **4.8** by treatment with a 33% HBr in acetic acid solution. The crude bromide was then treated with silver carbonate and benzyl alcohol to yield the desired β -benzyl lactoside **4.64** in 58% yield over 2 steps. Unlike the first-generation approach, chromatographic separation of **4.64** from any reaction by-product(s) proved facile. Reaction of **4.64** with NaOMe in methanol followed by reaction with excess 2,2-DMP and catalytic pTsOH in acetone furnished the 3',4'-acetonide **4.66** in 76% over the 2-step sequence;⁷⁴ the 4',6'-

acetone (not pictured) was rarely observed. Interestingly, use of an extreme excess of 2,2-DMP (≥ 10 eq.) resulted in very low yields of **4.66** ($< 10\%$). Instead, the major products were suspected (based on NMR analysis) to be the 3',4'-acetone wherein a molecule of 2,2-DMP was appended to the C6 alcohol (**4.67**), C6' alcohol (**4.68**), or both alcohols (**4.69**) (**Scheme 4.33B**). From 3',4'-acetone **4.66**, lactose acceptor **4.53** could be accessed via perbenzylation of **4.66** followed by acid-mediated acetone removal to reveal the diol (**Scheme 4.33A**).



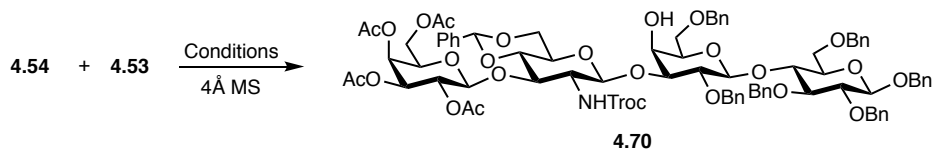
Scheme 4.33. Synthesis of lactose acceptor **4.53**. **(A)** Reaction sequence to **4.53**. **(B)** Suspected side-products in formation of 3',4'-acetone **4.66** when using ≥ 10 eq. of 2,2-dimethoxypropane (2,2-DMP).

It is important to note that although the C3' and C4' alcohols of acceptor **4.53** were both free, we hypothesized that glycosylation would occur selectively at the equatorial C3' alcohol over the axial C4' alcohol. Indeed, this selectively had been demonstrated in previous reports from the Danishefsky and Schmidt laboratories.^{68, 74, 75}

4.5.5 Synthesis of Lacto-N-Tetraose

For the initial attempt at uniting LNB donor **4.54** and lactose acceptor **4.53** to yield tetrasaccharide **4.70**, we elected to use catalytic TMSOTf as the promoter, dichloromethane as the reaction solvent, and a reaction temperature of 0 °C due to the success of these conditions in the first glycosylation between galactose trichloroacetimidate donor **4.18** and glucosamine acceptor **4.52**. Surprisingly, these conditions gave rise to a complex product mixture (**Table 4.2**). Attempts to lower the reaction temperature to -65 °C and further dilute the reaction did not remedy the situation as complex product mixtures were again observed.

Table 4.2. Attempted Glycosylations to Yield LNT Tetrasaccharide **4.70**



Entry	Promoter	Conc. (M)	Temp (°C)	Result
1	TMSOTf (cat.)	0.2	-5	complex mixture
2	TMSOTf (cat.)	0.05	-65	complex mixture
3	BF ₃ •OEt ₂ (cat.)	0.05	-20	low reactivity
4	BF ₃ •OEt ₂ (xs)	0.05	-20	decomposition
5	AgOTf (xs)	0.1	r.t.	no reactivity
6	MeOTf (cat.)	0.05	-35	low reactivity
7	MeOTf (xs)	0.05	-15 to r.t.	decomposition
8	TfOH (cat.)	0.05	-65	complex mixture
9	TfOH (cat.)	0.025	-20	decomposition

Due to the failure of TMSOTf to promote a clean reaction at a range of temperatures, more mild promoters were tested including BF₃•OEt₂, AgOTf, and MeOTf (**Table 4.2**). Unfortunately, glycosylation with these promoters largely suffered from an

apparent lack of donor activation, and increasing the amount of promoter did not improve glycosylation outcome. Subsequent attempts at uniting donor **4.54** and acceptor **4.53** relied on TfOH as the promoter. As a stronger promoter than $\text{BF}_3 \cdot \text{OEt}_2$, AgOTf, and MeOTf, we reasoned that TfOH-mediated glycosylations would not suffer from a lack of donor activation. While TMSOTf is a similarly strong activator, the difficulties encountered in storing this Lewis acid and the continued need for distillation of the reagent prompted the switch to TfOH. Once again, however, complex product mixtures were observed in TfOH-promoted glycosylations between **4.54** and **4.53** at reaction temperatures ranging from -70 to -20 °C.

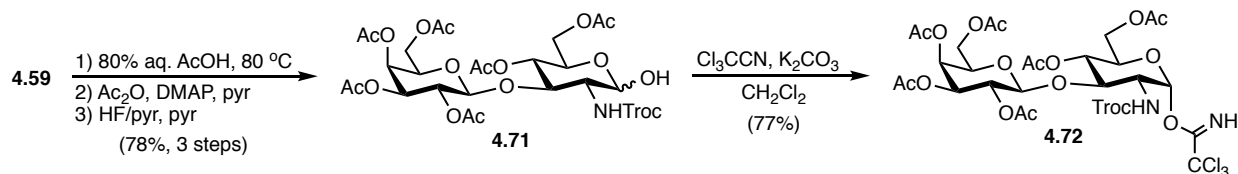
Though NMR analysis of the product mixtures did not allow for a definite judgment of whether or not the desired tetrasaccharide was formed, there was evidence that we had united the LNB and lactose components. However, the configuration of this union remained unknown. Indeed, the LNB component could have been added to either the C3' or C4' alcohol of lactose acceptor **4.53**, or both. Moreover, though it was hypothesized that any newly formed glycosidic linkage would be β -oriented due to the Troc protecting group at the C2 amine of donor **4.54**, NMR analysis did not allow us to rule out the possibility that an α -linkage had formed. Finally, although we observed no compatibility issues with the benzylidene acetal in glycosylations between glucosamine acceptor **4.52** and galactose donor **4.18**, we nevertheless hypothesized that this acetal might not be compatible in the current glycosylation and that this lack of compatibility could be contributing to the observed glycosylation product mixture.

In an attempt to deconvolute the product mixtures resulting from TfOH-promoted glycosylations, we treated the mixtures with acetic anhydride to “cap” any remaining free

alcohols. Unfortunately, while this step did separate some byproducts from others, it never facilitated isolation and characterization of single compounds or characterization of single compounds within in a mixture. Moreover, attempts to carry the various acetylated glycosylation product mixtures through to the Troc removal step were similarly unfruitful.

4.5.6 Second-Generation Approach to Lacto-N-Tetraose

As discussed previously in section 4.3.3, cyclic protecting groups like the benzylidene acetal are known to have a disarming effect on glycosyl donors. Indeed, this class of donor rigidifies the ring which serves to restrict formation of the oxocarbenium ion intermediate.^{33, 34, 76} We therefore hypothesized that the benzylidene acetal of donor **4.54** was responsible for the low donor reactivity observed in several of the aforementioned glycosylation attempts. We further hypothesized that due to this lowered reactivity, the glycosylation promoters employed might be engaging the oxygens of the acetal and consequently facilitating various levels of acetal cleavage. Importantly, this result would be at least partially responsible for the mixture of products observed.



Scheme 4.34. Synthesis of second-generation, peracetylated LNB donor **4.72**.

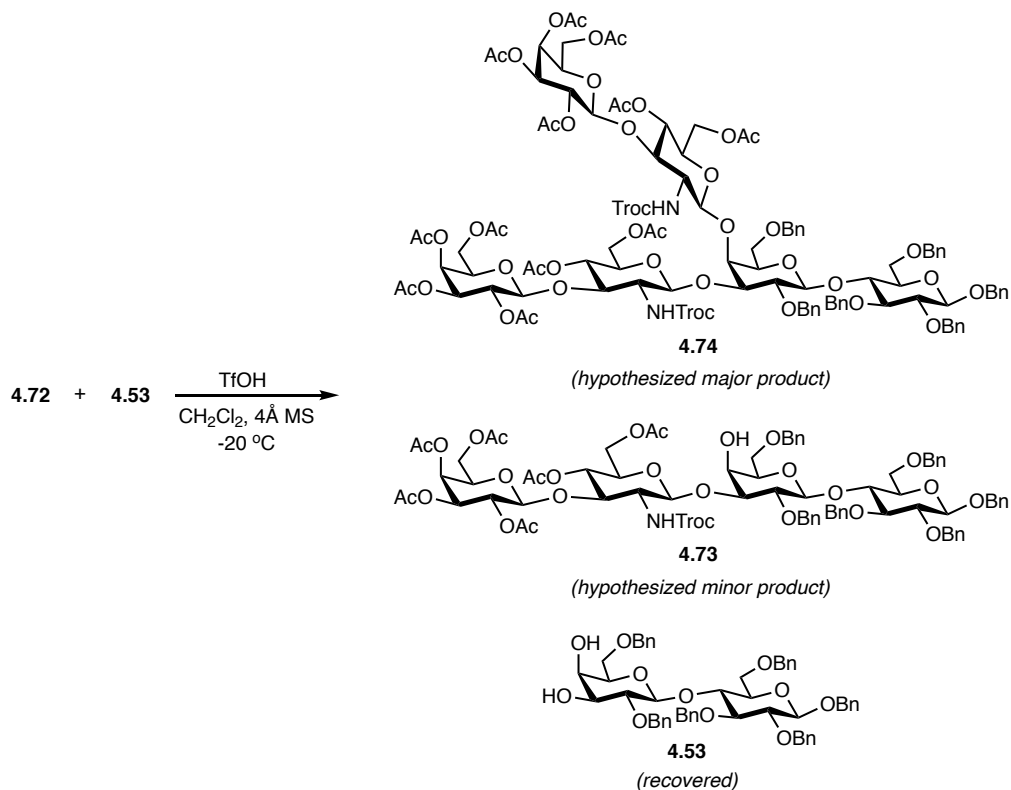
To circumvent the poor reactivity of acetal donor **4.54**, the acetal was first removed via treatment of **4.59** with 80% aqueous acetic acid at 80 °C (**Scheme 4.34**). The resulting crude diol was then acetylated followed by HF-mediated removal of the β -silyl ether to

yield lactol **4.71** in 78% over the 3-step sequence. Finally, lactol **4.71** was converted to α -trichloroacetimidate donor **4.72** in 77% yield by treatment with potassium carbonate and trichloroacetonitrile; although this method is characteristic of β -trichloroacetimidate formation, prolonged reaction times allow for equilibration to the more stable α -imidate. It is important to note that initial attempts to form α -imidate **4.72** did rely on typical DBU and trichloroacetonitrile conditions. Surprisingly however, these conditions proved unreliable as frequent decomposition was observed. Thus, in an attempt to lessen this degradation, potassium carbonate and prolonged reaction times were used to generate the desired imidate.

With new LNB donor **4.72** in hand, we once again attempted to glycosylate with lactose diol acceptor **4.53** to form the final glycosidic linkage to furnish LNT tetrasaccharide **4.73**. Due to the strong electron-withdrawing nature of donor **4.72**, TfOH was again selected as the glycosylation promoter. While TMSOTf is a similarly strong activator, TfOH was once again selected owing to its increased ease of continued use and storage compared to TMSOTf. Unfortunately, glycosylation between donor **4.72** and acceptor **4.53** did not proceed as smoothly as expected as once again multiple glycosylation products were obtained (**Scheme 4.35**).

Notably, the product mixture obtained for the current glycosylation was much simpler than that seen in the first-generation approach to LNT. Indeed, although we were unable to fully characterize and thus confirm formation of the desired tetrasaccharide **4.73**, extensive NMR analysis and low-resolution mass spectral data suggested that **4.73** had in fact been formed. However, similar analyses suggested that this tetrasaccharide was not the major product formed. Rather, it appeared as if hexasaccharide **4.74**, resulting

from glycosylation at both the C3' and C4' alcohols of acceptor **4.53**, was the prime glycosylation product (**Scheme 4.35**). The recovery of significant quantities of unreacted acceptor **4.53** further supported this conclusion

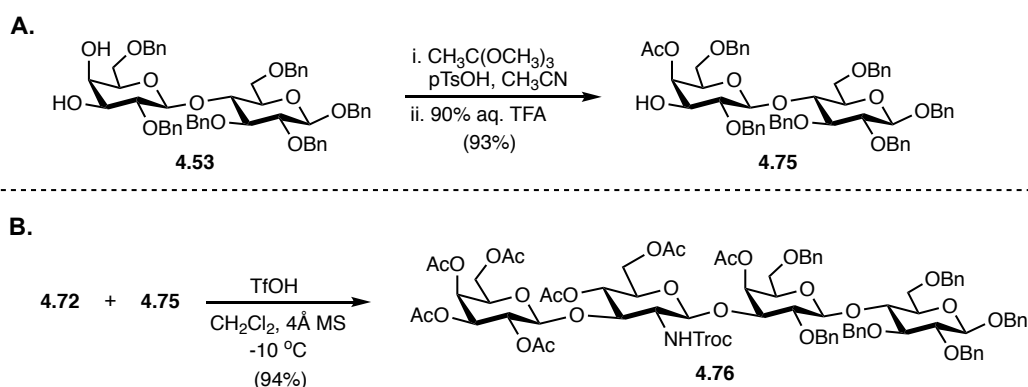


Scheme 4.35. Hypothesized result of second-generation glycosylation towards LNT tetrasaccharide **4.73**.

In an attempt to better exploit the hypothesized increased reactivity of the equatorial C3' alcohol over the axial C4' alcohol and consequently mitigate formation of the suspected di-glycosylated **4.74**, donor **4.72** was added dropwise to a solution of acceptor **4.53** and TfOH in dichloromethane. Despite numerous attempts at this order of addition, hexasaccharide **4.74** remained the suspected major glycosylation product. The lack of selective reactivity at the C3' over C4' alcohols was later found to be consistent with prior reports of glycosylations using extensively benzylated, electron-rich acceptors like **4.53**.⁶⁸ We therefore hypothesized that glycosylation would be improved by protecting

the C4' alcohol of diol acceptor **4.53**. Notably, the aforementioned chemical syntheses of LNT by the Tejumia and Schmidt laboratories as well as the chemical synthesis of LNT-Pro₃ reported by the Chen laboratory featured lactose acceptors with only the C3' alcohol free.

Selective C4' alcohol protection of lactose diol **4.53** was accomplished using a simple two-step, one-pot procedure reported previously by Nicolaou et al.⁷⁷ Treatment of diol **4.53** with trimethyl orthoacetate and pTsOH followed by treatment with 90% aqueous trifluoroacetic acid (TFA) furnished known C4' acetate **4.75** in 93% yield (**Scheme 4.36**).⁷⁸ With new lactose acceptor in hand, we once again attempted glycosylation with peracetylated, trichloroacetimidate LNB donor **4.72**. Satisfyingly, use of TfOH, dichloromethane, and a reaction temperature of -10 °C cleanly yielded the desired tetrasaccharide **4.76** in 88% on the first attempt to give 73 mg of **4.76**. Notably, with these conditions, glycosylation with **4.72** and **4.75** was performed to yield 850 mg of tetrasaccharide **4.76** in a single glycosylation event which corresponded to an improved yield of 94%.

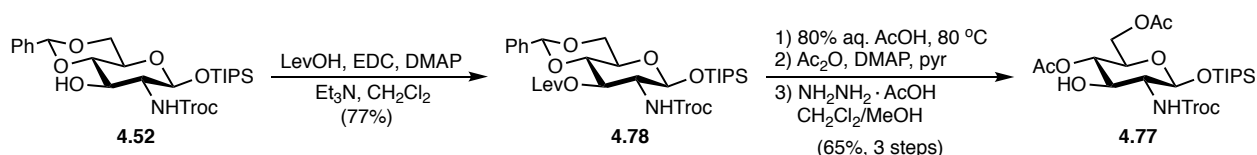


Scheme 4.36. Synthesis of fully protected LNT tetrasaccharide **4.76**. **(A)** Synthesis of second-generation axially-acetylated lactose acceptor **4.75**. **(B)** Glycosylation between peracetylated LNB trichloroacetimidate donor **4.72** and lactose acceptor **4.45** to yield tetrasaccharide **4.76**.

From fully protected tetrasaccharide **4.76**, a three-step deprotection sequence was envisioned to yield LNT (**2.4**). Prior to deprotection attempts, however, we attempted to improve the route to **4.76** by revisiting the first glycosylation to yield an LNB disaccharide.

4.5.7 Second-Generation Approach to Lacto-*N*-Biose Donor **4.72**

In the first-generation route to donor **4.72**, the benzylidene acetal of the glucosamine residue was removed after glycosylation between glucosamine acceptor **4.52** and galactose donor **4.18** (see **Scheme 4.34**). As previously described, this manipulation proved particularly advantageous in the campaign to access a protected LNT-derivative cleanly and in high yields. While the two-step conversion of LNB acetal **4.59** to the corresponding diacetate was high yielding, we noted that it would be preferential to perform these manipulations on a simpler substrate, i.e. remove the glucosamine acetal from monosaccharide **4.52** as opposed to LNB disaccharide **4.59**, which was obtained through glycosylation.

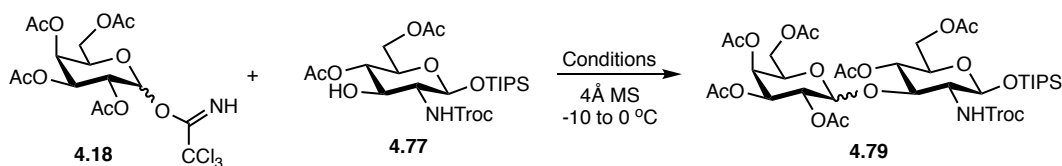


Scheme 4.37. Synthesis of second-generation, acetylated glucosamine acceptor **4.77**.

Synthesis of second-generation, peracetylated glucosamine acceptor **4.77** began with protection of the free C3 alcohol of glucosamine acceptor **4.52** as the corresponding levulinic (Lev) ester (**Scheme 4.37**). This transformation was accomplished by 1-ethyl-3-(3-dimethylaminopropyl)carbodiimide (EDC)-mediated coupling of glucosamine alcohol **4.52** with levulinic acid to yield Lev ester **4.78** in 77% yield. The benzylidene acetal of **4.78** was then cleaved through treatment with 80% aqueous acetic acid at 80 °C and the

corresponding diol treated with acetic anhydride in pyridine to yield the diacetate (structure not pictured). Lev deprotection using hydrazine acetate then furnished second-generation, acetylated glucosamine acceptor **4.77** in 65% over the three-step sequence.

Table 4.3. Attempted Glycosylations to Yield LNB Disaccharide **4.79**



Entry	Donor	Promoter	Solvent	Conc. (M)	% Yield	α : β	% R.A. ^a
1	α ; 1.3 eq.	TMSOTf (cat.)	CH ₂ Cl ₂	0.08	39	1:2.5	0
2	α ; 2.0 eq.	BF ₃ •OEt ₂ (cat.)	CH ₂ Cl ₂	0.08	trace	--	≥ 50
3	α ; 1.5 eq.	TfOH (cat.)	CH ₂ Cl ₂	0.08	72	1:7	14
4	α ; 2.0 eq.	TfOH (cat.)	CH ₂ Cl ₂	0.08	72	1:2.8	15
5	α / β , 1.5 eq.	TfOH (cat.)	CH ₂ Cl ₂	0.08	70	1:2.3	16
6	α ; 2.0 eq.	TfOH (xs)	CH ₂ Cl ₂	0.08	83	1:2.8	9
7	α ; 1.5 eq.	TfOH (cat.)	PhCH ₃ /CH ₂ Cl ₂ (1.2:1)	0.05	76	1:4.4	6
8	α ; 2.0 eq.	TfOH (cat.)	PhCH ₃ /CH ₂ Cl ₂ (3.7:1)	0.05	74	1:4.3	12
9	α ; 1.5 eq.	TfOH (xs)	PhCH ₃ /CH ₂ Cl ₂ (1.9:1)	0.08	71	1:2	0
10	α ; 2.0 eq.	TfOH (xs)	PhCH ₃ /CH ₂ Cl ₂ (2.8:1)	0.08	85	1:3.2	trace

^aR.A. = recovered acceptor

Glycosylation of new glucosamine acceptor **4.77** with galactose donor **4.18** to yield LNB disaccharide **4.79** initially employed the conditions used for the first-generation approach to LNB disaccharide **4.59**: TMSOTf (cat.) as the promoter, dichloromethane as the solvent, and a reaction temperature between -10 and 0 °C (specifically -5 °C in the present glycosylation) (**Table 4.3**). Notably, under these conditions, a lack of product

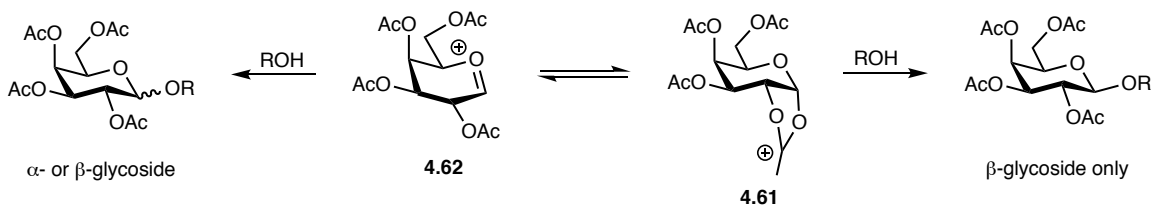
formation was observed and unreacted acceptor **4.77** remained. Thus, additional TMSOTf was added to push the reaction to completion. Although the reaction proceeded to completion, an unexpected result emerged.

Although donor **4.18** featured a C2 acetate capable of NGP that facilitates β -glycoside formation, a mixture of the α and β isomers of disaccharide **4.79** was isolated. The desired β -anomer was the major product isolated in 28% yield while the α -anomer was isolated in only 11% yield (**Table 4.3**); the diminished overall yield is hypothesized to be due to product decomposition resulting from treatment with an excess of TMSOTf. It is important to note, that due to similar polarities, the α and β products proved difficult to separate from one another. Moreover, attempts to carry the anomeric mixture through to the next reaction in the hopes that this would facilitate separation were unfruitful.

A lack of reactivity and corresponding product formation was again seen when $\text{BF}_3 \cdot \text{OEt}_2$ was used as the promoter (**Table 4.3**). Despite the use of excess $\text{BF}_3 \cdot \text{OEt}_2$, and excess donor, only a trace amount of either the α or β disaccharide was isolated. In agreement with this result, a significant amount of unreacted acceptor was recovered. Interestingly, based on NMR analysis, it was suspected that the acetylated galactosyl α -fluoride was a minor byproduct of the reaction. This result would agree with previous reports of glycosyl trichloroacetimidates being transformed into their corresponding fluorides upon treatment with $\text{BF}_3 \cdot \text{OEt}_2$.^{45, 79, 80} It has been proposed that this conversion is caused by reaction of the trichloroacetimidate donor with HF present in the $\text{BF}_3 \cdot \text{OEt}_2$. Moreover, literature precedent suggests that conversion to the fluoride is more likely to occur when using a significantly disarmed donor or a weakly nucleophilic acceptor.

Due to the obvious need for a strong activator, we next elected to test TfOH as the glycosylation promoter. Unfortunately, although activation with catalytic TfOH increased overall yield, it did not prevent formation of the α -linked disaccharide (**Table 4.3**). The highest α/β product ratio that could be obtained was 1:7. This result was accomplished using catalytic TfOH in dichloromethane with 1.5 equivalencies of donor. It is important to note, however, that this result proved highly variable. Indeed, in a later attempt on a larger scale, these conditions gave a comparable overall yield of 78%, but the α/β ratio was a mere 1:2.1. Finally, use of an α/β imidate donor **4.18** mixture (1:6, α/β) did little to improve reaction selectivity. This donor mixture also failed to solve another shortcoming of the reaction: recovered unreacted acceptor.

In all cases, treatment with catalytic TfOH was accompanied by the recovery of unreacted acceptor. Although this material could be recycled, its presence further complicated purification of the desired β -glycoside. Surprisingly, increasing the amount of donor did little to mitigate recovery of unreacted acceptor (**Table 4.3**). As a final note, increasing the equivalences of TfOH did little to improve α/β product ratios or to decrease the amount of acceptor recovered.



Scheme 4.38. Proposed mechanistic explanation for the formation of both α and β glycosides despite a C2 participating functionality on galactose donor **4.18**.

Formation of the unexpected α -anomer is hypothesized to be a result of the decreased nucleophilicity of acceptor **4.77**; nucleophilicity is decreased due to the

addition of electron-withdrawing acetate protecting groups at the C4 and C6 alcohols. As illustrated generically in **Scheme 4.4** in section 4.5.3 and recapitulated specifically for the present reaction conditions in **Scheme 4.38**, glycosylation with peracetylated trichloroacetimidate donor **4.18** proceeds through acyloxonium ion intermediate **4.61** (generated by NGP by the C2 acetate). Subsequent S_N2-like attack of a glycosyl acceptor at the anomeric center of intermediate **4.61** generates the β -glycoside. Importantly, acyloxonium ion intermediate **4.61** is in equilibrium with oxocarbenium ion intermediate **4.62**. Thus, it is possible that in the presence of a particularly unreactive acceptor, a portion of intermediate **4.61** has ample time to convert back to **4.62**. Unlike attack at the anomeric center of acyloxonium ion **4.61**, attack at the anomeric center of oxocarbenium ion **4.62** can generate either the α or β glycoside (**Scheme 4.38**).

Due to the previously encountered issues with orthoacetate formation when using the participating, highly-polar acetonitrile as the glycosylation solvent, we decided to investigate the effect of toluene, a solvent with a lower polarity than dichloromethane, on the outcome of the current glycosylation. Low solubilities of **4.18** and **4.77** in toluene, however, precluded exclusive use of toluene as the sole reaction solvent. Therefore, reactions were run in a mixture of toluene and dichloromethane. Unfortunately, this did little to improve the α/β product ratios or the amount of unreacted acceptor recovered (**Table 4.3**).

As a result of the inability to prevent α -glycoside formation as well as the difficulties encountered in separating the α and β products from one another, the second-generation route to LNB donor **4.72** was abandoned in favor of the first-generation route.

4.5.8 Deprotection of Tetrasaccharide **4.76** to Afford Lacto-N-Tetraose

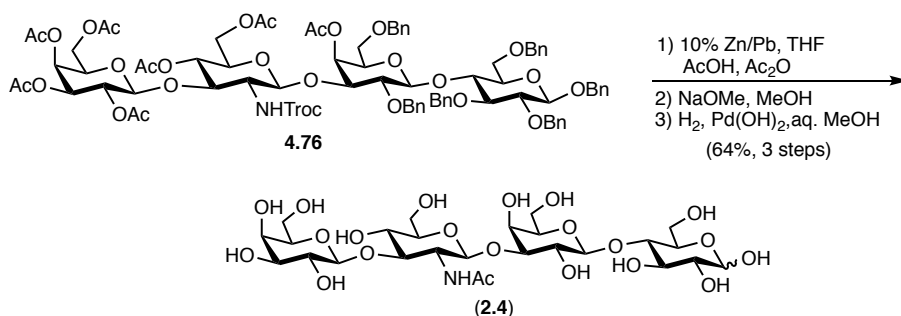
As previously mentioned, a three-step deprotection sequence was hypothesized to yield LNT (**2.4**) from fully protected LNT tetrasaccharide **4.76**. The first step of this deprotection sequence consisted of Troc cleavage with *in situ* acetamide formation. For this transformation, we initially employed standard Zn/AcOH/Ac₂O in THF conditions.⁸¹⁻⁸⁵ While these conditions did yield the desired acetamide (not pictured), the reactions generally failed to proceed to completion even when using an extreme excess of activated Zn and extended reaction times (≥ 24 h). Moreover, formation of the desired product was often accompanied by the formation of unknown side-products, which forced chromatographic purification of the desired acetamide. Importantly, this purification proved difficult and contributed to low yields of the desired acetamide.

In an attempt to improve reaction outcome, several reaction parameters were altered; in all cases, an extreme excess of activated zinc was used. First, different ratios of THF/AcOH/Ac₂O were investigated. Unfortunately, deviation from the original 3:2:1 THF/AcOH/Ac₂O, including removal of THF altogether, had little effect on reaction outcome. Second, we investigated the effect of delayed addition of Ac₂O.⁶⁸ Once again, this change did little to improve reaction outcome. Finally, various zinc activation methods were employed including activation with 2% and 5% HCl solutions, elemental iodine (I₂), and a combination of HCl and I₂ activation. While zinc activated by these various methods proved effective on simpler substrates, they did not improve the outcome of Troc deprotection and acetamide formation on tetrasaccharide **4.76**.

While Zn/AcOH is a standard method for Troc deprotection, it has been shown that this method often results in only partial cleavage of the carbamate.^{84, 85} Reexamination of

the literature, however, revealed a less conventional Zn-mediated cleavage method that was shown to have success. In separate reports from the Overman and Boger laboratories, a 10% Zn/Pb couple in THF and AcOH was found to effect efficient and high-yielding conversions of Troc-protected amines into the corresponding free amines.^{86, 87} Satisfyingly, treatment of tetrasaccharide **4.76** with 10% Zn/Pb couple in 3:2:1 THF/AcOH/Ac₂O resulted in full conversion to the corresponding amide without the formation of detectable side-products (**Scheme 4.39**). It has been hypothesized that formation of a Zn/metal couple serves to increase the surface area of the reactive zinc thus facilitating Zn-mediated reduction. Notably, use of a 10% Cd/Pb couple gave comparable results.⁸⁸

Following clean Troc deprotection and acetamide formation, deacetylation of the crude acetamide was affected by treatment with NaOMe. Finally, hydrogenation using Pearlman's catalyst facilitated cleavage of the benzyl ethers to yield fully deprotected, crude LNT (**2.4**). Purification of the crude tetrasaccharide using size exclusion chromatography ultimately furnished LNT in 64% over the three-step deprotection sequence (**Scheme 4.39**).



Scheme 4.39. Deprotection of fully protected LNT tetrasaccharide **4.76** to yield LNT (**2.4**).

4.6 Conclusion

In summary, LNT was synthesized from three readily accessible building blocks using a two-glycosylation approach. Notably, both glycosylations relied on the use of trichloroacetimidate donors to yield the desired β -glycosides reliably and in high yields. In these glycosylations, the protecting group strategies of the glucosamine and lactose moieties proved to be particularly impactful. In the first glycosylation between galactose donor and glucosamine acceptor, the 4,6-benzylidene acetal-protected glucosamine acceptor was superior to the corresponding 4,6-diacetate variant in generating the desired β -linked LNB disaccharide selectively and in high yield. The 4,6-benzylidene acetal-protected LNB disaccharide was then readily converted to the corresponding trichloroacetimidate donor for glycosylation with a lactose diol acceptor.

In this second glycosylation, both the 4,6-benzylidene acetal of the LNB donor and the presence of two free alcohols on the lactose acceptor proved problematic. Initial attempts demonstrated that the LNB acetal was incompatible with the glycosylation conditions employed. While conversion of the acetal to the corresponding diacetate improved glycosylation outcome, selective glycosylation at the equatorial C3' alcohol over the axial C4' alcohol of the lactose acceptor was never achieved. This selectivity issue was easily remedied by selectively acetylating the axial alcohol to generate a lactose acceptor featuring only the free C3' alcohol. Indeed, use of this second-generation lactose acceptor with the 4,6-diacetate LNB donor produced a fully-protected LNT derivative reliably and in high yield. Of note is the fact that this reaction was conducted to produce ca. 1 g of fully-protected LNT in a single glycosylation event.

From the fully-protected LNT derivative, a three-step deprotection sequence furnished LNT. The first step of this sequence, the Troc carbamate removal with *in situ* acetamide formation, was originally attempted using activated Zn. Unfortunately, this method proved to be slow, unreliable, and often resulted in incomplete conversion to the desired acetamide. However, substitution of the Zn for either a 10% Zn/Pb or 10% Cd/Pd couple resulted in faster, more reliable, and complete conversion to the acetamide. Subsequent deacetylation and debenzylation proceeded smoothly to generate LNT in consistent yields of over 50% (after final purification) for the three-step deprotection sequence. To date, our synthetic efforts towards LNT using the route described herein have yielded around 150 mg of fully deprotected LNT.

4.7 Experimental Methods

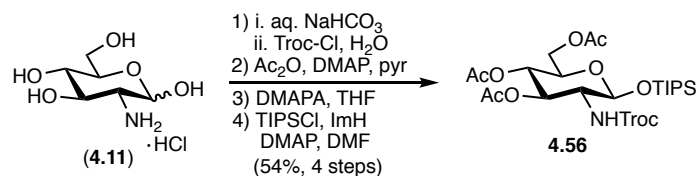
General Methods

Commercial reagents were used as received. Anhydrous solvents were taken from an MBRAUN solvent purification system (MB SPS) and stored over 4 Å or 3 Å molecular sieves. All moisture-sensitive reactions were performed in flame- or oven-dried round bottom flasks under an argon atmosphere. All air- or moisture-sensitive liquids were transferred via oven-dried stainless-steel syringes or cannula. Reaction temperatures were monitored and controlled via thermocouple thermometer and corresponding hot plate stirrer. Flash column chromatography was performed as described by Still et. al. using silica gel 230-400 mesh. Analytical thin-layer chromatography (TLC) was performed on glass-backed Silica gel 60 F₂₅₄ plates (EMD/Merck KGaA) and visualized using UV, cerium ammonium molybdate stain, and anisaldehyde stain.

Instrumentation

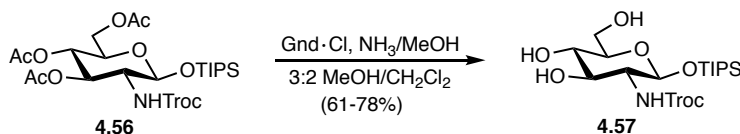
¹H NMR spectra were obtained on a Bruker 400 or 600 MHz spectrometer with reporting relative to deuterated solvent signals. ¹H NMR spectral data are presented as follows: chemical shifts (δ ppm), multiplicity (s=singlet, d=doublet, dd=doublet of doublets, t=triplet, q=quartet, p=pentet, m=multiplet, br=broad, app=apparent), coupling constants (J in Hz), integration, proton assignment. Deuterated chloroform was calibrated to 7.26 ppm. Deuterated methanol was calibrated to 3.31 ppm. Deuterium oxide was calibrated to 4.79 ppm. ¹³C NMR spectra were obtained on a Bruker 100 MHz or 150 MHz spectrometer with reporting relative to deuterated solvent signals. ¹³C NMR spectral data are presented as follows: chemical shifts (δ ppm), carbon assignment. Deuterated chloroform was calibrated to 77.16 ppm. Deuterated methanol was calibrated to 49.0 ppm. Proton and carbon assignments were made with the aid of 2D NMR techniques (COSY, HSQC, and HMBC). High resolution mass spectra were recorded on a high resolution Thermo Electron Corporation MAT 95XP-Trap by use of electro-spray ionization (ESI) by the Indiana University Mass Spectrometry facility and a SYNAPT G2 or SYNAPT G2-S spectrometer (Waters, for TOF-MS) by the McLean lab of Vanderbilt University. Low resolution mass spectra were recorded on a Thermo Scientific Dionex Ultimate 3000 HPLC system with MSQ Plus Mass Detector. Optical rotations were obtained using a Perkin Elmer 341 polarimeter.

Compound preparation



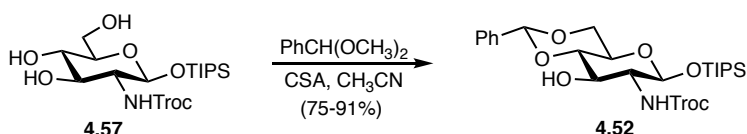
(2R,3S,4R,5R,6S)-2-(acetoxymethyl)-5-(((2,2,2-trichloroethoxy)carbonyl) amino)-6-((triisopropylsilyl)oxy)tetrahydro-2H-pyran-3,4-diyl diacetate (4.56). To a suspension of D-(+)-glucosamine hydrochloride (**4.11**) (1.0 eq, 3.0 g, 14 mmol) in H₂O (30 mL) was added NaHCO₃ (3.0 eq, 3.5 g, 42 mmol) at room temperature and the resulting mixture was stirred 1 H. 2,2,2-trichloroethyl chloroformate (5.0 eq, 9.4 mL, 70 mmol) was then added dropwise over 20 minutes. The reaction was stirred an additional 3 H after which a white solid had formed. The reaction was filtered, washed with additional H₂O (250 mL), and allowed to dry overnight. The crude Troc-protected glucosamine was coevaporated with benzene (3x) then dissolved in pyridine (130 mL) and acetic anhydride (5.0 eq, 6.6 mL, 70 mol) was added dropwise over 5 minutes. The resulting solution was stirred 6 H then was diluted with EtOAc (250 mL), washed with 2 N HCl (6 x 90 mL), brine (1 x 90 mL), dried (MgSO₄), filtered, and concentrated *in vacuo* to yield a pale-yellow foam. The crude tetraacetate was dissolved in THF (70 mL) and 3-(dimethylamino)-1-propylamine (DMAPA) (5.0 eq, 8.8 mL, 70 mmol) was added. The reaction was stirred 1 H and 15 minutes then was diluted with CH₂Cl₂ (130 mL), washed with 2 N HCl (2 x 60 mL), dried (MgSO₄), filtered, and concentrated *in vacuo* to yield a white foam. The crude lactol was dissolved in DMF (90 mL) and imidazole (2.0 eq, 1.9 g, 28 mmol), DMAP (cat), and chlorotriisopropylsilane (1.2 eq, 3.6 mL, 17 mmol) were added sequentially. The resulting solution was stirred 16 H then additional chlorotriisopropylsilane was added (1.5 mL). The reaction stirred an additional 22 H then was diluted with EtOAc (180 mL), washed with

H₂O (3 x 80 mL), 2N HCl (1 x 80 mL), brine (1 x 80 mL), dried (MgSO₄), filtered, and concentrated *in vacuo*. The crude product was purified via flash column chromatography (2:1 hexanes/EtOAc) to yield anomeric silyl ether **4.56** (4.87 g, 7.65 mmol, 55% over 4 steps) as a white solid: R_f 0.48 (2:1 hexanes/EtOAc); ¹H NMR (400 MHz, CDCl₃) δ 5.23 (t, *J*=10.1 Hz, 1H, H-3), 5.06 (d, *J*=8.6 Hz, 1H, NH), 5.04 (t, *J*=9.6 Hz, 1H, H-4), 4.89 (d, *J*=7.8 Hz, 1H, H-1), 4.75 (d, *J*=12.0 Hz, 1H, Troc CH), 4.61 (d, *J*=12.0 Hz, 1H, Troc CH), 4.15 (d, *J*=4.2 Hz, 2H, H-6a, H-6b), 3.72-3.61 (m, 2H, H-2, H-5), 2.06 (s, 3H, COCH₃), 2.03 (s, 3H, COCH₃), 2.02 (s, 3H, COCH₃), 1.12-1.01 (m, 21H, TIPS), 1.60 (s, H₂O); ¹³C (100 MHz, CDCl₃) δ 170.9 (COCH₃), 170.8 (COCH₃), 169.7 (COCH₃), 154.1 (Troc CO), 96.1 (C-1), 95.4 (Troc CCl₃), 74.8 (Troc CH₂), 72.1 (C-3), 71.9 (C-5), 69.1 (C-4), 62.6 (C-6), 58.7 (C-2), 20.8 (COCH₃), 17.9 (TIPS), 17.8 (TIPS), 12.3 (TIPS). HRMS (ESI) calcd for C₂₄H₄₀Cl₃NO₁₀Si [M+Na]⁺ 658.1385, found 658.1356.



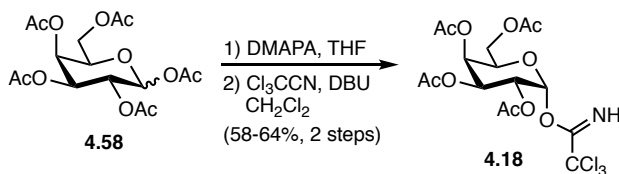
2,2,2-trichloroethyl((2S,3R,4R,5S,6R)-4,5-dihydroxy-6-(hydroxymethyl)-2-((triisopropylsilyl)oxy)tetrahydro-2H-pyran-3-yl)carbamate (4.57). To a solution of **4.56** (1.0 eq, 4.0 g, 6.3 mmol) in CH₂Cl₂ (60 mL) and MeOH (60 mL), was added guanidine hydrochloride (5.0 eq, 3.0 g, 31 mmol) and 7 N NH₃/MeOH (12.0 eq, 8.4 mL, 75 mmol) sequentially. The resulting solution was stirred 21 H then was neutralized with AcOH and concentrated *in vacuo*. The crude product was purified via flash column chromatography (10:1 CHCl₃/MeOH) to yield triol **4.57** (2.45 g, 4.80 mmol, 76%) as a white solid: R_f 0.41 (10:1 CH₂Cl₂/MeOH); ¹H NMR (400 MHz, MeOD) δ 4.73 (d, *J*=7.7 Hz, 1H, H-1), 4.70 (s,

2H, Troc CH, Troc CH), 3.84 (dd, $J=2.6, 11.8$ Hz, 1H, H-6a), 3.72 (dd, $J=5.0, 11.8$ Hz, 1H, H-6b), 3.47-3.33 (m, 3H, H-2, H-3, H-4), 3.23 (ddd, $J=2.6, 5.0, 9.0$ Hz, 1H, H-5), 1.16-1.07 (m, 21 H, TIPS), 1.98 (s, AcOH); ^{13}C (100 MHz, MeOD) δ 156.9 (Troc CO), 97.7 (C-1), 97.0 (Troc CCl_3), 77.7 (C-5), 75.8 (Troc CH_2), 75.7 (C-3), 72.3 (C-4), 62.8 (C-6), 61.5 (C-2), 18.4 (TIPS), 18.4 (TIPS), 13.5 (TIPS). HRMS (ESI) calcd for $\text{C}_{18}\text{H}_{34}\text{Cl}_3\text{NO}_7\text{Si}$ $[\text{M}+\text{Na}]^+$ 532.1068, found 532.1059.

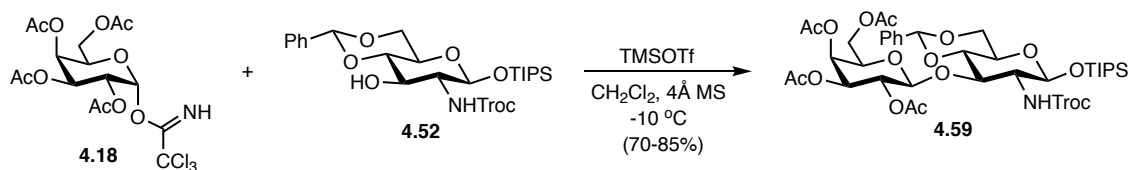


2,2,2-trichloroethyl((2R,4aR,6S,7R,8R,8aS)-8-hydroxy-2-phenyl-6-((triisopropylsilyl)oxy)hexahydropyrano[3,2-d][1,3]dioxin-7-yl)carbamate (4.52). To a solution of **4.57** (1.0 eq, 1.5 g, 2.9 mmol) in CH_3CN (30 mL) was added benzaldehyde dimethyl acetal (2.0 eq, 0.88 mL, 5.9 mmol). The reaction pH was adjusted between 2-4 using DL-10-camphorsulfonic acid and the reaction heated to 60°C . The reaction was stirred 2 H then was neutralized with Et_3N , diluted with EtOAc (70 mL), washed with water (2 x 30 mL), brine (1 x 30 mL), dried (MgSO_4), filtered, and concentrated *in vacuo*. The crude product was purified via flash column chromatography (6:1 hexanes/ EtOAc) to yield benzylidene acetal **4.52** (1.6 g, 3.0 mmol, 91%) as a white foam: R_f 0.60 (1:1 hexanes/ EtOAc); ^1H NMR (400 MHz, CDCl_3) δ 7.50-7.48 (m, 2H, aromatic), 7.40-7.36 (m, 3H, aromatic), 5.55 (s, 1H, benzylidene CH), 5.15 (d, $J=5.9$ Hz, 1H, NH), 4.92 (d, $J=7.5$ Hz, 1H, H-1), 4.74 (app d, $J=12.0$ Hz, 1H, Troc CH), 4.66 (app d, $J=11.9$ Hz, 1H, Troc CH), 4.29 (dd, $J=10.5, 4.9$ Hz, 1H, H-6a), 4.06-4.02 (m, 1H, H-3), 3.78 (t, $J=10.2$ Hz, 1H, H-6b), 3.58 (t, $J=9.2$ Hz, 1H, H-4), 3.49-3.36 (m, 2H, H-5, H-2), 1.15-1.03 (m, 21H, TIPS); ^{13}C (100 MHz, CDCl_3)

δ 154.6 (Troc CO), 137.2 (aromatic), 129.5 (aromatic), 128.5 (aromatic), 126.5 (aromatic), 102.1 (benzylidene CH), 96.2 (C-1), 95.3 (Troc CCl₃), 81.7 (C-4), 75.0 (Troc CH₂), 71.0 (C-3), 68.7 (C-6), 66.3 (C-5), 61.3 (C-2), 17.9 (TIPS), 12.3 (TIPS). HRMS (ESI) calcd C₂₅H₃₈Cl₃NO₇Si [M+Na]⁺ 620.1381, found 620.1367.



(2R,3S,4S,5R,6R)-2-(acetoxymethyl)-6-(2,2,2-trichloro-1-iminoethoxy)tetrahydro-2H-pyran-3,4,5-triyl triacetate (4.18). To a solution of **4.58** (1.0 eq, 1.0 g, 2.6 mmol) in THF (13 mL) was added 3-(dimethylamino)-1-propylamine (DMAPA) (5.0 eq, 1.6 mL, 12.8 mmol). The reaction was stirred 1.5 H then was diluted with CH₂Cl₂ (20 mL), washed with 2 N HCl (2 x 10 mL), dried (MgSO₄), filtered, and concentrated *in vacuo*. The crude lactol was dissolved in CH₂Cl₂ (18 mL) and cooled to 0 °C. To the cooled solution was added trichloroacetonitrile (5.0 eq, 1.3 mL, 13 mmol) followed by 1,8-diazabicyclo[5.4.0]undec-7-ene (DBU) (0.25 eq, 0.96 mL, 0.64 mmol). After 30 minutes, the reaction was allowed to warm to room temperature and stir an additional 5.5 H. The reaction was then filtered and concentrated *in vacuo*. The crude product was purified via flash column chromatography (1:1 hexanes/EtOAc) to yield α -trichloroacetimidate **4.18** (0.81 g, 1.6 mmol, 64% over 2 steps) as a pale-yellow foam: *R_f* 0.50 (1:1 hexanes/EtOAc). ¹H and ¹³C spectroscopy data were in accordance with literature data.⁵⁶



(2R,3S,4S,5R,6R)-2-(acetoxymethyl)-6-(((2R,4aR,6S,7R,8R,8aS)-2-phenyl-7-(((2,2,2-trichloroethoxy)carbonyl)amino)-6-((triisopropylsilyl)oxy)hexahydro pyrano[3,2-

d][1,3]dioxin-8-yl)oxy)tetrahydro-2H-pyran-3,4,5-triyl triacetate (4.59). Donor **4.18**

(1.4 eq, 1.46 g, 3.0 mmol) and acceptor **4.52** (1.0 eq, 1.27 g, 2.1 mmol) were

coevaporated with benzene (2 x 8 mL) and placed in a vacuum desiccator containing

P₂O₅ overnight. The donor/acceptor mixture was dissolved in CH₂Cl₂ (14 mL) and the

resulting solution was cannulated into a reaction flask containing 4 Å powdered molecular

sieves (2.7 g). The mixture was stirred under argon 1 h then cooled to -10 °C and TMSOTf

(0.1 eq, 0.038 mL in 0.2 mL CH₂Cl₂) was added. The reaction was stirred 10 minutes then

quenched with Et₃N. The reaction was diluted with CH₂Cl₂, filtered through celite, dried

(MgSO₄), filtered, and concentrated *in vacuo*. The crude residue was purified via flash

column chromatography (2:1 hexanes/EtOAc) to yield disaccharide **4.59** (1.59 g, 1.71

mmol, 81%) as a white foam: R_f 0.35 (1:1 hexanes/EtOAc); ¹H NMR (400 MHz, CDCl₃) δ

7.49-7.45 (m, 2H, aromatic), 7.40-7.34 (m, 3H, aromatic), 5.54 (s, 1H, benzylidene CH),

5.29 (d, *J*=2.8 Hz, 1H, H-4'), 5.19 (dd, *J*=8.4, 10.4 Hz, 1H, H-2'), 5.18 (d, *J*=8.0 Hz, NH),

5.11 (d, *J*=7.8 Hz, H-1), 4.92 (dd, *J*=3.4, 10.4 Hz, 1H, H-3'), 4.69 (s, 2H, Troc CH, Troc

CH), 4.68 (d, *J*=8.6 Hz, H-1'), 4.32 (t, *J*=9.2 Hz, H-3), 4.27 (dd, *J*=5.0, 10.6 Hz, 1H, H-6a),

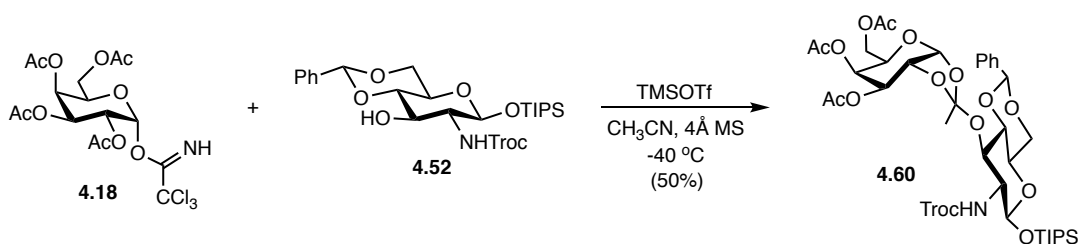
4.11 (q, EtOAc), 4.06 (dd, *J*=8.4, 10.6 Hz, 1H, H-6'a), 3.83 (dd, *J*=5.4, 10.7 Hz, 1H, H-

6'b), 3.78 (t, *J*=10.4 Hz, H-6b), 3.72 (t, *J*=9.2 Hz, 1H, H-4), 3.64 (t, *J*=6.7 Hz, 1H, H-5'),

3.50-3.44 (ddd, *J*=4.9, 9.7, 9.7 Hz, 1H, H-5), 3.28 (q, *J*=8.0 Hz, 1H, H-2), 2.11 (s, 3H,

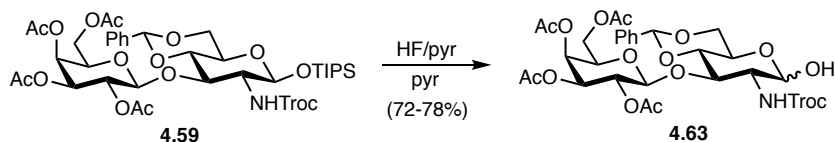
COCH₃), 2.04 (s, EtOAc), 2.03 (s, 3H, COCH₃), 1.95 (s, 3H, COCH₃), 1.93 (s, 3H, COCH₃),

1.62 (s, H₂O), 1.25 (t, EtOAc), 1.12-1.00 (m, 21H, TIPS), 0.06 (s, silicone grease); ¹³C (100 MHz, CDCl₃) δ 170.4 (COCH₃), 170.3 (COCH₃), 170.2 (COCH₃), 169.6 (COCH₃), 153.9 (Troc CO), 137.2 (aromatic), 129.4 (aromatic), 128.5 (aromatic), 126.2 (aromatic), 101.5 (benzylidene CH), 101.0 (C-1'), 95.3 (C-1), 95.2 (Troc CCl₃), 80.4 (C-4), 78.2 (C-3), 74.9 (Troc CH₂), 71.1 (C-3'), 70.6 (C-5'), 69.4 (C-2'), 68.8 (C-6), 67.0 (C-4'), 66.2 (C-5), 61.0 (C-6'), 60.7 (C-2), 20.9 (COCH₃), 20.8 (COCH₃), 20.7 (COCH₃), 20.7 (COCH₃), 17.9 (TIPS), 17.9 (TIPS), 12.3 (TIPS). HRMS (ESI) calcd for C₃₉H₅₆Cl₃NO₁₆Si [M+Na]⁺ 950.2332, found 950.2311.



(3aR,5R,6S,7S,7aR)-5-(acetoxymethyl)-2-methyl-2-(((2R,4aR,6S,7R,8R,8aS)-2-phenyl-7-(((2,2,2-trichloroethoxy)carbonyl)amino)-6-((triisopropylsilyl)oxy) hexahydro pyrano[3,2-d][1,3]dioxin-8-yl)oxy)tetrahydro-5H-[1,3]dioxolo[4,5-b]pyran-6,7-diyl diacetate (4.60). Donor **4.18** (1.3 eq, 0.16 g, 0.33 mmol) and acceptor **4.52** (1.0 eq, 0.15 g, 0.25 mmol) were coevaporated with benzene (2 x 4 mL) and placed in a vacuum desiccator containing P₂O₅ overnight. The donor/acceptor mixture was dissolved in CH₃CN (1.25 mL) and the resulting solution was cannulated into a reaction flask containing 4 Å powdered molecular sieves (0.4 g). The mixture was stirred under argon 1 H then cooled to -40 °C and TMSOTf (1 drop) was added. The reaction was stirred 1 H then quenched with Et₃N. The reaction was diluted with EtOAc (25 mL), filtered through celite, washed with water (3 x 10 mL), brine (1 x 10 mL), dried (MgSO₄), filtered, and

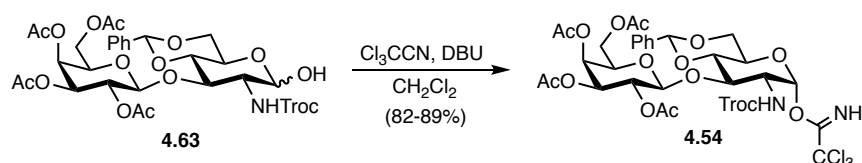
concentrated *in vacuo*. The crude residue was purified via flash column chromatography (2:1 hexanes/EtOAc) to yield orthoacetate **4.60** (0.115 g, 0.124 mmol, 50%) as a white foam: R_f 0.48 (2:1 hexanes/EtOAc); ^1H NMR (400 MHz, CDCl_3) δ 7.45-7.43 (m, 2H, aromatic), 7.35-7.33 (m, 3H, aromatic), 5.82 (d, $J=4.8$ Hz, 1H, H-1'), 5.51 (s, 1H, benzylidene CH), 5.33 (dd, $J=1.5, 3.2$ Hz, 1H, H-4'), 5.26 (d, $J=8.7$ Hz, 1H, NH), 4.94 (d, $J=7.2$ Hz, 1H, H-3'), 4.93 (d, $J=7.1$ Hz, 1H, H-1), 4.83 (d, $J=11.9$ Hz, 1H, Troc CH), 4.55 (d, $J=12.0$ Hz, 1H, Troc CH), 4.30-4.23 (m, 3H, H-6a, H-2', H-5'), 4.11-4.05 (m, 3H, H-6'a, H-3, H-6'b), 3.76 (t, $J=10.2$ Hz, 1H, H-6b), 3.60 (t, $J=9.3$ Hz, 1H, H-4), 3.45-3.36 (m, 2H, H-5, H-2), 2.08 (s, 3H, COCH_3), 2.04 (s, 3H, COCH_3), 2.01 (s, 3H, COCH_3), 1.65 (orthoacetate CH_3), 1.25 (m, grease), 0.06 (s, silicone grease), 1.11-1.02 (m, 21H, TIPS); ^{13}C (100 MHz, CDCl_3) δ 170.6 (COCH_3), 170.1 (COCH_3), 170.0 (COCH_3), 154.0 (Troc CO), 137.2 (aromatic), 129.2 (aromatic), 128.3 (aromatic), 126.2 (aromatic), 120.5 (orthoacetate C), 101.7 (benzylidene CH), 98.4 (C-1'), 96.6 (C-1), 95.2 (Troc CCl_3), 80.5 (C-4), 75.0 (Troc CH_2), 72.5 (C-2'), 71.6 (C-3'), 71.6 (C-3), 69.0 (C-5'), 68.7 (C-6), 66.5 (C-5), 65.8 (C-4'), 61.6 (C-6'), 60.3 (C-2), 25.1 (orthoacetate CH_3), 20.9 (COCH_3), 20.8 (COCH_3), 20.8 (COCH_3), 17.9 (TIPS), 17.8 (TIPS), 12.3 (TIPS). HRMS (TOF) calcd for $\text{C}_{39}\text{H}_{56}\text{Cl}_3\text{NO}_{16}\text{Si}$ $[\text{M}+\text{Na}]^+$ 950.2326, found 950.2365.



(2R,3S,4S,5R,6R)-2-(acetoxymethyl)-6-(((2R,4aR,6R,7R,8R,8aS)-6-hydroxy-2-phenyl-7-(((2,2,2-trichloroethoxy)carbonyl)amino)hexahydropyrano[3,2-d][1,3]dioxin-8-yl)oxy)tetrahydro-2H-pyran-3,4,5-triyl triacetate (4.63**). To a solution **4.59** (1.0 eq, 1.0**

g, 1.1 mmol) in pyridine (11 mL) cooled to 0 °C was added 70% HF in pyridine (5.4 mL) dropwise over 5 minutes. The solution was stirred 30 minutes then was allowed to warm to room temperature and stir an additional 4.5 H. The reaction was diluted with water (40 mL) and extracted with EtOAc (4 x 15 mL). The combined organics were quenched with solid NaHCO₃, and saturated NaHCO₃ solution, washed with 2 N HCl (3 x 20 mL), brine (1 x 20 mL), dried (MgSO₄), filtered, and concentrated *in vacuo*. The crude residue was purified via flash column chromatography (2:3 hexanes/EtOAc) to yield lactol **4.63** (0.64 g, 0.83 mmol, 77%) (α/β 2.2:1) as a white foam: *R*_f 0.38 (1:1 hexanes/EtOAc); ¹H NMR (400 MHz, CDCl₃) δ (α anomer) 7.48-7.45 (m, 2H, aromatic), 7.38-7.35 (m, 3H, aromatic), 5.55 (s, 1H, benzylidene CH), 5.54 (s, 0.45 H, minor anomer), 5.30-5.25 (m, 2H, H-1, H-4'), 5.19 (dd, *J*=8.0, 10.4 Hz, minor anomer), 5.17 (dd, *J*=8.0, 10.4 Hz, H-2'), 4.96 (d, *J*=12.0 Hz, 1H, Troc CH), 4.92 (dd, *J*=3.4, 10.5 Hz, 1H, H-3'), 4.80 (d, *J*=11.9 Hz, 0.45 H, minor anomer), 4.71 (m, 0.45 H, minor anomer), 4.69 (d, *J*=8.0 Hz, 1H, H-1'), 4.59 (d, *J*=12.1 Hz, 1H, Troc CH), 4.43 (m, 0.45 H, minor anomer), 4.33 (dd, *J*=4.9, 10.5 Hz, 0.45 H, minor anomer), 4.24 (dd, *J*=4.8, 10.3 Hz, 1H, H-6a), 4.14-3.98 (m, 4H, H-5, H-2, H-3, H-6'a), 3.83-3.71 (m, 3H, H-6'b, H-6b, H-4), 3.57 (t, *J*=6.7 Hz, 1H, H-5'), 3.52 (d, *J*=3.2 Hz, 1H, OH), 3.53-3.47 (m, 0.9 H, minor anomer), 2.11 (s, 1.35 H, minor anomer), 2.10 (s, 3H, COCH₃), 2.06 (s, 3H, COCH₃), 1.97 (s, 1.35 H, minor anomer), 1.95 (s, 1.35 H, minor anomer), 1.95 (s, 3H, COCH₃), 1.91 (s, 3H, COCH₃), 1.75 (br s, 0.45 H, minor anomer OH), 1.25 (m, grease), 0.06 (s, silicone grease); ¹³C (100 MHz, CDCl₃) δ 170.5 (COCH₃), 170.4 (minor anomer), 170.4 (COCH₃), 170.3 (COCH₃), 169.7 (COCH₃), 154.2 (Troc CO), 137.2 (aromatic), 137.0 (minor anomer), 129.5 (minor anomer), 129.4 (aromatic), 128.5 (aromatic), 126.2 (minor anomer), 126.1 (aromatic), 126.1 (aromatic),

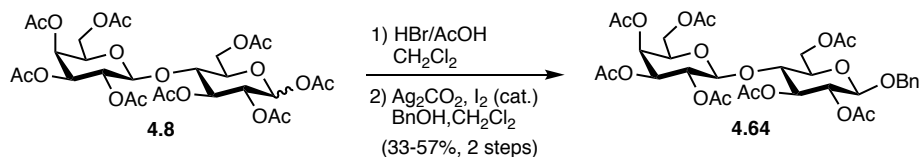
101.6 (minor anomer), 101.6 (benzylidene CH), 101.2 (C-1'), 95.5 (Troc CCl₃), 95.3 (minor anomer), 92.5 (C-1), 80.8 (C-4), 77.3 (C-3), 75.0 (Troc CH₂), 71.1 (C-3'), 71.0 (minor anomer), 70.8 (minor anomer), 70.6 (C-5'), 69.6 (C-2'), 69.4 (minor anomer), 69.0 (C-6), 68.7 (minor anomer), 66.9 (C-4'), 66.5 (minor anomer), 62.7 (C-5), 60.9 (C-6'), 54.8 (C-2), 20.8 (COCH₃), 20.8 (COCH₃), 20.7 (COCH₃). HRMS (ESI) calcd for C₃₀H₃₆Cl₃NO₁₆ [M+Na]⁺ 794.0997, found 794.1010.



(2R,3S,4S,5R,6R)-2-(acetoxymethyl)-6-(((2R,4aR,6R,7R,8R,8aS)-2-phenyl-6-(2,2,2-trichloro-1-iminoethoxy)-7-(((2,2,2trichloroethoxy)carbonyl)amino) hexahydro pyrano [3,2-d][1,3]dioxin-8-yl)oxy)tetrahydro-2H-pyran-3,4,5-triyl triacetate (4.54).

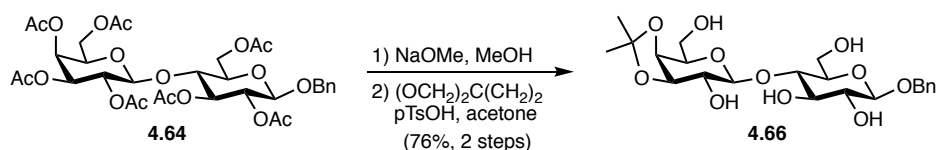
To a solution of **4.63** (1.0 eq, 0.35 g, 0.45 mmol) in CH₂Cl₂ (6.2 mL) cooled to 0 °C was added trichloroacetonitrile (10 eq, 0.45 mL, 4.5 mmol) followed by 1,8-diazabicyclo[5.4.0]undec-7-ene (DBU) (cat.). The reaction was stirred 1 H then was allowed to warm to room temperature and stir an additional 1 H. The reaction was concentrated and the crude residue purified via flash column chromatography (1:1 hexanes/EtOAc) to yield α -trichloroacetimidate **4.54** (0.36 g, 0.40 mmol, 89%) as a pale yellow powder: *R_f* 0.71 (1:1 hexanes/EtOAc); ¹H NMR (400 MHz, CDCl₃) δ 8.78 (s, 1H, imidate NH), 7.52-7.45 (m, 2H, aromatic), 7.40-7.35 (m, 3H, aromatic), 6.40 (d, *J*=3.8 Hz, H-1), 5.60 (s, 1H, benzylidene CH), 5.32 (d, *J*=3.0 Hz, 1H, H-4'), 5.21 (dd, *J*=7.9, 10.4 Hz, H-2'), 5.12 (d, *J*=8.6 Hz, 1H, NH), 4.97 (dd, *J*=3.4, 10.5 Hz, H-3'), 4.94 (d, *J*=11.9 Hz, 1H, Troc CH), 4.80 (d, *J*=7.9 Hz, 1H, H-1'), 4.56 (d, *J*=12.0 Hz, 1H, Troc CH), 4.34 (dd, *J*=4.6,

10.3 Hz, 1H, H-6a), 4.25 (ddd, $J=3.8, 10.2, 10.2$ Hz, 1H, H-2), 4.12-4.04 (m, 2H, H-3, H-6'a), 3.98 (ddd, $J=4.7, 9.7, 9.7$ Hz, H-5), 3.92-3.84 (m, 2H, H-6'b, H-4), 3.82 (t, $J=10.3$ Hz, 1H, H-6b), 3.72 (t, $J=6.7$ Hz, H-5'), 2.12 (s, 3H, COCH₃), 2.01 (s, 3H, COCH₃), 1.96 (s, 3H, COCH₃), 1.95 (s, 3H, COCH₃), 1.56 (s, H₂O), 1.25 (m, grease); ¹³C (100 MHz, CDCl₃) δ 170.4 (COCH₃), 170.3 (COCH₃), 169.6 (COCH₃), 160.5 (imidate CNH), 154.1 (Troc CO), 136.9 (aromatic), 129.5 (aromatic), 128.5 (aromatic), 126.1 (aromatic), 101.6 (benzylidene CH), 100.9 (C-1'), 95.4 (Troc CCl₃), 95.3 (C-1), 90.9 (imidate CCl₃), 79.8 (C-4), 76.8 (C-3), 74.9 (Troc CH₂), 71.0 (C-3'), 70.9 (C-5'), 69.8 (C-2'), 68.6 (C-6), 66.8 (C-4'), 65.2 (C-5), 61.0 (C-6'), 54.4 (C-2), 20.8 (COCH₃), 20.7 (COCH₃), 20.7 (COCH₃). HRMS (ESI) calcd for C₃₂H₃₆Cl₆N₂O₁₆ [M+Na]⁺ 937.0094, found 937.0067.



(2R,3S,4S,5R,6S)-2-(acetoxymethyl)-6-(((2R,3R,4S,5R,6R)-4,5-diacetoxy-2-(acetoxymethyl)-6-(benzyloxy)tetrahydro-2H-pyran-3-yl)oxy)tetrahydro-2H-pyran-3,4,5-triyl triacetate (4.64). To a solution of lactose octaacetate (**4.8**) (1.0 eq, 4.0 g, 5.9 mmol) in CH₂Cl₂ (4.5 mL) cooled to 0°C was added HBr/AcOH (33 wt%) (2.7 eq, 4.5 mL, 16 mmol) dropwise over 30 minutes. The reaction was slowly allowed to warm to room temperature and stir 2.5 H. The reaction was diluted with CH₂Cl₂ and water, quenched with saturated NaHCO₃ solution, and extracted with additional CH₂Cl₂ (4 x 10 mL). The combined organics were washed with saturated NaHCO₃ solution (3 x 20 mL), water (1 x 20 mL), brine (1 x 20 mL), dried (MgSO₄), filtered, and concentrated *in vacuo* to yield a white foam. The crude anomeric bromide was dissolved in CH₂Cl₂ (20 mL) and added to a suspension

of Ag_2CO_3 (2.6 eq, 4.1 g, 15 mmol), 4Å molecular sieves (3.0 g), and a crystal of I_2 in CH_2Cl_2 (10 mL). Benzyl alcohol (5.0 eq, 3.0 mL 29 mmol) was added and the resulting mixture stirred in the dark for 17.5 H then was filtered through a plug of celite and concentrated *in vacuo*. The crude residue was purified via flash column chromatography (1:1 hexanes/EtOAc) to yield anomeric benzyl ether **4.64** (2.5 g, 3.4 mmol, 58% over 2 steps) as a white foam: *Rf* 0.40 (1:1 hexanes/EtOAc); ^1H (400 MHz, CDCl_3) δ 7.37-7.25 (m, 5H, aromatic), 5.34 (dd, $J=1.1, 3.5$ Hz, 1H, H-4'), 5.15 (dd, $J=9.3, 9.2$ Hz, 1H, H-3), 5.10 (dd, $J=7.9, 10.4$ Hz, 1H, H-2'), 4.97 (dd, $J=7.8, 9.8$ Hz, 1H, H-2), 4.95 (dd, $J=3.3, 9.8$ Hz, 1H, H-3'), 4.86 (d, $J=12.3$ Hz, PhCH), 4.59 (d, $J=12.3$ Hz, PhCH), 4.53 (dd, $J=2.0, 12.8$ Hz, 1H, H-6a), 4.52 (d, $J=8.0$ Hz, 1H, H-1), 4.48 (d, $J=7.9$ Hz, 1H, H-1'), 4.15-4.05 (m, 3H, H-6'a, H-6b, H-6'b), 3.88-3.84 (ddd, $J=2.0, 4.9, 7.0$ Hz, 1H, H-5), 2.14 (s, 3H, COCH_3), 2.14 (s, 3H, COCH_3), 2.05 (s, 3H, COCH_3), 2.04 (s, 3H, COCH_3), 2.03 (s, 3H, COCH_3), 2.00 (s, 3H, COCH_3), 1.96 (s, 3H, COCH_3), 1.59 (s, H_2O), 1.25 (m, grease); ^{13}C (100 MHz, CDCl_3) δ 170.5 (COCH_3), 170.5 (COCH_3), 170.3 (COCH_3), 170.2 (COCH_3), 169.9 (COCH_3), 169.8 (COCH_3), 169.2 (COCH_3), 136.8 (aromatic), 128.6 (aromatic), 128.2 (aromatic), 127.9 (aromatic), 101.2 (C-1'), 99.2 (C-1), 76.4 (C-4), 72.9 (C-3), 72.8 (C-5), 71.8 (C-2), 71.1 (C-3'), 70.9 (C-5'), 70.8 (PhCH₂), 69.3 (C-2'), 66.7 (C-4'), 62.1 (C-6), 61.0 (C-6'), 21.0 (COCH_3), 21.0 (COCH_3), 20.8 (COCH_3), 20.8 (COCH_3), 20.7 (COCH_3). LRMS calcd for $\text{C}_{33}\text{H}_{42}\text{O}_{18}$ $[\text{M}+\text{Na}]^+$ 749.23, found 749.44.



(2R,3R,4R,5S,6R)-2-(benzyloxy)-5-(((3aS,4R,6S,7R,7aR)-7-hydroxy-4-(hydroxymethyl)-2,2-dimethyltetrahydro-4H-[1,3]dioxolo[4,5-c]pyran-6-yl)oxy)-6-(hydroxymethyl) tetrahydro-2H-pyran-3,4-diol (4.66).⁷⁴ To a solution of **4.64** (1.0 eq, 1.8 g, 2.5 mmol) in

MeOH was added a concentrated NaOMe solution. The reaction was stirred 15 H then neutralized with Dowex 50Wx8, filtered, and concentrated *in vacuo* to yield a white solid.

The crude deacetylated anomeric benzyl ether (1.0 eq, 1.0 g, 2.3 mmol) was suspended in acetone (18 mL) and 2,2-dimethoxypropane (8.5 eq, 2.4 mL, 20 mmol) and p-toluenesulfonic acid (0.1 eq, 0.04 g, 0.23 mmol) were added sequentially. The resulting

mixture was stirred 16 H. The reaction was concentrated *in vacuo* and purified via flash column chromatography (13:1 EtOAc/MeOH) to yield 3',4'-acetonide **4.66** (0.89 g, 1.9

mmol, 76%) as a white solid: *R*_f 0.35 (9:1 EtOAc/MeOH); ¹H (400 MHz, CDCl₃) δ 7.43-

7.41 (m, 2H, aromatic), 7.35-7.27 (m, 3H, aromatic), 4.92 (d, *J*=11.8 Hz, 1H, PhCH), 4.67

(d, *J*=11.8 Hz, 1H, PhCH), 4.39 (d, *J*=7.7 Hz, 1H, H-1), 4.37 (d, *J*=8.0 Hz, 1H, H-1'), 4.19

(dd, *J*=2.0, 5.5 Hz, 1H, H-4'), 4.05 (dd, *J*=5.6, 7.2 Hz, 1H, H-3'), 3.95-3.92 (m, 1H, H-5'),

3.90 (dd, *J*=2.4, 12.1 Hz, 1H-H-6a), 3.86-3.73 (m, 3H, H-6a, H-6'a, H-6'b), 3.59 (dd, *J*=8.8,

9.3 Hz, 1H, H-4), 3.53 (t, *J*=8.9 Hz, 1H, H-3), 3.45 (dd, *J*=7.5, 8.0 Hz, 1H, H-2), 3.43-3.38

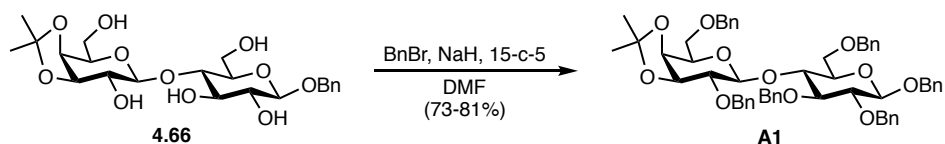
(m, 1H, H-5), 1.47 (s, 3H, CCH₃), 1.32 (s, 3H, CCH₃); ¹³C (100 MHz, CDCl₃) δ 139.0

(aromatic), 129.3 (aromatic), 129.2 (aromatic), 128.7 (aromatic), 111.1 (C(CH₃)₂), 104.2

(C-1'), 103.1 (C-1), 81.0 (C-4), 80.9 (C-3'), 76.5 (C-5), 76.4 (C-3), 75.4 (C-5'), 75.1 (C-4'),

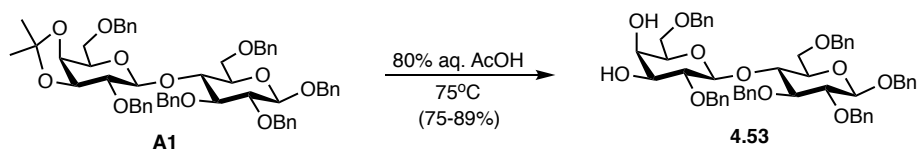
74.9 (C-2), 74.5 (C-2'), 71.8 (PhCH₂), 62.4 (C-6'), 61.9 (C-6), 28.4 (CCH₃), 26.5 (CCH₃).

LRMS calcd for C₂₂H₃₂O₁₁ [M+H]⁺ 473.20, found 473.28.



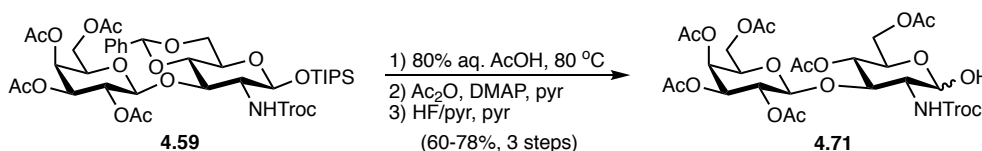
(3aS,4R,6S,7R,7aS)-7-(benzyloxy)-4-((benzyloxy)methyl)-2,2-dimethyl-6-(((2R,3R,4S,5R,6R)-4,5,6-tris(benzyloxy)-2-((benzyloxy)methyl)tetrahydro-2H-pyran-3-yl)oxy)tetrahydro-4H-[1,3]dioxolo[4,5-c]pyran (A1).⁷⁴ To a solution of **4.66** (1.0 eq, 0.60 g, 1.3 mmol) in DMF (13 mL) cooled to 0 °C was added benzyl bromide (10 eq, 1.5 mL, 13 mmol) followed by solid NaH (60 wt%) (7.5 eq, 0.38 g, 9.5 mmol) and 15-crown-5 (cat.). The reaction was slowly allowed to warm to room temperature and stir 4.5 H. The reaction was poured onto ice water (40 mL) and extracted with EtOAc (4 x 15 mL). The combined organics were washed with water (1 x 20 mL), brine (1 x 20 mL), dried (MgSO₄), filtered, and concentrated *in vacuo*. The crude residue was purified via flash column chromatography (4:1 hexanes/EtOAc) to yield benzylated acetonide **A1** (0.95 g, 1.0 mmol, 81%) as a clear, sticky oil: *R_f* 0.72 (2:1 hexanes/EtOAc); ¹H (400 MHz, CDCl₃) δ 7.39-7.21 (m, 30H, aromatic), 4.96 (d, *J*=12.2 Hz, 1H, PhCH), 4.94 (d, *J*=11.2 Hz, 1H, PhCH), 4.91 (d, *J*=11.2 Hz, 1H, PhCH), 4.80 (d, *J*=11.8 Hz, 1H, PhCH), 4.74 (d, *J*=10.5 Hz, 1H, PhCH), 4.73 (d, *J*=10.8 Hz, 1H, PhCH), 4.68 (d, *J*=11.8 Hz, 1H, PhCH), 4.67 (d, *J*=12.1 Hz, 1H, PhCH), 4.60 (d, *J*=12.1 Hz, 1H, PhCH), 4.52 (d, *J*=12.1 Hz, 1H, PhCH), 4.51 (d, *J*=7.7 Hz, 1H, H-1), 4.45 (d, *J*=12.0 Hz, 1H, PhCH), 4.43 (d, *J*=8.0 Hz, 1H, H-1'), 4.32 (d, *J*=12.1 Hz, 1H, PhCH), 4.12 (dd, *J*=1.6, 5.6 Hz, 1H, H-4'), 4.04 (dd, *J*=5.8, 6.5 Hz, 1H, H-3'), 3.99 (dd, *J*=9.3, 9.4, 1H, H-4), 3.84 (dd, *J*=4.2, 11.0 Hz, 1H, H-6a), 3.76 (dd, *J*=1.6, 10.9 Hz, 1H, H-6b), 3.71-3.66 (m, 2H, H-6'a, H-5'), 3.59-3.33 (m, 5H, H-2', H-6'b, H-3, H-5, H-2), 1.36 (s, 3H, CCH₃), 1.40 (s, 3H, CCH₃); ¹³C (100 MHz, CDCl₃) δ 139.1 (aromatic), 138.7 (aromatic), 138.7 (aromatic), 138.6 (aromatic), 138.4 (aromatic), 137.7 (aromatic),

128.5 (aromatic), 128.5 (aromatic), 128.4 (aromatic), 128.4 (aromatic), 128.3 (aromatic), 128.3 (aromatic), 128.2 (aromatic), 128.0 (aromatic), 128.0 (aromatic), 127.8 (aromatic), 127.7 (aromatic), 127.7 (aromatic), 127.6 (aromatic), 127.6 (aromatic), 127.6 (aromatic), 127.4 (aromatic), 109.9 (C(CH₃)₂), 102.7 (C-1), 102.0 (C-1'), 83.2 (C-3), 82.0 (C-2), 80.8 (C-2'), 79.5 (C-3'), 76.5 (C-4), 75.6 (PhCH₂), 75.3 (C-5), 75.2 (PhCH₂), 73.7 (C-4'), 73.5 (PhCH₂), 73.4 (PhCH₂), 73.3 (PhCH₂), 72.1 (C-5'), 71.1 (PhCH₂), 69.0 (C-6'), 68.4 (C-6), 28.1 (CCH₃), 26.6 (CCH₃). LRMS calcd for [M+H]⁺ 923.43, found 923.45.



(2R,3R,4S,5R,6S)-5-(benzyloxy)-2-((benzyloxy)methyl)-6-(((2R,3R,4S,5R,6R)-4,5,6-tris(benzyloxy)-2-((benzyloxy)methyl)tetrahydro-2H-pyran-3-yl)oxy)tetrahydro-2H-pyran-3,4-diol (4.53). A solution of **A1** (1.0 eq, 1.5 g, 1.7 mmol) in 80% aqueous acetic acid (16 mL) was heated to 75 °C. The reaction was stirred 4 H then diluted with water (40 mL) and extracted with CH₂Cl₂ (4 x 15 mL) while solid NaHCO₃ was added. The combined organics were washed with a saturated aqueous NaHCO₃ solution (3 x 20 mL), brine (1 x 20 mL), dried (MgSO₄), filtered, and concentrated *in vacuo*. The crude residue was purified via flash column chromatography (1:1 hexanes/EtOAc) to yield diol **4.53** (1.2 g, 1.4 mmol, 82%) as a dense white solid: *R_f* 0.13 (2:1 hexanes/EtOAc); ¹H (400 MHz, CDCl₃) δ 7.39-7.22 (m, 30H, aromatic), 4.98 (d, *J*=11.0 Hz, 1H, PhCH), 4.96 (d, *J*=12.1 Hz, 1H, PhCH), 4.91 (d, *J*=10.8 Hz, 1H, PhCH), 4.81 (d, *J*=11.6 Hz, 1H, PhCH), 4.77 (d, *J*=11.0 Hz, 1H, PhCH), 4.73 (d, *J*=10.8 Hz, 1H, PhCH), 4.67 (d, *J*=11.6 Hz, 1H, PhCH), 4.66 (d, *J*=12.1 Hz, 1H, PhCH), 4.62 (d, *J*=12.2 Hz, 1H, PhCH), 4.50 (d, *J*=7.8 Hz, 1H, H-

1), 4.47 (d, $J=12.2$ Hz, 1H, PhCH), 4.45 (d, $J=7.2$ Hz, 1H, H-1'), 4.45 (d, $J=11.8$ Hz, 1H, PhCH), 4.39 (d, $J=12.2$ Hz, 1H, PhCH), 4.03 (t, $J=9.3$ Hz, 1H, H-3), 3.95 (d, $J=1.7$ Hz, H-4'), 3.84 (dd, $J=4.1, 11.1$ Hz, 1H, H-6a), 3.77 (dd, $J=1.8, 11.0$ Hz, H-6b), 3.64-3.57 (m, 2H, H-6'a, H-3), 3.52-3.48 (m, 2H, H-2, H-6'b), 3.44-3.39 (m, 3H, H-3', H-2', H-5), 3.37 (q, $J=5.8$ Hz, 1H, H-5'), 2.46 (br s, 1H, OH), 2.38 (br s, 1H, OH); ^{13}C (100 MHz, CDCl_3) δ 139.3 (aromatic), 138.7 (aromatic), 138.5 (aromatic), 138.4 (aromatic), 138.1 (aromatic), 137.7 (aromatic), 128.7 (aromatic), 128.6 (aromatic), 128.5 (aromatic), 128.5 (aromatic), 128.4 (aromatic), 128.2 (aromatic), 128.2 (aromatic), 128.1 (aromatic), 128.0 (aromatic), 128.0 (aromatic), 127.9 (aromatic), 127.8 (aromatic), 127.7 (aromatic), 127.7 (aromatic), 127.4 (aromatic), 102.7 (C-1'), 102.6 (C-1), 83.0 (C-3), 82.0 (C-2'), 76.7 (C-4), 75.4 (PhCH₂), 75.3 (C-5), 75.1 (PhCH₂), 75.0 (PhCH₂), 73.7 (PhCH₂), 73.6 (C-3'), 73.4 (PhCH₂), 73.0 (PhCH₂), 68.9 (C-4'), 68.8 (C-6'), 68.4 (C-6). LRMS calcd for $[\text{M}+\text{H}]^+$ 883.41, found 883.79.

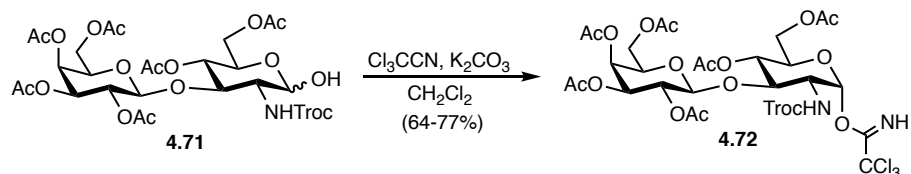


(2R,3S,4S,5R,6R)-2-(acetoxymethyl)-6-(((2R,4aR,6R,7R,8R,8aS)-6-hydroxy-2-phenyl-7-(((2,2,2trichloroethoxy)carbonyl)amino)hexahydropyrano[3,2-d][1,3]dioxin-8-yl)oxy)tetrahydro-2H-pyran-3,4,5-triyl triacetate (4.71). A solution of **4.59** (1.0 eq, 1.45 g, 1.56 mmol) in 80% aqueous acetic acid (15 mL) was heated to 80 °C and stirred 5 H and 15 minutes. The reaction was diluted with water (40 mL) and extracted with EtOAc (4 x 15 mL) while solid NaHCO_3 was added. The combined organics were washed with a saturated aqueous NaHCO_3 solution (4 x 20 mL), brine (1 x 20 mL), dried (MgSO_4),

filtered, and concentrated *in vacuo* to yield a white solid. The crude diol was dissolved in pyridine (16 mL) and acetic anhydride (2.5 eq, 0.37 mL, 3.9 mmol) and DMAP (cat.) were added. The reaction was stirred 1 H and 15 minutes then diluted with EtOAc (50 mL), washed with 2 N HCl (4 x 20 mL), brine (1 x 20 mL), dried (MgSO₄), filtered, and concentrated *in vacuo* to yield a white foam. The crude diacetate was dissolved in pyridine (15 mL) and the resulting solution cooled to 0 °C. 70% HF in pyridine (8 mL) was added dropwise over 5 minutes. The reaction was stirred 1 H then allowed to warm to room temperature and stir an additional 5 H. The reaction was diluted with water (40 mL) and extracted with EtOAc (4 x 15 mL) while solid NaHCO₃ was added. The combined organics were quenched with saturated NaHCO₃ solution, washed with 2 N HCl (4 x 20 mL), brine (1 x 20 mL), dried (MgSO₄), filtered, and concentrated *in vacuo*. The crude residue was purified via flash column chromatography (2:3 hexanes/EtOAc) to yield lactol **4.71** (0.94 g, 1.2 mmol, 78% over 3 steps) (α/β 8:1) as a white foam: *R*_f 0.20 (1:1 hexanes/EtOAc); ¹H NMR (400 MHz, CDCl₃) δ (α anomer) 5.36 (m, 1H, *NH*), 5.35 (d, *J*=3.2 Hz, 1H, H-4'), 5.25 (t, *J*=2.9 Hz, 1H, H-1), 5.05 (dd, *J*=7.8, 10.4 Hz, 1H, H-2'), 4.99 (t, *J*=8.8 Hz, H-4), 4.92 (dd, *J*=3.4, 10.5 Hz, 1H, H-3'), 4.74 (s, 2H, Troc CH, Troc CH), 4.65 (d, *J*=7.8 Hz, H-1'), 4.24-4.15 (m, 4H, H-6'a, H-5, H-6a, H-6b), 4.07-4.00 (m, 3H, H-3, H-6'b, H-2), 3.90 (dd, *J*=7.0, 6.7 Hz, 1H, H-5'), 3.35 (d, *J*=3.0, 1H, OH), 2.14 (s, 3H, COCH₃), 2.10 (s, 3H, COCH₃), 2.07 (s, 3H, COCH₃), 2.06 (s, 3H, COCH₃), 2.06 (s, 3H, COCH₃), 1.95 (s, 3H, COCH₃); ¹³C (100 MHz, CDCl₃) δ (α anomer) 171.1 (COCH₃), 170.6 (COCH₃), 170.3 (COCH₃), 170.3 (COCH₃), 169.8 (COCH₃), 169.5 (COCH₃), 154.1 (Troc CO), 100.7 (C-1'), 95.3 (Troc CCl₃), 92.1 (C-1), 75.4 (C-3), 74.9 (Troc CH₂), 70.9 (C-3'), 70.6 (C-5'), 69.1 (C-2'), 68.8 (C-4), 67.9 (C-5), 67.0 (C-4'), 62.5 (C-6), 61.0 (C-6'), 55.2 (C-2), 21.0

(COCH₃), 20.9 (COCH₃), 20.9 (COCH₃), 20.8 (COCH₃), 20.8 (COCH₃), 20.7 (COCH₃).

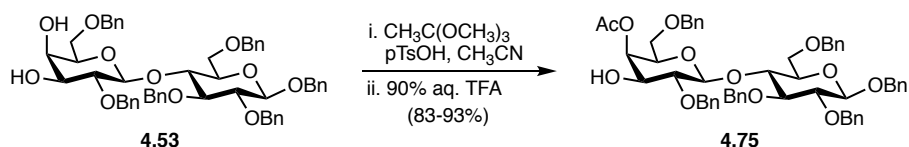
HRMS (ESI) calcd for C₂₇H₃₆Cl₃NO₁₈ [M+Na]⁺ 790.0896, found 790.0905.



(2R,3R,4S,5S,6R)-2-(((2R,3S,4R,5R,6R)-3-acetoxy-2-(acetoxymethyl)-6-(2,2,2-trichloro-1-iminoethoxy)-5-(((2,2,2-trichloroethoxy)carbonyl)amino) tetrahydro-2H-pyran-4-yl)oxy)-6-(acetoxymethyl)tetrahydro-2H-pyran-3,4,5-triyl triacetate (4.72).

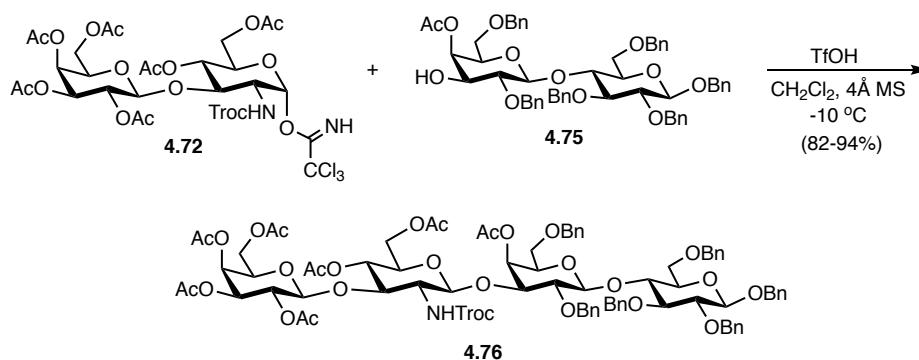
To a solution of **4.71** (1.0 eq, 0.30 g, 0.39 mmol) in CH₂Cl₂ (5.6 mL) was added potassium carbonate (3.0 eq, 1.6 g, 1.2 mmol) and trichloroacetonitrile (10 eq, 0.39 mL, 3.9 mmol) sequentially. The reaction was stirred 22 H then diluted with CH₂Cl₂, filtered through celite, and concentrated *in vacuo*. The crude residue was purified via flash column chromatography (1:1 hexanes/EtOAc) to yield α -trichloroacetimidate **4.72** (0.27 g, 0.30 mmol, 77%) as a white foam: *R_f* 0.38 (1:1 hexanes/EtOAc); ¹H (400 MHz, CDCl₃) δ 8.83 (s, 1H, imidate NH), 6.31 (d, *J*=3.7 Hz, 1H, H-1), 5.37 (dd, *J*=0.8, 3.5 Hz, 1H, H-4'), 5.14-5.05 (m, 3H, H-2', H-4, NH), 4.96 (dd, *J*=3.4, 10.4 Hz, 1H, H-3'), 4.78 (d, *J*=12.0 Hz, 1H, Troc CH), 4.70 (d, *J*=7.5 Hz, 1H, H-1'), 4.69 (d, 12.2 Hz, 1H, Troc CH), 4.29 (td, *J*=3.8, 10.1, 10.1 Hz, 1H, H-2), 4.23-4.17 (m, 2H, H-6'a, H-6a), 4.14-4.02 (m, 4H, H-6b, H-5, H-3, H-6'b), 3.96 (t, *J*=6.7 Hz, 1H, H-5'), 2.15 (s, 3H, COCH₃), 2.08 (s, 3H, COCH₃), 2.07 (s, 3H, COCH₃), 2.06 (s, 3H, COCH₃), 2.04 (s, 3H, COCH₃), 1.96 (s, 3H, COCH₃), 1.66 (s, H₂O), 1.25 (m, grease), 0.06 (s, silicon grease); ¹³C (100 MHz, CDCl₃) δ 170.9 (COCH₃), 170.5 (COCH₃), 170.2 (COCH₃), 170.2 (COCH₃), 169.5 (COCH₃), 169.5 (COCH₃), 160.4

(imidate CNH), 154.0 (Troc CO), 100.6 (C-1'), 95.2 (Troc CCl₃), 90.9 (imidate CCl₃), 75.8 (C-3), 75.0 (Troc CH₂), 70.9 (C-5'), 70.8 (C-3'), 70.3 (C-5), 69.3 (C-2'), 68.0 (C-4), 67.0 (C-4'), 61.8 (C-6), 61.2 (C-6'), 54.7 (C-2), 20.9 (COCH₃), 20.9 (COCH₃), 20.8 (COCH₃), 20.8 (COCH₃), 20.8 (COCH₃), 20.7 (COCH₃). HRMS (ESI) calcd for C₂₉H₃₆Cl₆N₂O₁₈ [M+Na]⁺ 932.9992, found 932.9962.



(2R,3R,4S,5R,6S)-5-(benzyloxy)-2-((benzyloxy)methyl)-4-hydroxy-6-(((2R,3R,4S,5R,6R)-4,5,6-tris(benzyloxy)-2-((benzyloxy)methyl)tetrahydro-2H-pyran-3-yl)oxy)tetrahydro-2H-pyran-3-yl acetate (4.75).^{77, 89} To a solution of **4.53** (1.0 eq, 0.9 g, 1.0 mmol) in CH₃CN (10 mL) was added trimethyl orthoacetate (3.0 eq, 0.38 mL, 3.0 mmol) and p-toluenesulfonic acid (0.1 eq, 0.02 g, 0.1 mmol). The reaction was stirred 25 minutes then 90% trifluoroacetic acid (0.36 mL) was added. The resulting solution was stirred 20 minutes then diluted with water (15 mL) and extracted with EtOAc (4 x 5 mL). The combined organics were washed with a saturated NaHCO₃ solution (2 x 7 mL), brine (1 x 7 mL), dried (MgSO₄), filtered, and concentrated *in vacuo*. The crude residue was purified via flash column chromatography (2:1 hexanes/EtOAc) to yield axial acetate **4.75** (0.87 g, 0.94 mmol, 93%) as a white foam: *R*_f 0.32 (2:1 hexanes/EtOAc); ¹H (600 MHz, CDCl₃) δ 7.34-7.13 (m, 30H, aromatic), 5.30 (d, *J*=3.2 Hz, 1H, H-4'), 4.93 (d, *J*=10.5 Hz, 1H, PhCH), 4.91 (d, *J*=11.9 Hz, 1H, PhCH), 4.87 (d, *J*=10.9 Hz, 1H, PhCH), 4.76 (d, *J*=11.4 Hz, 1H, PhCH), 4.71 (d, *J*=10.6 Hz, 1H, PhCH), 4.69 (d, *J*=10.9 Hz, 1H, PhCH), 4.63 (d, *J*=11.3 Hz, 1H, PhCH), 4.62 (d, *J*=12.1 Hz, 1H, PhCH), 4.59 (d, *J*=12.1 Hz, 1H,

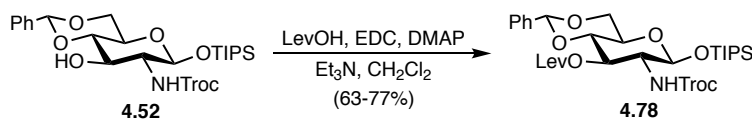
PhCH), 4.45 (d, $J=7.8$ Hz, 1H, H-1), 4.44 (d, $J=7.7$ Hz, 1H, H-1'), 4.42 (d, $J=11.4$ Hz, 1H, PhCH), 4.41 (d, $J=12.1$ Hz, 1H, PhCH), 4.20 (d, $J=12.0$ Hz, 1H, PhCH), 3.99 (t, $J=9.2$ Hz, 1H, H-4), 3.77 (dd, $J=4.0, 11.0$ Hz, 1H, H-6a), 3.71 (dd, $J=1.2, 10.7$ Hz, H-6b), 3.60 (dd, $J=3.4, 9.6$ Hz, 1H, H-3'), 3.53 (t, $J=9.1$ Hz, 1H, H-3), 3.48 (t, $J=6.6$ Hz, 1H, H-5'), 3.45 (dd, $J=7.9, 8.9$ Hz, 1H, H-2), 3.36 (dd, $J=7.9, 9.4$ Hz, 1H, H-2'), 3.33 (ddd, $J=1.6, 3.8, 9.5$ Hz, 1H, H-5), 3.30 (d, $J=6.7$ Hz, 2H, H-6'a, H-6'b), 2.20 (br s, 1H, OH), 1.99 (s, 3H, COCH₃), 1.53 (s, H₂O); ¹³C (100 MHz, CDCl₃) δ 171.1 (COCH₃), 139.2 (aromatic), 138.7 (aromatic), 128.4 (aromatic), 138.3 (aromatic), 138.1 (aromatic), 137.6 (aromatic), 128.6 (aromatic), 128.5 (aromatic), 128.5 (aromatic), 128.4 (aromatic), 128.2 (aromatic), 128.1 (aromatic), 128.0 (aromatic), 128.0 (aromatic), 127.9 (aromatic), 127.8 (aromatic), 127.8 (aromatic), 127.8 (aromatic), 127.7 (aromatic), 127.5 (aromatic), 102.7 (C-1), 102.5 (C-1'), 82.9 (C-3), 81.9 (C-2), 80.3 (C-2'), 76.5 (C-4), 75.4 (PhCH₂), 75.2 (PhCH₂), 75.2 (C-5), 73.6 (PhCH₂), 73.4 (PhCH₂), 72.6 (C-3'), 72.1 (C-5'), 71.1 (PhCH₂), 69.7 (C-4'), 68.3 (C-6), 67.4 (C-6'), 20.9 (COCH₃). LRMS calcd for C₅₆H₆₀O₁₂ [M+NH₄]⁺ 942.44, found 942.56.



(2R,3R,4S,5S,6R)-2-(((2R,3S,4R,5R,6S)-3-acetoxy-6-(((2R,3S,4S,5R,6S)-3-acetoxy-5-(benzyloxy)-2-((benzyloxy)methyl)-6-(((2R,3R,4S,5R,6R)-4,5,6-tris(benzyloxy)-2-((benzyloxy)methyl)tetrahydro-2H-pyran-3-yl)oxy)tetrahydro-2H-pyran-4-yl)oxy)-2-

(acetoxymethyl)-5-(((2,2,2-trichloroethoxy)carbonyl)amino)tetrahydro-2H-pyran-4-yl)oxy)-6-(acetoxymethyl)tetrahydro-2H-pyran-3,4,5-triyl triacetate (4.76). Donor **4.72** (1.1 eq, 0.55 g, 0.60 mmol) and acceptor **4.75** (1.0 eq, 0.50 g, 0.54 mmol) were coevaporated with benzene (2 x 6 mL) and placed in a vacuum desiccator containing P₂O₅ overnight. The donor/acceptor mixture was dissolved in CH₂Cl₂ (18 mL) and the resulting solution was cannulated into a reaction flask containing 4Å powdered molecular sieves (1.1 g). The mixture was stirred under argon 1 h then cooled to -10 °C and TfOH (cat.) was added. The reaction was stirred 12 minutes then quenched with Et₃N. The reaction was diluted with CH₂Cl₂, filtered through celite, dried (MgSO₄), filtered, and concentrated *in vacuo*. The crude residue was purified via flash column chromatography (1:1 hexanes/EtOAc) to yield tetrasaccharide **4.76** (0.85 g, 0.51 mol, 94%) as a white foam: *R_f* 0.35 (1:1 hexanes/EtOAc); ¹H (400 MHz, CDCl₃) δ 7.48-7.44 (m, 2H, aromatic), 7.38-7.25 (m, 25H, aromatic), 7.23-7.16 (m, 3H, aromatic), 5.42 (d, *J*=3.6 Hz, 1H, H-4'), 5.33 (d, *J*=3.0 Hz, H-4'''), 5.01-4.82 (m, 7H, H-3''', H-2''', Troc CH, PhCH, PhCH, PhCH, PhCH), 4.77-4.69 (m, 5H, PhCH, PhCH, PhCH, H-1'', H-4''), 4.64 (d, *J*=12.3 Hz, 1H, PhCH), 4.61 (d, *J*=13.2 Hz, 1H, PhCH), 4.49-4.42 (m, 4H, PhCH, PhCH, H-1', H-1), 4.32 (d, *J*=12.1 Hz, 1H, Troc CH), 4.28 (d, *J*=11.8 Hz, PhCH), 4.23-4.14 (m, 4H, H-6''a, H-1'', H-6''a, H-6''b), 4.10-4.03 (m, 3H, H-6''b, H-4, NH), 3.81-3.77 (m, 2H, H-5''', H-6a), 3.71-3.60 (m, 3H, H-5'', H-3', H-6b), 3.58-3.52 (m, 3H, H-5', H-2', H-3), 3.49-3.42 (m, 3H, H-3'', H-2'', H-2), 3.36-3.31 (m, 3H, H-6a, H-6b, H-5), 2.13 (s, 3H, COCH₃), 2.12 (s, 3H, COCH₃), 2.07 (s, 3H, COCH₃), 2.02 (s, 3H, COCH₃), 1.99 (s, 3H, COCH₃), 1.96 (s, 3H, COCH₃), 1.95 (s, 3H, COCH₃), 1.64 (s, H₂O), 1.26 (m, grease); ¹³C (100 MHz, CDCl₃) δ 171.0 (COCH₃), 170.5 (COCH₃), 170.3 (COCH₃), 170.3 (COCH₃), 169.8 (COCH₃), 169.3

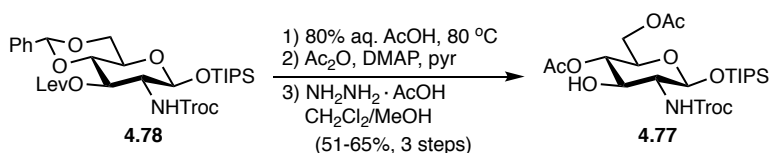
(COCH₃), 169.3 (COCH₃), 153.9 (Troc CO), 139.3 (aromatic), 139.1 (aromatic), 138.7 (aromatic), 138.2 (aromatic), 138.1 (aromatic), 137.6 (aromatic), 128.9 (aromatic), 128.6 (aromatic), 128.5 (aromatic), 128.4 (aromatic), 128.3 (aromatic), 128.2 (aromatic), 128.2 (aromatic), 128.1 (aromatic), 128.0 (aromatic), 128.0 (aromatic), 127.9 (aromatic), 127.9 (aromatic), 127.8 (aromatic), 127.7 (aromatic), 127.5 (aromatic), 126.9 (aromatic), 102.6 (C-1), 102.0 (C-1'), 100.9 (C-1'''), 100.7 (C-1''), 95.6 (Troc CCl₃), 82.8 (C-3), 81.9 (C-2'), 81.7 (C-2), 77.2 (C-3'''), 76.7 (C-3'), 76.0 (C-4), 75.5 (PhCH₂), 75.2 (PhCH₂), 75.1 (C-5), 74.6 (PhCH₂), 74.3 (Troc CH₂), 73.7 (PhCH₂), 73.7 (PhCH₂), 72.8 (C-5'), 71.7 (C-5''), 71.0 (PhCH₂), 70.9 (C-3'''), 70.5 (C-5'''), 69.4 (C-4'), 69.4 (C-4''), 68.8 (C-2'''), 68.1 (C-6), 68.0 (C-6'), 66.9 (C-4'''), 62.5 (C-6''), 61.1 (C-6'''), 57.5 (C-2''), 21.0 (COCH₃), 21.0 (COCH₃), 20.8 (COCH₃), 20.8 (COCH₃), 20.8 (COCH₃), 20.7 (COCH₃), 20.7 (COCH₃). HRMS (ESI) calcd for C₈₃H₉₄Cl₃NO₂₉ [M+Na]⁺ 1696.4875, found 1696.4839.



(2R,4aR,6S,7R,8R,8aS)-2-phenyl-7-(((2,2,2-trichloroethoxy)carbonyl)amino)-6-((triisopropylsilyl)oxy)hexahydropyrano[3,2-d][1,3]dioxin-8-yl 4-oxopentanoate (4.78).

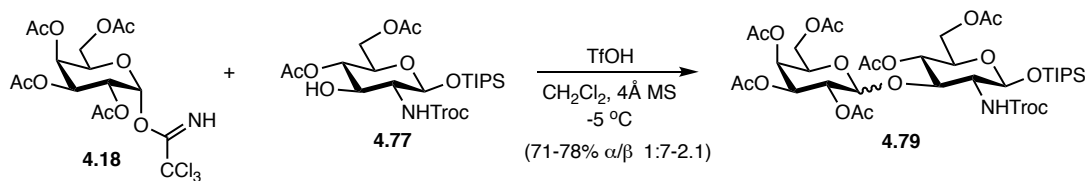
To a solution of **4.52** (1.0 eq, 1.45 g, 2.43 mmol) in CH₂Cl₂ (25 mL) cooled to 0 °C was added levulinic acid (3.0 eq, 0.746 mL, 7.29 mmol), Et₃N (4.5 eq, 1.5 mL, 11 mmol), DMAP (cat.), and 1-ethyl-3-(3-dimethylaminopropyl)carbodiimide (EDC) (3.0 eq, 1.46 g, 7.29 mmol) sequentially. After 1 H, the reaction was allowed to warm to room temperature and stir an additional 20 H. The reaction was diluted with CH₂Cl₂ (50 mL), washed with water (3 x 20 mL), saturated aq. NaHCO₃ solution (1 x 20 mL), brine (1 x 20 mL), dried

(MgSO₄), filtered, and concentrated *in vacuo*. The crude product was purified via flash column chromatography (4:5 hexanes/EtOAc) to yield levulinic ester **4.78** (1.31 g, 1.88 mmol, 77%) as a white foam: R_f 0.35 (1:1 hexanes/EtOAc); ¹H (400 MHz, CDCl₃) δ 7.46-7.43 (m, 2H, aromatic), 7.37-7.33 (m, 3H, aromatic), 5.51 (s, 1H, benzylidene CH), 5.30 (t, J=10.0 Hz, 1H, H-3), 4.73 (m, 2H, Troc CH, Troc CH), 4.93 (d, J=7.8 Hz, 1H, H-1), 4.30 (dd, J=5.0, 10.5 Hz, 1H, H-6a), 3.80 (t, J=10.2 Hz, 1H, H-6b), 3.72 (t, J=9.4 Hz, 1H, H-4), 3.67 (q, J=9.0 Hz, 1H, H-2), 3.50 (td, J=5.0, 9.8 Hz, H-5), 2.84-2.51 (m, 4H, Lev CH, Lev CH, Lev CH, Lev CH), 1.56 (s, H₂O) 1.12-1.03 (m, 21H, TIPS); ¹³C (100 MHz, CDCl₃) δ 206.2 (Lev CO), 172.8 (Lev COO), 154.3 (Troc CO), 137.1 (aromatic), 129.3 (aromatic), 128.4 (aromatic), 126.4 (aromatic), 101.3 (benzylidene CH), 96.8 (C-1), 95.5 (Troc CCl₃), 79.0 (C-4), 74.9 (Troc CH₂), 71.5 (C-3), 68.6 (C-6), 66.6 (C-5), 59.5 (C-2), 38.1 (Lev CH₂), 29.9 (Lev CH₃), 28.1 (Lev CH₂), 17.9 (TIPS), 17.8 (TIPS), 12.2 (TIPS). HRMS (ESI) calcd for C₃₀H₄₄Cl₃NO₉Si [M+Na]⁺ 718,1749, found 718.1725.



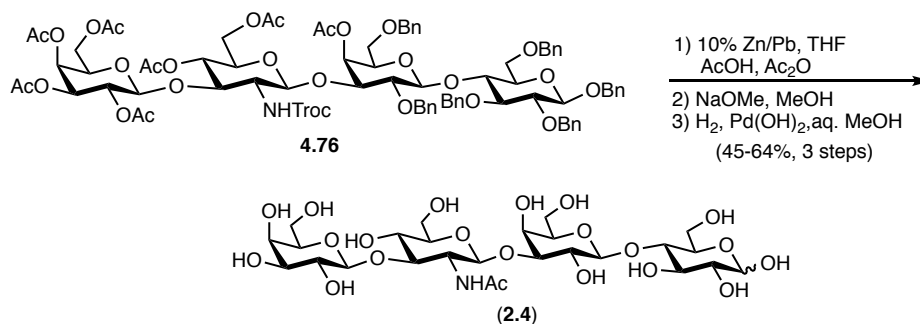
((2R,3S,4R,5R,6S)-3-acetoxy-4-hydroxy-5-(((2,2,2-trichloroethoxy)carbonyl)amino)-6-((triisopropylsilyl)oxy)tetrahydro-2H-pyran-2-yl)methyl acetate (4.77). A solution of **4.78** (1.0 eq, 1.7 g, 2.4 mmol) in 80% aqueous acetic acid (20 mL) was heated to 80 °C and stirred 5 H. The reaction was diluted with water (40 mL) and extracted with EtOAc (4 x 15 mL) while solid NaHCO₃ was added. The combined organics were washed with a saturated aqueous NaHCO₃ solution (5 x 20 mL), brine (1 x 20 mL), dried (MgSO₄), filtered, and concentrated *in vacuo* to yield a white solid. The crude diol was dissolved in

pyridine and DMAP and acetic anhydride were added sequentially. The reaction was stirred 5.5 H then was diluted with EtOAc (50 mL), washed with 2 N HCl (5 x 20 mL), brine (1 x 20 mL), dried (MgSO₄), filtered, and concentrated *in vacuo* to yield a dense, off-white solid. The crude diacetate was dissolved in a mixture of CH₂Cl₂ (24 mL) and MeOH (4.8 mL) and hydrazine acetate was added. The reaction was stirred 7 H then was diluted with CH₂Cl₂ (50 mL), washed with water (3 x 20 mL), brine (1 x 20 mL), dried (MgSO₄), filtered, and concentrated *in vacuo*. The crude product was purified via flash column chromatography (3:2 hexanes/EtOAc) to yield alcohol **4.77** (1.0 g, 1.7 mmol, 65% over 3 steps) as a light, white solid: R_f 0.46 (1:1 hexanes/EtOAc); ¹H (400 MHz, CDCl₃) δ 5.26 (br s, 1H, NH), 4.88 (d, J=4.88 Hz, 1H, H-1), 4.88 (t, J=9.3 Hz, 1H, H-4), 4.69 (m, 2H, Troc CH, Troc CH), 4.16 (m, 2H, H-6a, H-6b), 3.95 (t, J=8.5 Hz, 1H, H-3), 3.66 (m, 1H, H-5), 3.34 (q, J=7.4, 7.4 Hz, H-2), 2.12 (s, 3H, COCH₃), 2.05 (s, 3H, COCH₃), 1.17-1.04 (m, 21H, TIPS); ¹³C (100 MHz, CDCl₃) δ 170.9 (COCH₃), 170.8 (COCH₃), 154.9 (COCH₃), 95.4 (Troc CO), 95.3 (C-1), 75.0 (Troc CH₂), 72.5 (C-3), 72.0 (C-5), 71.9 (C-4), 62.9 (C-6), 61.4 (C-2), 21.0 (COCH₃), 20.8 (COCH₃), 18.0 (TIPS), 17.9 (TIPS), 12.3 (TIPS). HRMS (ESI) calcd for C₂₂H₃₈Cl₃NO₉Si [M+Na]⁺ 616.1279, found 616.1277.



(2R,3R,4S,5S,6R)-2-(((2R,3S,4R,5R,6S)-3-acetoxy-2-(acetoxymethyl)-5-(((2,2,2-trichloroethoxy)carbonyl)amino)-6-((triisopropylsilyl)oxy)tetrahydro-2H-pyran-4-yl)oxy)-6-(acetoxymethyl)tetrahydro-2H-pyran-3,4,5-triyl triacetate (4.79**). Donor **4.18****

(1.5 eq, 1.24 g, 2.52 mmol) and acceptor **4.77** (1.0 eq, 1.00 g, 1.68 mmol) were coevaporated with benzene (2 x 7 mL) and placed in a vacuum desiccator containing P₂O₅ overnight. The donor/acceptor mixture was dissolved in CH₂Cl₂ (17 mL) and the resulting solution was cannulated into a reaction flask containing 4Å powdered molecular sieves (1.5 g). The mixture was stirred under argon 1 h then cooled to -5 °C and TfOH (cat.) was added. The reaction was stirred 15 minutes then quenched with Et₃N. The reaction was diluted with CH₂Cl₂, filtered through celite, dried (MgSO₄), filtered, and concentrated *in vacuo*. The crude residue was purified via flash column chromatography (3:2 to 1:1 hexanes/EtOAc) to yield disaccharide **4.79** (1.20 g, 1.30 mmol, 78%) (α/β 1:2.1) as a white foam: R_f 0.60 (α), 0.40 (β) (1:1 hexanes/EtOAc); ¹H (400 MHz, CDCl₃) δ (β anomer) 5.33 (dd, J=0.8, 3.5 Hz, 1H, H-4'), 5.11-5.05 (m, 2H, H-2', NH), 4.96 (d, J=8.2 Hz, 1H, H-1), 4.94-4.88 (m, 2H, H-3', H-4), 4.71 (q, J=12.0 Hz, 2H, Troc CH, Troc CH), 4.62 (d, J=7.8 Hz, 1H, H-1'), 4.22 (t, J=9.6 Hz, H-3), 4.19-4.04 (m, 4H, H-6a, H-6b, H-6a, H-6b), 3.85 (td, J=0.5, 6.8 Hz, 1H, H-5'), 3.68 (m, 1H, H-5), 3.33 (d, J=8.2, 10.2 Hz, 1H, H-2), 2.14 (s, 3H, COCH₃), 2.08 (s, 3H, COCH₃), 2.07 (s, 3H, COCH₃), 2.06 (s, 3H, COCH₃), 2.04 (s, 3H, COCH₃), 1.96 (s, 3H, COCH₃), 1.58 (s, H₂O), 1.12-1.02 (m, 21 H, TIPS); ¹³C (100 MHz, CDCl₃) δ (β anomer) 170.8 (COCH₃), 170.5 (COCH₃), 170.3 (COCH₃), 170.2 (COCH₃), 169.6 (COCH₃), 169.5 (COCH₃), 154.0 (Troc CO), 101.0 (C-1'), 95.3 (Troc CCl₃), 95.1 (C-1), 77.4 (C-3), 74.8 (Troc CH₂), 71.8 (C-5), 71.0 (C-3'), 70.7 (C-5'), 69.6 (C-4), 69.2 (C-2'), 67.0 (C-4'), 62.9 (C-6), 61.2 (C-6'), 60.5 (C-2), 21.0 (COCH₃), 21.0 (COCH₃), 20.8 (COCH₃), 20.8 (COCH₃), 20.8 (COCH₃), 20.7 (COCH₃), 17.9 (TIPS), 17.9 (TIPS), 14.3 (TIPS), 12.3 (TIPS). HRMS (ESI) calcd for C₃₆H₅₆Cl₃NO₁₈Si [M+Na]⁺ 946.2230, found 946.2243.



N-((2S,3R,4R,5S,6R)-2-(((2R,3S,4S,5R,6S)-3,5-dihydroxy-2-(hydroxymethyl)-6-(((2R,3S,4S,5R,6R)-4,5,6-trihydroxy-2-(hydroxymethyl)tetrahydro-2H-pyran-3-yl)oxy)tetrahydro-2H-pyran-4-yl)oxy)-5-hydroxy-6-(hydroxymethyl)-4-(((2R,3R,4S,5R,6R)-3,4,5-trihydroxy-6-(hydroxymethyl)tetrahydro-2H-pyran-2-yl)oxy)tetrahydro-2H-pyran-3-yl)acetamide (2.4). To a solution of **4.76** (1.0 eq, 0.10 g, 0.06 mmol) in THF (1.5 mL) was added acetic acid (1.0 mL) and acetic anhydride (0.5 mL) followed by 10% Zn/Pb couple solid (0.24 g).^{87, 88} The resulting mixture was stirred 6 H and 15 min then was diluted with CH₂Cl₂ (20 mL), filtered through celite, washed with saturated NaHCO₃ solution (3 x 7 mL), brine (1 x 7 mL), dried (MgSO₄), filtered, concentrated *in vacuo*, and coevaprotated with toluene to yield a white foam. The crude acetamide was suspended in MeOH (2 mL) and a concentrated NaOMe solution was added. The reaction was stirred 2 H then neutralized with Dowex 50Wx8, filtered, and concentrated *in vacuo* to yield a white solid. The crude heptanol was suspended in MeOH (2 mL) and H₂O (1 mL) and Pd(OH)₂ was added (2.0 eq, 0.083 g, 0.119 mmol). The reaction was stirred under H₂ for 3 days then was diluted with H₂O and MeOH, filtered through celite, concentrated *in vacuo*, coevaporated with toluene, and lyophilized to yield lacto-*N*-tetraose (**2.4**) (0.027 g, 0.038 mmol, 64% over 3 steps) as a white solid: [α]_D²⁰ +13.5 (c 0.26, DMSO); ¹H and ¹³C spectroscopy data were in accordance with literature data.⁹⁰ HRMS (TOF) calcd for C₂₆H₄₅NO₂₁ [M+Na]⁺ 730.2382, found 730.3188.

4.8 References

1. Craft, K. M.; Townsend, S. D., The Human Milk Glycome as a Defense Against Infectious Diseases: Rationale, Challenges, and Opportunities. *ACS Infect. Dis.* **2017**, *4* (2), 77-83.
2. Boltje, T. J.; Buskas, T.; Boons, G. J., Opportunities and challenges in synthetic oligosaccharide and glycoconjugate research. *Nat. Chem.* **2009**, *1* (8), 611-22.
3. Nijman, R. M.; Liu, Y.; Bunyatratthata, A.; Smilowitz, J. T.; Stahl, B.; Barile, D., Characterization and Quantification of Oligosaccharides in Human Milk and Infant Formula. *J. Agric. Food Chem.* **2018**, *66* (26), 6851-6859.
4. Kunz, C.; Rudloff, S.; Baier, W.; Klein, N.; Strobel, S., Oligosaccharides in human milk: structural, functional, and metabolic aspects. *Ann. Rev. Nutr.* **2000**, *20*, 699-722.
5. Urashima, T.; Asakuma, S.; Leo, F.; Fukuda, K.; Messer, M.; Oftedal, O. T., The predominance of type I oligosaccharides is a feature specific to human breast milk. *Adv. Nutr.* **2012**, *3* (3), 473S-82S.
6. Ninonuevo, M. R.; Park, Y.; Yin, H.; Zhang, J.; Ward, R. E.; Clowers, B. H.; German, J. B.; Freeman, S. L.; Killeen, K.; Grimm, R.; Lebrilla, C. B., A strategy for annotating the human milk glycome. *J. Agric. Food Chem.* **2006**, *54* (20), 7471-80.
7. Aly, M. R. E.; Ibrahim, E. S. I.; El Ashry, E. S. H.; Schmidt, R. R., Synthesis of lacto-*N*-neotetraose and lacto-*N*-tetraose using the dimethylmaleoyl group as amino protective group. *Carbohydr. Res.* **1999**, *316* (1-4), 121-132.
8. Hahm, H. S.; Liang, C. F.; Lai, C. H.; Fair, R. J.; Schuhmacher, F.; Seeberger, P. H., Automated Glycan Assembly of Complex Oligosaccharides Related to Blood Group Determinants. *J. Org. Chem.* **2016**, *81* (14), 5866-77.
9. Takamura, T. C., T.; Ishihara, H.; Tejima, S., Chemical Modification of Lactose. XIII. Synthesis of Lacto-*N*-tetraose. *Chem. Pharm. Bull.* **1980**, *28* (6), 1804-1809.
10. Sherman, A. A.; Yudina, O. N.; Mironov, Y. V.; Sukhova, E. V.; Shashkov, A. S.; Menshov, V. M.; Nifantiev, N. E., Study of glycosylation with *N*-trichloroacetyl-*D*-glucosamine derivatives in the syntheses of the spacer-armed pentasaccharides sialyl lacto-*N*-neotetraose and sialyl lacto-*N*-tetraose, their fragments, and analogues. *Carbohydr. Res.* **2001**, *336* (1), 13-46.

11. Shengshu, H.; Hai, Y.; Xi, C., Chemoenzymatic synthesis of α 2-3-sialylated carbohydrate epitopes. *Sci. China Chem.* **2011**, *54* (1), 117-128.
12. Yao, W.; Yan, J.; Chen, X.; Wang, F.; Cao, H., Chemoenzymatic synthesis of lacto-*N*-tetrasaccharide and sialyl lacto-*N*-tetrasaccharides. *Carbohydr. Res.* **2015**, *401*, 5-10.
13. Hsu, Y.; Lu, X. A.; Zulueta, M. M.; Tsai, C. M.; Lin, K. I.; Hung, S. C.; Wong, C. H., Acyl and silyl group effects in reactivity-based one-pot glycosylation: synthesis of embryonic stem cell surface carbohydrates Lc₄ and IV²Fuc-Lc₄. *J. Am. Chem. Soc.* **2012**, *134* (10), 4549-52.
14. Han, N. S.; Kim, T. J.; Park, Y. C.; Kim, J.; Seo, J. H., Biotechnological production of human milk oligosaccharides. *Biotechnol. Adv.* **2012**, *30* (6), 1268-78.
15. Auge, C.; Crout, D. H., Chemoenzymatic synthesis of carbohydrates. *Carbohydr. Res.* **1997**, *305* (3-4), 307-12.
16. Wong, C-H.; Halcomb, R. L.; Ichikawa, Y.; Kajimoto, T., Enzymes in Organic Synthesis-Application to the Problems of Carbohydrate Recognition (Part 2). *Angew. Chem. Int. Ed.* **1995**, *34*, 521-546.
17. Muthana, S.; Cao, H.; Chen, X., Recent progress in chemical and chemoenzymatic synthesis of carbohydrates. *Curr. Opin. Chem. Biol.* **2009**, *13* (5-6), 573-81.
18. Koeller, K. M.; Wong, C. H., Synthesis of complex carbohydrates and glycoconjugates: enzyme-based and programmable one-pot strategies. *Chem. Rev.* **2000**, *100* (12), 4465-94.
19. Yu, H.; Chokhawala, H. A.; Huang, S.; Chen, X., One-pot three-enzyme chemoenzymatic approach to the synthesis of sialosides containing natural and non-natural functionalities. *Nat. Protoc.* **2006**, *1* (5), 2485-92.
20. Boons, G-J.; Hale, K. J., Organic Synthesis with Carbohydrates. Blackwell Science Inc.: Malden, 2000.
21. Mydock, L. K.; Demchenko, A. V., Mechanism of chemical *O*-glycosylation: from early studies to recent discoveries. *Org. Biomol. Chem.* **2010**, *8* (3), 497-510.

22. Adero, P. O.; Amarasekara, H.; Wen, P.; Bohe, L.; Crich, D., The Experimental Evidence in Support of Glycosylation Mechanisms at the S_N1-S_N2 Interface. *Chem. Rev.* **2018**, *118* (17), 8242-8284.
23. Schmidt, R. R.; Kinzy, W., Anomeric-Oxygen Activation for Glycoside Synthesis: The Trichloroacetimidate Method. *Adv. Carbohydr. Chem. Biochem.* **1994**, *50*, 21-123.
24. Gorenstein, D. G., Stereoelectronic Effects in Biomolecules. *Chem. Rev.* **1987**, *87* (5), 1047-1077.
25. Edward, J. T., Stability of glycosides to acid hydrolysis. *Chem. Ind. (London)* **1955**, 1102-1104.
26. Edward, J. T., Anomeric Effect How It Came To Be Postulated. *ACS Symp. Ser.* **1993**, *539*, 1-5.
27. Lemieux, R. U., Effects of unshared pairs of electrons and their solvation on conformational equilibria. *Pure Appl. Chem.* **1971**, *25* (3), 527-548.
28. Guo, J.; Ye, X. S., Protecting groups in carbohydrate chemistry: influence on stereoselectivity of glycosylations. *Molecules* **2010**, *15* (10), 7235-65.
29. Fraserreid, B.; Wu, Z. F.; Udodong, U. E.; Ottosson, H., Armed-Disarmed Effects in Glycosyl Donors - Rationalization and Sidetracking. *J. Org. Chem.* **1990**, *55* (25), 6068-6070.
30. Mootoo, D. R.; Konradsson, P.; Fraserreid, B., *N*-Pentenyl Glycosides Facilitate a Stereoselective Synthesis of the Pentasaccharide Core of the Protein Membrane Anchor Found in Trypanosoma-Brucei. *J. Am. Chem. Soc.* **1989**, *111* (22), 8540-8542.
31. Mootoo, D. R.; Konradsson, P.; Udodong, U.; Fraser-Reid, B., "Armed" and "Disarmed" -Pentenyl Glycosides in Saccharide Couplings Leading to Oligosaccharides. *J. Am. Chem. Soc.* **1988**, *110*, 5583-5584.
32. Douglas, N. L.; Ley, S. V.; Lucking, U.; Warriner, S. L., Tuning glycoside reactivity: New tool for efficient oligosaccharide synthesis. *J. Chem. Soc. Perkin Trans. 1* **1998**, (1), 51-65.

33. Fraserreid, B.; Wu, Z. F.; Andrews, C. W.; Skowronski, E.; Bowen, J. P., Torsional Effects in Glycoside Reactivity - Saccharide Couplings Mediated by Acetal Protecting Groups. *J. Am. Chem. Soc.* **1991**, *113* (4), 1434-1435.
34. Jensen, H. H.; Nordstrom, L. U.; Bols, M., The disarming effect of the 4,6-acetal group on glycoside reactivity: torsional or electronic? *J. Am. Chem. Soc.* **2004**, *126* (30), 9205-13.
35. Toshima, K., Glycosyl fluorides in glycosidations. *Carbohydr. Res.* **2000**, *327* (1-2), 15-26.
36. Demchenko, A. V., Stereoselective chemical 1,2-cis O-glycosylation: From 'sugar ray' to modern techniques of the 21st century. *Synlett* **2003**, (9), 1225-1240.
37. Schmidt, R. R.; Behrendt, M.; Toepfer, A., Nitriles as Solvents in Glycosylation Reactions - Highly Selective β -Glycoside Synthesis. *Synlett* **1990**, (11), 694-696.
38. Nicolaou, K. C.; Mitchell, H. J., Adventures in Carbohydrate Chemistry: New Synthetic Technologies, Chemical Synthesis, Molecular Design, and Chemical Biology. *Angew. Chem. Int. Ed.* **2001**, *40* (9), 1576-1624.
39. Igarashi, K., The Koenigs-Knorr Reaction. *Adv. Carbohydr. Chem. Biochem.* **1977**, *34*, 243-283.
40. Lemieux, R. U.; Hendriks, K. B.; Stick, R. V.; James, K., Halide Ion Catalyzed Glycosidation Reactions Syntheses of α -Linked Disaccharides. *J. Am. Chem. Soc.* **1975**, *97* (14), 4056-4062.
41. Lemieux, R. U.; Hayami, J., The mechanism of the anomerization of the tetra-O-acetyl-D-glucopyranosyl chlorides. *Can. J. Chem.* **1965**, *43* (8), 2162-2173.
42. Mukaiyama, T.; Murai, Y.; Shoda, S., An Efficient Method for Glucosylation of Hydroxy Compounds Using Glucopyranosyl Fluoride. *Chem. Lett.* **1981**, (3), 431-432.
43. Schmidt, R. R.; Michel, J., Facile Synthesis of α - and β -O-Glycosyl Imidates; Preparation of Glycosides and Disaccharides. *Angew. Chem.* **1980**, *19* (9), 731-732.
44. Zhu, X.; Schmidt, R. R., New principles for glycoside-bond formation. *Angew. Chem.* **2009**, *48* (11), 1900-34.

45. Nielsen, M. M.; Stougaard, B. A.; Bols, M.; Glibstrup, E.; Pedersen, C. M., Glycosyl Fluorides as Intermediates in $\text{BF}_3 \cdot \text{OEt}_2$ -Promoted Glycosylation with Trichloroacetimidates. *Eur. J. Org. Chem.* **2017**, 2017 (9), 1281-1284.
46. Codee, J. D.; Litjens, R. E.; van den Bos, L. J.; Overkleeft, H. S.; van der Marel, G. A., Thioglycosides in sequential glycosylation strategies. *Chem. Soc. Rev.* **2005**, 34 (9), 769-82.
47. Zhang, Z. Y.; Ollmann, I. R.; Ye, X. S.; Wischnat, R.; Baasov, T.; Wong, C. H., Programmable one-pot oligosaccharide synthesis. *J. Am. Chem. Soc.* **1999**, 121 (4), 734-753.
48. Murata, T.; Inukai, T.; Suzuki, M.; Yamagishi, M.; Usui, T., Facile enzymatic conversion of lactose into lacto-*N*-tetraose and lacto-*N*-neotetraose. *Glycoconj. J.* **1999**, 16 (3), 189-195.
49. Baumgartner, F.; Conrad, J.; Sprenger, G. A.; Albermann, C., Synthesis of the human milk oligosaccharide lacto-*N*-tetraose in metabolically engineered, plasmid-free *E. coli*. *Chembiochem.* **2014**, 15 (13), 1896-900.
50. Auge, C.; Veyrieres, A., Synthesis of a disaccharide oxazoline- 2-methyl-[4,6-di-O-acetyl-1,2-dideoxy-3-O-(2,3,4,6-tetra-O-acetyl- β -d-galactopyranosyl)- α -d-glucopyrano][2',1'-4,5]-2-oxazoline. *Carbohydr. Res.* **1976**, 46, 293-298.
51. Dea, I. C. M., Aryl glycosides of oligosaccharides Part II. Bromo-, chloro-, and iodo-phenyl beta-D-glycosides of some disaccharides. *Carbohydr. Res.* **1970**, 12, 297-299.
52. Tejima, S.; Chiba, T., Synthesis of 6-Acetamide-6-deoxy lactose Derivatives. *Chem. Pharm. Bull.* **1973**, 21 (3), 546-551.
53. Chiba, T.; Haga, M.; Tejima, S., Studies on the Reactivities of the Secondary Hydroxyl Groups in 1,6-Anhydro-4',6'-O-Benzylidene- β -Lactose by Selective Benzoylation. *Carbohydr. Res.* **1975**, 45, 11-18.
54. Takamura, T.; Tejima, S., Chemical Modification of Lactose. VIII. Studies on the Reactivities of the Secondary Hydroxyl Groups in 1,6-Anhydro-4',6'-O-benzylidene- β -lactose by selective p-Toluenesulfonylation. *Chem. Pharm. Bull.* **1978**, 26 (4), 1117-1122.

55. Aly, M. R. E.; Castro-Palomino, J. C.; Ibrahim, E. S. I.; El-Ashry, E. S. H.; Schmidt, R. R., The dimethylmaleoyl group as amino protective group - Application to the synthesis of glucosamine-containing oligosaccharides. *Eur. J. Org. Chem.* **1998**, (11), 2305-2316.
56. Schmidt, R. R.; Stumpp, M., Synthese von 1-Thioglycosiden. *Liebigs Ann. Chem.* **1983**, 7, 1249-1256.
57. Jung, K-H.; Hoch, M.; Schmidt, R. R., Selectively Protected Lactose and 2-Azido Lactose, Building Blocks for Glycolipid Synthesis. *Liebigs. Ann.* **1989**, 1989, 1099-1106.
58. Schmidt, R. R.; Michel, J., Facile Synthesis of α - and β -Glycosyl Imidates; Preparation of Glycosides and Disaccharides. *Angew. Chem. Int. Ed.* **1980**, 19 (9), 731-732.
59. Barczai-Martos, M.; Korosy, F., Preparation of Acetobrome-Sugars. *Nature (London)* **1950**, 165, 369.
60. Agnihotri, G.; Tiwari, P.; Misra, A. K., One-pot synthesis of per-O-acetylated thioglycosides from unprotected reducing sugars. *Carbohydr. Res.* **2005**, 340 (7), 1393-6.
61. Baer, H. H.; Abbas, S. A., Synthesis of O- α l-fucopyranosyl-(1 \rightarrow 3)-O- β -d-galactopyranosyl-(1 \rightarrow 4)-d-glucose (3'-O- α -l-fucopyranosyllactose), and an improved route to its β -(1'' \rightarrow 3')-linked Isomer. *Carbohydr. Res.* **1980**, 84, 53-60.
62. Yudina, O. N.; Sherman, A. A.; Nifantiev, N. E., Synthesis of propyl and 2-aminoethyl glycosides of α -D-galactosyl-(1 \rightarrow 3')- β -lactoside. *Carbohydr. Res.* **2001**, 332 (4), 363-71.
63. Wang, Z.; Zhou, L.; El-Boubbou, K.; Ye, X. S.; Huang, X., Multi-component one-pot synthesis of the tumor-associated carbohydrate antigen Globo-H based on preactivation of thioglycosyl donors. *J. Org. Chem.* **2007**, 72 (17), 6409-20.
64. Huang, T. Y.; Zulueta, M. M.; Hung, S. C., One-pot strategies for the synthesis of the tetrasaccharide linkage region of proteoglycans. *Org. Lett.* **2011**, 13 (6), 1506-9.
65. Hsu, C. H.; Chu, K. C.; Lin, Y. S.; Han, J. L.; Peng, Y. S.; Ren, C. T.; Wu, C. Y.; Wong, C. H., Highly α -selective sialyl phosphate donors for efficient preparation of natural sialosides. *Chemistry* **2010**, 16 (6), 1754-60.

66. Liu, X. W.; Xia, C.; Li, L.; Guan, W. Y.; Pettit, N.; Zhang, H. C.; Chen, M.; Wang, P. G., Characterization and synthetic application of a novel β 1,3-galactosyltransferase from *Escherichia coli* O55:H7. *Bioorg. Med. Chem.* **2009**, *17* (14), 4910-5.
67. Craft, K. M.; Townsend, S. D., Synthesis of lacto-*N*-tetraose. *Carbohydr. Res.* **2017**, *440-441*, 43-50.
68. Dullenkopf, W.; CastroPalomino, J. C.; Manzoni, L.; Schmidt, R. R., *N*-Trichloroethoxycarbonyl-glucosamine derivatives as glycosyl donors. *Carbohydr. Res.* **1996**, *296*, 135-147.
69. Andersen, S. M.; Heuckendorff, M.; Jensen, H. H., 3-(Dimethylamino)-1-propylamine: a cheap and versatile reagent for removal of byproducts in carbohydrate chemistry. *Org. Lett.* **2015**, *17* (4), 944-7.
70. Corey, E. J.; Venkateswarlu, A., Protection of Hydroxyl Groups as Zeri-Butyldimethylsilyl Derivatives. *J. Am. Chem. Soc.* **1972**, *94* (17), 6190-6191.
71. Kunesch, N.; Miet, C.; Poisson, J., Utilisation de la guanidine comme agent désacétylant sélectif-une méthode de désacétylation instantanée applicable aux sucres. *Tetrahedron Lett.* **1987**, *28* (31), 3569-3572.
72. Ellervik, U.; Magnusson, G., Guanidine/guanidinium nitrate; A mild and selective *O*-deacetylation reagent that leaves the *N*-Troc group intact. *Tetrahedron Lett.* **1997**, *38* (9), 1627-1628.
73. Maiti, K. K.; Decastro, M.; El-Sayed, A. B.; Foote, M. I.; Wolfert, M. A.; Boons, G. J., Chemical synthesis and proinflammatory responses of monophosphoryl lipid A adjuvant candidates. *Eur. J. Org. Chem.* **2010**, *2010* (1), 80-91.
74. Danishefsky, J. R. A. a. S. J., New Applications of the *n*-Pentenyl Glycoside Method in the Synthesis and Immunoconjugation of Fucosyl GM1: A Highly Tumor-Specific Antigen Associated with Small Cell Lung Carcinoma. *J. Am. Chem. Soc.* **1999**, *121*, 10875-10882.
75. Martin, T. J.; Schmidt, R. R., Efficient Sialylation with Phosphite as Leaving Group. *Tetrahedron Lett.* **1992**, *33* (41), 6123-6126.

76. Crich, D.; de la Mora, M.; Vinod, A. U., Influence of the 4,6-O-benzylidene, 4,6-O-phenylboronate, and 4,6-O-polystyrylboronate protecting groups on the stereochemical outcome of thioglycoside-based glycosylations mediated by 1-benzenesulfinyl piperidine/triflic anhydride and *N*-iodosuccinimide/trimethylsilyl triflate. *J. Org. Chem.* **2003**, *68* (21), 8142-8.
77. Nicolaou, K. C.; Bockovich, N. J.; Carcanague, D. R., Total Synthesis of Sulfated Le(X) and Le(a)-Type Oligosaccharide Selectin Ligands. *J. Am. Chem. Soc.* **1993**, *115* (19), 8843-8844.
78. Lay, L.; Manzoni, L.; Schmidt, R. R., Synthesis of *N*-acetylglucosamine containing Lewis A and Lewis X building blocks based on *N*-tetrachlorophthaloyl protection--synthesis of Lewis X pentasaccharide. *Carbohydr. Res.* **1998**, *310*, 157-171.
79. Marandube, A.; Veyrieres, A., Glycosylation of lactose: Synthesis of branched oligosaccharides involved in the biosynthesis of glycolipids having blood-group I activity*. *Carbohydr. Res.* **1986**, *151*, 105-119.
80. Vanboeckel, C. A. A.; Delbressine, L. P. C.; Kaspersen, F. M., The Synthesis of Glucuronides Derived from the Antidepressant Drugs Mianserin and Org 3770. *Recl. Trav. Chim. Pays-Bas* **1985**, *104* (10), 259-265.
81. Just, G.; Grozinger, K., A Selective, Mild Cleavage of Trichloroethyl Esters, Carbamates, and Carbonates to Carboxylic Acids, Amines, and Phenols using Zinc:Tetrahydrofuran:pH 4.2-7.2 Buffer. *Synthesis* **1976**, *1976* (7), 457-458.
82. Pratt, M. R.; Bertozzi, C. R., Syntheses of 6-sulfo sialyl Lewis X glycans corresponding to the L-selectin ligand "sulfoadhesin". *Org. Lett.* **2004**, *6* (14), 2345-8.
83. Cochrane, S. A.; Findlay, B.; Bakhtiary, A.; Acedo, J. Z.; Rodriguez-Lopez, E. M.; Mercier, P.; Vederas, J. C., Antimicrobial lipopeptide tridecaptin A1 selectively binds to Gram-negative lipid II. *PNAS* **2016**, *113* (41), 11561-11566.
84. Ghosh, S.; Nishat, S.; Andreana, P. R., Synthesis of an Aminoxy Derivative of the Tetrasaccharide Repeating Unit of *Streptococcus dysgalactiae* 2023 Polysaccharide for a PS A1 Conjugate Vaccine. *J. Org. Chem.* **2016**, *81* (11), 4475-84.
85. Wuts, P. G. M., *Greene's Protective Groups in Organic Synthesis*, 5th Ed. John Wiley & Sons, Inc.:Hoboken, 2014.

86. Overman, L. E.; Freerks, R. L., A short total synthesis of (+/-)-perhydrogephyrotoxin. *J. Org. Chem.* **1981**, *46*, 2833-2835.
87. Boger, D. L.; Kim, S. H.; Mori, Y.; Weng, J.-H.; Rogel, O.; Castle, S. L.; McAtee, J. J., First and Second Generation Total Synthesis of the Teicoplanin Aglycon. *J. Am. Chem. Soc.* **2001**, *123*, 1862-1871.
88. Dong, Q.; Anderson, E.; Ciufolini, M. A., Reductive Cleavage of TROC Groups Under Neutral Conditions with Cadmium-Lead Couple. *Tetrahedron Lett.* **1995**, *36* (32), 5681-5682.
89. Lay, L.; Manzoni, L.; Schmidt, R. R., Synthesis of *N*-acetylglucosamine containing Lewis A and Lewis X building blocks based on *N*-tetrachlorophthaloyl protection--synthesis of Lewis X pentasaccharide. *Carbohydr. Res.* **1998**, *310*, 157-171.
90. Strecker, G.; Wieruszkeski, J.-M.; Michalski, J.-C.; Montreuil, J., Assignment of the ¹H- and ¹³C-NMR Spectra of Eight Oligosaccharides of the Lacto-*N*-tetraose and Neotetraose Series. *Glycoconj. J.* **1989**, *6*, 67-83.

Appendix A2:
Spectra Relevant to Chapter 4

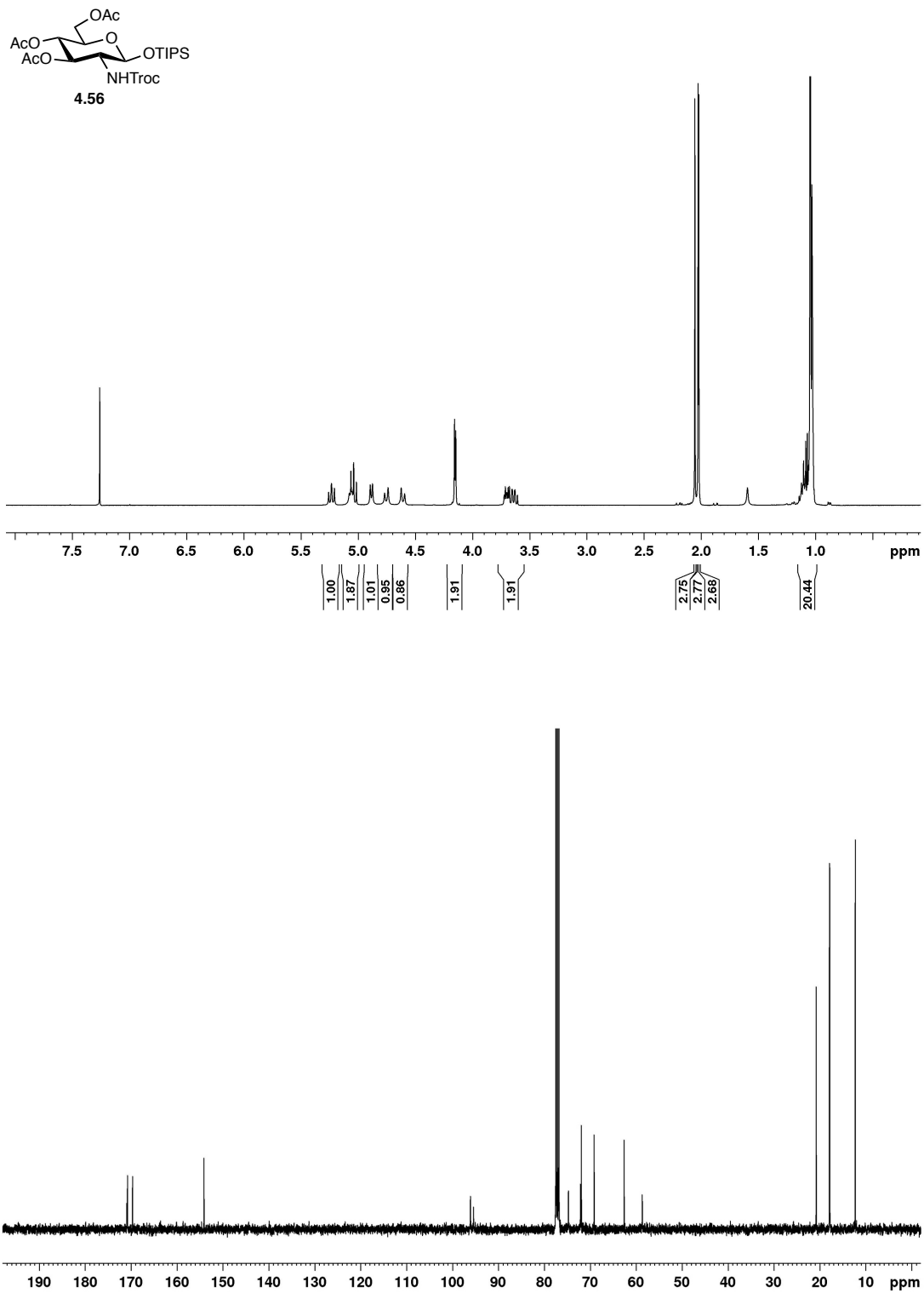


Figure A2.1. ^1H NMR (400 MHz, CDCl_3) and ^{13}C (100 MHz, CDCl_3) spectra of **4.56**.

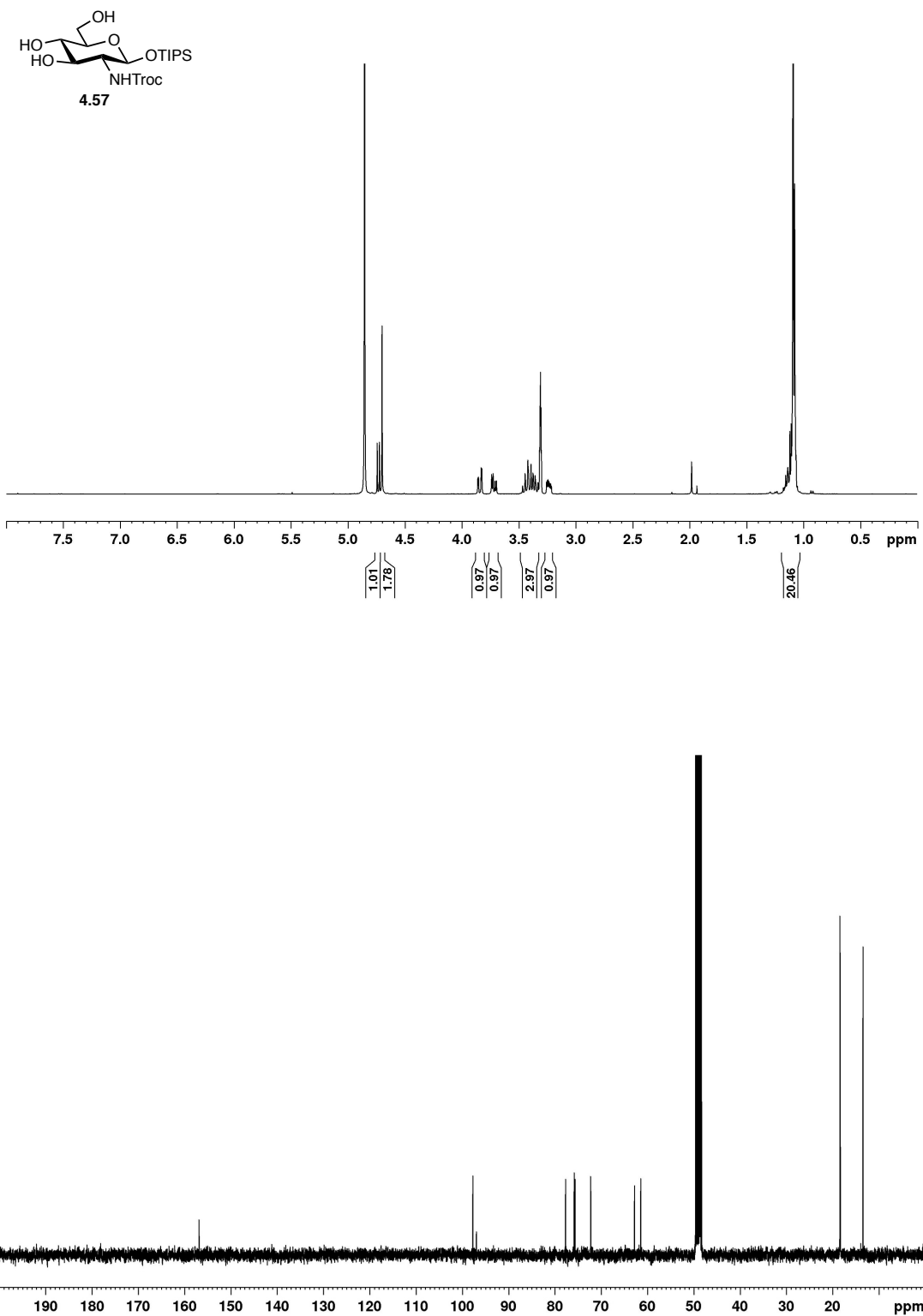


Figure A2.2. ¹H NMR (400 MHz, MeOD) and ¹³C (100 MHz, MeOD) spectra of **4.57**.

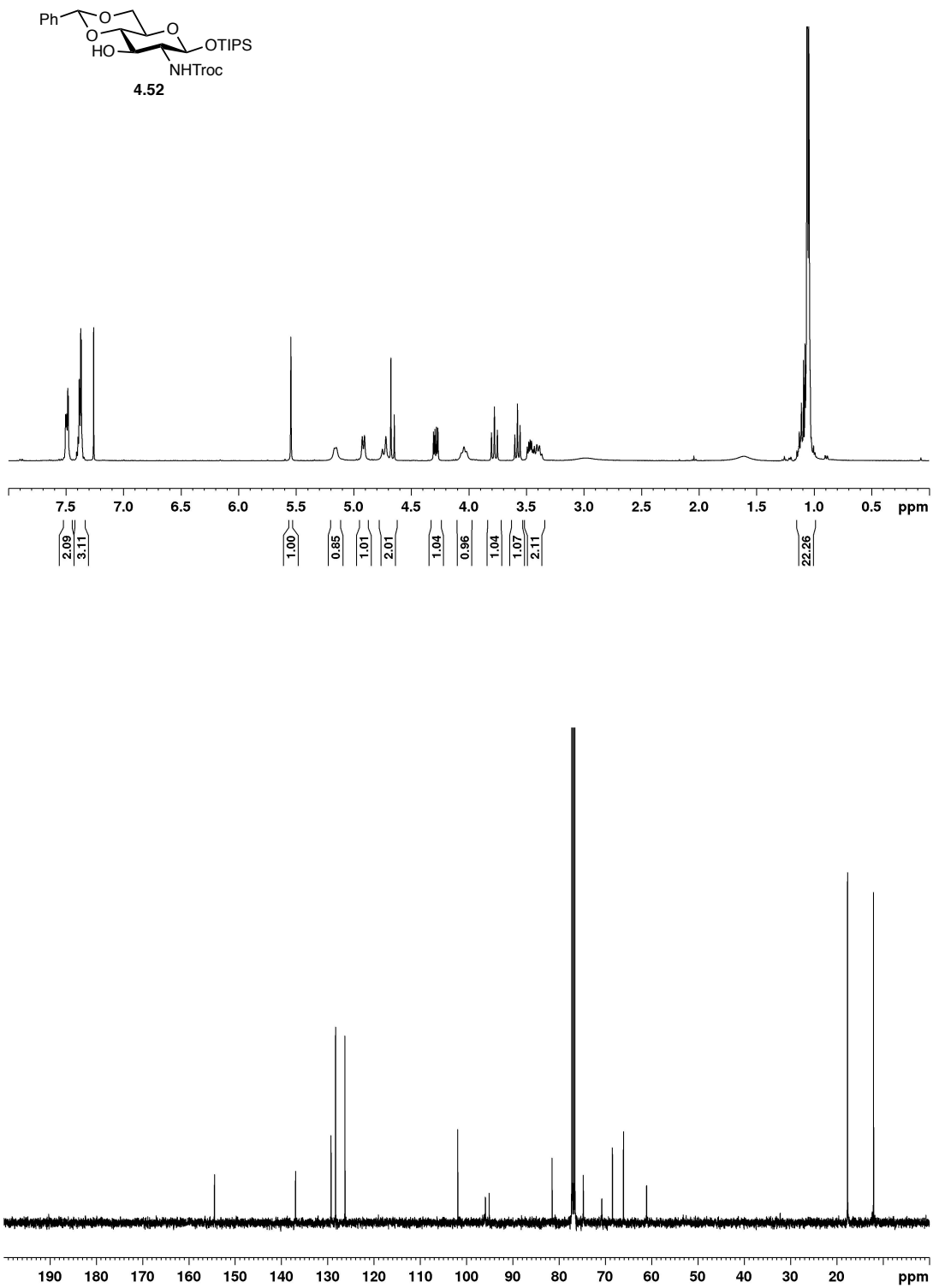


Figure A2.3. ¹H NMR (400 MHz, CDCl₃) and ¹³C (100 MHz, CDCl₃) spectra of **4.52**.

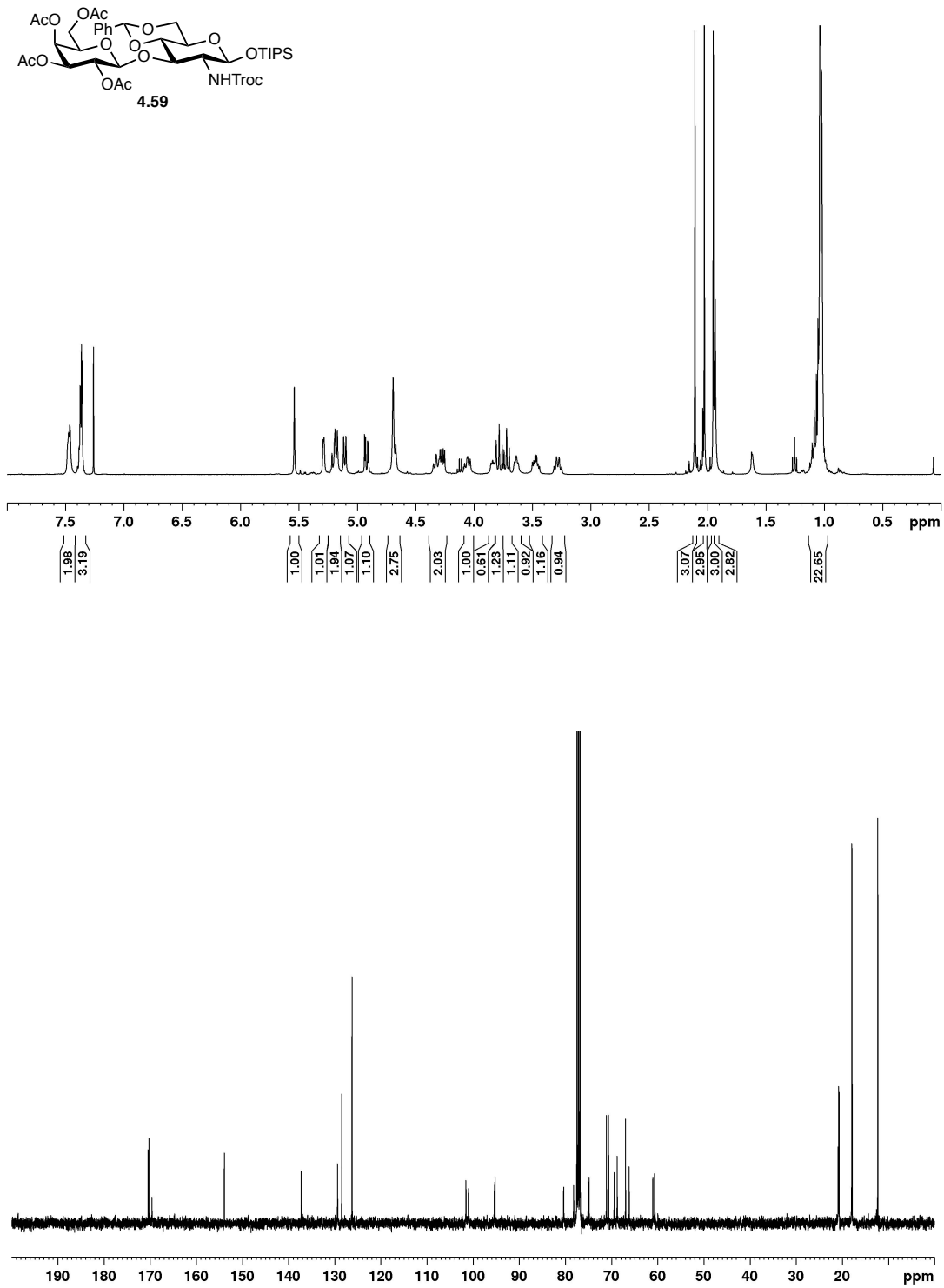


Figure A2.4. ¹H NMR (400 MHz, CDCl₃) and ¹³C (100 MHz, CDCl₃) spectra of **4.59**.

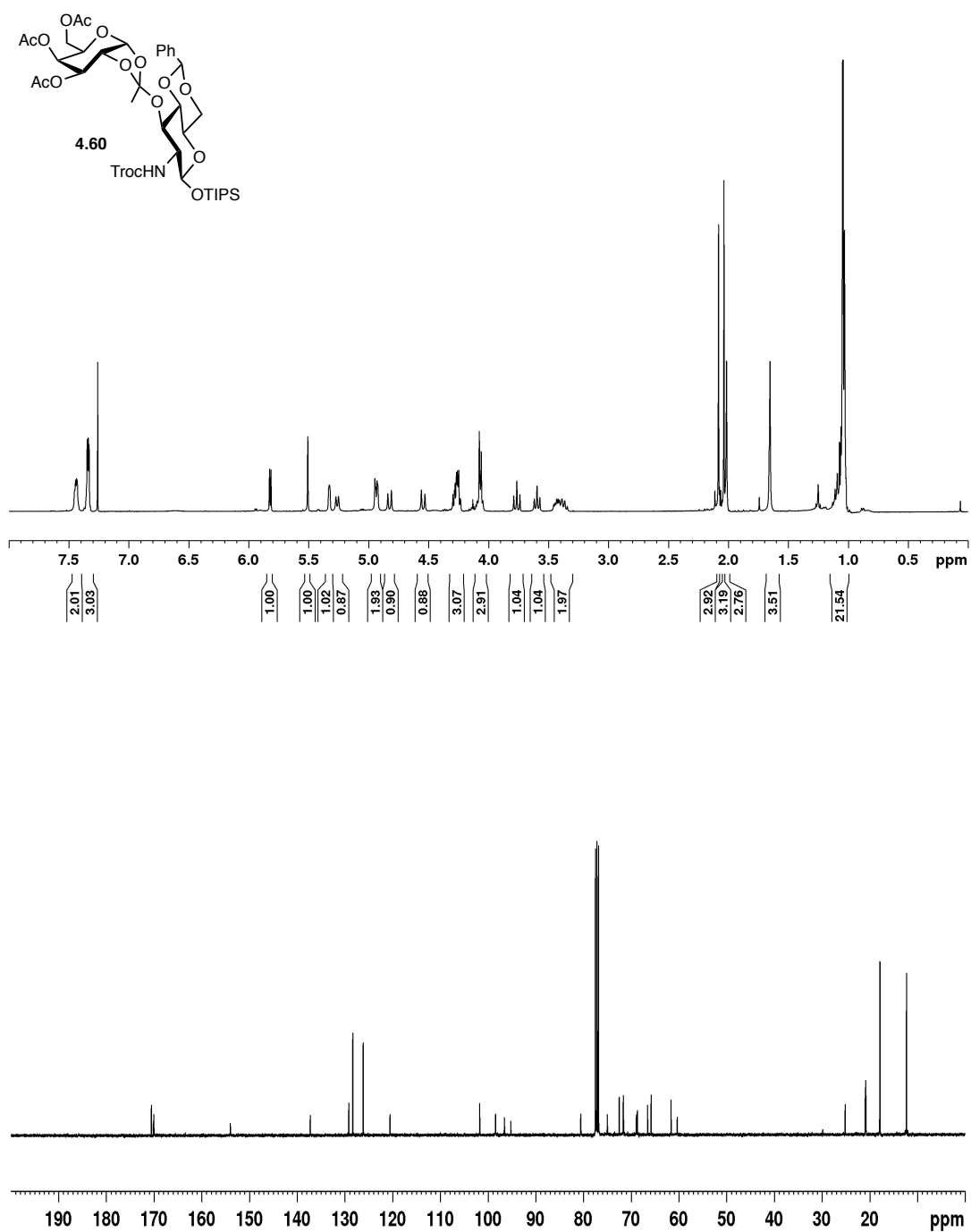


Figure A2.5. ^1H NMR (400 MHz, CDCl_3) and ^{13}C (100 MHz, CDCl_3) spectra of **4.60**.

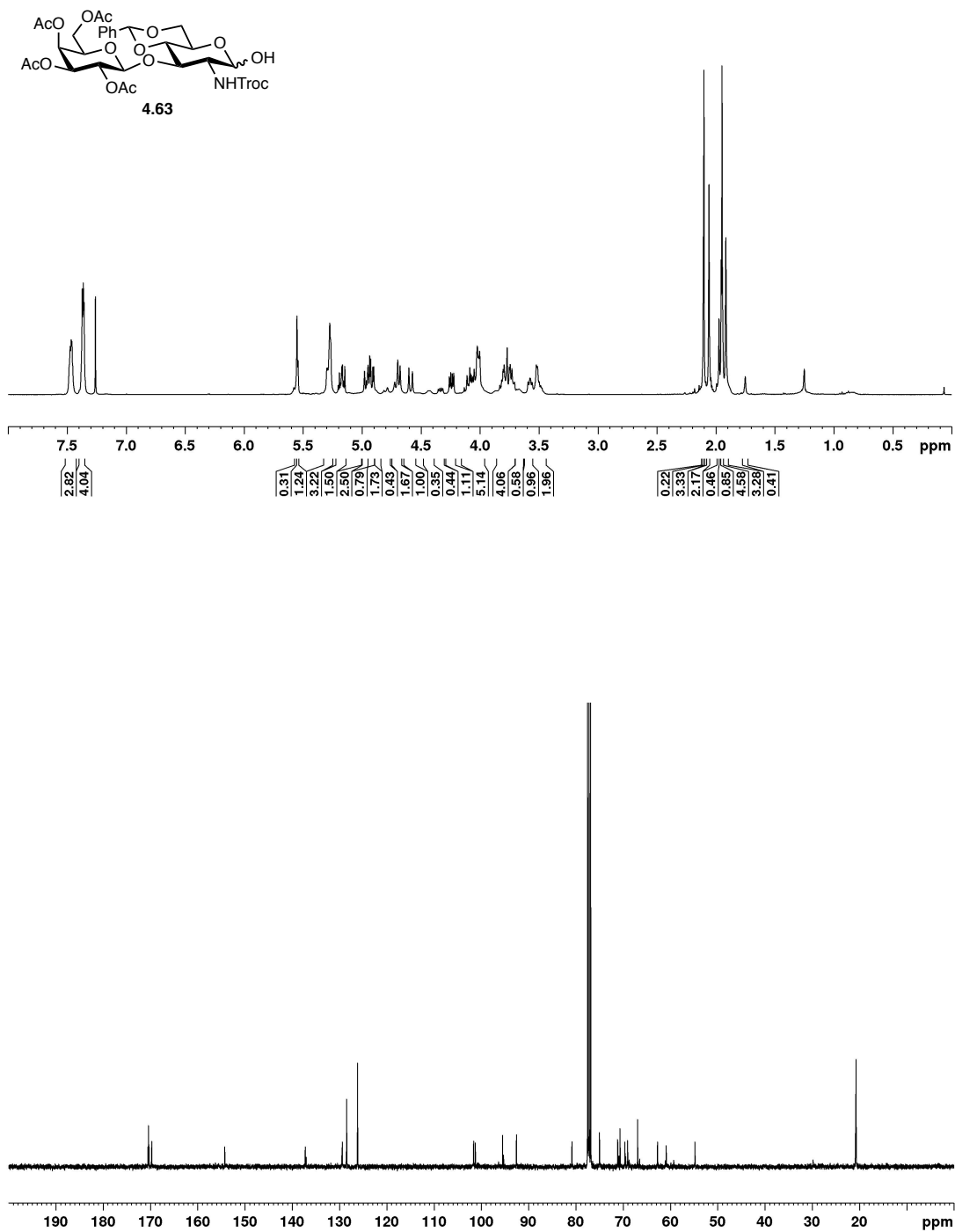


Figure A2.6. ¹H NMR (400 MHz, CDCl₃) and ¹³C (100 MHz, CDCl₃) spectra of **4.63**.

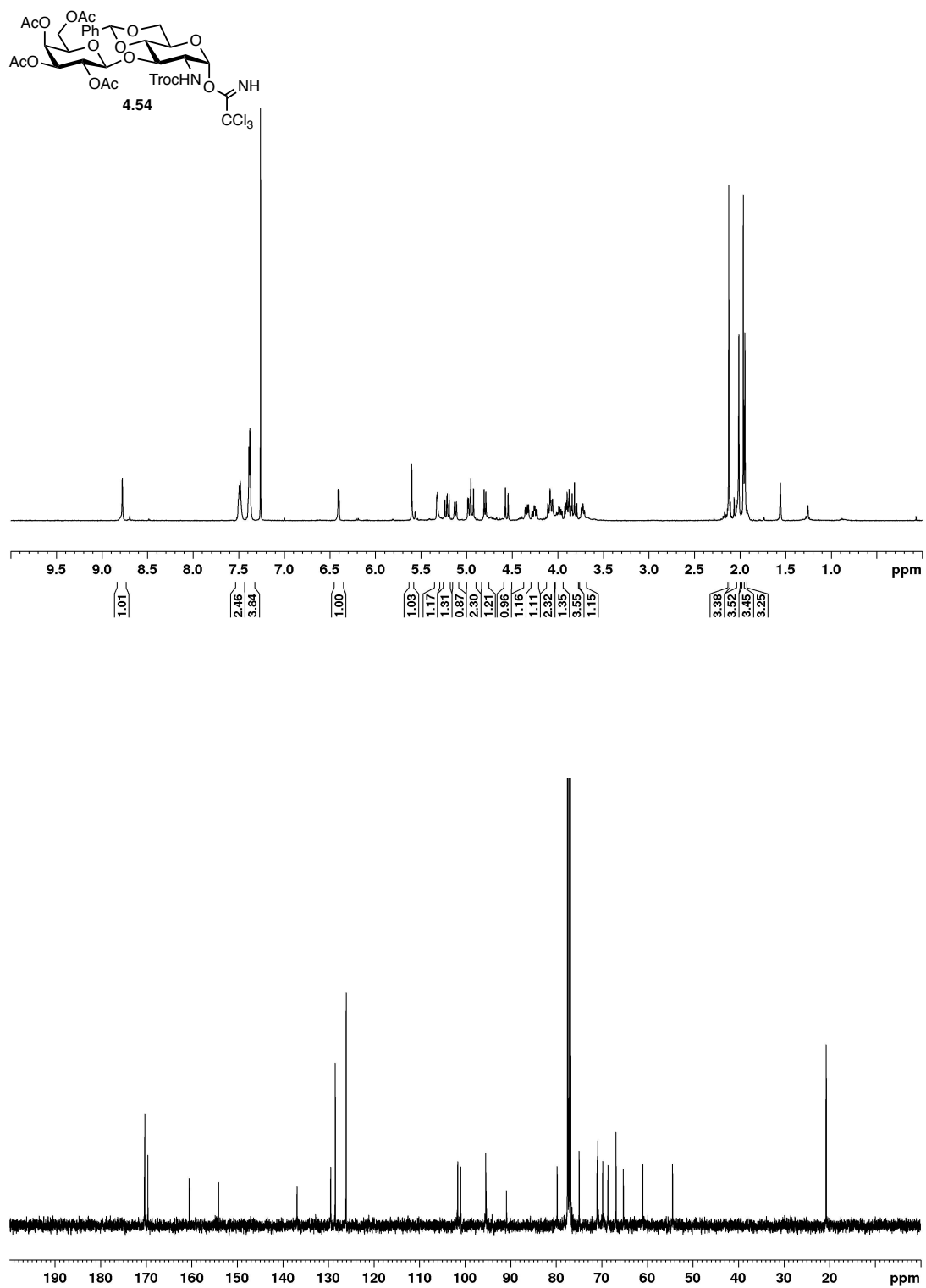


Figure A2.7. ^1H NMR (400 MHz, CDCl_3) and ^{13}C (100 MHz, CDCl_3) spectra of 4.54.

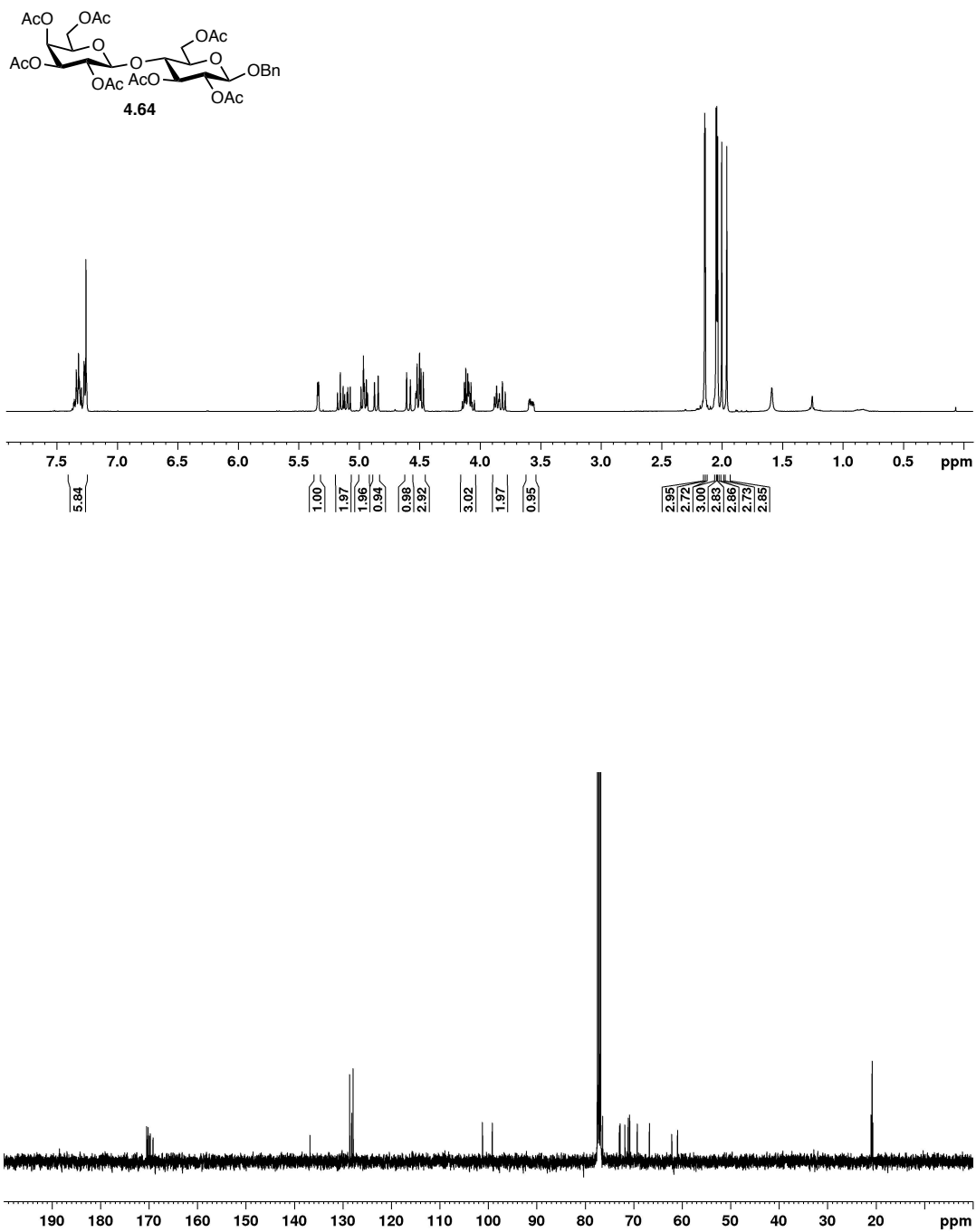


Figure A2.8. ¹H NMR (400 MHz, CDCl₃) and ¹³C (100 MHz, CDCl₃) spectra of **4.64**.

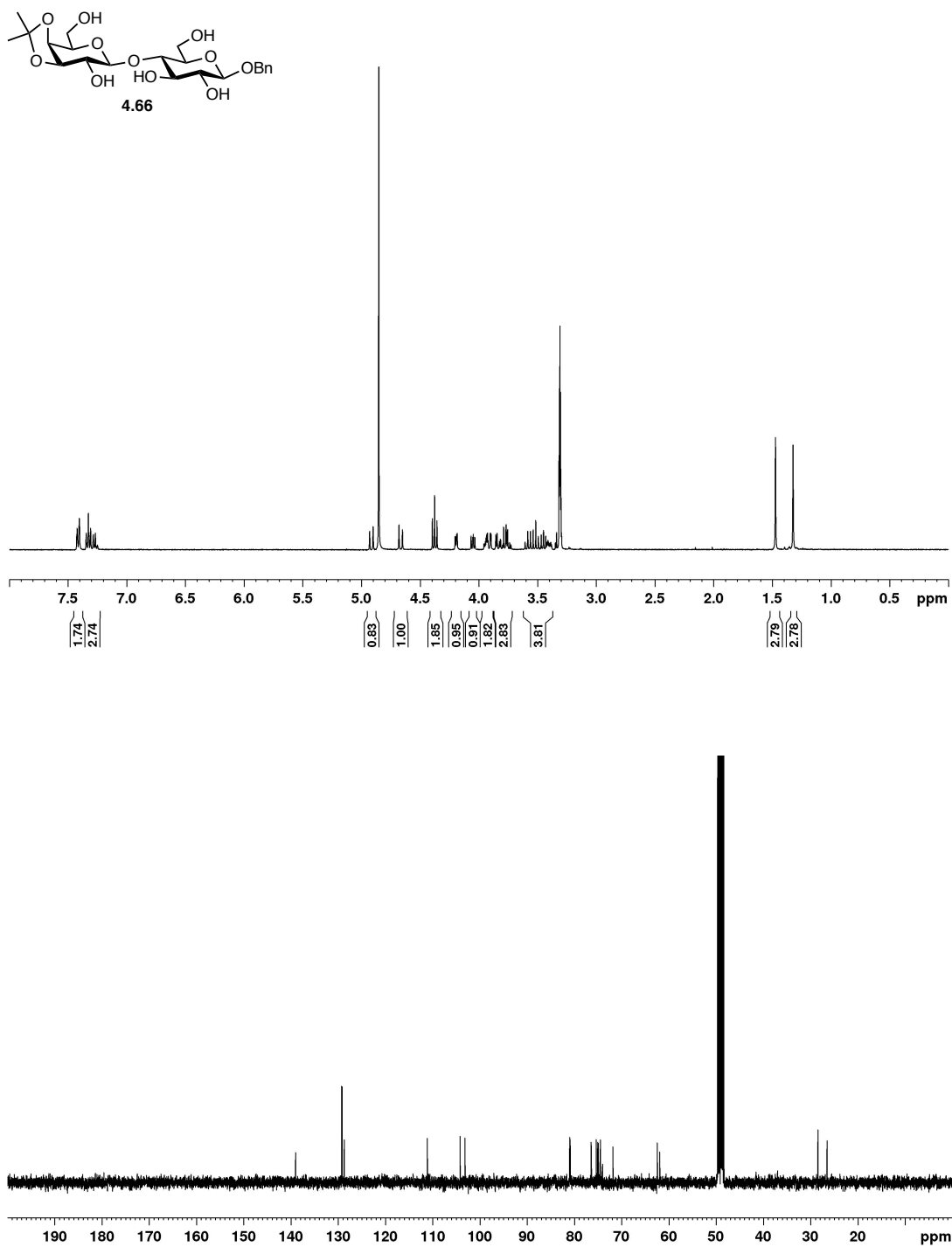


Figure A2.9. ^1H NMR (400 MHz, CDCl_3) and ^{13}C (100 MHz, CDCl_3) spectra of **4.66**.

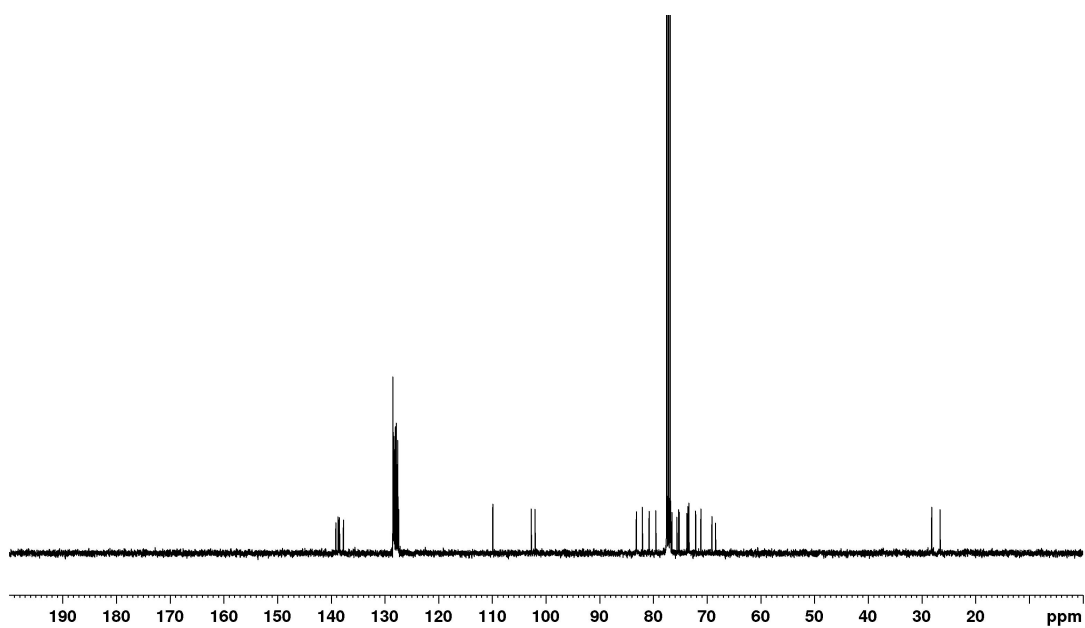
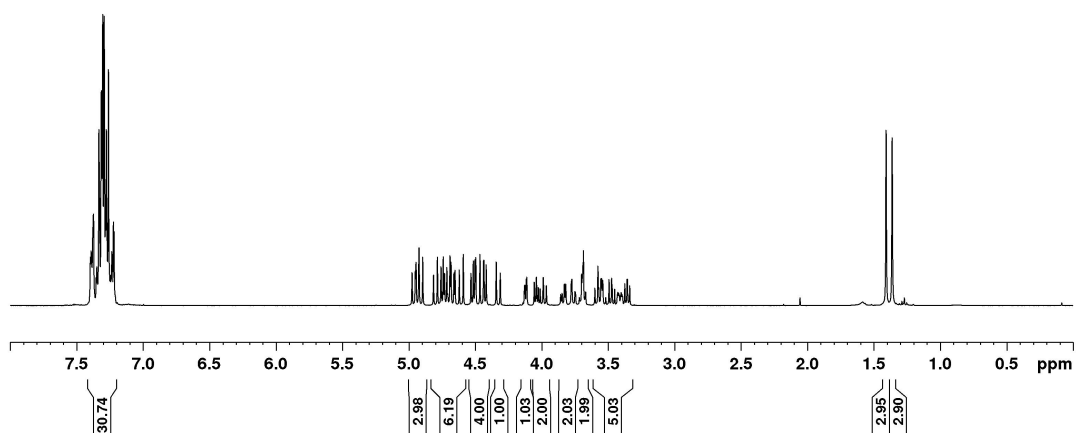
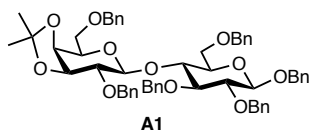


Figure A2.10. ^1H NMR (400 MHz, CDCl_3) and ^{13}C (100 MHz, CDCl_3) spectra of **A1**.

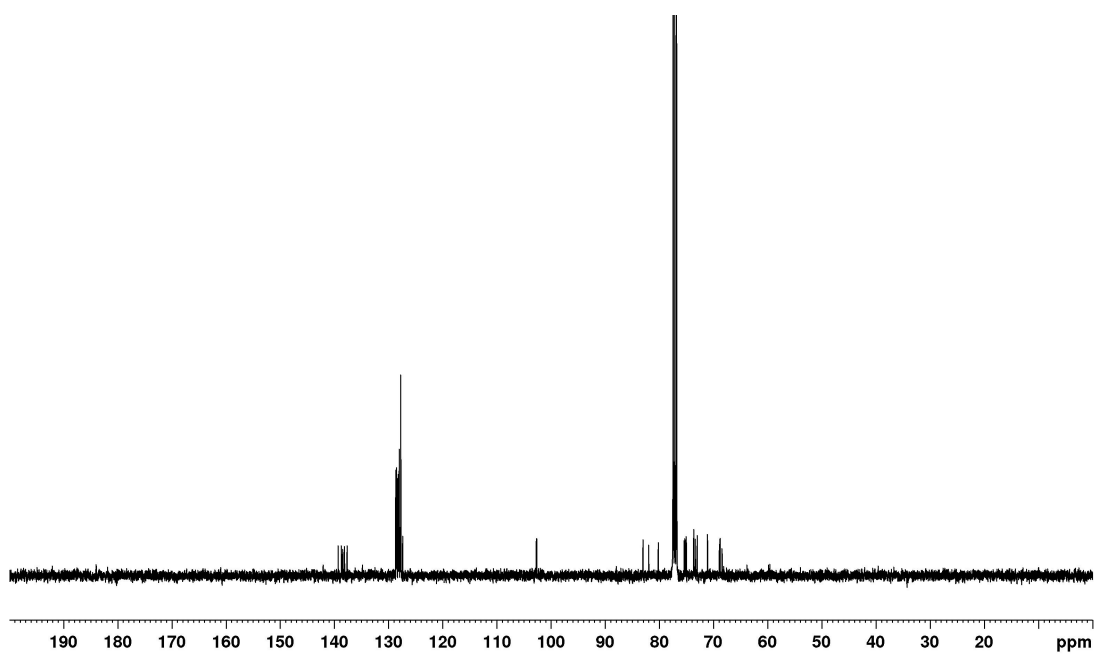
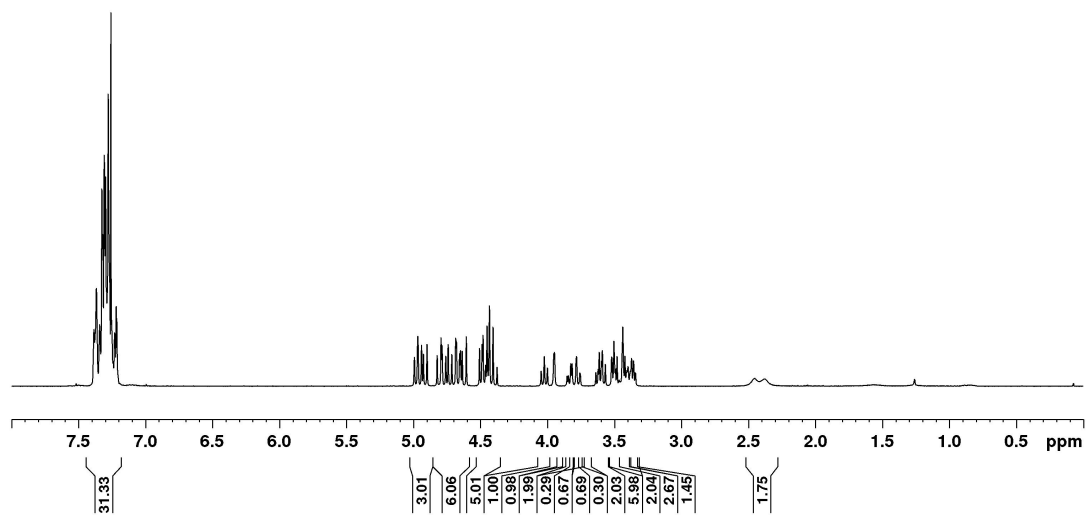
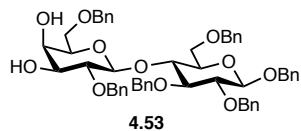


Figure A2.11. ^1H NMR (400 MHz, CDCl_3) and ^{13}C (100 MHz, CDCl_3) spectra of **4.53**.

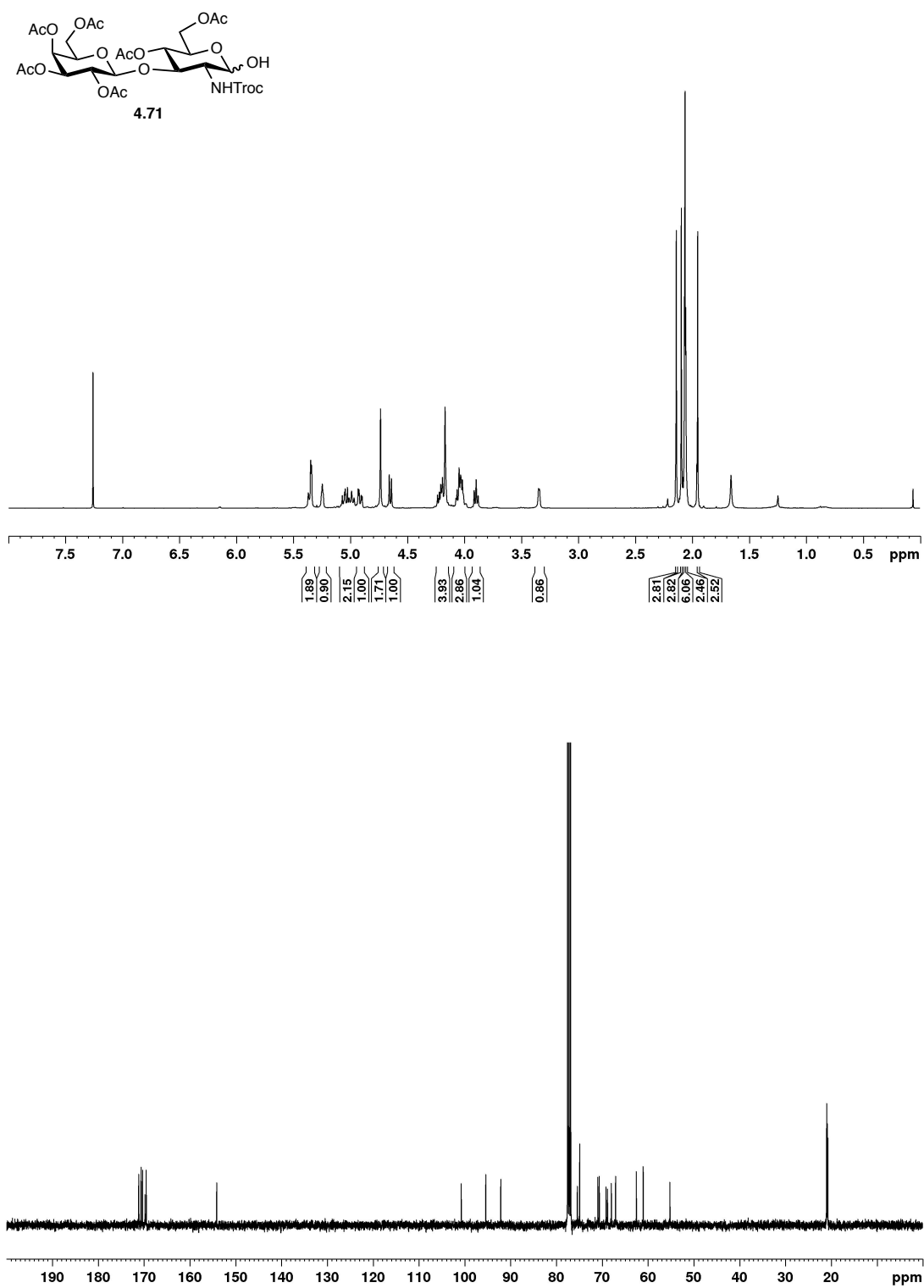


Figure A2.12. ¹H NMR (400 MHz, CDCl₃) and ¹³C (100 MHz, CDCl₃) spectra of **4.71**.

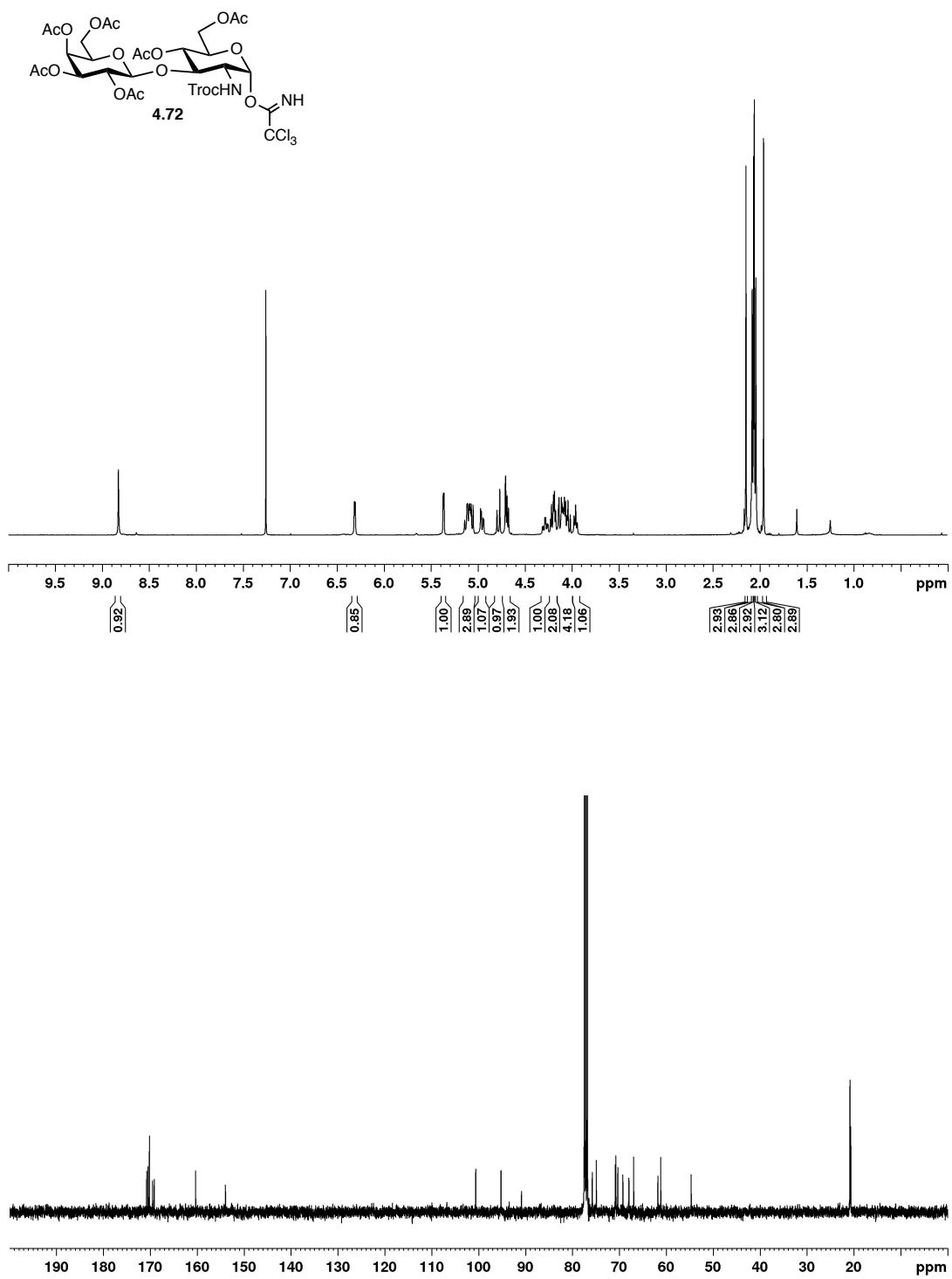


Figure A2.13. ¹H NMR (400 MHz, CDCl₃) and ¹³C (100 MHz, CDCl₃) spectra of **4.72**.

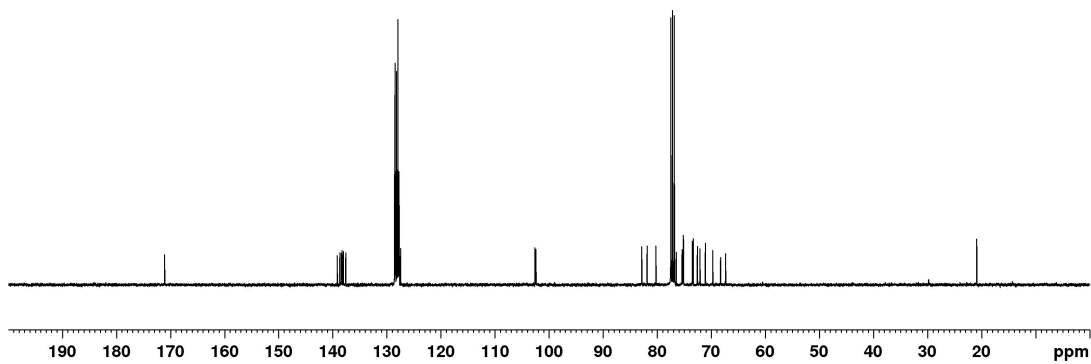
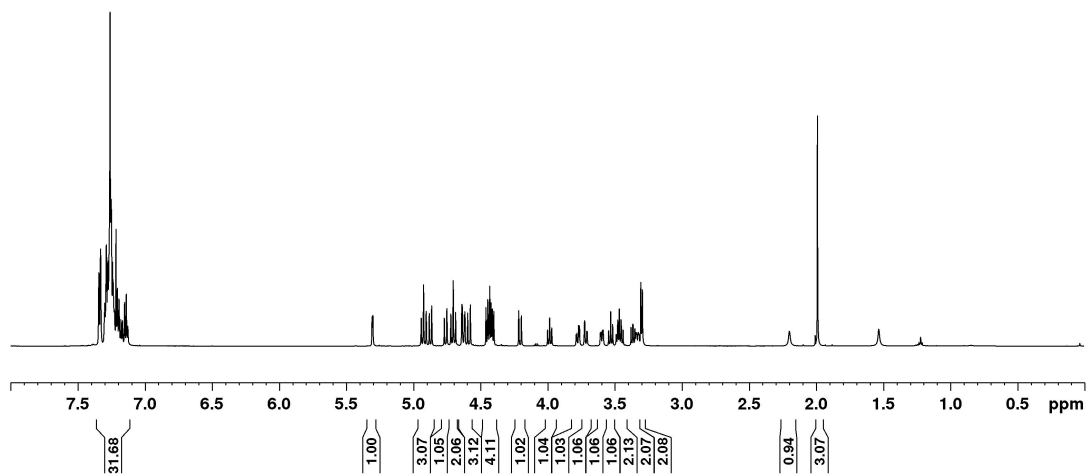
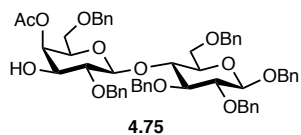


Figure A2.14. ^1H NMR (600 MHz, CDCl_3) and ^{13}C (100 MHz, CDCl_3) spectra of **4.75**.

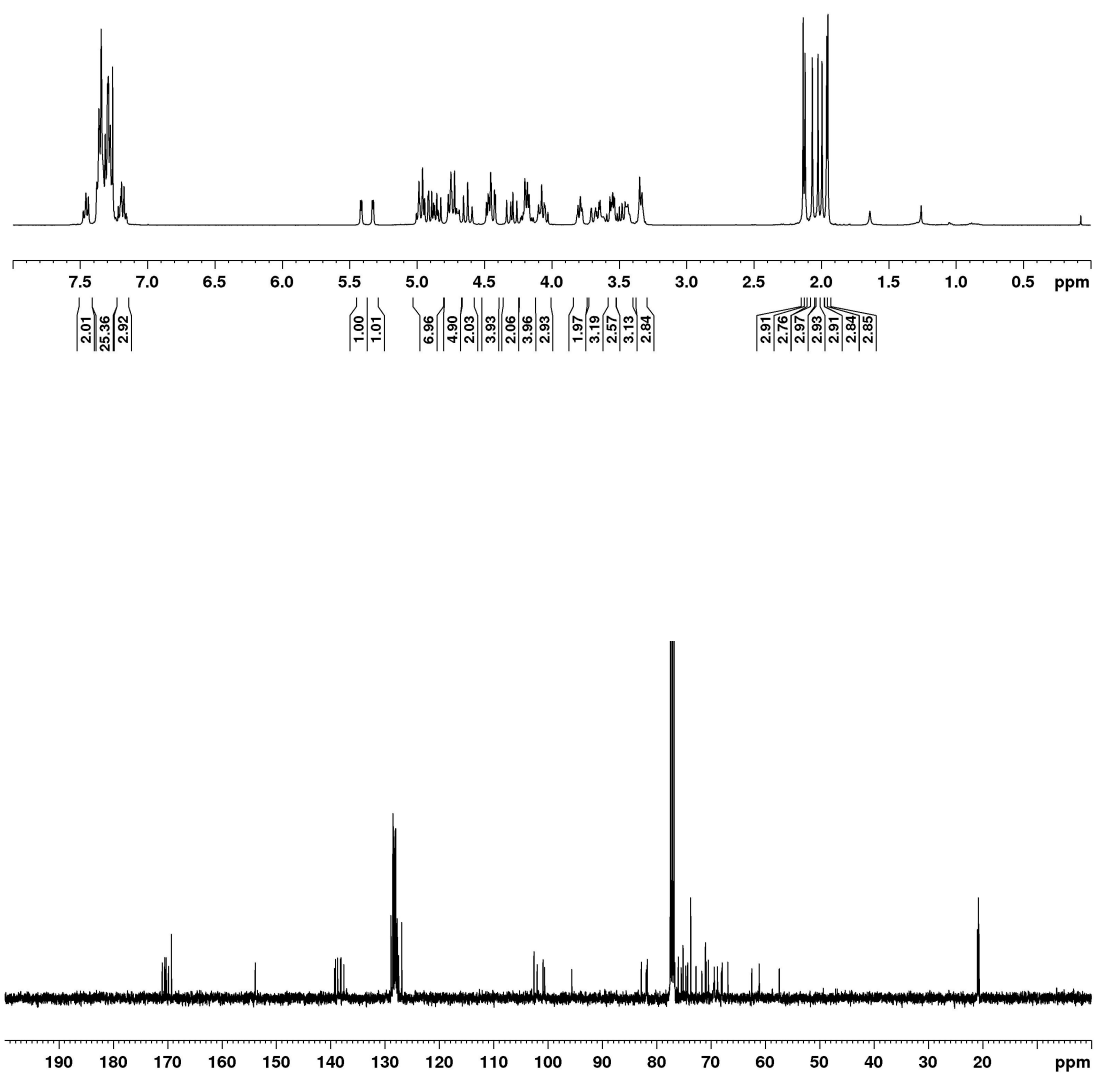
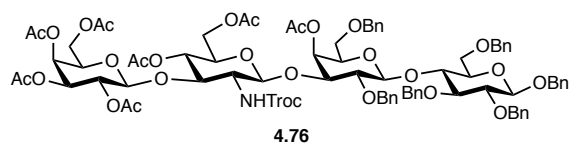


Figure A2.15. ¹H NMR (400 MHz, CDCl₃) and ¹³C (100 MHz, CDCl₃) spectra of **4.76**.

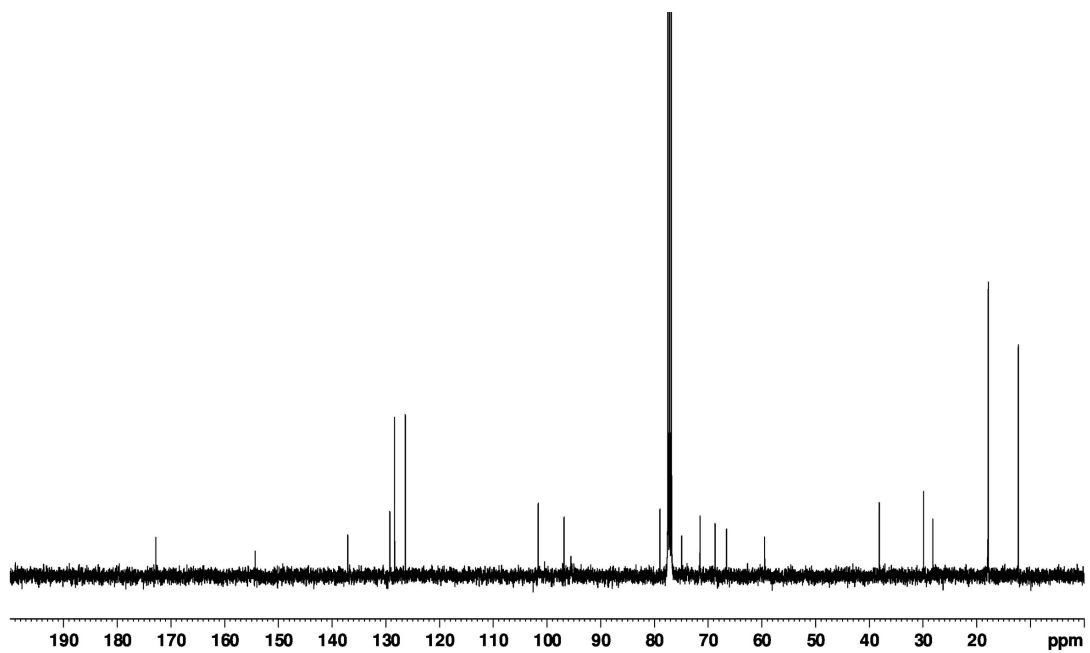
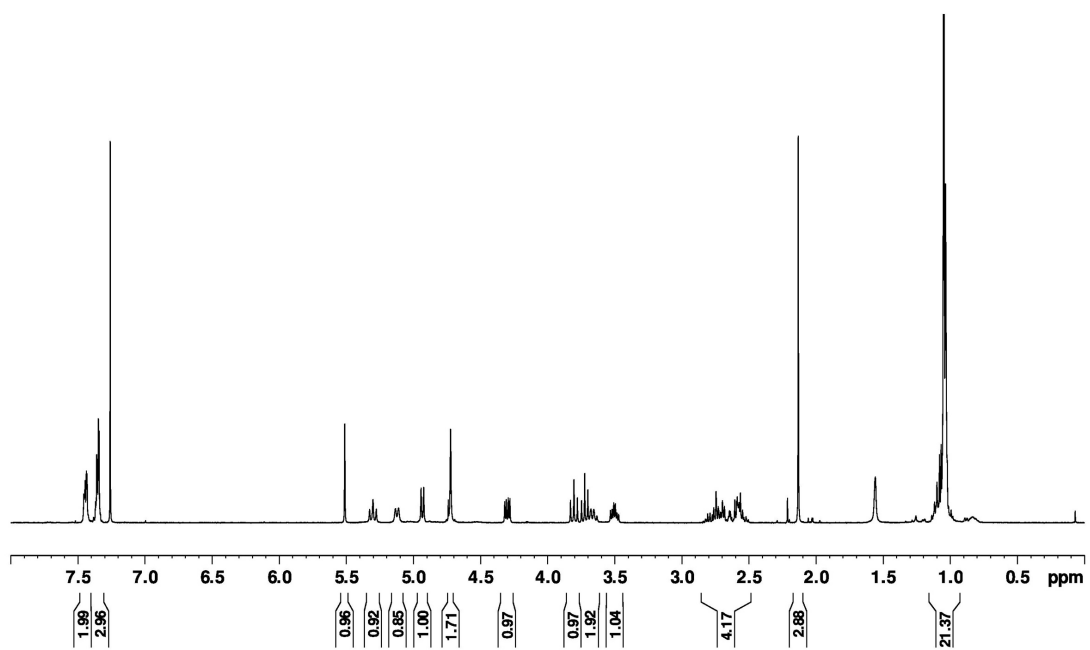
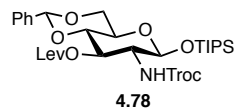


Figure A2.16. ^1H NMR (400 MHz, CDCl_3) and ^{13}C (100 MHz, CDCl_3) spectra of **4.78**.

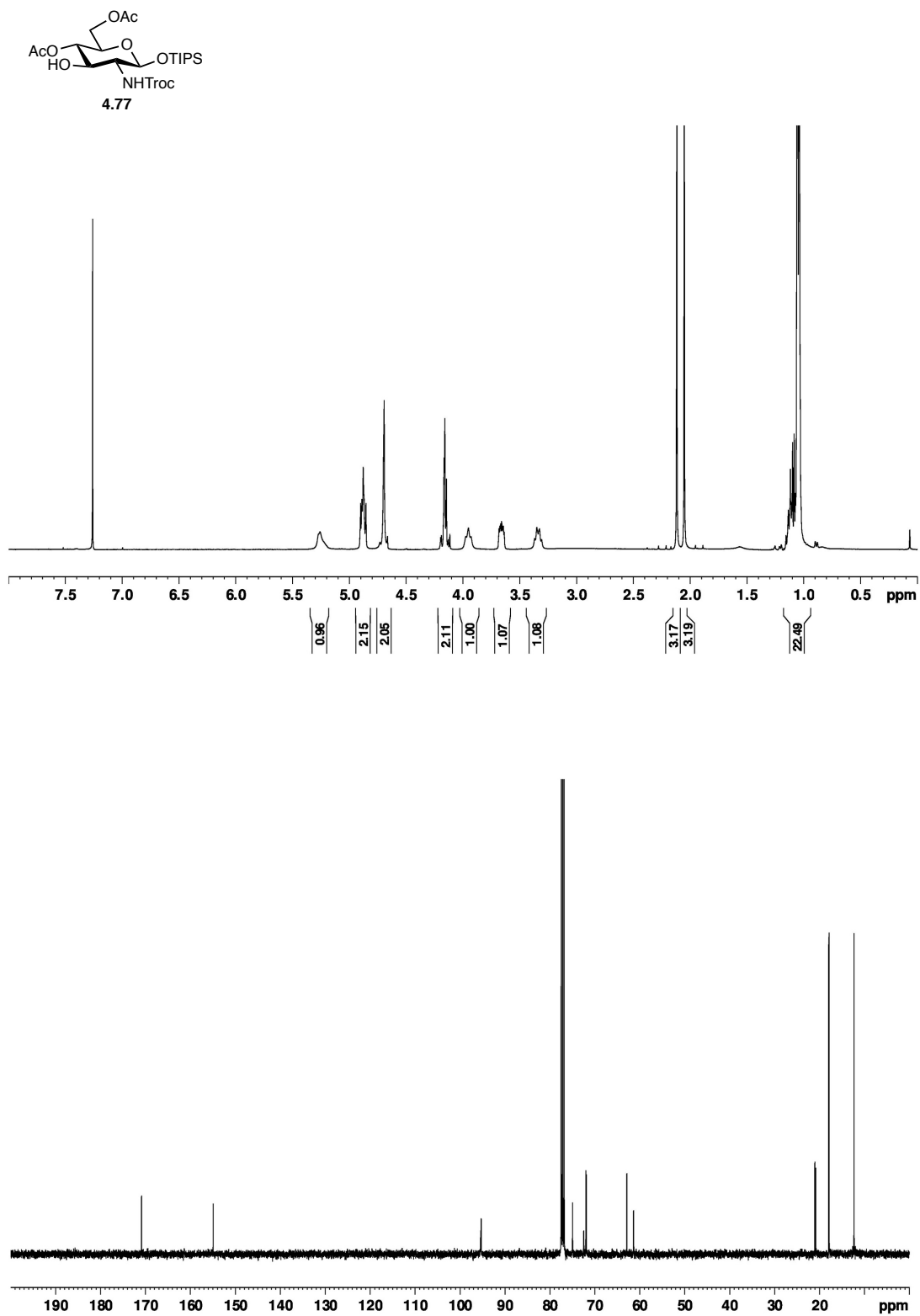


Figure A2.17. ¹H NMR (400 MHz, CDCl₃) and ¹³C (100 MHz, CDCl₃) spectra of **4.77**.

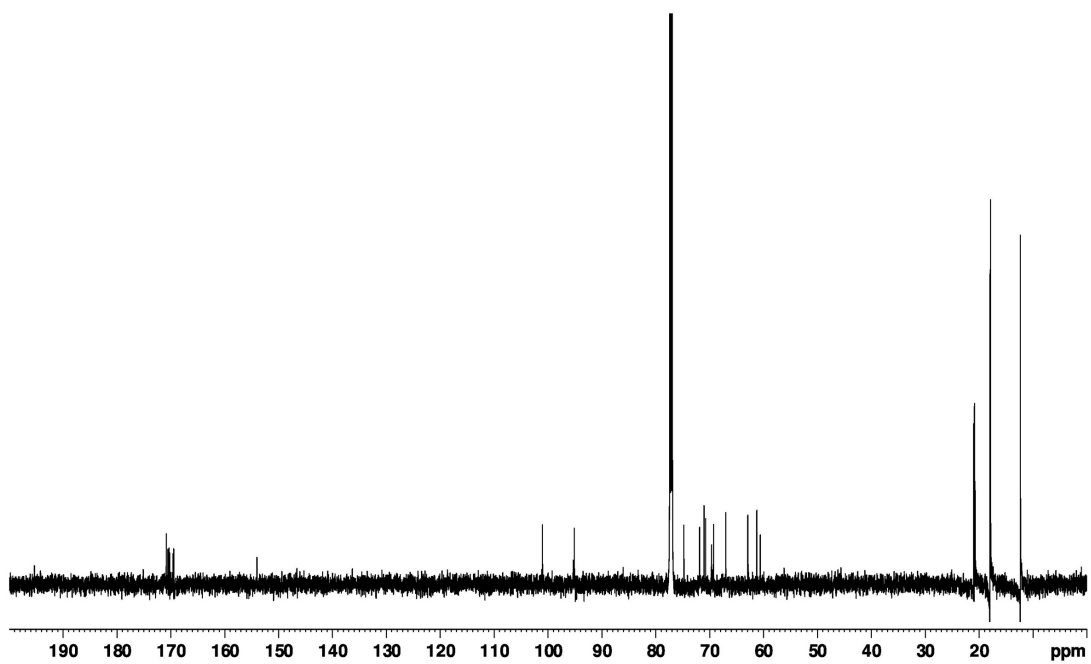
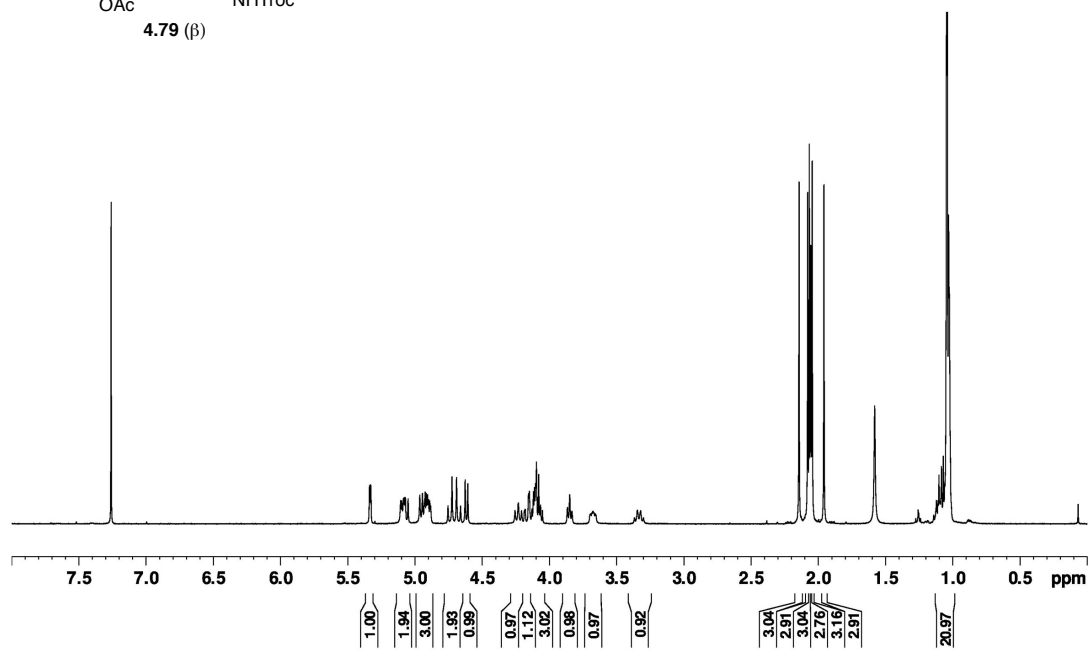
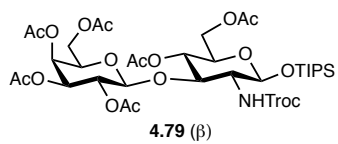


Figure A2.18. ^1H NMR (400 MHz, CDCl_3) and ^{13}C (150 MHz, CDCl_3) spectra of **4.79** (β).

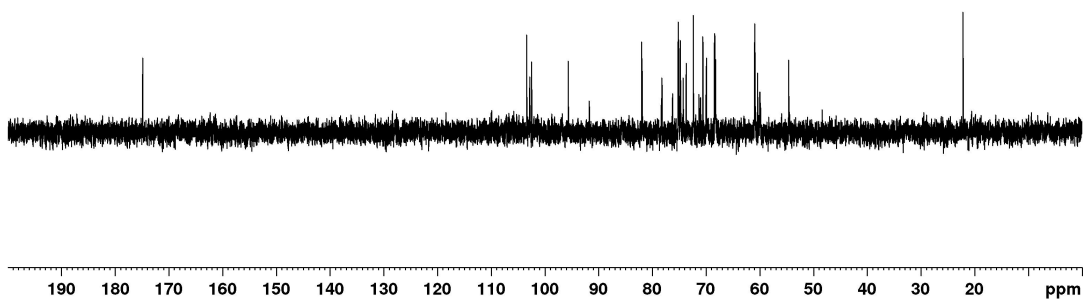
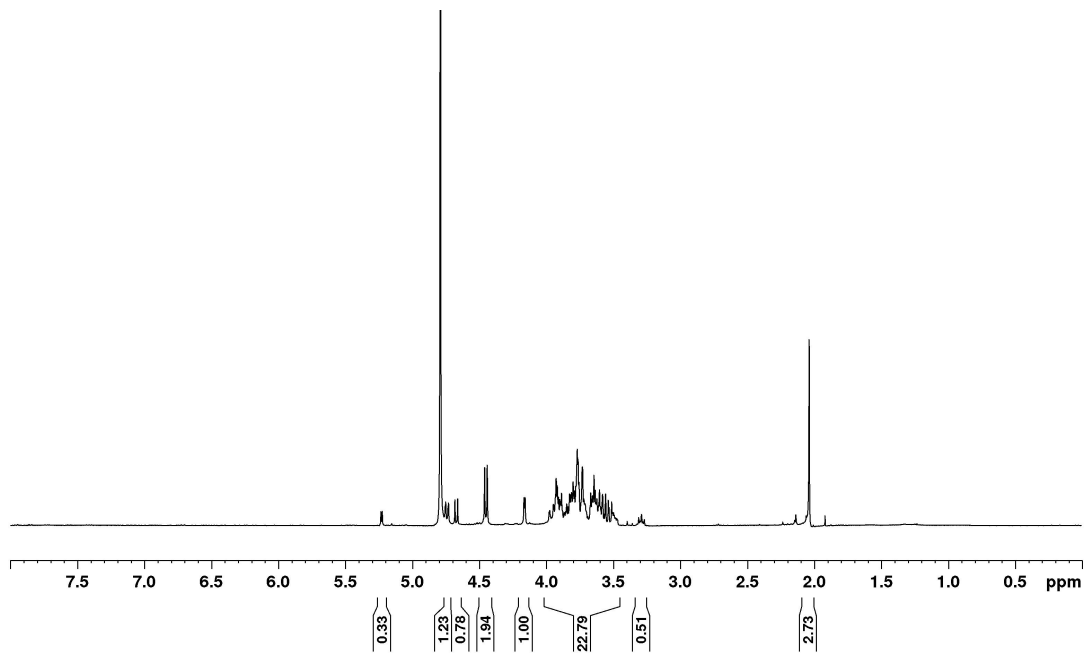
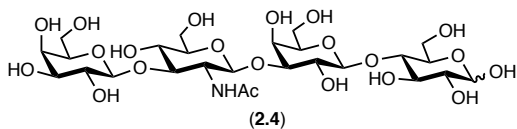
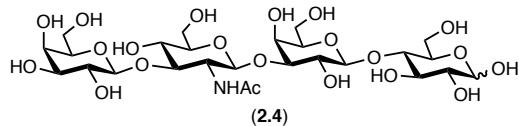


Figure A2.19. ^1H NMR (400 MHz, D_2O) and ^{13}C (100 MHz, D_2O) spectra of (2.4).

Table A2.1. Synthetic and Natural Lacto-*N*-Tetraose (LNT, **2.4**) in D₂O



Literature (400 MHz, D ₂ O) ^a		Synthetic (400 MHz, D ₂ O)	
δH	δC	δH (multiplicity, <i>J</i> / Hz)	δC
5.128	176.13	5.23 (d, <i>J</i> =3.8 Hz)	174.9
4.736	104.70	4.74 (d, <i>J</i> =8.4 Hz)	103.4
4.732	104.15	4.74 (d, <i>J</i> =8.4 Hz)	102.8
4.655	104.12	4.67 (d, <i>J</i> =8.0 Hz)	102.8
4.436	103.73	4.45 (d, <i>J</i> =7.8 Hz)	102.5
4.436	96.98	4.45 (d, <i>J</i> =7.8 Hz)	95.6
4.146	93.04	4.16 (d, <i>J</i> =3.2 Hz)	91.7
3.94	83.38	3.98-3.46 (m)	82.0
3.92	83.21	3.29 (m)	81.9
3.912	79.73	2.04 (s)	81.9
3.898	79.63		78.3
3.88	76.51		78.2
3.87	76.44		76.2
3.829	76.13		75.2
3.816	76.02		75.1
3.79	75.60		74.8
3.76	75.50		74.7
3.76	73.73		74.2
3.732	72.64		73.7
3.71	72.40		72.4
3.70	71.94		71.3
3.64	71.36		71.0
3.64	71.27		70.6
3.64	71.25		70.5
3.636	69.78		70.0
3.596	69.72		69.9
3.595	69.58		69.9
3.573	69.55		68.4
3.56	62.28		68.3
3.526	62.21		68.2
3.477	61.80		68.2
3.278	61.38		60.9
2.025	61.26		60.9
	55.95		60.4
	23.54		60.0
			59.8
			54.6
			22.1

^aStrecker, G.; Wieruszkeski, J-M.; Michalski, J-C.; Montreuil, J., *Glycoconj. J.* **1989**, *6*, 67-83.

CHAPTER 5

Evaluation of the Antibacterial Properties of Homogeneous Human Milk Oligosaccharides Against *Streptococcus agalactiae*

5.1 Introduction

In Chapter 3, our efforts to decipher the antibacterial properties of heterogeneous HMOs were presented. Briefly, we demonstrated that HMOs possess antimicrobial and/or antibiofilm activity against several pathogens, and that the antimicrobial activity was a result of increased cell membrane permeability. As noted in the concluding remarks of Chapter 3, while these studies demonstrated the therapeutic utility of HMOs, they lacked descriptions of the activities of homogeneous, single-entity compounds. Moreover, though an antimicrobial mechanism of action was identified, the specific HMO cellular targets remained unknown. To address these limitations, the work presented herein describes our efforts to identify the antibacterial activities of numerous single-entity HMOs against *Streptococcus agalactiae* (Group B Strep, GBS). These include neutral, non-fucosylated; neutral, fucosylated; and acidic, sialylated HMOs. Importantly, these studies were enabled by our synthetic efforts towards lacto-*N*-tetraose (LNT, **2.4**) (detailed in Chapter 4) as well as the donation of numerous HMOs by the Danish biotech company, Glycom. Additionally, this work was completed with the help of Harrison C. Thomas.

5.2 Rationale for Inclusion of Acidic, Sialylated HMOs

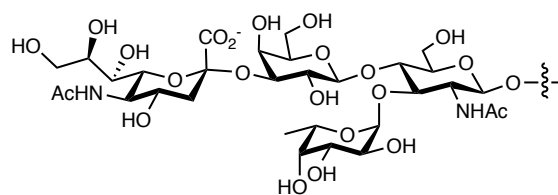
As previously mentioned in section 2.2.3 of Chapter 2, HMOs can be divided into two groups: neutral and acidic. The acidic fraction accounts for around 10-20% of total

HMO concentration and is comprised of HMOs that feature one or more sialic acid residues (specifically *N*-acetylneuraminic acid, Neu5Ac) linked to a core carbohydrate chain via α 2-3 and/or α 2-6 glycosidic linkages.^{1,2}

In terms of biological activity, sialylated HMOs are of particular interest as a number of microbial pathogens, including *Escherichia coli* and *Helicobacter pylori*, are known to bind this class of oligosaccharide (see section 2.5.2 of Chapter 2).^{3,4} Additionally, a study by Angeloni et al. provided evidence that sialylated HMOs may also directly modulate host intestinal epithelial cell responses to microbes⁵. In their study, Angeloni and co-workers found that incubation of cultured human intestinal epithelial cell lines with 3'-sialyllactose (3'-SL, **2.28**) led to decreased sialylation levels of cell surface glycans due to lowered gene expression of numerous sialyltransferases. They further demonstrated that the decreased prevalence of sialylated cell surface glycans significantly lowered adhesion levels of enteropathogenic *E. coli* (EPEC).

It has also been shown that sialylated HMOs decrease the binding of leukocytes to endothelial cells.⁶ This is thought to be due to the similarity of some sialylated HMO structures to sialyl-Lewis X (sLe^x, **5.1**), the binding determinant for selectins (**Figure 5.1**); leukocyte rolling, which is needed for the attachment of leukocytes to endothelial cells, is mediated by the interaction between selectins and their carbohydrate ligands. Moreover, it has been postulated that this decrease in leukocyte binding is one of the reasons for the lower rates of necrotizing enterocolitis (NEC) seen in breastfed infants compared to formula-fed infants. NEC, one of the most common and often fatal disorders in preterm infants, is a disease where the intestinal walls are invaded by bacteria which leads to infection and inflammation that can ultimately lead to destruction of the intestinal wall.⁷ As

a result of this destruction, stool and bacteria can enter the bloodstream and cause life-threatening infections. A link between NEC and sialylated HMOs was also detailed in a series of studies by the Bode and Chen laboratories. In these studies, it was shown that disiallacto-*N*-tetraose (DSLNT, **5.2**; **Figure 5.2**) contributed to the ability of HMO extracts to prevent NEC in a neonatal rat model.⁸⁻¹⁰ Concurrently, a clinical cohort study found this molecule to be associated with a lower risk of NEC.¹¹ Finally, sialylated HMOs are thought to be important for proper postnatal brain development as they serve as a rich source of sialic acid, which is an essential nutrient for brain development and cognition.¹²⁻¹⁴



Sialyl-Lewis X (sLe^X, **5.1**)

Figure 5.1. Structure of sialyl-Lewis X (sLe^X, **5.1**).

While there exist studies such as those from the Angeloni, Bode, and Chen laboratories that describe the biological effects of single-entity sialylated HMOs, it remains that the benefits conferred by this class of carbohydrate are largely restricted to broad descriptions of the class as a whole.¹⁵ This lack of specificity is due in large part to the difficulties of obtaining single-entity HMOs through isolation from milk or through total synthesis. Indeed, we found this reality to be the case concerning the relationship between sialylated HMOs and GBS. Despite the high structural similarity of numerous sialylated HMOs to GBS capsular polysaccharides (CPS) (see section 3.1.4 of chapter 3), prior to initiation of our studies, we were unable to find any reports detailing structure activity relationships for this class of HMO with regard to GBS antibacterial activity. There

was, however, a report from the Bode laboratory detailing the antimicrobial activity of heterogenous sialylated HMO extracts against GBS.

In their report, Bode et al. found that the acidic, sialylated portion of HMO extracts dosed at 10 mg/mL was devoid of antimicrobial activity against a GBS serotype III strain over 6 h.¹⁶ Despite this seemingly bleak outlook for the potential of sialylated HMOs to protect against GBS, we hypothesized that the use of single-entity compounds might uncover activity that would otherwise be lost when evaluating a complex mixture. In a similar vein, we hypothesized that screening against multiple GBS strains of varying serotypes might reveal previously undisclosed activity. As a final note, the Bode study did not address any HMO antibiofilm activity. Thus, in addition to accessing sialylated HMOs for antimicrobial activity, we also elected to assay for antibiofilm activity.

The acidic, sialylated HMOs used in the present study are shown in **Figure 5.2**. 3'-SL **2.28** and 6'-sialyllactose (6'-SL, **2.27**) are sialylated lactose trisaccharides that have both been shown to possess anti-inflammatory and prebiotic activities.¹⁷ 3'-SL tends to be slightly less abundant in human milk with concentrations typically ranging from 0.1 to 0.3 g/L while 6'-SL is typically found between 0.3 and 0.5 g/L.¹⁸ The remaining three compounds are of increased complexity. Disialyllacto-*N*-tetraose (DSLNT, **5.2**) is a hexasaccharide that, as previously mentioned, has been shown to protect against NEC. DSLNT has been reported to occur in human milk between 0.2 and 0.6 g/L.¹⁸ LS-tetrasaccharide a (LST a, **3.1**), like DSLNT, is a sialylated lacto-*N*-tetraose (LNT, **2.4**) derivative, while LS-tetrasaccharide c (LST c, **5.3**) is a sialylated lacto-*N*-neotetraose (LNnT, **2.5**) derivative. LST a and c have previously been shown to play a role in the modulation of intestinal epithelial cell maturation.¹⁹ Additionally, it was recently shown that

sialyllacto-*N*-tetraose (corresponding to three structural isomers) could be consumed by the infant-associated commensal *Bifidobacterium longum* subsp. *infantis*.²⁰ LST a is typically found in lower concentrations than LST c as these isomers have been reported to occur in human milk between 0.03 to 0.2 g/L and 0.1 to 0.6 g/L, respectively.¹⁸

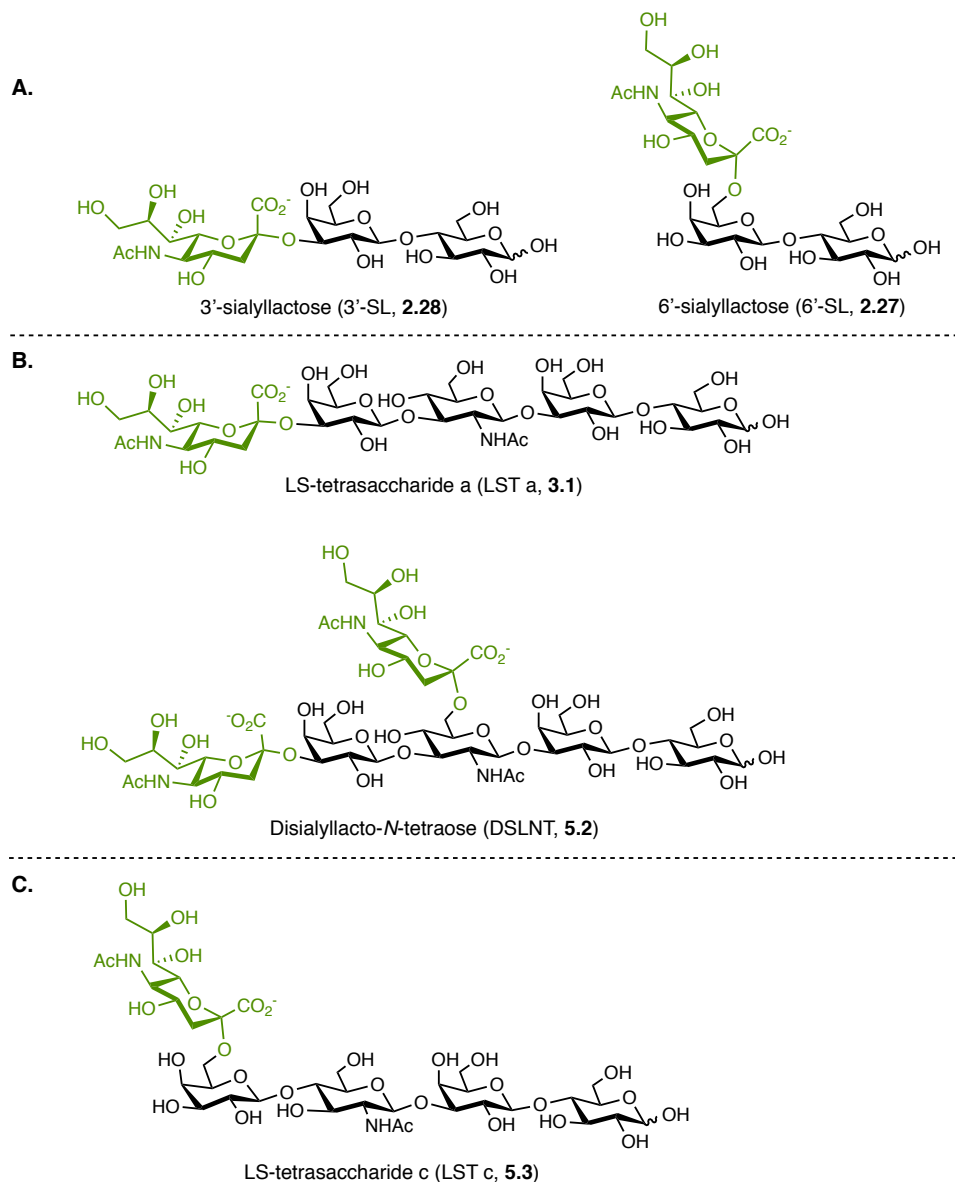


Figure 5.2. Structures of sialylated HMOs evaluated for antibacterial activity against GBS. **(A)** Structures of sialylated lactose (Lac, **2.1**) HMOs 3'-sialyllactose (3'-SL, **2.28**) and 6'-sialyllactose (6'-SL, **2.27**). **(B)** Structures of sialylated lacto-*N*-tetraose (LNT, **2.4**) HMOs LS-tetrasaccharide a (LST a, **3.1**) and disialyllacto-*N*-tetraose (DSLNT, **5.2**). **(C)** Structure of sialylated lacto-*N*-neotetraose (LNnT, **2.5**) HMO LS-tetrasaccharide c (LST c, **5.3**). Lac, LNT, and LNnT core structures are in black, sialic acid residues are highlighted in green.

5.3 Antimicrobial and Antibiofilm Activities of Homogenous Acidic, Sialylated HMOs¹⁵

To determine whether any observed antibacterial effects were strain-specific, we elected to assay against two strains of GBS of differing serotypes. As detailed in section 3.1.4 of Chapter 3, GBS strains can be classified into one of ten serotype classes (Ia, Ib, II-IX) based on the structure of their capsular polysaccharides (see **Figure 3.2**, section 3.1.4 of chapter 3).^{21, 22} For the presently described study, we selected GBS strains GB590 and GB2 which are serotype III and Ia strains, respectively. GB590 was selected due to the global relevance of serotype III strains to GBS disease; serotype III strains account for the greatest number of GBS infections of any serotype.²² GB2 was selected for two reasons. One, GB2 is a serotype Ia strain, and this serotype is one of the five types that account for more than 85% of the global GBS disease burden.²² Two, in our earlier studies investigating the antibacterial activities of heterogenous HMO mixtures, GB2 was the strain most susceptible to HMO supplementation.^{21, 23}

Antimicrobial activity was evaluated by monitoring GBS growth and viability over 24 h. Growth was quantified spectrophotometrically at OD₆₀₀ while viability was assessed by serial dilution of bacterial cultures and plating onto blood agar plates followed by enumeration of colony forming units (CFUs) the following day. GBS was grown in media alone (Todd-Hewitt Broth, THB) or THB supplemented with ca. 5 mg/mL HMO. This HMO concentration was selected for numerous reasons. First, in the course of our studies investigating the use of HMOs in antibiotic combination therapies (see section 3.3.1 of Chapter 3), we found the IC₅₀ of heterogenous HMO extracts against GB590 and GB2 to be around 5 mg/mL.²⁴ Thus, we hypothesized that dosing HMOs at this concentration would allow us to observe potential antibacterial activity without obliterating bacterial

growth. Furthermore, this concentration is physiologically relevant as HMOs are typically found in milk between 5 and 25 mg/mL. Finally, given the “irreplaceable” nature of the HMOs evaluated for this study, testing at the low end of physiological concentration enabled a thorough evaluation of antibacterial activity.

In addition to the five sialylated HMOs shown in **Figure 5.2**, the core carbohydrate structures lactose, LNT, and LNnT were included in the present evaluation. As previously mentioned, lactose serves as the core structure for 3'-SL and 6'-SL, LNT serves as the core structure for LST a and DSLNT, and LNnT serves as the core structure for LST c. Thus, inclusion of these neutral structures allowed for determination of whether any observed antibacterial activity of the sialylated HMOs was in fact contingent on the presence of sialic acid. Finally, as multiple laboratories including our own have found that HMO mixtures possess stronger antimicrobial activity than single HMOs, we also elected to assay against an HMO mixture composed of whole HMO extracts from multiple donor samples.¹⁰ This allowed for evaluation of whether any single compound was more effective than a heterogeneous HMO mixture.

Against both GB590 and GB2, the HMO mixture proved to be the most effective at reducing bacterial growth and viability (**Figures 5.3** and **5.4**). Compared to bacteria grown in media alone, the mixture was able to reduce GB590 growth by up to 99% and viability by up to 38% (**Figure 5.3**). Against GB2, growth reductions reached as high as 96% while viability was reduced by upwards of 36% (**Figure 5.4**). While impressive in its magnitude, this strong activity was not observed over the entire 24 h time frame. Indeed, by 24 h, bacterial growth had begun to recover; at 24 h, growth had rebounded to around 70% that of bacteria grown in media alone. This result was, however, in agreement with previous

findings from both our laboratory and the Bode laboratory that HMOs serve as bacteriostatic rather than bactericidal agents against GBS when they are dosed at the low end of physiological concentration.^{16, 23-25}

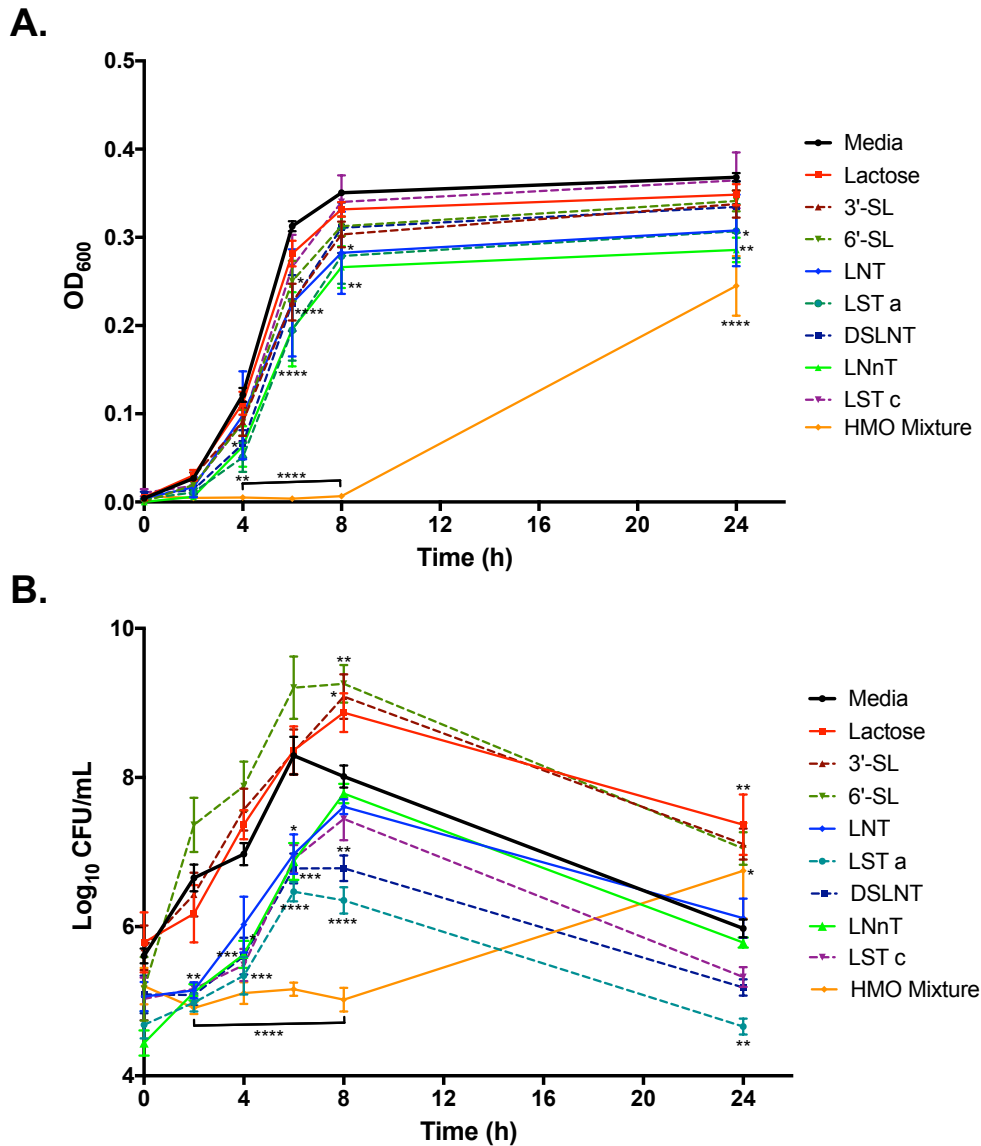


Figure 5.3. Effects of homogenous and heterogenous HMOs dosed at ca. 5 mg/mL on the growth and viability of GB590 in Todd-Hewitt Broth. **(A)** OD₆₀₀ readings were taken at 0, 2, 4, 6, 8, and 24 h. Mean OD₆₀₀ for each HMO source and time point is indicated by the respective symbols. **(B)** Enumeration of CFU/mL was performed at 0, 2, 4, 6, 8, and 24 h corresponding to the OD values graphed in (A). Mean log₁₀CFU/mL for each HMO source and time point is indicated by the respective symbols. Data displayed represent the mean OD₆₀₀ or log₁₀CFU/mL ± SEM of at least three independent experiments, each with 3 technical replicates. **** represents $p < 0.0001$ by 2-way ANOVA with *posthoc* Dunnett's multiple comparison test comparing the growth and viability of GB590 in each HMO supplementation condition to the growth and viability of GB590 in media alone.

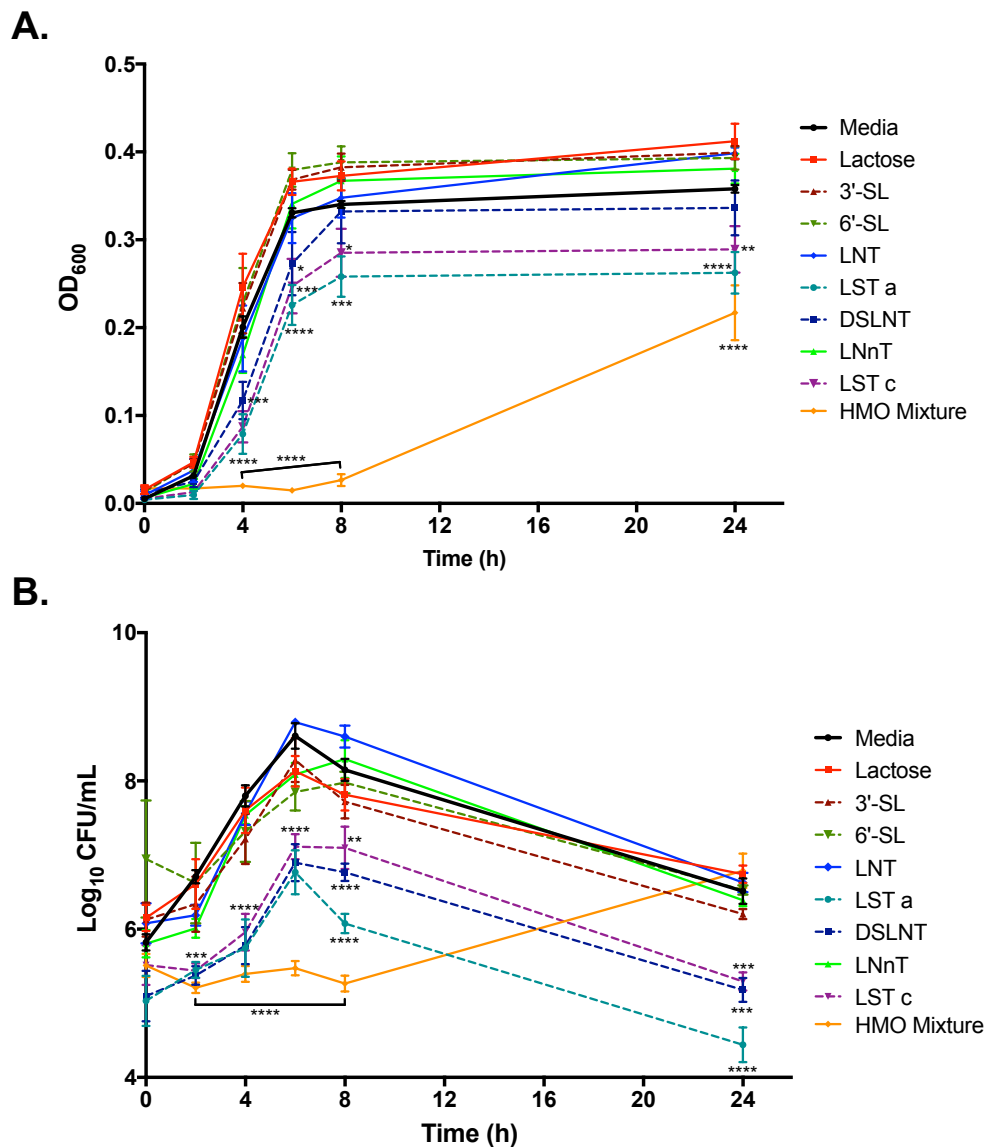


Figure 5.4. Effects of homogenous and heterogenous HMOs dosed at ca. 5 mg/mL on the growth and viability of GB2 in Todd-Hewitt Broth. **(A)** OD₆₀₀ readings were taken at 0, 2, 4, 6, 8, and 24 h. Mean OD₆₀₀ for each HMO source and time point is indicated by the respective symbols. **(B)** Enumeration of CFU/mL was performed at 0, 2, 4, 6, 8, and 24 h corresponding to the OD values graphed in (A). Mean log₁₀CFU/mL for each HMO source and time point is indicated by the respective symbols. Data displayed represent the mean OD₆₀₀ or log₁₀CFU/mL \pm SEM of at least three independent experiments, each with 3 technical replicates. **** represents $p < 0.0001$ by two-way ANOVA with *posthoc* Dunnett's multiple comparison test comparing the growth and viability of GBS in each HMO supplementation condition to the growth and viability of GBS in media alone.

Another notable finding was the difference in activity observed for LST a and DSLNT compared to their core neutral structure LNT as well as the difference between LST c and its core neutral structure LNnT (**Figures 5.3 and 5.4**). For the LNT-derived HMOs, as a general trend, LST a and DSLNT proved more effective at reducing growth and viability for both GB590 and GB2 than LNT. This trend was particularly pronounced for GB2. Against GB2, LNT did not significantly decrease growth or viability at any time point while LST a and DSLNT significantly reduced both growth and viability over several hours. Similarly, LST c was significantly more effective at reducing GB2 growth and viability than LNnT; LNnT did not reduce GB2 growth or viability at any point during the 24 h time frame. However, a different trend was seen against GB590 for LNnT and LST c. Against this strain, LNnT significantly decreased growth over several hours while LST c failed to significantly decrease GB590 growth at any time point. Interestingly, LNnT and its monosialylated derivative did cause comparable decreases in GB590 viability. Taken together, these results demonstrate that the sialic acid residue(s) of LST a, DSLNT, and LST c are indeed largely important for antimicrobial activity.

In addition to being generally more effective antimicrobial agents than their respective neutral core counterparts, LST a, DSLNT, and LST c proved much more effective than the monosialylated lactose-derivative 3'-SL and 6'-SL (**Figures 5.3 and 5.4**). Aside from 3'-SL and 6'-SL significantly reducing GB590 growth at 6 h, neither of these compounds showed any antimicrobial activity against either GBS strain. In fact, both 3'-SL and 6'-SL were found to significantly increase GB590 viability by 8 h. Importantly, we hypothesize that this lack of antimicrobial activity seen for 3'-SL and 6'-SL might be responsible for the lack of activity observed by Bode and co-workers for the acidic fraction

of HMOs against a serotype III strain.¹⁶ Given the results of the presently described study, it is possible that LST a, DSLNT, and LST c, which are strongly antimicrobial, did not constitute large enough portions of the acidic fraction to significantly alter bacterial growth in the original Bode study. This possibility is made more likely if 3'-SL and 6'-SL, which are largely devoid of antimicrobial activity, constituted a large portion of the acidic HMO fraction.

Notably, our findings represent the first report of single-entity sialylated HMOs possessing antimicrobial activity against GBS. Moreover, we showed that this antimicrobial activity was not limited to a single strain. Finally, the findings disclosed herein support our original hypothesis that testing single-entity sialylated compounds can uncover activity that would otherwise be lost when evaluating a complex mixture.

As a final point of study, we investigated the effects of single-entity HMO supplementation on GBS biofilm production (**Figure 5.5**). Biofilm production was assessed after 24 h of growth using the plate-based biofilm assay previously introduced in section 3.2.2 of Chapter 3. Again, this assay allows for quantification of bacterial growth via spectrophotometric reading at OD₆₀₀ followed by crystal violet staining of adherent bacteria and subsequent spectrophotometric reading at OD₅₆₀ to quantify biofilm production. As before, to account for any accompanying antimicrobial activity, results are expressed as a ratio of biofilm produced to the number of bacterial cells present (biomass).

Of the compounds tested, LNT, LST a, and LNnT were the only compounds found to significantly alter bacterial biofilm production (**Figure 5.5**). Against GB590, LNT and LNnT both increased biofilm production. Against GB2, LST a increased production while LNT decreased production.

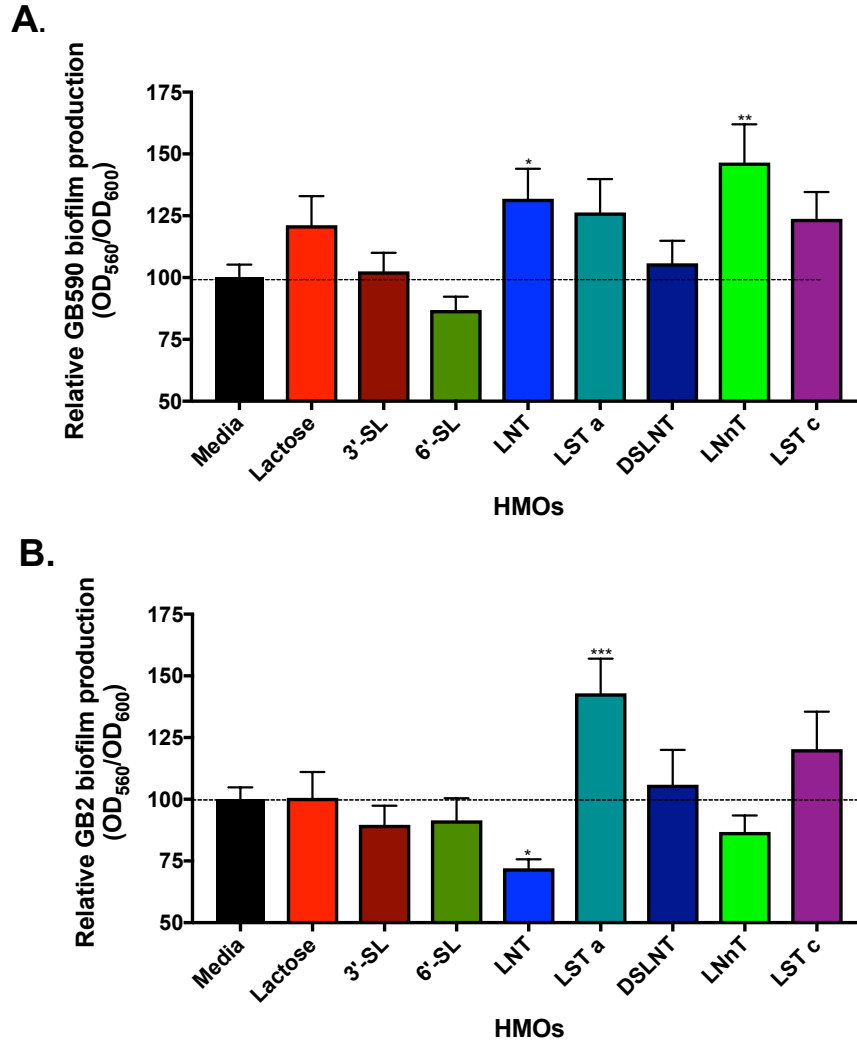


Fig. 5.5 Effects of homogeneous HMOs dosed at ca. 5 mg/mL on GBS biofilm production after 24 h of growth in Todd-Hewitt Broth. **(A)** Biofilm production, denoted by the ratio of biofilm/biomass (OD_{560}/OD_{600}), by GB590 in the presence of homogeneous HMOs relative to biofilm production in media alone. Data displayed represent the relative mean biofilm/biomass ratio \pm SEM of at least three independent experiments, each with 3 technical replicates, wherein biofilm production of GB590 in media alone is assigned a value of 100%. ** represents $p = 0.0020$ by one-way ANOVA, $F = 3.536$ with *posthoc* Dunnett's multiple comparison test comparing biofilm production of GB590 in each HMO supplementation condition to biofilm production of GB590 in media alone. **(B)** Biofilm production, denoted by the ratio of biofilm/biomass (OD_{560}/OD_{600}), by GB2 in the presence of homogeneous HMOs relative to biofilm production in media alone. Data displayed represent the relative mean biofilm/biomass ratio \pm SEM of at least three independent experiments, each with 3 technical replicates, wherein biofilm production of GB2 in media alone is assigned a value of 100%. **** represents $p < 0.0001$ by one-way ANOVA, $F = 4.955$ with *posthoc* Dunnett's multiple comparison test comparing biofilm production of GB2 in each HMO supplementation condition to biofilm production of GB2 in media alone. Mean GBS biofilm production levels in media alone are marked with a dotted line.

The promotion of biofilm production by LST a-supplementation was not wholly unexpected. Biofilm production, as detailed in section 3.1.4 of Chapter 3, is a well-known and common strategy used by bacterial pathogens to evade the action of antimicrobial agents, like antibiotics. Indeed, the ESKAPE pathogens (first discussed in section 1.4 of Chapter 1), which are notorious for their abilities to resist antimicrobial action, are also prolific biofilm producers.^{26, 27} Thus, it is possible that when challenged by a strong antimicrobial agent like LST a, GBS increases biofilm production in an attempt to protect itself against antimicrobial action. This line of reasoning could also be used to explain the patterns of altered biofilm production observed for LNT and LNnT. It remains unclear, however, why LST c and DSLNT, both of which showcased stronger antimicrobial activity than LNT, did not significantly increase biofilm formation.

5.4 Rationale for Inclusion of Neutral, Fucosylated and Non-Fucosylated HMOs

The neutral HMO fraction comprises around 80-90% of total HMO concentration. Moreover, over half of neutral HMOs are fucosylated.^{1, 28} As detailed previously in section 2.5.2 of Chapter 2, several neutral fucosylated HMOs are well-known for their ability to protect infants from pathogenic colonization.²⁹ Briefly, fucosylated HMOs share structural homology with host epithelial cell surface glycans and thus can serve as soluble receptor analogs that compete for bacterial binding with intestinal mucosa (see **Figure 2.18** in section 2.5.2 of chapter 2). For example, 2'-fucosyllactose (2'-FL, **2.8**) inhibits the binding of *Campylobacter jejuni* to intestinal cells and the binding of noroviruses to histo-blood group antigens (HBGAs).^{30, 31} 2'-FL as well as 3-fucosyllactose (3'-FL, **2.9**) inhibit

adhesion of *Pseudomonas aeruginosa* to epithelial cells.³² Furthermore, 3-FL and difucosyllactose (DFL, **2.12**) inhibit the adhesion of *Escherichia coli* to epithelial cells.^{33, 34}

Neutral HMOs, both fucosylated and non-fucosylated, have also been previously shown by the Le Doare and Bode laboratories to protect against GBS infection (briefly introduced in section 3.1.6 of chapter 3).^{16, 35} Using both *in vivo* and *in vitro* experiments, Le Doare and co-workers found that the presence of lacto-*N*-difucohexaose I (LNDFH I, **2.26**; **Figure 5.6**) correlated to reduced GBS growth; the presence of HMOs like LNDFH I and 2'-FL in various milk samples was determined using ¹H NMR spectroscopy.³⁵ While this study supports the protective effect of fucosylated HMOs against GBS, no evaluations were performed using single compounds, and the concentrations of individual HMOs in the milk extracts that were used were known. Indeed, the authors were aware of these and other limitations of their report and thus expressed the need for further studies not only to validate their findings but also to more clearly define the HMOs involved in protecting against GBS.

In contrast to the Le Doare study, Bode and co-workers assayed both HMO mixtures and several single-entity neutral, fucosylated and neutral, non-fucosylated HMOs against GBS.¹⁶ Initial screens showed that the neutral HMO portion of HMO extracts significantly slowed the growth of serotype III, Ia, and V GBS strains over 6 h. In an attempt to identify the HMO(s) responsible for this activity, Bode et al. next assayed the following HMOs for activity against GBS (serotype not specified): lacto-*N*-tetraose (LNT, **2.4**), lacto-*N*-neotetraose (LNnT, **2.5**), lacto-*N*-neoheptaose (LNnH, **2.14**), lacto-*N*-fucopentaose I (LNFP I, **2.10**), lacto-*N*-difucohexaose II (LNDFH II, **5.4**), lacto-*N*-neooctaose (LNnO, **5.5**), lacto-*N*-neodifucohexaose (LNnDFH, **5.6**), lacto-*N*-

neofucopentaose (LNnFP, **5.7**), and lacto-*N*-fucopentaose V (LNFP V, **5.8**) (**Figures 5.6** and **5.7**). Treatment with LNT and LNFP I dosed at 5 mg/mL resulted in significantly reduced GBS growth at 2 h. Once again, while this study provided evidence for the protective effects of neutral HMOs, it was limited in its scope. For example, bacterial growth was only evaluated after a very short growth period (2-6 h), the lone GBS serotype used for single-compound evaluation was not specified, and no fucosylated lactose-derived HMOs were tested for activity despite their prevalence in milk.

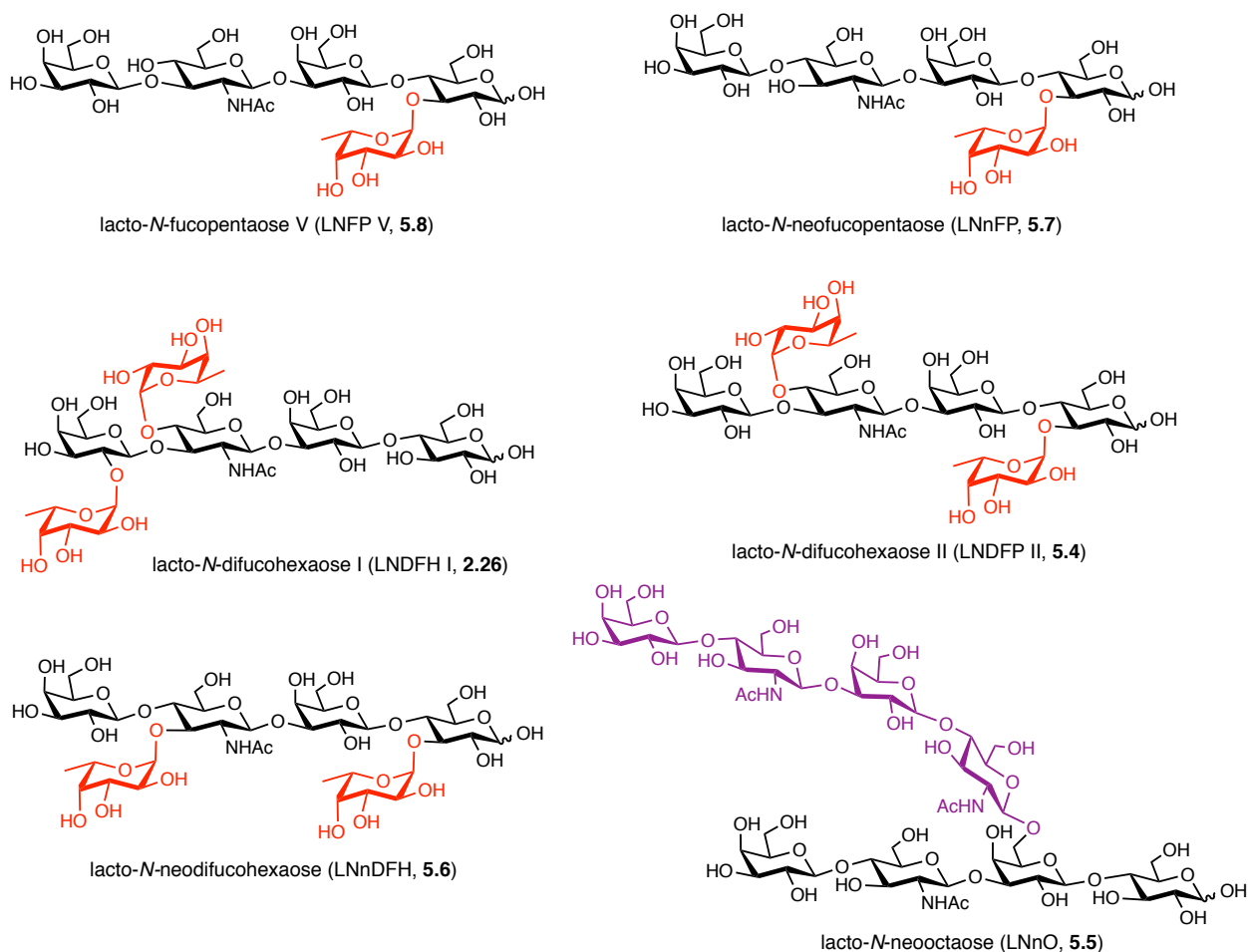


Figure 5.6. Structures of neutral HMOs previously assayed for antimicrobial activity against GBS. HMO core structures are in black, fucose residues are highlighted in red, non-fucosylated elongations of HMO core structures are highlighted in purple.

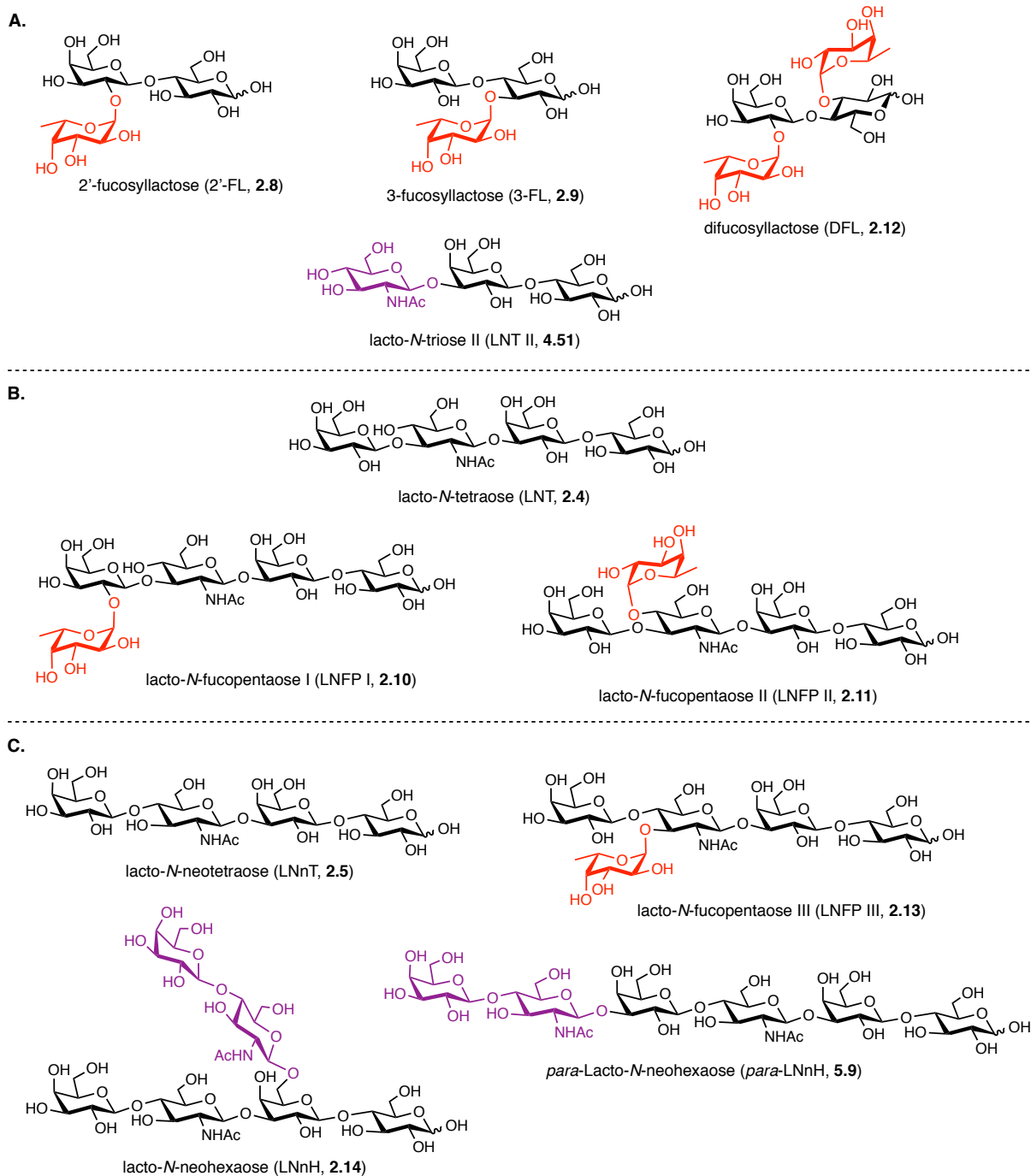


Figure 5.7. Structures of neutral HMOs assayed for antibacterial activity against GBS. **(A)** Structures of elongated lactose-derived HMOs 2'-fucosyllactose (2'-FL, **2.8**), 3-fucosyllactose (3-FL, **2.9**), difucosyllactose (DFL, **2.12**), and lacto-*N*-triose II (LNT II, **4.51**). **(B)** Structures of lacto-*N*-tetraose (LNT, **2.4**) and fucosylated LNT-derived HMOs lacto-*N*-fucopentaose I (LNFP I, **2.10**), and lacto-*N*-fucopentaose II (LNFP II, **2.11**). **(C)** Structures of elongated lacto-*N*-neotetraose (LNnT, **2.5**) and LNnT-derived HMOs lacto-*N*-fucopentaose III (LNFP III, **2.13**), lacto-*N*-neohexaose (LNnH, **2.14**), and *para*-lacto-*N*-neohexaose (*para*-LNnH, **5.9**), HMO core structures are in black. Fucose residues are highlighted in red. Non-fucosylated elongations of core structures are highlighted in purple.

To expand on the findings of the Le Doare and Bode laboratories and to address some limitations of their respective studies, we elected to screen a variety of neutral fucosylated and non-fucosylated HMOs, including several fucosylated-lactose derivatives, against two GBS strains (**Figure 5.7**). We hypothesized that increasing the time frame of the activity screens would provide a more comprehensive and useful account of HMO-mediated protection against GBS. Thus, growth and viability were monitored over 24 h. Finally, as HMO antibiofilm activity was not addressed in any prior study, we also elected to evaluate GBS biofilm production when grown in the presence of the various single-entity HMOs.

5.5 Antimicrobial and Antibiofilm Activities of Homogenous Neutral, Fucosylated and Non-Fucosylated HMOs³⁶

Analogous to our studies with sialylated single-entity HMOs, for the present study, we assayed the neutral HMOs shown in **Figure 5.7** for antibacterial activity against GBS strains GB590 and GB2; as before, HMOs were dosed at ca. 5 mg/mL (see section 5.3 for further explanation). Once again, antimicrobial activity was assessed by examining GBS growth and viability in THB over 24 h, while antibiofilm activity was assessed at 24 h of growth (see section 5.3 for more detail).

The antimicrobial activities of HMOs against GB590, as determined by changes in GBS growth and viability compared to GBS grown in media alone, are shown in **Figures 5.8** and **5.9**. As was observed with the sialylated HMOs, while numerous neutral single-entity HMOs were found to significantly reduce bacterial growth and viability, no single compound had as profound an effect as the heterogenous HMO mixture. As previously

described (see section 5.3), the mixture decreased GB590 growth by over 80% for the entirety of the first 8 h and significantly reduced viability for the first 8 h with reductions reaching almost 40%.

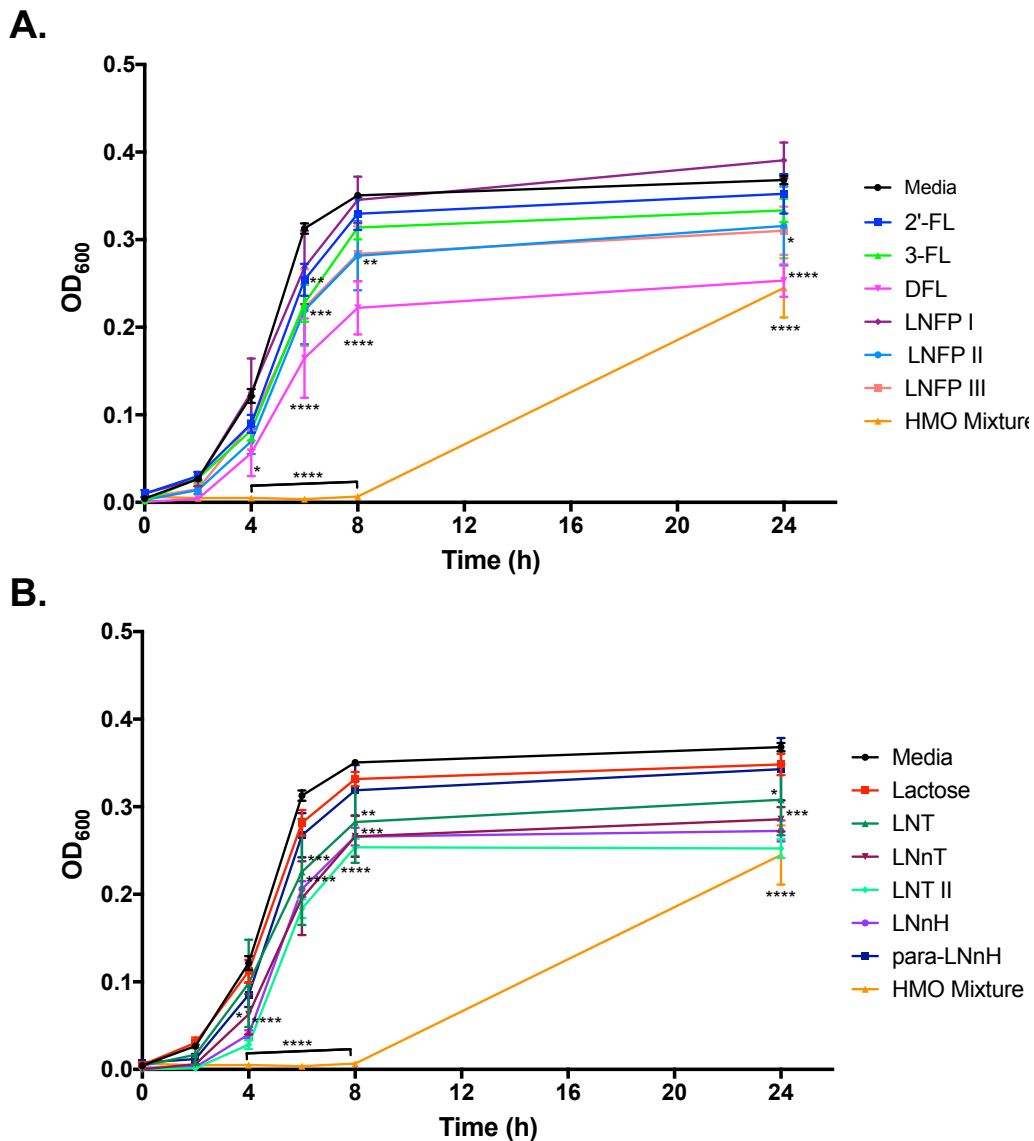


Figure 5.8. Effects of single-entity, neutral HMOs dosed at ca. 5 mg/mL on the growth of GB590 in Todd-Hewitt Broth. Growth was measured via OD_{600} readings taken at 0, 2, 4, 6, 8, and 24 h. Mean OD_{600} for each HMO source and time point is indicated by the respective symbols. **(A)** Growth of GB590 (OD_{600}) in the presence of neutral, fucosylated HMOs and an HMO mixture. **(B)** Growth of GB590 (OD_{600}) in the presence of neutral, nonfucosylated HMOs, lactose, and an HMO mixture. Data displayed represent the mean $OD_{600} \pm SEM$ of at least three independent experiments, each with three technical replicates. **** represents $p < 0.0001$ by two-way ANOVA with *posthoc* Dunnett's multiple comparison test comparing the growth and viability of GBS in each HMO supplementation condition to the growth and viability of GBS in media alone.

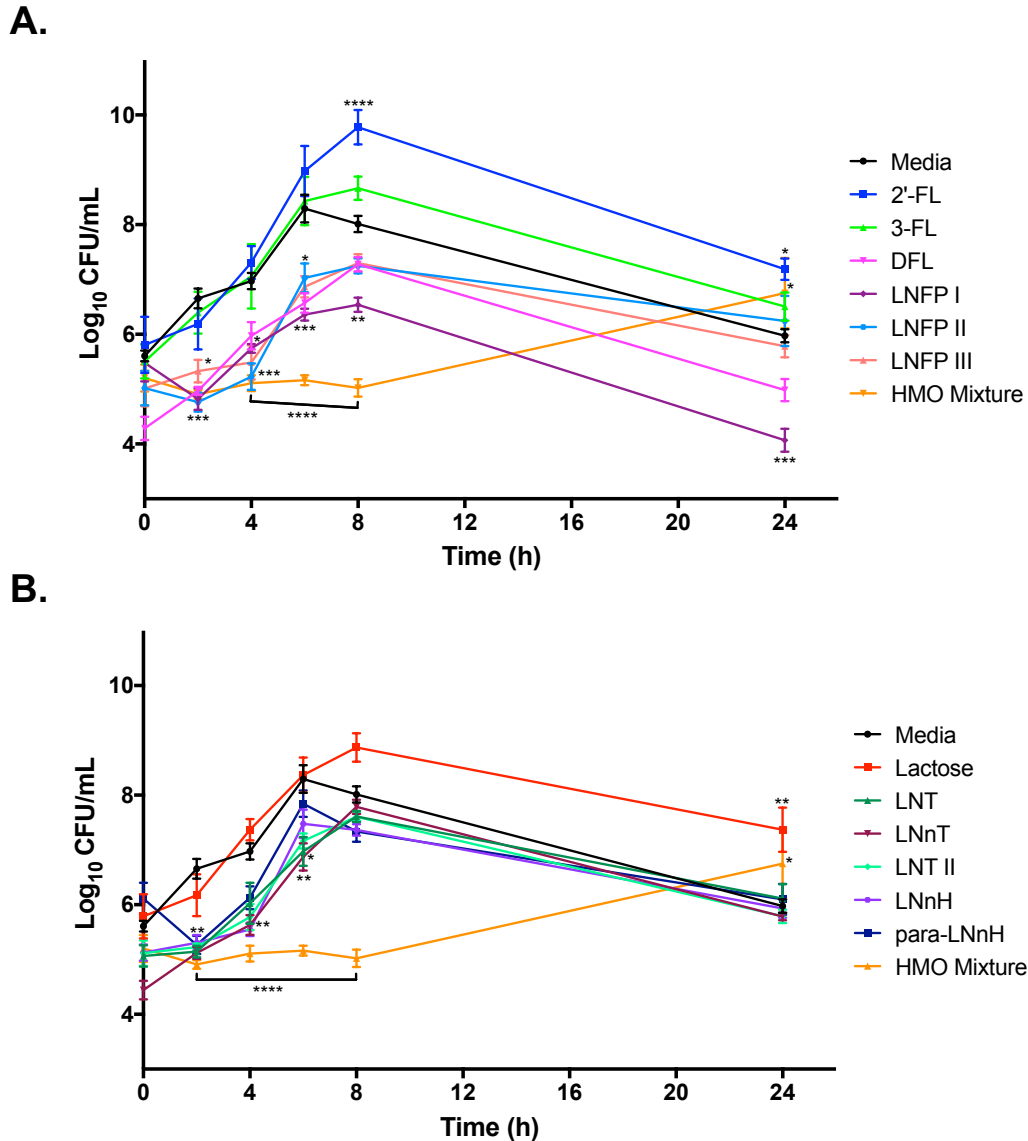


Figure 5.9. Effects of single-entity, neutral HMOs dosed at ca. 5 mg/mL on the viability of GB590 in Todd-Hewitt Broth. Viability was assessed via enumeration of CFU/mL performed at 0, 2, 4, 6, 8, and 24 h. Log₁₀CFU/mL for each HMO source and time point is indicated by the respective symbols. **(A)** Viability of GB590 (CFU/mL) corresponding to the OD values graphed in Figure 5.8A. **(B)** Viability of GB590 (CFU/mL) corresponding to the OD values graphed in Figure 5.8B. Data displayed represent the mean OD₆₀₀ or log₁₀CFU/mL ± SEM of at least three independent experiments, each with three technical replicates. **** represents $p < 0.0001$ by two-way ANOVA with *posthoc* Dunnett's multiple comparison test comparing the growth and viability of GBS in each HMO supplementation condition to the growth and viability of GBS in media alone.

For individual compounds, the presence or absence of fucose on a molecule was not a predictor of antimicrobial activity against GB590. For example, LNFP II and III displayed similar levels and patterns of growth and viability depressions as their nonfucosylated counterparts LNT and LNnT, respectively (**Figures 5.8 and 5.9**). Likewise, aside from significant growth reductions at 6 h, 2'-FL and 3-FL showed no more antimicrobial activity than lactose (which was inactive). Furthermore, the nonfucosylated HMOs LNT II and LNnH showed fairly similar levels of antimicrobial activity to LNFP II and LNFP III. In fact, these nonfucosylated compounds tended to suppress growth to a greater extent on average than LNFP II and III.

Although the absence of fucose did not correlate to lessened antimicrobial activity, the location and number of fucose residues did appear to have an effect. For instance, while LNFP II significantly reduced GB590 growth between 6 and 24 h, LNFP I did not significantly reduce growth at any point in the 24 h time frame (**Figure 5.8**); LNFP I and LNFP II are each monofucosylated LNT derivatives that differ only in the location of the fucose residue (see **Figure 5.7**). Interestingly, despite not significantly decreasing growth, LNFP I treatment did significantly reduce viability between 2 and 24 h with reductions reaching as high as 30% (**Figure 5.9**). Additionally, it was the only HMO source, including the HMO mixture, to significantly decrease viability at 24 h. Conversely, LNFP II only significantly decreased viability between 2 and 6 h. It is important to note, however, that between 2 and 6 h, both fucosylated LNT derivatives showed comparable viability reductions.

Comparison of the effects of DFL on GB590 growth and viability with those of 2'-FL and 3-FL further highlighted the importance of location and number of fucose residues.

As mentioned, aside from significant growth reductions at 6 h, 2'-FL and 3-FL were devoid of antimicrobial activity. DFL on the other hand significantly reduced growth between 4 and 24 h and significantly reduced viability at 2 and 6 h; growth reductions ranged from around 30-50%, while viability reductions were around 20% (**Figures 5.8** and **5.9**). As shown in **Figure 5.7**, DFL incorporates the functional aspects of both 2'-FL and 3-FL. That is, DFL features α 1-2-linked fucose residues at both the C2' and C3 positions of lactose. Based on these results, it appears as though both fucose residues are necessary for antimicrobial activity of fucosylated lactose derivatives against GB590.

For the activities of non-fucosylated HMOs against GB590, a few notable trends emerged. First, LNT and LNnT, structural isomers differing only by the glycosidic linkage between the terminal Gal and subterminal GlcNAc residues (see **Figure 5.7**), had fairly similar levels and patterns of antimicrobial activity (**Figures 5.8** and **5.9**). Conversely, LNnH and *para*-LNnH, structural isomers differing only by the location of one LacNAc (*N*-acetyllactosamine) unit (see **Figure 5.7**), did showcase noticeable differences in antimicrobial activity. Although neither compound was able to significantly reduce viability past 4 h, LNnH did significantly reduce growth between 4 and 24 h, while *para*-LNnH failed to significantly reduce growth at any point.

Moving from GB590, the antimicrobial activities of HMOs against GB2 are shown in **Figures 5.10** and **5.11**. The HMO mixture was again the most operative antimicrobial agent against GB2. As first described in section 5.3, treatment with the HMO mixture resulted in GB2 growth and viability reductions of up to 95% and 36%, respectively. As for the specific effects of single-entity compounds, as expected based on previous work, the effects of homogenous HMOs were indeed found to be strain-specific.

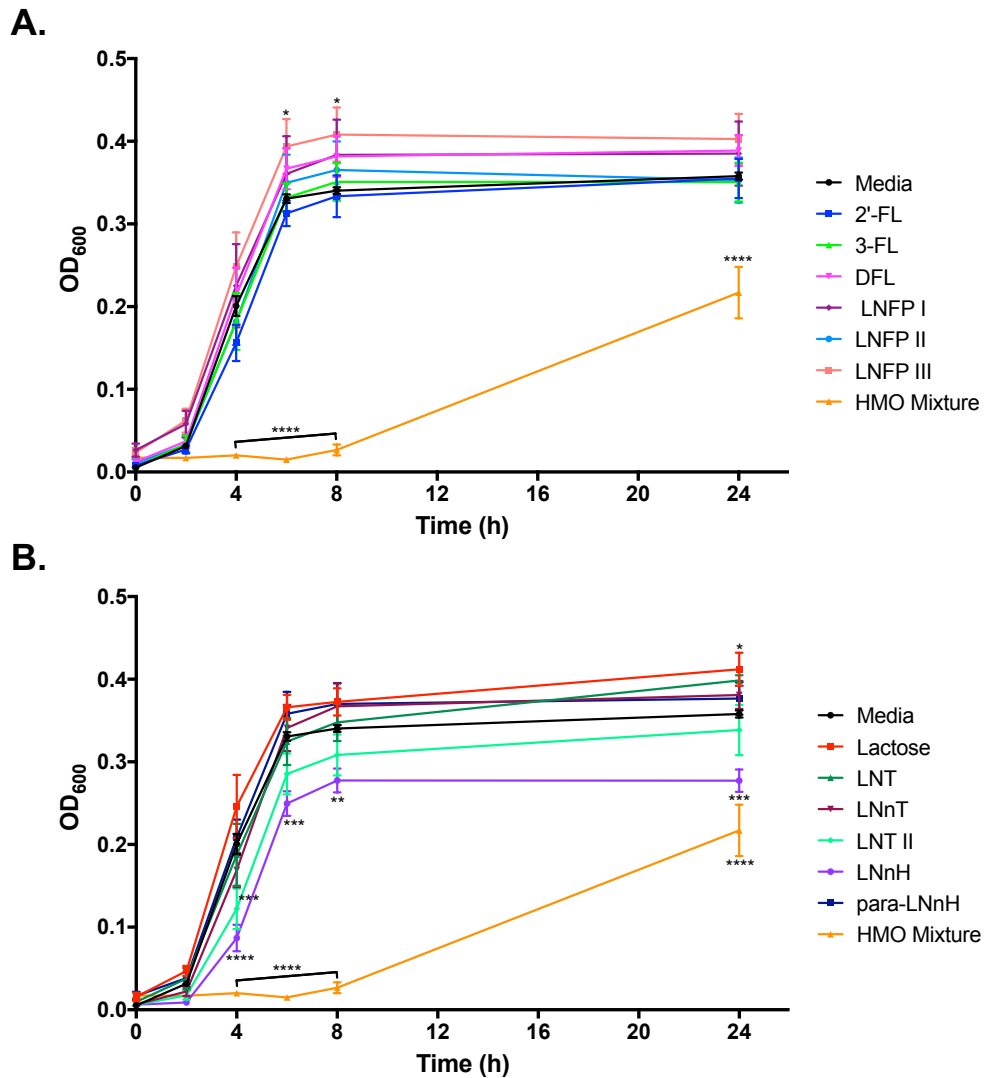


Figure 5.10. Effects of single-entity, neutral HMOs dosed at ca. 5 mg/mL on the growth of GB2 in Todd-Hewitt Broth. Growth was measured via OD_{600} readings taken at 0, 2, 4, 6, 8, and 24 h. Mean OD_{600} for each HMO source and time point is indicated by the respective symbols. **(A)** Growth of GB2 (OD_{600}) in the presence of neutral, fucosylated HMOs and an HMO mixture. **(B)** Growth of GB2 (OD_{600}) in the presence of neutral, nonfucosylated HMOs, lactose, and an HMO mixture. Data displayed represent the mean $OD_{600} \pm SEM$ of at least three independent experiments, each with three technical replicates. **** represents $p < 0.0001$ by two-way ANOVA with *posthoc* Dunnett's multiple comparison test comparing the growth and viability of GBS in each HMO supplementation condition to the growth and viability of GBS in media alone.

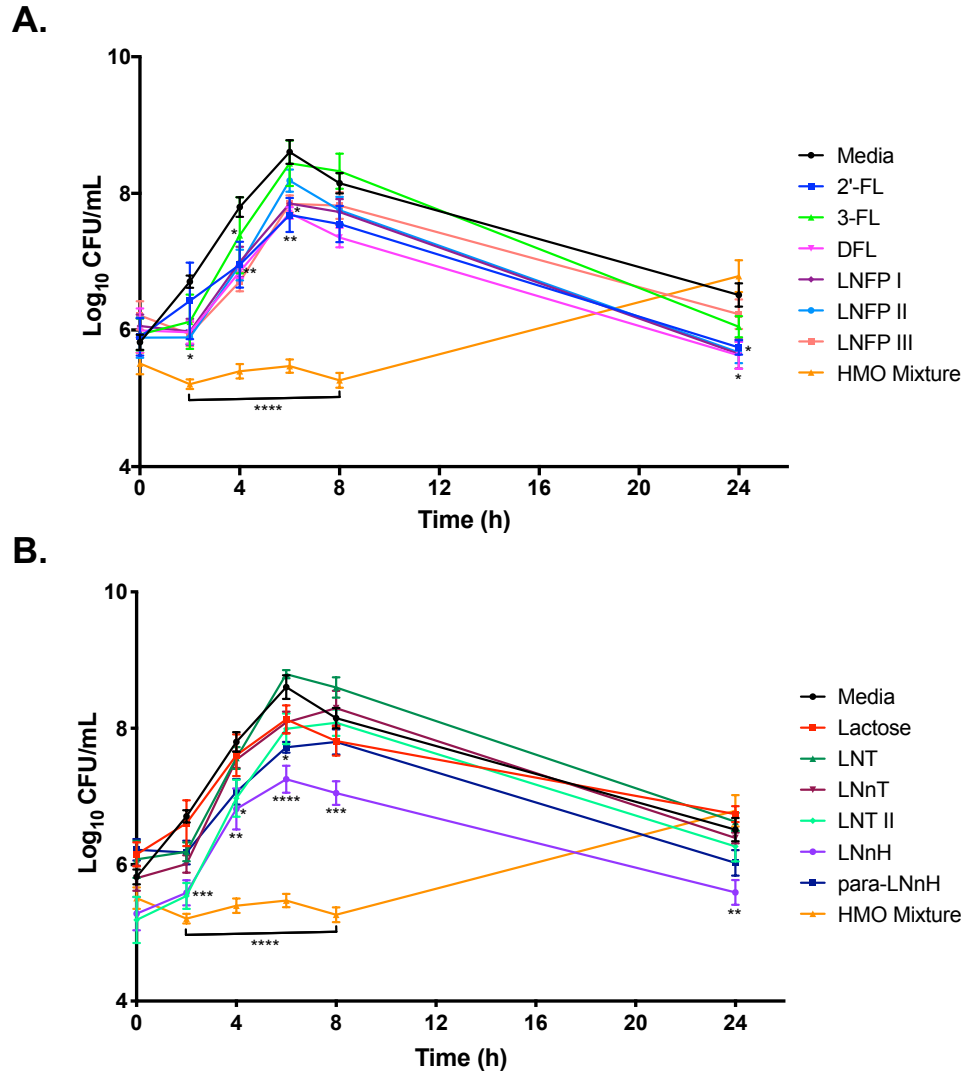


Figure 5.11. Effects of single-entity, neutral HMOs dosed at ca. 5 mg/mL on the viability of GB2 in Todd-Hewitt Broth. Viability was assessed via enumeration of CFU/mL performed at 0, 2, 4, 6, 8, and 24 h. Log₁₀CFU/mL for each HMO source and time point is indicated by the respective symbols. **(A)** Viability of GB2 (CFU/mL) corresponding to the OD values graphed in Figure 5.10A. **(B)** Viability of GB2 (CFU/mL) corresponding to the OD values graphed in Figure 5.10B. Data displayed represent the mean OD₆₀₀ or log₁₀CFU/mL ± SEM of at least three independent experiments, each with three technical replicates. **** represents $p < 0.0001$ by two-way ANOVA with *posthoc* Dunnett's multiple comparison test comparing the growth and viability of GBS in each HMO supplementation condition to the growth and viability of GBS in media alone.

Although LNT and LNnT significantly reduced GB590 growth and viability at several time points, neither of these compounds had any effect on the growth or viability of GB2 (**Figures 5.10** and **5.11**). Similarly, LNFP I, II, and III all saw reduced antimicrobial

activity against GB2. In fact, generally speaking, GB2 was found to be less susceptible to individual HMO supplementation than GB590. Indeed, LNT II and LNnH were the only single compounds to significantly reduce growth during the 24 h window. Interestingly, LNFP III was even found to significantly increase growth from 6 to 8 h. Impressively and uniquely, LNnH decreased growth from 4 to 24 h with reductions ranging on average around 20-50%.

In contrast to the minimal effect on GB2 growth, numerous individual HMOs did significantly reduce GB2 viability (**Figure 5.11**). As with growth, LNnH was the most effective at reducing cellular viability. LNnH decreased GB2 viability by around 15% over the entire 24 h period. Aside from 3-FL, all fucosylated compounds significantly reduced viability over several hours. Additionally, while LNT and LNnT did not reduce viability at any point, LNT II, LNnH, and *para*-LNnH did significantly reduce cellular viability over several hours. Although numerous compounds significantly decreased viability, it is important to note that the magnitudes of these reductions were universally smaller than those observed for GB590. This trend also held true for the magnitudes of growth reductions seen for the two strains.

Comparison of the antimicrobial activities of lactose, LNT, and LNnT against GB2 with their respective fucosylated derivatives showed that fucose generally appeared to increase antimicrobial activity. However, in some cases, such as with LNFP III, improvements in antimicrobial activity were minimal. Furthermore, it is notable that LNT II, a lactose-derived HMO lacking a fucose residue, significantly reduced GB2 growth and viability. Nevertheless, despite the general significance of fucose, it is not clear what effects fucose location and number of residues have on antimicrobial activity.

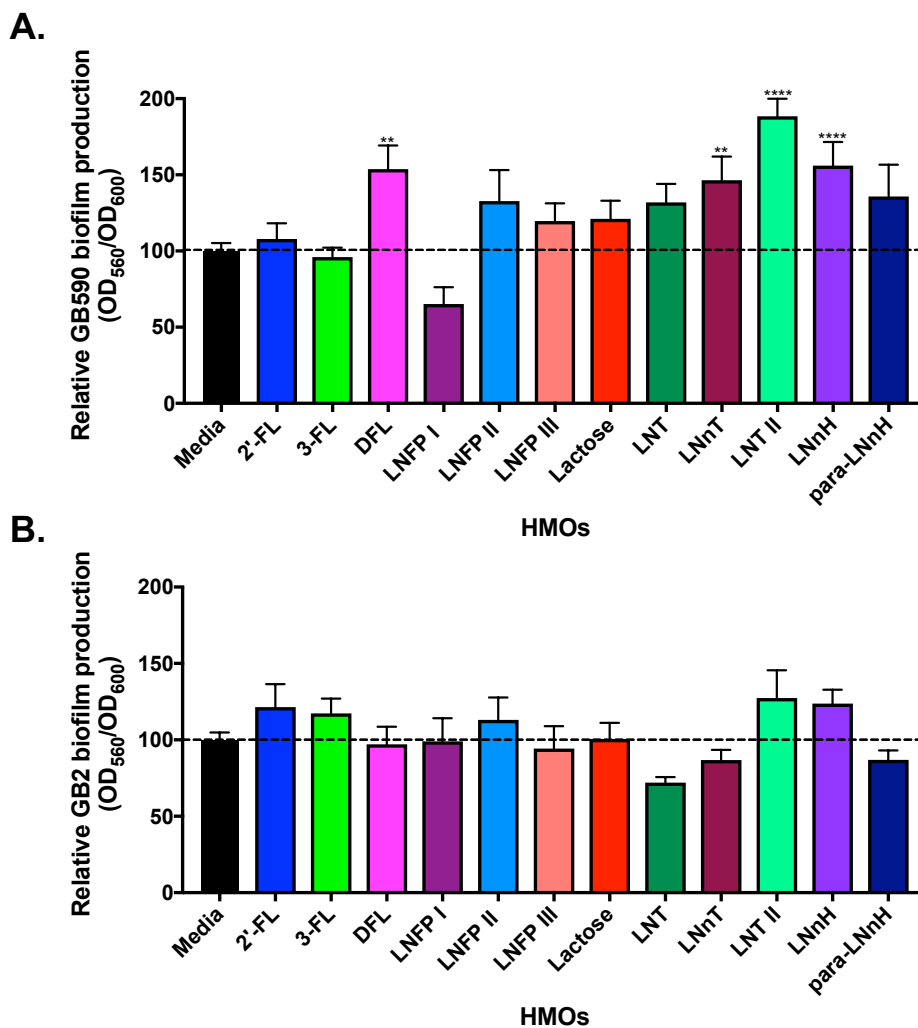


Figure 5.12. Effects of single-entity, neutral HMOs dosed at ca. 5 mg/mL on GBS biofilm production after 24 h of growth in Todd-Hewitt Broth. **(A)** Biofilm production, denoted by the ratio of biofilm/biomass (OD_{560}/OD_{600}), by GB590 in the presence of single-entity HMOs relative to biofilm production in media alone. Data displayed represent the relative mean biofilm/biomass ratio \pm SEM of at least three independent experiments, each with three technical replicates, wherein biofilm production of GB590 in media alone is assigned a value of 100%. **** represents $p < 0.0001$ by one-way ANOVA, $F = 9.811$ with *posthoc* Dunnett's multiple comparison test comparing biofilm production of GB590 in each HMO supplementation condition to biofilm production of GB590 in media alone. **(B)** Biofilm production, denoted by the ratio of biofilm/biomass (OD_{560}/OD_{600}), by GB2 in the presence of homogeneous HMOs relative to biofilm production in media alone. Data displayed represent the relative mean biofilm/biomass ratio \pm SEM of at least three independent experiments, each with three technical replicates, wherein biofilm production of GB2 in media alone is assigned a value of 100%. ** represents $p < 0.005$ by one-way ANOVA, $F = 2.527$ with *posthoc* Dunnett's multiple comparison test comparing biofilm production of GB2 in each HMO supplementation condition to biofilm production of GB2 in media alone. Mean GBS biofilm production levels in media alone are marked with a dotted line.

As a final evaluation of antibacterial activity, we evaluated the effects of individual neutral HMOs on GBS biofilm production (**Figure 5.12**). As detailed in section 5.3, antibiofilm activity was evaluated at 24 h using a plate-based assay that enables quantification of bacterial growth and biofilm production. For the neutral HMOs tested, no compound was found to significantly decrease biofilm formation for either GBS strain. Conversely, DFL, LNnT, LNT II, and LNnH significantly increased biofilm formation in GB590. Notably, these compounds also showcased some of the largest and most prolonged growth repressions. Given this result, we once again hypothesize that when challenged by strong antimicrobial agents, GBS increases biofilm production in order to evade antimicrobial action.

5.6 Summary of Homogenous HMO Evaluation Results³⁷

A summary of the antimicrobial and anti-biofilm activities of all single-entity HMOs tested is provided in **Table 5.1** (see Appendix A3 for more detail). While varying levels of activity were observed for the compounds, several general trends emerged. First and foremost, while numerous single compounds were potent antimicrobials, overall, no single compound was as effective of an antimicrobial as the heterogenous HMO mixture. Second, as was observed in previous studies using HMO mixtures, we found that different GBS strains had different susceptibilities to single-entity HMO-supplementation, i.e. HMO antimicrobial activity is strain-dependent. Overall, GB590 appeared to be more susceptible to treatment with single compounds, both neutral and acidic, than GB2.

Table 5.1. Summary of Antimicrobial and Antibiofilm Activities of Single-Entity HMOs Against Two Strains of GBS^a

Human Milk Oligosaccharide	<i>S. agalactiae</i> GB590			<i>S. agalactiae</i> GB2		
	Average Growth Reduction ^b	Average Viability Reduction ^b	Average Biofilm Reduction ^c	Average Growth Reduction ^b	Average Viability Reduction ^b	Average Biofilm Reduction ^c
Lactose (Lac)	3%	0%	0%	0%	2%	0%
2'-Fucosyllactose (2'-FL)	8%	0%	0%	9%	9%	0%
3-Fucosyllactose (3-FL)	15%	0%	0%	0%	4%	0%
Difucosyllactose (DFL)	51%	17%	0% ^d	0%	11%	0%
Lacto- <i>N</i> -triose II (LNT II)	54%	12%	0% ^d	22%	8%	0%
3'-Sialyllactose (3'-SL)	13%	0%	0%	0%	5%	0%
6'-Sialyllactose (6'-SL)	18%	0%	0%	0%	4%	0%
Lacto- <i>N</i> -tetraose (LNT)	24%	11%	0% ^d	0%	0%	28%
Lacto- <i>N</i> -fucopentaose I (LNFP I)	1%	24%	35%	0%	10%	0%
Lacto- <i>N</i> -fucopentaose II (LNFP II)	31%	15%	0%	0%	9%	0%
<i>LS</i> -tetrasaccharide <i>a</i> (LST <i>a</i>)	38%	23%	0% ^d	42%	25%	0% ^d
<i>Disialyllacto-N</i> -tetraose (DSLNT)	28%	18%	0%	18%	21%	0%
Lacto- <i>N</i> -neotetraose (LNnT)	42%	13%	0% ^d	5%	4%	0%
Lacto- <i>N</i> -fucopentaose III (LNFP III)	26%	14%	0%	0%	9%	0%
Lacto- <i>N</i> -neohexaose (LNnH)	48%	12%	0% ^d	39%	15%	0%
<i>para</i> -Lacto- <i>N</i> -neo hexaose (<i>para</i> -LNnH)	23%	9%	0%	0%	8%	0%
<i>LS</i> -tetrasaccharide <i>c</i> (LST <i>c</i>)	15%	16%	0%	35%	18%	0%
Heterogeneous HMO extract	82%	23%	N/A	73%	24%	N/A

^astrongest activity is bolded and highlighted in blue. ^baverage over 24 h of growth. ^caverage at 24 h of growth. ^dsignificantly increased biofilm formation.

In a similar vein, while neutral and acidic HMOs tended to have generally comparable levels of antimicrobial activity against GB590, against GB2, the larger acidic HMOs (LST a, DSLNT, and LST c) were superior antimicrobials than the neutral compounds. For example, against GB2, LST a, DSLNT, and LST c were all significantly better antimicrobials than LNT and LNnT; LST a and DSLNT are mono and disialylated LNT derivatives, respectively, while LST c is a monosialylated LNnT derivative. We hypothesize that the stronger antimicrobial activity of LST a, DSLNT, and LST c is related to the high structural similarity seen between these compounds and the CPS of G590 (serotype III) and GB2 (serotype Ib) (see **Figure 3.2**, section 3.1.4 of Chapter 3). The mechanism underlying this hypothesized activity, however, is currently unclear. As a final note, the strain-specificity observed for HMO treatment supports the possibility of developing narrow-spectrum antimicrobial compounds.

These studies also demonstrated that, as is characteristic of HMO antimicrobial activity *in vivo*, HMO antimicrobial activity *in vitro* is highly dependent on HMO structure. Indeed, we found that small differences in HMO structure could drastically alter antimicrobial activity. For example, we observed against GB590 that DFL possessed strong antimicrobial activity while the structurally similar 2'-FL and 3-FL were generally devoid of activity. Additionally, the isomeric LST a and LST c possessed varying levels of activity against GB590 both in terms of growth and viability. We also found that the simpler, monosialylated and monofucosylated lactose derivatives were significantly less effective antimicrobials than the larger HMOs derived from LNT and/or LNnT.

Initially, the lack of 2'-FL antimicrobial activity was surprising. However, a review of the extensive literature detailing the protective effects of 2'-FL against pathogenic

colonization offers a potential explanation for the lack of observed activity.²⁹ As previously described, 2'-FL is particularly well-known for its ability to protect infants from infection. This ability is attributable to the structural similarity of 2'-FL to numerous epithelial cell surface glycans that serve as sites for pathogen binding. This allows 2'-FL to serve as a soluble decoy receptor and inhibit initial pathogen binding; the binding of pathogens to epithelial cells is the first step towards pathogen colonization and proliferation. This knowledge in combination with the results of our studies suggests that the environment wherein 2'-FL encounters a pathogen is perhaps as important to the antimicrobial capabilities of this HMO as its molecular structure. Thus, we hypothesize that any antimicrobial activity of 2'-FL against GBS would likely be attributable to an ability to prevent bacterial adhesion to epithelial cells. This mechanism of action would not, however, have been assessable with the assays employed in our studies thus far.

Finally, in contrast to the often high levels of antimicrobial activity observed, the vast majority of HMOs did not reduce GBS biofilm production for either strain tested. In fact, numerous compounds actually increased biofilm production. As previously mentioned, this result is hypothesized to be the result of a high level of antimicrobial activity as biofilm production is a common pathogen defense mechanism.

5.7 Antimicrobial and Antibiofilm Activities of Simple HMO Mixtures³⁶

Given the strong antimicrobial activity of several single-entity HMOs, we hypothesized that challenging GBS with an HMO mixture consisting of the most active compounds would yield antimicrobial activity equal or superior to that of whole HMO extracts. Importantly, as HMO antimicrobial activity was found to be strain-specific,

different combinations of HMOs were used for GB590 and GB2. The GB590-specific mixture consisted of the following HMOs in equal quantities: LNFP I, LNFP II, LNFP III, LNnT, and LST a; this mixture is denoted as GB590 HMO mixture in **Figures 5.13** and **5.15**. The GB2-specific mixture consisted of the following HMOs in equal quantities: DSLNT, LST a, LST c, LNT II, and DFL; this mixture is denoted as GB2 HMO mixture in **Figure 5.14** and **5.15**.

In addition to mixtures consisting of the five most potent antimicrobial HMOs for each strain, we also screened an HMO mixture that attempted to mimic the general composition of whole HMO extracts; this mixture is denoted as HMO extract mimic in **Figures 5.13, 5.14, and 5.15**.^{2, 18, 28} The goal of this simplified mixture was to duplicate, to the best of our abilities, concentrations of the various classes of HMOs present in human milk. While whole milk extracts can contain over 100 different HMOs, the HMO extract mimic contained only 10 (**Table 5.2**).

Table 5.2. HMO Extract Mimic Composition

General HMO Classes and Concentrations	Individual HMO Components and Concentrations
<i>Neutral, Fucosylated HMOs (60%)</i>	2'-FL (20%)
	LNFP I (20%)
	DFL (20%)
<i>LNT (15%)</i>	LNT (15%)
<i>Neutral, Nonfucosylated HMOs (excluding LNT) (15%)</i>	LNnT (5%)
	LNT II (5%)
	<i>Para-LNnH (5%)</i>
<i>Acidic, Sialylated HMOs (10%)</i>	3'-SL (3.3%)
	6'-SL (3.3%)
	DSLNT (3.3%)

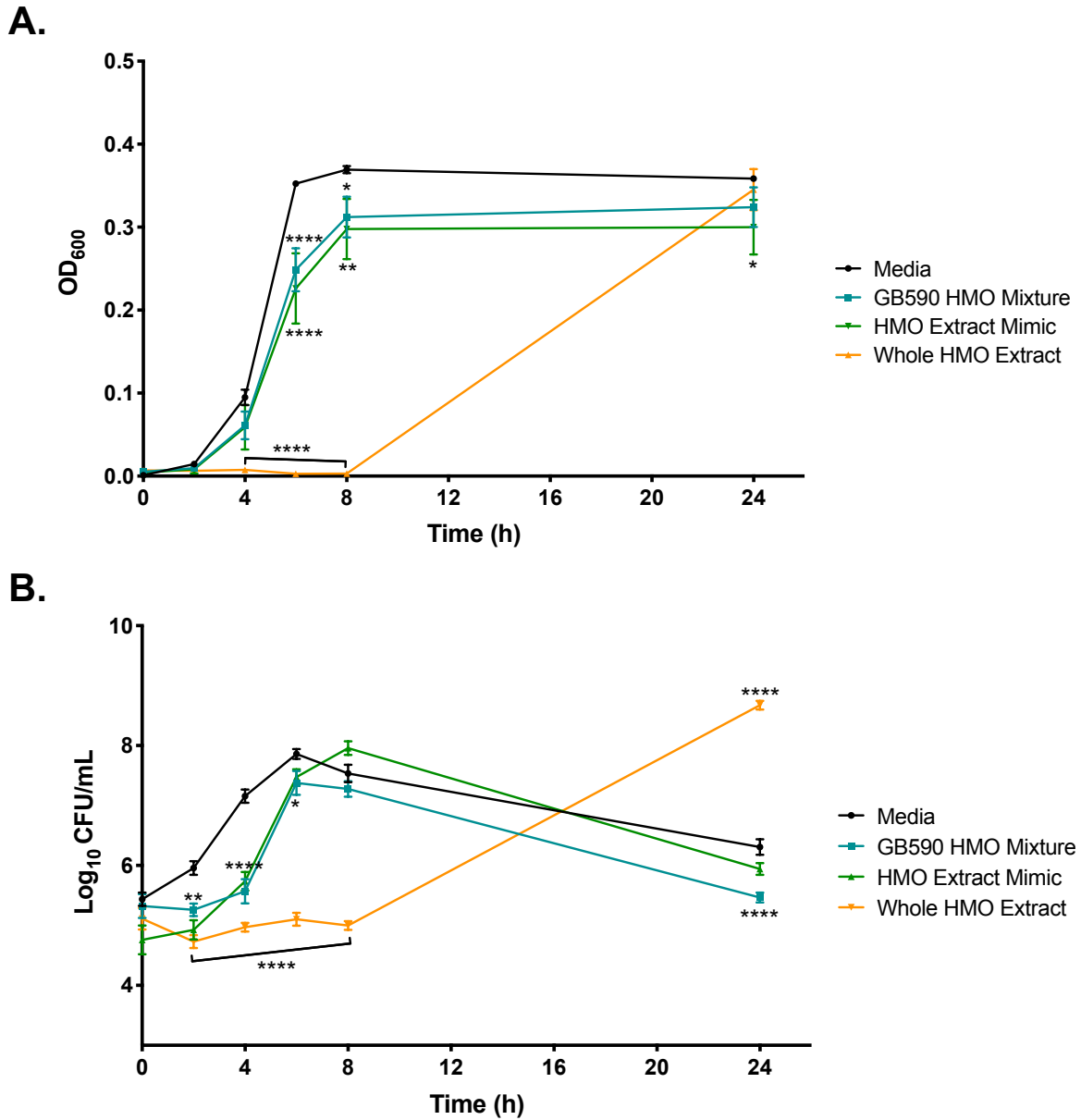


Figure 5.13. Effects of heterogeneous HMO mixtures dosed at ca. 5 mg/mL on the growth and viability of GB590 in Todd-Hewitt Broth. **(A)** OD₆₀₀ readings were taken at 0, 2, 4, 6, 8, and 24 h. Mean OD₆₀₀ for each HMO source and time point is indicated by the respective symbols. **(B)** Enumeration of CFU/mL was performed at 0, 2, 4, 6, 8, and 24 h corresponding to the OD values graphed in (A). Mean log₁₀CFU/mL for each HMO source and time point is indicated by the respective symbols. Data displayed represent the mean OD₆₀₀ or log₁₀CFU/mL ± SEM of at least three independent experiments, each with 3 technical replicates. **** represents $p < 0.0001$ by two-way ANOVA with *posthoc* Dunnett's multiple comparison test comparing the growth and viability of GBS in each HMO supplementation condition to the growth and viability of GBS in media alone.

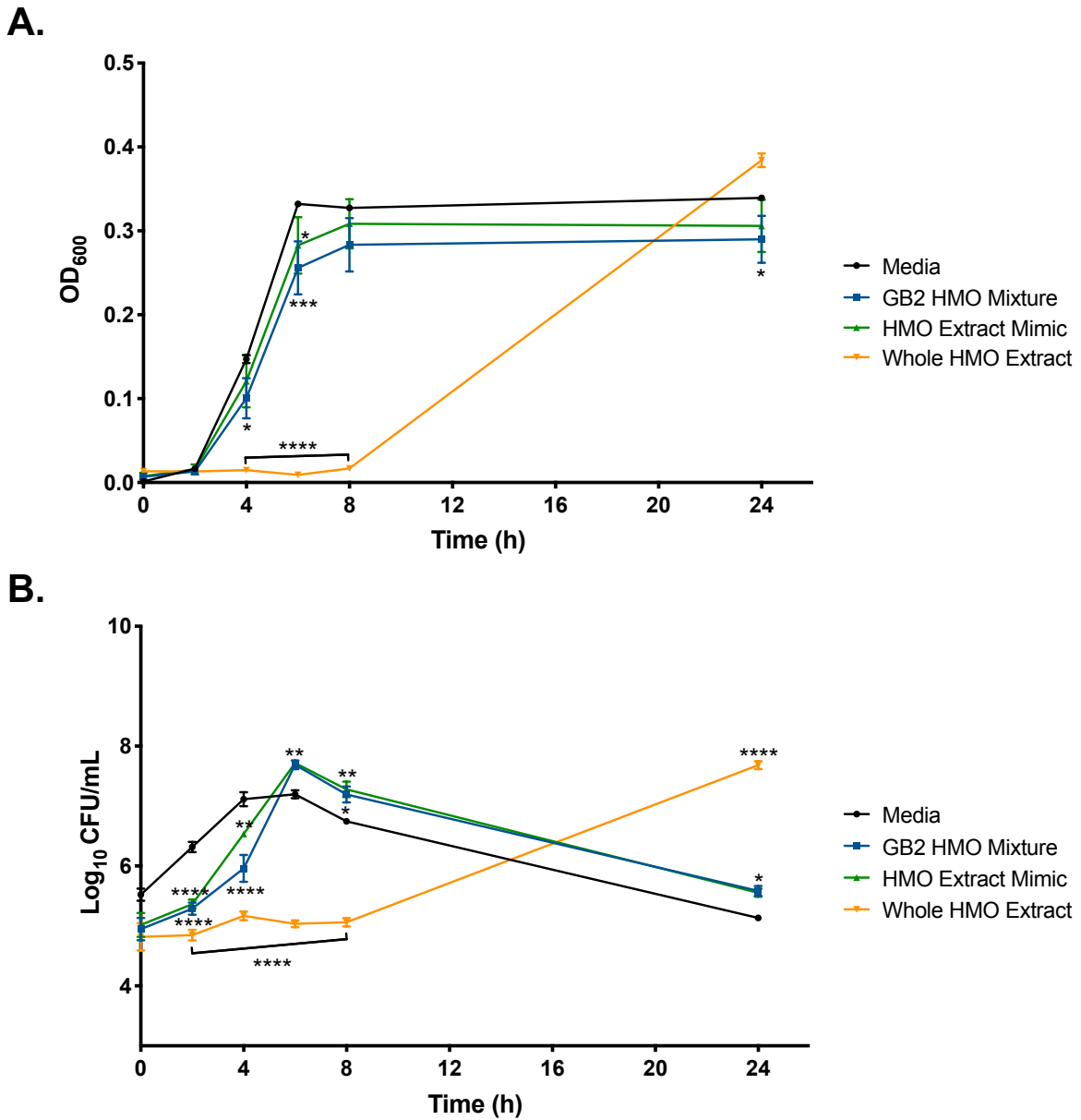


Figure 5.14 Effects of heterogenous HMO mixtures dosed at ca. 5 mg/mL on the growth and viability of GB2 in Todd-Hewitt Broth. **(A)** OD₆₀₀ readings were taken at 0, 2, 4, 6, 8, and 24 h. Mean OD₆₀₀ for each HMO source and time point is indicated by the respective symbols. **(B)** Enumeration of CFU/mL was performed at 0, 2, 4, 6, 8, and 24 h corresponding to the OD values graphed in (A). Mean log₁₀CFU/mL for each HMO source and time point is indicated by the respective symbols. Data displayed represent the mean OD₆₀₀ or log₁₀CFU/mL ± SEM of at least three independent experiments, each with 3 technical replicates. **** represents $p < 0.0001$ by two-way ANOVA with *posthoc* Dunnett's multiple comparison test comparing the growth and viability of GBS in each HMO supplementation condition to the growth and viability of GBS in media alone.

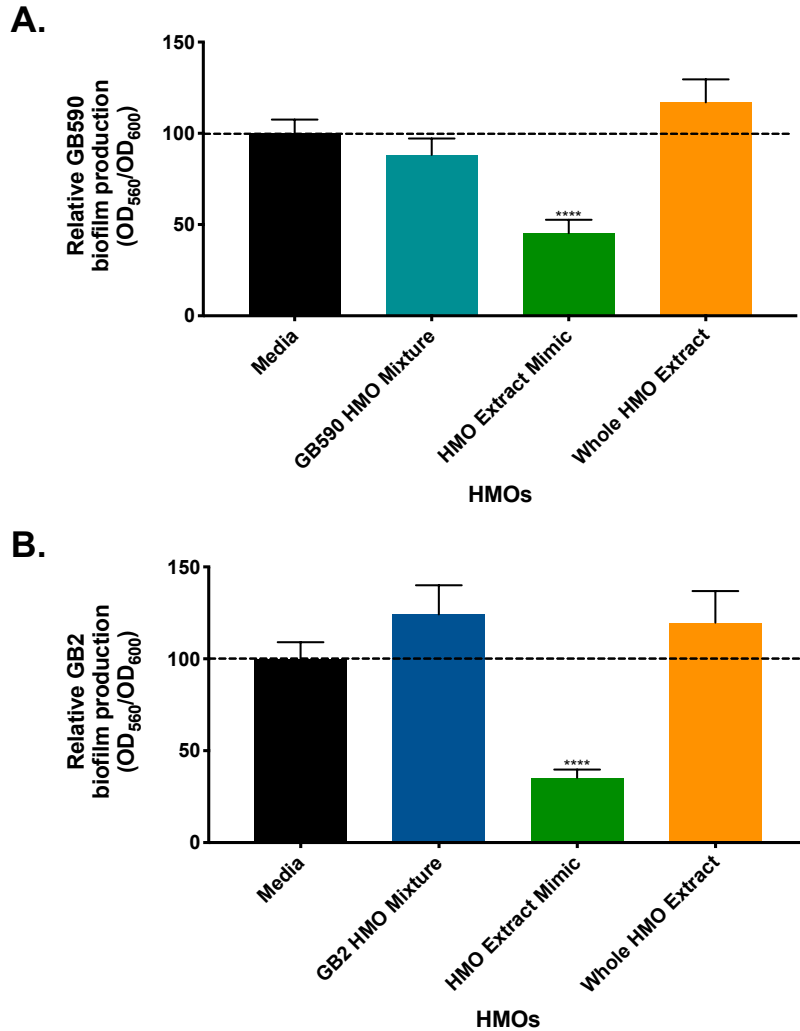


Figure 5.15. Effects of heterogeneous HMO mixtures dosed at ca. 5 mg/mL on GBS biofilm production after 24 h of growth in Todd-Hewitt Broth. **(A)** Biofilm production, denoted by the ratio of biofilm/biomass (OD_{560}/OD_{600}), by GB590 in the presence of single-entirety HMOs relative to biofilm production in media alone. Data displayed represent the relative mean biofilm/biomass ratio \pm SEM of at least three independent experiments, each with 3 technical replicates, wherein biofilm production of GB590 in media alone is assigned a value of 100%. **** represents $p < 0.0001$ by one-way ANOVA, $F = 14.47$ with *posthoc* Dunnett's multiple comparison test comparing biofilm production of GB590 in each HMO supplementation condition to biofilm production of GB590 in media alone. **(B)** Biofilm production, denoted by the ratio of biofilm/biomass (OD_{560}/OD_{600}), by GB2 in the presence of homogeneous HMOs relative to biofilm production in media alone. Data displayed represent the relative mean biofilm/biomass ratio \pm SEM of at least three independent experiments, each with 3 technical replicates, wherein biofilm production of GB2 in media alone is assigned a value of 100%. **** represents $p < 0.0001$ by one-way ANOVA, $F = 14.4$ with *posthoc* Dunnett's multiple comparison test comparing biofilm production of GB2 in each HMO supplementation condition to biofilm production of GB2 in media alone. Mean GBS biofilm production levels in media alone are marked with a dotted line.

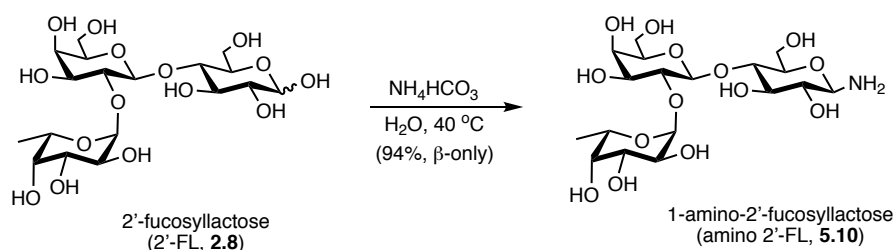
Analogous to prior experiments, each HMO mixture was dosed at ca. 5 mg/mL. Surprisingly, while each custom mixture significantly reduced GB590 or GB2 growth and viability, none of these mixtures displayed comparable antimicrobial activity to that of the whole HMO extract; the custom mixtures possessed similar levels and patterns of activity to one another (**Figures 5.13** and **5.14**). Interestingly, against GB2, the HMO extract mimic and the GB2 HMO mixture actually significantly increased GB2 viability from 6 to 24 h (**Figure 5.14**). In terms of antibiofilm activity, for both GB590 and GB2, the HMO mimic extract was the only mixture capable of significantly decreasing biofilm production (**Figure 5.15**). On average, this mixture decreased biofilm formation by over 50%. Given the similar magnitudes and patterns of antimicrobial activity for the HMO extract mimic and the GBS strain-specific HMO mixtures, it is unclear why only the HMO extract mimic reduced biofilm formation. This result is made even more interesting considering the fact that no individual compound in the HMO extract mimic was previously found to reduce biofilm formation.^{15, 36} Contrarily, several of these HMOs were found to increase GB590 biofilm formation.

5.8 Antimicrobial and Antibiofilm Activities of 1-Amino-2'-Fucosyllactose³⁸

Intrigued by the general lack of antibiofilm activity observed for the homogenous HMOs, we elected to investigate whether the natural structures could be minimally modified to yield superior antibiofilm compounds. Due to its widespread availability, we selected 2'-FL (**2.8**) as our HMO scaffold to modify. This selection was also favorable for the current investigation given the inability of 2'-FL to significantly increase or decrease GBS biofilm formation. We hypothesized that 2'-FL could be converted to an effective

antibiofilm compound by incorporating a positive charge into the structure. This hypothesis was founded on the premise that biofilm matrices are largely composed of anionic polymeric substances and negatively charged extracellular DNA. Given this characteristic, cationic small molecules are known to disrupt the biofilm matrix.³⁹⁻⁴⁷

The most facile method to incorporate a positive charge into the structure of 2'-FL (or the reducing end of any saccharide) is to convert the anomeric alcohol to an amine using the Kochetkov amination.⁴⁸ To achieve this conversion, 2'-FL was exposed to ammonium carbonate and heated for 72 hours to generate amine **5.10** in near quantitative yield as the β -anomer exclusively (**Scheme 5.1**); this work was completed by Prof. Townsend.



Scheme 5.1. Synthesis of 1-amino-2'-fucosyllactose (amino 2'-FL, **5.10**).

Gratifyingly, while the effects of amino 2'-FL derivative **5.10** on GB590 and GB2 growth and viability were generally comparable to those of 2'-FL (**Figures 5.16** and **5.17**), compound **5.10** was a significantly more effective antibiofilm compound than the parent 2'-FL (**Figure 5.18**). Impressively, exposure of GBS to ca. 5 mg/mL of amine **5.10** resulted in an average biofilm production decrease of 37% and 46% for strains GB590 and GB2, respectively. It is important to note that compound **5.10** does not decompose under the assay conditions used. As a final note, although assays to confirm the mechanism behind

the observed antibiofilm activity have not yet been initiated, we hypothesize that the positively charged carbohydrate could serve as a surfactant.

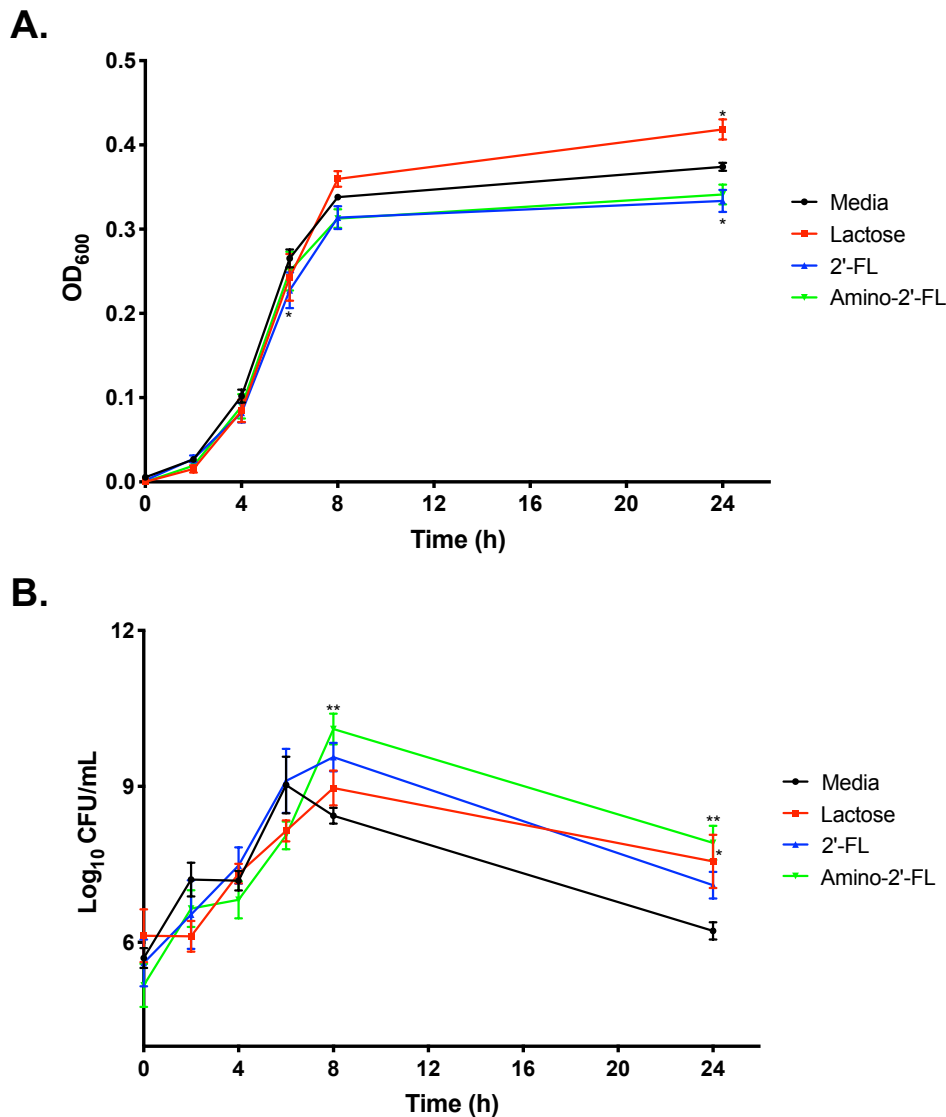


Figure 5.16. Effects lactose (2.1), 2'-FL (2.8), and amino 2'-FL (5.10) dosed at ca. 5 mg/mL on the growth and viability of GB590 in Todd-Hewitt Broth. **(A)** OD₆₀₀ readings were taken at 0, 2, 4, 6, 8, and 24 h. Mean OD₆₀₀ for each HMO source and time point is indicated by the respective symbols. **(B)** Enumeration of CFU/mL was performed at 0, 2, 4, 6, 8, and 24 h corresponding to the OD values graphed in (A). Mean log₁₀CFU/mL for each HMO source and time point is indicated by the respective symbols. Data displayed represent the mean OD₆₀₀ or log₁₀CFU/mL ± SEM of at least three independent experiments, each with 3 technical replicates. **, ***, and **** represent $p = 0.0037$, $p = 0.0005$, and $p < 0.0001$ respectively in (A), and ***, **** represent $p = 0.0007$ and $p < 0.0001$ respectively in (B) by 2-way ANOVA with *posthoc* Dunnett's multiple comparison test comparing the growth and viability of GB590 in each HMO supplementation condition to the growth and viability of GB590 in media alone.

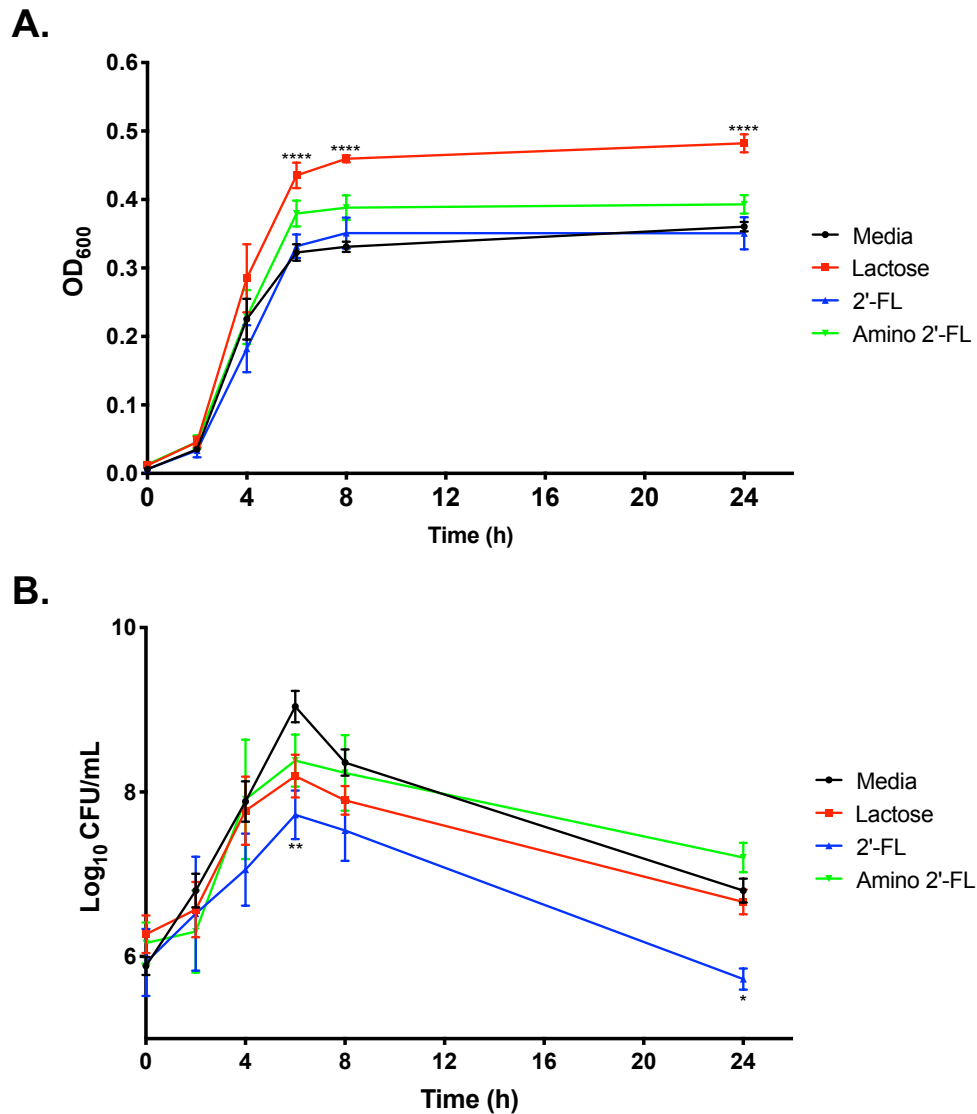


Figure 5.17. Effects of lactose (2.1), 2'-FL (2.8), and amino 2'-FL (5.10) dosed at ca. 5 mg/mL on the growth and viability of GB2 in Todd-Hewitt Broth. (A) OD₆₀₀ readings were taken at 0, 2, 4, 6, 8, and 24 h. Mean OD₆₀₀ for each HMO source and time point is indicated by the respective symbols. (B) Enumeration of CFU/mL was performed at 0, 2, 4, 6, 8, and 24 h corresponding to the OD values graphed in (A). Mean log₁₀CFU/mL for each HMO source and time point is indicated by the respective symbols. Data displayed represent the mean OD₆₀₀ or log₁₀CFU/mL ± SEM of at least three independent experiments, each with 3 technical replicates. * and **** represent $p = 0.0142$ and $p < 0.0001$ respectively in (A), and *** and **** represent $p = 0.0005$ and $p < 0.0001$ respectively in (B) by 2-way ANOVA with *posthoc* Dunnett's multiple comparison test comparing the growth and viability of GB2 in each HMO supplementation condition to the growth and viability of GB2 in media alone.

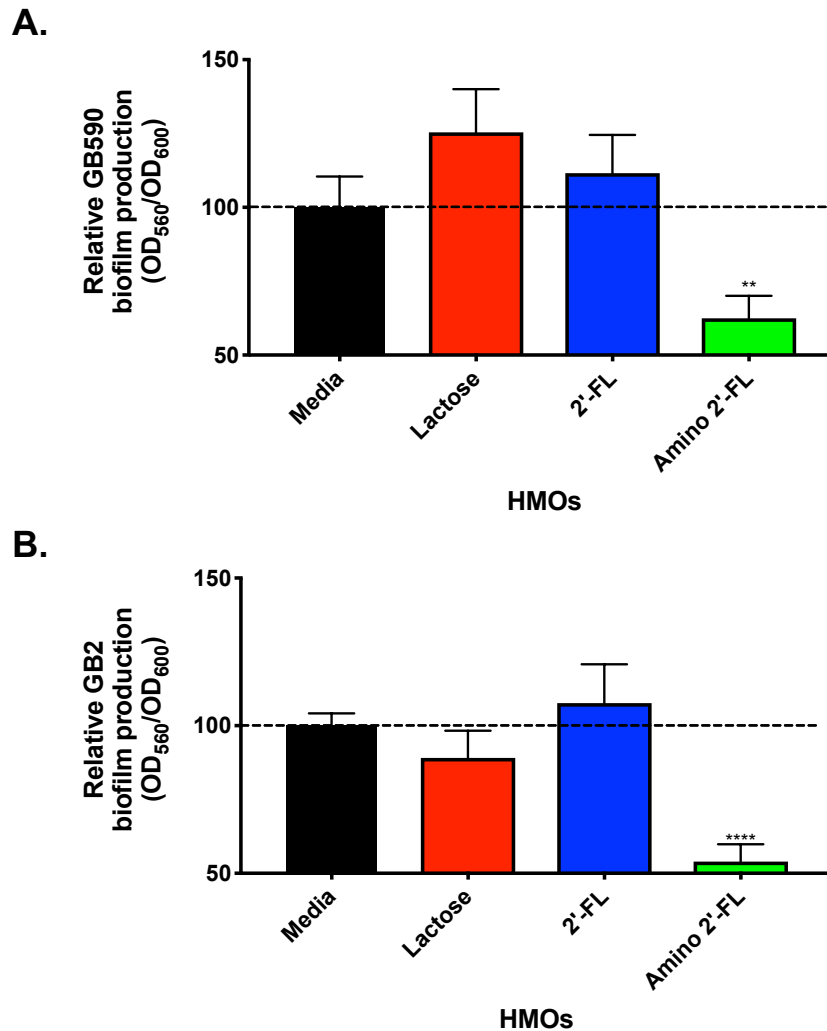


Figure 5.18. Effects of lactose (2.1), 2'-FL (2.8), and amino 2'-FL (5.10) dosed at ca. 5 mg/mL on GBS biofilm production after 24 h of growth in Todd-Hewitt Broth. **(A)** Biofilm production, denoted by the ratio of biofilm/biomass (OD₅₆₀/OD₆₀₀), by GB590 in the presence of various carbohydrates relative to biofilm production in media alone. Data displayed represent the relative mean biofilm/biomass ratio \pm SEM of at least three independent experiments, each with 3 technical replicates, wherein biofilm production of GB590 in media alone is assigned a value of 100%. *** represents $p = 0.0004$ by one-way ANOVA, $F = 7.562$ with *posthoc* Dunnett's multiple comparison test comparing biofilm production of GB590 in each carbohydrate supplementation condition to biofilm production of GB590 in media alone. **(B)** Biofilm production, denoted by the ratio of biofilm/biomass (OD₅₆₀/OD₆₀₀), by GB2 in the presence of various carbohydrates relative to biofilm production in media alone. Data displayed represent the relative mean biofilm/biomass ratio \pm SEM of at least three independent experiments, each with 3 technical replicates, wherein biofilm production of GB2 in media alone is assigned a value of 100%. **** represents $p < 0.0001$ by one-way ANOVA, $F = 9.961$ with *posthoc* Dunnett's multiple comparison test comparing biofilm production of GB2 in each carbohydrate supplementation condition to biofilm production of GB2 in media alone. Mean GBS biofilm production levels in media alone are marked with a dotted line.

5.9 Conclusions and Future Outlook

The work with neutral and acidic homogenous HMOs presented in this chapter has revealed that several single-entity HMOs possess strong antimicrobial activity against Group B *Streptococcus* (*Streptococcus agalactiae*, GBS). In agreement with previous reports from our laboratory and several others, the antimicrobial activity of single compounds was generally found to be lesser than that of whole heterogenous HMO extracts. Moreover, as with heterogenous HMO mixtures, the activity of homogenous HMOs was found to be strain-specific.

Having identified several active HMOs, the next goal will be to use these compounds as tools to identify specific HMO cellular targets. Indeed, although we have uncovered the mechanism of action of HMO antimicrobial activity, we have yet to uncover the targets engaged by HMOs to affect this activity. To address this void, future work will be focused on the synthesis of minimally-modified HMO-based chemoproteomic tools to identify the interacting partners of HMOs.

5.10 Experimental Methods

Materials

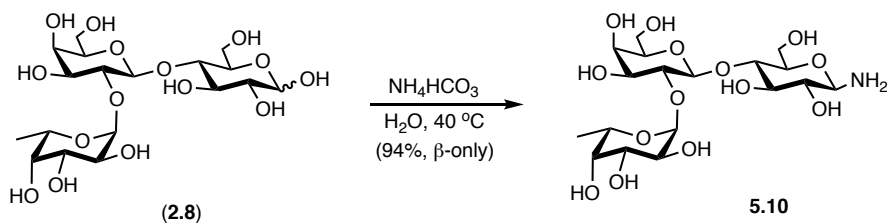
2'-fucosyllactose (2'-FL), 3-fucosyllactose (3-FL), difucosyllactose (DFL), lacto-*N*-fucopentaose I (LNFP I), lacto-*N*-fucopentaose II (LNFP II), lacto-*N*-fucopentaose III (LNFP III), lacto-*N*-neohexaose (LNnH), *para*-lacto-*N*-hexaose (*para*-LNnH), LS-tetrasaccharide a (LST a) sodium salt, LS-tetrasaccharide c (LST c) sodium salt, and disialyllacto-*N*-tetraose (DSLNT) disodium salt were generously donated by Glycom. Lacto-*N*-triose II (LNT II), lacto-*N*-neotetraose (LNnT), 3'-sialyllactose (3'-SL) sodium salt

and 6'-sialyllactose (6'-SL) sodium salt were purchased from Carbosynth. D-lactose monohydrate was purchased from Sigma Aldrich. Lacto-*N*-tetraose was synthesized previously (see Chapter 4).⁴⁹

Instrumentation

¹H NMR spectra were obtained on a Bruker 400 MHz spectrometer with reporting relative to deuterated solvent signals. ¹H NMR spectral data are presented as follows: chemical shifts (δ ppm), multiplicity (s=singlet, d=doublet, dd=doublet of doublets, t=triplet, q=quartet, p=pentet, m=multiplet, br=broad, app=apparent), coupling constants (Hz), integration, proton assignment. Deuterium oxide was calibrated to 4.79 ppm. ¹³C NMR spectra were obtained on a Bruker 100 MHz spectrometer with reporting relative to deuterated solvent signals. ¹³C NMR spectral data are presented as follows: chemical shifts (δ ppm). Proton assignments were made with the aid of 2D COSY NMR. Mass spectral data were recorded on an Ultraflex TOF MS in reflectron positive mode.

Compound Preparation



(2S,3S,4R,5S,6S)-2-(((2S,3R,4S,5R,6R)-2-(((2R,3S,4R,5R,6R)-6-amino-4,5-dihydroxy-2-(hydroxymethyl)tetrahydro-2H-pyran-3-yl)oxy)-4,5-dihydroxy-6-(hydroxymethyl)tetrahydro-2H-pyran-3-yl)oxy)-6-methyltetrahydro-2H-pyran-3,4,5-triol (5.10).

2'-FL (**2.8**) (1.0 eq, 0.49 g, 1.00 mmol) was dissolved in water (10 mL) and (NH₄)HCO₃ (10.0 eq, 0.79 g, 10.0 mmol) was added. The resultant slurry was warmed to 40 °C and stirred for three days. The clear supernatant was filtered through a plug of cotton, frozen, and lyophilized. Lyophilization was determined to be complete when the mass of the product remained constant. Glycosyl amine **5.10** (0.46 g, 0.94 mmol, 94%, 9:1 ratio of product to starting material) was obtained as a white solid: *R_f* 0.15 (60:30:3:5 CHCl₃:CH₃OH:AcOH:H₂O); ¹H NMR (400 MHz, D₂O) δ 5.31 (d, *J* = 2.2 Hz, 1H, H-1''), 4.55 (dd, *J* = 26.6, 8.5 Hz, 1H, H-1), 4.40 (d, *J* = 7.7 Hz, 1H, H-1'), 4.18 – 4.06 (m, 1H), 3.90 – 3.14 (m, 15H), 1.12 (t, *J* = 7.4 Hz, 3H); ¹³C NMR (100 MHz, D₂O) δ 100.1, 99.2, 84.9, 82.9, 76.1, 75.9, 75.1, 74.9, 73.9, 73.5, 71.5, 69.5, 69.0, 68.0, 66.76, 61.0, 60.2, 15.2. (M + Na)⁺ calcd for C₁₈H₃₂NNaO₁₄ 510.179, found 510.170.

Bacterial Strains and Culture Conditions

Clinical strains of *S. agalactiae* (GB590 and GB2) were generously provided by Dr. Shannon Manning at Michigan State University. All strains were grown on tryptic soy agar plates supplemented with 5% sheep blood (blood agar plates) at 37°C in ambient air overnight. All strains were subcultured from blood agar plates into 5 mL of Todd-Hewitt broth (THB) and incubated under shaking conditions at 180 RPM at 37°C overnight. Following overnight incubation, bacterial density was quantified through absorbance readings at 600 nm (OD₆₀₀) using a Promega GloMax-Multi Detection System plate reader. Bacterial numbers were determined using the predetermined coefficient of 1 OD₆₀₀ = 10⁹ CFU/mL.

HMO isolation

Human milk was obtained from 21 healthy, lactating women between 3 days and 3 months postnatal and stored between -80 and -20 °C. Deidentified milk was provided by Dr. Jörn-Hendrik Weitkamp from the Vanderbilt Department of Pediatrics, under a collection protocol approved by the Vanderbilt University Institutional Review Board (IRB#100897), and Medolac. Milk samples were thawed then centrifuged for 45 min. Following centrifugation, the resultant top lipid layer was removed. The proteins were then removed by diluting the remaining sample with roughly 1:1 v/v 180 or 200 proof ethanol, chilling the sample briefly, and centrifuging for 45 min followed by removal of the resulting HMO- containing supernatant. Following concentration of the supernatant in vacuo, the HMO-containing extract was dissolved in phosphate buffer (pH 6.5, 0.2 M) and heated to 37 °C.^{50, 51} β -galactosidase from *Kluyveromyces lactis* was added, and the reaction was stirred until lactose hydrolysis was complete. The reaction mixture was diluted with roughly 1:0.5 v/v 180 or 200 proof ethanol, chilled briefly, then centrifuged for 30 min. The supernatant was removed and concentrated in vacuo, and the remaining salts, glucose, and galactose were separated from the oligosaccharides using P-2 Gel (H_2O elutant). The oligosaccharides were then dried by lyophilization. HMO extracts from the 21 donor samples were pooled together to create an HMO cocktail.²⁴

Bacterial strains and culture conditions

Clinical strains of *S. agalactiae* (GB590 and GB2) were generously provided by Dr. Shannon Manning at Michigan State University. All strains were grown on tryptic soy agar plates supplemented with 5% sheep blood (blood agar plates) at 37 °C in ambient air

overnight. All strains were subcultured from blood agar plates into 5 mL of Todd-Hewitt broth (THB) and incubated under shaking conditions at 180 RPM at 37 °C overnight. Following overnight incubation, bacterial density was quantified through absorbance readings at 600 nm (OD₆₀₀) using a Promega GloMax-Multi Detection System plate reader. Bacterial numbers were determined using the predetermined coefficient of 1 OD₆₀₀= 10⁹ CFU/mL.

Bacterial growth and viability assays

S. agalactiae strains GB590 and GB2 were grown overnight as described above and used to inoculate fresh THB or THB supplemented with ca. 5 mg/mL HMO. Inoculation was performed at a multiplicity of infection (MOI) of 10⁶ colony forming units per 200 µL of growth medium in 96 well tissue culture treated, sterile polystyrene plates (Corning, Inc.). Cultures were grown under static conditions at 37 °C in ambient air. Bacterial growth was quantified through spectrophotometric readings at OD₆₀₀. Bacterial viability was evaluated by serial dilution and plating onto blood agar plates followed by quantification of viable colony forming units per mL of culture (CFU/mL).

Bacterial biofilm assay

S. agalactiae strains GB590 and GB2 were grown overnight as described and used to inoculate fresh THB or THB supplemented with ca. 5 mg/mL HMO. Inoculation was performed at a multiplicity of infection (MOI) of 10⁶ colony forming units per 200 µL of growth medium in 96 well tissue culture treated, sterile polystyrene plates (Corning, Inc.). Cultures were incubated under static conditions at 37 °C in ambient air for 24 h. Following

spectrophotometric reading at OD₆₀₀, culture media was removed and the wells were gently washed once with phosphate-buffered saline (PBS, pH 7.4) to removed non-adherent cells. Adherent cells were next stained with a 10% crystal violet solution for 10 minutes. Excess stain was removed and the wells were gently washed once with PBS then allowed to dry at room temperature for at least 30 minutes. The crystal violet stain was solubilized with an 80% ethanol/20% acetone solution and biofilm formation was quantified through spectrophotometric reading at OD₅₆₀.²⁵

Statistical analysis

All data shown represent at least 3 independent experiments each with 3 technical replicates. Data are expressed as the mean \pm SEM. Statistical analyses were performed in GraphPad Prism Software v. 7.0c. Statistical significance for growth and viability measurements were determined using two-way ANOVA with *posthoc* Dunnett's multiple comparison test comparing growth and viability in the presence of HMOs to growth and viability in media alone. Statistical significance for biofilm production was determined using one-way ANOVA with *posthoc* Dunnett's multiple comparison test comparing biofilm production in the presence of HMOs to biofilm production in media alone.

5.11 References

1. Bode, L., Human milk oligosaccharides: every baby needs a sugar mama. *Glycobiology* **2012**, 22 (9), 1147-62.
2. Ninonuevo, M. R.; Park, Y.; Yin, H.; Zhang, J.; Ward, R. E.; Clowers, B. H.; German, J. B.; Freeman, S. L.; Killeen, K.; Grimm, R.; Lebrilla, C. B., A strategy for annotating the human milk glycome. *J. Agric. Food Chem.* **2006**, 54 (20), 7471-80.

3. Parkkinen, J.; Finne, J.; Achtman, M.; Vaisanen, V.; Korhonen, T. K., *Escherichia coli* strains binding neuraminyl alpha2-3 galactosides. *Biochem. Biophys. Res. Comm.* **1983**, *111* (2), 456-461.
4. Autran, C. A.; Schoterman, M. H.; Jantscher-Krenn, E.; Kamerling, J. P.; Bode, L., Sialylated galacto-oligosaccharides and 2'-fucosyllactose reduce necrotising enterocolitis in neonatal rats. *Br. J. Nutr.* **2016**, *116* (2), 294-9.
5. Angeloni, S.; Ridet, J. L.; Kussy, N.; Gao, H.; Crevoisier, F.; Guinchard, S.; Kochhar, S.; Sigrist, H.; Sprenger, N., Glycoprofiling with micro-arrays of glycoconjugates and lectins. *Glycobiology* **2005**, *15* (1), 31-41.
6. Bode, L.; Kunz, C.; Muhly-Reinholz, M.; Mayer, K.; Seeger, W.; Rudloff, S., Inhibition of monocyte, lymphocyte, and neutrophil adhesion to endothelial cells by human milk oligosaccharides. *Thromb. Haemost.* **2004**, *92* (6), 1402-10.
7. Neu, J.; Walker, W. A., Necrotizing Enterocolitis. *N Engl J Med* **2011**, *364*, 255-264.
8. Yu, H.; Lau, K.; Thon, V.; Autran, C. A.; Jantscher-Krenn, E.; Xue, M.; Li, Y.; Sugiarto, G.; Qu, J.; Mu, S.; Ding, L.; Bode, L.; Chen, X., Synthetic disialyl hexasaccharides protect neonatal rats from necrotizing enterocolitis. *Angew. Chem.* **2014**, *53* (26), 6687-91.
9. Jantscher-Krenn, E.; Zhrebtsov, M.; Nissan, C.; Goth, K.; Guner, Y. S.; Naidu, N.; Choudhury, B.; Grishin, A. V.; Ford, H. R.; Bode, L., The human milk oligosaccharide disialyllacto-*N*-tetraose prevents necrotising enterocolitis in neonatal rats. *Gut* **2012**, *61* (10), 1417-25.
10. Yu, H.; Yan, X.; Autran, C. A.; Li, Y.; Etzold, S.; Latasiewicz, J.; Robertson, B. M.; Li, J.; Bode, L.; Chen, X., Enzymatic and Chemoenzymatic Syntheses of Disialyl Glycans and Their Necrotizing Enterocolitis Preventing Effects. *J. Org. Chem.* **2017**, *82* (24), 13152-13160.
11. Autran, C. A.; Kellman, B. P.; Kim, J. H.; Asztalos, E.; Blood, A. B.; Spence, E. C. H.; Patel, A. L.; Hou, J.; Lewis, N. E.; Bode, L., Human milk oligosaccharide composition predicts risk of necrotising enterocolitis in preterm infants. *Gut* **2018**, *67* (6), 1064-1070.
12. Wang, B.; McVeagh, P.; Petocz, P.; Brand-Miller, J., Brain ganglioside and glycoprotein sialic acid in breastfed compared with formula-fed infants. *Am. J. Clin. Nutr.* **2003**, *78* (5), 1024-9.

13. Wang, B.; Yu, B.; Karim, M.; Hu, H.; Sun, Y.; McGreevy, P.; Petocz, P.; Held, S.; Brand-Miller, J., Dietary sialic acid supplementation improves learning and memory in piglets. *Am. J. Clin. Nutr.* **2007**, *85* (2), 561-9.
14. Wang, B., Sialic acid is an essential nutrient for brain development and cognition. *Ann. Rev. Nutr.* **2009**, *29*, 177-222.
15. Craft, K. M.; Thomas, H. C.; Townsend, S. D., Sialylated variants of lacto-*N*-tetraose exhibit antimicrobial activity against Group B *Streptococcus*. *Org. Biomol. Chem.* **2018**, *17* (7), 1893-1900.
16. Lin, A. E.; Autran, C. A.; Szyszka, A.; Escajadillo, T.; Huang, M.; Godula, K.; Prudden, A. R.; Boons, G. J.; Lewis, A. L.; Doran, K. S.; Nizet, V.; Bode, L., Human milk oligosaccharides inhibit growth of group B *Streptococcus*. *J. Biol. Chem.* **2017**, *292* (27), 11243-11249.
17. Tarr, A. J.; Galley, J. D.; Fisher, S. E.; Chichlowski, M.; Berg, B. M.; Bailey, M. T., The prebiotics 3'Sialyllactose and 6'Sialyllactose diminish stressor-induced anxiety-like behavior and colonic microbiota alterations: Evidence for effects on the gut-brain axis. *Brain Behav. Immun.* **2015**, *50*, 166-177.
18. Kunz, C.; Rudloff, S.; Baier, W.; Klein, N.; Strobel, S., Oligosaccharides in human milk: structural, functional, and metabolic aspects. *Ann. Rev. Nutr.* **2000**, *20*, 699-722.
19. Kuntz, S.; Rudloff, S.; Kunz, C., Oligosaccharides from human milk influence growth-related characteristics of intestinally transformed and non-transformed intestinal cells. *Br. J. Nutr.* **2008**, *99* (3), 462-71.
20. Sela, D. A.; Li, Y.; Lerno, L.; Wu, S.; Marcobal, A. M.; German, J. B.; Chen, X.; Lebrilla, C. B.; Mills, D. A., An infant-associated bacterial commensal utilizes breast milk sialyloligosaccharides. *J. Biol. Chem.* **2011**, *286* (14), 11909-18.
21. Cieslewicz, M. J.; Chaffin, D.; Glusman, G.; Kasper, D.; Madan, A.; Rodrigues, S.; Fahey, J.; Wessels, M. R.; Rubens, C. E., Structural and genetic diversity of group B *streptococcus* capsular polysaccharides. *Infect. Immun.* **2005**, *73* (5), 3096-103.
22. Melin, P.; Efstratiou, A., Group B streptococcal epidemiology and vaccine needs in developed countries. *Vaccine* **2013**, *31 Suppl 4*, D31-42.

23. Ackerman, D. L.; Doster, R. S.; Weitkamp, J. H.; Aronoff, D. M.; Gaddy, J. A.; Townsend, S. D., Human Milk Oligosaccharides Exhibit Antimicrobial and Antibiofilm Properties against Group B *Streptococcus*. *ACS Infect. Dis.* **2017**, *3* (8), 595-605.
24. Craft, K. M.; Gaddy, J. A.; Townsend, S. D., Human Milk Oligosaccharides (HMOs) Sensitize Group B *Streptococcus* to Clindamycin, Erythromycin, Gentamicin, and Minocycline on a Strain Specific Basis. *ACS Chem. Biol.* **2018**, *13* (8), 2020-2026.
25. Ackerman, D. L.; Craft, K. M.; Doster, R. S.; Weitkamp, J. H.; Aronoff, D. M.; Gaddy, J. A.; Townsend, S. D., Antimicrobial and Antibiofilm Activity of Human Milk Oligosaccharides against *Streptococcus agalactiae*, *Staphylococcus aureus*, and *Acinetobacter baumannii*. *ACS Infect. Dis.* **2018**, *4* (3), 315-324.
26. Pendleton, J. N.; Gorman, S. P.; Gilmore, B. F., Clinical relevance of the ESKAPE pathogens. *Expert Rev. Anti. Infect. Ther.* **2013**, *11* (3), 297-308.
27. Santajit, S.; Indrawattana, N., Mechanisms of Antimicrobial Resistance in ESKAPE Pathogens. *Biomed. Res. Int.* **2016**, *2016*, 2475067.
28. Nijman, R. M.; Liu, Y.; Bunyatratchata, A.; Smilowitz, J. T.; Stahl, B.; Barile, D., Characterization and Quantification of Oligosaccharides in Human Milk and Infant Formula. *J. Agric. Food Chem.* **2018**, *66* (26), 6851-6859.
29. Craft, K. M.; Townsend, S. D., The Human Milk Glycome as a Defense Against Infectious Diseases: Rationale, Challenges, and Opportunities. *ACS Infect. Dis.* **2017**, *4* (2), 77-83.
30. Ruiz-Palacios, G. M.; Cervantes, L. E.; Ramos, P.; Chavez-Munguia, B.; Newburg, D. S., *Campylobacter jejuni* binds intestinal H(O) antigen (Fuc α 1, 2Gal β 1, 4GlcNAc), and fucosyloligosaccharides of human milk inhibit its binding and infection. *J. Biol. Chem.* **2003**, *278* (16), 14112-20.
31. Schrotten, H.; Hanisch, F. G.; Hansman, G. S., Human Norovirus Interactions with Histo-Blood Group Antigens and Human Milk Oligosaccharides. *J. Virol.* **2016**, *90* (13), 5855-9.
32. Weichert, S.; Jennewein, S.; Hufner, E.; Weiss, C.; Borkowski, J.; Putze, J.; Schrotten, H., Bioengineered 2'-fucosyllactose and 3-fucosyllactose inhibit the adhesion of *Pseudomonas aeruginosa* and enteric pathogens to human intestinal and respiratory cell lines. *Nutr. Res.* **2013**, *33* (10), 831-8.

33. Cravioto, A.; Tello, A.; Villafan, H.; Ruiz, J.; del Vedovo, S.; Neeser, J. R., Inhibition of localized adhesion of enteropathogenic *Escherichia coli* to HEp-2 cells by immunoglobulin and oligosaccharide fractions of human colostrum and breast milk. *J. Infect. Dis.* **1991**, *163* (6), 1247-55.
34. Coppa, G. V.; Zampini, L.; Galeazzi, T.; Facinelli, B.; Ferrante, L.; Capretti, R.; Orazio, G., Human milk oligosaccharides inhibit the adhesion to Caco-2 cells of diarrheal pathogens: *Escherichia coli*, *Vibrio cholerae*, and *Salmonella fytis*. *Pediatr. Res.* **2006**, *59* (3), 377-82.
35. Andreas, N. J.; Al-Khalidi, A.; Jaiteh, M.; Clarke, E.; Hyde, M. J.; Modi, N.; Holmes, E.; Kampmann, B.; Mehring Le Doare, K., Role of human milk oligosaccharides in Group B *Streptococcus* colonisation. *Clin. Transl. Immunology* **2016**, *5* (8), e99.
36. Craft, K. M.; Thomas, H. C.; Townsend, S. D., Interrogation of Human Milk Oligosaccharide Fucosylation Patterns for Antimicrobial and Antibiofilm Trends in Group B *Streptococcus*. *ACS Infect. Dis.* **2018**, *4* (12), 1755-1765.
37. Craft, K. M.; Townsend, S. D., Mother Knows Best: Deciphering the Antibacterial Properties of Human Milk Oligosaccharides. *Acc. Chem. Res.* **2019**, *Ahead of print*.
38. Craft, K. M.; Townsend, S. D., 1-Amino-2'-fucosyllactose inhibits biofilm formation by *Streptococcus agalactiae*. *J. Antibiot. (Tokyo)* **2019**, *Ahead of print*.
39. de la Fuente-Nunez, C.; Korolik, V.; Bains, M.; Nguyen, U.; Breidenstein, E. B.; Horsman, S.; Lewenza, S.; Burrows, L.; Hancock, R. E., Inhibition of bacterial biofilm formation and swarming motility by a small synthetic cationic peptide. *Antimicrob. Agents Chemother.* **2012**, *56* (5), 2696-704.
40. del Pozo, J. L.; Patel, R., The challenge of treating biofilm-associated bacterial infections. *Clin. Pharmacol. Ther.* **2007**, *82* (2), 204-9.
41. Donelli, G.; Francolini, I.; Piozzi, A.; Di Rosa, R.; Marconi, W., New polymer-antibiotic systems to inhibit bacterial biofilm formation: a suitable approach to prevent central venous catheter-associated infections. *J. Chemother.* **2002**, *14* (5), 501-7.
42. Jain, T.; Muktapuram, P. R.; Sharma, K.; Ravi, O.; Pant, G.; Mitra, K.; Bathula, S. R.; Banerjee, D., Biofilm inhibition and anti-Candida activity of a cationic lipobenzamide molecule with twin-nonyl chain. *Bioorg. Med. Chem. Lett.* **2018**, *28* (10), 1776-1780.

43. Meeker, D. G.; Wang, T.; Harrington, W. N.; Zharov, V. P.; Johnson, S. A.; Jenkins, S. V.; Oyibo, S. E.; Walker, C. M.; Mills, W. B.; Shirtliff, M. E.; Beenken, K. E.; Chen, J.; Smeltzer, M. S., Versatility of targeted antibiotic-loaded gold nanoconstructs for the treatment of biofilm-associated bacterial infections. *Int. J. Hyperthermia* **2018**, *34* (2), 209-219.
44. Perez-Soto, N.; Moule, L.; Crisan, D. N.; Insua, I.; Taylor-Smith, L. M.; Voelz, K.; Fernandez-Trillo, F.; Krachler, A. M., Engineering microbial physiology with synthetic polymers: cationic polymers induce biofilm formation in *Vibrio cholerae* and downregulate the expression of virulence genes. *Chem. Sci.* **2017**, *8* (8), 5291-5298.
45. Saini, H.; Vadekeetil, A.; Chhibber, S.; Harjai, K., Azithromycin-Ciprofloxacin-Impregnated Urinary Catheters Avert Bacterial Colonization, Biofilm Formation, and Inflammation in a Murine Model of Foreign-Body-Associated Urinary Tract Infections Caused by *Pseudomonas aeruginosa*. *Antimicrob. Agents Chemother.* **2017**, *61* (3).
46. Takahashi, H.; Nades, E. T.; Kuroda, K., Cationic Amphiphilic Polymers with Antimicrobial Activity for Oral Care Applications: Eradication of *S. mutans* Biofilm. *Biomacromolecules* **2017**, *18* (1), 257-265.
47. Wu, H.; Moser, C.; Wang, H. Z.; Hoiby, N.; Song, Z. J., Strategies for combating bacterial biofilm infections. *Int. J. Oral. Sci.* **2015**, *7* (1), 1-7.
48. Likhoshesterov, L. M.; Novikova, O. S.; Derevitskaja, V. A.; Kochetkov, N. K., A New Simple Synthesis of Amino Sugar β -D-Glycosylamines. *Carbohydr. Res.* **1986**, *146* (1), C1-C5.
49. Craft, K. M.; Townsend, S. D., Synthesis of lacto-*N*-tetraose. *Carbohydr. Res.* **2017**, *440-441*, 43-50.
50. Santibáñez, L.; Fernández-Arrojo, L.; Guerrero, C.; Plou, F. J.; Illanes, A., Removal of lactose in crude galacto-oligosaccharides by β -galactosidase from *Kluyveromyces lactis*. *J. Mol. Cat. B: Enzym.* **2016**, *133*, 85-91.
51. Ramirez-Macias, D.; Shaw, K.; Ward, R.; Galvan-Magana, F.; Vazquez-Juarez, R., Isolation and characterization of microsatellite loci in the whale shark (*Rhincodon typus*). *Mol. Ecol. Resour.* **2009**, *9* (3), 798-800.

Appendix A3:
Data and Spectra Relevant to Chapter 5

Table A3.1. Effects of Sialylated HMOs on GB590 Growth Over 24 h^{a,b}

Time (h)	Media (Control)	Lactose	3'-SL	6'-SL	LNT	LST a	DSLNT	LNnT	LST c	HMO Mixture
	Difference from Control (%) ± SEM									
0	0.00 ± 22.37	23.88 ± 55.76	8.42 ± 62.34	-100.00 ±	-4.86 ± 84.35	-22.14 ± 56.83	71.47 ± 99.55	-100.00 ±	142.08 ± 102.11	51.10 ± 44.78
2	0.00 ± 10.13	13.33 ± 24.40	9.22 ± 18.52	-27.83 ± 14.53	-37.00 ± 43.61	-59.00 ± 17.54	-47.42 ± 18.71	-77.52 ± 11.25	-31.30 ± 21.33	-82.26 ± 5.06
4	0.00 ± 9.13	-7.78 ± 12.34	-25.12 ± 14.02	-26.12 ± 12.88	-19.02 ± 41.44	-58.30 ± 13.91	-45.80 ± 13.41	-48.23 ± 19.34	-25.14 ± 18.59	-95.83 ± 1.10
6	0.00 ± 2.63	-9.96 ± 4.99	-27.53 ± 6.80	-19.95 ± 7.53	-27.85 ± 19.47	-37.73 ± 11.09	-27.91 ± 10.20	-37.42 ± 13.54	-14.78 ± 11.77	-98.79 ± 0.41
8	0.00 ± 1.37	-5.35 ± 2.51	-13.46 ± 4.22	-10.79 ± 3.27	-19.41 ± 13.36	-20.42 ± 9.05	-11.28 ± 8.21	-24.05 ± 6.77	-2.92 ± 8.67	-98.12 ± 0.95
24	0.00 ± 1.84	-5.40 ± 3.50	-8.28 ± 4.37	-7.35 ± 3.42	-16.36 ± 11.06	-16.63 ± 8.36	-9.16 ± 8.02	-22.40 ± 3.92	-0.94 ± 8.74	-33.47 ± 9.23

^aSignificant reductions from control are bolded and highlighted in blue ($P < 0.05$, by two-way ANOVA with *posthoc* Dunnett's multiple comparison test).

^bSignificant increases from control are highlighted in red ($P < 0.05$, by two-way ANOVA with *posthoc* Dunnett's multiple comparison test).

Table A3.2. Effects of Sialylated HMOs on GB2 Growth Over 24 h^{a,b}

	Media (Control)	Lactose	3'-SL	6'-SL	LNT	LST a	DSLNT	LNnT	LST c	HMO Mixture
Time (h)	Difference from Control (%) ± SEM									
0	0.00 ± 22.37	23.88 ± 55.76	8.42 ± 62.34	-100.00 ±	-4.86 ± 84.35	-22.14 ± 56.83	71.47 ± 99.55	-100.00 ±	142.08 ± 102.11	51.10 ± 44.78
2	0.00 ± 10.13	13.33 ± 24.40	9.22 ± 18.52	-27.83 ± 14.53	-37.00 ± 43.61	-59.00 ± 17.54	-47.42 ± 18.71	-77.52 ± 11.25	-31.30 ± 21.33	-82.26 ± 5.06
4	0.00 ± 9.13	-7.78 ± 12.34	-25.12 ± 14.02	-26.12 ± 12.88	-19.02 ± 41.44	-58.30 ± 13.91	-45.80 ± 13.41	-48.23 ± 19.34	-25.14 ± 18.59	-95.83 ± 1.10
6	0.00 ± 2.63	-9.96 ± 4.99	-27.53 ± 6.80	-19.95 ± 7.53	-27.85 ± 19.47	-37.73 ± 11.09	-27.91 ± 10.20	-37.42 ± 13.54	-14.78 ± 11.77	-98.79 ± 0.41
8	0.00 ± 1.37	-5.35 ± 2.51	-13.46 ± 4.22	-10.79 ± 3.27	-19.41 ± 13.36	-20.42 ± 9.05	-11.28 ± 8.21	-24.05 ± 6.77	-2.92 ± 8.67	-98.12 ± 0.95
24	0.00 ± 1.84	-5.40 ± 3.50	-8.28 ± 4.37	-7.35 ± 3.42	-16.36 ± 11.06	-16.63 ± 8.36	-9.16 ± 8.02	-22.40 ± 3.92	-0.94 ± 8.74	-33.47 ± 9.23

^aSignificant reductions from control are bolded and highlighted in blue ($P < 0.05$, by two-way ANOVA with *posthoc* Dunnett's multiple comparison test).

^bSignificant increases from control are highlighted in red ($P < 0.05$, by two-way ANOVA with *posthoc* Dunnett's multiple comparison test).

Table A3.3. Effects of Sialylated HMOs on GB590 Viability Over 24 h^{a,b}

Time (h)	Media (Control)	Lactose	3'-SL	6'-SL	LNT	LST a	DSLNT	LNnT	LST c	HMO Mixture
	Difference from Control (%) ± SEM									
0	0 ± 2.48	3.27 ± 7.42	1.94 ± 5.64	-7.84 ± 7.75	-9.70 ± 3.84	-16.47 ± 3.57	-9.19 ± 4.76	-20.80 ± 3.33	-10.28 ± 5.34	-7.21 ± 4.66
2	0 ± 3.83	-7.22 ± 6.29	-3.37 ± 5.11	10.69 ± 6.26	-22.67 ± 2.65	-25.11 ± 2.72	-23.60 ± 2.95	-23.05 ± 2.65	-22.38 ± 2.47	-26.24 ± 2.35
4	0 ± 3.04	5.69 ± 3.61	8.57 ± 4.65	13.09 ± 5.33	-13.55 ± 5.68	-23.37 ± 3.97	-19.60 ± 3.93	-19.25 ± 3.14	-21.32 ± 3.53	-26.71 ± 2.63
6	0 ± 4.29	0.87 ± 4.92	0.56 ± 4.76	10.96 ± 6.08	-15.92 ± 4.09	-22.01 ± 2.83	-18.26 ± 3.46	-17.13 ± 3.91	-16.72 ± 3.39	-37.76 ± 2.18
8	0 ± 2.60	10.67 ± 3.83	13.37 ± 4.27	15.50 ± 3.81	-5.04 ± 2.15	-20.74 ± 2.66	-15.34 ± 2.66	-2.85 ± 2.41	-7.08 ± 3.97	-37.34 ± 2.28
24	0 ± 2.88	23.30 ± 7.24	18.97 ± 4.24	17.94 ± 4.39	2.32 ± 4.88	-22.01 ± 2.38	-13.25 ± 2.55	-3.17 ± 2.28	-10.88 ± 2.87	12.97 ± 10.97

^aSignificant reductions from control are bolded and highlighted in blue ($P < 0.05$, by two-way ANOVA with *posthoc* Dunnett's multiple comparison test).

^bSignificant increases from control are highlighted in red ($P < 0.05$, by two-way ANOVA with *posthoc* Dunnett's multiple comparison test).

Table A3.4. Effects of Sialylated HMOs on GB2 Viability Over 24 h^{a,b}

Time (h)	Media (Control)	Lactose	3'-SL	6'-SL	LNT	LST a	DSLNT	LNnT	LST c	HMO Mixture
0	0 ± 2.67	5.67 ± 3.63	5.29 ± 4.42	19.32 ± 13.78	4.41 ± 5.05	-13.53 ± 6.06	-12.45 ± 6.08	-0.32 ± 3.68	-5.25 ± 4.95	-5.36 ± 3.25
2	0 ± 1.88	-1.47 ± 5.17	-5.53 ± 5.69	-1.27 ± 8.19	-7.75 ± 2.41	-18.73 ± 1.92	-19.89 ± 2.15	-10.40 ± 2.25	-18.91 ± 1.83	-22.36 ± 1.47
4	0 ± 2.62	-2.51 ± 4.33	-7.47 ± 4.65	-6.16 ± 5.54	-3.01 ± 2.72	-26.36 ± 5.17	-25.92 ± 3.48	-3.33 ± 2.37	-23.60 ± 3.47	-30.80 ± 1.88
6	0 ± 2.85	-5.52 ± 3.06	-3.77 ± 3.95	-8.78 ± 3.43	2.20 ± 2.17	-21.35 ± 3.79	-19.85 ± 3.32	-6.02 ± 2.63	-17.36 ± 2.57	-36.40 ± 1.71
8	0 ± 2.57	-4.11 ± 3.15	-5.25 ± 3.28	-2.11 ± 2.53	5.50 ± 2.65	-25.42 ± 2.09	-16.97 ± 2.08	1.79 ± 3.64	-12.91 ± 3.86	-35.39 ± 1.78
24	0 ± 3.71	3.49 ± 3.26	-4.75 ± 2.71	0.24 ± 2.79	1.78 ± 3.35	-31.82 ± 4.03	-20.47 ± 3.25	-1.87 ± 2.85	-18.71 ± 2.84	4.25 ± 4.49

^aSignificant reductions from control are bolded and highlighted in blue ($P < 0.05$, by two-way ANOVA with *posthoc* Dunnett's multiple comparison test).

^bSignificant increases from control are highlighted in red ($P < 0.05$, by two-way ANOVA with *posthoc* Dunnett's multiple comparison test).

Table A3.5. Effects of Sialylated HMOs on GB590 Biofilm Production at 24 h^{a,b}

Media (Control)	Lactose	3'-SL	6'-SL	LNT	LST a	DSLNT	LNnT	LST c
0 ± 5.23	21.14 ± 11.78	2.527 ± 7.47	-13.07 ± 5.33	31.87 ± 12.15	26.31 ± 13.55	5.77 ± 9.10	46.48 ± 15.48	23.76 ± 10.87
Difference from Control (%) ± SEM								

^aSignificant reductions from control are bolded and highlighted in blue ($P < 0.05$, by one-way ANOVA with *posthoc* Dunnett's multiple comparison test). ^bSignificant increases from control are highlighted in red ($P < 0.05$, by one-way ANOVA with *posthoc* Dunnett's multiple comparison test).

Table A3.6. Effects of Sialylated HMOs on GB2 Biofilm Production at 24 h^{a,b}

Media (Control)	Lactose	3'-SL	6'-SL	LNT	LST a	DSLNT	LNnT	LST c
0 ± 4.81	0.57 ± 10.52	-10.34 ± 7.73	-8.51 ± 8.93	-27.95 ± 3.66	42.90 ± 14.11	5.89 ± 14.10	-13.25 ± 6.69	20.32 ± 15.14
Difference from Control (%) ± SEM								

^aSignificant reductions from control are bolded and highlighted in blue ($P < 0.05$, by one-way ANOVA with *posthoc* Dunnett's multiple comparison test). ^bSignificant increases from control are highlighted in red ($P < 0.05$, by one-way ANOVA with *posthoc* Dunnett's multiple comparison test).

Table A3.7. Effects of Neutral, Fucosylated HMOs on GB590 Growth Over 24 h^{a,b}

	Media (Control)	2'-FL	3-FL	DFL	LNFP I	LNFP II	LNFP III	HMO Mixture
Time (h)	Difference from Control (%) ± SEM							
0	0 ± 22.37	129.91 ± 102.25	-54.29 ± 46.27	-87.42 ± 12.74	134.50 ± 86.80	-34.56 ± 42.88	20.89 ± 61.46	51.10 ± 44.78
2	0 ± 10.13	12.46 ± 18.82	2.08 ± 17.08	-85.36 ± 13.16	0.11 ± 31.39	-47.28 ± 16.41	-43.17 ± 23.46	-82.26 ± 5.06
4	0 ± 9.13	-26.18 ± 9.64	-32.48 ± 10.42	-53.65 ± 21.77	3.41 ± 32.56	-42.54 ± 12.58	-25.25 ± 25.52	-95.83 ± 1.10
6	0 ± 2.63	-18.75 ± 6.08	-27.26 ± 6.91	-47.32 ± 14.55	-14.22 ± 13.52	-29.83 ± 12.46	-28.87 ± 14.07	-98.79 ± 0.41
8	0 ± 1.37	-5.95 ± 5.36	-10.46 ± 3.96	-36.61 ± 8.69	-1.47 ± 7.65	-19.63 ± 11.30	-18.97 ± 8.99	-98.12 ± 0.95
24	0 ± 1.84	-4.28 ± 6.24	-9.45 ± 3.78	-31.24 ± 5.09	6.11 ± 5.69	-14.28 ± 12.28	-15.77 ± 7.56	-33.47 ± 9.23

^aSignificant reductions from control are bolded and highlighted in blue ($P < 0.05$, by two-way ANOVA with *posthoc* Dunnett's multiple comparison test). ^bSignificant increases from control are highlighted in red ($P < 0.05$, by two-way ANOVA with *posthoc* Dunnett's multiple comparison test).

Table A3.8. Effects of Neutral, Nonfucosylated HMOs on GB590 Growth Over 24 h^{a,b}

	Media (Control)	Lactose	LNT	LNT	LNT II	LNnH	para-LNnH	HMO Mixture
Time (h)	Difference from Control (%) ± SEM							
0	0.00 ± 22.37	23.88 ± 55.76	-4.86 ± 84.35	-100.00 ± 0.00	-100.00 ± 0.00	-55.13 ± 25.62	77.39 ± 93.00	51.10 ± 44.78
2	0.00 ± 10.13	13.33 ± 24.40	-37.00 ± 43.61	-77.52 ± 11.25	-95.16 ± 3.62	-90.48 ± 3.39	-55.75 ± 22.58	-82.26 ± 5.06
4	0.00 ± 9.13	-7.78 ± 12.34	-19.02 ± 41.44	-48.23 ± 19.34	-76.74 ± 4.33	-67.04 ± 4.49	-29.89 ± 12.35	-95.83 ± 1.10
6	0.00 ± 2.63	-9.96 ± 4.99	-27.85 ± 19.47	-37.42 ± 13.54	-41.30 ± 3.59	-34.17 ± 3.18	-14.50 ± 8.22	-98.79 ± 0.41
8	0.00 ± 1.37	-5.35 ± 2.51	-19.41 ± 13.36	-24.05 ± 6.77	-27.60 ± 2.87	-24.13 ± 2.96	-9.03 ± 8.25	-98.12 ± 0.95
24	0.00 ± 1.84	-5.40 ± 3.50	-16.36 ± 11.06	-22.40 ± 3.92	-31.47 ± 3.11	-26.01 ± 3.41	-6.89 ± 9.74	-33.47 ± 9.23

^aSignificant reductions from control are bolded and highlighted in blue ($P < 0.05$, by two-way ANOVA with *posthoc* Dunnett's multiple comparison test). ^bSignificant increases from control are highlighted in red ($P < 0.05$, by two-way ANOVA with *posthoc* Dunnett's multiple comparison test).

Table A3.9. Effects of Neutral, Fucosylated HMOs on GB2 Growth Over 24 h^{a,b}

	Media (Control)	2-FL	3-FL	DFL	LNFP I	LNFP II	LNFP III	HMO Mixture
Time (h)	Difference from Control (%) ± SEM							
0	0.00 ± 18.61	52.58 ± 70.23	26.07 ± 64.43	134.99 ± 82.02	407.83 ± 165.37	105.41 ± 93.86	353.48 ± 126.29	231.24 ± 72.30
2	0.00 ± 8.72	-13.99 ± 16.11	6.60 ± 32.86	17.32 ± 25.91	83.61 ± 52.11	4.33 ± 28.95	96.66 ± 47.25	-46.05 ± 8.52
4	0.00 ± 8.51	-22.18 ± 11.89	-9.26 ± 17.90	6.08 ± 18.30	12.29 ± 25.91	-9.41 ± 15.03	23.81 ± 21.94	-89.97 ± 1.23
6	0.00 ± 2.25	-5.42 ± 4.92	0.33 ± 5.49	10.94 ± 7.71	9.08 ± 13.92	5.79 ± 10.46	19.11 ± 10.23	-95.48 ± 0.77
8	0.00 ± 1.66	-1.99 ± 7.54	3.10 ± 6.78	12.19 ± 7.42	12.70 ± 12.61	7.33 ± 10.20	19.90 ± 9.76	-92.18 ± 1.97
24	0.00 ± 1.71	-0.85 ± 6.71	-2.04 ± 6.68	8.58 ± 5.43	7.58 ± 10.94	-1.34 ± 7.74	12.49 ± 8.61	-39.38 ± 8.74

^aSignificant reductions from control are bolded and highlighted in blue ($P < 0.05$, by two-way ANOVA with *posthoc* Dunnett's multiple comparison test). ^bSignificant increases from control are highlighted in red ($P < 0.05$, by two-way ANOVA with *posthoc* Dunnett's multiple comparison test).

Table A3.10. Effects of Neutral, Nonfucosylated HMOs on GB2 Growth Over 24 h^{a,b}

Time (h)	Media (Control)	Lactose	LNT	LNnT	LNT II	LNnH	para-LNnH	HMO Mixture
0	0.00 ± 18.61	201.51 ± 103.76	82.64 ± 91.27	23.75 ± 69.83	14.63 ± 63.10	16.75 ± 47.39	222.71 ± 103.07	231.24 ± 72.30
2	0.00 ± 8.72	48.76 ± 21.49	19.34 ± 41.89	-29.47 ± 18.52	-44.36 ± 16.84	-71.57 ± 9.50	21.92 ± 22.77	-46.05 ± 8.52
4	0.00 ± 8.51	22.66 ± 20.35	-6.50 ± 19.50	-15.72 ± 11.50	-39.11 ± 12.84	-56.67 ± 8.44	3.89 ± 12.53	-89.97 ± 1.23
6	0.00 ± 2.25	10.71 ± 4.87	-1.83 ± 8.72	3.13 ± 8.63	-13.69 ± 7.60	-24.51 ± 4.67	8.33 ± 8.21	-95.48 ± 0.77
8	0.00 ± 1.66	9.51 ± 5.04	2.19 ± 6.73	7.88 ± 8.26	-9.41 ± 7.38	-18.44 ± 4.35	8.74 ± 7.56	-92.18 ± 1.97
24	0.00 ± 1.71	15.12 ± 5.78	11.35 ± 2.26	6.43 ± 4.91	-5.44 ± 8.57	-22.57 ± 3.91	5.21 ± 5.65	-39.38 ± 8.74

^aSignificant reductions from control are bolded and highlighted in blue ($P < 0.05$, by two-way ANOVA with *posthoc* Dunnett's multiple comparison test). ^bSignificant increases from control are highlighted in red ($P < 0.05$, by two-way ANOVA with *posthoc* Dunnett's multiple comparison test).

Table A3.11 . Effects of Neutral, Fucosylated HMOs on GB590 Viability Over 24 h^{a,b}

	Media (Control)	2'-FL	3-FL	DFL	LNFP I	LNFP II	LNFP III	HMO Mixture
Time (h)	Difference from Control (%) ± SEM							
0	0 ± 2.48	3.59 ± 9.30	-1.82 ± 5.80	-23.60 ± 4.03	-2.25 ± 6.28	-10.49 ± 5.81	-10.59 ± 6.00	-7.21 ± 4.66
2	0 ± 3.83	-7.00 ± 7.45	-3.91 ± 6.29	-25.34 ± 2.30	-27.55 ± 3.58	-28.42 ± 3.26	-19.90 ± 3.80	-26.24 ± 2.35
4	0 ± 3.04	4.84 ± 4.88	1.23 ± 8.68	-14.34 ± 4.02	-17.63 ± 2.11	-25.02 ± 3.84	-21.30 ± 4.77	-26.71 ± 2.63
6	0 ± 4.29	8.26 ± 6.44	1.65 ± 6.15	-20.76 ± 3.21	-23.32 ± 2.67	-15.24 ± 4.11	-17.23 ± 3.45	-37.76 ± 2.18
8	0 ± 2.60	22.03 ± 4.53	8.12 ± 3.33	-9.18 ± 2.33	-18.40 ± 2.20	-9.56 ± 2.38	-8.94 ± 2.64	-37.34 ± 2.28
24	0 ± 2.88	20.26 ± 4.10	8.91 ± 4.86	-16.59 ± 3.81	-31.89 ± 3.79	4.47 ± 7.96	-3.25 ± 3.96	12.97 ± 10.97

^aSignificant reductions from control are bolded and highlighted in blue ($P < 0.05$, by two-way ANOVA with *posthoc* Dunnett's multiple comparison test). ^bSignificant increases from control are highlighted in red ($P < 0.05$, by two-way ANOVA with *posthoc* Dunnett's multiple comparison test).

Table A3.12. Effects of Neutral, Nonfucosylated HMOs on GB590 Viability Over 24 h^{a,b}

Time (h)	Media (Control)	Lactose	LNT	LNnT	LNT II	LNnH	para-LNnH	HMO Mixture
	Difference from Control (%) ± SEM							
0	0 ± 2.48	3.27 ± 7.42	-9.70 ± 3.84	-20.80 ± 3.33	-8.75 ± 4.52	-8.56 ± 3.10	9.04 ± 5.53	-7.21 ± 4.66
2	0 ± 3.83	-7.22 ± 6.29	-22.67 ± 2.65	-23.05 ± 2.65	-21.44 ± 2.36	-20.27 ± 3.01	-20.85 ± 3.28	-26.24 ± 2.35
4	0 ± 3.04	5.69 ± 3.61	-13.55 ± 5.68	-19.25 ± 3.14	-17.19 ± 3.87	-20.43 ± 2.41	-12.14 ± 3.55	-26.71 ± 2.63
6	0 ± 4.29	0.87 ± 4.92	-15.92 ± 4.09	-17.13 ± 3.91	-13.61 ± 3.11	-9.85 ± 4.16	-5.45 ± 4.10	-37.76 ± 2.18
8	0 ± 2.60	10.67 ± 3.83	-5.04 ± 2.15	-2.85 ± 2.41	-5.07 ± 1.96	-8.08 ± 2.15	-8.43 ± 2.90	-37.34 ± 2.28
24	0 ± 2.88	23.30 ± 7.24	2.32 ± 4.88	-3.17 ± 2.28	-3.11 ± 2.84	-0.72 ± 3.48	2.07 ± 5.13	12.97 ± 10.97

^aSignificant reductions from control are bolded and highlighted in blue ($P < 0.05$, by two-way ANOVA with *posthoc* Dunnett's multiple comparison test). ^bSignificant increases from control are highlighted in red ($P < 0.05$, by two-way ANOVA with *posthoc* Dunnett's multiple comparison test).

Table A3.13. Effects of Neutral, Fucosylated HMOs on GB2 Viability Over 24 h^{a,b}

	Media (Control)	2'-FL	3-FL	DFL	LNFP I	LNFP II	LNFP III	HMO Mixture
Time (h)	Difference from Control (%) ± SEM							
0	0 ± 2.67	1.36 ± 5.10	1.95 ± 4.45	2.97 ± 5.84	4.08 ± 3.49	1.14 ± 5.43	6.73 ± 4.12	-5.36 ± 3.25
2	0 ± 1.88	-4.19 ± 8.46	-8.75 ± 6.04	-11.07 ± 2.76	-10.90 ± 3.04	-12.16 ± 2.01	-11.45 ± 2.89	-22.36 ± 1.47
4	0 ± 2.62	-10.81 ± 4.60	-5.29 ± 7.37	-12.13 ± 1.98	-10.28 ± 3.30	-10.89 ± 3.33	-14.00 ± 2.40	-30.80 ± 1.88
6	0 ± 2.85	-10.69 ± 3.42	-1.91 ± 4.34	-10.36 ± 2.05	-8.75 ± 1.88	-4.87 ± 2.70	-8.81 ± 2.34	-36.40 ± 1.71
8	0 ± 2.57	-7.33 ± 3.67	2.16 ± 3.67	-9.77 ± 2.41	-5.19 ± 2.90	-4.86 ± 2.95	-4.02 ± 2.95	-35.39 ± 1.78
24	0 ± 3.71	-11.77 ± 2.83	-7.15 ± 3.40	-13.56 ± 3.79	-13.25 ± 4.00	-12.92 ± 3.34	-4.32 ± 4.18	4.25 ± 4.49

^aSignificant reductions from control are bolded and highlighted in blue ($P < 0.05$, by two-way ANOVA with *posthoc* Dunnett's multiple comparison test). ^bSignificant increases from control are highlighted in red ($P < 0.05$, by two-way ANOVA with *posthoc* Dunnett's multiple comparison test).

Table A3.14. Effects of Neutral, Nonfucosylated HMOs on GB2 Viability Over 24 h^{a,b}

	Media (Control)	Lactose	LNT	LNnT	LNT II	LNnH	para-LNnH	HMO Mixture
Time (h)	Difference from Control (%) ± SEM							
0	0 ± 2.67	5.67 ± 3.63	4.41 ± 5.05	-0.32 ± 3.68	-10.86 ± 6.06	-9.28 ± 4.56	6.82 ± 3.38	-5.36 ± 3.25
2	0 ± 1.88	-1.47 ± 5.17	-7.75 ± 2.41	-10.40 ± 2.25	-17.38 ± 3.03	-16.69 ± 2.98	-7.88 ± 2.86	-22.36 ± 1.47
4	0 ± 2.62	-2.51 ± 4.33	-3.01 ± 2.72	-3.33 ± 2.37	-10.59 ± 3.85	-12.59 ± 4.19	-9.36 ± 2.92	-30.80 ± 1.88
6	0 ± 2.85	-5.52 ± 3.06	2.20 ± 2.17	-6.02 ± 2.63	-7.14 ± 3.21	-15.72 ± 2.85	-10.28 ± 2.02	-36.40 ± 1.71
8	0 ± 2.57	-4.11 ± 3.15	5.50 ± 2.65	1.79 ± 3.64	-0.83 ± 2.96	-13.48 ± 2.65	-4.29 ± 2.86	-35.39 ± 1.78
24	0 ± 3.71	3.49 ± 3.26	1.78 ± 3.35	-1.87 ± 2.85	-3.79 ± 4.24	-14.12 ± 3.58	-7.48 ± 3.77	4.25 ± 4.49

^aSignificant reductions from control are bolded and highlighted in blue ($P < 0.05$, by two-way ANOVA with *posthoc* Dunnett's multiple comparison test). ^bSignificant increases from control are highlighted in red ($P < 0.05$, by two-way ANOVA with *posthoc* Dunnett's multiple comparison test).

Table A3.15. Effects of Neutral, Fucosylated HMOs on GB590 Biofilm Production at 24 h^{a,b}

Media (Control)	2'-FL	3-FL	DFL	LNFP I	LNFP II	LNFP III
Difference from Control (%) ± SEM						
0 ± 5.23	7.84 ± 10.36	-3.95 ± 6.12	53.77 ± 15.53	-34.86 ± 11.05	32.72 ± 20.35	19.66 ± 11.66

^aSignificant reductions from control are bolded and highlighted in blue ($P < 0.05$, by two-way ANOVA with *posthoc* Dunnett's multiple comparison test). ^bSignificant increases from control are highlighted in red ($P < 0.05$, by two-way ANOVA with *posthoc* Dunnett's multiple comparison test).

Table A3.16. Effects of Neutral, Nonfucosylated HMOs on GB590 Biofilm Production at 24 h^{a,b}

Media (Control)	Lactose	LNT	LNnT	LNT II	LNnH	para-LNnH
Difference from Control (%) ± SEM						
0 ± 5.23	21.15 ± 11.78	31.87 ± 12.15	46.49 ± 15.49	88.45 ± 11.46	55.99 ± 15.52	35.76 ± 20.86

^aSignificant reductions from control are bolded and highlighted in blue ($P < 0.05$, by two-way ANOVA with *posthoc* Dunnett's multiple comparison test). ^bSignificant increases from control are highlighted in red ($P < 0.05$, by two-way ANOVA with *posthoc* Dunnett's multiple comparison test).

Table A3.17. Effects of Neutral, Fucosylated HMOs on GB2 Biofilm Production at 24 h^{a,b}

Media (Control)	2'-FL	3-FL	DFL	LNFP I	LNFP II	LNFP III
Difference from Control (%) ± SEM						
0 ± 4.81	21.45 ± 15.04	17.34 ± 9.69	-2.97 ± 11.57	-0.93 ± 15.15	13.04 ± 14.71	-5.70 ± 14.62

^aSignificant reductions from control are bolded and highlighted in blue ($P < 0.05$, by two-way ANOVA with *posthoc* Dunnett's multiple comparison test). ^bSignificant increases from control are highlighted in red ($P < 0.05$, by two-way ANOVA with *posthoc* Dunnett's multiple comparison test).

Table A3.18. Effects of Neutral, Nonfucosylated HMOs on GB2 Biofilm Production at 24 h^{a,b}

Media (Control)	Lactose	LNT	LNnT	LNT II	LNnH	para-LNnH
Difference from Control (%) ± SEM						
0 ± 4.81	0.57 ± 10.52	-27.95 ± 3.66	-13.25 ± 6.69	27.39 ± 18.18	23.71 ± 9.17	-13.11 ± 6.23

^aSignificant reductions from control are bolded and highlighted in blue ($P < 0.05$, by one-way ANOVA with *posthoc* Dunnett's multiple comparison test). ^bSignificant increases from control are highlighted in red ($P < 0.05$, by one-way ANOVA with *posthoc* Dunnett's multiple comparison test).

Table A3.19. Effects of HMO Mixtures on GB590 Growth Over 24 h^{a,b}

	Media (Control)	GB590 HMO Mixture	HMO Extract Mimic	Whole HMO Extract
Time (h)	Difference from Control (%) ± SEM			
0	0 ± 53.26	435.37 ± 320.79	326.07 ± 345.94	605.46 ± 363.47
2	0 ± 10.76	-34.25 ± 23.89	-43.73 ± 35.22	-56.22 ± 13.26
4	0 ± 14.00	-35.54 ± 18.84	-38.07 ± 29.03	-92.10 ± 2.46
6	0 ± 1.21	-29.48 ± 7.37	-35.85 ± 12.01	-99.22 ± 0.41
8	0 ± 1.67	-15.49 ± 6.75	-19.38 ± 9.86	-99.17 ± 0.50
24	0 ± 1.32	-9.57 ± 6.73	-16.34 ± 9.23	-3.69 ± 6.99

^aSignificant reductions from control are bolded and highlighted in blue ($P < 0.05$, by two-way ANOVA with *posthoc* Dunnett's multiple comparison test). ^bSignificant increases from control are highlighted in red ($P < 0.05$, by two-way ANOVA with *posthoc* Dunnett's multiple comparison test).

Table A3.20. Effects of HMO Mixtures on GB590 Viability Over 24 h^{a,b}

	Media (Control)	GB590 HMO Mixture	HMO Extract Mimic	Whole HMO Extract
Time (h)	Difference from Control (%) ± SEM			
0	0 ± 2.90	-2.09 ± 4.16	-12.49 ± 4.79	-5.99 ± 3.83
2	0 ± 2.72	-11.73 ± 2.43	-17.33 ± 3.16	-20.64 ± 2.37
4	0 ± 2.21	-22.18 ± 3.08	-19.84 ± 2.51	-30.55 ± 1.49
6	0 ± 1.49	-6.17 ± 2.73	-4.93 ± 1.95	-35.11 ± 1.56
8	0 ± 2.71	-3.43 ± 2.52	5.60 ± 2.51	-33.67 ± 1.60
24	0 ± 2.93	-13.35 ± 2.21	-5.78 ± 2.49	37.52 ± 3.08

^aSignificant reductions from control are bolded and highlighted in blue ($P < 0.05$, by two-way ANOVA with *posthoc* Dunnett's multiple comparison test). ^bSignificant increases from control are highlighted in red ($P < 0.05$, by two-way ANOVA with *posthoc* Dunnett's multiple comparison test).

Table A3.21. Effects of HMO Mixtures on GB2 Growth Over 24 h^{a,b}

	Media (Control)	GB2 HMO Mixture	HMO Extract Mimic	Whole HMO Extract
Time (h)	Difference from Control (%) ± SEM			
0	0 ± 68.10	511.18 ± 361.67	575.82 ± 493.49	1078.82 ± 657.40
2	0 ± 6.04	-20.09 ± 23.47	-4.61 ± 36.12	-20.15 ± 18.34
4	0 ± 4.66	-31.69 ± 16.50	-17.98 ± 21.37	-89.92 ± 2.16
6	0 ± 1.60	-22.94 ± 9.58	-14.87 ± 10.22	-97.22 ± 0.77
8	0 ± 0.87	-13.43 ± 9.73	-5.76 ± 9.00	-94.84 ± 0.77
24	0 ± 0.81	-14.52 ± 8.26	-9.78 ± 9.20	13.28 ± 2.50

^aSignificant reductions from control are bolded and highlighted in blue ($P < 0.05$, by two-way ANOVA with *posthoc* Dunnett's multiple comparison test). ^bSignificant increases from control are highlighted in red ($P < 0.05$, by two-way ANOVA with *posthoc* Dunnett's multiple comparison test).

Table A3.22. Effects of HMO Mixtures on GB2 Viability Over 24 h^{a,b}

	Media (Control)	GB2 HMO Mixture	HMO Extract Mimic	Whole HMO Extract
Time (h)	Difference from Control (%) ± SEM			
0	0 ± 2.57	-10.38 ± 3.76	-9.13 ± 3.96	-12.73 ± 4.41
2	0 ± 1.94	-16.27 ± 1.97	-15.10 ± 1.68	-23.29 ± 1.76
4	0 ± 2.36	-16.21 ± 3.44	-8.17 ± 1.65	-27.35 ± 1.59
6	0 ± 1.33	6.85 ± 1.43	7.25 ± 1.24	-30.03 ± 1.04
8	0 ± 1.04	6.66 ± 2.10	7.90 ± 2.11	-24.97 ± 1.17
24	0 ± 1.09	8.77 ± 1.80	8.18 ± 1.58	49.65 ± 1.76

^aSignificant reductions from control are bolded and highlighted in blue ($P < 0.05$, by two-way ANOVA with *posthoc* Dunnett's multiple comparison test). ^bSignificant increases from control are highlighted in red ($P < 0.05$, by two-way ANOVA with *posthoc* Dunnett's multiple comparison test).

Table A3.23. Effects of HMO Mixtures on GB590 Biofilm Production at 24 h^{a,b}

Media (Control)	GB590 HMO Mixture	HMO Extract Mimic	Whole HMO Extract
Difference from Control (%) ± SEM			
0.00 ± 7.52	-11.76 ± 8.90	-54.65 ± 7.31	16.98 ± 12.61

^aSignificant reductions from control are bolded and highlighted in blue ($P < 0.05$, by one-way ANOVA with *posthoc* Dunnett's multiple comparison test). ^bSignificant increases from control are highlighted in red ($P < 0.05$, by one-way ANOVA with *posthoc* Dunnett's multiple comparison test).

Table A3.24. Effects of HMO Mixtures on GB2 Biofilm Production at 24 h^{a,b}

Media (Control)	GB590 HMO Mixture	HMO Extract Mimic	Whole HMO Extract
Difference from Control (%) ± SEM			
0.00 ± 9.03	24.12 ± 15.80	-64.72 ± 4.50	19.68 ± 17.16

^aSignificant reductions from control are bolded and highlighted in blue ($P < 0.05$, by one-way ANOVA with *posthoc* Dunnett's multiple comparison test). ^bSignificant increases from control are highlighted in red ($P < 0.05$, by one-way ANOVA with *posthoc* Dunnett's multiple comparison test).

Table A3.25. Effects of 1-Amino-2'-Fucosyllactose (Amino-2'-FL) on GB590 Growth Over 24 h^{a,b}

	Media (Control)	Lactose	2'-FL	Amino-2'-FL
Time (h)	Difference from Control (%) ± SEM			
0	0 ± 36.75	-98.91 ± 1.12	-63.77 ± 37.43	-100.00 ± 0.00
2	0 ± 13.85	-42.01 ± 17.65	2.06 ± 18.38	-27.84 ± 15.30
4	0 ± 10.66	-17.11 ± 14.45	-19.44 ± 12.82	-11.85 ± 15.75
6	0 ± 5.64	-8.51 ± 11.03	-14.28 ± 8.69	-5.66 ± 9.48
8	0 ± 1.62	6.36 ± 3.00	-7.18 ± 4.14	-7.53 ± 3.43
24	0 ± 1.83	11.85 ± 3.50	-10.88 ± 3.72	-8.81 ± 3.36

^aSignificant reductions from control are bolded and highlighted in blue ($P < 0.05$, by two-way ANOVA with *posthoc* Dunnett's multiple comparison test). ^bSignificant increases from control are highlighted in red ($P < 0.05$, by two-way ANOVA with *posthoc* Dunnett's multiple comparison test).

Table A3.26. Effects of 1-Amino-2'-Fucosyllactose (Amino-2'-FL) on GB590 Viability Over 24 h^{a,b}

	Media	Lactose	2'-FL	Amino-2'-FL
Time (h)	Difference from Control (%) ± SEM			
0	0 ± 4.80	7.55 ± 9.61	-1.64 ± 8.57	-9.19 ± 7.93
2	0 ± 6.36	-15.13 ± 5.61	-9.34 ± 10.03	-7.77 ± 6.44
4	0 ± 3.69	1.91 ± 3.75	4.06 ± 5.57	-5.08 ± 5.56
6	0 ± 8.55	-9.74 ± 5.90	0.88 ± 9.15	-10.72 ± 6.15
8	0 ± 2.53	6.29 ± 4.44	13.35 ± 3.83	19.76 ± 4.12
24	0 ± 3.79	21.46 ± 8.85	14.13 ± 5.14	27.20 ± 6.27

^aSignificant reductions from control are bolded and highlighted in blue ($P < 0.05$, by two-way ANOVA with *posthoc* Dunnett's multiple comparison test). ^bSignificant increases from control are highlighted in red ($P < 0.05$, by two-way ANOVA with *posthoc* Dunnett's multiple comparison test).

Table A3.27. Effects of 1-Amino-2'-Fucosyllactose (Amino-2'-FL) on GB2 Growth Over 24 h^{a,b}

	Media	Lactose	2'-FL	Amino 2'-FL
Time (h)	Difference from Control (%) ± SEM			
0	0 ± 35.56	91.90 ± 63.02	7.47 ± 59.56	116.09 ± 77.58
2	0 ± 18.97	30.06 ± 27.95	-4.66 ± 31.50	30.25 ± 32.91
4	0 ± 18.69	26.48 ± 27.77	-19.23 ± 18.56	1.39 ± 22.08
6	0 ± 5.24	34.86 ± 7.65	2.77 ± 6.60	17.55 ± 7.34
8	0 ± 3.18	38.82 ± 3.50	5.99 ± 7.26	17.21 ± 6.10
24	0 ± 2.70	33.78 ± 4.48	-2.72 ± 6.78	9.03 ± 4.24

^aSignificant reductions from control are bolded and highlighted in blue ($P < 0.05$, by two-way ANOVA with *posthoc* Dunnett's multiple comparison test). ^bSignificant increases from control are highlighted in red ($P < 0.05$, by two-way ANOVA with *posthoc* Dunnett's multiple comparison test).

Table A3.28. Effects of 1-Amino-2'-Fucosyllactose (Amino-2'-FL) on GB2 Viability Over 24 h^{a,b}

	Media	Lactose	2'-FL	Amino 2'-FL
Time (h)	Difference from Control (%) ± SEM			
0	0 ± 2.65	6.55 ± 4.38	0.75 ± 7.17	4.75 ± 4.67
2	0 ± 4.26	-3.40 ± 5.72	-4.12 ± 10.58	-7.33 ± 7.86
4	0 ± 4.42	-1.40 ± 6.09	-10.50 ± 6.23	0.33 ± 9.73
6	0 ± 2.98	-9.36 ± 3.45	-14.58 ± 3.74	-7.27 ± 4.02
8	0 ± 2.71	-5.50 ± 2.76	-9.90 ± 4.76	-1.50 ± 5.83
24	0 ± 3.01	-2.04 ± 3.04	-15.81 ± 2.61	5.90 ± 3.48

^aSignificant reductions from control are bolded and highlighted in blue ($P < 0.05$, by two-way ANOVA with *posthoc* Dunnett's multiple comparison test). ^bSignificant increases from control are highlighted in red ($P < 0.05$, by two-way ANOVA with *posthoc* Dunnett's multiple comparison test).

Table A3.29. Effects of 1-Amino-2'-Fucosyllactose (Amino-2'-FL) on GB590 Biofilm Production at 24 h^{a,b}

Media	Lactose	2'-FL	Amino 2'-FL
Difference from Control (%) ± SEM			
0 ± 10.47	25.38 ± 14.61	11.61 ± 12.89	-37.57 ± 7.61

^aSignificant reductions from control are bolded and highlighted in blue ($P < 0.05$, by one-way ANOVA with *posthoc* Dunnett's multiple comparison test). ^bSignificant increases from control are highlighted in red ($P < 0.05$, by one-way ANOVA with *posthoc* Dunnett's multiple comparison test).

Table A3.30. Effects of 1-Amino-2'-Fucosyllactose (Amino-2'-FL) on GB2 Biofilm Production at 24 h^{a,b}

Media	Lactose	2'-FL	Amino 2'-FL
Difference from Control (%) ± SEM			
0 ± 4.16	-10.89 ± 9.20	7.62 ± 13.20	-46.01 ± 5.82

^aSignificant reductions from control are bolded and highlighted in blue ($P < 0.05$, by one-way ANOVA with *posthoc* Dunnett's multiple comparison test). ^bSignificant increases from control are highlighted in red ($P < 0.05$, by one-way ANOVA with *posthoc* Dunnett's multiple comparison test).

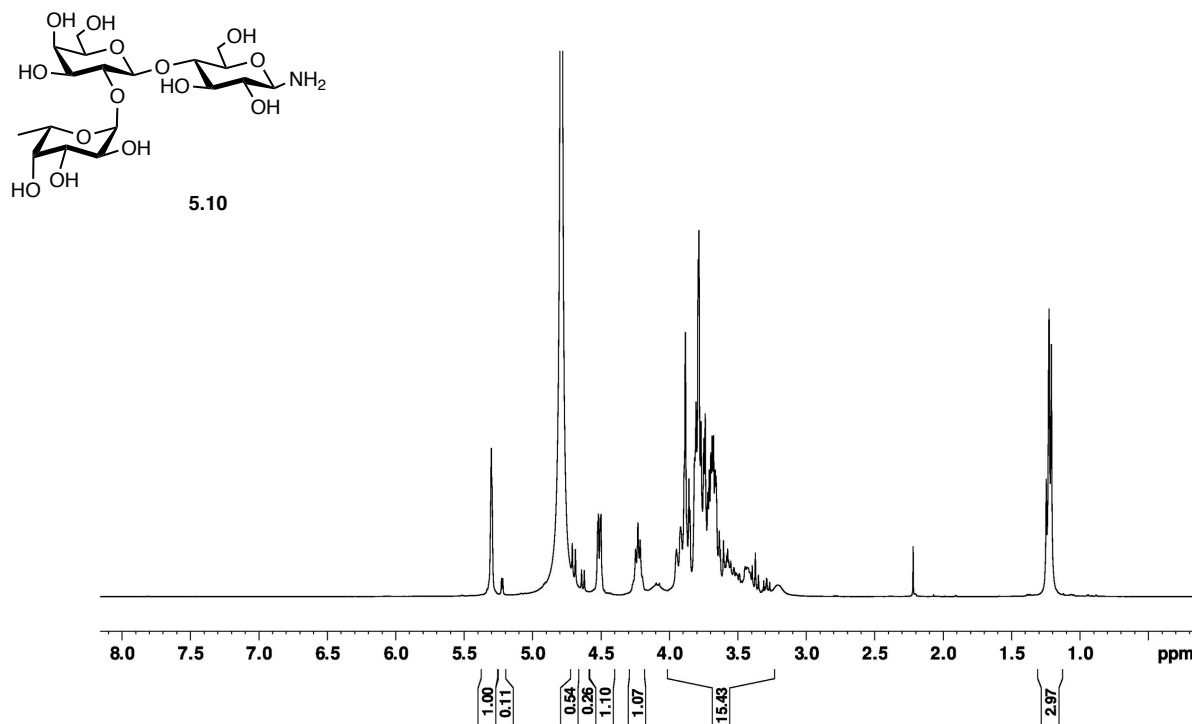
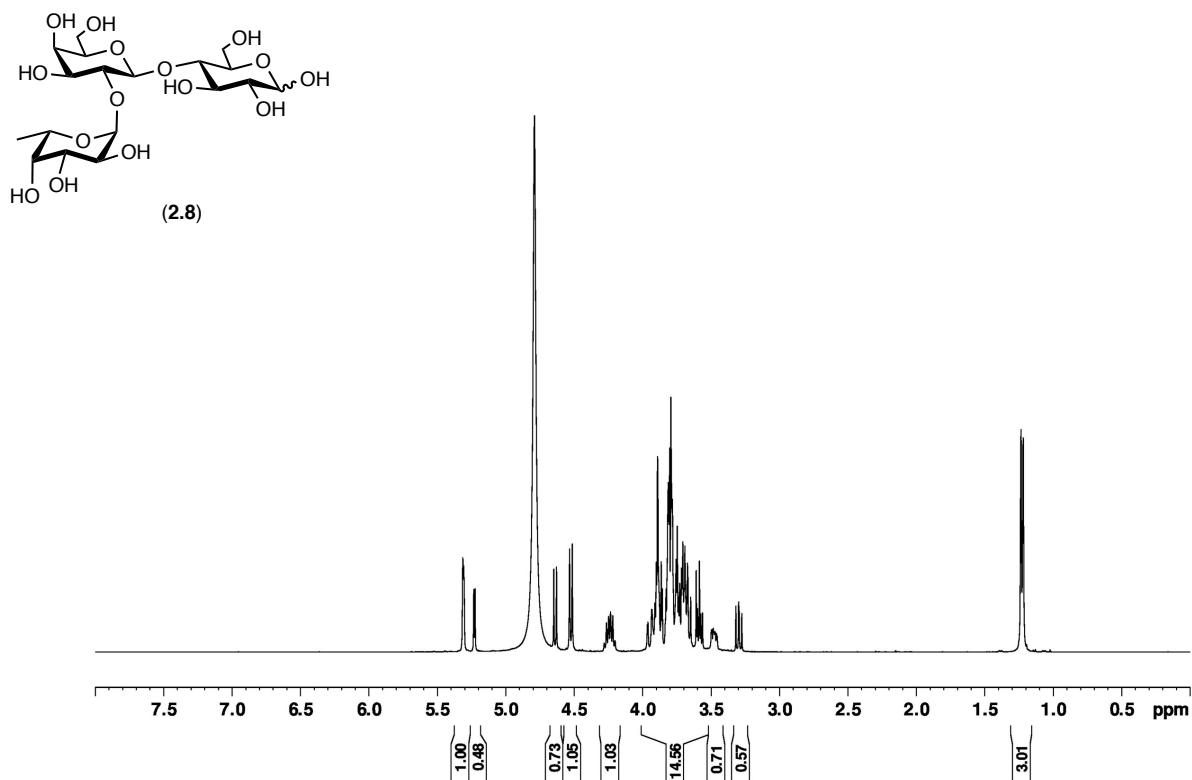


Figure A3.1. ¹H NMR (400 MHz, D₂O) comparison of 2'-FL (2.8) and 1-amino-2'-FL, 5.10.

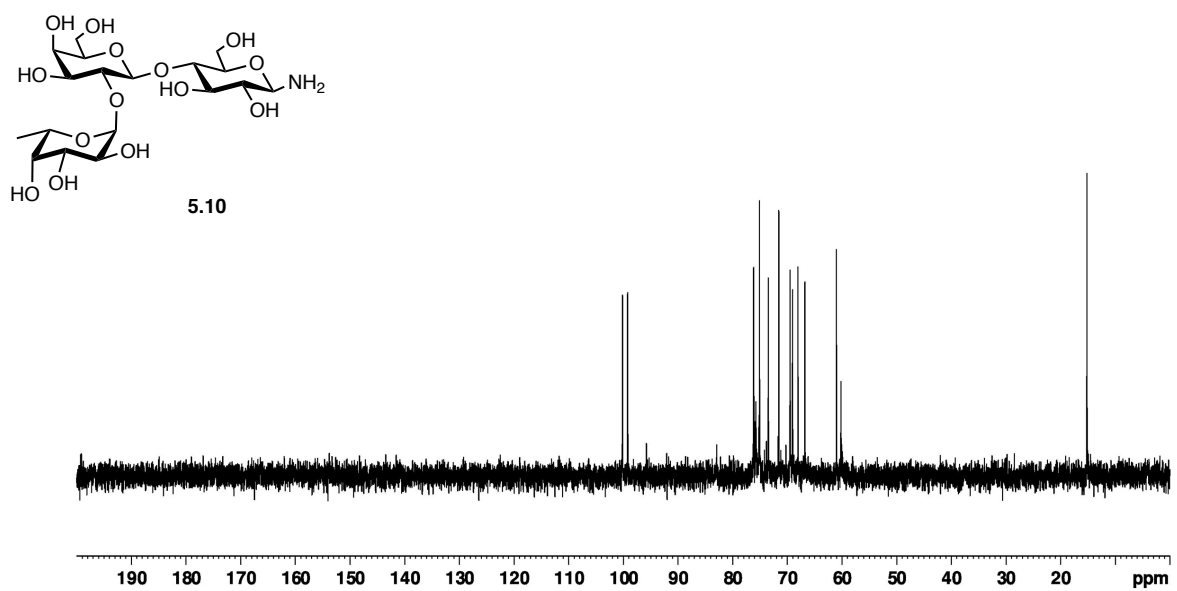
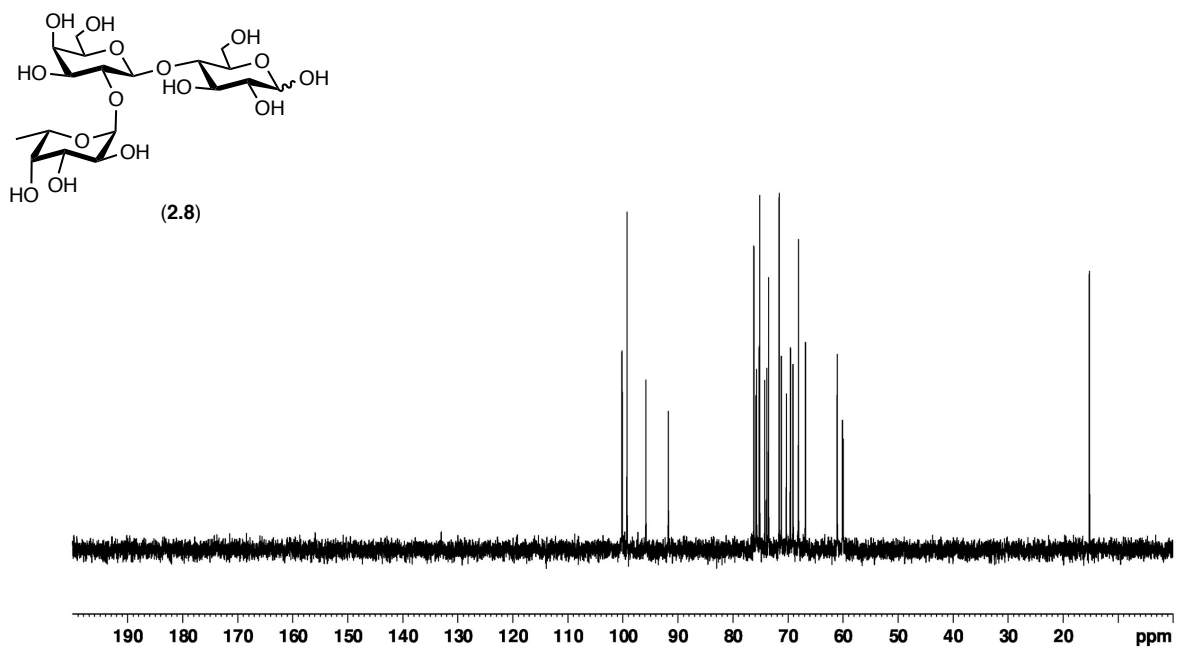


Figure A3.2 ^{13}C NMR (100 MHz, D_2O) comparison of 2'-FL (2.8) and 1-amino-2'-FL, 5.10.